

OPTIMAL DESIGN AND CONTROL OF  
MINE SITE ENERGY SUPPLY SYSTEMS

by

Alberto Romero

A thesis submitted in partial fulfillment

of the requirements for the degree of

Doctor of Philosophy (PhD) in Natural Resources Engineering

Faculty of Graduate Studies

Laurentian University

Sudbury, Ontario, Canada

© Alberto Romero, 2016

**THESIS DEFENCE COMMITTEE/COMITÉ DE SOUTENANCE DE THÈSE**  
**Laurentian Université/Université Laurentienne**  
Faculty of Graduate Studies/Faculté des études supérieures

Title of Thesis Titre de la thèse	OPTIMAL DESIGN AND CONTROL OF MINE SITE ENERGY SUPPLY SYSTEMS	
Name of Candidate Nom du candidat	Romero, Alberto	
Degree Diplôme	Doctor of Philosophy	
Department/Program Département/Programme	Natural Resources Engineering	Date of Defence Date de la soutenance August 26, 2016

**APPROVED/APPROUVÉ**

Thesis Examiners/Examineurs de thèse:

Dr. Dean Millar  
(Co-supervisor/Co-directeur de thèse)

Dr. Monica Carvalho  
(Co-supervisor/Co-diretrice de thèse)

Dr. Brent Livers  
(Committee member/Membre du comité)

Dr. Marc Aresnault  
(Committee member/Membre du comité)

Dr. Alan Fung  
(External Examiner/Examineur externe)

Dr. Youssou Gningue  
(Internal Examiner/Examineur interne)

Approved for the Faculty of Graduate Studies  
Approuvé pour la Faculté des études supérieures  
Dr. Shelley Watson  
Madame Shelley Watson  
Acting Dean, Faculty of Graduate Studies  
Doyenne intérimaire, Faculté des études  
supérieures

**ACCESSIBILITY CLAUSE AND PERMISSION TO USE**

I, **Alberto Romero**, hereby grant to Laurentian University and/or its agents the non-exclusive license to archive and make accessible my thesis, dissertation, or project report in whole or in part in all forms of media, now or for the duration of my copyright ownership. I retain all other ownership rights to the copyright of the thesis, dissertation or project report. I also reserve the right to use in future works (such as articles or books) all or part of this thesis, dissertation, or project report. I further agree that permission for copying of this thesis in any manner, in whole or in part, for scholarly purposes may be granted by the professor or professors who supervised my thesis work or, in their absence, by the Head of the Department in which my thesis work was done. It is understood that any copying or publication or use of this thesis or parts thereof for financial gain shall not be allowed without my written permission. It is also understood that this copy is being made available in this form by the authority of the copyright owner solely for the purpose of private study and research and may not be copied or reproduced except as permitted by the copyright laws without written authority from the copyright owner.

## Abstract

The mining sector has seen an increase in costs associated with the use of energy in recent decades. Due to lower ore grade, deeper mineralization, or more remote location new mines generally require more energy to produce the same amount of mineral. Mining operations require reliable and cost-effective energy supply, without which extraction becomes economically risky, as well as unsafe for miners.

Commercial software and research-oriented computer models are now available to assist in the decision making process regarding the optimal selection of Energy Supply Systems (ESS) and associated costs. However, software and models present limitations: some are designed to minimize the cost of supplying only heat and electricity, while others are custom applications for the residential and commercial sectors. Most computer tools assume invariable operating conditions, e.g. energy supply and demand profiles that do not change throughout the lifetime of the mine, or conditions whose variations can be perfectly predicted. As a result, the optimization of ESS can yield designs that lack robustness to deal with real life, changing environments.

Under the same approach, the Optimal Mine Site Energy Supply (OMSES) concept was originally developed as a deterministic mathematical programming tool to find the optimal combination of energy technologies and sources that could meet final energy demands. The solution also included the optimal operation strategy based on typical energy demands of a specific mine site.

This thesis expands OMSES to address the robustness of the solution, by considering the uncertainty and variability of real operating conditions. A method is proposed herein, based on

the optimal solution obtained by OMSES and utilizing Model Predictive Control (MPC). The MPC-based simulation under changing environmental conditions ensures that energy demands are met at all times, taking into account energy demands and supply forecast, as well as their inherent variability. Results show that near optimal, more robust design solutions are obtained when the system is simulated under uncertain, more realistic operational conditions, leaving MPC in charge of exploring under-capacity events and of redesigning the system to ensure feasibility with minimum cost increase. This new method has been termed MPC-OMSES dynamic redesign.

This thesis also reports on research work to adapt OMSES formulation to account for varying demands throughout the life of the mine, as a consequence of the natural process of mine development and extraction, which means deeper operations over time. This process entails a progressive increase in energy demands, and therefore the energy supply system must be planned accordingly. The proposed Long Term OMSES (LTOMSES) shows the advantages of considering an investment plan for the ESS, especially in the case of capital-intensive renewable energy technologies.

Other concepts that have been integrated in OMSES and are covered in this thesis include: (i) material flows with considerable impact in the energy consumption have been included in the mathematical formulation, in combination with the corresponding technologies, such as pumps, fans and mobile equipment; (ii) energy and material storage have been also included, along with complex utility tariff structures, and grid and pipeline extensions. More innovative and integrated solutions can be considered by expanding the feasibility region of the optimization

problem, as shown in a case study covering the integration of battery-powered electric underground mobile equipment.

Overall, this thesis provides insight and tools to assist engineers in the important task of designing comprehensive and cost-effective energy supply systems for underground mines. Future work suggested includes: the development of a methodology to design fully adaptive ESS (not considering a pre-existing optimal or sub-optimal design); the simultaneous optimization of the production plan (ore extracted per day) and the design and operation of the ESS; and a dynamic approach to review the investment plan in the face of long-term environmental operating conditions.

## **Keywords**

Mining, energy supply systems, renewable energy, energy storage, model predictive control

## Acknowledgments

This work is the result of many people's effort led by my supervisor and friend Dr. Dean Millar. I am deeply grateful for his patience, insight and guidance, and that of my co-supervisor Dr. Monica Carvalho, who has also provided me with excellent advice and support in the most challenging times of this journey.

I would like thank the sponsors of the SUMIT program for the support generously given through MIRARCO and the Center for Excellence in Mining Innovation (CEMI). Particularly helpful and rewarding was the time I spent at BESTECH, a principal sponsor of my research, under the supervision of Mr. Dan Dumais.

Many thanks are also due for the advice and comments provided by my thesis committee members (and also some apologies for the extension of this dissertation.) Each of them has elevated the quality of the final document which was highly improved in its early draft versions by Ms. Lafontaine, to whom I owe a debt of gratitude, not only for her valuable advice, but also for her support.

This fruitful adventure would not have been as personally rewarding without the people I have had the opportunity to work with. The Laurentian University staff, from the librarians to my favorite caffeine provider, has been fundamental in providing their kind service and care. To everyone I have had the chance to speak to, laugh with and share a pitcher with, many thanks.

Thanks especially to Michael McBride, Salina, A.J., Marta, Javier, Diane and David, and to all those who generously opened their hearts and gifted me with their friendship.

The greatest gratitude, for their encouragement and love, is owed to my dear family and friends I left in my homeland, I particular, to my parents Aurelio y Mercedes, my brother Luis and my sister Carmen. Finally, to Jenny, for your unconditional love and support, and for patiently waiting and generously forgiving the long periods of absence, thank you for always being there.

Alberto Romero

September 2016

## Co-Authorship Statement

The following includes a list of the publications containing material reproduced in this thesis, with the nature and scope of work from co-authors.

Romero, A., Carvalho, M., and Millar, D.L. 2014. Application of a Polygeneration Optimization Technique for a Hospital in Northern Ontario. *Transactions of the Canadian Society for Mechanical Engineering*, 38 (1) pp. 45–62.

A. Romero was responsible for obtaining data on hospital energy demands in Northern Ontario, provincial market structure and prices of gas and electricity, and provincial support programs for cogeneration. A. Romero also extended where needed the computer code developed by M. Carvalho. M. Carvalho collected information on equipment costs. The document was written with equal contribution by the three co-authors. The content of this publication is included and extended in Chapter 3 and Appendix 1 of this thesis.

Carvalho, M., Romero, A., Shields, G., and Millar, D. 2014. Optimal Synthesis of Energy Supply Systems for Remote Open Pit Mines. *Applied Thermal Engineering*, 64 (1) pp. 315–30. doi:<http://dx.doi.org/10.1016/j.applthermaleng.2013.12.040>.

This paper extends the analysis presented in a paper by M. Carvalho and D. Millar. Equipment costs and energy demands of the open pit mine studied were then defined. A. Romero was responsible for the implementation of the grid extension and the electricity price structure, as well as the energy storage formulation as part of the optimization problem. A. Romero defined, calculated and analyzed the scenarios

included in the paper. The document was written with equal contribution by M. Carvalho, A. Romero and D. Millar, and was reviewed by G. Shields. A previous congress version was presented by A. Romero on August 2013 at the World Mining Congress, Montreal, Quebec. The content of this publication is included and extended in Chapter 7 and Appendix 2 of this thesis.

Romero, A., Millar, D., Carvalho, M., Maestre, J.M., and Camacho, E.F. 2015. A Comparison of the Economic Benefits of Centralized and Distributed Model Predictive Control Strategies for Optimal and Sub-Optimal Mine Dewatering System Designs. *Applied Thermal Engineering*, 90 pp. 1172–83. doi:<http://dx.doi.org/10.1016/j.applthermaleng.2015.01.031>.

A. Romero was responsible for developing the models and the computer algorithms, and defined, simulated and analyzed the several scenarios discussed in the paper. Generous advice and many comments regarding Model Predictive Control were given by J. M. Maestre and E. F. Camacho. D. Millar reviewed the document in its several versions and made meaningful comments until the final version. The document was mainly written by A. Romero, completed by D. Millar, and reviewed by the remaining co-authors. The content of this publication is included and extended in Chapter 8 of this thesis.

Millar, D., Romero, A., Carvalho, M., and Levesque, M. 2015. Optimal Mine Site Energy Supply. In *Responsible Mining: Case Studies in Managing Social & Environmental Risks in the Developed World*, Jarvie-Eggart (Ed.), SME, pp. 389.

This book chapter includes work published by the co-authors in previous publications. The task of summarizing and completing the document was mainly done by D. Millar

and A. Romero. M. Carvalho and M. Levesque reviewed the final document. The content of this publication is included Chapter 4 of this thesis.

Romero, A., Carvalho, M., and Millar, D. 2016. Optimal Design and Control of Wind-Diesel Hybrid Energy Systems for Remote Arctic Mines. Journal of Energy Resources Engineering, 138 (6):062004-062004-10

A. Romero was responsible for modeling, simulating and analyzing the results obtained. The manuscript, written by A. Romero, was reviewed in the several draft stages by D. Millar, which made many comments and suggestions that enriched the study and the corresponding document. M. Carvalho reviewed as well the manuscript before submission. A peer review version, after an invitation for submission, has been accepted for publication in the Journal of Energy Resources Technologies. The content of this publication is included and extended in Chapters 9 and 10 of this thesis.

# Table of contents

<b>Thesis Defense Committee .....</b>	<b>ii</b>
<b>Abstract.....</b>	<b>iii</b>
<b>Keywords.....</b>	<b>v</b>
<b>Acknowledgments .....</b>	<b>vi</b>
<b>Co-Authorship Statement .....</b>	<b>viii</b>
<b>Table of contents .....</b>	<b>xi</b>
<b>List of Tables .....</b>	<b>xv</b>
<b>List of Figures.....</b>	<b>xvi</b>
<b>Nomenclature .....</b>	<b>xx</b>
<b>1 Introduction .....</b>	<b>1</b>
1.1 Optimal Mine Site Energy Supply .....	1
1.2 Control and Operational Optimization of Energy Supply Systems .....	3
1.3 OMSES practical limitations.....	4
1.4 Key Research Questions.....	5
1.5 Objectives and Structure of the Thesis.....	6
<b>2 Literature review.....</b>	<b>15</b>
2.1 Energy Demand Characterization in the Mining Industry .....	15
2.2 Polygeneration Systems as a Means to Use Energy More Efficiently .....	16
2.3 Optimization of Energy Supply Systems .....	20
2.4 Model Predictive Control in Energy Supply Systems.....	24
<b>3 Optimal Mine Site Energy Supply Basic Formulation.....</b>	<b>30</b>
3.1 Introduction .....	30
3.1.1 <i>Decision Variables and Scale of the Problem</i> .....	32
3.1.2 <i>Time Scale Considerations</i> .....	34
3.2 Objective Function .....	35
3.2.1 <i>Fixed Costs</i> .....	36
3.2.2 <i>Variable Cost</i> .....	37
3.3 Problem Constraints .....	37
3.3.1 <i>Installed Capacity and Equipment Production Limits</i> .....	37
3.3.2 <i>Energy Balance Constraint Across Technologies</i> .....	38
3.3.3 <i>Energy Balance Constraints across Utilities</i> .....	39
3.3.4 <i>Constraints on the Flows of Utilities</i> .....	41
3.3.5 <i>Grid Capacity Constraints</i> .....	42
3.3.6 <i>Demand Charge Minimization</i> .....	43
<b>4 Extensions of Basic OMSES Formulation .....</b>	<b>47</b>
4.1 Renewable Energy.....	48
4.1.1 <i>Biomass</i> .....	49
4.1.2 <i>Wind Power</i> .....	51
4.2 Spinning Reserve.....	61
4.3 Power to Gas Technologies.....	64
4.4 Material Flow Utilities .....	66
4.4.1 <i>Dewatering</i> .....	67
4.4.2 <i>Demand Management via Material Storage</i> .....	69
4.4.3 <i>Ventilation</i> .....	70
4.5 Energy Storage Technologies.....	72
4.5.1 <i>Storage Balance across Typical Days for a Month</i> .....	72
4.5.2 <i>Seasonal Storage for OMSES' Basic Formulation</i> .....	76
4.5.3 <i>Seasonal Storage for One Year Hourly Definition</i> .....	77

4.6	Seasonal Storage in the Form of Hydrogen Gas from Water Electrolysis.....	77
4.7	Mobile Technologies for Loading and Hauling.....	80
4.7.1	<i>Electric Powered Vehicles in Mining</i> .....	81
4.7.2	<i>Hydrogen-Based Technologies for Mobile and Stationary Applications in Mining</i> .....	82
4.7.3	<i>More Conventional Mobile Plant Technology Alternatives in Mining</i> .....	83
4.7.4	<i>Mobile Work Demand Integration in OMSES</i> .....	84
4.8	Summary.....	88
<b>5</b>	<b>OMSES Integration with Optimal Control in Dynamic Environments.....</b>	<b>89</b>
5.1	MPC Theoretical Basis.....	89
5.2	OMSES and MPC Comparison.....	94
5.3	Characteristic Disturbances and Forecast.....	98
5.4	MPC Feedback Control.....	98
5.5	Dynamic Design.....	100
5.5.1	<i>MPC Algorithm to Allow for Design Modifications</i> .....	103
5.5.2	<i>Methodology of Validation of the Dynamic Design Using MPC</i> .....	104
5.5.3	<i>Limitations of Higher Time Resolution OMSES Model to Obtain Optimal Solutions</i> .....	108
5.6	Applications of Various Modifications of MPC Used in Combination with OMSES.....	109
5.7	Conclusion.....	115
<b>6</b>	<b>Development of Long Term OMSES.....</b>	<b>116</b>
6.1	Comparison with Other Optimization Tools with Interannual System Variation.....	116
6.2	Extended Formulation Using a Static Algorithm.....	118
6.2.1	<i>Decision Variables and Scale of the Problem</i> .....	118
6.2.2	<i>Objective Function</i> .....	118
6.3	A suggestion for an Extended Formulation Using a Dynamic Algorithm.....	121
<b>7</b>	<b>Remote Mines and Biomass.....</b>	<b>123</b>
7.1	Mine Description.....	123
7.2	Mine Demands Characterization.....	125
7.3	Summary of Scenarios Considered.....	131
7.4	Results.....	135
7.5	Discussion.....	137
7.5.1	<i>Discussion of Specific Results for Optimal Mine Site Energy Supply</i> .....	137
7.5.2	<i>Discussion of Further Trade-offs Investigated</i> .....	143
7.5.3	<i>Discussion of the Findings of this Study to General Energy Supply Optimization Studies</i> .....	146
7.6	Conclusion.....	147
<b>8</b>	<b>Mine Dewatering Systems Design and Control Optimization.....</b>	<b>150</b>
8.1	Demand Side Management in Underground Mines.....	150
8.1.1	<i>Water System's Optimization</i> .....	151
8.1.2	<i>Water Systems Control Using MPC</i> .....	153
8.2	Design and Control Strategies Improving Traditional Methods.....	156
8.2.1	<i>Optimal Design</i> .....	157
8.2.2	<i>Extensions for Robust Optimality in Operations</i> .....	159
8.3	Problem Formulation.....	164
8.3.1	<i>Design Problem</i> .....	164
8.3.2	<i>Control Problem</i> .....	165
8.4	Framework for Assessment.....	167
8.4.1	<i>Economic Environment</i> .....	168
8.4.2	<i>Water Inflow</i> .....	170
8.4.3	<i>Variable Speed Pump Implementation</i> .....	171
8.4.4	<i>Design and Control Cases Explored</i> .....	173
8.5	Results.....	178
8.6	Discussion.....	181
8.7	Conclusions.....	184
<b>9</b>	<b>Remote Mining and Wind Power.....</b>	<b>186</b>

9.1	Mine Description.....	186
9.1.1	<i>Mine Utility Demands</i> .....	187
9.1.2	<i>Economic Data</i> .....	190
9.1.3	<i>Environmental Data at the Mine Site</i> .....	191
9.1.4	<i>Mine’s Actual Wind Farm</i> .....	192
9.2	Scenarios Investigated.....	194
9.3	Design Results Using OMSES.....	199
9.3.1	<i>Wind Analysis Results</i> .....	199
9.3.2	<i>Optimal Design for the Scenarios Considered</i> .....	201
9.4	Further Parametrical Analysis Using OMSES.....	203
9.4.1	<i>Total Annual Savings as a Function of Wind Turbines Installed</i> .....	203
9.4.2	<i>Electricity Storage Influence in the Optimal Design</i> .....	204
9.4.3	<i>Total Annual Savings as a Function of the Mine’s Life and the Number of Wind Turbines</i> .....	206
9.5	Simulation Results.....	207
9.5.1	<i>Optimal Operation of Scenario VI Design</i> .....	207
9.5.2	<i>Wind Forecast Analysis</i> .....	209
9.5.3	<i>Wind Penetration, Spinning Reserve and Curtailment Analysis</i> .....	210
9.6	Discussion.....	211
9.7	Conclusions.....	215
<b>10</b>	<b>Applications of MPC to Mitigate OMSES Model Inaccuracies .....</b>	<b>218</b>
10.1	Introduction.....	219
10.2	Detailed Modeling of the Heat Storage System for Improved MPC-Based ESS Operation.....	220
10.2.1	<i>Heat Storage Modeling</i> .....	220
10.2.2	<i>Model Predictive Control Layout</i> .....	222
10.2.3	<i>Results</i> .....	224
10.3	Analysis of Diesel Generators Waste Heat Bypass in Stand-Along Systems with Renewable Energy..	227
10.3.1	<i>Cogeneration and Heat Recovery Bypass Modeling Options</i> .....	227
10.3.2	<i>Heat Storage Management</i> .....	229
10.3.3	<i>Investigated Scenarios</i> .....	229
10.3.4	<i>Results</i> .....	231
10.4	MPC to Improve the Design.....	236
10.4.1	<i>Case Study</i> .....	236
10.4.2	<i>Results</i> .....	240
10.5	Conclusions.....	247
<b>11</b>	<b>Electrical Vehicles in Underground Mines .....</b>	<b>250</b>
11.1	Mine Description.....	250
11.1.1	<i>Mine Utility Demands</i> .....	251
11.1.2	<i>Economic Data</i> .....	255
11.1.3	<i>Scenarios Investigated</i> .....	258
11.2	Results.....	261
11.2.1	<i>Summary of the Results</i> .....	261
11.2.2	<i>Seasonal Storage of Propane</i> .....	263
11.2.3	<i>Reduction of Demand Charges</i> .....	264
11.2.4	<i>Battery Management</i> .....	265
11.3	Discussion.....	267
11.4	Conclusions.....	269
<b>12</b>	<b>An Example Application of Long Term OMSES .....</b>	<b>271</b>
12.1	Mine Description.....	271
12.1.1	<i>Mine Utility Demands</i> .....	272
12.1.2	<i>Economic Data</i> .....	272
12.1.3	<i>Scenarios Investigated</i> .....	273
12.2	Results.....	276
12.3	Discussion.....	278
12.4	Conclusions.....	281

<b>13</b>	<b>Contributions and Future Work</b>	<b>283</b>
13.1	Contributions to the Current State of Knowledge	283
13.2	Future work	289
<b>14</b>	<b>References</b>	<b>291</b>
<b>Appendices</b>		<b>309</b>
A1.	Polygeneration in a hospital in Northern Ontario	310
A2.	Victor Mine demand series	347
A3.	Ontario Power demand, Humidex and Community Power Consumption	355
A4.	Connection Capacity and Wind Power parametrical analysis	361
A5.	Propane, Natural Gas, Diesel and Electricity Infrastructure options for a remote mine	364
A6.	Comparison of OMSES and HOMER Results	368
A7.	100% Renewable supply of electricity, heat and cooling for a remote mine	384
A8.	Flowcharts and Algorithms for MPC and Long Term OMSES Implementation	407

## List of Tables

Table 3-1 Example membership of set U for utilities.....	32
Table 3-2 Example membership of set V for technologies.....	33
Table 3-3 Decision Variable Information.....	33
Table 3-4 Selected equipment and matrix of production coefficients.....	39
Table 4-1 State decision variables for energy storage.....	73
Table 5-1 MPC and OMSES formulation – equations and variable comparison.....	97
Table 7-1 Remote open pit mine energy demands, per representative day.....	125
Table 7-2 Selected equipment and matrix of production coefficients, $K_{uv}$ .....	126
Table 7-3 Optimal solutions for Scenarios 0, 1 and 2 – Diesel @ 130 CAD/MWh; Biomass (Peat) @ 30 CAD/MWh; Electricity: HOEP and GA considered.....	136
Table 8-1 Inputs for design problem.....	176
Table 8-3 Summary of optimized operation using CMPC.....	179
Table 8-4 MPC comparison with increased systems design robustness.....	180
Table 8-5 Non centralized controllers setup.....	180
Table 9-1 Equipment and matrix of production coefficients.....	191
Table 9-2 Problem inputs.....	194
Table 9-3 Wind speed data and wind turbine output (Inner Whaleback year 2012).....	200
Table 9-4 Scenario results from the design optimization problem (mine life 10 years).....	203
Table 9-5 Average diesel used for electricity generation [MWh/day].....	208
Table 9-6 Variable costs savings (relative to Scenario II).....	209
Table 9-7 Wind speed forecast influence on diesel consumption.....	210
Table 10-1 Diesel consumption in January to maintain the storage temperature above 50°C.....	231
Table 10-2 Summary of scenarios for the evaluation of MPC redesign.....	237
Table 10-3 Detailed model and dynamic redesign results.....	244
Table 11-1 Mine information.....	254
Table 11-2 Equipment information considered in the conservative superstructure.....	255
Table 11-3 Storage technologies information.....	257
Table 11-4 Allowed mobile technologies for the different scenarios.....	259
Table 11-5 Summary of scenarios.....	262
Table 12-1 Scenario results for a mine with different demands throughout its life and different economic environment.....	277

## List of Figures

Figure 1-1 Thesis ‘road-map’ .....	13
Figure 1-2 Representation of the topics addressed in this thesis .....	14
Figure 2-1 Representation of energy conversion systems (arrows represent different energy forms) .....	17
Figure 2-2 Multigeneration system with n output streams, adapted from Dincer and Zamfirescu (2014).....	17
Figure 2-3 Relationship among ESS concepts.....	19
Figure 3-1 Example of a superstructure – Vertical lines represent technologies, horizontal lines represent utilities, a positive sign symbolizes production, and a negative sign denotes consumption .....	31
Figure 3-2 Utility balance scheme implemented in the optimization module .....	40
Figure 3-3 Non conditional and conditional weighting factors expressing the likelihood of a peak demand event within a given hour of the day considering June, July and August .....	44
Figure 4-1 Example of wind speed characterization for Sudbury Airport; data for April 2012 (top) and diurnal cycle for several years (bottom) .....	54
Figure 4-2 Wind speed spectrum for Sudbury Airport (2012) .....	55
Figure 4-3 Wind speed spectrum for Pickle Lake weather station (2012) .....	56
Figure 4-4 Wind speed spectrum for Inner Whaleback weather station (2012).....	56
Figure 4-5 January wind speed and corresponding monthly spectrum (2012).....	57
Figure 4-6 Monthly root mean cube wind speed for several years at Sudbury Airport (top) and Inner Whaleback (bottom).....	58
Figure 4-7 Examples of different wind profiles for a typical day.....	60
Figure 4-8 Power to gas concept illustrated by a power to methane plant including diverse CO <sub>2</sub> sources (Sterner, 2009) .....	65
Figure 4-9 Storage scheme implemented in the optimization module .....	74
Figure 4-10 Scheme of the ventilation subsystem’s interaction with mechanical work.....	86
Figure 4-11 Subdivision of shifts in working periods for a 3 packs split battery system for a typical day.....	87
Figure 5-1 MPC receding horizon for tracking.....	92
Figure 5-2 MPC implementation example (Shi et al., 2005).....	99
Figure 5-3 OMSES typical days problem 1, versus actual ESS problem, 2 – Optimal solutions are O1 and O2....	105
Figure 5-4 Optimal solutions for typical days problem (O1) and actual problem (O2) .....	106
Figure 5-5 Optimal solutions for typical days problem (O1) and actual problem (O2); Pathway followed during simulation in actual environment.....	107
Figure 5-6 Convexity issues in MILP problems in ESS; the feasibility region of the whole problem (P2) results from the union of both ovals .....	108

Figure 5-7 Example of wind forecast with varying prediction and control intervals duration; the first 20 intervals span 1 hour, the next 3 hours, and the last 3 intervals 24 hours. Total number of intervals=24; total horizon=96 hours.....	110
Figure 5-8 MPC for tracking used to ensure that the level of storage at the end of the horizon stays within the desired range (dashed lines) or as close as possible to the reference (solid line) .....	112
Figure 5-9 Production adjustment to ensure feasible operation.....	113
Figure 6-1 Long term OMSES (LTOMSES) with dynamic feedback .....	122
Figure 7-1 Victor Diamond Mine location (source: Google) .....	124
Figure 7-2 Superstructure illustrating all potential conversion pathways considered .....	127
Figure 7-3 Scenario 1 Hourly Ontario Electricity Price (HOEP) in four different months.....	138
Figure 7-4 Scenario 1 Hourly electricity stored in four different months .....	139
Figure 7-5 Scenario 1 Global Adjustment approach influence in July electricity imports.....	141
Figure 7-6 Steam flows in January period Scenario 2 .....	142
Figure 7-7 Steam flows in July period Scenario 2 .....	143
Figure 7-8 Connection distance parametrical analysis .....	146
Figure 8-1 Underground dewatering system.....	151
Figure 8-2 Simple dewatering scheme; Arrows express direction of the flow. Each rectangle represents a reservoir and its pump station .....	155
Figure 8-3 Dewatering system with two lifting stages in an underground mine .....	158
Figure 8-4 Centralized control scheme .....	160
Figure 8-5 Distributed control scheme .....	161
Figure 8-6 Decentralized control scheme .....	162
Figure 8-7 Traditional control scheme.....	163
Figure 8-8 HOEP June 2011; Actual (dotted line) Vs average (continuous line) hourly profile .....	169
Figure 8-9 Water inflows; Top: Monthly infiltration inflows (constant flow) for each reservoir; Bottom: water inflow associated with mine production activities into the lower reservoir.....	171
Figure 8-10 Example of power-flow curves for a variable speed pump: cubic (continuous line) and linear (dashed line) approximations .....	172
Figure 8-11 Dewatering system optimization & control simulation hierarchical summary, illustrating design, optimization and simulation cases considered (cases abbreviated with emboldened letters).....	174
Figure 9-1 Environmental data sources (Google 2014).....	187
Figure 9-2 Normalized electricity demand profile.....	189
Figure 9-3 Enercon E-70 Wind turbine curves (Enercon website, 2015) ( $\rho_{air}=1.225 \text{ kg/m}^3$ ) - $P_{nom}$ is the turbine power output; $C_p$ is the <i>power coefficient</i> .....	193
Figure 9-4 Conservative superstructure for an underground mine .....	198
Figure 9-5 <i>Root mean cubic (rmc)</i> speed for the months of the year considered (2012) measured at the Inner Whaleback weather station .....	201

Figure 9-6 OMSES result superstructure with the installed technologies .....	202
Figure 9-7 Optimal wind turbine units influence total annual cost and variable cost savings .....	204
Figure 9-8 Electric storage influence optimal number of wind turbine units .....	205
Figure 9-9 Project life influence on optimal wind turbine units and variable costs (without <i>spinning reserve</i> nor electric storage) .....	206
Figure 9-10 Spinning reserve and wind power curtailment during January .....	211
Figure 9-11 Spinning reserve in absence of electric storage. $P_{wind}$ is the power produced by each turbine, in MW, SR is the spinning reserve, and $PR$ is the penetration ratio. ....	213
Figure 9-12 Influence of control horizon on the electric storage and the spinning reserve .....	214
Figure 9-13 State of charge and penetration ratio relationship for different turbulence intensity levels ( $TI$ ) .....	215
Figure 10-1 Cogeneration plant schematic, adapted from ASHRAE (2012) .....	219
Figure 10-2 Thermal model of the heat storage system .....	221
Figure 10-3 Cogeneration plant with heat storage and high-to-medium temperature heat exchange, adapted from (ASHRAE, 2012) .....	223
Figure 10-4 Heat storage temperature with three feedback alternatives: 1) feedback in temperature of the reservoir and heat losses to the ambient; 2) only feedback in temperature; 3) no feedback .....	225
Figure 10-5 Heat storage level with three feedback alternatives: 1) feedback in temperature of the reservoir and heat losses to the ambient; 2) only feedback in temperature; 3) no feedback .....	226
Figure 10-6 Temperature and heat level of the heat storage system in January, no heat recovery bypass, no information feedback .....	232
Figure 10-7 Temperature and heat level of the heat storage system in January, no heat recovery bypass, with information feedback .....	233
Figure 10-8 Temperature and heat level of the heat storage system in January, with heat recovery bypass, no feedback information .....	234
Figure 10-9 Temperature and heat level of the heat storage system in January, with heat recovery bypass, and feedback information .....	235
Figure 10-11 Scenario 11 Mechanical chiller and cooling tower evolution; engine exhaust bypass, $T_{set} = 10^{\circ}\text{C}$ ....	241
Figure 10-12 Scenario 12 Mechanical chiller and cooling tower evolution; No engine exhaust bypass, $T_{set} = 10^{\circ}\text{C}$ .....	241
Figure 10-13 Scenario 21 Mechanical chiller and cooling tower evolution; engine exhaust bypass, $T_{set} = 15^{\circ}\text{C}$ ....	242
Figure 10-14 Scenario 22 Mechanical chiller and cooling tower evolution; No engine exhaust bypass, $T_{set} = 15^{\circ}\text{C}$ .....	242
Figure 10-15 July optimal operation results for the detailed demand model with summer $T_{set} = 15^{\circ}\text{C}$ and bypass allowed .....	245
Figure 10-16 Local wind speed and ambient temperature .....	246
Figure 11-1 Musselwhite Mine location .....	251
Figure 11-2 Normalized profiles for electricity and mechanical work .....	252

Figure 11-3 Scenario 11 Propane storage level .....	263
Figure 11-4 Purchased electricity in Scenario 4a .....	264
Figure 11-5 Purchased electricity in Scenario 4b .....	264
Figure 11-6 Scenario 4a Battery pack 1.....	266
Figure 11-7 Scenario 4a Battery pack 2.....	266
Figure 11-8 Scenario 4a Battery pack 3.....	267
Figure 11-9 Total annual cost for the different scenarios depicted in Table 11-4.....	268

## Nomenclature

### *Abbreviations*

AA	ambient air utility
AC	alternate current
ACRW	absorption chiller
ADSM	active demand side management
ARIMA	autoregressive integrated moving average
ARX	auto regressive external
BAU	“business as usual”
BM	biomass utility
CAD	Canadian dollar
CAM	custom adoption model (DER-CAM)
CCG	conservative conversion grid
CESOP	clean energy standard offer program
CHP	combined heat and power
CHPSOP	combined heat and power standard offer program
CMPC	centralized model predictive control
CTCW	cooling tower (alternatively CT)
CW	cooling water utility
DcMPC	decentralized model predictive control
DEHW	diesel engine
DER	distributed energy resources
DG	distributed generation
DI	diesel utility
DMG	distributed multi generation
DMPC	distributed model predictive control
DPM	diesel particulate matter
DSM	demand side management
DTSM	diesel turbine with steam generator
DW	dewatering (water) utility
EAM	enterprise asset management
EE	electricity utility
ESS	energy supply system
EV	electric vehicle
EZ	electrolyzer
FC	fuel cell
FR	feasibility region
FTDI	Fischer-Tropsch plant
FTS	Fischer-Tropsch synthesis
GA	global adjustment
GEHW	gas engine
GFBM	biomass gasifier

GHG	greenhouse gas
GIS	geographic information system
GTSM	gas turbine with steam generator
HOEP	hourly Ontario energy price
HOMER	Hybrid optimization of multi energy resources
HW	hot water utility
HWBM	hot water biomass boiler
HWEE	electric boiler
HWNG	hot water boiler
HX	heat exchanger
ICE	internal combustion engine
IESO	Independent Electricity System Operator
IGCC	integrated gasification combined cycle
IP	integer programming
IWB	Inner Whaleback (weather station)
LCOE	levelized cost of energy
LFP	lithium iron phosphate (LiFePO <sub>4</sub> )
LHD	load-haul-dump vehicle
LP	linear programming
LTOMSES	Long Term OMSES
MCRW	mechanical chiller (alternatively MC)
MES	multi-energy system
MILP	mixed integer linear programming
MIMO	multiple input – multiple output
MPC	model predictive control
NG	natural gas utility
NN	neural net (network)
NRCan	Natural Resources Canada
OD	optimal design
OF	objective function
OMSES	optimal mine site energy supply
OP	open pit
OPA	Ontario Power Authority
ORC	organic Rankine cycle
P2G	power-to-gas technology
PEM	polymer electrolyte membrane (fuel cell technology)
PID	proportional integral derivative (controller)
PR	propane utility
PV	photovoltaic
RE	renewable energy
RW	chilled water utility
SAPS	stand alone power system
SHW	sanitary hot water
SM	steam utility
SMBM	steam biomass boiler

SMDI	steam diesel boiler
SMNG	steam boiler
SOC	state of charge
STG	start-up fuel consumption [MWh/MW]
STSM	steam turbine
SY	syngas fuel utility
TAC	total annual cost
TD	traditional design
TI	turbulence intensity
ToU	time of use
TURN	technologies and urban resources network
UG	underground
VA	Steam (water vapor)
Wd	weekday (labor day)
We	weekend
WT	wind turbine

### *Symbols*

a	cost constant [CAD/MW], demand charge histogram coefficients [-]
A	heat transfer area [m <sup>2</sup> ]
b	cost constant [CAD/MW-km]
c	cost [CAD]
C	cost [CAD] ([CAD/year]), utility conversion coefficient
CF	capacity factor [-]
CHR	contract heat rate [MWh <sub>thermal</sub> / MWh <sub>electric</sub> ]
C <sub>p</sub>	specific heat [J/kg-K]
d	number of typical days (in the typical year)
DC	demand charges [CAD]
E	energy, envelope coefficients for demand charges
f	idling fuel consumption index (dimensionless)
h	number of typical hours (in the typical day), hour
H	horizon (referred to model predictive control)
HHV	high heating value [J/kg] ([J/litre])
NRSL	net revenue support level [CAD/MW-month]
i	interest, discount term
j	inflation
J	cost function
k	constant term, conductivity [W/m-K], time interval in the rolling horizon [-]
K	coefficient matrix
l	losses (energy)
L	capacity limit (import/export), constraint function (MPC), time, water/pump level
LHV	low heating value [J/kg] ([J/litre])

M	mass [kg]
$\dot{m}$	mass flow rate [kg/s]
mCp	capacity coefficient [W/K]
n	time discretization: hours per day, days per year
N	number of intervals in the rolling horizon
O	optimum
p	purchase price [CAD/MWh], pressure
P	power [MW], rated output ([m <sup>3</sup> /h], [kg/s]), problem (mathematical programming)
PR	penetration ratio [-]
q	sale price [CAD/MWh], volumetric flowrate [m <sup>3</sup> /s]
Q	volumetric flow rate [m <sup>3</sup> /s], heat flow [J/s]
r	elements considered for the calculation of demand charges
R	reservoir
REV	revenue
SR	strip ration [tonnes of waste / tonnes of ore]
t	time
T	time set, temperature [C] ([K])
u	manipulated variable
U	utility set
UA	heat exchange coefficient [W/K]
v	speed [m/s]
V	technology set, volume [m <sup>3</sup> ]
VOM	operation and maintenance cost under CHPSOP [CAD/MWh]
w	disturbance variable
WPADF	wind power air density factor [-]
x	state variable
y	output signal
Y	energy exchange constraining parameter

### *Subscripts*

c	control (rolling horizon)
d	discount, design
e	energy, equality (constraints)
fix	fixed (non variable)
h	inequality (constraints)
i	day
ic	indirect costs
inf	infrastructure
inv	investment
j	hour
net	network (infrastructure not connected with the external energy grids)
nom	nominal, nameplate

o	operation
O&M	operation and maintenance (not included fuel consumption)
op	equipment in operation mode (in contrast to spinning reserve, sr)
p	prediction (rolling horizon), pump index
peak	peak power (Ontario demand)
PM	prime mover
pw	present worth
r	auxiliary hour index
ref	reference value
rf	(capital) recovery factor
rnc	root mean cube
s	auxiliary day index
set	setpoint
sr	equipment in spinning reserve
STH	heat storage
sup	support
t	auxiliary month index
tot	total
TRANS	transmission
u	utility
v	technology
var	variable
y	year

### *Superscripts*

ch	charge
con	consumed
dem	demand
ds	discharge
pro	produced
pur	purchase
sel	selling
sto	storage
was	wasted

### *Greek letters*

$\alpha$	production rate compared to nominal [-], specific energy use correction factor [-]
$\beta_u$	specific utility use (per unit of mined product) [kWh/tonne] ([kg/tonne], [m <sup>3</sup> /ton]...)
$\beta_{u,0}$	specific utility use as reported by the consumer

$\Gamma$	utility connection rating [MW]
$\delta$	auxiliary binary variable [-]
$\Delta$	demand charges or economic support [CAD]
$\varepsilon$	error
$\eta$	efficiency [-]
$\mu$	number of pieces of technology installed
$\Pi$	energy produced by a technology (characteristic utility for each technology) [MWh]
$\rho$	density [ $\text{kg/m}^3$ ]
$\sigma$	standard deviation
$\Phi$	energy exchanged [MWh]
$X$	energy exchanged by a technology [MWh]
$\Psi$	energy stored [MWh]

# Chapter 1

## 1 Introduction

Despite technological improvements, energy consumption in mining has been steadily increasing in the last decades both in absolute and relative terms (per unit mass of product) (Mudd, 2007; Levesque et al., 2014). This has occurred fundamentally as a result of lower quality ores (Chapman and Roberts, 1983). In the search for higher concentration of mineral deposits, greater energy costs in mining are further driven by the fact that new deposits are increasingly found in remote locations that lack prior infrastructure, or deeper into the Earth's crust.

Since the nature of a mineral deposit (grade, depth, and geographic location) determines the practical minimal energy to obtain the desired final product, it also influences the economic viability of resource extraction and processing. The ores that are cheaper to extract, both economically and energetically, are exploited first (Crowson, 2011). As a result, the average ore grade of mined deposits has been steadily decreasing over the last century (Chapman and Roberts, 1983; Mudd, 2007; Northey et al., 2014).

### 1.1 Optimal Mine Site Energy Supply

Optimal Mine Site Energy Supply (OMSES) is a concept developed to provide a tool to mitigate the problem of increasing energy costs and energy demands in the mining industry (Carvalho and Millar, 2012). Until 2012, no other study and approach had been presented with the objective of integrating the problem of supply of several energy demands present in mines and optimizing the Energy Supply System (ESS) based on cost. Being more an application of current energy

optimization tools than a novel one, OMSES successfully identified and applied the specific constraints to which mines are subject to, particularly for remote mines where the lack of energy sources or energy infrastructure can significantly increase the cost of energy, and hence, the cost of mineral production.

The seminal work by Carvalho and Millar (2012), developed from Carvalho's previous work regarding ESS's optimization (Carvalho, 2011), pointed to the opportunities from which mines could benefit regarding their energy procurement and use. This includes demand and supply side management, which allows them – as energy consumers and frequently also as producers of energy and owners of energy transportation and distribution networks – to optimize the design and operation of their energy infrastructure, given a set of historical energy demands. This optimization was focused on the minimization of energy costs, but could also consider the reduction of energy-related greenhouse gas (GHG) emissions.

The main contribution was that of applying to mining the concept of polygeneration (see Section 2.2) and energy systems optimization (Section 2.3) through mathematical programming-based tools (Serra et al., 2009). Furthermore, the diversity and magnitude of energy flows of mines highlighted by Carvalho and Millar led to more general formulations, of broader applicability, than systems in which the demands are limited to, for example, electricity, heating, and cooling. However, OMSES presented a limited scope regarding some energy transformations at the mine site, not providing a suitable method to compare, for example, different technologies for hauling operations consuming different forms and amounts of energy for the same task.

## 1.2 Control and Operational Optimization of Energy Supply Systems

OMSES, as well as other optimization tools developed hitherto to optimize ESS designs (see Section 2.3), both research-oriented and commercial software, provide solutions that remain optimal as long as energy demands and energy prices after commissioning remain equal to those used in the design optimization step (Mancarella, 2014; Mendes et al., 2011). These tools reflect valuable conceptual advances, but do not necessarily produce systems that remain optimal when the environmental operational parameters change, which must be expected over the life of the ESS. These environmental parameters include factors affecting mainly the energy demands, from ambient temperature to production output (e.g., tonnes of ore per day extracted).

Several authors have recently explored the use of Stochastic and Robust Optimization to produce improved solutions under uncertainty (Majewski et al., 2015; Bungener et al., 2015). However, there is still a lack of research in the area of simulation of optimal ESS operations and scheduling – few authors have addressed the question of what challenges arise to previously-optimized ESS under variable and uncertain operating environments, and how these challenges can be mitigated.

Literature examples of simulation of optimized ESS are scarce, but two do exist and both are extreme simplifications of ESS in contrast to the general formulations in this thesis. Collazos et al. (2009) and Torreglosa et al. (2015) simulate optimized ESS designs with the aim of evaluating the control strategy under uncertain operating conditions. The framework used in both works is Model Predictive Control (MPC) which is a control approach for systems where mathematical models are available and where constraints exist that challenge the use of other methods, for example, a simple feedback control (i.e., proportional-integral-derivative, or PID, controllers) or relays based on hysteresis cycles.

These and other works (see Section 2.4) support the use of MPC to control ESS due to the nature of the optimization problem to be solved, i.e., optimal scheduling problems under potentially uncertain operational conditions, in addition to the typical state equations representing conservation of energy, typical of energy storage technologies. Among other objectives, this thesis explores the benefits of using MPC beyond mere control purposes, in order to evaluate under which conditions (environmental, economic or user-related) the optimized design will reach operational limitations.

### **1.3 OMSES practical limitations**

In addition to the aforementioned, OMSES' concept presented some limitations partly shared by other ESS optimization tools. These limitations can be summarized as follows:

- The use of typical demands: through the process of averaging, peak demands are reduced and, consequently, even a successful optimization is potentially solving a different problem than the real one at hand.
- The use of last year's demands; OMSES perfectly optimizes an ESS using historical demand data, which is acceptable providing future demand is the same. Even if future demand just follows the same pattern as previous years, there is no guarantee that the optimal ESS will remain optimal for these future demands. It is not simply the issue of optimality that is at stake in this context either. As will be shown subsequently (Chapter 10), the optimal ESS identified using last year's demand data may not even be feasible.
- OMSES produces an optimal operational plan as part of its solution. In applying this operational plan one has to an assumption that future demands will be known perfectly,

implying no treatment of uncertainty known to be so characteristic of the mining process in particular

- No consideration of mechanical/transportation energy demand, the technologies that provide it, or their interaction with other energy flows.
- No consideration of energy storage.
- The consideration of one year of energy demand to characterise potential seasonal variability, and so, disregarding that mines vary their production rate throughout their lives. The original formulation therefore ignores the possibility of incremental capital investment, which can be advantageous from an economic point of view.

## **1.4 Key Research Questions**

The key research questions that thus arise in pursuit of resolving or mitigating these weaknesses are:

- What kind of uncertainties can and should be addressed, and how? Example: mine life, production uncertainty, wind and solar variability, future costs...
- Can MPC be used to evaluate the robustness and resilience of optimal polygeneration design and, when possible, improve it?
- If so, how?
- How can renewable energy sources with output that can vary over very short time scales be integrated with in OMSES' typical day formulations while keeping problem sizes small?
- Can polygeneration systems' optimization be extended to accommodate mobile equipment, which is so important in the mine production processes?

- Is it possible to use material or energy storage for Demand Side Management (DSM) strategies and integrate these into a polygeneration system optimization for mine sites?
- Can seasonal energy storage be integrated in OMSES?
- Can a typical day approach accommodate seasonal storage, or is a more detailed definition of the time frame required?

Aside from specific technical issues associated with methodological development, some more general questions arise:

- Could a mine be fueled 100% with renewable energy?
- What happens with the period in which the mine still does not produce ore (just development)?
- How should energy be optimally supplied during mine development?

## **1.5 Objectives and Structure of the Thesis**

The concepts and tools covered in this work will be of interest to those responsible of reducing energy related costs in mining. Hopefully, the reader will find valuable material throughout the thesis, depending on the specific economic and technical constraints of the mine site. However, only the reader familiar with linear algebra, mathematical programming, differential equations and control theory will find few obstacles to rapidly implement any of the solutions or methods described here. Many of the results articulated in this thesis, some published by the author and his collaborators as peer review articles, are already delivering economic value for mine operators who were part of the SUMIT consortium.

The implementation of the concepts covered here can be carried out in any optimization solver capable of solving MILP problems in combination with a programming language allowing the

user to solve iteratively time dependent problems or parametrical analyses. However, is advised that author's choice of Lingo (Lindo Systems, 2007) solver and Matlab as programming tools is not arbitrary. Lingo allows the user to define optimization problems symbolically, which makes it easy to step from the problem definition and the computer implementation, and avoids the necessary discussion on results reliability because it is a well established optimization tool.

The choice of the Branch and Bound algorithm available in Lingo ensures global optimality of the solution, providing the problem is feasible and bounded. Matlab, in which this work relies extensively, is also a well tested and widely used programming language whose functions or sub-routines have been optimized and de-bugged. To help the reader interested in replicating each of the case studies, 'recipe lists' have been provided previous to each results section of each chapter, which connecting the mathematical formulation to whatever computer tools the reader choose to use.

This thesis is structured so to provide a progressive introduction to the concepts upon which the novel tools developed here rest. The thesis begins with a brief literature review, provided in Chapter 2, which helps the reader less familiar with concepts such as polygeneration, ESS, optimization, and mining to become familiar and up to date with the latest advances in the optimization of ESS and the use of MPC to control them.

Chapter 3 describes the basic formulation of OMSES, providing a suitable mathematical framework, absent in the work of Carvalho and Millar (2012). This framework makes possible a more compact definition of the problem without loss of the generality needed to allow for the expansions presented described in the following chapters.

The first OMSES expansions focused on the use of less conventional and renewable energy sources and technologies, such as biomass, gasification, and liquid fuel synthesis. Chapter 4 describes these renewable sources, and includes extensions to OMSES concerning energy storage technologies, key material flows within the energy supply system, and a more detailed definition of a mine's energy demand. The incorporation of mobile equipment technologies (mainly trucks and loaders) into the energy system is also considered in this chapter.

Chapter 5 and 6 discuss important drawbacks to the core formulation of OMSES, then propose and evaluate several methods to resolve the weaknesses. OMSES was initially proposed on the basis of perfect knowledge of the mine's energy demands over well-defined time intervals characterizing typical operation patterns. Three simplifications were then made:

- The first relates to the magnitude of the demand, which, due to a process of averaging applied within a month to arrive at a typical daily profile for that month, yields system designs that would not be able to meet extreme high energy demand periods.
- The second entails an ideal perfect knowledge of the system's demand over the complete optimization time frame. Any system, while operating, will do so without the absolute certainty of future demands, for any given future time horizon of seconds, hours, days, and even months. This in turn is a scheduling or control problem, which also encompasses the uncertainty about variable renewable energy input (wind speed or solar radiation), or the state of stored energy and mass. This control problem can also be considered an optimization problem, where at any given instant, a set of planned actions exists that yields the minimum cost of operation.
- Finally, OMSES' assumption of equal annual energy demand profiles for the whole life of the mine was always a transitional oversimplification. Mine energy demands are better

represented in an extended formulation, where different years exist with different demand profiles, in addition to the time subdivision in hours and days.

Thus, Chapter 5 examines the first two issues, proposing the use of the energy supply system model with the design obtained with OMSES in a simulation scheme with uncertainty in the system's environment forecasts.

Chapter 6 considers the implications of interannual energy demand variation during a mine's life. This variation arises from two main factors: production ramp up, which can take several years, and mine deepening. It is considered that everything else remains constant if not specified. The ore grade, for instance, may change, but the model at this stage is not granular enough as to reflect this change. Prices of energy resources are likely to increase, and such variations over several years can be accounted for more appropriately with this approach.

The extensions and new methods described in Chapters 4, 5, and 6 are applied in illustrative case studies in the remaining chapters. Chapter 7 describes how OMSES is used to calculate the optimal design and operation of a remote open pit mine in Northern Ontario. The basic formulation is upgraded with energy storage and the addition of biomass to the set of available energy sources. The analysis of the optimal design for the scenario that best describes the actual mine and its techno-economic environment is complemented with a parametrical analysis, in which the distance to the closest grid connection point is flexed and the consequent changes in optimal ESS design configuration are analyzed.

Chapter 8 implements a methodology to optimally control the complete mine energy supply system in one of the most flexible and fundamental parts of mine operations: the dewatering system. The relationship between water flows, mine depth, and power requirements is studied.

The optimal design and operational plans are calculated using OMSES' extended formulation, including storage. The optimal design is simulated under more realistic price dynamics and under different control approaches for several interconnected pumps and reservoirs. The control approaches considered are centralized MPC, decentralized MPC, and distributed MPC, and the three scenarios progressively reflect a deterioration of data communication systems that may occur at a mine, over time.

Chapter 9 builds on the findings of Chapter 8 to illustrate the generalization of MPC to the complete mine energy supply system. In addition to water and heat storage (OMSES basic formulation extension), the problem includes wind energy as an available local renewable energy source and the use of spinning reserve to mitigate wind variability. The optimal design solution was compared with the conventional design, which relies exclusively on diesel to meet all energy requirements. Data from a real mine with a hybrid wind-diesel energy supply system, Diavik Diamond Mine (Northwest Territories, Canada), was used to validate the optimization process, which included a simulation and optimal control of the energy system through MPC.

Using the same case study of Chapter 9, Chapter 10 further analyzes the behavior and feasibility of the optimal design under uncertainties, both in the plant model and the environmental conditions of wind and temperature. The method described in Chapter 5 to improve the robustness of OMSES design is also applied, ensuring the feasibility under realistic operating conditions.

Chapter 11 presents research on the use of different vehicle technologies in underground mines, and how techno-economic and climatic environmental parameters may affect the choice of using, for example, electric or diesel powered equipment. Using OMSES' extended formulation, the

optimal ESS for an underground mine is calculated under different scenarios defined by varying constraints in choices of technologies and cooling demands underground. The investigations are designed so that the impact on underground cooling demand, due to varying heat release by the various mobile technologies, could be estimated, and the optimal ESS for the mine can be calculated.

Chapter 12 presents the final case study of the thesis, which illustrates the difficulties and advantages of considering varying energy demands for different years of the mine's life. Results demonstrate the economic benefit of considering production ramp-up in mines regarding their ESS investment plan, particularly when high investment costs in renewable energy precludes its use, despite long term savings from reduced operating costs.

Chapter 13 presents the contributions of the present thesis and suggests areas for future work.

Finally, several appendices have been included in order to support the many assumptions and conclusions obtained through the different case studies.

In order to transition and generalise from the work of Carvalho (2011) applied to a specific jurisdiction (Spain), Appendix 1 considers the case of a hospital in Northern Ontario with its complex electrical tariff system. Its energy demands were calculated and the economic environment was studied in depth to find the optimal energy supply system. The discussion focuses on the electric tariff structure and the regional support program designed to encourage the use of cogeneration approaches.

Appendix 2 brings additional information about Northern Ontario's electric system, mainly regarding the effect of the ambient temperature on the power consumed in the province. Appendix 3 describes the energy demand profiles used in Chapters 7 and 13. Appendix 4

expands the analysis of Chapter 9, including additional diesel price and mine location scenarios for which the optimal ESS is calculated. Appendix 5 is used to illustrate the addition of several fuel sources for remote applications, in addition to diesel, as studied in Chapters 7 and 9.

Appendix 6 covers the optimization and simulation case study analyzed in Chapter 9, this time using the computer tool HOMER (Hybrid Optimization of Multi Energy Resources), the current standard in commercial software for energy systems design and simulation optimization when renewable energy sources are available.

Appendix 7 applies the formulation of seasonal energy storage to the mine described in Chapter 9, and assesses the possibility of meeting the mine's energy demands exclusively from wind power. While the results show that it is technically feasible, the discussion considers if it is true given the OMSES model's limitations and the cost implied in such 100% renewable systems.

Appendix 8 includes charts and portions of the computer code programmed for the MPC-based simulations, in particular for Chapter 9, as well as for the Long Term OMSES analysis described in Chapter 6 and applied in Chapter 12.

Figure 1-1 illustrates the 'road-map' for alternative reading options depending on how familiar or interested is the reader with the topics included in this thesis. A graphical representation of the topics addressed in this thesis in relation to the concepts of polygeneration and distributed energy resources is shown in Figure 1-2, where the dashed line, rather than representing a set boundary, is a link that connects all the circles of the periphery, which are derivations of Distributed Energy Resources (DER) systems (see Chapter 2). Semi-transparent ellipsoids emphasize some of the most important contributions throughout the circular link. This link is, in short, the present thesis.

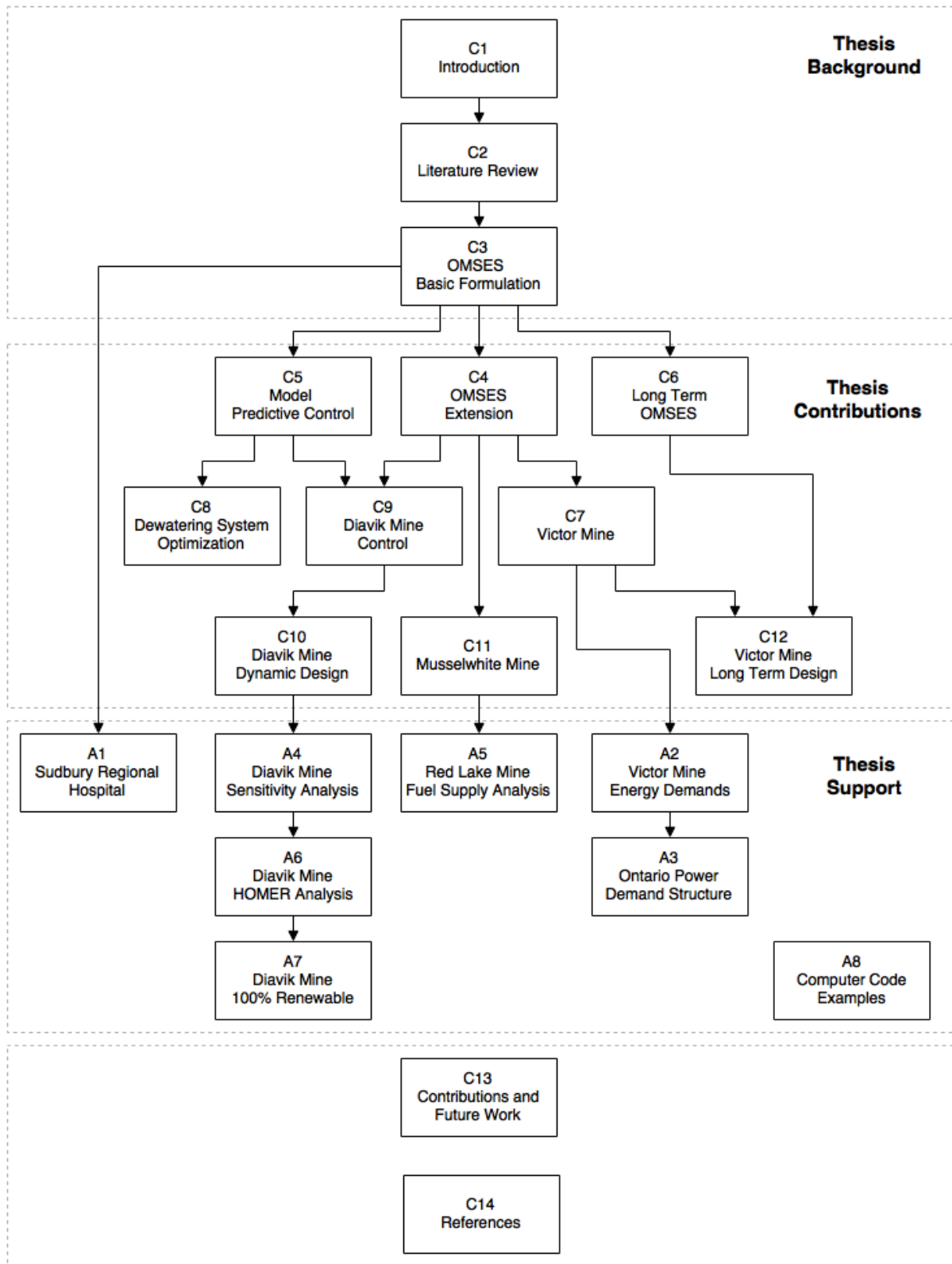


Figure 1-1 Thesis 'road-map'

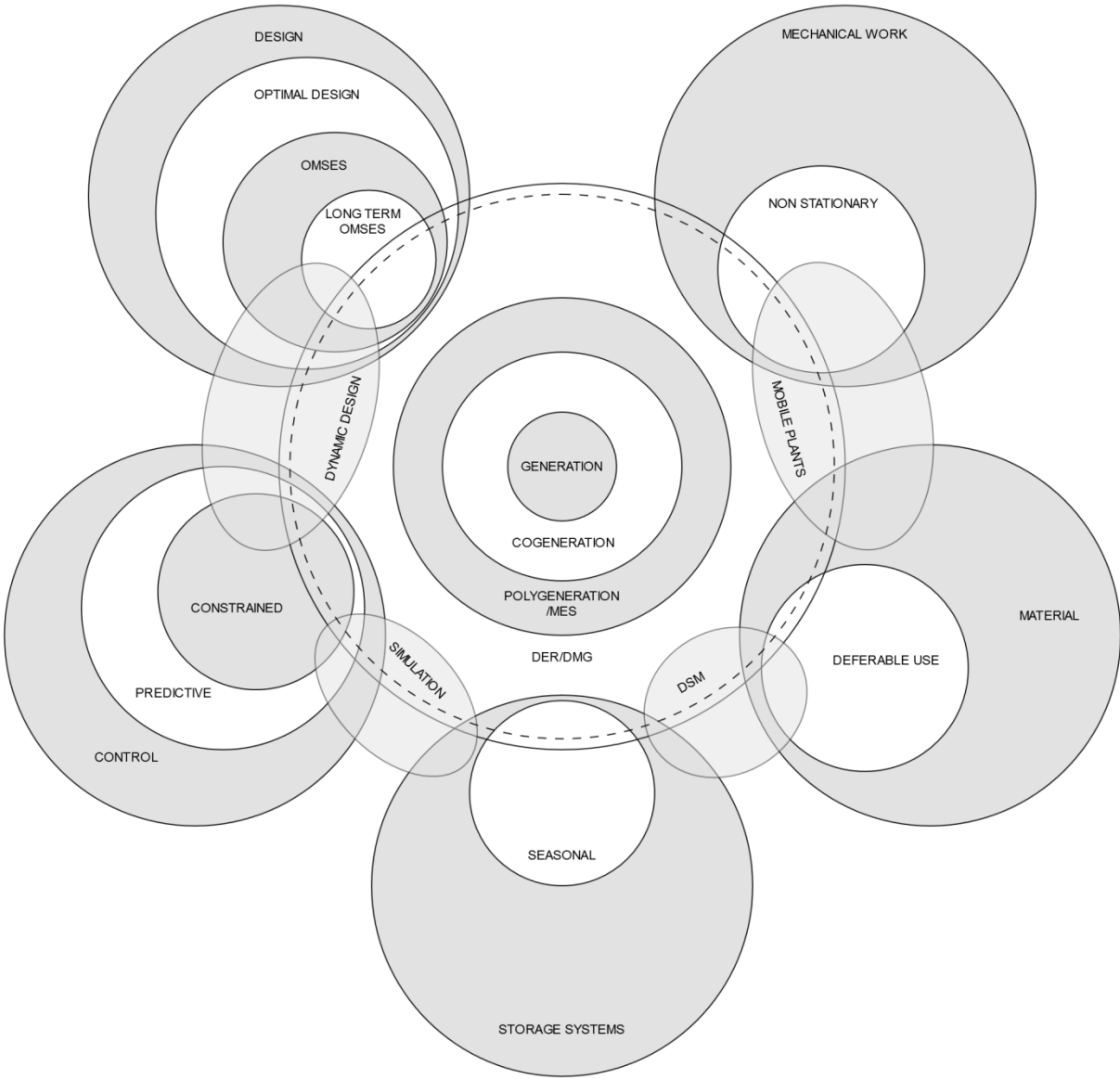


Figure 1-2 Representation of the topics addressed in this thesis

# Chapter 2

## 2 Literature review

The chapter begins with some insights on mines' energy demands and the relationships of these with the processes involved in ore extraction. Subsequently, the general concept of polygeneration as a methodology to integrate more efficiently several energy processes is presented, including the family of derived concepts usually covered when dealing with ESS. Finally, an up-to-date summary regarding research on ESS design and scheduling optimization is presented, followed by an overview on the use of Model Predictive Control in the field of ESS.

### 2.1 Energy Demand Characterization in the Mining Industry

To understand the structure of the energy demand of a particular mine, one must know where energy is being consumed, which technologies are available at the site to produce the type of energy required to support mineral production (electricity, heating, cooling, diesel, natural gas, etc.), and which energy resources are available on site.

Typically, the total energy supplied to a mine is obtained from multiple sources, and is then allocated to different uses (i.e., where there is an energy demand). For instance, diesel fuel was the primary source of energy for the task of loading and hauling in some iron, aluminum, and copper mines studied by Norgate and Haque (2010), where trucks are used for such purpose. Although there are other hauling technology alternatives available (electrically driven trucks, conveyor belts, etc.), it is usually assumed in the preliminary stages of mine planning that one type is to be used.

Through auditing and benchmarking, the energy intensity of mining processes, i.e., energy units per ton extracted, hoisted, crushed, etc., can be assessed. For some of these processes, there exists an inverse relationship with the grade of the ore and the stripping ratio, which is the ratio of waste rock volume to ore tonnage (Chapman and Roberts, 1983; Levesque et al., 2014). Using available energy intensity data, the energy demand of a mine as a function of its characteristic ore grade and output, depth, stripping ratio, etc., can be estimated. Such energy intensity factors indicate the level of efficiency with which energy is consumed by the mining operation and may help reduce costs through comparison of their values for different processes, technologies or even minable deposits.

## **2.2 Polygeneration Systems as a Means to Use Energy More Efficiently**

Cogeneration is the process by which a single input stream of energy, commonly fuel, is transformed into heat and electrical energy in a single site (Chicco and Mancarella, 2009). Cogeneration is also referred to as Combined Heat and Power, or CHP. It builds upon the concept of a generator that converts an energy form into a different one (Figure 2-1). In some cases, mechanical energy can replace electricity definition (Directive 2004/8/EC on the Promotion of Cogeneration Based on a Useful Heat Demand, 2004; ASHRAE, 2012).

Polygeneration's concept is derived from cogeneration, and involves the production of three or more output energy streams (Mancarella, 2014) (Figure 2-1). The terms multigeneration, polygeneration, or multi energy systems (MES) can be used interchangeably and refer to an energy supply system (ESS) that meets multiple energy demands of a consumer center imposed beforehand (Lozano and Valero, 1993; Mancarella, 2014).

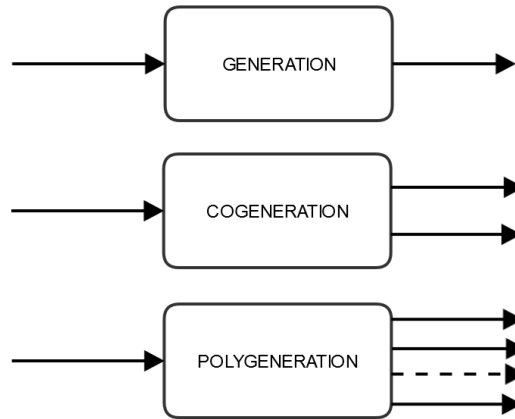


Figure 2-1 Representation of energy conversion systems (arrows represent different energy forms)

The concept of polygeneration includes not only energy streams or vectors among their inputs and outputs, but also material flows (Österreicher and Pol, 2007). The most common material flow is the production of fresh water through desalination (Kyriakarakos et al., 2011; Rubio-Maya et al., 2011b). Material flows are added when they interact with the ESS while either producing or consuming significant amounts of energy. A more detailed representation of a polygeneration system is shown in Figure 2-2.

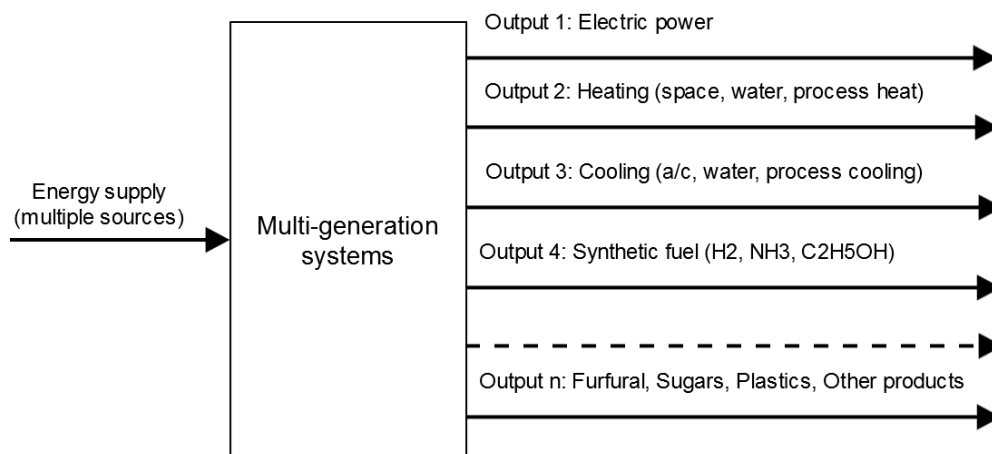
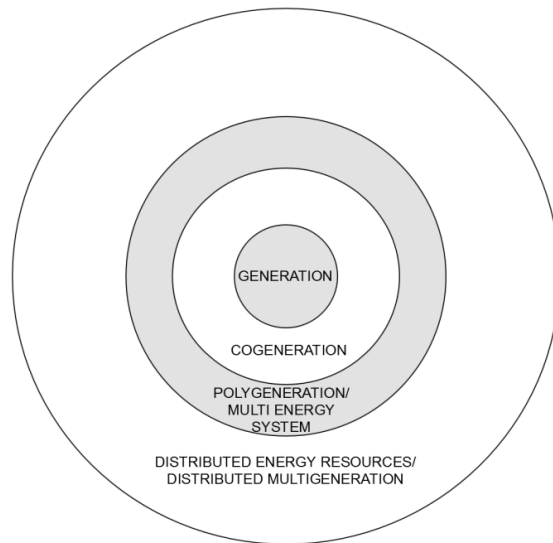


Figure 2-2 Multigeneration system with n output streams, adapted from Dincer and Zamfirescu (2014)

A further expansion of polygeneration leads to more complex concepts, when the energy resources, producers, and consumers are geographically distributed (Chicco and Mancarella, 2009). This is the case of Distributed Energy Resources (DER), which currently receive significant attention (Mancarella, 2014; Mendes et al., 2011; Manfren et al., 2011; Liu et al., 2011). DER focuses on geographically distributed sources of energy, emphasizing the use of renewable energy (RE) where locally economically attractive.

In conjunction with the concept of DER, and with emphasis on the use of renewable energy sources, energy storage, and smart management of energy demand, multigeneration gives way to distributed multigeneration (DMG). DMG systems refer to medium-to-large size clusters of energy consumers, from neighbourhoods, through cities, to regions, and can even be considered on the scale of entire countries (Henning and Palzer, 2014). DMG can be seen as an extension of Distributed Generation (DG), which focuses on the problem of electricity generation in a geographically distributed fashion, as opposed to centralized generation in conventional power plants (coal, nuclear, etc.), to supply geographically spread consumers. The interactions between distributed generators and consumers give rise to the concept of so-called “smart grids”. As well as electricity, DMG includes the generation of other useful energy forms such as heating and cooling, and thus integrates polygeneration techniques.

Given this differentiation, polygeneration (or MES) could equally fit with DER and DMG, if the goal was to try to capture all the technical, economical, and environmental advantages of energy integration (Mancarella, 2014). A Venn diagram illustrating the relationship among the previous concepts is shown in Figure 2-3.



**Figure 2-3 Relationship among ESS concepts**

Polygeneration's importance is fundamentally linked with the opportunity to integrate energy streams of different levels of exergy (i.e., minimum work required to reach a given thermodynamic state from the environment conditions) to reduce the cost of supplying the energy demands (Lozano and Valero, 1993). The efficiency through which the ESS meets the demands of the consumers is related to the exergy of the input and output streams. Accordingly, the theory of the exergetic cost was developed to allocate the thermodynamic cost of the final and intermediate energy/exergy flows to individual elements of the ESS (Valero et al., 1986; Lozano and Valero, 1993). The theory of exergetic cost made its most important contribution in the field of thermoeconomics, recognized as the "science of energy savings" (Lozano et al., 1993); it permits a better, even optimal, use of the energy resources to be proposed, both energetically and economically. Having decided on an ESS construct – whether it be DER or a conceptual variation – it is natural to consider how such systems can be optimized to reduce costs or emissions, or to increase profitability of energy supply.

## 2.3 Optimization of Energy Supply Systems

Mathematical techniques to find maximum and minimum values of analytical functions had been developed well before the 1950s. Some of these techniques had been used to find the solution of systems of equations. However, it was with the development of linear programming (LP) and in particular the Simplex Method (Dantzig, 1948; Dantzig et al., 1955) that linear problems involving a large number of constraints, expressed as inequalities, could be solved. The parallel development of electronics and computing power made it possible to find optimized solutions to large decision making problems in various fields (Dantzig, 1963), from warfare, through contract bidding, to airlift routing.

Linear programming has been used in energy-related fields as early as the 1950s. In Massé and Gibrat (1957), LP was used to investigate the optimal investment plan for the national electric power industry. Since then, problems dealing with investment, operation planning, and control of ESS have been studied by means of mathematical programming. Once stated, these problems can be solved using different solution search algorithms. These are generally chosen depending on the computational resources available, especially when the formulated problems include non-linear expressions. A comparison between different optimization algorithms used currently, as well as different computer software to solve for optimal ESS, can be found in Mendes et al. (2011). Among the software options available discussed, two are worth mentioning here due to their relevance for the present work: the Hybrid Optimization Model for Electric Renewables (HOMER) (Lambert et al., 2006) (reviewed and applied in Appendix 6), and Distributed Energy Resources Customer Adoption Model (DER-CAM) (Stadler et al., 2008) (see Chapter 4).

The synthesis problem of an ESS involves the identification of a design which is capable of supplying the final energy demands of the consumers. This includes the specifications of the structure or configuration of the system, including which technologies are present, the rating of each piece of equipment, and the operational schedule (Petruschke et al., 2014). When optimizing an ESS, the goal is usually to obtain the least total annual cost (TAC) throughout the life of the ESS, this being the sum of investment and operation costs (Yokoyama et al., 2002; Lozano et al., 2009; Ren and Gao, 2010; Zhou et al., 2013; Carvalho, 2011; Romero et al., 2014).

Using optimization techniques on the synthesis problem generally leads to mathematical programming problems, which can be single or multiple objective optimizations. Multi-objective optimization of ESS involves the use of weighting functions grouping not only monetary, but also environmental or performance-related parameters. Examples of an environmental objective function include a straightforward minimization of CO<sub>2</sub> emissions originating from the ESS during its life, or a more complex function of the impact of the system quantifying economic, environmental, and social parameters (Postels et al., 2015).

The constraints to which ESSs are subject are diverse. The principal constraint involves the strict supply of the energy to meet that which is demanded. The equipment installed, whose operation makes that possible, may also be subject to certain capacity constraints, such as a minimum partial load, or a minimum operational time. Operational constraints generally depend on the degree of complexity with which the real equipment is modeled. Simple strict linear models will not support partial load constraints because the expressions that define the fuel or the electricity consumed by the equipment become non-linear (Mendes et al., 2011). Thus, piecewise (linearized) (Yokoyama et al., 2002; Negenborn, 2007) or quadratic models (Rubio-Maya et al., 2011a) can be adopted at the expense of higher computational effort when solving the problem.

The decision variables in synthesis problems are of two natures:

- 1) One quantifying the design, including which technologies are installed, their number and their rating, and
- 2) the other regarding the operation of the selected equipment, interval by interval and the associated energy flows exchanged throughout the ESS, as well as the interaction with the environment.

Many authors have expressed concerns regarding the use of optimization techniques applied to ESS (Collazos et al., 2009; Voll et al., 2013). The problem to be solved requires the identification of the energy demands of the consumers. Collazos et al. (2009) have highlighted the errors that can arise when identifying typical user demands with averages; the error translates into solutions which choose equipment with insufficient capacity to supply peak demands. Voll et al. (2013) suggest the use of additional peak demand constraints, by which the system can be appropriately sized. However, peak demands for various utilities do not necessarily take place simultaneously. Therefore, the strategies already explored to deal with the weakness of typical demands leave room for further improvement.

In order to deal with this shortcoming, various methods have been proposed, among which Stochastic Optimization and Robust Optimization stand out. The former is used when there are known probability functions for the most likely environment from which the optimal solution is obtained, as in Monte Carlo Techniques (Dantzig and Thapa, 1997; Koltsaklis et al., 2015). Robust Optimization, as implemented by Majewski et al. (2015), makes allowances for the uncertainties (in this case in energy demands and prices) but yields solutions that are generally too conservative, and, for ESS, results in oversized equipment or systems. The use of the

conservative design approach of Robust Optimization generally results in higher TAC than non-robust optimization, unless the actual, free from uncertainty, operating cost results dominate over investment costs of both the robust and non-robust designs. This effect is seen in Majewski et al. (2015), although it is not explicitly emphasized there.

Identification of the optimal energy supply for a mine (or for any other energy consumer), whether measured in monetary, energy, or even environmental units, is a complex task. In general, a significant number of assumptions and simplifications are made to maintain computational tractability (e.g., assumption of fixed daily demand patterns as opposed to considering all possible energy demand combinations).

DER or MES optimization has been extended in recent works to include not only the typical energy demands in systems – namely electricity, heating, and cooling – but also demand for other non-energy forms of resource, such as fresh water (Menon et al., 2013). Examples of desalination integrated in polygeneration schemes can be found in the literature. Recently, Rubio-Maya et al. (2011a) and Rubio-Maya et al. (2011b) investigated on the use of polygeneration for a hotel where the main demands are for electricity, heating, cooling and fresh water, proposing a sequential methodology to optimize the ESS. In Kyriakarakos et al. (2011), hydrogen is produced in a standalone power system as an energy carrier; hydrogen is used both as a transportation fuel purposes and an energy carrier with which to seasonally store energy from renewable energy. Ilic et al. (2012) include the production of biofuels with which to cover transportation demands. Finally, Palzer and Henning (2014a) study a DER problem in which, in addition to meeting electricity and heating demands for commercial and industrial consumers, demand from a transportation sector (excluding railway) is supplied in the forms of hydrogen, synthetic methane, and electricity. These studies indicate both economic and thermodynamic

advantages of polygeneration combined with optimization techniques, stressing the importance of the integration of local renewable energy sources.

As a result of these and previous works, several optimization tools have emerged, such as the already mentioned HOMER and DER-CAM, with the aim of calculating optimal ESS designs that ultimately address the economical problem of resource allocation (Mendes et al., 2011).

## **2.4 Model Predictive Control in Energy Supply Systems**

ESS designs based on past operating conditions, especially when using averaged typical demand profiles, do not ensure the optimality, nor even the feasibility, of the ESS while in operation (in a Mathematical Programming sense). As expressed by Collazos et al. (2009), perfect knowledge of demands is *“not acceptable when implementing the optimal management strategy for an existing system since these profiles are stochastic and are not perfectly predictable.”* The same observation holds even if the profiles are free of random character, but simply vary from prior patterns. In other words, an optimal design based on typical past demands may yield unfeasible operating conditions/system states as soon as demand varies from their empirical levels in absence of auxiliary sources (energy routes), if these sources were not present in the optimal design. This is especially important in isolated energy systems where, in order to mitigate this problem, ESS optimal designs normally have much higher rated equipment than infrastructure connected systems, in order to deal with extremes of load and source variability.

Assuming that the system can be designed using typical conditions (for example using OMSES), the question is: How can one evaluate the robustness of such designs and determine the best operational management strategy for post-commissioning stages? Before answering this question, it is important to remember that: *“...from the control systems view, smart grids are*

*essentially predictive optimal control problems, which can be formulated as optimizing the cost, the use of storage, the use of wind/PV source, and to match the production with the consumption in a predictive horizon”* (Zong et al., 2012). This assertion, although referring to smart grids, can be extended to energy systems in general, and reinforces the selection of MPC among other control approaches.

Several authors have investigated the use of MPC in ESS for control and scheduling purposes (e.g., Collazos et al. (2009), Zong et al. (2012), Avci et al. (2013), Mayhorn et al. (2013), Pereira et al. (2013), and Torreglosa et al. (2015)). Although MPC is generally applied in tracking problems, where certain output variables are required to stay close to a reference value, scheduling problems can also take advantage of the special characteristics of this control approach. The existence of a fixed system design is assumed and its operation can be optimally scheduled over a given time horizon. Its ability to deal with physical constraints, the prediction of the problem inputs, the use of simplified mathematical models for the real plant, and its consideration of cost functions suitable for optimization, makes of MPC a useful approach for energy scheduling optimization (Camacho and Bordons, 2004). MPC can not only include cost functions related exclusively to energy, but it can also accommodate penalty functions regarding certain variables taking values that can move freely, within a certain range. This is the case, for example, in the work of Collazos et al. (2009), where an MPC implementation, in addition to minimizing energy costs, maintains indoor temperature conditions within set point limits by means of a penalty function.

MPC can be used to simulate and optimally operate a previously optimized design, given that both problems (design and control) include, in their respective time horizons, the same operational constraints applied to the components of the system (see Chapter 5 for a detailed

description of MPC). While the design problem is concerned with time horizons of years, which are then discretized to obtain typical operating conditions in the form of daily profiles, the control problem involves operation horizons no longer than several days. Collazos et al. (2009), for example, apply MPC to a previously calculated optimal polygeneration design following the methodology used in Weber et al. (2006). The work is distinguished by the following: an autoregressive external (ARX) input method to characterize the second order model of the thermal dynamic of a single family house (the consumer); the use of comfort penalties, these being a linear expression of the indoor temperature; the use of a piece-wise (non linear) model of the cogeneration plant; and minimum running time and start up costs. The grid connected system is controlled to minimize energy costs and user discomfort. In doing so, the MPC based control system is capable of exploiting the system's thermal inertia in a smart fashion, leading, technically, to a load shift. The study includes electricity consumption and outdoor temperature forecasts (the latter based on the previous 30 days) in order to take better operational decisions.

In Torreglosa et al. (2015), the system simulated and controlled had also been previously optimized. However, the only energy demand considered was electricity; heating and cooling were not considered.

The retrospective formulation of OMSES, i.e., considering past operational conditions to optimize the design, leads to very large problem sizes as the discrete time interval considered becomes smaller in approaches aiming to optimize design and operation simultaneously. MPC offers more flexibility in this respect, as optimization and simulation consider a finite time horizon that is typically shorter than even abbreviated year-round formulations.

The application of MPC on existing, non optimized designs is more common (Avci et al., 2013; Mayhorn et al., 2013; Pereira et al., 2013; Zong et al., 2012). In Zong et al. (2012), for instance, the use of MPC to control an intelligent building and its energy supply system is presented, to develop what these authors refers to as “active demand-side management” (ADSM). In the case considered, the system had two electricity sources: electricity grid and solar photovoltaic (PV). With a given design imposed, the aim of the work was to demonstrate maximization of the use of PV to heat the house (first order linear model) while reducing the energy cost and maintaining the indoor thermal comfort, penalizing the deviation from a temperature setpoint. The controller, which considered environmental parameters (solar radiation, ambient temperature, and wind speed) and electricity price forecasts, is capable of using the thermal storage capacity of the building to reduce external consumption of electricity from the grid.

In Mayhorn et al. (2013) a hybrid wind-diesel stand alone energy system with battery energy storage and high penetration of renewable energy is simulated and optimally controlled using MPC. Uncertainty in load and wind speed is considered for the look-ahead dispatch problem. The goal of the controller is to minimize a weighted function of: the fuel cost; the change in power output of the existing diesel generators (two units); the battery’s state of charge, penalizing low level; and the inability of isochronous generators to provide real-time balancing.

When applying MPC to ESS, it is important to recognize how finely discretized the considered control horizon should be. The control and forecast (Chapter 5) horizon can be divided into segments of ten minutes as suggested by Zong et al. (2012), or longer, like in Collazos et al. (2009) (15 minutes and 1 hour). Power control or scheduling generally require shorter intervals (high control frequency) than thermal problems, for which effective control can be achieved using longer intervals (low control frequency); e.g., intervals are taken from minutes to hours for

thermal problems, as opposed to one to ten minutes for power scheduling, or milliseconds to seconds to power quality control. When dealing with power systems and formulations aiming to control power quality, the dynamics of the actual system may require intervals of .25 seconds (Negenborn, 2007). Generally, the frequency of the control (i.e., the length of the discrete intervals) will be determined by the length of the control horizon, the ability to obtain a reliable forecast in the given horizon, and the computational complexity.

An example of longer discrete time intervals in power systems is found in del Real et al. (2014). The reason for such selection is that the required control and forecast horizons are longer because the problem is more focused on the reduction of the power generation cost and the reduction of greenhouse gas emissions than on the instantaneous control of power quality parameters (e.g., voltage and frequency). In general, the dynamic of large power systems in terms of daily variations is slow, especially when meeting aggregated demand from multiple consumers with appreciable diversity in their demand patterns. Furthermore, the assumption can be made that the optimal schedule is valid for each planned hour. Del Real et al. (2014) extend the concept of distributed energy resources (DER) to the control of several energy hubs of producers and/or consumers. Thus, a distributed model predictive control (DMPC) (see Chapter 8 for examples on centralized and distributed MPC) approach is used to coordinate power production and exchange among the hubs, so that the overall system can achieve near optimal operation in comparison with a centralized control system approach.

In an uncertain environment where conditions defining demand are changing continuously, the optimal energy system can be tested through simulation. This enables one to determine its feasibility, including whether the system can effectively supply the energy demanded in a timely manner, and whether it does so with the expected annual cost that was anticipated in the design

stage. MPC provides a suitable scheme to evaluate the solutions obtained with OMSES, because the definition of the problem in terms of plant model and cost function is expressed identically to the design optimization problem (Carvalho et al., 2014b). Furthermore, as shown previously in the available literature, MPC represents an excellent candidate for optimal control of the operation of the system. The case of mine energy systems is of special importance given the variety of the forms of demands for energy and the potential uncertainties associated with them, as shown in this thesis.

# Chapter 3

## 3 Optimal Mine Site Energy Supply Basic Formulation

Carvalho and Millar (2012) presented the original OMSES formulation and development roadmap, together with simplified illustrative case study examples. This work did not offer a self-contained mathematical description of the optimization problem, but instead, drew upon the polygeneration optimization formulation presented in Carvalho (2011). In this chapter, the necessary self-contained OMSES formulation is presented. The mathematical expressions and additional support information defining the optimization problem, i.e., decision variables, objective function and constraints, are set out as they are used in this thesis. Although not a formal literature review-type chapter of the thesis, the Chapter nevertheless constitutes a detailed review of the mathematical programming technique required for the work.

### 3.1 Introduction

The general problem of design optimization of an energy supply system for a generic mine is addressed in this chapter. The mine is treated as an energy system whose final demands have to be met using available resources at the site and some combination of available technologies. The optimization problem is formulated using Mixed Integer Linear Programming (MILP).

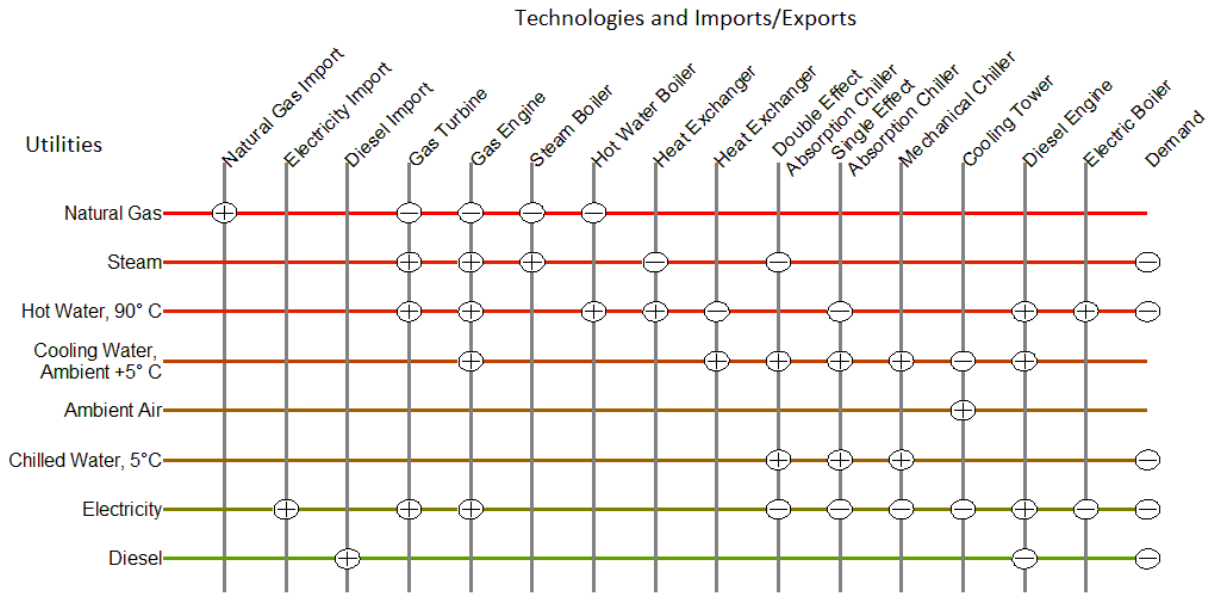


**Figure 3-1 Example of a superstructure – Vertical lines represent technologies, horizontal lines represent utilities, a positive sign symbolizes production, and a negative sign denotes consumption**

The energy system is composed of a set of technologies that produce and exchange energy *utilities* so that the right type and quantity of energy required is delivered to the demand center at the appropriate time and place. A *utility* is a good that is exchanged in the ESS, typically a form of energy, such as electricity, natural gas, or heat. Figure 3-1 describes the interactions between technologies and energy sources (denoted “Imports”) and utility flows in the mine. Such representations are referred to herein as grid superstructures or simply *superstructures*. Each vertical line represents a technology (or an import). A *technology* produces or consumes *utilities* delivered across the site by physical distribution systems, the latter represented by horizontal lines. Each technology consumes a utility if their intersection has a node with a negative sign. Alternatively, a technology produces a utility if their lines cross with a node with a positive sign. Should there not be any node, the technology does not produce nor consume that utility. Technologies (and imports) are labeled on the top side of the graph, while utilities are labeled on the left side. The last vertical column of nodes on the right hand side of the graph (without a vertical line) is reserved for utilities for which the demand center, in this case a mine, has a

*demand* (negative sign). If those demands are not met, the mine cannot operate. The utilities demanded are represented by nodes with a negative sign because they represent consumption of utilities. If the superstructure includes all the technologies that are available in the problem and all utilities including an ambient air utility, then it is termed a Conservative Conversion Grid (CCG) superstructure, or simply *conservative superstructure*. The term ‘conservative’ refers to the necessity of ensuring conservation of energy or energy flow across the utilities and within the technologies. Mathematically, such conservation is articulated through the prescription of constraints. The ambient air utility represents the ultimate sink for all sources of energy featuring in the superstructure.

### 3.1.1 Decision Variables and Scale of the Problem

Subscripts  $u$ ,  $v$ ,  $i$  and  $j$  are used respectively in reference to sets of utilities (U), technologies (V), and representative days and hours (T). The defined set for each variable is expressed in Eq. 3-1 and are exemplified in Table 3-1 and Table 3-2. The use of  $u$  in lower case denotes that is a *variable (formally element or object)*, while U represents the *set*; the same applies to V and T. In other words,  $u$  takes all the possible values contained in the set U, and so on.

$$u \in U, v \in V, (i,j) \in T \quad (3-1)$$

**Table 3-1 Example membership of set U for utilities**

Utilities (U)	Abbreviation
Biomass	BM
Electricity	EE
Syngas	SY
Natural Gas	NG
Diesel/Syndiesel	DI
Steam	SM
Hot Water	HW
Cooling Water	CW
Chilled Water	RW
Ambient Air	AA

**Table 3-2 Example membership of set V for technologies**

Technologies (V)	Abbreviation
Gasifier	GFBM
Fischer-Tropsch	FTDI
Gas Turbine	GTSM
Diesel Turbine	DTSM
Steam Turbine	STSM
Gas Engine	GEHW
Diesel Engine	DEHW
Steam Boiler	SMNG
Hot Water Boiler	HWNG
Biomass Boiler (Steam)	SMBM
Biomass Boiler (Hot water)	HWBM
Electric Boiler	HWEE
Diesel Boiler	SMDI
Absorption Chiller	ACRW
Mechanical Chiller	MCRW
Cooling Tower	CTCW

In this work, decision variables (the variables for which values are obtained from the optimization process) use Greek capital letters for energy-related variables, and lower case Greek letters for dimensionless variables. Table 3-3 includes the main features of each of the variables used, which are further described in the following sections.

**Table 3-3 Decision Variable Information**

Variable	Units	Description	Set	Type
$\mu_v$	-	Number of units of each technology	$V$	Integer
$\Phi_{uij}$	MWh	Utility flow	$U, T$	Real
$\Pi_{vij}$	MWh	Production by technology	$V, T$	Real
$X_{uvij}$	MWh	Utility flows by technology	$U, V, T$	Real
$\Gamma_u$	MW	Utility connection rating	$U$	Real
$\delta_{uij}$	-	Auxiliary variable charge/discharge	$U, T$	Binary
$\Delta_{uij}$	CAD	Demand charges	$U, T$	Real

### 3.1.2 Time Scale Considerations

The problem is formulated so that the variables must find a value inside the feasibility region defined, among others, by energy balance equations which form the principal constraints of the problems. The balance is applied over each time interval. Therefore, given such a time interval, the balance may be applied in terms of energy or power. In this work, it is assumed that the equipment delivers steady power in each interval, and the balance during each one is expressed in MWh.

The time discretization methodology used in the present work is called “hierarchical uniform time discretization” (Samsatli and Jennings, 2013). This formulation requires definition of the time domain as a series of hierarchically related time levels. Here, a year is divided into  $d$  representative days, and each representative day into  $h$  time intervals with the identical duration of  $\Delta t = 24/h$  hours. It is here considered that the unit system for each time level is *days* and *hours*; i.e., subsequent time discretization of each of the levels represents fractions of days and hours respectively. If  $n_i$  is the day fraction (generally integer values) of  $i^{th}$  day type ( $i=1\dots d$ ), and  $n_j$  is the hour fraction (integer or real) of the  $j^{th}$  hour type ( $j=1\dots h$ ), the characteristic duration of the interval  $(i,j)$  will be given by

$$t_{ij} = n_i \cdot n_j \quad (3-2)$$

Following Samsatli and Jennings (2013), the number of repetitions of typical days, providing each typical day represents one of the twelve months of a typical year, is equal to the days that this month contains and, furthermore,  $\sum_{i=1}^d n_i = 365$ . Similarly, it can be observed that the following is true:  $\sum_{j=1}^h n_j = \sum_{j=1}^h \Delta t = \sum_{j=1}^h 24/h = 24$ , when the lower level, time intervals are 24 and equally distributed ( $h=24$ ).

For instance, if 12 typical days are used to define the demands of each month of a typical year, then  $n_i = 31, 28, 31 \dots 31$  for each  $i = 1, 2, 3 \dots 12$ . If the number of intervals within a day is 24, then  $n_j = 1$  for all  $j=1, 2, 3 \dots 24$ . Different time discretization can be accommodated to increase or decrease granularity in the energy demands of consumers (Samsatli and Jennings, 2013).

Formally, the unit in which  $t_{ij}$  is expressed depends on the product involved – days times hours. However, in order to maintain consistency among all the equations that follow,  $t_{ij}$  is considered dimensionless.

In the following formulation, a quantity  $x$  that varies over time is designated by  $x_{ij}$  at the  $j^{th}$  time interval of the  $i^{th}$  representative day of the year. The generalisation of temporal division will be discussed in later sections. For a temporal distribution including years, which therefore includes typical years, days, and hours, the reader is referred to Chapter 6. For a full year problem, with 365 consecutive days of 24 hours each, the reader will find more information in Section 4.5.3 and a case study in Appendix 7.

### 3.2 Objective Function

The problem to solve is the minimization of all the costs that, throughout the operating life of the mine, are related to energy consumption and the way energy is procured and used. The objective function considered is the annualized cost in monetary units (e.g., CAD):

$$\text{Minimise } C_{tot} = C_{fix} + C_{var} \quad (3-3)$$

where  $C_{tot}$  is the total annual cost, defined as the sum of the annuitized fixed cost  $C_{fix}$  (equipment and infrastructure) and the annual variable cost,  $C_{var}$ .

### 3.2.1 Fixed Costs

The annuitized fixed cost is expressed by

$$C_{fix} = k_{rf} \cdot (1 + k_{ic}) \cdot [ \sum_v \mu_v \cdot C_{inv,v} + \sum_u C_{inf,u} + \sum_u C_{net,u} ] \quad (3-4)$$

$$k_{rf} = i_d \cdot (1 + i_d)^y / ((1 + i_d)^y - 1) \quad (3-5)$$

where  $k_{rf}$  is the annuitization factor, calculated using an expected discount rate  $i_d$  and a project life  $y$  (years) (Eq. 3-5). The right hand side of Eq. 3-4, except  $k_{rf}$ , represents the capital expenditure. The coefficient  $k_{ic}$  accounts for engineering and supervision expenses, legal expenses, contractor's fees and contingencies, which may be assumed to be some percentage of the equipment investment costs.  $\mu_v$  and  $C_{inv,v}$  are, respectively, the number of pieces of equipment installed and the capital cost of each unit of technology  $v$ .  $C_{inf,u}$  is the cost of installing or building the required external infrastructure in order to have access to the utility  $u$ . Finally,  $C_{net,u}$  represents the cost associated with an internal distribution network for each utility, which may be a cost already assumed by the consumer, e.g., heating grid in a building.  $C_{net,u}$  takes a 0 value if the utility is not present in the solution of the problem. Generally, the cost of both external infrastructure and internal distribution networks are a function of their capacity and length. As an example of an infrastructure cost function, the capital cost of an electricity connection may be expressed as follows:

$$C_{inf,u} = \Gamma_u \cdot (a_{inf,u} + D_{TRANS} \cdot b_{inf,u}) \quad (3-6)$$

where  $\Gamma_u$  is the rating or capacity (MW) of the connection, e.g., the capacity of the transmission line and transformer system (free variable, to be defined by the optimization procedure) in case of electricity, and  $D_{TRANS}$  is the distance between the site and the nearest existing connection.  $a_{inf,u}$  and  $b_{inf,u}$  have units of CAD/MW and CAD/MW/km, respectively.

### 3.2.2 Variable Cost

The annual variable cost is expressed by

$$C_{var} = \sum_{ij} c_{e,ij} \cdot t_{ij} + \sum_{vij} c_{O\&M,v} \cdot \Pi_{vij} \cdot t_{ij} + \sum_{uij} \Delta_{uij} \quad (3-7)$$

where  $c_{e,ij}$  is the energy cost (CAD) for every time interval arising from imported and exported energy forms: diesel, biomass, natural gas, electricity, etc.  $c_{O\&M,v}$  is the operating cost (CAD/MWh) for the technology  $v$ ,  $\Pi_{vij}$  the produced characteristic utility (MWh) during a given time interval by the technology  $v$ , and  $\Delta_{uij}$  is the demand charge or extra revenues (CAD) expressed as a payment or income that may be different for each time interval, and generically different for each utility. This demand charge generally depends on how much utility is purchased and when, and therefore is a variable cost dependent on the jurisdiction regulation.

The hourly variable cost of energy is expressed as a function of the commodity flows purchased and sold:

$$c_{e,ij} = \sum_u p_{uij} \cdot \Phi_{uij}^{pur} + \sum_u q_{uij} \cdot \Phi_{uij}^{sel} \quad (3-8)$$

Equation 3-8 contains the cost of importing and exporting each utility in the market and the respective amounts of flows. Energy purchase and sale prices are  $p$  and  $q$  respectively, and the imported and exported flows are  $\Phi_{uij}^{pur}$  and  $\Phi_{uij}^{sel}$ .

## 3.3 Problem Constraints

### 3.3.1 Installed Capacity and Equipment Production Limits

The installed power ( $P_v$ ) for each technology  $v$  is given by

$$P_v = \mu_v \cdot P_{nom,v} \quad (3-9)$$

where  $P_{\text{nom},v}$  is the nominal power (MW) of the equipment representing the technology  $v$ . Technology operation is subject to production limits as set out in Carvalho (2011). The actual output of each technology is expressed, however, in MWh. Thus, the capacity limit constraint for each technology is expressed as follows, considering  $n_j$  the duration in hours of the corresponding time interval  $(i,j)$ :

$$\Pi_{vij} \leq P_v \cdot n_j \quad (3-10)$$

### 3.3.2 Energy Balance Constraint Across Technologies

According to its design, each technology interacts with the superstructure by consuming and producing utilities. A technology is actually defined by the utilities it consumes and produces, and in which proportion to the main utility produced, which is also defined as a characteristic. Equation 3-11 represents the utility balance for every technology:

$$X_{uvij} = K_{uv} \cdot \Pi_{vij} \quad (3-11)$$

where  $X_{uvij}$  (MWh) is the energy flow of utility  $u$  consumed or produced by technology  $v$  in the period  $(i,j)$  and  $K_{uv}$  is the production coefficient matrix that defines the energy/mass balance of each equipment. An example for  $K_{uv}$  is shown in, being the units of each coefficient “MWh of utility produced (consumed if negative) per MWh of main utility produced”.

**Table 3-4 Selected equipment and matrix of production coefficients**

Equipment <sup>1</sup>	Electricity	Natural gas	Steam	Hot Water	Cooling Water	Chilled Water	Ambient Air
Gas Turbine	<b>1</b>	-3.03	0.59	0.66			
Gas Engine	<b>1</b>	-2.44	0.70	0.41	0.23		
Steam Boiler		-1.18	<b>1</b>				
Hot Water Boiler		-1.22		<b>1</b>			
Steam-HW HX			-1	<b>1</b>			
HW-CW HX				-1	<b>1</b>		
Absorption Chiller	-0.01			-1.36	2.36	<b>1</b>	
Mechanical Chiller	-0.17				1.17	<b>1</b>	
Cooling Tower	-0.01				1		<b>1</b>

<sup>1</sup>*Solar turbines, Caterpillar gas engines, SMARDT electrical chillers, York hot water absorption chillers, Cleaver Brooks hot water boilers, Vapour Power steam boilers and Marley cooling towers*

Table 3-4 illustrates the quantitative relationship among the utilities produced and consumed by each technology. The positive and negative signs represent produced and consumed utilities. Each technology produces a characteristic utility (bold), in a quantity that is represented with the variable  $\Pi_{vij}$ . It should be noted that, given a superstructure representation (Figure 3-1), coefficient signs are redundant. In general for OMSES, signs will be mathematically substituted by defining production and consumption matrices, described in the next subsection.

### 3.3.3 Energy Balance Constraints across Utilities

Figure 3-2 shows a detailed representation of the scheme implemented in the optimization model, using the superstructure-based methodology for a generic utility. The horizontal line represents the energy balance for a particular utility for all intervals that are members of  $T$ .

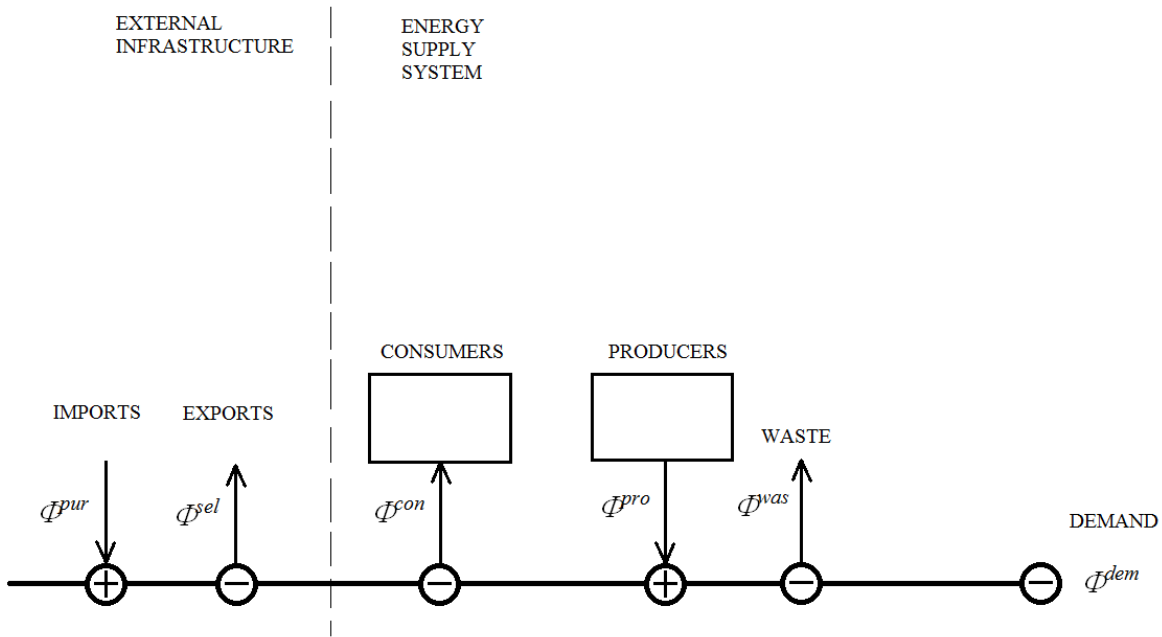


Figure 3-2 Utility balance scheme implemented in the optimization module

The balance equations across time and utility are expressed as follows:

$$\Phi_{uij}^{pro} + \Phi_{uij}^{pur} - \Phi_{uij}^{con} - \Phi_{uij}^{sel} - \Phi_{uij}^{was} - \Phi_{uij}^{dem} = 0 \quad (3-12)$$

$$\Phi_{uij}^{pro} = \sum_v X_{uvij} \cdot K_{uv}^{pro} \quad (3-13)$$

$$\Phi_{uij}^{con} = \sum_v X_{uvij} \cdot K_{uv}^{con} \quad (3-14)$$

where the terms on the left hand side of Equation 3-12 are, respectively, the production, consumption, purchase, sale, waste, and demand of utility ( $u$ ) in the period ( $i,j$ ).  $K_{uv}^{pro}$  and  $K_{uv}^{con}$  are binary matrices that define the sense of each of the terms in  $X_{uvij}$ .  $K_{uv}^{pro}$  is 1 when technology ( $v$ ) produces utility ( $u$ ) (otherwise 0), and  $K_{uv}^{con}$  is 1 when technology ( $v$ ) consumes utility ( $u$ ) (otherwise 0).

Production (*pro*) and consumption (*con*) correspond to internal utility flows whereas purchase (*pur*), sale (*sel*), waste (*was*), and demand (*dem*) represent exchanges of utilities between the energy supply system and the environment.

### 3.3.4 Constraints on the Flows of Utilities

Constraints may apply depending on the problem addressed on the flows purchased, consumed, wasted, etc. There are cases where limitations on annual purchase may apply on certain utilities, for example, diesel. Generally, the limitation imposed on the amount of a utility consumed (or purchased) in a certain time ( $i, j \in \hat{T}$ ) is specified as:

$$\sum_{ij} \Phi_{uij}^{con(pur)} \cdot t_{ij} \leq L_u \quad (3-15)$$

where  $L_u$  is the limit amount of the utility  $u$  that is allowed to be consumed (purchased) in the period  $\hat{T}$ . This period, which is a subset of  $T$ , may correspond to time constraints on the supply chain which impose limitations on bunkering activities. Diesel bunkering management, for example, is very important when considering remote mining operations, especially where access can be poor because of a challenging landscape and climatic environment. For example, a mine may only be accessible by temporary trail in the winter, or by air; a winter-road may only be open in February, a period in which diesel is safely allowed to be trucked in. The threshold on storage tank sizing can be mathematically expressed as:

*For each day of January (month 1) and any day of March or later ( $\geq$  month 3):*

$$\sum_{ij} \Phi_{DI,ij}^{con} \cdot t_{ij} \leq L_{DI} \quad (3-16)$$

$$\hat{T}: i \in \{1, 3 \dots 12\} \cap j \in \{1 \dots 24\}$$

where  $\Phi_{DI,ij}^{con}$  refers here to hourly consumption of diesel. This cumulative sum must be lower than  $L_{DI}$ , the capacity of the storage tank.

$\Phi_{uij}^{was}$  represents any flow leaving the ESS which passes into the surrounding environment. *Waste* flows are those leaving the energy supply system without meeting any demand or being consumed by any equipment, in a controlled manner. This is the case of the low-temperature heat released by a cooling tower (or similar technology); the utility *ambient air*, which cannot be used by any technology, is generally a useless form of energy. In general, the user of OMSES decides whether or not  $\Phi_{uij}^{was}$  participates in the energy balance of any of the utilities, providing there exist a technology adapted for such purpose.

### 3.3.5 Grid Capacity Constraints

As explained in Section 3.2.1, the ESS may have access to an external utility source by means of the corresponding infrastructure, such as transmission line in the case of electricity, or a pipeline in the case of natural gas. The amount of utility that can be transported is the capacity of the grid,  $\Gamma_u$ . This capacity value, which determines the cost of the grid connection, also imposes a constraint on the imports and exports of the utility it transports. If it is assumed that the utility flow limits are the same for imports and exports, the capacity constraints can be expressed as follows:

$$\Phi_{uij}^{pur} \leq Y_u^{pur} \cdot \Gamma_u \cdot n_j \quad (3-17)$$

$$\Phi_{uij}^{sel} \leq Y_u^{sel} \cdot \Gamma_u \cdot n_j \quad (3-18)$$

$Y_u^{pur}$  and  $Y_u^{sel}$  are binary variables and respectively express the possible restrictions in purchase and sale of a utility and constraints defined as external boundary conditions.

### 3.3.6 Demand Charge Minimization

In addition to the cost of the energy supplied, utility companies charge other costs associated with grid operation and maintenance, company's salaries and profits, etc. Additional services may be charged, such as enhanced supply reliability for consumers whose energy demands must be guaranteed (hospitals) or are willing to pay the increased cost (some factories). However, the most common term utility companies charge is related to the maximum instantaneous consumption (power) and is called the *demand charge* (DC). Demand charges are common in electric markets, but can also apply to the supply of other energy forms.

In Ontario, the amounts paid by large electricity consumers for capacity (DC) depend on the power they draw from the system during the peak power demand at provincial level, which happens at times that cannot be precisely predicted. In this jurisdiction DC are also referred to as Global Adjustment (GA) charges. Traditionally, the provincial power demand peaks either during the coldest or the warmest hours of the year (see Appendix 1). The scheme within OMSES for this jurisdiction to deal with DC involves the computation of a series of weighting factors that permit the likely DC to be predicted for any hour of operation. The weighting factors are computed as follows: suppose that  $x$  is an ordered set of couplets:

$$x = \{(P_1, h_1), (P_2, h_2), \dots, (P_j, h_j), \dots, (P_N, h_N)\} \quad (3-19)$$

where  $P_j$  is the provincial demand (Ontario) in MWh/h and  $h_j$  is the hour of the day at which this demand occurs.  $h_j$  can assume values (labels) from 01 to 24.  $x$  is ordered by the decreasing value of  $P_j$  so that  $P_1$  is the highest demand in the period of  $N$  contiguous hours of sampled couplets.  $N$  could assume a value of 8760 if a full year is considered. For the first  $r$  elements of  $x$ , a histogram of incidence of each hour of the day can be prepared:

$$F_r = \{a_{01,r}, a_{02,r}, \dots a_{024,r}\} \quad (3-20)$$

where, for instance,  $a_{02,r}$  represents the number of times 02:00hrs was a peak hour in the set of  $r$  elements, normalized by  $r$ . When multiple histograms are prepared, each adopting a different value of  $r$ , an envelope to them all can be defined:

$$E_j = \max (a_{j,r}) \quad (3-21)$$

and the weighting coefficients arise by normalizing:

$$DC_j = \frac{E_j}{\sum_{k=1}^{24} E_k} \quad (3-22)$$

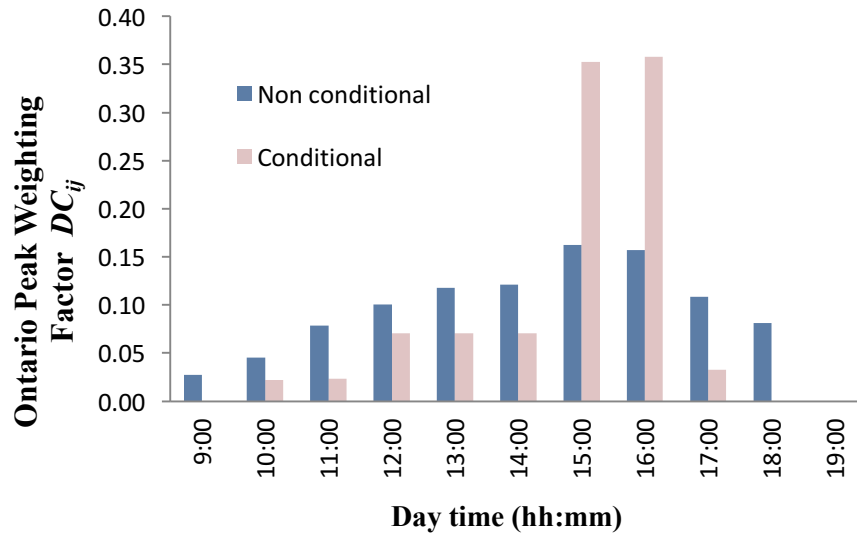


Figure 3-3 Non conditional and conditional weighting factors expressing the likelihood of a peak demand event within a given hour of the day considering June, July and August

When  $r = \{10, 20, 30, 40, 50, 60, 100\}$  and using hourly demand data for Ontario in 2012 (IESO, 2012), the weighting coefficients adopted in subsequent calculations are labeled ‘non-conditional’ in Figure 3-3. The statistical analysis to produce Figure 3-3 included exclusively data for June, July and August in 2012. Similarly, a ‘conditional’ set of weighting coefficients (Figure 3-3) can be formed by revising set  $x$  so that it contains only the highest demand hour in each day of the year and following the same scheme (Equations 3-20, 3-21, and 3-22). The

‘conditional’ approach is used because the demand charges of large electricity consumers depend on their power demand in the five hours of the greatest provincial electricity demand (see Chapter 7 and Appendix 1 and Appendix 3), on different days. ‘Non-conditional’ means the power demand in hours of the same day can be considered.

Observation of Figure 3-3 reveals the following aspects: the highest power demand in Ontario in the year 2012 was most likely to occur between 15:00 and 16:00 hours. If only the highest demand for each day is considered (‘conditional’ bars) the peak is at 16:00. If this condition is relaxed, the distribution is smoother (‘non-conditional’ bars) and the peak is at 15:00. The practical consequence follows: if one were to avoid only one hour of consumption each day to minimize demand charges, 16:00 should be the hour of the day selected. If the possibility of reducing consumption for over several hours of each day is to be considered, ‘non-conditional’ weighting may be adopted in the optimization process.

When applied, the weighting functions allow for the calculation of demand charges with the result that the optimization process results tends to avoid electricity consumption during peak periods. Recommendations for load peak clipping or load shifting emerge in the results of optimization. As there are no means to differentiate demands, load shifting would be achieved by accumulating purchased electricity for a later use; peak clipping would take place whenever the systems substitute electricity purchased from the grid by self-generated electricity.

For simplicity in illustration of the optimization formulation in the forthcoming scenarios covered in this thesis, the weighting factors,  $DC_{ij}$ , are applied only to the month of July. For Ontario, this is when the highest demands are expected, due to weather conditions. Therefore, the weighted consumption of externally purchased electricity ( $\Phi_{peak}^{pur}$ ) is calculated as follows:

$$\Phi_{peak}^{pur} = \sum_{ij} DC_{ij} \cdot \Phi_{uij}^{pur} \quad (3-23)$$

where  $\Phi_{peak}^{pur}$  is the demand level that is used to estimate the operation's demand charge, calculated for July and electricity purchase.  $DC_{ij}$  expresses the subjective likelihood of a transmission and distribution system peak, illustratively established from historical data of summer months of 2012 for Ontario in Figure 3-3. If the maximum provincial demand can take place in winter, historical data from the respective months should be used to calculate different  $DC_{ij}$  coefficients and use accordingly, i.e., to calculate potential  $\Delta_{uij}$  originated in winter time (this has actually happened in 2014; see Appendix 3 for more information).

For the jurisdiction considered, the fraction that  $\Phi_{peak}^{pur}$  is of the system demand, apportions the fraction of the total annual system costs allocated to the operation. This cost is paid by the consumer on a monthly basis, as indicated in Eq. 3-7. Generally,  $\Delta_{uij}$  is a function of  $\Phi_{peak}^{pur}$ , established by the utility company that can vary from one jurisdiction to another.

# Chapter 4

## 4 Extensions of Basic OMSES Formulation

While Chapter 3 served principally to review the basic formulation of Carvalho and Millar (2012), it did introduce important variations to generalize the tariff structures that can be accommodated so that OMSES can be particularized to the jurisdiction where the ESS is to be deployed. In this and the following two Chapters, the work done to bring OMSES to its current level of development is explained. The OMSES extensions described in this chapter are:

- Renewable energy sources and technologies (Section 4.1)
- Spinning reserve (Section 4.2)
- Power to gas technologies (Section 4.3)
- Material flow utilities (Section 4.4)
- Storage systems, short and long term (Section 4.5 and 4.6)
- Mobile technologies for material transport (Section 4.7)

which renders its overall utility superior to mainstream ESS optimization tools. The present chapter describes the necessary modifications to the initial formulation of OMSES. Each section describes the fundamental basis on which the modifications are made, as well as the justification for why the new modifications become specifically interesting in the area of mine energy systems. Content regarding ventilation and mechanical work utilities has been published in Romero et al. (2015a). The energy storage formulation was applied in Carvalho et al. (2014b),

and renewable energy formulation in Carvalho et al. (2014a), for solar energy, and in Romero et al. (2015a), for wind energy.

## **4.1 Renewable Energy**

Renewable energy can be an option to reduce energy costs in mining. The cost of energy from wind power and solar photovoltaics has already been found to be cost-competitive in some regions, although this depends on the life of the project, the cost of competing conventional sources of energy, and the structure and size of the demand. Generally, investment costs are the main obstacle for RE deployment. Arriaga et al. (2013) evaluated the potential of RE technologies (wind power and photovoltaics) in Northern Ontario to supply electricity to remote communities, arriving at the conclusion that those are already economically “break-even.” Because of the reduced carbon emissions compared to conventional solutions (mainly diesel engines), a carbon pricing scheme would make conventional sources a more expensive alternative. A complete summary of the challenges of remote area power supply systems, not only financial but also technical, can be found in Tan et al. (2014).

Remoteness, however, can be a relative concept, especially when addressing the problem of energy supply. In some instances, building a transmission line or a pipeline becomes a cost-effective investment (Carvalho et al., 2014b), instead of, or in addition to, other local renewable energy sources.

In this section, two particular renewable energy sources are investigated: wind power and biomass. Examples of solar technologies in the field of energy systems are abundant, generally focusing on solar thermal technologies for low temperature domestic water (Carvalho et al., 2014b), and solar photovoltaic (Stadler et al., 2008). Solar power, whether thermal or

photovoltaic, is used today in some remote mines where solar irradiation is especially abundant (e.g., South Africa, Chile) (Judd, 2015b; Judd, 2015a; Jacobsen, 2015; Dube, 2015; “Exploring the Benefits of the Mining-Solar Collaboration in Chile,” 2015; “Solar for Mines: Providing Baseload Solutions,” 2015).

This section shows the way in which OMSES can accommodate the technologies associated with two renewable sources which are different in terms of their uncertainty, variability, and their readiness for generation (Scott, 2005). For biomass, constant availability can be considered, as long as biomass related constraints are met, such as maximum amount that can be purchased or stored monthly or annually (Carvalho et al., 2014b). On the other hand, wind power varies significantly on an hourly and daily basis (variability), although mean monthly power generation can be considered fairly constant interannually. It is also difficult to predict wind speed beyond the next 24 hours (uncertainty). Therefore, it may be possible to use OMSES’ ‘typical-days’ approach in conjunction with wind power, although results are successful only under low penetration conditions, as will be demonstrated.

#### **4.1.1 Biomass**

Whether it concerns mining or not, the use of biomass either as a fuel to produce heat and power, or as a feedstock to produce synthetic fuels, remains controversial. An in-depth analysis about the preferred conversion pathways for different biomass products and their final uses can be found in Sterner (2009). For the present work, only two types of conversion of purposefully grown biomass feedstock are discussed and used in OMSES – gasification and the Fischer-Tropsch process (Carvalho et al., 2014b).

Biomass gasification systems operate by heating biomass in an oxygen depleted environment where the solid biomass breaks down to form syngas, a combustible gas (Basu, 2010). Syngas is very versatile, as it can be used in boilers, process heaters, turbines, engines, and fuel cells, or distributed in pipelines, and blended with natural gas or other gaseous fuels.

Gasification processes can be designed to handle a wide range of biomass feedstock – from woody residues, to agricultural residues, to dedicated crops – without major changes in the basic process (Aggarwal, 2013). The variable economics of biomass farming, collection, and distribution make the economic viability of the technology particularly site-specific (Rubio-Maya et al., 2011b).

The Fischer–Tropsch Synthesis (FTS) process (Aggarwal, 2013; Basu, 2010) can convert syngas into a wide variety of hydrocarbon products, from gases to waxes, including liquid hydrocarbons of commercial interest such as syndiesel. FTS processes using biomass-derived syngas have received a great deal of interest in recent years as a suitable means of high-quality production fuels (free of sulfur, nitrogen, and aromatics) for different applications, since they are compatible and capable of being blended with conventional fuels, and thus offer the possibility to utilize existing fuel infrastructure (Ilic et al., 2012).

By considering gasification plants and FTS plants as technologies admissible into the OMSES infrastructure, further integration approaches can be considered to reduce the energy supply costs due to the uniqueness of mines' energy demand structure which, as indicated in Chapter 1, intensely depend on diesel fuel. Producing syndiesel onsite is also interesting because it is a form of energy easy to store. In addition, trucks, excavators, shovels, loaders, and some types of static

prime movers can draw from the diesel/syndiesel utility to generate electricity, while other types of prime movers can draw directly from the syngas utility.

The implementation of biomass technologies in OMSES is straightforward when it is assumed that biomass is ready to be used throughout the year without restriction on the hourly flow. Thus, the ESS designer can proceed as with any other energy technology when choosing the set of those technologies present in the conservative superstructure. However, some additional constraints such as biomass seasonal bunkering may apply. Biomass fuels present relatively low energy density (up to, but typically less than, 20 MJ/kg of dry substance (Dahlquist, 2013)), and therefore the storage of large volumes is usually required. For example, a fixed-sized biomass storage tank can be considered, applying the constraint reflecting complete annual consumption:

$$\sum_{ij} \Phi_{BM,ij}^{con} \cdot t_{ij} \leq L_{BM} \quad (4-1)$$

where  $\Phi_{BM,ij}^{con}$  refers to the hourly consumption of biomass, with an annual sum lower than  $L_{BM}$ , which is the size of the storage. Constraints such as this can also be defined for specific time intervals, not necessarily for a complete year.

#### 4.1.2 Wind Power

OMSES' original formulation lies on the identification of typical time series that, when repeated, describe with sufficient accuracy mines' energy demands, as well as other environmental factors (prices of energy resources, ambient temperatures, etc.). For wind power, diurnal cycles can be generally identified, even from a single year of data (Manwell et al., 2009). The use of hourly data from a single year, although apparently limited, can be used to obtain typical wind diurnal patterns suitable for OMSES.

However, there are areas where diurnal cycles are not predominant. Daily based wind cycles are originated by local and global heating and cooling of the atmosphere by the solar irradiation (Manwell et al., 2009), which may not take place in extreme latitudes, where insolation is limited or absent during half of the year.

The limitation of hourly data – typical of meteorological stations whose data are available online from several institutions, such as Environment Canada (2014) – is that it is impossible to quantify important factors such as turbulence intensity (TI) (Hunter et al., 2001), and therefore the resource evaluation may provide optimistic results. In case of hourly data, the power produced by each installed wind turbine can be calculated based on the hourly wind speed. When using optimization tools such as OMSES, typical daily wind profiles may be calculated for each representative month. By having a daily profile that varies hourly, the ESS is better able to account for the hours in which the renewable resource is not available.

The typical wind profiles have to be adjusted not to represent average speeds within the considered interval, but a value that better defines the typical power output of the wind turbines, i.e., the root mean cube speed  $v_{rmc}$  [m/s] (Patel, 2005). Thus, when diurnal cycles can be identified, and a wind speed profile calculated, this should be normalized and multiplied by the corresponding typical  $v_{rmc}$ .

To build those typical profiles, the hourly data for a full year are categorized so that  $v_{rst}$  represented the wind speed at the  $r^{th}$  hour, of the  $s^{th}$  day of the  $t^{th}$  month. The methodology used in this work to calculate the characteristic wind speed each hour of the representative days is described as follows in 7 steps:

1. Collect wind speed data for one year (e.g., (Environment Canada website, 2014)), with a resolution of 1 hour.
2. Calculate the average wind speed  $\bar{v}_{st}$  for each day (Eq. 4-2).
3. Within a day, divide each hourly value by its corresponding daily average wind speed (Eq. 4-3), obtaining  $\hat{v}_{rst}$ .
4. Within month  $t$ , use  $\hat{v}_{rst}$  to calculate an average hourly normalized profile  $\hat{v}_{rt}$  (Eq. 4-4).  
For example, let us assume the third month ( $t=3$ ) consist of two days ( $n_{st} = n_{s3} = 2$ ). If  $\hat{v}_{113}$ , the normalized speed of the first hour ( $r=1$ ) of the first day ( $s=1$ ), is 0.5, and for the first hour of the second day  $\hat{v}_{123}$  is 0.7, then the resulting first hour normalized speed for this month is, therefore,  $\hat{v}_{rt} = \hat{v}_{13} = \frac{0.5+0.7}{n_{s3}} = \frac{0.5+0.7}{2} = 0.6$ .
5. Once the profile is calculated for each typical day (for each month), the hourly values are divided by the total sum. The sum of the components is therefore 1..
6. Multiply the resulting 24 hour normalized profiles of each month by the *rmc* monthly wind speed (Patel, 2005).
7. Using the resulting *rmc* profiles (step 5) and given a wind turbine curve, calculate the power output per wind turbine.

$$\bar{v}_{st} = \frac{1}{n_r} \sum_{r=1}^{n_r} v_{rst} \quad (4-2)$$

$$\hat{v}_{rst} = \frac{v_{rst}}{\bar{v}_{st}} \quad (4-3)$$

$$\hat{v}_{rt} = \frac{1}{n_{st}} \sum_{s=1}^{n_{st}} \hat{v}_{rst} \quad (4-4)$$

The methodology to calculate typical wind profiles for each month assumes that wind varies based on cyclic atmospheric behavior. Thus, as an interval of 24 hours must be selected, it may start with the first minute of the local standard time, solar time, or any other 24 hour cycle that

correlates with the atmospheric variations that cause air flows. Here, the local standard time was selected.

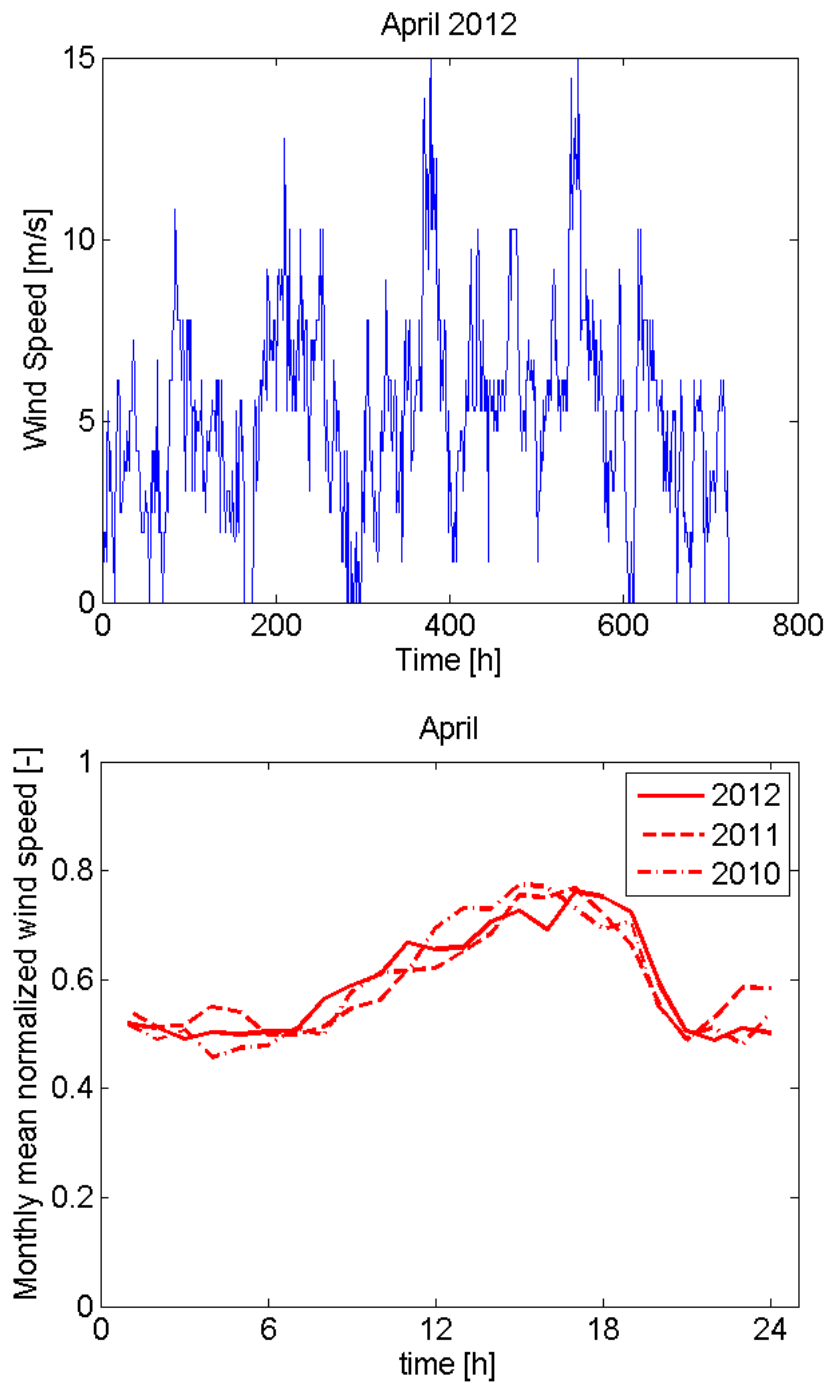


Figure 4-1 Example of wind speed characterization for Sudbury Airport; data for April 2012 (top) and diurnal cycle for several years (bottom)

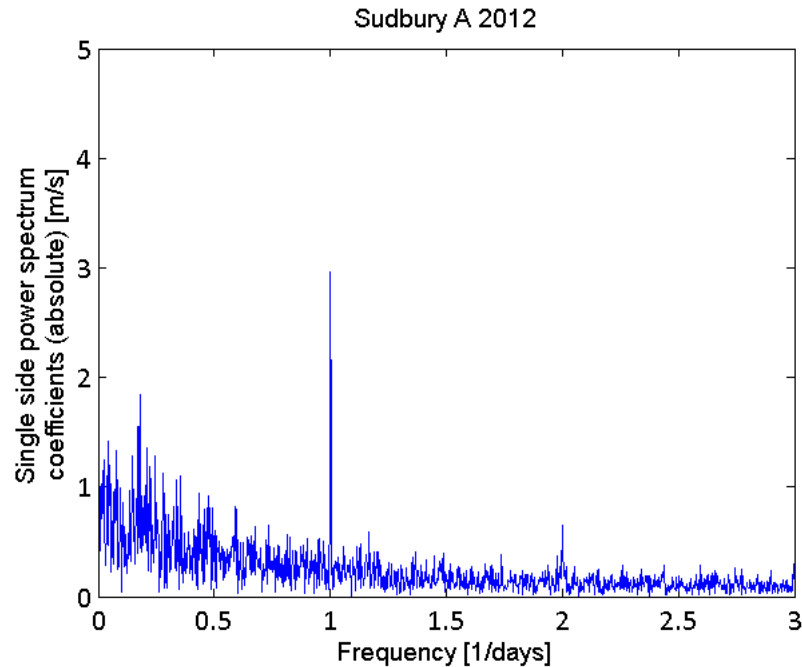


Figure 4-2 Wind speed spectrum for Sudbury Airport (2012)

Figure 4-1 shows the wind speed in April of 2012 and the diurnal cycle (step 4) for several years at Sudbury’s Airport (Ontario, CA) (Environment Canada, 2014). The diurnal cycle shows consistency between years for this particular month.

Matlab® Fast Fourier Transform function was used to calculate the single power spectrum of the wind speed of a complete year (2012), showing in Figure 4-2 that a consistent diurnal wind cycle exists (spectrum spike at the frequency  $1 \text{ day}^{-1}$ ) (Langreder and Bade, 2012), and a possible lunar effect may also take place (spectrum spike at the frequency  $2 \text{ day}^{-1}$ ). Figure 4-3 exemplifies another case of diurnal cycle (using spectral analysis) in a different site, Pickle Lake weather station, (Environment Canada, 2014).

As anticipated, not all sites present daily cycles, at least not throughout all seasons. Figure 4-4 shows the spectrum for a different location, Inner Whaleback (IWB) weather station (Latitude

61.92°N, Longitude 113.73°W). The absence of diurnal cycle is evident, potentially being substituted in some months (e.g., January) by other atmosphere-related effects (Figure 4-5).

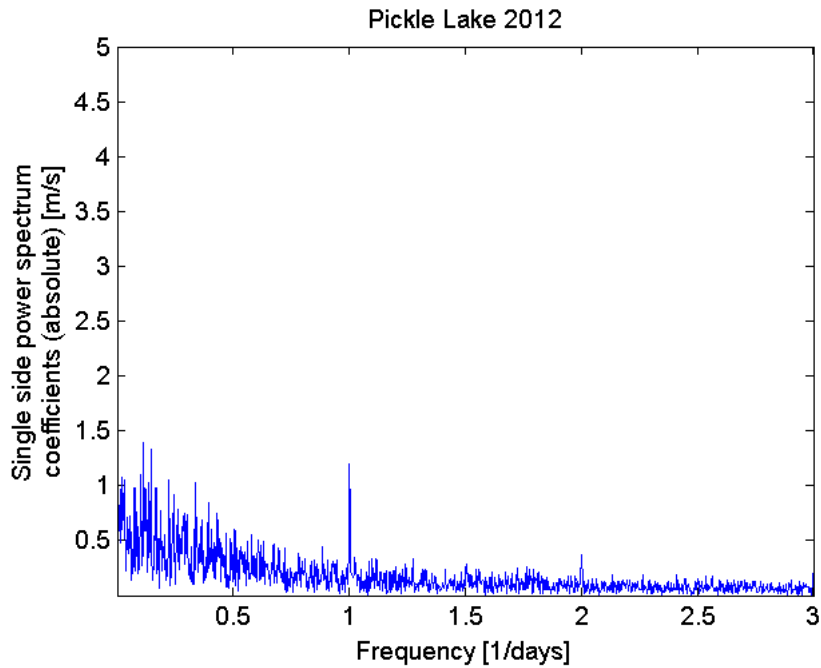


Figure 4-3 Wind speed spectrum for Pickle Lake weather station (2012)

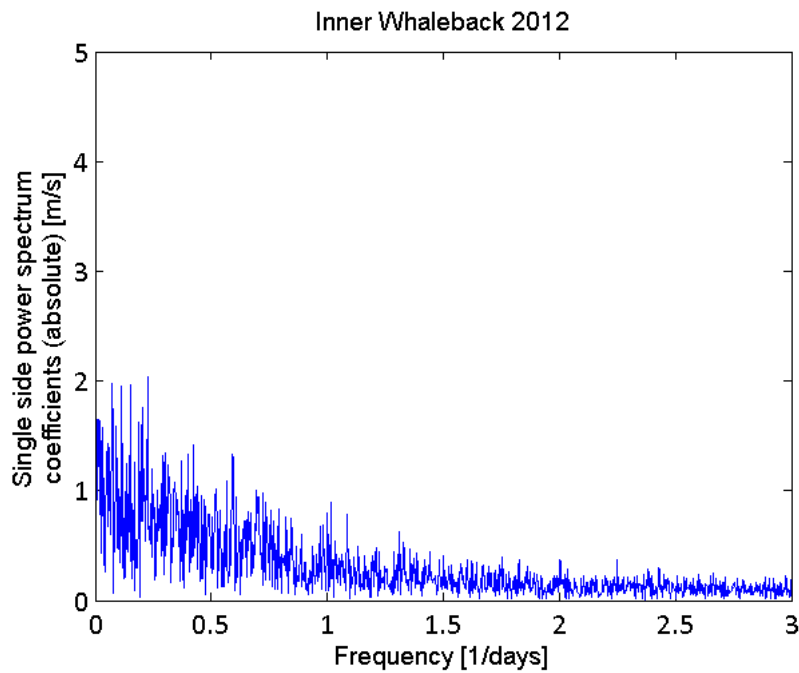


Figure 4-4 Wind speed spectrum for Inner Whaleback weather station (2012)

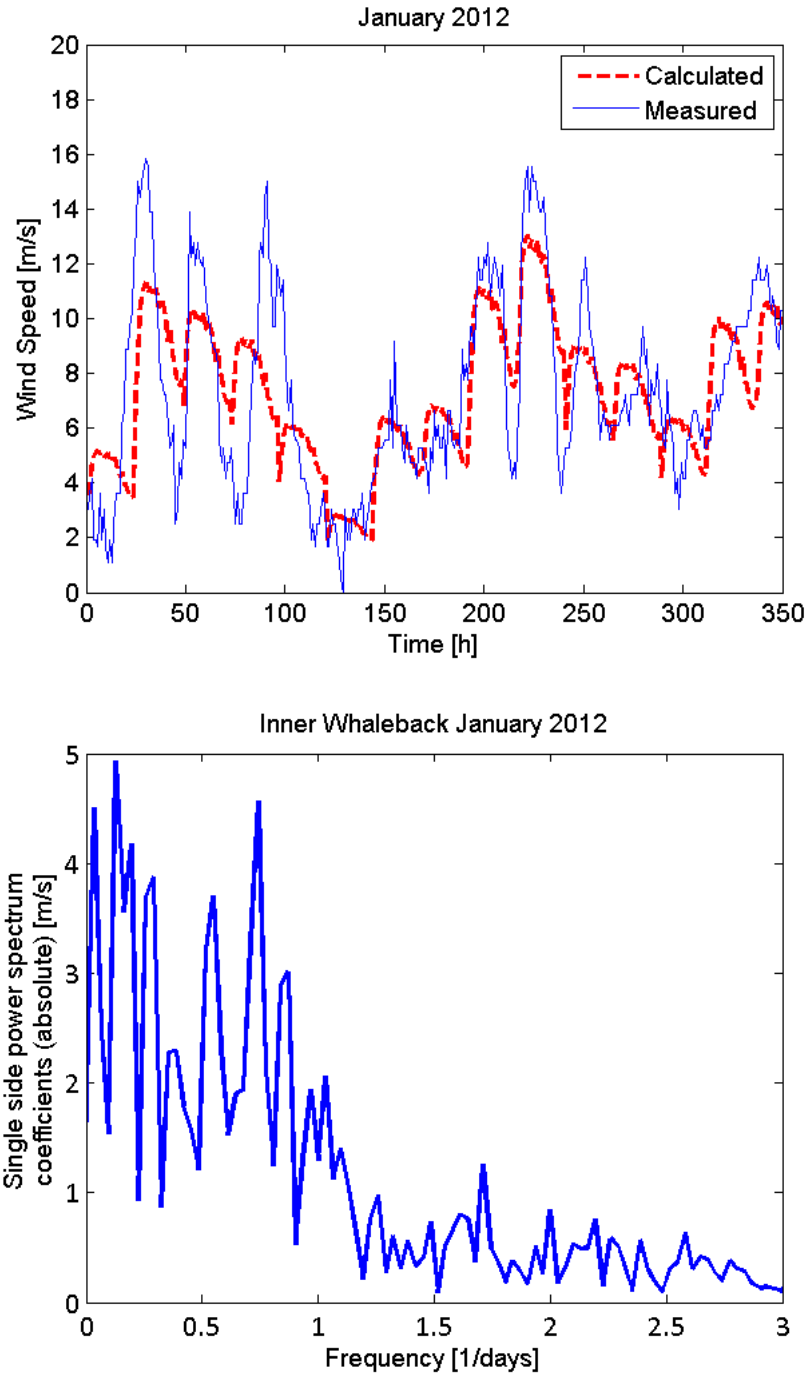


Figure 4-5 January wind speed and corresponding monthly spectrum (2012)

Figure 4-5 shows the wind speed at IWB for January 2012 (Environment Canada, 2014). The corresponding spectrum (bottom) indicates the possible existence of a super diurnal cycle (frequency lower than 24 hours), which can be appreciated the first days of the month

represented, where the calculated diurnal profile is also plotted (top, dashed line) calculated in this case by multiplying the normalized profile by the average wind speed of the day.

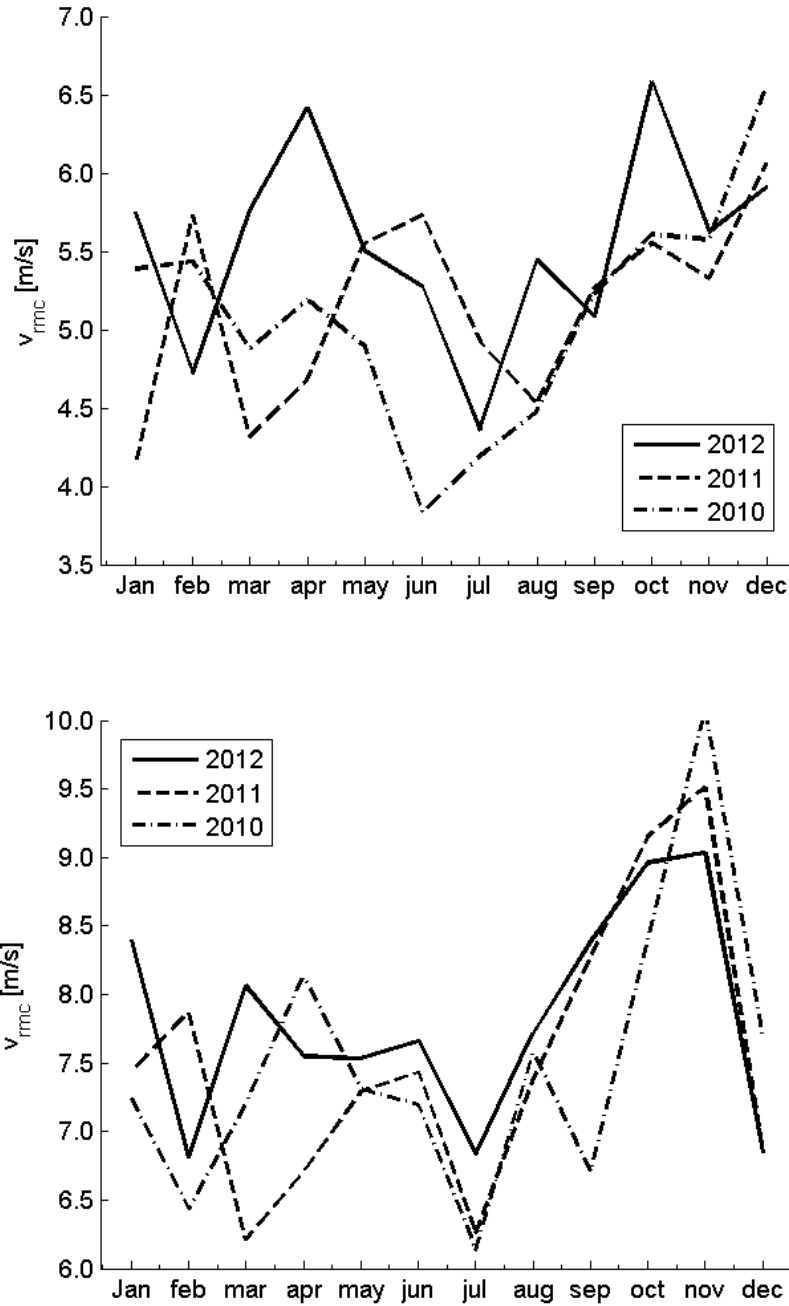


Figure 4-6 Monthly root mean cube wind speed for several years at Sudbury Airport (top) and Inner Whaleback (bottom)

Despite the absence of diurnal cycles, sites generally present seasonal patterns that can be estimated with up to 90% confidence with one year worth of data (Manwell et al., 2009). Figure

4-6 illustrates three years of data for the previously referred sites. It is worth mentioning that the site without a clear diurnal pattern (IWB) presents higher consistency among the years studied.

In the context of OMSES, low and medium wind penetration systems (defined here when the instantaneous power output for wind meets less than 50% of the base load electrical demand of the site) can be optimized when diurnal wind profiles are available or can be calculated. However, the designer may have to impose constraints that ensure that the optimal solution always has enough backup power capacity to meet the electrical demands in case of null (0 MW) wind power output. This is particularly important in case of stand-alone power systems, for the use of typical wind profiles may introduce the false information that wind is always blowing (Figure 4-2). For higher penetration of wind power, further precautions when modeling and optimizing the system must be taken to constantly maintain the nominal voltage and frequency values of the grid, as well as when including short or long term energy storage systems (Chapter 12).

In cases where diurnal wind patterns can't be found because of the lack of locally monitored wind speed, synthetic sinusoidal profiles can be designed to represent the potential yield of the resource and the time dependency. The wind profiles used to obtain the energy produced by the wind turbines can be calculated according to the proposed approach (Figure 4-7, wind profile 1), or by making use of sinusoidal profiles (Figure 4-7, curves Wind profile 2 and Wind profile 3). The profiles must be adjusted so that, when multiplied by the monthly *rmc* speeds, the energy obtained in the three cases is equal. The process of averaging hourly data to obtain the hourly profiles for each month yields fairly constant curves, where a daily cyclical variation can be observed. Sinusoidal profiles can be adjusted to better reproduce interday typical variations that result in more reliable results when designing the system, especially regarding spinning reserve

requirements and energy storage (Section 4.5). The use and effectiveness of these will be analyzed in Chapter 12.

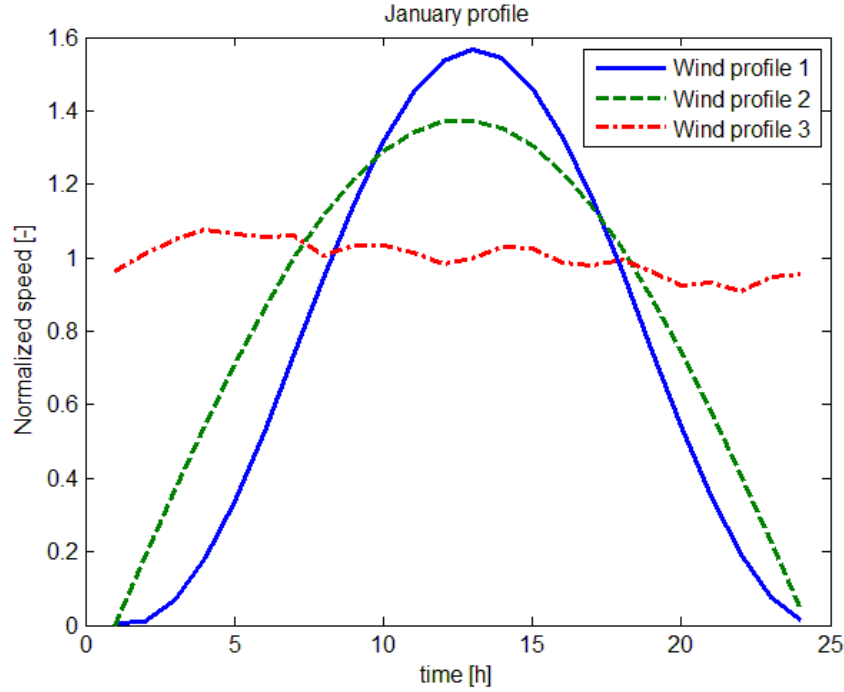


Figure 4-7 Examples of different wind profiles for a typical day

To integrate a source of electricity production with uncertain variability and intermittency into the OMSES formulation, two methods can be followed. Firstly, considering wind energy as an intermittent resource would entail the definition of a new utility (i.e., wind power) and introducing an appropriate conversion technology (i.e., wind turbine) to convert it to electricity. Second, a less invasive alternative is to consider an additional source of electric power,  $\Phi_{uij}^{RE}$ , in the energy balance (Eq. 4-5), which is constrained by the availability of wind power due to hourly wind speed fluctuations (Eq. 4-6). With the latter approach, and considering the utility balance for electricity ( $u=EE$ ), the energy balance equation is expressed as follows:

$$\Phi_{uij}^{pro} + \Phi_{uij}^{pur} - \Phi_{uij}^{con} - \Phi_{uij}^{sel} - \Phi_{uij}^{was} - \Phi_{uij}^{dem} + \Phi_{uij}^{RE} = 0 \quad (4-5)$$

$$\Phi_{uij}^{RE} \leq \mu_{WT} \cdot P_{WT,ij}(v_{ij}) \cdot (1 - l_{dist}) \quad (4-6)$$

Equation 4-6 includes the decision variable for the number of units of a given turbine model installed,  $\mu_{WT}$ , the available energy at any given time by such turbine as a function of the wind speed,  $P_{WT,ij}(v_{ij})$ , the actual energy produced by the wind farm,  $\Phi_{uij}^{RE}$ , and the losses produced by the auxiliary equipment associated with the wind farm, including the distribution losses ( $l_{dist}$ ). The inequality expresses the possibility, otherwise constrained using an ‘=’ sign, of curtailing the output of wind power production.

The extra source of electricity  $\Phi_{uij}^{RE}$  does not entail an hourly O&M cost in the same way as for actual *technologies* (Equation 3-7, Chapter 3). Alternatively, the costs associated with the maintenance and operation of the wind farm are here included in the investment cost. The maintenance is added as a percentage of the investment, which OMSES then annuitizes, for it is here assumed that the annual hours of operation of the hypothetical wind farm are known at the time of the investment decision.

## 4.2 Spinning Reserve

When balancing energy supply and demand, special attention must be paid to the variability of renewable energy output, as well as the continuous changes to some systems’ loads. Standalone power systems with high RE penetration are good examples of challenging management exercises. In this section, the emphasis is put on solving the issues with energy systems that include wind turbines. The problem is that sudden wind speed drops can affect the quality of the power while backup technology switches on, and measures are required to deal with this.

The spinning reserve is considered a power management tool to deal with drops in renewable power generation or sudden changes in load. Mines' electrical loads are generally free from large-scale uncertain variability, but large loads are switched on and off on a regular basis. There are two ways in which the reserve is achieved, even in the absence of renewable energy sources and in the presence of high load variability and uncertainty: synchronized generators (on 'stand-by' mode) and electricity storage systems.

The drop in power generation from the wind turbine depends on the turbulence intensity ( $TI$ ).  $TI$  is a function of the mean wind speed ( $v$ ) in a given interval and its standard deviation in said interval ( $\sigma$ ), i.e.,  $TI = \sigma/v$ . The characterization of  $TI$  requires a wind speed measurement resolution of at least minutes, preferably seconds, since  $v$  is calculated as the 10 minute speed average, and  $\sigma$  its characteristic deviation. Given particular values for  $TI$ , the spinning reserve that compensates for almost any power reduction from the wind farm can be determined, assuming that the drop in wind speed expected is some function of  $\sigma$ . Throughout this work,  $TI = 0.2$  is used with a conservative wind drop of  $2\sigma$ . These are conservative parameters defining  $TI$ , which lies between 0.05 and 0.40, but usually remains low (0.10) for wind speeds above 5 m/s (Langreder and Bade, 2012).

Knowing the lowest value of the expected wind provides the value of the maximum expected power drop, which must be countered by a combination of: 1) the remaining capacity of the active generators; 2) the available electric energy stored and its discharge power; and 3) the generators in spinning reserve (synchronized with the micro-grid). System loads that can be deferred or curtailed can also be considered as a mechanism to compensate for RE output drops. This option, when possible, is more economic than 2) and 3), but involves a management effort that requires specific analysis.

Equations 4-7 through 4-11 impose the constraints necessary to update the existing model in order to include the spinning reserve.

$$c_{e,ij}^{sr} = p_{DI} \cdot f_{idle} \cdot \mu_{PM,ij}^{sr} \cdot P_{nom,PM} / \eta_{PM} \quad (4-7)$$

$$\Phi_{PM,ij}^{pro} \leq \mu_{PM,ij}^{op} \cdot P_{nom,PM} \quad (4-8)$$

$$\Phi_{PM,ij}^{pro} \geq (\mu_{PM,ij}^{op} - 1) \cdot P_{nom,PM} \quad (4-9)$$

$$(\mu_{PM,ij}^{sr} + \mu_{PM,ij}^{op}) \cdot P_{nom,PM} - \Phi_{PM,ij}^{pro} + \Psi_{EE,ij}^{sto} \geq \mu_{WT,ij}^{op} \cdot (\Phi_{WT,ij}^{pro}|_{high} - \Phi_{WT,ij}^{pro}|_{low}) \quad (4-10)$$

$$\mu_{PM,ij}^{sr} + \mu_{PM,ij}^{op} \leq \mu_{PM} \quad (4-11)$$

The number of engines synchronized at every interval is  $\mu_{PM,ij}^{sr}$ , while the number of generators supplying power is  $\mu_{PM,ij}^{op}$ . The consumption of the generators idling can be calculated by means of the factor  $f_{idle}$  (dimensionless) and the thermal efficiency,  $\eta_{PM}$  (dimensionless). The cost incurred by the spinning reserve is calculated using Equation 4-7. Equations 4-8 and 4-9 are needed to constrain the output of the operating prime movers (actually producing electricity), while Equation 4-10 imposes the total spinning reserve as a function of the maximum wind variability,  $\Phi_{WT,ij}^{pro}|_{high} - \Phi_{WT,ij}^{pro}|_{low}$ , the stored electricity in any interval  $ij$ ,  $\Psi_{EE,ij}^{sto}$ , and the remaining capacity of the prime movers producing (energy storage and its formulation in OMSES is later discussed in Section 4.5). The active generators and those in spinning reserve cannot be more in number than the units installed (Equation 4-11). High ( $\Phi_{WT,ij}^{pro}|_{high}$ ) and low ( $\Phi_{WT,ij}^{pro}|_{low}$ ) wind power output are calculated using  $+2\sigma$  increase and  $-2\sigma$  decrease from the actual wind speed at each time interval.

The formulation just presented regarding spinning reserve and wind power is used in a case study developed in Chapter 9.

### 4.3 Power to Gas Technologies

Power to Gas (P2G) technologies can be included in the OMSES framework through the introduction of two new technologies and associated processes:

- 1) The electrolysis of water to produce diatomic hydrogen (gas) from water molecules;
- 2) A methanation process by which, when adding carbon dioxide ( $\text{CO}_2$ ), the available hydrogen will react to yield methane ( $\text{CH}_4$ ) in the so called Sabatier Process (Stern, 2009).

Conversion efficiencies depend on several parameters, such as pressure of the products of the reaction, source of  $\text{CO}_2$  and source of electrical power (Stern, 2009). In general, the water electrolysis process can be carried out by electrolyzers which, having as inputs water and electricity, produce a stream of low to high pressure hydrogen gas. Electrolyzer efficiencies can be as high as 80% (LHV) (Stern, 2009; Zakeri and Syri, 2015), defined as hydrogen energy divided by the electrical energy consumed. The net efficiency, as well as the costs, depends on the technology: solid oxide, alkaline or polymer electrolyte membrane (PEM). For example, 1,820 CAD/kW (1,400 US\$/kW from the source, considering an exchange rate of 1.3 CAD/US\$) can be assumed for alkaline, and 767 CAD/kW (590 US\$/kW) (projected for 2020) for solid oxide electrolyzers (Zakeri and Syri, 2015).

Power to methane assumes further conversion of  $\text{H}_2$  to methane ( $\text{CH}_4$ ) through methanation (Figure 4-8). The chemical reactions that take place (water-gas shift and methanation) constitute

the basis of different processes, such as coal and biomass gasification, that allow the methanation of CO<sub>2</sub> and CO, obtaining CH<sub>4</sub>, in the presence of H<sub>2</sub> or any syngas stream (Sterner, 2009).

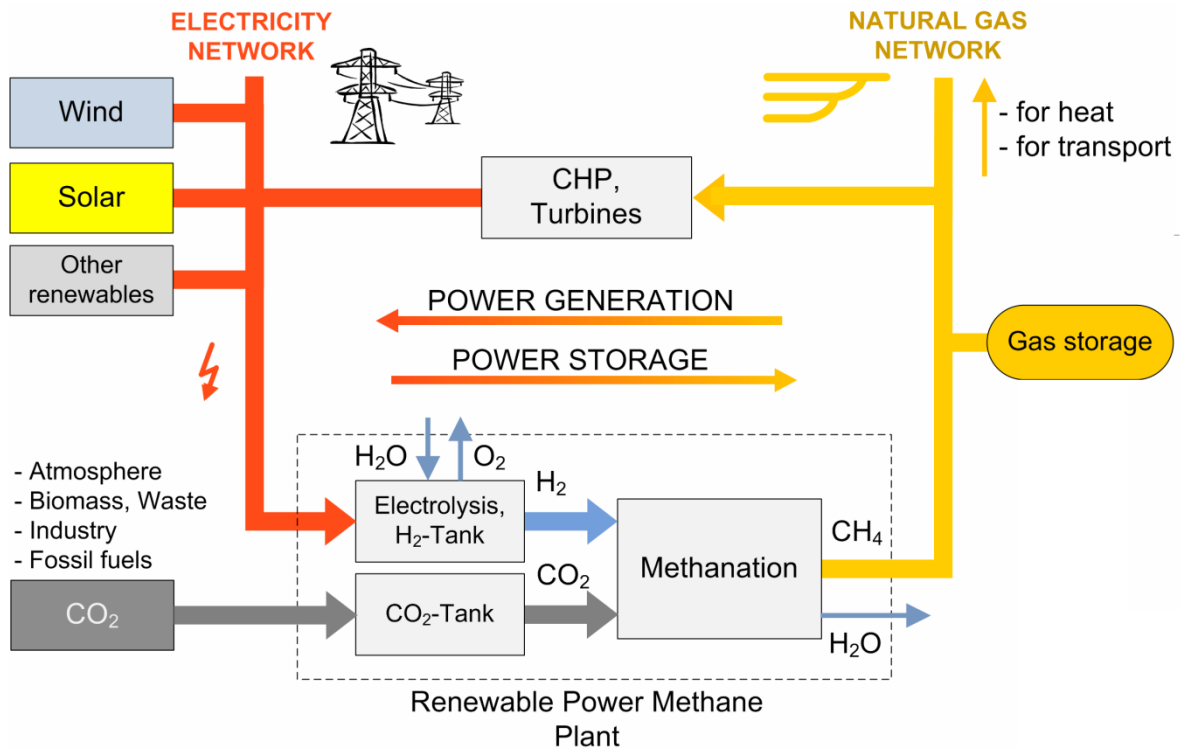


Figure 4-8 Power to gas concept illustrated by a power to methane plant including diverse CO<sub>2</sub> sources (Sterner, 2009)

Methanation's usefulness lies in the potential to produce synthetic natural gas from more abundant (non-renewable) fossil fuels such as coal (Meyer et al., 1982), as well as from (renewable) biomass. When used in combination with water electrolysis, synthetic methane production has a conversion round-trip efficiency in the range of 33-40% (electricity-to-electricity), increasing the costs of electrolysis by another 1,300 CAD/ kW<sub>e</sub> (1000\$/kW<sub>e</sub>) (Zakeri and Syri, 2015), though this last figure depends on the source of CO<sub>2</sub> (Sterner, 2009). Fixed operation and maintenance costs for hydrogen-based technologies, including storage, can be as high as 11.4 CAD/MWh (8 €/MWh from source, considering an exchange rate of 0.7 CAD/€ as

of September 2016) (Stern, 2009) for renewable power methane (RPM), and averaging 5 CAD/MWh (3 to 4 €/MWh) for hydrogen-based storage and conversion through fuel cell or gas turbine when considering 8760 hours of operation per year (Zakeri and Syri, 2015).

In addition to electric power, other inputs such as water, carbon dioxide, or biomass residues, are needed to practically obtain synthetic fuels. These material flows can be introduced as additional utilities without loss of generality. Furthermore, the use of some sources of power may provide solutions with lower efficiencies or higher emissions (Stern, 2009), but remain important where synthetic fuel production is a must. Thus, these concepts have been recently developed as a solution to store and disperse variable renewable energy sources, such as wind and solar power (Stern, 2009; Henning and Palzer, 2014). Power to gas technologies are frequently only cost-effective if the investment cost burden is spread throughout an assumed long life of the ESS (Palzer and Henning, 2014b; Palzer and Henning, 2014a). In general, mines do not have a production life longer than 10-20 years, which may act against their adoption.

The conversion technologies regarding P2G can be treated in the same fashion described in the basic formulation of OMSES (Chapter 3).

#### **4.4 Material Flow Utilities**

There are several processes in mines where material is transported and stored in reservoirs: water in dams, rock in piles, even gold ingots on shelves. Due to the changing marginal cost of the different types of energy - both outside and within the system - the transportation or processing of the material flows can be more economic during certain time intervals. This arises from the interaction among energy and material flows: the power consumed by pumps to drain water, by the hoist in lifting rock, or by the mills and electrochemical plants in processing the different

streams. In mines, buffer system stores exist that can be economically deployed, in addition to serving in case of equipment down-time, so that the whole mine does not stop production.

Different material flows can be included in the superstructure without losing generality as an energy system. They have a meaning for the model in the sense that the energy required for the material handling and storage is significant and can be optimized. By way of example, this section addresses the use of water as a material flow that can be stored and whose handling facility, the dewatering system, can be managed in an optimal manner. Ventilation air, although it cannot be stored, plays an important role in underground mines' ESS, as will be discussed later in this chapter.

Balance equations for material flows are implemented following Equations 3-9 to 3-18. Material flows will affect the units in which the coefficients in  $K_{uv}$  are expressed. When material flows are present the units of each coefficient are “mass/volume/energy of utility produced (consumed) per mass/volume/energy of main utility produced”. Material flows not necessarily have mass units such as kg or tonnes, but can also be expressed volumetric units, such as cubic meters ( $m^3$ ) or litres, transported (e.g., hauled, displaced) during the considered time interval  $t_{ij}$ .

#### **4.4.1 Dewatering**

The dewatering system's function is to collect and remove water from the mine, in order to maintain a safe operating environment. The water collected comes from several sources, among which the most important are meteorological precipitation, ground water seepage, and service water used for drilling, dust control, washing and even pipeline leaks (de la Vergne, 2003). The term inflow will be used here to refer to them.

The nature of the inflows can result in daily and even seasonally varying flow profiles. Service water for production processes can be estimated by knowing how much water each productive task requires and, together with the expected seepage, the pumping operation may be scheduled.

Dewatering facilities include different elements such as pipes, valves, pumps, water reservoirs, and sumps, among others. The system is designed to meet specified performance requirements, mainly expressed in terms of water flowrate and head. Due to the particular characteristics of the fluid pumped, water containing solid particles and dissolved chemical substances, as well as the uncertainty in inflows and permitted times of operation, the design and operation of a mine dewatering system can quickly become complex.

Underground mines, up to thousands of meters deep, collect the water in sumps from where it is pumped up to the surface or to an intermediate sump level, where another pumping plant is located. These plants consist of one or more pumps, normally connected in parallel, and include the necessary valves, by-passes, and filters to permit proper setup, operation, and maintenance. Due to the solid content of the pumped water, it is necessary to provide proper settling and decantation capacity.

Dewatering in the context of OMSES can be treated as a material flow utility that interacts with energy flow by means of pumps. The formulation to describe water balances in reservoirs is given in Section 4.5. Economical parameters include the cost of building an underground dam (expressed in economic units per unit of volumetric storage capacity), the investment in pumps, and the cost of running them.

It is assumed that each dam or water reservoir receives a constant inflow over a given interval  $t_{ij}$ . The inflow can be approximated by considering a water flow term dependent on production

(drilling, washing, etc.) and a term dependent on infiltration from lakes, aquifers, rain, and snow, among others. The former may have a daily pattern; the latter could be relatively constant throughout the day representative of each month, but with seasonal variations from month to month (or from representative day to representative day).

Although critical to the production process, the dewatering system is not completely constrained to the pace of other mining processes. This is in contrast to, for example, hoisting services and ventilation of underground mines, or rock loading and hauling in open pit mines. In other words, there exists some flexibility to decide when and how to operate the dewatering system, but nevertheless it must be operated within its own design limits, e.g., water reservoir dimensions cannot be overtopped and pumping flow rates and head available must be respected. This flexibility makes it possible to use water management in order to run the pumps when it is more convenient in the economic sense, which involves the use of concepts such as Demand Side Management.

#### **4.4.2 Demand Management via Material Storage**

Demand side management (DSM) strategies are those operational actions on the load of the mine, for certain processes that can be rescheduled in time to take advantage of, for example, lower prices of energy during certain time intervals. DSM can also be used to reduce the peak load of an ESS when importing energy from the grid, for this can originate certain charges, often proportional to the peak load. More information on the different supply and demand side management strategies, recognized in general as load management, can be found in Abaravičius and Pyrko (2006).

Details about the use of demand-side management to reduce energy costs associated to the dewatering system are presented in Chapter 8. Optimal design and control strategies are discussed, among which centralized and decentralized options are included. Advantages of considering mass storage in ESS include the lower cost of storage and the management strategy of operating the material system when energy is available at a lower cost.

In Section 4.5, the equations that describe the storage management of the different utilities are presented. Without loss of generality, the same equations can be applied to material and energy utilities. In fact, there is some similarity with mass and volumetric storage used in the field of ESS, for example, as a means to defer energy use in desalination plants (Rubio-Maya et al., 2011b; Kyriakarakos et al., 2011).

#### **4.4.3 Ventilation**

This section deals with underground mine ventilation. Fresh air is required underground to ensure adequate air quality in the working areas for health and safety reasons. Air is circulated to dilute toxic gases and dust generated due to mining activities, including blasting and rock handling.

Due to its overwhelming impact on the energy consumption of some underground mines, ventilation can be introduced to the OMSES superstructure as a utility for the air flow, in these volumetric units, and considering fans as power-consuming, ventilation air-producing technology. Fans consume most of the power (electricity), which is one of the most expensive energy forms. A ventilation system may have installed up to 10 MW of ventilation power (de Souza, 2015). Furthermore, the air pushed or pulled into the mine by the surface fans may

require thermal treatment, either heating or cooling, which adds energy and cost to the auxiliary process of the mine's ventilation.

Cooling is often required locally underground. The objective is normally to offset local heat flows, such as mobile equipment waste heat, source rock heat flow, as well as heat from the broken rock after a blast, to maintain a comfortable working environment. Ventilation air conditioning can offset part of the thermal loads underground, but some constraints exist on how much the air can be 'treated'. This is illustrated in winter (in Canada for instance), when some mines heat the air up to a temperature setpoint, while deep underground areas still require cooling. The setpoint temperature may be determined by constraints related to icing, comfort, machine tolerances, etc., at the fresh air mine inlet and below. A lower temperature setpoint would save cooling requirements underground, but may violate some of the constraints mentioned on surface. An example of temperature setpoint can be found in several case studies in Chapters 9, 10, and 11.

Temperatures underground can reach up to 40°C (Tonnoo and Allen, 2008); once surpassed, working is challenging and, under some regulations, forbidden (regulations may also impose working rest regimes for workers as a function of the workplace temperature and humidity (MHSA website, 2015)). The range of temperatures under which cooling is required may, through conventional air conditioning systems, release as by-product a medium grade heat (60 – 90°C) that can be used for bulk air heating elsewhere. On the surface, the heat released by combustion engines through their cooling systems (water/refrigerant and lubricating oil) as well as heat flow in exhausts is of sufficient quality to heat the air up to the typical fresh air conditions in underground mines. The low temperature demand brings the opportunity to use waste heat as well as heat regeneration from, for example, ventilation exhaust from the mine.

## **4.5 Energy Storage Technologies**

Energy storage is not only useful when a variable such as renewable energy is introduced in an energy system. Regarding electricity, it is also important to improve grid stability and quality, as well as regulate voltage and frequency when sudden load changes cannot be accommodated rapidly by electric generators. It also improves the overall efficiency of cogeneration plants with non simultaneous demands for heat and power, and purchasing and storing energy when prices are lower reduces the energy bill. In the context of DER, energy storage can play an important role, although the high cost of these technologies may act as a disincentive to its implementation. Furthermore, its implementation and use (i.e., charging and discharging) can compete with renewable energy in certain circumstances (Stadler et al., 2008). However, it is widely recognized that energy storage is the appropriate complement to variable, uncertainty related renewable energy, and where energy collected can be stored for later use if it is not needed at the time of its production. There is more than one type of energy storage technology, although it is not the aim of this study to address or determine which is the best for a mine energy system; this could be decided through OMSES when given as technological options.

### **4.5.1 Storage Balance across Typical Days for a Month**

The general expressions that describe how energy is stored are presented in this section. The temporal scale used is based in the concept of typical days divided in equal intervals of one hour. For a system in which energy demands and energy price environment do not vary significantly throughout the year from one day to the next, this approach (typical or characteristic days) yields reasonable results when designing energy supply systems with energy storage. The problem becomes more complex if renewable energy sources are included, such as wind or solar, for the assumption of ‘typical days’ cannot generally be assumed.

The approach taken involves the addition of state variables ( $\Psi_{uij}$ ) necessary to define the state of charge of the storage technologies at every time step (Table 4-1).

**Table 4-1 State decision variables for energy storage**

Variable	Units	Description	Set	Type
$\Psi_{uij}$	MWh	Stored utility level	$U, T$	Real
$\Psi_{u,max/min}$	MWh	Storage capacity limits	$U$	Real

The annuitized fixed cost when energy storage technologies are considered is restated as follows:

$$C_{fix} = k_{rf} \cdot (1 + k_{ic}) \cdot [ \sum_v \mu_v \cdot C_{inv,v} + \sum_u C_{inf,u} + \sum_u C_{sto,u} ] \quad (4-12)$$

where  $C_{sto,u}$  is the cost of installing storage for the utility  $u$ . The capital cost of installing storage may be expressed as:

$$C_{sto,u} = c_{sto,u} \cdot \Psi_{u,max} \quad (4-13)$$

where  $\Psi_{u,max}$  is the size of the utility store (rated storage capacity here expressed in MWh because hourly intervals are always considered), which is determined by the optimization procedure, and  $c_{sto,u}$  is the specific cost in currency per unit of storable energy (e.g., CAD/MWh).

With storage involved (Figure 4-9), decisions made in any specific interval ( $i,j$ ) affect subsequent intervals. OMSES' energy balance is updated as indicated in (Eq. 4-14). The flow regarding storage,  $\Phi_{uij}^{sto}$ , is considered a negative value when energy is being stored, and positive if the energy is extracted from the storage system.

$$\Phi_{uij}^{pro} + \Phi_{uij}^{pur} - \Phi_{uij}^{con} - \Phi_{uij}^{sel} - \Phi_{uij}^{was} - \Phi_{uij}^{dem} + \Phi_{uij}^{sto} = 0 \quad (4-14)$$

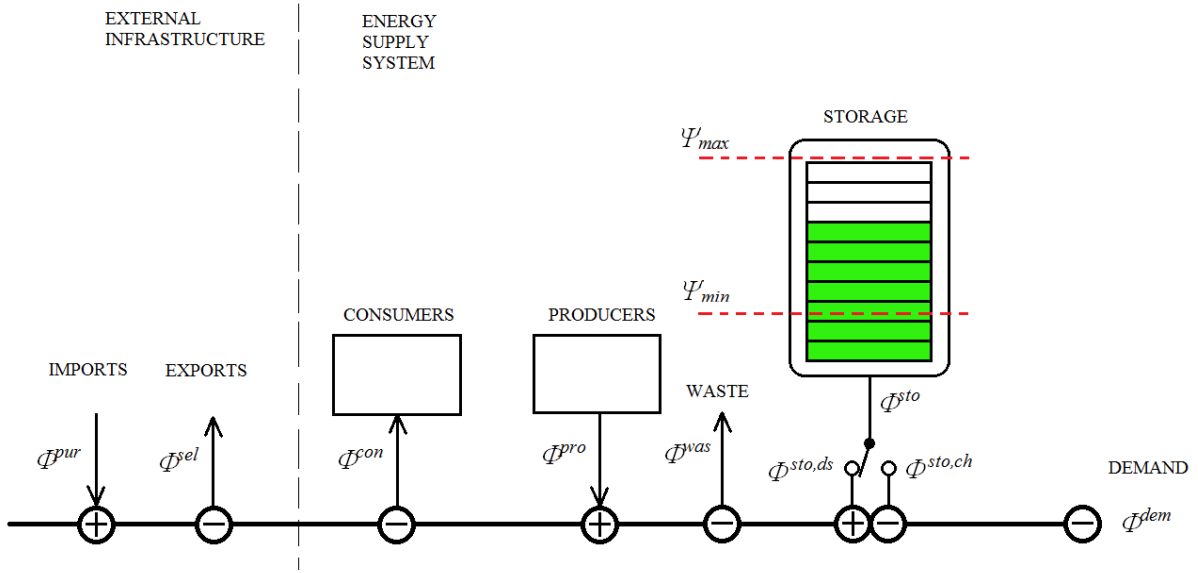


Figure 4-9 Storage scheme implemented in the optimization module

Energy storage parameters are described as follows, where the superscripts *ch* and *ds* refer to charge and discharge:

$$\Phi_{uij}^{sto} = \Phi_{uij}^{sto,ch} - \Phi_{uij}^{sto,ds} \quad (4-15)$$

$$\Phi_{uij}^{sto} \leq \delta_{uij}^{sto} \cdot HS_u \quad (4-16)$$

$$\Phi_{uij}^{sto} \leq -(1 - \delta_{uij}^{sto}) \cdot HS_u \quad (4-17)$$

$$\Phi_{uij}^{sto,ch} \leq \Phi_{u,max}^{sto,ch} \quad (4-18)$$

$$\Phi_{uij}^{sto,ds} \leq \Phi_{u,max}^{sto,ds} \quad (4-19)$$

Equation 4-15 is introduced in order to avoid non-linearity; discharge and charge flow directions have different efficiencies, which require the definition of two different variables for charge and discharge flows. The values of these variables cannot be simultaneously higher than 0 and, therefore, Eq. 4-16 and 4-17 are introduced.  $\delta_{uij}^{sto}$  is a binary variable indicating the direction of the flow (charge 1, discharge 0) and  $HS_u$  is an integer, one order of magnitude higher than  $\Phi_{uij}^{sto}$ .

$HS_u$  is introduced to avoid the nonlinearity if we were to use a single decision variable. Maximum discharge and charge flow constraints are expressed in Eq. 4-18 and 4-19.  $\Phi_{u,max}^{sto,ch}$  is the maximum charge rate (i.e., energy charged within the balance interval) that can be transferred to the store in one time interval.  $\Phi_{u,max}^{sto,ch}$  may be set, defining it as a fraction of the storage capacity ( $\Psi_{u,max}$ ). The same applies to  $\Phi_{u,max}^{sto,ds}$  for the maximum discharge rate (i.e., energy discharged within the balance interval).

Energy conservation in the storage system imposes relationships (energy balances) between the states of energy stores in consecutive time intervals (Eq. 4-20). This includes a constraint that couples the last hour of each day, the 24<sup>th</sup>, with the first hour of the following day, effectively imposing a daily cycle when the utility demands in a given month are stationary. Where abbreviated representations of annual operational performance are adopted within implementation of the formulation (for example, when the system performance is evaluated using twelve 24-hour days, where each of these days is taken to be representative of every day in the corresponding month), the application of Eq. 4-20 may lead to a small discrepancy in the formulation across months (representative days), having a different impact on the results depending on the problem evaluated that has to be analyzed. There is no constraint on the state of charge (or discharge) of any store, other than that their states should respect their maximum and minimum storage capacities (Eq. 4-21), and so the optimization formulation will only approximate the optimum charge and discharge paths for the stores.

$$\Psi_{uij} = \eta_{decay,u} \cdot \Psi_{ui,j-1} - \frac{\Phi_{uij}^{sto,ds}}{\eta_{ds,u}} + \Phi_{uij}^{sto,ch} \cdot \eta_{ch,u} \quad (4-20)$$

$$\Psi_{u,min} \leq \Psi_{uij} \leq \Psi_{u,max} \quad (4-21)$$

$\Psi_{uij}$  represents the energy state of the storage system, for the utility  $u$  in the time interval  $i,j$ ,  $\eta_{decay,u}$  is included to represent the energy losses non-related to the charge and discharge processes,  $\eta_{ds,u}$  is the discharging efficiency (portion of energy output from storage that is usefully discharged), and  $\eta_{ch,u}$  is the charging efficiency (portion of energy input to storage that is usefully charged). Maximum storable energy ( $\Psi_{u,max}$ ) is limited by the storage capacity (e.g., MWh), while the minimum ( $\Psi_{u,min}$ ) is usually a fraction (e.g., 40% in a lead-acid electric battery) of the rated capacity of  $\Psi_{u,max}$ . These limits are applied for every interval (Eq. 4-21).

#### 4.5.2 Seasonal Storage for OMSES' Basic Formulation

When seasonal energy storage is to be considered, a different approach has to be taken, for the division in typical days cannot directly apply to, for example, inter-month or inter-season mass balance.

In order to deal with the problem of lack of continuity in the energy balance (i.e., from one month to the next) for energy storage subsystems, two solutions are proposed for OMSES. The first solution is intended for inter-month energy storage balance. A set of equations is established in order to deal with inter-month energy storage, decoupling the daily balance of energy storage for each typical day, but integrating for a whole month the amount of energy extracted from and provided to the storage system. Then, the balance for consecutive months is established. Equations 4-22 and 4-23 illustrate this approach. Again, the charge and discharge profiles will be the same within each typical day, but now more energy can be drawn than charged as long as enough energy was stored in the previous month.

$$\Psi_{ui} = \eta_{decay,u} \cdot \Psi_{u,i-1} + \sum_j \left( -\frac{\Phi_{uij}^{sto,ds}}{\eta_{ds,u}} + \Phi_{uij}^{sto,ch} \cdot \eta_{ch,u} \right) \cdot n_j \quad (4-22)$$

$$\Psi_{u,min} \leq \Psi_{ui} \leq \Psi_{u,max} \quad (4-23)$$

This formulation has been applied in Chapter 11, as well as in a case study covered in Appendix 5.

### 4.5.3 Seasonal Storage for One Year Hourly Definition

The second solution for seasonal storage is based on an exhaustive definition of the model through a set of 8760 consecutive hours. The OMSES formulation does not change significantly when considering a full year model. The daily time definition is again one hour. The balances, in this case, are established for every hour and every pair of consecutive days. In contrast, the typical day formulation included first and last hour balances for each day. In the 8760 hour model an additional balance can be established between the last and the first hour of the year to assure continuity of some important storage variables, such as heat or fuels if there is a strong seasonality in the level of storage.

This solution provides another advantage; in addition to seasonal storage balance, it also permits the use of a higher temporal resolution (less than an hour) of renewable energy sources, avoiding the use of typical days of solar radiation or wind speed. Thus, hourly series of wind speed for a given year can be used directly and effectively in OMSES, which will find more realistic, optimal design solutions. These issues will be further explored in Chapter 11.

## 4.6 Seasonal Storage in the Form of Hydrogen Gas from Water Electrolysis

The concept of a 100% renewable energy supply system is technically feasible (Henning and Palzer, 2014) and desirable (Sterner, 2009), but not always cost effective. Until recently, in fact, the majority of the papers addressing fully renewable power systems for remote areas, observed the lower costs of the alternative, i.e., systems based partially or entirely in fossil fuel

technologies (mainly diesel). The trend in costs of technologies and fuels brought and brings today hope for economical feasibility for systems that rely solely on solar or wind technologies.

Although feasible, the design of standalone energy systems that can reliably operate for several years using photovoltaic modules and/or wind turbines is challenging. Despite exhaustive theoretical and experimental research, the effort is ongoing, currently focusing on battery reliability, optimized control, and improved conversion efficiency. In order to obtain standalone renewable energy systems, storage is essential. In the absence of storage, these systems do not generally compete with the economics of conventional energy supply solutions. Demand and supply do not usually match unless consumers adapt their demand patterns or generation is curtailed. Short term storage (batteries, flywheels, etc.) can store energy to be released in oncoming days, but for long term storage, different storage technologies and energy vectors are needed.

Among all the system configurations for long term storage, one that stands out for its tangible achievements is the standalone renewable-hydrogen based system. This concept has been repeatedly studied and several experimental pilot plants have been operating with optimal design and control. The experience gained is enough to consider it a practical concept. However, at well below 1 MW, the scale at which it has been tested is still small. Systems for isolated households or pump stations, telecommunication apparatus, etc., have been the principal subjects of study.

Hydrogen storage has several advantages over other types of energy storage. In practice, the most advantageous characteristics are its mass energy density and chemical stability (Zakeri and Syri, 2015), despite some technical challenges that affected hydrogen leakage, which can be solved with adequate storage materials. These two properties allow for seasonal storage,

providing certain seasonal variability of already cost-effective renewable energy technologies. There may be some exceptions to this assertion; seasonal storage could transform an otherwise non-economically feasible renewable technology into a cost-effective state, although this is dependent on the quality of the local renewable resource to produce hydrogen, as well as the cost of this combination of technologies. Short term storage, generally electrochemical batteries, cannot reliably store energy in high quantities (MWh) for long periods of time, i.e., months or years. Therefore, seasonal storage such as hydro-power and stable synthetic fuels are needed if fully renewable based energy systems are to be developed.

Although batteries or similar short term energy storage systems cannot play a major role in seasonal energy storage, they enable a better use of the renewable energy resource and, at the same time, they help in reducing the size of the conversion technologies, i.e., electrolyzer and fuel cells, if hydrogen is considered as the seasonal energy carrier. This conclusion is shown in several papers briefly discussed below, and highlights the need for optimization tools to calculate the integrated storage and production solutions that cost the least.

As of now, no mining facility that stores energy in the form of H<sub>2</sub> has been reported. A small scale demonstration plant is projected at Raglan Mine, in Quebec (Canada), which is not used for seasonal storage (Simon, 2014). If a mine is to be operated with energy supplied solely from renewable sources with daily and seasonal variability, some sort of long term, physical and chemically stable, energy storage is required. Electric batteries do not represent a practical and cost-effective solution for this objective.

## 4.7 Mobile Technologies for Loading and Hauling

Rock transportation in open pit and underground mining relies on different technological solutions. Technologies such as loaders, trucks, conveyor belts or hoists interact differently with the energy supply system, consuming and developing different mass and energy flows to make possible mining processes such as mucking, loading, hauling and dumping, or hoisting,. The main flows when analyzing these technologies are the fuel or electricity consumed and the mechanical work developed. This mechanical work is actually the measure of the final use of the equipment. This chapter focuses on mobile technology used to load, haul or dump rock in underground mines, although the methods here developed can be extended to the remaining technologies in charge of transporting rock within mines, whether surface or underground operations.

Coal mines have a long tradition of electrification centered around “continuous miners” and conveyor belts. The same can be said of other soft rock mining, such as phosphate and potash mining, which adopt similar methods and equipment. In other, harder rock mining, electrification is limited to some rock handling operations and some mining operations (i.e., hoisting and conveyor belts), and underground equipment heavily relies on diesel in those production activities that require additional flexibility during operation. Generally, the rock in these mines will be blasted, mucked, and loaded by LHD (load-haul-dump) units, and then either transported to chutes that send it to crushers or hoists or dumped on hauling trucks. These will transport the rock towards the surface or, as in the previous case, dump it in underground crushing systems or hoists. There are currently two alternatives to diesel power machinery: electric vehicles and hydrogen fueled vehicles.

#### 4.7.1 Electric Powered Vehicles in Mining

Of the multiple advantages of using electrical vehicles (EV) underground in mining, the potential increase in air quality and comfort is the most significant (Paraszczak et al., 2014). Until recently, fully battery-powered electrical underground heavy duty machinery (loaders or trucks) were not available, and tethered and trolley assisted vehicles were the only electric alternatives to diesel powered vehicles (Bétournay et al., 2011). Today, several commercial battery-based alternatives are available (Paraszczak et al., 2014; General Electric Transportation website, 2015). Information about the RDH Muckmaster 300EB Evolution loader, for example, is fairly complete and accessible (Paraszczak et al., 2014; Ewing, 2015; RDH website, 2015). The battery technology used (Lithium Iron Phosphate, LiFePO<sub>4</sub>, or LFP) was already anticipated in Bétournay et al. (2011) as a good candidate for these type of vehicles. Operational details can be found in Ewing (2015).

Electrical powered vehicles are locally emission free, and have the advantage of a higher conversion ratio of energy than other pathways - around 30% for ICE and 80% for electric vehicles ('pump to wheel') (Sterner, 2009; Kelly et al., 2011). Furthermore, the use of battery electric vehicles allows demand side management strategies to be explored as is done in Chapter 11.

Details for the electric trolley and tethered vehicles can be found in Paraszczak et al. (2014). They are perceived to have limited flexibility in the underground environment and the infrastructural constraints make direct comparison with other vehicle technologies more difficult or limited to specific types of mines and mining methods. For an older but insightful analysis of the potential vehicle options (some of them in use, others discarded, and others still in

development stage), the reader is directed to the work of Robertson (1985), which gives the reader an indication that the technological choices have not changed much since then.

The economical environment, i.e., the prices of electricity and diesel and operating conditions, heavily affect the outcome of studies concerned with whether this technology can be substituted for diesel powered technologies (Paraszczak et al., 2014). Considerable research effort has been expended over the last 20 years to develop and improve the technology associated with electrical vehicles, particularly regarding batteries, charging systems, drives, control, etc. The result is a technology that, in principle, marginally competes in cost with internal combustion engine (ICE) vehicles, although only for those willing to increase the investment cost to save on fuel.

#### **4.7.2 Hydrogen-Based Technologies for Mobile and Stationary Applications in Mining**

Hydrogen as a fuel for mobile equipment is contemplated as a solution to improve air quality in mines. The use of hydrogen as a fuel for underground use is not exempt from great hazard (Ulleberg et al., 2010; Verhelst and Wallner, 2009; Miller et al., 2012), but adequate safety measures can mitigate them so that they may meet current mining safety standards.

Fuel cells, both for stationary and automotive applications, generally have higher efficiencies. In practice, 50% thermal efficiency (LHV) can be considered for automotive applications (Kelly et al., 2011); 60% for stationary power plants can be reasonably expected (Pilavachi et al., 2009).

These values, some of them associated with laboratory and computer simulation tests rather than commercial equipment, are consistent with actual available technologies operating in different applications. For example, Miller et al. (2012) reported on a fuel cell powered mine locomotive with a mean thermodynamic efficiency of 51%. However, from the remaining information

provided in the cited work (mean observed net power and mean fuel usage), the low and high heating value efficiencies are 45% and 39% respectively.

Other FC mining vehicles exist at the prototyping stage. Fuel cells have been tested in more flexibly operated LHD vehicles, this time hybridized with electric batteries (Bétournay et al., 2011). The purpose of using batteries is two-fold; it allows for a steadier power output of fuel cells or internal combustion engines, as the battery can be charged when the load required by the vehicle is low. It also delivers peak power when needed, meaning that centralized plants can have lower installed capacity (FC or ICE). Overall efficiencies of the plant vehicle can be as high as 51% when fuel cells are used in hybrid systems (Bétournay et al., 2011).

#### **4.7.3 More Conventional Mobile Plant Technology Alternatives in Mining**

A similar strategy has also been applied in a hybrid diesel-battery underground loader (Bétournay et al., 2011). In addition to achieving higher load factors compared to fully diesel powered mobile plants, and therefore achieving higher mean efficiencies, ventilation requirements in UG mines may be reduced significantly due to better combustion conditions that lead to dramatic reductions of diesel particulate matter (DPM) content in the exhaust gases (Lajunen, 2014; Paraszczak et al., 2014).

These alternatives to conventional diesel plants present advantages in the area of fuel economy, maintenance costs, and ventilation requirements. However, cost advantages have to be evaluated on a case by case basis, due to the inherent diversity of operating conditions among different mines (Bétournay et al., 2005).

#### 4.7.4 Mobile Work Demand Integration in OMSES

This work assumes that safety challenges are solved for any of the technologies modeled and included in the optimization problem. There is enough evidence in the literature that those included are practical technologies in underground mines, although each of them present particular challenges for their implementation. Because an integrated approach is followed, hidden advantages may arise in terms of energy cost savings.

Here follows a description of the interaction of diesel mobile technology with other utilities within the model superstructure in the context of an underground mine. For the purpose of this work, ventilation is considered a *utility*, used for the removal (or dilution) of contaminant gases (CO, CO<sub>2</sub>, NO<sub>x</sub>, PM) and dust underground. There may be a final demand for ventilation, but the utility is mainly “consumed” by underground diesel mobile equipment that is meeting a mechanical utility demand (e.g., drilling, mucking, loading, or hauling rock). This mobile equipment, therefore, simultaneously needs an input of diesel (or electricity, H<sub>2</sub>, etc.) and the corresponding ventilation rate required by Health and Safety regulations. In addition, ventilation may consume heating or cooling power, depending on the ambient temperature and the temperature setpoint in the fresh air raise at the surface level. This shows how utility demands are interrelated: what is conventionally considered a demand for diesel – e.g., Carvalho et al. (2014) – heating, cooling, and electricity in an underground mine, is actually a single demand for *mechanical work*.

Figure 4-10 describes the interactions of the technologies *ventilation fan* and *diesel mobile equipment*. As mentioned, the air supplied underground may need heating or cooling, which will depend on whether the ambient temperature is lower or higher than the temperature setpoint ( $T_{set}$ ).

As special attention is given to ventilation, the coefficients that relate the ventilation utility and thermal flows (cooling and heating) change every hour with ambient temperature. These coefficients are, therefore, functions of the form  $C(T)=C_p \cdot (T-T_{set})$ , where  $T$  is the ambient temperature,  $T_{set}$  the temperature setpoint, and  $C_p$  the specific heat for air, considered constant and in convenient units (in units MW/Mm<sup>3</sup>/h-°C, where Mm<sup>3</sup> = 10<sup>6</sup>m<sup>3</sup>). In this work, the heating required for some consumers can be a low grade heat type; ventilation heating can be met by low temperature waste heat from a diesel generator, for the temperature to which the ventilation air is heated is normally low.

The need for heating or cooling of the ventilation air is shown in Figure 4-10, where it can be observed how the ventilation air delivered (positive sign node for the “Ventilation Fan” technology) involves the consumption (negative sign nodes) of either chilled water (refrigeration) or cooling water (considered a source of low grade heat suitable for heating, otherwise rejected via cooling towers), as well as the necessary electrical power to drive the fans.

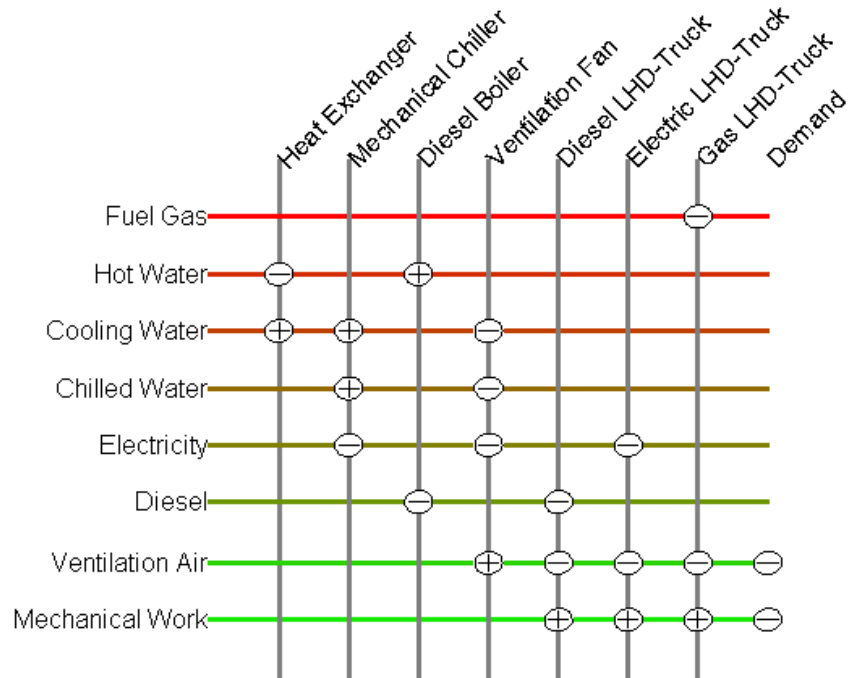


Figure 4-10 Scheme of the ventilation subsystem's interaction with mechanical work

Additional constraints in OMSES' formulation must be added to link the use of electric batteries and the electric vehicles. The power consumed by these must equal the discharge flow of the batteries. When considering the split system (several packs), further constraints are needed (Ewing, 2015). These are charging and discharging time constraints. Regarding discharging, no two of them can discharge simultaneously during the day, each of them providing power only in their respective and consecutive working time. For example, for three packs, three consecutive subshifts of even length should be set (Figure 4-11). Regarding charge of both single and split systems, the charge can be done at any time except during their working time. The formulation that defines the management of the split battery system may differ among electric mobile equipment manufacturers at the request of mine operators.

OMSES considers the battery pack as a storage device that includes the batteries for every mobile plant operating during a specific subshift.

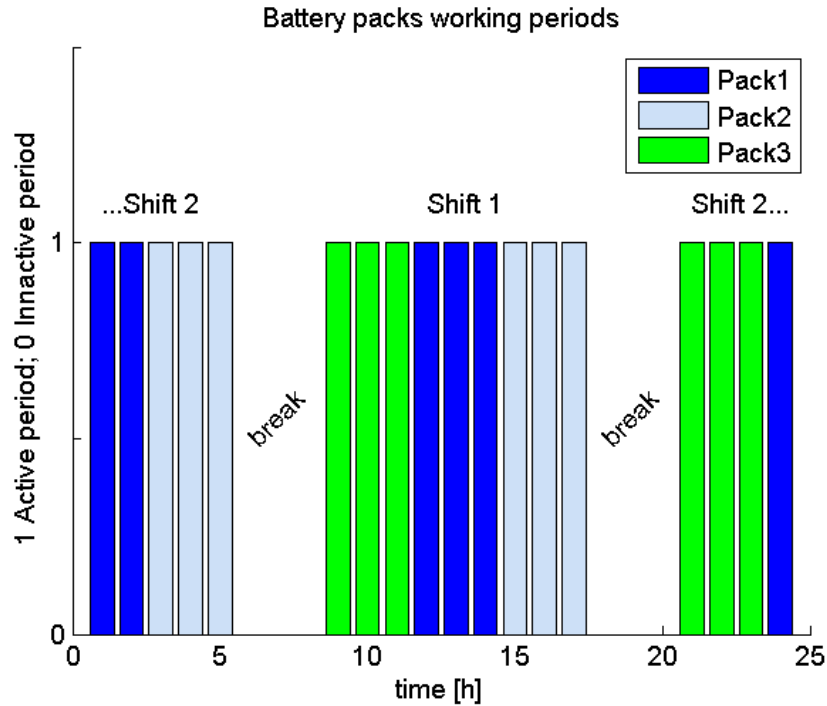


Figure 4-11 Subdivision of shifts in working periods for a 3 packs split battery system for a typical day

The number of packs can be estimated from the experience reported by the operators of these vehicles, i.e., the mining companies. In general, due to the technological level currently available batteries (energy and power density), the duty of the vehicle to deliver and the vehicle tonnage, several battery packs have to be exchanged (swapped) once the state of charge reaches the minimum value, which in some cases is after 3-4 hours (Paraszczak et al., 2014; Ewing, 2015).

The alternative to several removable batteries is to use the single mounted battery, which entails a third of the investment compared with the previous case. The advantages of having several packs are increased vehicle availability (in case of battery downtime) and improved charging management in the forms of refrigerated packs ready to be connected and lower charging power which reduces overheating, mainly in the case of lead-acid. The main disadvantage of several packs comes from the loading and unloading time, which reduces shift time and may require

special equipment. Despite this, minimal loading time has been reported by operators of battery-powered loaders when exchanging the packs (Ewing, 2015).

## **4.8 Summary**

In this chapter, several formulation extensions have been added to increase the scope of technologies and energy sources from which OMSES, as an ESS optimization tool, can benefit to produce more sustainable, as well as cost effective, integrated solutions. It should be pointed out, however, that the use of beforehand known, past demands, either for material or energy utilities remained unaltered. This assumption, which involves a retrospective design of the ESS, is revised in the next section.

# Chapter 5

## 5 OMSES Integration with Optimal Control in Dynamic Environments

The general characteristics of MPC were outlined in Section 2.4. The current chapter defines more precisely what model predictive control is and why it is chosen to complement OMSES' basic formulation to control mine site energy supply systems. The usual algorithms through which MPC is implemented to network systems are introduced first. Then, the formulations for both the design and the control problem are compared in order to illustrate how both share to a large extent the same mathematical models. Finally, the uses of MPC in the field of mine ESS are presented; these include the control of the ESS, an algorithm to detect and correct design limitations inherited from the application of OMSES, and the modification of the mining production plan based on ESS operating constraints.

In Romero et al. (2015c), results of the design and control optimization of a dewatering system were included, considering different levels of control centralization. The application of MPC for the control of the ESS of a remote Arctic mine including wind energy appeared in (Romero et al., 2015a).

### 5.1 MPC Theoretical Basis

Energy supply systems can be regarded as networks where energy and potentially materials or utilities are transported, exchanged, transformed, produced, consumed, etc. The optimal management of the networks is a complex engineering problem with many applications and where MPC has been successfully applied. Power networks (Negenborn, 2007), water systems

(Alvarado et al., 2011), or natural gas grids (Alkano et al., 2014), are typical examples of network control optimization.

The solutions obtained from the OMSES methodology are essentially networks whose operating schedule, calculated for certain average conditions, has to be recalculated for the conditions in which the ESS will have to operate and be controlled. Thus, it makes sense to take advantage of a control approach formulated in the same terms as MPC. This approach is characterized by the use of the following information (Negenborn, 2007):

- 1) an objective function quantifying the performance of the control actions or inputs;
- 2) a (mathematical) prediction model of the real plant to be controlled, including states and possible future disturbances;
- 3) constraints on the states, inputs, and outputs of the system;
- 4) direct or indirect measurement of the state of the system at the beginning of the control cycle.

In order to control the system, out of all the possible control actions, there is a particular set of them which must be found and that will minimise the objective function. The existence of a cost minimising set of control actions depends upon the assumptions of the convexity and linearity of the problem modeled and a linear cost function, and whether these safely apply to the case of OMSES (Camacho and Bordons, 2004).

The control algorithm can be summarized in three steps (Negenborn, 2007):

- 1) measuring the current state of the system;
- 2) determining which actions optimize the performance over the prediction horizon by solving the control optimization problem:

*minimize* the objective function in terms of actions over the prediction horizon,  
*subject to* the dynamics of the whole network, the constraints on flows and states, the measuring of the initial state of the network at the beginning of the current control cycle.

3) implementing the actions until the next control cycle and returning to step 1).

MPC assumes the repetition of the control optimization problem with a certain frequency. When the controlled system has evolved using the planned actions in the previous interval  $k-1$ , the optimal set of actions at  $k$  for the next  $N_c$  time intervals are computed (Figure 5-1). However, the actions actually applied at each iteration are only those for the first time interval of the horizon. This method is applied in what is called the receding horizon, which always includes the next  $N_c$  discrete time intervals. For this reason, MPC is also known as receding horizon control or moving horizon control (Negenborn, 2007). The prediction horizon ( $N_p$ ), alternatively, includes as many intervals as the operating conditions may require regarding, for instance, the disturbances. As indicated previously, the objective function generally includes the control effort over the prediction horizon.

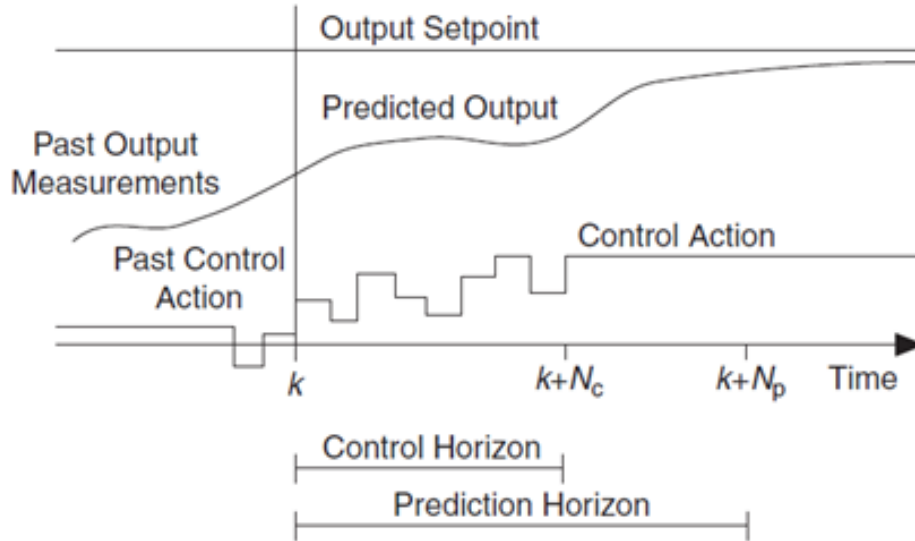


Figure 5-1 MPC receding horizon for tracking

As represented in Figure 5-1, the control action in the last interval within the control horizon may be assumed constant, especially in tracking control problems where an output setpoint is defined. Examples of MPC problems for tracking include water storage management (Alvarado et al., 2011) and indoor comfort temperature (Collazos et al., 2009). MPC does not necessarily deal only with tracking problems, but also may be applied to scheduling or planning problems. Examples of these include Goodwin et al. (2006) in the field of mine planning, and Romero et al. (2015c) on mine dewatering.

Although the measurement of the state of the system is central in the MPC formulation, this does not necessarily mean that the controlled system (the physical plant) can be accessed for measurement. Thus, more detailed models of the plant than the prediction model can be used to ensure closed loop control in absence of access to the physical plant output or state.

The formulation of the control problem, which is repeated at each  $k$  (Figure 5-1), is presented below:

$$\text{Minimize} \quad J^{MPC} = \sum_{i=0}^{N_p-1} J_i(x_k, u_k, y_k) \quad (5-1)$$

$$\text{Subject to} \quad x_{k+1} = \mathbf{A}x_k + \mathbf{B}u_k + \mathbf{D}w_k \quad (5-2)$$

$$y_k = \mathbf{C}x_k \quad (5-3)$$

$$L_e(x_k, u_k, y_k) = 0 \quad (5-4)$$

$$L_h(x_k, u_k, y_k) \leq 0 \quad (5-5)$$

$$x_k \equiv x_k(k + i|k) \quad (5-6)$$

When assumed linear, the objective function or performance index, represented by  $J^{MPC}$  (Equation 5-1) is the weighted sum throughout the prediction horizon of the actions applied  $u_k$ , the states of the system  $x_k$ , and the output signals from the system  $y_k$ . Equation 5-2 describes the state equation for a system, i.e., how the actions and disturbances ( $w_k$ ) affect the controlled system, at least at the model level. The variables described and the problem formulation itself can be used for single input – single output (SISO) and multiple input – multiple output (MIMO) systems (Camacho and Bordons, 2004; Maciejowski, 2002). MPC formulation is generally simplified, without loss of generality, through Equation 5-6, which expresses the fact that the problem is repeatedly solved in for increasing values of  $k$  (for consistency with other works,  $i$  has been kept as the index for the intervals in the rolling horizon, and should not be confused with the day index in OMSES formulation).

The present work considers the state equations (Equation 5-2) as the energy and mass balances linking the state of the system ( $x_k$ ) and the manipulated variables ( $u_k$ ). Examples of these might be the level of a water tank and the mass flowrates in and out, or the temperature of a heat storage system and the heat flows entering and leaving the system. Output variables can also be calculated using known relationships (Equation 5-3) and used to specify variable related costs

(Equation 5-1) or constraints defined either as equality or inequalities (Equation 5-4 and 5-5). Matrices **A**, **B**, **C**, and **D** mathematically describe the system aimed to be controlled.

When model predictive control is used in energy systems, the cost function generally includes those costs related to the purchase of energy and equipment maintenance, as well as those costs associated with desirable or undesirable states of the system. The latter may be expressed in linear (Collazos et al., 2009; Zong et al., 2012; Halvgaard et al., 2012) or quadratic form (Pichler et al., 2014). Other examples of cost functions include power tracking quadratic costs (Mayhorn et al., 2012) or demand charges costs (Salsbury et al., 2013; Romero et al., 2015c).

Equality and inequality constraints (Equations 5-4 and 5-5) also refer to energy balances. OMSES' criteria regarding energy balances (Chapter 3) generally apply for the balances across networks and individual energy converters. Additional constraints that are site-specific or process-specific may also apply, such as running hours for equipment (Xenos et al., 2016) or ramp-up for some technologies (del Real et al., 2014). Not uncommon is the relaxation of some constraints through the introduction of penalty cost (added to the objective function) associated with the violation of such constraints. These are turned into so called soft-constraints, extensively used in complex MIMO and multi-agent systems and applied on system states and output variables (Wang, 2009).

## **5.2 OMSES and MPC Comparison**

A comparison between the definitions of OMSES and MPC regarding their use in energy systems is next presented. The optimal design problem (OMSES) is formulated as a MILP that relies on a mathematical model and a cost function that includes, in addition to energy and operating costs, the annuitized investment in equipment and infrastructure. The time horizon in

which this problem is solved is generally one year, which is divided into  $d$  non-consecutive typical days, which are further divided into  $h$  consecutive time intervals (i.e., 24 intervals of 1 hour duration).

There are three main differences between the OMSES design problem of Chapter 3 and the MPC optimization problem discussed here.

- 1) MPC repetitively solves its optimization problem in a receding horizon while OMSES solves the design problem, once, in a fixed static horizon.
- 2) MPC assumes a specified plant design (here provided by OMSES); therefore, unlike OMSES, the amount of equipment or infrastructure ratings are not decision variables for MPC, and do not appear in its objective function.
- 3) OMSES assumes that all inputs within the operation horizon are perfectly known, while for MPC, only a forecast is available at every control time step.

OMSES' formulation (Chapter 3) has been adapted to MPC nomenclature, illustrating the parallelisms and differences drawn in the previous paragraphs.

$$\text{Minimize} \quad J^{OMSES} = \sum_{k=(1,1)}^{(d,h)} J(x_k, u_{d,k}, u_{o,k}, y_k) \quad (5-7)$$

$$\text{Subject to} \quad x_{k+1} = \mathbf{A}'x_k + \mathbf{B}'_d u_{d,k} + \mathbf{B}'_o u_{o,k} + \mathbf{D}'w_k \quad (5-8)$$

$$y_k = \mathbf{C}'x_k \quad (5-9)$$

$$L'_e(x_k, u_k, y_k) = 0 \quad (5-10)$$

$$L'_h(x_k, u_k, y_k) \leq 0 \quad (5-11)$$

$$u_k = u_{d,k} + u_{o,k} \quad (5-12)$$

$$\mathbf{B}'u_k = \mathbf{B}'_d u_{d,k} + \mathbf{B}'_o u_{o,k} = \begin{bmatrix} \mathbf{B}'_d & \mathbf{0} \\ \mathbf{0} & \mathbf{B}'_o \end{bmatrix} \begin{bmatrix} u_{d,k} \\ u_{o,k} \end{bmatrix} \quad (5-13)$$

Energy supply systems can be categorized as MIMO systems. Thus, all the variables  $(x_k, u_{d,k}, u_{o,k}, y_k)$  will typically represent vectors. Equation 5-7 refers to the objective function, which mainly depends on the decision variables of the original problem: the design variables,  $u_{d,k}$ , and the operation variables for the typical days,  $u_{o,k}$ . Generally, Equation 5-8 will apply to storage systems, which for OMSES depend mainly on the net flow into the system, included in  $u_{o,k}$ . Thus,  $\mathbf{B}'_d$  will typically be the null matrix. Losses in the storage systems can be characterized as disturbances ( $w_k$ ). However, when losses can be quantified as charging and discharging efficiencies or as a function of the level of storage, matrices  $\mathbf{A}'$  and  $\mathbf{B}'_o$  will define them. The design variables,  $u_{d,k}$ , do not depend on the time horizon in OMSES, but the subscript remains in case the design could be modified on a seasonal basis, e.g., if there are equipment rentals.

Equation 5-10 includes the essential energy and mass balance across utilities, as well as the output and inputs of utilities for every technology. An example of Equation 5-11 is the limitation of utility production below the installed capacity, for every technology installed.

The subscript  $k$  is defined in MPC as the starting time interval of every iteration. Here, it expresses the time index representing the couple (day, hour or  $i,j$ ). Because not all the time intervals are consecutive in OMSES' typical formulation, it is more convenient to leave Equation 5-7 as an abstract sum of terms in order to better appreciate the parallelisms with MPC, rather than expressing explicitly the sum of fixed costs and variable costs, already done in Chapter 3. Splitting the summation into design and operation costs results into two cost functions,  $J_d(u_{d,k})$  and  $J_o(x_k, u_{o,k}, y_k)$  respectively.

In OMSES, the definition of identical typical days for each month leads to a cyclical operation, which translates into linking the states at the end and the beginning of the typical day. The operation conditions, actual or simulated with MPC, require the relaxation of such a terminal constraint. Using mathematical notation, the following equation included in OMSES is omitted in MPC:

$$x_{(i,1)} = \mathbf{A}'x_{(i,24)} + \mathbf{B}'u_{(i,24)} + \mathbf{C}'w_{(i,24)} \quad (5-14)$$

It is not the aim of the thesis to reformulate the OMSES problem using the mathematical expressions characteristic of MPC. Rather, this section's aim is to draw common features and remain attached to OMSES formulation. To this end, what follows is a non exhaustive equivalency list (Table 5-1) between this section and the equations and variables presented in Chapters 3 and 4.

**Table 5-1 MPC and OMSES formulation – equations and variable comparison**

	MPC		OMSES
	Section 5.2	Chapter 3	Chapter 4
<b>Equation Description</b>			
Cost function	Eq. 5-7	Eq. 3-3 to 3-8	
Auxiliary variables	Eq. 5-9	Eq. 3-4 to 3-9 Eq. 3-23	Eq. 4-7 Eq. 4-12, 4-13 Eq. 4-15
State relationships	Eq. 5-8	-	Eq. 4-20 Eq. 4-22
Equality constraints	Eq. 5-10	Eq. 3-11 to 3-14	Eq. 4-5 Eq. 4-14
Inequality constraints	Eq. 5-11	Eq. 3-10 Eq. 3-15 to 3-18	Eq. 4-1 Eq. 4-6 Eq. 4-8 to 4-11 Eq. 4-16, 4-19 Eq. 4-21 and Eq. 4-23
<b>Variable</b>			
State variable	$x_k$	-	$\Psi_{uij}$
System design	$u_{d,k}$	$\mu_v, \Gamma_u$	$\Psi_{u,max}$
Control action	$u_{o,k}$	$\Pi_{vij}$	$\Phi_{uij}^{sto,ch(ds)}$

### **5.3 Characteristic Disturbances and Forecast**

In terms of which model disturbances can be predicted, and to what extent, there are several approaches in MPC. In the present work, it will be assumed that all energy demand forecasts are perfect. Furthermore, if it is assumed that the control actions are maintained throughout each time interval, any variation from the predicted demand can be dealt with by more specific controllers (e.g., programmable logic controller) and that the mean value of the demand will be close to that predicted. This approach is known as hierarchical control (Negenborn, 2007).

Other disturbances, such as ambient temperature, solar radiation, wind speed, or energy price in dynamic markets, require a different approach. For instance, electricity prices may be known for the next 24 hours, but beyond that an approximation may be available using the previous day's information. For ambient temperature, accepted forecasting methods include previous days information (Collazos et al., 2009), meteorological forecasts (Zong et al., 2012) or, as proposed here, local statistical data using the Erbs coefficients (Erbs et al., 1983). Renewable energy related variables (wind speed and solar radiation) are associated with greater variability and uncertainty, therefore making forecasting more difficult. A ten minute interval forecast for several hours is obtained in Mayhorn et al. (2012) using an Autoregressive Integrated Moving Average (ARIMA) model, while an actual meteorological forecast is used in Zong et al. (2012) to predict PV output.

### **5.4 MPC Feedback Control**

The use of information feedback from the real system or from another process model will be discussed in this section. Figure 5-2 shows the mechanism of MPC feedback control.

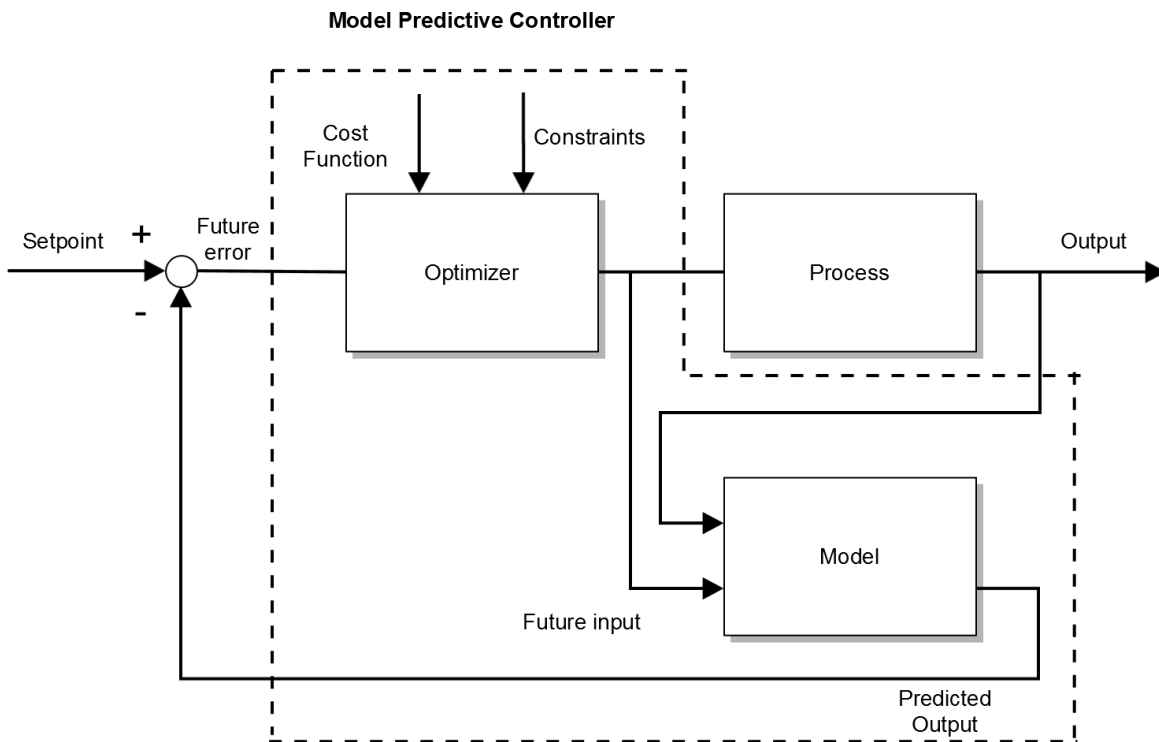


Figure 5-2 MPC implementation example (Shi et al., 2005)

MPC is formulated so that some feedback information can be taken directly or indirectly from the actual plant to overcome the inherent inaccuracy of the simplified prediction model upon which the optimal series of actions are derived. Thus, it can be expected that there will be some deviation of the trajectory of the model's future states from the actual plant's evolution once the control actions are applied. Providing information on the plant state to the model making predictions, given the control actions, forms a feedback loop so that the control actions can be modified and control of the plant maintained. The need for feedback control increases with the complexity of the plant's dynamic. The feedback information is used mainly to update the state of the system. In some instances, the system's state update can be taken from a more detailed dynamic model than that used by the MPC controller as opposed to the actual plant, reducing the need for additional monitoring.

OMSES assumes zero order dynamic models (no time delay in the response) for the equipment installed and for the storage facilities. In addition, technologies' performance depends linearly on the control actions. This reduces the ability of the formulation to define partial load operation of the equipment or inertial effects during load variations. Chapter 9 illustrates the use of more detailed models to improve systems' operation through feedback, which in addition allows for richer simulation results with which to evaluate the performance and adequacy of the controller and the MPC system's model.

## 5.5 Dynamic Design

Among all of the OMSSES basic formulation's weaknesses, the consideration of average values for the demands is especially problematic. The averaging process takes place on two levels:

- 1) The minimum interval is typically chosen as an hour, where a constant demand is considered, although actually it may fluctuate significantly around the mean value;
- 2) The use of typical weekdays or weekends, or simply days characterizing a month (or a season) assumes all days to be equal, which does not account for, e.g., variable ambient temperature, solar radiation, wind speed, user's load, etc. across days.

The direct consequence is the design of subsystems (e.g., the cooling system, heating system, dewatering system, etc.) that may not be able to deal with peak loads. This section attempts to overcome this limitation by using a simulation approach in which the design, i.e., the technologies installed, may change in size and number while solving the MPC-based optimal control problem.

Several strategies can be adopted to mitigate the problem of designing an ESS for every possible operating condition. The usual approach is to consider as a constraint that the ESS must be able

to supply the highest peak demand considering the worst case of simultaneity of all consumer centers within the system (Majewski et al., 2015). This approach has also been used, for example, by Voll et al. (2013), and involves augmenting the set of ‘typical days’ with additional days for which the daily operating costs are not considered in the calculation of the objective function, and their demands must be met. Thus, in addition to, for example, one typical day for each month of the year, a 13<sup>th</sup> might be defined in order to capture a high ambient temperature day in summer, perhaps using a certain percentile of confidence. Such an approach would ensure that the optimal equipment combination is still achieved, and would take extreme demand profiles into account.

Subsystems (cooling, heating, etc.) may also be designed to deliver the “worst case scenario” load or demand. OMSES can accommodate such constraints over specific technologies (e.g., mechanical chiller, boiler, etc.), but in general the peak load will be unknown when the technologies installed are in fact the answer of the problem, as well as the internal energy flows (production and consumption; see Chapter 3).

Following either approach is useless when energy or material storage is considered to reduce peak demands (loads). Furthermore, the more modeling effort is put into satisfying *final demands* (e.g., mechanical work, compressed air, potential energy, etc.) as opposed to *demands* (electricity, heating, cooling, etc.), the more technological solutions and combinations appear, and the less straightforward the calculation of peak demands becomes.

The advantages of load shedding in the context of energy supply design and operation optimization have been recently addressed by Bungener et al. (2015). Thus, the authors of that work recognise the problems of *undercapacity* or *supply shortage* that existing energy systems

may suffer from, which, in general, apply to both optimized and non-optimized systems. In their analysis of mitigation alternatives they show how certain combinations of investment in new equipment and load shedding yield feasible, near-optimal, and more robust solutions for systems potentially facing undercapacity. However, two observations should be made of the methodology proposed, which are relevant for the present thesis. The first observation relates to the load period considered for the systems design and operation optimization. Bungener et al. (2015) consider a complete year of operation where the daily energy demands are perfectly known. This can be expressed as perfect demand knowledge in a scheduling problem considering one year prediction and control horizon, using MPC terminology. Although the uncertainty in demands is thus absent, they do consider the supply uncertainty by removing from the original design of the system several units (boilers). The second observation is that they do not consider energy storage in their formulation, suggesting it though in their conclusions. In their formulation, the load shed during a given period is not claimed in a later one. In contrast, when considering the use of energy storage consumers do not have to sacrifice their objectives of demand satisfaction even when the supply system faces undercapacity.

Not quite far from the work of Bungener et al. (2015), a third approach presented here proposes a dynamic design optimization within the same framework as the MPC problem to optimize the operation of ESS. The cost function for the MPC problem formulated in Section 5.1 only includes the costs incurred during the system's operation: the cost of energy and the costs of equipment operation and maintenance. The MPC cost function ( $J_i$ ) can be extended to include the cost of adding an extra piece of technology at every time step. Although computationally more demanding, this ensures that the optimization problem to be solved remains feasible. It is important to realise that this approach involves manipulation of the OMSES design hitherto

assumed to be the optimal design. System design improvement becomes part of the MPC problem, and thus the design process of the ESS becomes dynamic. The algorithm can be improved so that the extended MPC problem optimizations are only used when the problem becomes non-feasible and the original MPC cost function is used while the existing plant feasibility meets system demand. This approach permits consideration of uncertainty in both energy demand and supply; demands in energy systems involve certain variability, for example due to people's behavior, or weather variations; forecasts are also limited regarding the production from renewable sources (Section 4.1.2).

### 5.5.1 MPC Algorithm to Allow for Design Modifications

The formulation of the proposed alternative to deal with unfeasible operation is here presented. It uses a relaxation of the MPC-OMSES programming problem that allows for the addition of new capacity of the selected technologies. A flow chart showing how the algorithm is implemented using Matlab and Lingo can be found in Appendix 8.

$$P_v^{OMSES} = \mu_v^{OMSES} \cdot P_{nom,v} \quad (5-15)$$

$$\Pi_{vij} \leq P_v^{OMSES} + \Delta\mu_v \cdot P_{nom,v} \quad (5-16)$$

If  $P_v^{OMSES}$  is the capacity calculated by OMSES for each technology  $v$  (Equation 5-15), then the problem solved with MPC includes a variation of the maximum production by that technology (Equation 5-16) that adds an integer variable,  $\Delta\mu_v$ , which is in fact a new decision variable. Thus, the problem corresponding to the MPC-based simulation is relaxed to avoid the infeasibilities (instances in which the problem of control is infeasible) derived from, for example, a shortage in capacity or run out of a certain utility stored.

The choice of whether the relaxation is applied at every control step, or just when infeasibilities arise, depends on several factors, such as the available computational time and capacity, or the flags that softwares provide to indicate that the problem is infeasible. Other, less objective factors bring the problem of cost allocation to every increase in equipment or even to each marginal rating increase in the original pieces of equipment. The simplest option is to assign the annuitized cost of the corresponding technology and allow for additional units of each technology. The costs of operation and maintenance considered by MPC for the next 24 hours, for example, are significantly smaller than the annuitized cost of the equipment, so any long term investment regarding the use of wind turbines or seasonal energy storage is discarded for a cost reason. The method to weight both operation cost and investment is not addressed in this thesis, and, to the best knowledge of the author, it has not been covered in other works. It is suggested, however, that long term dynamic design would imply the allocation of some penalty cost for the long term energy stored at any given time, ensuring that enough energy is stored to be later drawn. How much energy is stored at any given time can be calculated with OMSES' typical days design using the seasonal formulation (Chapter 4), used for example in Chapter 11.

### **5.5.2 Methodology of Validation of the Dynamic Design Using MPC**

In order to validate this dynamic design approach, there needs to be a method to evaluate whether or not the optimal design is achieved, **or** one that, with the best knowledge of all operating conditions, arrives at a local minimum cost solution. In this work, the use of a better time-resolved demand definition should be used to test the results of the dynamic design approach, i.e., the use of demand profiles with 8760 sequential hours, as opposed to 12 days (Carvalho et al., 2014b) or 8 days (Romero et al., 2014), with 24 consecutive hourly intervals each, or any convenient discretization of the time frame where energy exchanges are defined.

To understand the issues with such an undertaking, the transition between solution spaces for the basic OMSES problem and that with better resolved demand definition needs some appreciation. Figure 5-3 illustrates the different problems to be solved -  $P1$  is the OMSES typical day formulation problem (e.g.,  $12 \times 24 = 288$  hours), while  $P2$  is the problem defined in the horizon comprising 8760 hours.

The feasibility regions for problems  $P1$  and  $P2$  are, respectively,  $FR1$  and  $FR2$ , while the objective function is represented by a hyperplane identical, as a first approximation, for both problems ( $OF1=OF2=OF$ ). Because the equations defining the mass and energy balances are almost identical - with the difference of the daily storage terminal constraint, assumed less critical -  $FR2$  can be considered included in  $FR1$ . The reason for this assumption is that the more constrained demands for the actual problem, for example when ambient temperatures deviate from the average, are used in  $P1$ . In set theory notation, if  $FR1 \subset FR2$ , and  $O2 \in FR2$ , then  $O2 \in FR1$ .

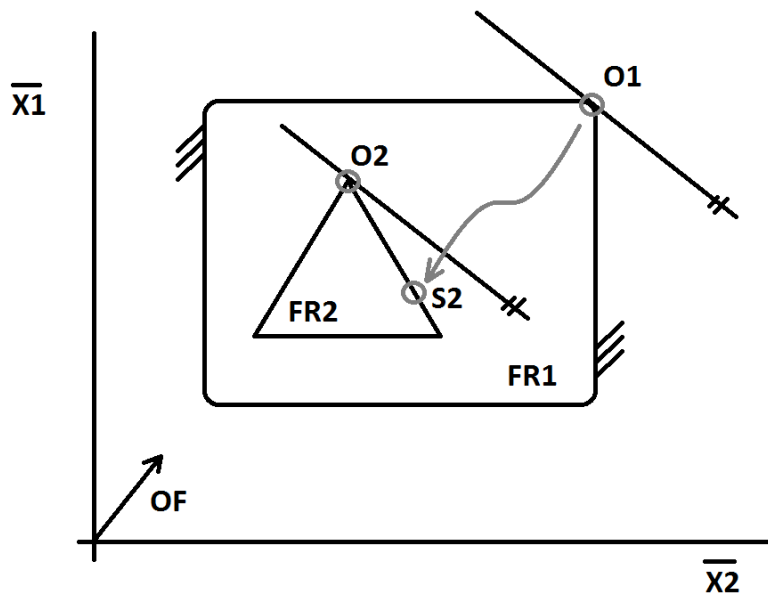


Figure 5-3 OMSES typical days problem 1, versus actual ESS problem, 2 – Optimal solutions are O1 and O2

This argument leaves aside the daily terminal balances for energy storage in OMSES, but these actually do not represent the optimal storage management if environmental conditions change on a daily basis.

The shape of *FR2* may be significantly different from *FR1* (Figure 5-3). There is no reason to think that the optimal design (and operation) defined by *O2* shall be qualitatively close to *O1*. Both regions have been represented as convex spaces, whose optimum results are found at the intersection (tangent) with the perpendicular of the objective function (OF). Both P1 and P2 are MILP problems, and therefore non-convex, despite the representation in Figure 5-4. However, optimization algorithms such as the Branch and Bound Method, which can solve MILP typical of ESS design optimization problems by splitting the solution space into combinations of convex regions over which the simplex algorithm can successfully find the optimal (Yokoyama et al., 2002). Both problems share the same integer and binary variables, and thus the convex regions can be considered similar.

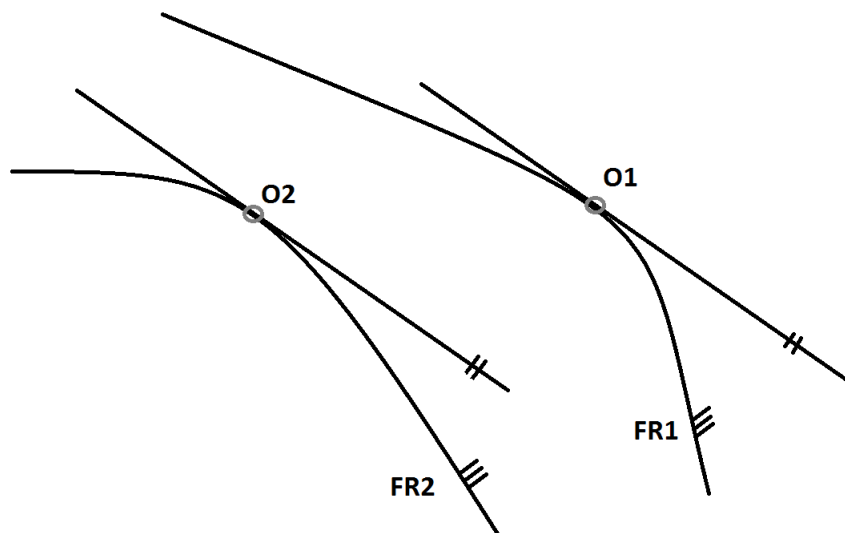


Figure 5-4 Optimal solutions for typical days problem (O1) and actual problem (O2)

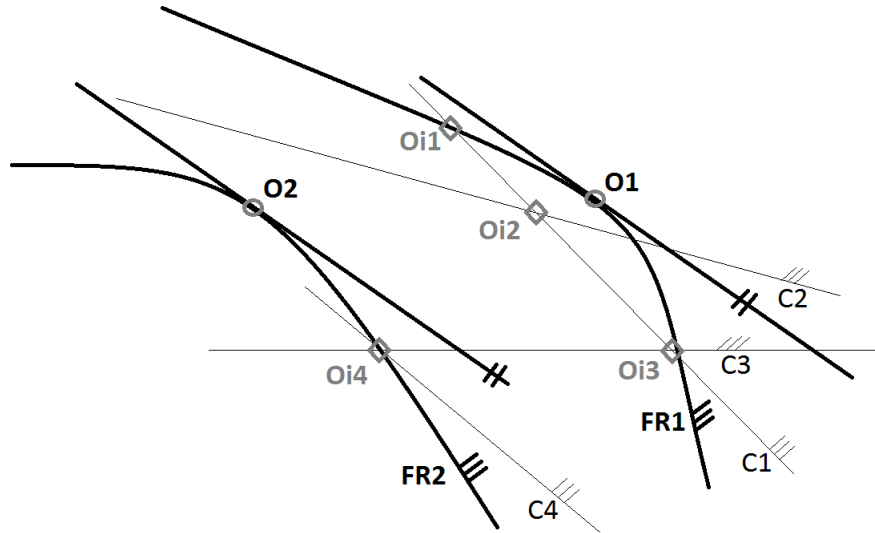


Figure 5-5 Optimal solutions for typical days problem (O1) and actual problem (O2); Pathway followed during simulation in actual environment

Figure 5-4 illustrates in a simplified manner the optimal solutions for both problems. Using the same representation, Figure 5-5 describes the process involved while moving towards  $O2$  from  $O1$ . The path proposed to reach  $O2$  is based on the progressive addition of constraints arising during the simulation of the ESS under actual or more realistic operation conditions. MPC can be used to guarantee feasibility in actual operating conditions, i.e., improving  $O1$  systematically until  $FR2$  is reached, but there is no certainty to whether it will end close enough to  $O2$  in the new feasibility region if  $OF_{MPC}$  only includes operating costs or if it is simply equal to  $OF1(=OF2)$ . The new feasibility region maybe more constrained than  $FR2$ , i.e., it is smaller in a multidimensional sense. Indeed,  $P2$  is essentially the same as the MPC problem when the latter considers investment costs, except for the prediction horizon (8760 hours for  $P2$  and usually less than 48 hours in MPC-based DER control problems), which continuously imposes a state constraint in the first interval, in particular for the storage systems.

The path for the intermediate optimal solutions ( $O_i$ ) (Figure 5-5) will be determined by the sequences of new constraints ( $C1$  to  $C4$ ). However, if the problem is convex (and to some extent we can consider it so while using the dynamic design approach because the design is fixed or incremental), then the order will not affect the final destination ( $O_{if}$ , in this case  $O_{i4}$ ) under the same constraints.

### 5.5.3 Limitations of Higher Time Resolution OMSES Model to Obtain Optimal Solutions

Even if problems are considered partially convex (Figure 5-6), solutions involving medium and long term storage or renewables cannot and will not be reached unless MPC considers long term horizons or leverages the cost of expensive renewables and storage compared with conventional technologies.

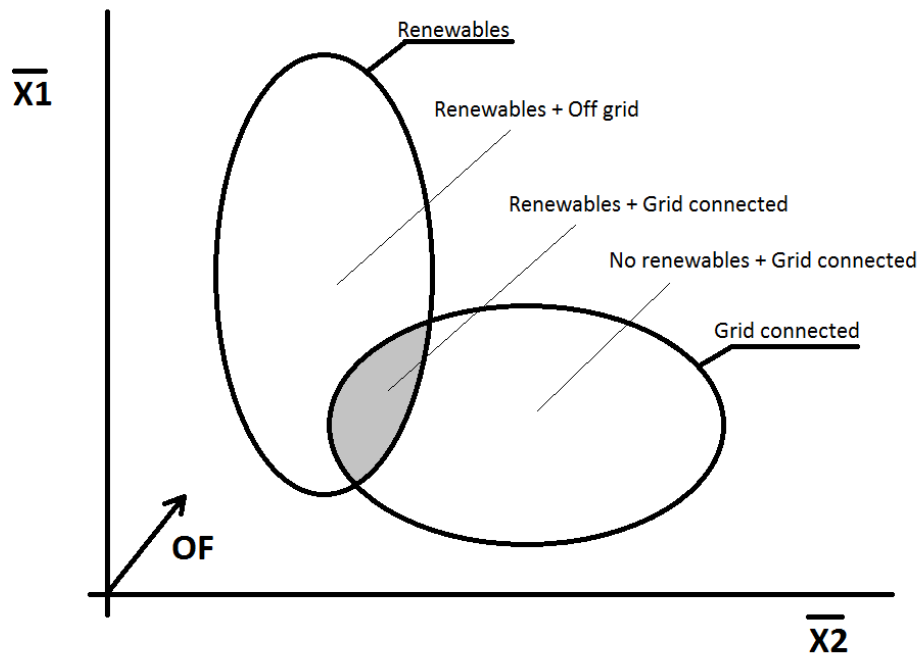


Figure 5-6 Convexity issues in MILP problems in ESS; the feasibility region of the whole problem (P2) results from the union of both ovals

The cost of infrastructure such as transmission lines also has to be leveraged to make it possible to get closer to  $O2$  if this includes investment in it, which  $O1$  did not. This brings back the discussion to the use of 8760h models, rather than 288h as was the case of OMSES' original idea. The main advantage of using 'typical days' lies in its compactness. The definition of the typical consumer's behavior is an approach accepted in engineering practice. However, when variable and uncertain renewable energy sources are added to the problem, it results in it being challenging or impossible to simultaneously define typical demands and renewable production over the same time frame.

Nevertheless, using higher granularity in the temporal characterization of demands and renewable energy output does not necessarily result in a better design. For example, optimizing an ESS using OMSES, assuming that the demands and the wind speed for the 8760 hours of a typical year are known, would yield a solution in terms of design and operation suboptimal compared to the real life problem in which forecasted information is limited to the next 1 to 5 days. That is, OMSES optimization problem considering 8760 hours is equivalent to an MPC problem with  $N_p=N_c=8760$ , solved simultaneously, also including the investment costs in the objective function, and applying the appropriate terminal constraint at the end of the year. This may result in solutions as unrealistic as when using typical days' OMSES formulation. This consideration applies for any selection of  $d$  and  $h$  when defining the OMSES model.

## **5.6 Applications of Various Modifications of MPC Used in Combination with OMSES**

If MPC is to be used as a tool to dynamically design a feasible (or improved) solution for the actual ESS problem, then, an interesting trade-off appears between the selection of the control

horizon, the partition of this horizon, the weighting of operation and investment costs, and the penalty costs used to induce a particular type of solution (e.g., one with more storage capacity or with higher renewable penetration).

In order to achieve solutions that account for the uncertainty in the output of renewable sources such as wind, the typical forecast length for power output is generally limited to 2 days, although it seems possible to have information that is useful for ESS scheduling for up to 5 days (Landberg et al., 2003). This is illustrated in Figure 5-7, where the prediction horizon has been extended to 4 days, involving 24 periods of variable length (a proved manageable size for an MES' scheduling purposes). In general, this approach considering variable length intervals in the prediction (and control) horizon is similar to others such as Goodwin et al. (2008), but would be applied to ESS instead of mine planning, the former demanding a lower temporal granularity (years).

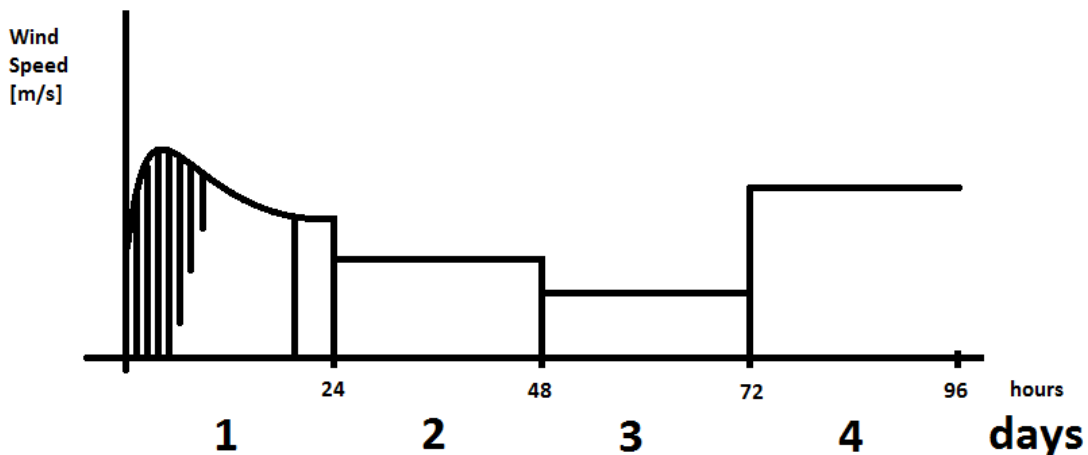


Figure 5-7 Example of wind forecast with varying prediction and control intervals duration; the first 20 intervals span 1 hour, the next 3 hours, and the last 3 intervals 24 hours. Total number of intervals=24; total horizon=96 hours

When OMSES is applied on a typical day's demand model in the presence of renewable energy sources, the characterization of these by typical profiles may result in unfeasible designs for the actual operational conditions, including the user's demands and renewable power output. The greater the energy flows associated with renewables, with their high variability, in the OMSES typical days solution, the more likely one should expect unfeasible designs. Having installed enough conventional power capacity using auxiliary constraints (i.e., diesel generators or grid connection capacity), the infeasibilities can be eliminated, although the solution thus calculated may be too conservative. The alternative approach consists of using storage as a means to mitigate the variability of renewable power output, relying on a limited conventional generation capacity. The system being simulated using MPC's relaxed dynamic design formulation (including the possibility to modify the design) would have the secondary objective of producing energy in excess and storing it (the primary is meeting the instantaneous demands).

Figure 5-8 depicts the method described being applied to seasonal storage. OMSES can accommodate seasonal energy storage (Chapter 4), which provides, at least as a first approximation to the actual problem ( $P2$ ), a reference level to be tracked by an MPC algorithm with terminal costs. In this case, the energy stored is the variable to be tracked, with the penalty applied only to the last control period. In addition to the flows that make possible the supply of the final energy demands in the control horizon, the manipulated variables include the increase, when needed, of the renewables and the storage installed capacity, being those conveniently weighted in the objective function considering the operational costs of the system. A tree-based MPC to account for possible forecast outcomes and produce more robust decisions could also be accommodated (Maestre et al., 2013).

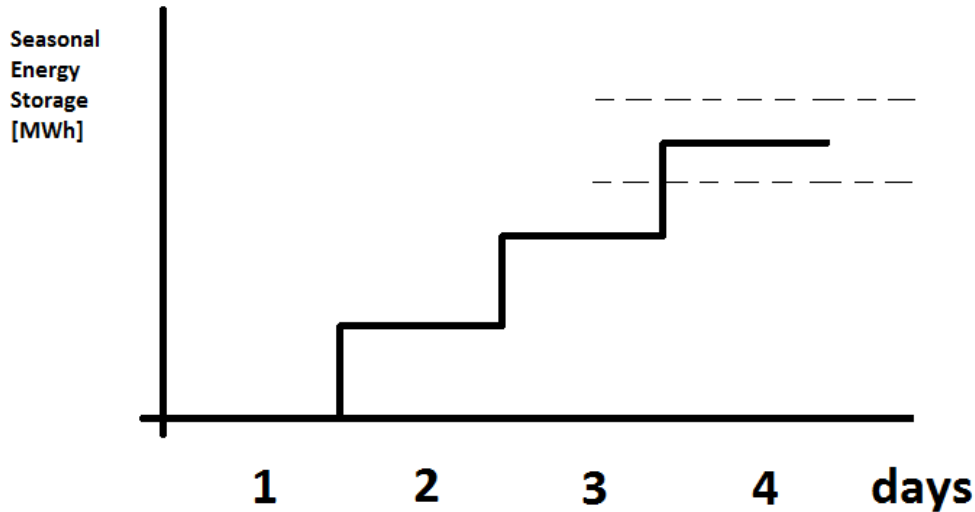


Figure 5-8 MPC for tracking used to ensure that the level of storage at the end of the horizon stays within the desired range (dashed lines) or as close as possible to the reference (solid line)

The last potential application of MPC in mining, which can be extended to any production process in the industry whose energy management were to be optimized, includes the variation of the scheduled production level in order to comply with all the constraints that appear during the operation of the ESS. The energy demands must be met, which may be substituted by the constraint imposing a certain production output every hour. This assumes that energy demands depend linearly on production (tonnes of ore per hour), which is generally true (Chapman and Roberts, 1983), if not instantly, at least integrated throughout time intervals such as hours.

Figure 5-9 shows a particular example in which operational constraints are relaxed, in this case not by increasing the capacity of any particular ESS parts, but by reducing the production (tonnes of ore extracted, from production plan  $p1$  to  $p2$ ), which reduces the energy demands, for production in general is the driver of utility needs at every given time. In Figure 5-9, the simulation of the optimal design ( $OI$ ) faces a first constraint that allows it to remain feasible by

modifying the operation schedule or the design (capacity increase) while maintaining the production plan  $p1$ . The second constraint that appears, however, makes the problem unfeasible unless the production plan is lowered to  $p2$ . A trade-off may appear if the operation is to remain feasible by a combination of mine output reduction or by capacity increase in some part of the ESS.

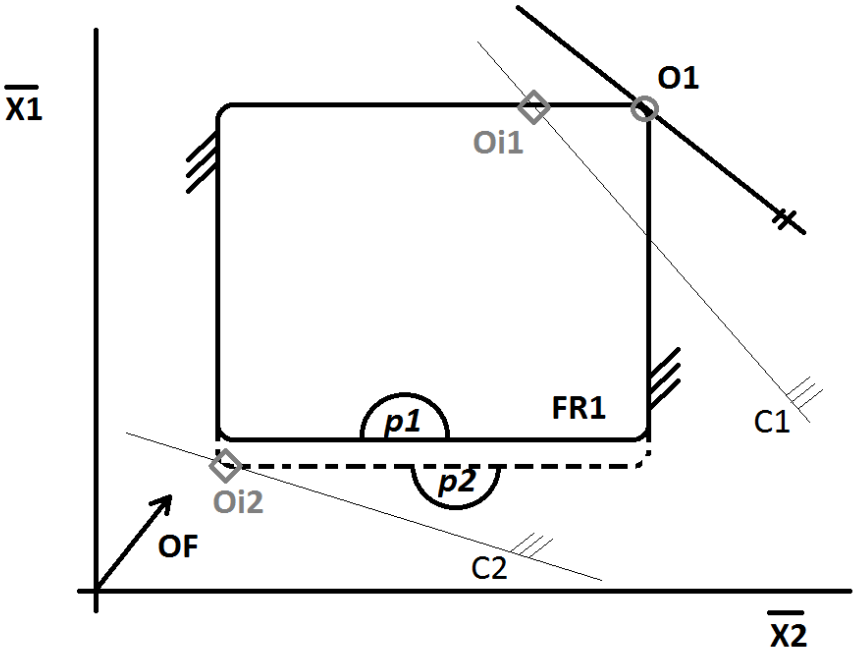


Figure 5-9 Production adjustment to ensure feasible operation

Special constraints on the ESS are common in the mining industry. For example, production of minerals in each mine commonly find bottlenecks in grid capacity or ability to deal with load variations, which causes power quality issues. Such was the case of LKAB mine in Sweden, where the activation of simultaneous loads (hoists in this case) led to inadmissible reactive power consumption from the point-of-view of the grid. These issues were solved by the installation of a Static Var Compensator (SVC), which can be considered part of the ESS. After the installation

of the SVC, the mine could increase the hoisting capacity by 20-30% (Grünbaum and Willemsen, 2013).

The formulation of utility demand constraints in light of variable production rates requires the modification of the balance equation (Equation 3-12). By production, or production plan, the parameter considered is the tonnage extracted, or milled, depending on the boundary applied to the energy supply system, as well as the best indicator of energy and material demands and flows.

$$\Phi_{uij}^{pro} + \Phi_{uij}^{pur} - \Phi_{uij}^{con} - \Phi_{uij}^{sel} - \Phi_{uij}^{was} = \alpha_{ij} \Phi_{uij}^{dem} \quad (5-16)$$

$$\alpha_{min} \leq \alpha_{ij} \leq \alpha_{max} \quad (5-17)$$

Equation 5-14 introduces the production correction factor,  $\alpha_{ij}$ , which as a decision variable relaxes the OMSES problem. It is allowed herein that the mine, from its nominal production capacity ( $\alpha_{ij} = 1$ ), can choose to vary it within a range (Equation 5-17), allocating perhaps a higher production rate to a specific hour, shift, or month. In practice, this allows the mine to shift load while complying with specific targets of annual production, providing that the elements not present in the ESS can vary the operating point within the required margin.

Additional constraints may be: the incapacity to increase production during the periods between shifts (Equation 5-18); annual production targets (Equation 5-19); or monthly production targets (Equation 5-20).

$$\alpha_{ij} = 1 \quad \forall (i, j) \notin t_{shift} \quad (5-18)$$

$$\sum_{ij} \alpha_{ij} \cdot n_i \cdot n_j = 365 \quad (5-19)$$

$$\sum_j \alpha_{ij} \cdot n_j = 24 \quad (5-20)$$

Production rate variation not only can be used in OMSES, but also while simulating and optimally controlling the ESS in the receding horizon, requiring a higher computational effort, but increasing the capacity of the controller to reduce operation costs, especially in the presence of fluctuating hourly energy prices or demand charges. Positive (load increasing) or negative (load shedding) variations may involve the use of the corresponding priority in equipment shedding and penalty costs to achieve more practical results (Bungener et al., 2015).

## **5.7 Conclusion**

This chapter, together with Section 2.4, has covered the characteristics of MPC that make it a suitable control approach for networked systems, such as ESS, mainly drawing from the work of other authors. Control and scheduling of OMSES' optimal designs seemed a reasonable next step to evaluate whether the optimal system design and the original operation schedule remain optimal, near-optimal, or feasible at all, under more realistic operating conditions.

An approach has been developed to extend MPC's formulation so that the capacity of the subsystems, as well as the production plan of the mine, could be varied to ensure feasibility while minimizing the total annual costs. Dynamic redesign is applied in Chapter 10, while production plan variation is left for future work.

# Chapter 6

## 6 Development of Long Term OMSES

So far the problem of optimal allocation of energy resources has been solved in two different time frames: the first considering one typical year, where the design and the operation were simultaneously optimized, and the second considering a control problem defined over a number of hours of operation in the immediate future. For mining, in contrast to production engineering, considering equal energy demands from one year to the next may not be an appropriate assumption or a justifiable simplification. In other cases, the interannual variation is related to the system's imposed evolution, such as the progressive implementation of energy efficiency measures. In short, this chapter addresses the OMSES problem defined when considering interannual demands variations. Further support documentation for this chapter is included in Appendix 8.

### 6.1 Comparison with Other Optimization Tools with Interannual System Variation

Some optimization tools exist today regarding energy systems optimization, although not all of them allow for interannual variation of demands and design. The general approach consists of defining a typical year for energy demands and, when considered, typical wind speed and solar radiation profiles. Given these, the optimal system's design and typical operation are calculated. This approach is used, for example, by HOMER (Lambert et al., 2006), DER-CAM (Stadler et al., 2008), and EAM (Engica Technology Systems International website, 2015). OMSES has the

same capability (Carvalho et al., 2014b). For a detailed review and comparison of the alternatives, see Mendes et al. (2011).

EnerGIS and TURN (Samsatli and Jennings, 2013) identify the optimal design for typical consumer demand, but allow for spatial distribution of individual consumers and energy sources, involving also the optimization of interconnecting energy grids.

In particular, TURN is also designed to consider interannual demand variations and system design evolution (Samsatli and Jennings, 2013). It does this by defining a temporal framework with various levels of definition, as in DER-CAM and OMSES. However, in addition to typical days divided into hourly intervals (or several intervals with variable duration within each day), TURN uses longer time periods (years) as attributes for the problem variables, such as energy flows and, more importantly, equipment and infrastructure installed, or a conservation measure (e.g., building envelope retrofit), on a yearly basis.

OMSES is here extended to include years as an added time attribute, despite being closer to DER-CAM in its economic assessment of the problem (considering annuitized investment costs, as opposed to TURN, which considers a constant, arbitrary weight equal for all years in the time horizon). The net present cost of future investment is considered in the new framework, as well as fuel cost inflation and O&M increase due to equipment degradation. This is different from TURN's approach of establishing technological retirement, which could make more sense for energy systems of a greater lifespan than those for mines (at least at project stage), which is generally lower than 20 years.

## 6.2 Extended Formulation Using a Static Algorithm

This section includes the formulation that makes possible the calculation of the optimal design for the case of a mine with interannual demand evolution.

### 6.2.1 Decision Variables and Scale of the Problem

OMSES's basic formulation is modified to accommodate the new time level: years. It can be seen in Eq. 6-1 that  $T$  is now the time horizon, which has grown in attributes, being  $y$  the index for years.

$$u \in U, v \in V, (i, j, y) \in T \quad (6-1)$$

Following the basic formulation, a quantity  $x$  concerning operational strategy is designated by  $x_{yij}$ , corresponding to the  $j^{\text{th}}$  sampling time interval of the  $i^{\text{th}}$  representative day of the  $y^{\text{th}}$  year. If  $n_i$  is the number of  $i$  type days per year, the annual operational intervals for the year  $y$  for the  $j^{\text{th}}$  sampling time on the  $i^{\text{th}}$  representative day will be:

$$t_{ij} = n_i \cdot n_j \cdot n_y \quad (6-2)$$

Following the same notation, the number of years that every period  $y$  contains is  $n_y$ . An example for the annual periods would be three multi-year periods, with 5, 5, and 10 years each. In this example,  $y$  takes values from the set  $\{1,2,3\}$ , and  $n_y$  from  $\{5,5,10\}$  respectively.

### 6.2.2 Objective Function

The consideration of multi-annual periods introduces further complexity in the calculation of the present worth of future investments and operation costs. Several strategies have been suggested for long term investment optimization in energy systems. In addition to TURN, which does not explicitly consider present worth nor annuitization, other works have proposed the use of

discounted present worth, such as the recent works by Koltsaklis et al. (2015) and Georgiou (2015). These two works use both annuitization and present worth calculation for the future series of investments, as well as present worth for the operation and maintenance. The question arises of whether annuitization makes sense when the life of the equipment considered (or the useful life for the mine) is comparable to the planned investment. In both these studies, the plants and the infrastructure considered have operating lives of around 40 years, while the planning horizon consist of 15 years (Koltsaklis et al. 2015) and 10 years (Georgiou 2015). In the case of a mining operation, such method considered for the investment will significantly reduce the investment weight when both investment and the series of annual operation costs are discounted and summed throughout the life of the mine.

For the reason explained, the approach followed to calculate the cost function is to use discounted costs for all the monetary flows throughout the life of the mine. The discounting process may consider the inflation rate ( $j$ ) to correct discount rates. Inflation accounts for the rise in costs of a commodity over time (Haberl, 1993). In the present work, equipment and energy inflate at different rates,  $j_r$  and  $j_e$  respectively.

The present cost of all fixed costs is expressed by:

$$C_{fix} = (1 + k_{ic}) \cdot \sum_y (k_{pw,y} \cdot \sum_v \mu_{vy} \cdot C_{inv,v}) \quad (6-3)$$

$$k_{pw,y} = f(i'_d, L_y) = 1/(1 + i'_d)^{(L_y-1)} \quad (6-4)$$

$$i'_d = (i_d - j_r)/(1 + j_r) \quad (6-5)$$

$$L_y = \sum_{\bar{y}=1}^{y-1} n_{\bar{y}} \quad (6-6)$$

$i_d$  is the discount rate. The coefficient  $k_{ic}$  refers to installation, engineering, etc. costs (Section 3.2.1).  $\mu_{vy}$  and  $C_{inv,v}$  are, respectively, the number of pieces of equipment installed in the

corresponding year ( $y$ ), and the capital cost of each piece of technology ( $v$ ). The present cost of future investment is calculated through  $k_{pw,y}$ , which uses the corrected discount rate ( $i'_d$ ) and the period passed since the production starts,  $L_y$ . For simplicity, the costs of storage and infrastructure have been omitted, but these could be generalized from Eq. 4-12, if required. Equations 6-4 through 6-6 have been formulated in agreement with Haberl (1993).

The annual variable cost is then expressed as follows:

$$C_{var} = \sum_{ijy} (C_{e,ijy} + \sum_v c_{O\&M,v} \cdot \Pi_{vijy|\hat{y}}) \cdot t_{ijy} \quad (6-7)$$

$$\Pi_{vijy|\hat{y}} = k_{O\&M,\hat{y}} \cdot \Pi_{vijy|1} + k_{O\&M,\hat{y}-1} \cdot \Pi_{vijy|2} + \dots + k_{O\&M,1} \cdot \Pi_{vijy|\hat{y}} \quad (6-8)$$

where  $C_{e,ijy}$  is the hourly energy cost arising from diesel, biomass, and electricity consumption,  $c_{O\&M,v}$  is the operating cost for the technology  $v$ ,  $\Pi_{vijy|\hat{y}}$  is the produced utility in a given time (year  $y$ , day  $i$ , hour  $j$ ) by the technology  $v$  installed at the year  $\hat{y}$ . The term  $k_{O\&M,\hat{y}}$  reflects the degradation factor, which progressively increases the operating and maintenance cost from the time the technology is installed. For simplicity, demand charges are omitted from the formulation. The cost of energy is adjusted to inflation ( $j_e$ ) according to Haberl (1993).

$$c_{e,ijy} = \sum_u k_{pw,y} \cdot p_{uij} \cdot k_{EIR,y} \cdot \Phi_{uij}^{pur} \quad (6-9)$$

$$i''_d = (i_d - j_e) / (1 + j_e) \quad (6-10)$$

$$k_{EIR,y} = \sum_{m=n_{y0}}^{n_{yf}} (1 + j_e)^m \quad (6-11)$$

$$n_{y0} = 1 + \sum_{\bar{y}=1}^{y-1} n_{\bar{y}} \quad (6-12)$$

$$n_{yf} = n_{y0} + n_y - 1 \quad (6-13)$$

Equation 6-10 assumes the use of  $i''_d$  to calculate the capital recovery factor  $k_{pw,y}$ . The energy inflation rate multiplier,  $k_{EIR,y}$ , is the cumulative sum of the inflation for every  $m^{th}$  year of the

period considered (Equation 6-11). For the first multi-annual period ( $y=1$ ), the sum is carried out for  $m= n_{10}=1$  to  $m=n_{1f}=n_1$ ; for the second period ( $y=2$ )  $n_{20}=1+ n_1$  and  $n_{2f}= n_{20} +n_2-1=n_1+n_2$ . Equations 6-12 and 6-13 generalize these calculations.

### **6.3 A suggestion for an Extended Formulation Using a Dynamic Algorithm**

The proposed algorithm to design more robust, long term design solutions involves the combination of the interannual varying demand formulation, and the simulation of each year subsequently, updating the design solution calculated using the extended MPC dynamic design problem. The approach is illustrated in Figure 6-1. The long term problem is solved in a receding horizon, but after each time, that problem is constrained with the more robust design for every given year obtained with MPC formulation. The approach is similar to what Goodwin et al. (2008) and Goodwin et al. (2006) propose for the problem of long term planning optimization. The distinction between investment and operating costs is what the present thesis identifies as a potential improvement in mine planning regarding the energy supply system when implemented as a dynamic optimization programming problem, although this method has not been implemented in this thesis.

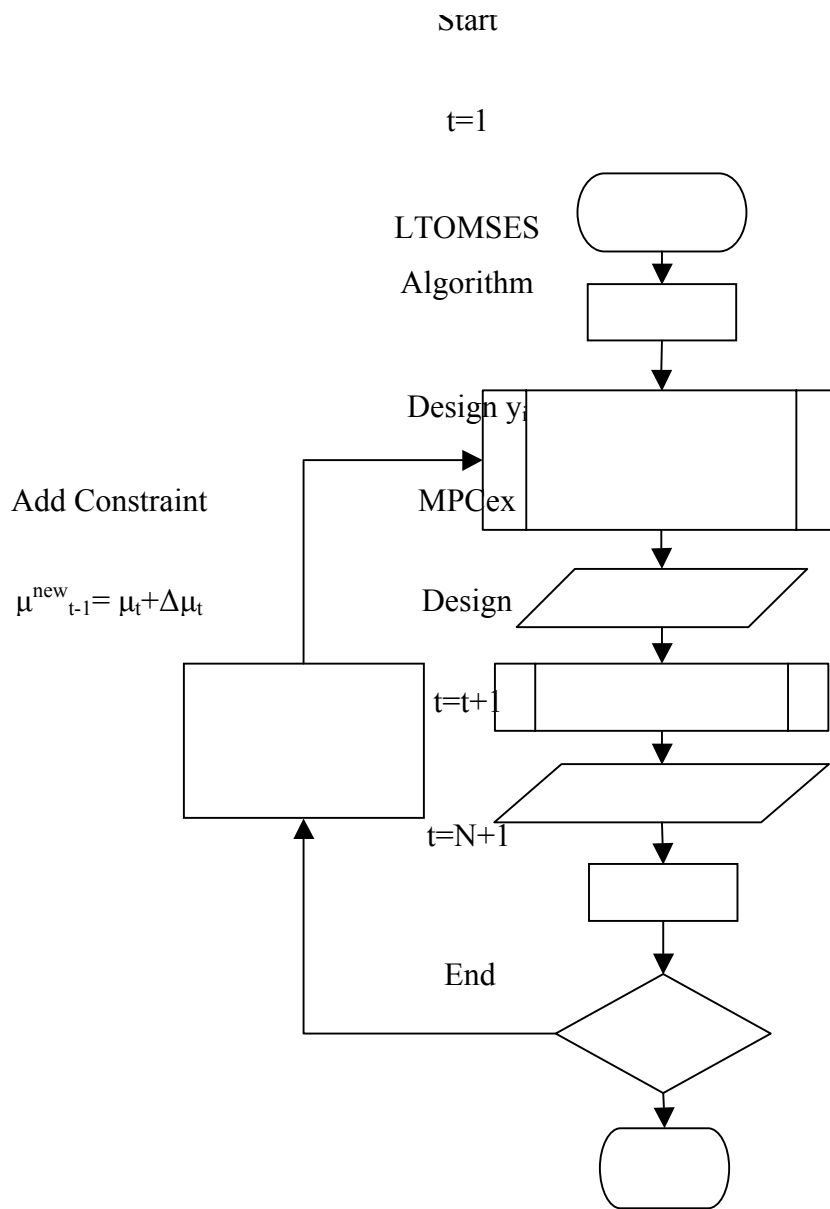


Figure 6-1 Long term OMSES (LTOMSES) with dynamic feedback

# Chapter 7

## 7 Remote Mines and Biomass

This chapter describes how OMSES is used to calculate the optimal design and operation of a remote open pit mine in Northern Ontario. The basic formulation is upgraded with energy storage and the addition of biomass to the set of available energy sources. Further features in this chapter include the production of diesel through biomass gasification and subsequent liquid fuel synthesis to meet the mine's diesel demand, the consideration of demand charges minimization through a novel approach for the considered jurisdiction, and the analysis of how the distance separating the mine site and the electricity network influences the optimal ESS.

The content of this chapter was first published in (Carvalho et al., 2014b).

### 7.1 Mine Description

Victor Mine is an open pit diamond mine (52.82°N, 83.90°W) situated 90 kilometers west from Attawapiskat, a community in Northern Ontario (Figure 7-1). According to De Beers Canada (2014), the mine can only be accessed by airplane for all but six weeks of the year, a period during which a seasonal ice road allows the mine to be supplied with equipment and materials needed for the next twelve months of operation.

The mine is connected to a privately-owned electricity transmission line, spanning 270 kilometers, from Moosonee (ON) to Attawapiskat (Five Nations Energy Inc. website, 2015). From the latter, a 115kV line runs to the mine site, with an estimated capacity of 20 MVA. On-site emergency diesel generators can supply up to 7.8 MVA (Powertel website, 2015). Diesel is

delivered to the mine site while the ice road is available and is stored in tanks. Other fuels are currently used in the operations, but in a quantity negligible for the purpose of this study (De Beers, 2014).

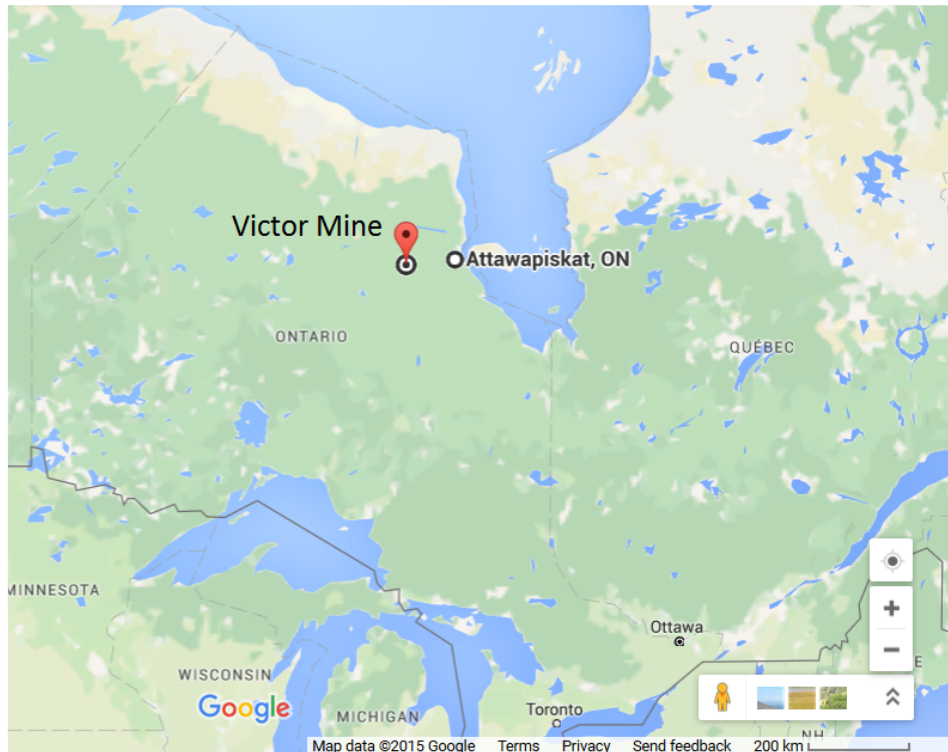


Figure 7-1 Victor Diamond Mine location (source: Google)

Ontario is known to hold significant peat resources which, in addition to horticultural uses, can also be processed to obtain synthetic fuels (Gleeson et al., 2006). Peat can be subject to transformations such as gasification and the Fischer-Tropsch process (Chapter 4), which can be used as a substitute for natural gas and diesel with moderate modification of the equipment being fueled. This case study explores the use of locally available peat that could complement electricity and imported diesel in the search for more economic alternatives than the conventional energy supply.

## 7.2 Mine Demands Characterization

The excavation of open pit mines (surface mining) is typically developed by diesel-hydraulic shovels with diesel fuelled trucks carrying both ore and waste. The materials excavated are later processed in several stages in which electricity is intensively used in operations such as, for example, crushing, milling, fluids pumping, and transporting solid materials on conveyor belts. Examples of heating and cooling demands in the mine include process steam and air conditioning of the existing facilities. A summary of the demands is briefly included in the following, although a more detailed description is included in Appendix 2.

Electricity and diesel consumption data from a real operation were available (De Beers Canada 2010; Shields 2013). In order to represent one operational year, the optimization model utilized 12 representative days (one 24-hour day per month). Demand data was taken from Carvalho and Millar (2012): 119,730 MWh/year of electricity, 2356 MWh/year of heat, 354 MWh/year of cooling, and 102,667 MWh/year of diesel. Total and mean energy demands are presented in Table 7-1.

**Table 7-1 Remote open pit mine energy demands, per representative day**

Day Type	$n_i$ (days/yr)	Heating demand		Cooling demand		Diesel demand		Electricity demand	
		Total MWh/day	Mean MW	Total MWh/day	Mean MW	Total MWh/day	Mean MW	Total MWh/day	Mean MW
January	31	10.54	0.44	0	0	386.55	16.11	364.97	15.21
February	28	9.64	0.40	0	0	413.34	17.22	372.67	15.53
March	31	9.37	0.39	0	0	298.88	12.45	315.76	14.35
April	30	6.58	0.27	0	0	236.86	9.87	326.55	13.61
May	31	4.85	0.20	0	0	232.20	9.67	309.83	12.91
June	30	3.89	0.16	1.80	0.16	212.24	8.84	278.22	11.59
July	31	3.22	0.13	5.41	0.32	224.22	9.34	297.37	12.39
August	31	3.43	0.14	4.25	0.27	224.88	9.37	293.89	12.25
September	30	4.27	0.18	0	0	241.82	10.07	326.55	13.61
October	31	5.34	0.22	0	0	249.54	10.40	316.96	13.21
November	30	7.20	0.30	0	0	277.44	11.56	369.53	15.40
December	31	9.30	0.39	0	0	385.20	16.05	367.59	15.32
		MWh/yr	MW	MWh/yr	MW	MWh/yr	MW	MWh/yr	MW
Year	365	2356	0.27	354	0.25	102,667	11.75	119,730	13.78

**Table 7-2 Selected equipment and matrix of production coefficients,  $K_{ij}$**

Equipment	Nominal Power (MW)	Capital Cost (10 <sup>3</sup> CAD)	O&M Cost (CAD/MWh)	Biomass	Electricity	Syngas	Diesel/Syndiesel	Steam	Hot Water	Cooling Water	Chilled Water	Ambient Air
Gasifier	3.0	3000	4.0	1.54		<b>1</b>		0.06				
Fischer-Tropsch	3.0	4000	6.0			1.25	<b>1</b>	0.60				
Gas Turbine	3.6	4000	7.5		<b>1</b>	3.03		0.59	0.66			
Diesel Turbine	3.6	4000	10.0		<b>1</b>		3.00	0.60	0.60			
Steam Turbine	5.6	2500	5.0		<b>1</b>			3.00	2.00			
Gas Engine	3.6	3600	10.0		<b>1</b>	2.44		0.70	0.41	0.33		
Diesel Engine	4.4	4400	5.0		<b>1</b>		2.27		0.80	0.20		
Steam Boiler	3.0	144	1.0			1.18		<b>1</b>				
Hot Water Boiler	3.9	150	1.0			1.22			<b>1</b>			
Biomass Boiler (HW)	2.0	200	4.0	1.25					<b>1</b>			
Biomass Boiler (VA)	3.5	492	4.0	1.40				<b>1</b>				
Electric Boiler	3.5	144	1.0		1.11				<b>1</b>			
Diesel Boiler	3.0	130	1.0				1.15		<b>1</b>			
Absorption Chiller*	1.5	280	5.0		0.01				1.36	2.36	<b>1</b>	
Mechanical Chiller	2.7	185	2.0		0.21					1.21	<b>1</b>	
Cooling Tower	5.0	82	5.0		0.02					1		<b>1</b>
VA-HW HX	5.0	50	1.0					1.1	<b>1</b>			
HW-CW HX	5.0	35	1.0						1.1	<b>1</b>		

\* Single Effect Absorption Chiller

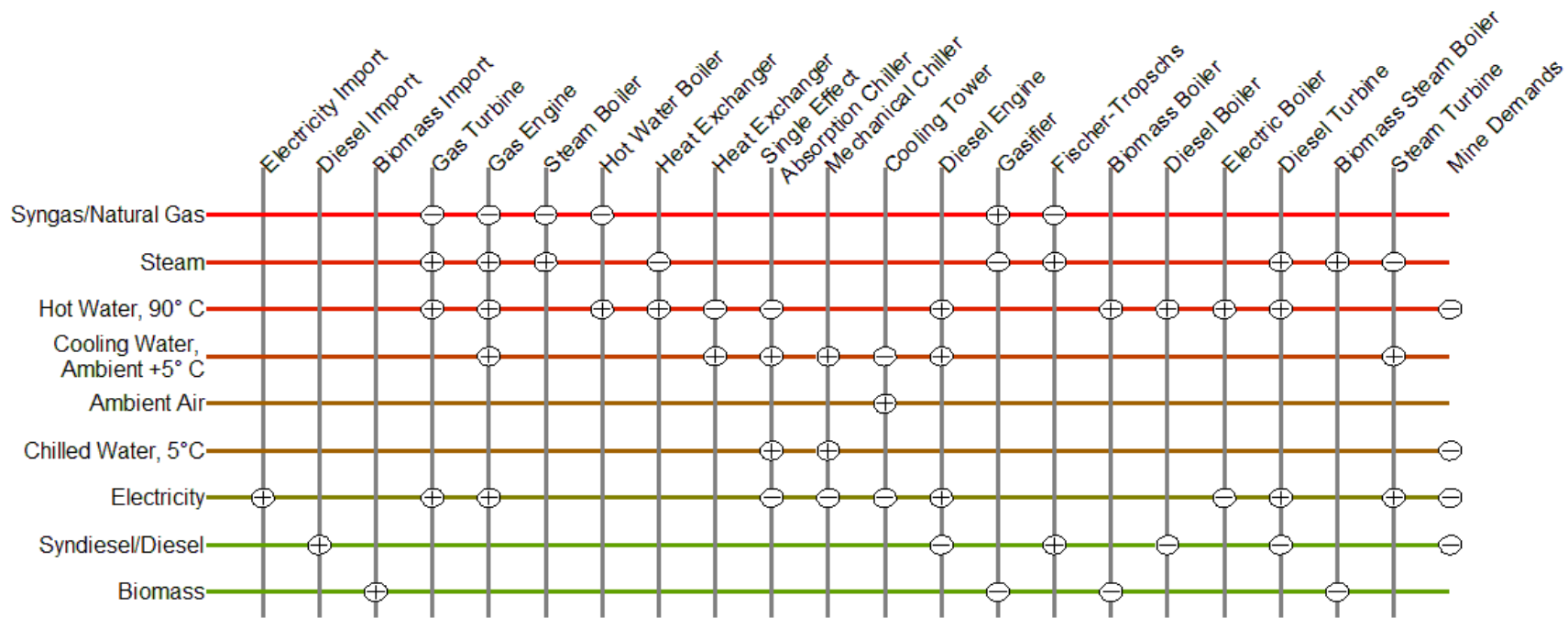


Figure 7-2 Superstructure illustrating all potential conversion pathways considered

Table 7-2 shows the information regarding the technology set from which OMSES selects the optimal combination. In the context of equipment performance, it should be noted that the coefficients of Table 7-2 correspond to design operation points. Nominal efficiencies can be obtained in a system when several pieces of equipment are run in parallel; this is assumed in this work following the approach of e.g., (Trapani and Millar, 2013). Thus, in order to meet increasing demand the system switches-on an additional unit. Once the optimal design and operation of the system is obtained, observation of the load factor of the optimal number of pieces of equipment can be used to select the appropriate size of each unit, and even the number of units, in order to select near-optimal solutions more practical. Rubio-Maya et al. (2011a) for example, model power, temperature, and exhaust gas mass flowrate output of an internal combustion engine as a function of the actual load (electrical), whereas Zhou et al. (2013) and Ren and Gao (2010) apply constant efficiencies. The same consideration regarding partial load operation applies to the remaining technologies included in this work. However, the rating of the equipment included could be reduced so that several units would have to be installed, and so the operation in partial load would be substituted by actuating units to increase the efficiency.

It should be noted that the coefficients listed in Table 7-2 reflect an assumption that, for example, the temperature of steam meets the needs of the technologies connected to this utility. Consequently, these coefficients present a simplification of reality in that a rather static thermodynamic condition is assumed.

The conservative superstructure is presented in Figure 7-2. The network includes three energy resources: electricity, diesel and biomass (peat). Through convenient transformations,

biomass can be used for heating purposes (using biomass boilers), electricity generation, or syndiesel production. Electricity can be generated with steam generation and subsequent use of steam turbines or through biomass gasification and subsequent operation of syngas fueled gas engines or gas turbines. Syngas can be further processed to obtain syndiesel for the operation of diesel fueled stationary engines (Diesel cycle or Brayton cycle) or to meet the diesel demand to operate trucks and other mobile equipment, including compressors, drill rigs, and engine driven pumps.

The nominal power, capital cost of the equipment, and operation and maintenance (O&M) costs estimates adopted in this study are also presented in Table 7-2. Within the formulation, such rates are adjustable to reflect case specific, or jurisdiction specific prices, but herein are presented in the specific context of the Ontario case study considered.

The capital cost estimates include transportation of equipment and installation. The lifetime of the system was considered to be 20 years and so the discount rate adopted, 10%, yields an annuitization factor of 0.12 year<sup>-1</sup>. The price for electricity purchased from the grid is the average for each hour of each month, based on the Hourly Ontario Energy Price (HOEP). It is assumed that the mine is considered an Ontario Class A customer (average demand above 5MW), although the installation of generators could lead to a notable reduction of the electricity purchased and a change to Class B classification. An example of Ontario's electricity price structure applied to a small consumer (Class B) in Appendix 1. Information about the provincial total power demand has been included in Appendix 2.

This study assumes that a connection point to the electricity transmission or distribution system is available for the mine site. While Victor Mine is actually grid connected, it is here

left for OMSES to find whether or not the deployment of a transmission line from the mine to the connection point is cost-effective. Consequently, within the polygeneration superstructure, the electric grid connection is itself considered as a supply technology that can be selected or not (connected or islanded) through a decision variable in the optimization procedure. Connection to the electric grid implies a connection cost,  $C_{inf,EE}$ , which comprises the cost of a transmission line from the existing 115 kV system (which may consider challenging development conditions such as line installation through peat lands and seasonal restrictions on working hours, as are present for the Northern Ontario case study considered), transformer costs and substation costs (including parallel redundancy, dynamic VAR compensation, and installation of emergency generators). For a mine site in Northern Ontario, depending on distance, the power line to site could cost up to CAD 15,000,000 and the substation, approximately CAD 20,000,000. For the scenario investigated, it is considered that the mine site is 100 km away from the 115 kV lines, and that the cost of transmission lines is 10,000 CAD/MW-km. Building the substation (including the transformer, security/backup equipment, foundation, switches) costs 1,000,000 CAD/MW, an estimate that includes connection redundancy for supply security reasons. All these economic values are derived mostly from Mason et al. (2012). Electric storage (lead-acid) is available at a cost of 190,000 CAD/MWh (Stadler et al., 2008).

The price of imported diesel was taken to be 130 CAD/MWh, which is approximately equivalent to 1.35 CAD/litre (Carvalho and Millar, 2012), the consumer pump price prevailing at the time of writing in Sudbury, Canada. The price of purpose grown solid biomass was 50 CAD/MWh, which is approximately equivalent to CAD 225 per tonne (at 16

MJ/kg, dry – an estimate that includes the cost of pelletizing and transportation) (Oo et al., 2012).

Peat was also considered at 30 CAD/MWh (equivalent to approximately 55 CAD/tonne). Herein a special case, specific to Northern Ontario, is made for the utilization of peat fuel, also considered biomass, which can be used in electricity generating stations and other facilities requiring a long-term assured supply of environmentally favorable, economically competitive and consistent quality fuel (Telford, 2009). One site in Northwestern Ontario, for example, contains over 155 million tonnes, which is sufficient to supply northern generating stations for more than 20 years (Telford, 2009).

### **7.3 Summary of Scenarios Considered**

Various scenarios were investigated to show the effect of adding different technologies as options for selection in the optimal mine site energy supply solution. The scenarios are defined by the availability of grid connection, the availability of biomass technologies, and a set of commodity prices. For all scenarios, natural gas imports are not considered due to the high cost of transportation to the mine site. In Figure 7-1, technologies using ‘gas’ are thus assumed to use of syngas.

Scenario 0 can be referred to as the “conventional scenario”, where biomass technology was prevented from being considered as an option and, therefore, diesel synthesis processes are not part of the solution. The mine is connected to the electric grid, with the connection point 100 km distant from the closest substation. Diesel imports were limited to 30,000 MWh, the maximum amount that can be transported along ice roads in February of each year.

Scenario 1 considers that it is possible, but not necessary, to connect the system to the closest substation, located 100 km away, with all the commodities and technologies available (including biomass gasification and syndiesel production); also, Scenario 1 implements the equation for demand charges (Equation 3-7 and Equations 3-19 through 3-23). In order to highlight the effect of the demand charging scheme, a modified formulation that fixes the value of electricity demand charges is presented as Scenario 1a. In Scenario 1a,  $\Phi_{peak}^{pur}$  is assigned a fixed value of 13 MW for the power consumed during the hours when demand charges are calculated.

Scenario 2 considers it technically impossible to build the electric connection. Consequently, the system operates in islanded mode. As in Scenario 1, all technologies are available including biomass imports. In Scenario 1 and 2, the technologies available are those contained in the conservative superstructure, including the possibility of energy storage (electricity or syngas or both). Again for logistical reasons, any biomass bunkering was limited to 400,000 MWh/year.

The Branch and Bound method from a commercial mathematical programming software package, Lingo 11.0 (Lindo Systems, 2007), was applied in the solution of these MILP problems. The size of the problem can be described by the number of decision variables. For scenario 1 this amounted to a total of 78388 variables, 1190 of them being integer variables. The solution was constrained by 51293 constraints in the decision variables. These numbers varied slightly from scenario to scenario. Generally, the runtime to solve the system with a personal computer with Intel i7 architecture was around 4 minutes and 40 seconds.

Results in the next section are confined to i) a report of the optimal mine site energy supply system configuration in terms of the number of units of the available technologies actually installed, and the total installed capacity of a technology, ii) annual sums of the energy imported onto or produced on the site in various forms, iii) capital costs associated with the equipment and the grid connection, if applicable, iv) annual costs for energy imported onto the site together with annuitized costs for the capital equipment.

Economic outcomes of the analyses can be principally assessed through comparison of the total annual cost figures, with the simultaneous understandings that each scenario meets the same demands for energy utility, in all forms, for every interval comprising the year modeled, and that the time value of money has been accommodated through the capital cost annuitization process. When comparing the total annual costs, lower, is better. Further comparisons between the figures for each of the scenarios may also be made to inform decision making. For example, if a mining operation, or other similar industrial venture, is capital constrained, the total capital expenditure required to realize one of the mine site energy supply solutions may be of over-riding importance.

**METHODOLOGICAL ASIDE:**

For each case study in this and the following five chapters, a ‘recipe sheet’ has been devised to compactly and concisely specify the mathematical program solved with a reference to the equations defined in Chapters 3 to 6. This serves as an intermediate link between the high level mathematical descriptions of OMSES (MPC-OMSES, LT-OMSES) and the computer code required to execute the solutions contained in Appendix 8.

**PROBLEM: REMOTE OPEN PIT MINE, NORTHERN ONTARIO  
ILLUSTRATION OF BASIC OMSES + BIOMASS**

<b>MINIMIZE</b>	<b>Equation</b>	<b>Inputs</b>
Total annual cost = Investment Cost	(3-4) (3-5) (3-6)	Section 7-2
+ Variable Cost	(4-12,13) storage	
+ Demand Charges	(3-7) (3-8)	Figure 3-3
<del>+ Support Revenues</del>		
<del>+ Penalties</del>		
<b>SUBJECT TO</b>		
Utility Energy Balance	(3-12,13,14)	Table 7-1
	(4-14) storage	Appendix 2
Equipment performance:		
- Conversion coefficients	(3-11)	Table 7-2
- Production limits	(3-9)	
o Maximum load	(3-10)	Table 7-2
<del>o Minimum load</del>		
Infrastructure Constraints	(3-17,18)	Scenario 2 – off grid
Storage Balance		
- Hourly	(4-15) to (4-23)	
<del>— Monthly</del>	<del>(4-22,23)</del>	
Scenario Based:		
- Resource Availability		
<del>o Wind</del>	<del>(4-5) (4-6)</del>	
o Biomass	(3-15,16)	Section 7-2
<del>— Spinning Reserve</del>	<del>(4-7) to (4-11)</del>	
<del>— Storage Charging/Discharging</del>		
- Demand Charge		Scenario 1
o Fixed		Scenario 1a
o Free		
- Terminal constraint on storage		
o Applied		
<del>o Not applied</del>		
<b>DECISION VARIABLES</b>		
Technologies Available		Scenario 0 – conventional technologies
Equipment Units		
- OMSES		
<del>— MPC-OMSES</del>		
<del>— LT-OMSES</del>		
Storage Size		
Grid Capacity		
Energy/Mass Flows		
- Typical days		
<del>— Rolling horizon</del>		
<del>Incremental Equipment units</del>	(5-6)	

## **7.4 Results**

Summaries of the optimal solutions for these scenarios are shown in Table 7-3. The precision of the values present in the Table, particularly financials and utility flows, are commensurate with the fact that the results are from a computer optimization process, and are not historical records of physically operating plants.

**Table 7-3 Optimal solutions for Scenarios 0, 1 and 2 – Diesel @ 130 CAD/MWh; Biomass (Peat) @ 30 CAD/MWh; Electricity: HOEP and GA considered**

	Scenario 0		Scenario 1a		Scenario 1		Scenario 2	
System Composition	Number (total power)							
Gasifier	0 (0 MW)		5 (15 MW)		5 (15 MW)		9 (27 MW)	
Fischer-Tropsch	0 (0 MW)		4 (12 MW)		4 (12 MW)		0 (0 MW)	
Gas turbine	0 (0 MW)							
Diesel turbine	0 (0 MW)							
Steam turbine	0 (0 MW)		1 (5.6 MW)		2 (11.2 MW)		1 (5.6 MW)	
Gas engine	0 (0 MW)		0 (0 MW)		0 (0 MW)		3 (10.8 MW)	
Diesel engine	2 (8.8 MW)		0 (0 MW)		0 (0 MW)		0 (0 MW)	
Steam boiler	0 (0 MW)							
Hot Water Boiler	0 (0 MW)							
Biomass boiler (HW)	0 (0 MW)							
Biomass boiler (VA)	0 (0 MW)		0 (0 MW)		7 (24.5 MW)		3 (10.5 MW)	
Electric boiler	1 (3.5 MW)		0 (0 MW)		0 (0 MW)		0 (0 MW)	
Diesel boiler	0 (0 MW)		0 (0 MW)		1 (3 MW)		1 (3 MW)	
Single Effect Abs Chiller	1 (1.5 MW)		0 (0 MW)		0 (0 MW)		1 (1.5 MW)	
Mechanical Chiller	0 (0 MW)		1 (2.7 MW)		1 (2.7 MW)		0 (0 MW)	
Cooling Tower	2 (10 MW)		1 (5 MW)		5 (25 MW)		4 (20 MW)	
VA-HW HX	0 (0 MW)		1 (5 MW)		1 (5 MW)		0 (0 MW)	
HW-CW HX	2 (10 MW)		0 (0 MW)		0 (0 MW)		1 (5 MW)	
Electricity connection capacity	15.79 MW		13.73 MW		13.52 MW		0	
Electricity storage	15.27 MWh		2.10 MWh		7.3 MWh		0	
Syngas storage	0		0		0		0	
Imported electricity	120,632 MWh/yr		105,134 MWh/yr		102,424 MWh/yr		--	
Imported diesel	108,364 MWh/yr		9,914 MWh/yr		10,089 MWh/yr		102,679 MWh/yr	
Imported biomass	--		178,548 MWh/yr		190,892 MWh/yr		399,493 MWh/yr	
Production of syngas	--		115,940 MWh/yr		116,971 MWh/yr		227,643 MWh/yr	
Production of syndiesel	--		92,752 MWh/yr		93,577 MWh/yr		--	
Capital cost of system	CAD	14,214,130.97	CAD	39,445,997.26	CAD	47,943,215.59	CAD	48,931,350.00
Connection to the electric grid	CAD	31,578,172.76	CAD	27,456,709.91	CAD	27,047,459.90	CAD	-
Annual cost of imported electricity	CAD/yr	4,347,118.85	CAD/yr	6,794,944.45	CAD/yr	3,471,087.06	CAD/yr	-
Annual cost of imported diesel	CAD/yr	14,087,316.74	CAD /yr	1,288,778.40	CAD/yr	1,311,613.19	CAD/yr	13,348,256.14
Annual cost of imported biomass	CAD/yr	-	CAD/yr	5,356,446.48	CAD/yr	5,726,765.08	CAD/yr	11,984,790.69
Annual O&M	CAD/yr	33,139.52	CAD/yr	1,255,926.50	CAD/yr	1,341,529.94	CAD/yr	2,769,403.01
Annuitized cost of equipment*	CAD/yr	5,570,864.06	CAD/yr	8,094,220.96	CAD/yr	9,063,794.96	CAD/yr	5,871,762.00
Total annual cost	CAD/yr	24,038,439.17	CAD/yr	22,790,316.80	CAD/yr	20,914,790.23	CAD/yr	33,974,211.84

\* Lifetime 20 years,  
Discount rate 10%

## 7.5 Discussion

### 7.5.1 Discussion of Specific Results for Optimal Mine Site Energy Supply

The implications are now discussed for each scenario and its corresponding optimal configuration and operation. The three scenarios can be considered as a reasonable evolution from a conventional or *BAU*, *Business as Usual*, scenario towards adoption of innovative configurations based on the use of biomass (Sterner, 2009).

Not one of the four scenarios should be considered the ‘best’. It must be appreciated that each column of results in Table 7-3 is the best (minimum total annual cost) under the set of special constraints that define the scenario. Thus, when interpreting the results for practical situations, the question that one should ask oneself is rather: *which scenario applies most closely to the circumstances at hand?*

Scenario 0 is of the type that occurs at most mine sites when gaseous fuels are not available. In these mines, diesel generators are installed to supply electricity to the mine as a main or back up source. The possibility of installing energy storage exists in Scenario 0 and the results for the optimal solution for this scenario include both a grid connection and electricity storage.

When biomass consumption and all technologies are available, in addition to an electric grid connection, Scenario 1 results in an optimal system which is distinct from Scenario 0. Biomass availability and hence price determines the solution, which favors selection of gas fired steam turbines over gas engines. In Scenario 1 the electric grid capacity does not reach the peak demand level and, like Scenario 0, electricity storage is included, but with half the previous capacity.

Figure 7-3 illustrates the price variations throughout the year. January and February have been included to illustrate cold months in which peak provincial demand occurs in the evening, when domestic demand for heating and a higher demand for illumination increase the HOEP to its maximum value. April represents a month of moderate power demand, before summer days bring an increasing demand for air conditioning, peaking generally in July, also represented. Higher provincial power demand during the central hours of the summer days causes the highest HOEP for the year considered, which can be also considered every year.

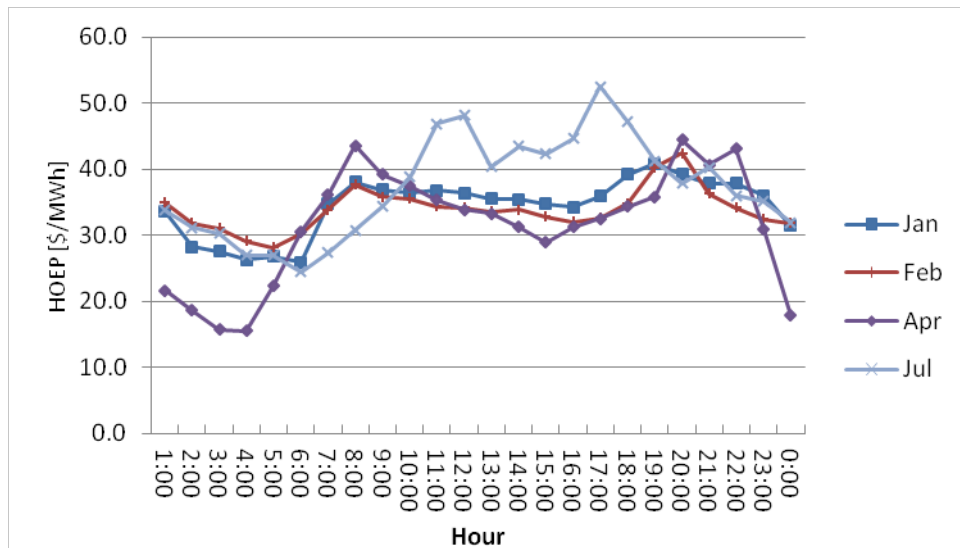


Figure 7-3 Scenario 1 Hourly Ontario Electricity Price (HOEP) in four different months

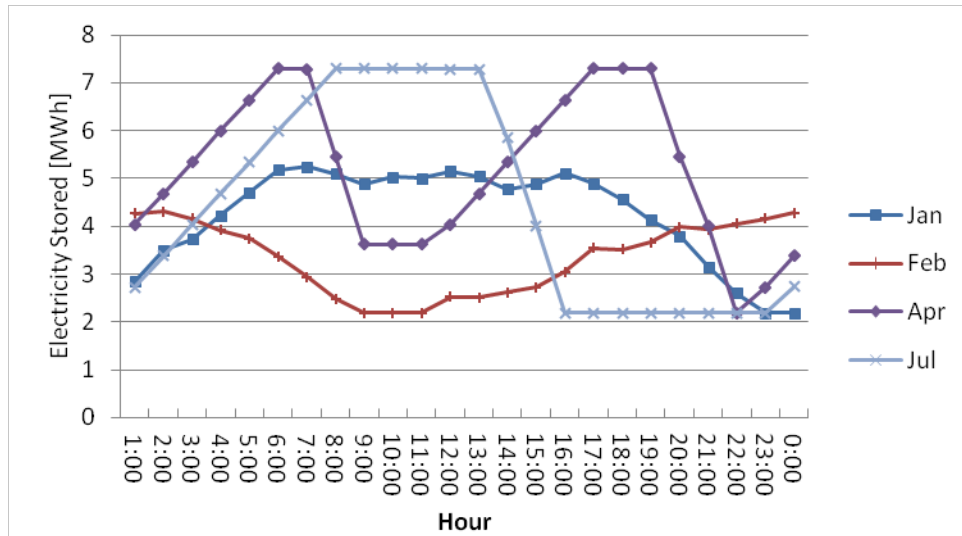


Figure 7-4 Scenario 1 Hourly electricity stored in four different months

The optimal mine site energy supply solution for Scenario 1 produces seasonal variations in the use of the electricity storage assets. In general, electricity is stored when the HOEP is lower (Figure 7-4, April), although other considerations may apply. In the summer months where there is appreciable price sensitivity due to Ontario’s GA demand charge allocation (Section 3.3.6), the optimal solution charges the electricity stores as rapidly as possible, to minimize electricity imports during the Ontario peak demand hours of the early afternoon (when air conditioning use in the Greater Toronto Area dominates the electricity system) (Figure 7-3). In non-peak demand months, the electricity storage system is utilized to balance off the system internally as cost sensitivity for the internal energy flows dominates rather than external price sensitivity.

As referred to earlier, according to the formulation, it is possible that the state of (dis-)charge of the electricity storage assets will have some bearing on the installed electricity storage capacity. For the months in which the maximum storage level or maximum SOC was not reached, illustrated by months January and February in Figure 7-4, the coupling (Equation 4-20) suffices without discrepancies in transitions between months having any effect within the cost minimization function. No constraint defining the initial state of charge at the beginning of the year is

necessary. Where the full range of the electricity storage may be cycled within a typical day of a month (e.g., months April and July, Figure 7-4) and when the charge state at the beginning of a month is close to maximum, coupling (Equation 4-20) may result in a higher installed electricity storage capacity. As the capital cost of storage relates to the installed capacity of electricity storage and so does appear in the cost function to be minimized, the state dependency may result in an increase of electrical storage capacity. However, in ‘worst-case’ sensitivity studies designed to explore this state dependency, no material increases of storage capacity were determined. The reason for this is that electricity pricing signals (Figure 7-3) are stronger determinants than any state dependency; for July, the overriding factor is demand charging.

In order to highlight the effect of the demand charges on electricity, Figure 7-5 compares the approach of implementing Equations 3-19 through 3-23. Scenario 1 considers that the mine is free to store or generate electricity on site by installing the appropriate technologies, and use it to reduce the imports of electricity during the hours in which demand charges for the mine are calculated. In contrast, Scenario 1a assumes that the mine is importing 13 MW during Ontario peak demand hours (Section 3.3.6), which fixes the amount paid for GA in the scenario. The approximate 48.9% electricity energy costs decrease from Scenario 1a to Scenario 1 (Table 7-3) corresponds to 8.2% less in annuitized capital cost, due to the load shedding effect. The savings in electricity costs are equivalent to 32 CAD/MWh applied to each MWh purchased. Figure 7-5 demonstrates that the former approach results in satisfactory and realistic operational modes of load shedding. Having the mine invested in enough capacity to generate electricity on site, this capacity can be used in other months where Ontario peak demand may take place actually such as June and August in summer, and even January or February in winter (see Appendix 3).

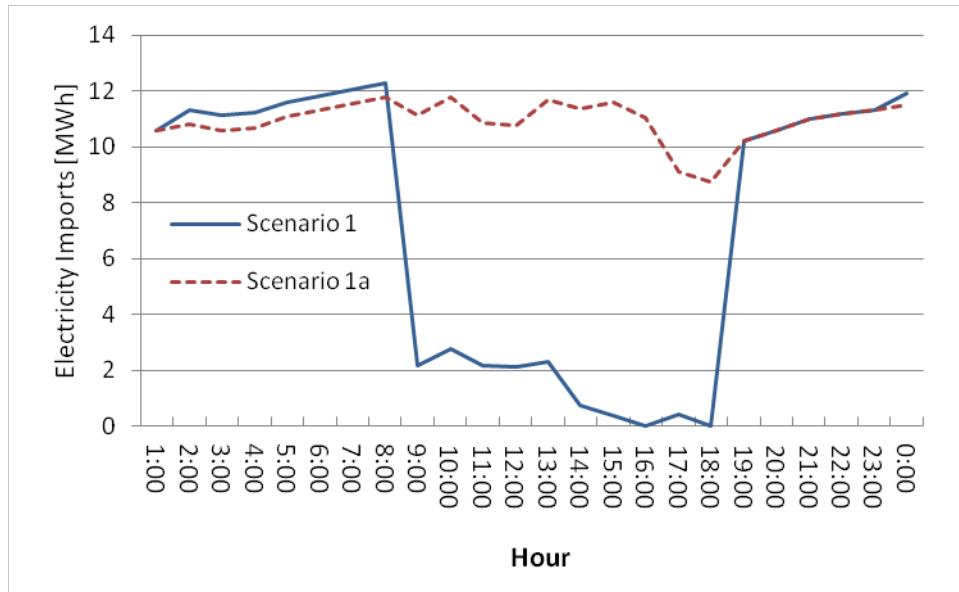


Figure 7-5 Scenario 1 Global Adjustment approach influence in July electricity imports

Compared with Scenario 0, the reduction in the annual cost in Scenario 1 is 16.7% (Table 7-3). This means that the conventional solution is not the cheapest option. The additional investment in equipment is recovered due to the biomass price, which is typical of the region and competitive, and because only 10% of the diesel required is imported, being the remaining diesel demand synthesized on-site.

Scenario 2 eliminates the possibility of an electric connection and therefore the operational strategy that forms part of the optimal mine site energy supply is quite distinct, as demand charge minimization within the objective function is no longer relevant. Electricity storage systems do not feature in the optimal mine site energy supply either as in Scenario 1, where the operational strategy that emerged was one that took advantage of occasional lower wholesale electricity prices (typically at night). For Scenario 2 all electricity is self-generated. For the conditions defined, the optimal mine site energy supply solution that emerged was based around an integrated gasification combined cycle (IGCC) plant comprising gas engines and steam turbines (for additional information about IGCC, see for example (Dincer and Zamfirescu, 2014)). This

result would clearly be different if biomass availability was restricted, or was available - but at a very high price.

High efficiencies of gas engines and the possibility of using high grade heat to generate steam introduced an unexpected, but understandable, result, illustrated by Figure 7-6 and Figure 7-7. These show steam flows for January (Figure 7-6) and July (Figure 7-7). In January, steam demand for electricity generation is supplied by recovering heat from gas engines and by the biomass boiler. In contrast, in July the biomass boilers only produce a relatively small amount in order to cover peak demands during the day, and the heat recovered from the gas engines supplies the steam base load. However, it is worthy to note that the steam turbine could be performing at undesirably low efficiency levels as a result of the assumption of constant efficiency, which could be easily restricted within the formulation using piece wise models (Negenborn, 2007).

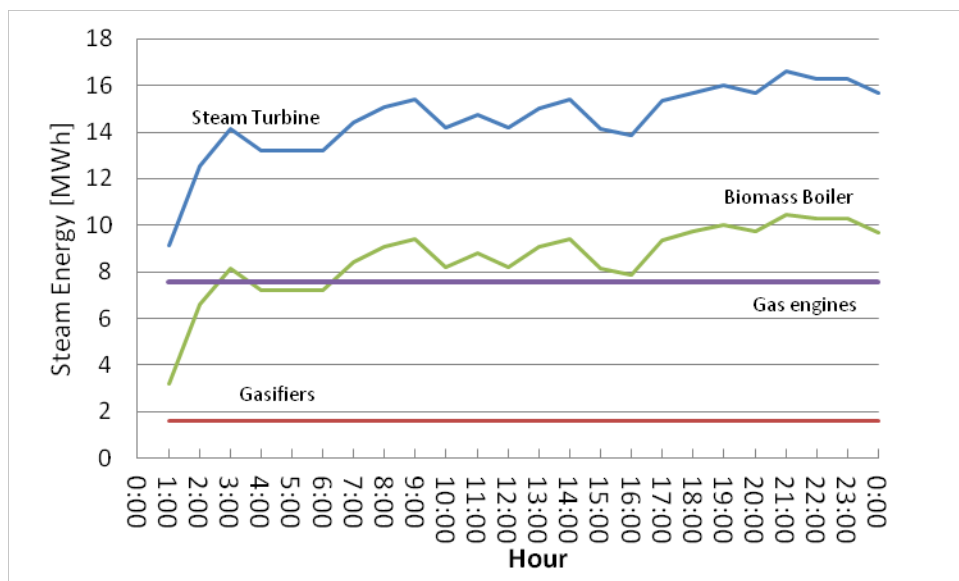


Figure 7-6 Steam flows in January period Scenario 2

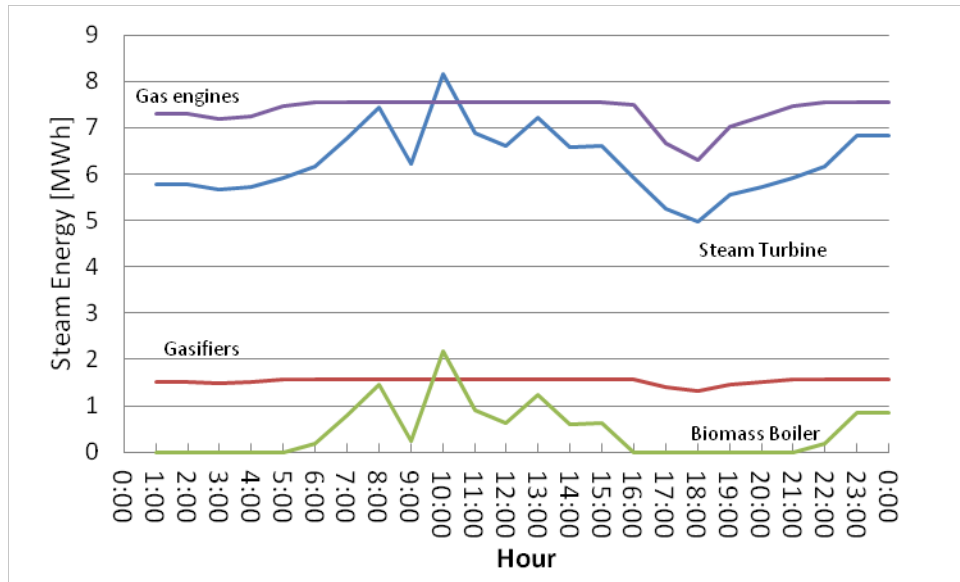


Figure 7-7 Steam flows in July period Scenario 2

Table 7-3 reports the biomass imported being very close to the maximum, meaning that bunkering capacity is heavily exhausted for Scenario 2. This suggests extended solutions if this limitation is removed, but these are not explored here. In other words, if electricity is generated from biomass, syndiesel cannot be produced. The conversion efficiency from biomass to electricity results 30% due to the bottoming steam cycle, slightly higher than the gasifier and the gas engine combined (26%). Total annual costs increased 65% in Scenario 2 compared with Scenario 1, which illustrates the advantage of Scenario 1’s grid connection.

### 7.5.2 Discussion of Further Trade-offs Investigated

The optimal mine site energy supply formulation may be used to investigate additional trade-offs through adjustment of scenario parameters, and the addition or removal of constraints. It is interesting to investigate whether a starting point exists for reduction in diesel procurement and consequent installation and operation of gasifiers coupled with FTS units (for self-production of syngas and syndiesel). The first study investigated on biomass conversion into diesel, including the use of biomass as a fuel to generate electricity at the conservative value of 50 CAD/MWh

(purpose grown biomass, instead of peat). Through repeated re-optimizations while increasing the diesel price, it was identified that when this increased to 150 CAD/MWh, the optimal solution installs one gasifier producing syngas and one Fischer-Tropsch unit along with electricity storage rated at 10 MWh; when the price increases to 200 CAD/MWh, the solution installs also a gas engine as well as gasifiers and FT units and electricity (10 MWh) and syngas (50 MWh) storage. The price for diesel considered throughout the work (130 CAD/MWh) is close to the breakeven point for gasifiers and FT plants when these are used exclusively to meet the mine's diesel demand.

It is also interesting to verify the biomass price starting point for the installation of gasifiers. In this case, the biomass procurement cost would be much reduced as the resource is close to, or on-site. At a price of 30 CAD/MWh for peat, maintaining all other prices constant, the re-optimized solution of the base case includes the purchase of biomass to feed gasifiers (4 units) and then Fischer-Tropsch (3 units) plants. This analysis assumed as well that biomass was exclusively used to produce syndiesel for the mobile plants and a price of 130 CAD/MWh for imported diesel.

Finally, the model was used to explore the impact of increasing connection distance, on the connection capacity, annualized cost and energy storage. As the connection distance increased, the optimal mine site energy supply solution was recomputed driven by a search for minimum total annual cost, all other things remaining equal. As expected, the minimum total annual cost increases with grid connection distance (Figure 7-8), principally driven by higher investment costs of the grid connection, however it is also interesting to examine how the optimal system design changes with connection distance. As distance increases, electricity storage capacity is

maintained as a beneficial technology until 500 km. Just beyond this range, the rating of the grid connection capacity reduces further but a connection is maintained to 1700 km.

The advantages of remaining connected to the grid even with long connection distances, with the increasing costs involved, arose from two factors: low HOEP and high GA. These were calculated considering the electricity consumed in a short period of time: in the worst case, 10 hours a day during the weekdays of three summer months, *i.e.*, 7% of the total hours of the year. This leads to the system consuming as much electricity from the grid as possible, providing that in all scenarios the energy system is able to generate its own electricity via thermal engines. Electricity or syngas storage, as well as internal generation capacity helps to avoid the entire, or at least the gross part of, GA charges, while for the remaining time the utility grid provides the maximum available power. Electricity storage is cost effective for connection distances below 500 km, and over 1700 km—when the system becomes islanded and electric storage is used for peak shaving.

Additionally, parametric analysis reveals the following trends:

- Syngas and electricity storage capacity did not feature in the various solutions simultaneously.
- Between connection distances of 800 and 1400 km biomass is gasified in order to generate sufficient supply for electricity generation and production of syndiesel.
- Four FT plants are installed for connection distances up to 800 km, and three FT plants are installed for further locations, until islanding at 1700km.
- For connection distances above 1400 km, the cost of generating syndiesel apparently increases until its market import price. This is an indirect consequence of higher cost of

levelized electricity (including connection), which encourages the alternative use of gas engines, which therefore reduces the annual available biomass import for syndiesel production. As an example, beyond 1700 km no FT plant is installed, but the annualized cost is almost the same as at 1400 km, where the optimal solution contains three FT plants (one FT is installed from 1500 to 1600 km).

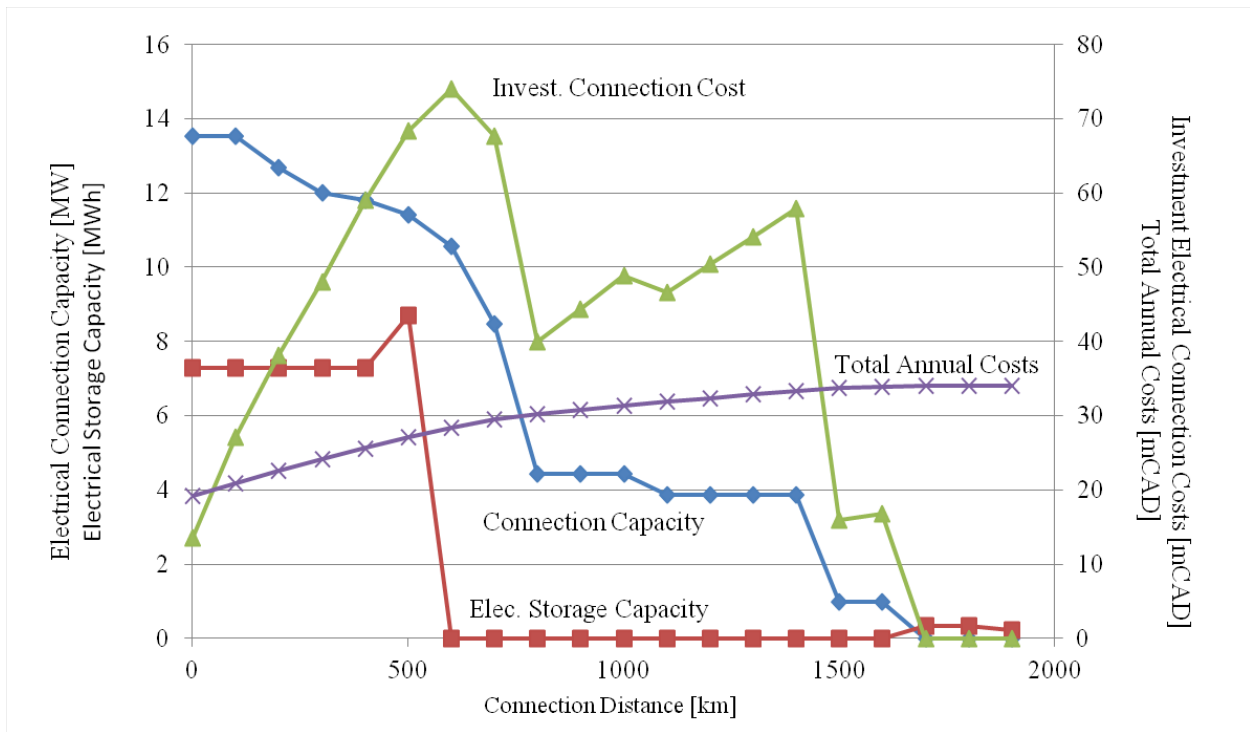


Figure 7-8 Connection distance parametrical analysis

### 7.5.3 Discussion of the Findings of this Study to General Energy Supply Optimization Studies

This study has identified scenarios in which more exotic technologies (such as FTS units or absorption chillers) are advantageous in polygeneration systems for mines. Determination of optimal mine site energy supply solutions of the nature set out in this chapter is of general relevance as its findings and methodologies will be applicable not only to any mine but also other large industrial users and remote communities, worldwide. Implementation of the

formulation can be scaled down to a public sector building or scaled up to consider a nation. The benefits obtained can be extended to any energy supply optimization study to reveal and understand: cost savings, carbon reduction, and security of energy supply.

The optimal mine site energy supply case study herein presented considers three levels of problems simultaneously: synthesis (which technologies), the design (rating or units installed) and the operation levels. At the synthesis level, it must be noted that the optimal configuration can be obtained not only for a new installation, but also for retrofitting to an existing solution.

The information requirements for the use of the optimal energy supply tool presented are the energy utility demands of the consumer center, herein exemplified for a mining operation, the available utilities and technologies, and the economic scenario (energy tariffs, price of utilities, existence of special government grant programs or incentives, and interest rates).

## **7.6 Conclusion**

This chapter has illustrated some of the features formulated for optimal mine site energy supply described in Chapter 3 and Chapter 4, such as:

- i) Consideration of partial electricity grid connection (in the case of finite import/export capacity limits governed by cable rating);
- ii) Avoidance of DC by reducing imports at times of peak demand for electrical power (when peaks are characterized by a weighting function). This advance represents a novel contribution in the field of DER;
- iii) Assimilation of complex electricity tariff arrangements (such as those in Ontario) into the formulation;

- iv) Use of biomass and related technologies, with the particular emphasis on peat resources available in Northern Ontario, with annual constraints on storage capacity;
- v) Integration of energy utility storage systems, exemplified by biomass and diesel bunkering and electricity and syngas storage.

Developments i), ii) and v) arose in facing the complexity of the mining operations, many times located in remote areas and account for some of the particularities of studying an open-pit mine in the province of Ontario.

The scenarios explored to illustrate the formulation permitted solutions that were different in character to emerge from the optimization process. The business-as-usual scenario of grid connection and diesel importation with locally available biomass resource utilization precluded was found to have total annual costs 15% more costly than the optimal solution that emerged when the local biomass resource was permitted to be utilized, where total annual costs included annuitization of the capital costs. In the latter scenario, the optimal system that emerged was one built around gasifiers and a steam turbine. A lower rating grid connection and electricity storage system also featured as part of a lower cost solution to balancing off the mine micro-grid at times of peak demand (even allowing for the complexities of the Ontario electricity demand charging system). The optimal mine site energy supply solution under these circumstances also included installation of a Fischer-Tropsch syndiesel production plant coupled to the gasifiers that reduced diesel imports to below 10% the business-as-usual scenario.

A final scenario that precluded an electrical grid connection returned an optimal mine site energy supply solution that was built around an integrated gasification combined cycle system utilizing gas engines and a steam turbine to cover heating and power utility demand with diesel being

imported. The total annual cost of this scenario was 63% higher than the ‘utilize local biomass’ scenario. The total capital costs for the scenarios were as follows: business-as-usual – CAD 45.7 million; utilize local biomass – CAD 74.9 million; islanded - CAD 48.9 million.

On the assumption that a regulatory system permitted all three scenarios as options, the choice of scenario for implementation would depend on the availability of capital. Without capital constraint, the ‘utilize local biomass’ scenario would be preferred as it leads to the lowest life cycle cost. With capital constraints, the business-as-usual scenario would prevail despite its higher lifecycle costs. If a grid connection was not possible, the islanded solution is the only choice.

The influence of the connection distance to the closest grid location was assessed, establishing how the optimal solution evolves towards an off-grid solution. This analysis is convenient due to the traditional remoteness of mine sites. Under biomass supply constraints, the mine would have to prioritize on electricity or syndiesel production. This behavior of the optimal solution significantly depends on the mine energy demands (not only configuration but also scale), although more research is required in order to obtain an insight into this dependence. It was verified that HOEP is sufficiently low to guarantee a connection to the electric grid and to compensate related costs, however presenting sufficient capacity for self-generation in order to avoid demand charges (Global Adjustment).

# Chapter 8

## 8 Mine Dewatering Systems Design and Control Optimization

Chapter 8 implements a methodology to optimally control the mine energy supply system using the dewatering system. The optimal design and operational plans are calculated using OMSES' extended formulation including storage. The operation of the optimal design is then simulated under more realistic price dynamics and under different control approaches for two interconnected pumps and reservoirs. These control approaches realistically illustrate the degree of communication achievable between pumping stages in the mine.

The content of this chapter was first published in (Romero et al., 2015c).

### 8.1 Demand Side Management in Underground Mines

A simplified representation of an underground mine dewatering system is shown in Figure 8-1. Dewatering pumps are located at different levels, some of them pumping water within the same level, some pumping toward higher levels and eventually to the surface. Initially, water is collected in the level sumps, from which it is delivered to pumping stations where a bigger reservoir or dam is located, before it is elevated. As Figure 8-1 shows, when the depth of the mine requires it, water is elevated in subsequent stages in different levels, until it reaches the surface, often being disposed into ponds.

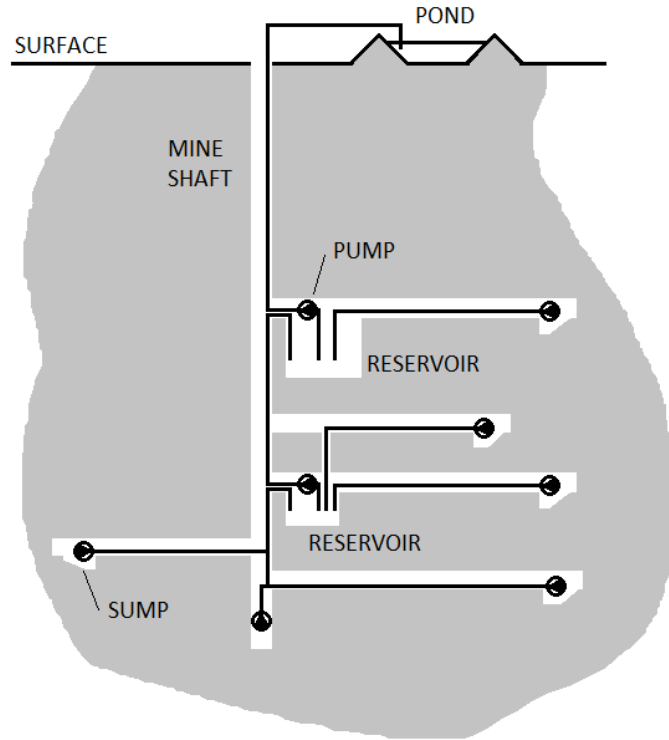


**Figure 8-1** Underground dewatering system

The ability of the dewatering to store water and defer pumping permits the application of load shifting (LS) and demand side management (DSM) strategies, especially in markets with tariffs that feature variable prices in different time intervals, for example, so-called *time of use* pricing (ToU), as well as *demand charges* (DC) (see Chapter 3). In order to apply DSM measures, the system operation needs to be optimized taking into account system design constraints, as well as the costs associated to the operation.

### **8.1.1 Water System's Optimization**

Optimization of pumping systems is not a new field of research, either for design or for operation purposes. Considerable effort has been expended on exploring and validating new control strategies during the last 20 years. This chapter introduces a methodology to assess the problem

of optimal design and operation of a water system subject to operational uncertainties, specifically regarding the case of a mine dewatering system.

Today, water system design does not receive as much attention from the academic community (Pulido-Calvo et al., 2006; H. Zhang et al., 2012; H. Zhang, 2011; Kurek and Ostfeld, 2013) as water system operation does (Zhuan and Xia, 2013; Vosloo et al., 2012; Van Staden et al., 2011; Chen and Coulbeck, 1991; du Plessis et al., 2013; J. Zhang and Xia, 2011; Yang and Børsting, 2010; Al-gwiaz et al., 2008; McCormick and Powell, 2003; Alvarado et al., 2011). When considered, design optimization focuses on pump arrangement and capacity (Pulido-Calvo et al., 2006; H. Zhang et al., 2012; H. Zhang, 2011) and, less frequently, on system components such as piping, valve selection or reservoir capacity (Kurek and Ostfeld, 2013). One of the reasons for this is that there are many robust and precise design tools available, such as Rossman (2000) or WaterCAD (2014) that render this design task straightforward.

Regarding design, Pulido-Calvo et al. (2006) optimize a fish farm pumping station design and operation schedule for one typical year of water demand to get the lowest total annual cost, including the corresponding investment and operation (electricity) costs. H. Zhang et al. (2012) optimize design of pump stations in a water system that has fixed reservoir size; H. Zhang (2011) does not optimize reservoir size but points out the advantage of larger reservoirs for greater cost savings through load shifting strategies. In the work presented by Kurek and Ostfeld (2013) a multi-objective optimization to a water distribution system is applied so that it selects the optimal reservoir size to obtain the least operation (pumping schedule) and investment cost, while assuring water quality. In these papers there is insufficient discussion, if any at all, on whether or not the optimal design will remain optimal when the reference, operating conditions are to

change. The system may be optimal for historical, known, conditions, but does it remain optimal in the face of future uncertainties?

There are many examples of pump operation scheduling, and these are generally cast as mathematical programming problems solved by means of one of many solver algorithms available (Genetic Algorithms, Particle Swarm Optimization, Branch and Bound Simplex, etc.) Examples of different approaches and applications can be found in several works (Zhuan and Xia, 2013; Vosloo et al., 2012; Van Staden et al., 2011; Chen and Coulbeck, 1991; du Plessis et al., 2013; J. Zhang and Xia, 2011; Yang and Børsting, 2010; Al-gwiaz et al., 2008; McCormick and Powell, 2003; Alvarado et al., 2011). Most of the approaches for these scheduling optimizations minimize operating costs based on ToU tariffs. Some also minimize the frequency of pump switching in a given interval of time (in fixed speed pumps repeated start-ups can cause overheating and excessive stress, that lead to premature failure). Demand Charges, which strictly depend on the power consumed by the system (a traditionally deterministic calculation based upon a defined tariff), can also be minimized. Fixed and variable speed pumps have been investigated in such studies, suggesting that variable speed pumps improve energy efficiency while load shifting can be either achieved with fixed or variable speed. Nevertheless, the optimality of the schedules calculated relies on existing, perhaps sub-optimal designs and, once again, they do not consider the effect of uncertain future operating conditions.

### **8.1.2 Water Systems Control Using MPC**

In recent years water system control has received attention, and more specifically optimal control. Model Predictive Control (Camacho and Bordons, 2004) is the preferred approach, for its ability to deal with system's constraints (pump capacity, reservoir limits, etc.) and to accommodate cost functions for either tracking purposes (e.g., to maintain water level or

flowrate) or simply to model operating costs. As repeated by Rossiter (2004), MPC also provides a control framework that is robust in systems with model and disturbances uncertainties. A MPC uses system models that normally do not require great precision or complexity to achieve successful control results.

Mine dewatering systems generally comprise several pumps associated with respective reservoirs at increasing levels. When it comes to the control of these systems, a centralized approach where all control actions are centrally computed and coordinated could be costly computationally, and in case of a control outage, the whole system will be affected. Given that dewatering systems are physically distributed a non-centralized MPC implementations was also considered. This way, the pumping of water will not stop completely even if there is a fault in the control system. Non-centralized control may be easier to implement physically in mines given the difficulty of deploying underground communication networks.

The idea behind non-centralized approaches is to divide the overall control problem into smaller components that are assigned to local controllers, also known as *agents*. The natural partition of the centralized control problem in this context is to consider that there is an agent for each tank (Figure 8-2), which controls the corresponding water level and governs the pumping of water out of the tank. In order to coordinate the control tasks of the different controllers, it is considered in this work that the agents may exchange some practical information related to the system and to other agents' operating state and planned actions by means of a communication network. The type and amount of information exchanged, if any, has to be defined according to practical criteria –pumps that discharge into other pumps' reservoirs may communicate – and taking into account the type of scheme used for the distribution of the centralized control problem, the action

of the later may consider the actions and intentions of the former. Figure 8-2 illustrates the proposed simplified scheme, with several pump levels exchanging water and information.

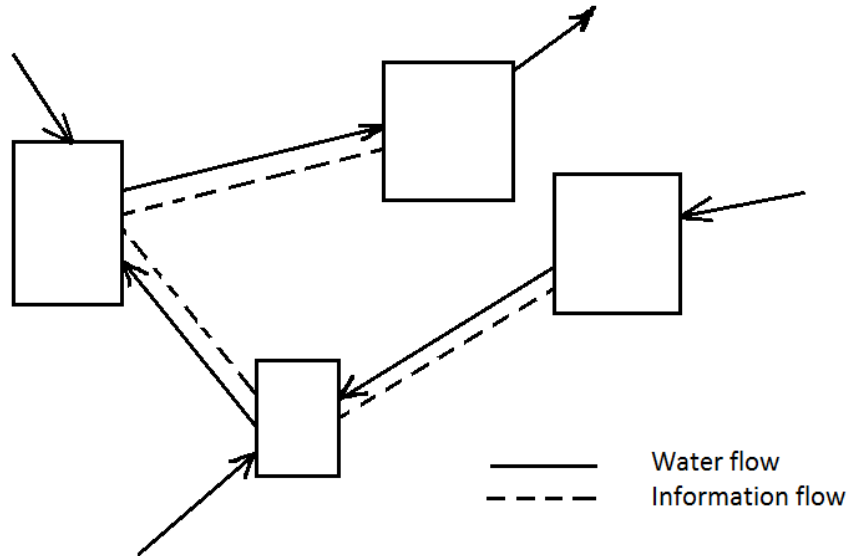


**Figure 8-2 Simple dewatering scheme; Arrows express direction of the flow. Each rectangle represents a reservoir and its pump station**

If complex systems are split into different control entities operating individually, while including some sort of communication, distributed and decentralized control can improve reliability and robustness of the overall system, reaching optimal or near optimal control. For further description of these approaches the reader is referred to Negenborn (2007) and Maestre and Negenborn (2014). Examples of MPC applied to water systems can be found in the recent literature (H. Zhang et al., 2012; H. Zhang, 2011; Middelberg et al., 2009). A case study of distributed control in water systems using different collaboration strategies among agents is presented in Alvarado et al. (2011).

In light of the reviewed literature, a lack of analysis of the complete optimization of energy systems has been found, especially those dealing with water systems. Attempts to link operation and design, but a good example can be found in Kookos and Perkins (2001). The methodology

proposed by Koolos and Perkins (2001), however, does not accommodate time-variant controllers, such as MPC, which is the approach considered in the present work.

Here, MPC is applied to a mine dewatering system, which has been initially optimized following the methodology used in Chapters 3 and 4. MPC deals with the existence of physical constraints and uncertain operation conditions of mining operations. The optimized design takes into account investment costs, ToU and DC. The latter is characterized statistically to account for the calculation methodology of Ontario electricity market (IESO, 2014) which is more sophisticated than most. MPC is used for the reasons already mentioned, but also permits investigation of DC's influence in the optimal design. The aim is to explore, using the approach taken by other authors, the gap between design optimization and optimal control of water systems as an example of ESS. This is a considered necessary and prior step that enables the generalization extension of MPC for the control of optimal mine site energy supply systems.

## **8.2 Design and Control Strategies Improving Traditional Methods**

Due to the natural variability, determining the actual water flow collected in mine sumps is challenging in advance of construction; however, it is not impossible to estimate it, with sufficient precision, to design safe and reliable dewatering systems and schedule the pumping.

The traditional approach for deciding upon underground dewatering system dam capacity is that they should store between 8 and 24 hours of water inflow at each dam without pumping. Pump discharge capacity at each level is designed to match the expected inflow. Normally, a higher capacity is installed to provide flexibility and backup pumps feature to increase safety in case of unexpectedly high inflows.

Underground mine pump operation is generally triggered by maximum and minimum water levels at each water reservoir (dams or sumps) where pumps are installed. The resulting pumping schedule can only be improved upon with deferred pumping strategies if enough storage and pumping capacity is available (H. Zhang, 2011; Vosloo et al., 2012). Regardless of the type of mine and pumping strategy, in case of emergency automatic signals activate pumps so that the mine environment is always properly dewatered.

### 8.2.1 Optimal Design

In the present work ‘design’ only affects the calculation of the dams’ capacity. The number of pumps, their arrangement, as well as the diameter and material of the pipe work can be capably left to common practice design. This consideration is based upon the fact that pump capacity is mainly determined on worst case scenario of pumping duty (high and constant inflows).

Optimized water reservoirs are calculated with the OMSES methodology assuming water inflows as an imposed utility mass flow *import* (see Chapter 3 and 4) for every tank. The system considered includes pumps as technologies, water and electricity as utilities, and water tanks as the only storage system. Dewatering needs, as well as electricity tariff, was characterized as though the dewatering system were the only energy system contemplated in the mine. Dewatering needs are treated as material flow utilities that interact with energy flow utilities by means of the pumps. Balance equations (constraints) in water and energy were implemented. Economic parameters of the problem include: the cost of building the dams, expressed in economic units per unit volume of storage capacity; the hourly electricity price; and the demand charges, calculated for individual hours of the year, as described in Chapter 3.

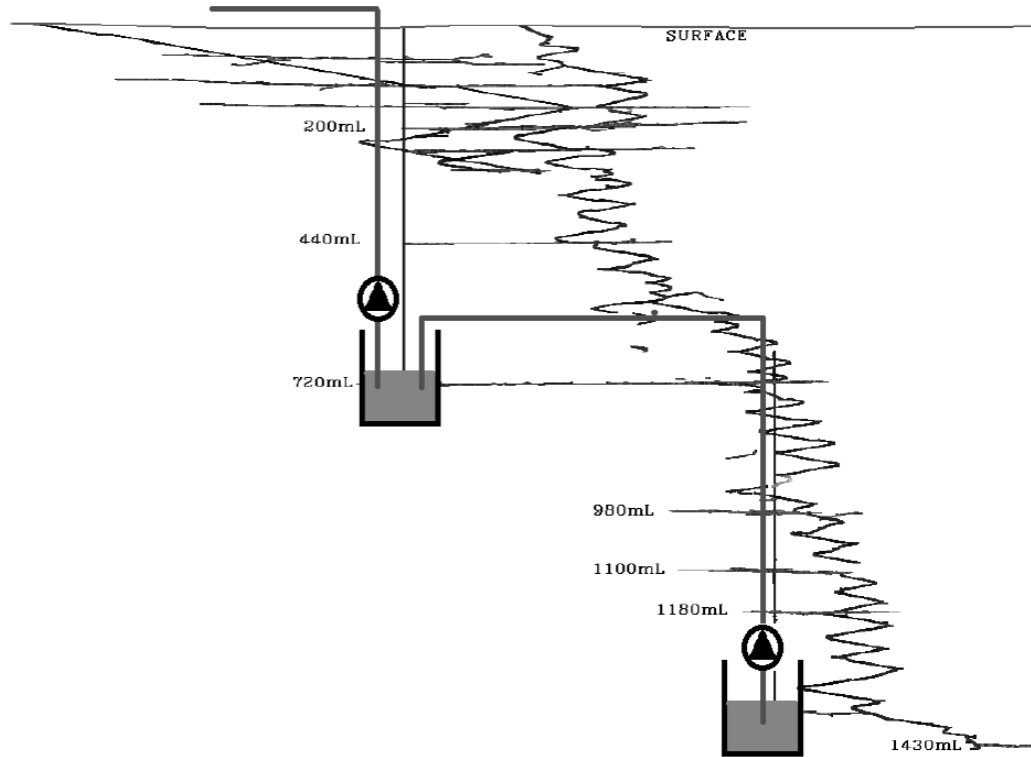


**Figure 8-3 Dewatering system with two lifting stages in an underground mine**

For illustrative purposes a complete dewatering system is split into two similar subsystems each comprising a pump and a reservoir (Figure 8-3). Pumps operate over the whole range of speeds admissible, leading to a corresponding range of discharge ( $\text{m}^3/\text{h}$ ), following H. Zhang (2011). Two pumps connected to their respective dams, or water reservoirs effect mine dewatering. The inflows are assumed known, as is the performance of the pumps (their relationship between flowrate and power consumed). Similarly, the hourly price of the electricity is also assumed known in advance. Consequently, the results will indicate a design conditioned by the expected environment in which it is going to operate.

One difference with previous models in the literature (H. Zhang, 2011) is the use of a linear approximation of the power-flowrate function for variable speed pumps, which is a reasonable approximation as will be explained in Section 8.4.3 and illustrated in Figure 8-10. In the case of

the design problem, the optimization problem remains linear; this is a desirable characteristic in terms of computational burden, and because the same model is used in the operation optimization problem, the coherency of the models permits direct comparison between both design and the operation problem results. It is also considered that there exist minimum operating flows given by, for instance, a requirement for a minimum rotational speed of the pump or minimum flow within the pipe work in order to avoid solids deposition. Maximum flow may be limited by the frequency converter or the requirement to avoid cavitations. Pumps can be activated or not, so the flow limits only apply when active.

### **8.2.2 Extensions for Robust Optimality in Operations**

In the present work the dewatering system is modeled as a zero-order dynamic system (no delays). In addition, the power-flow curve of each pump, linearly approximated for the tolerable operation range, i.e., between a minimum and maximum value of the nominal flow given by minimum and maximum rotational speeds of the pumps. The model used here is based on similar MPC works found in the literature (H. Zhang, 2011), and considers cases of centralized, distributed, and decentralized control.

### 8.2.2.1 Centralized Model Predictive Control (CMPC)

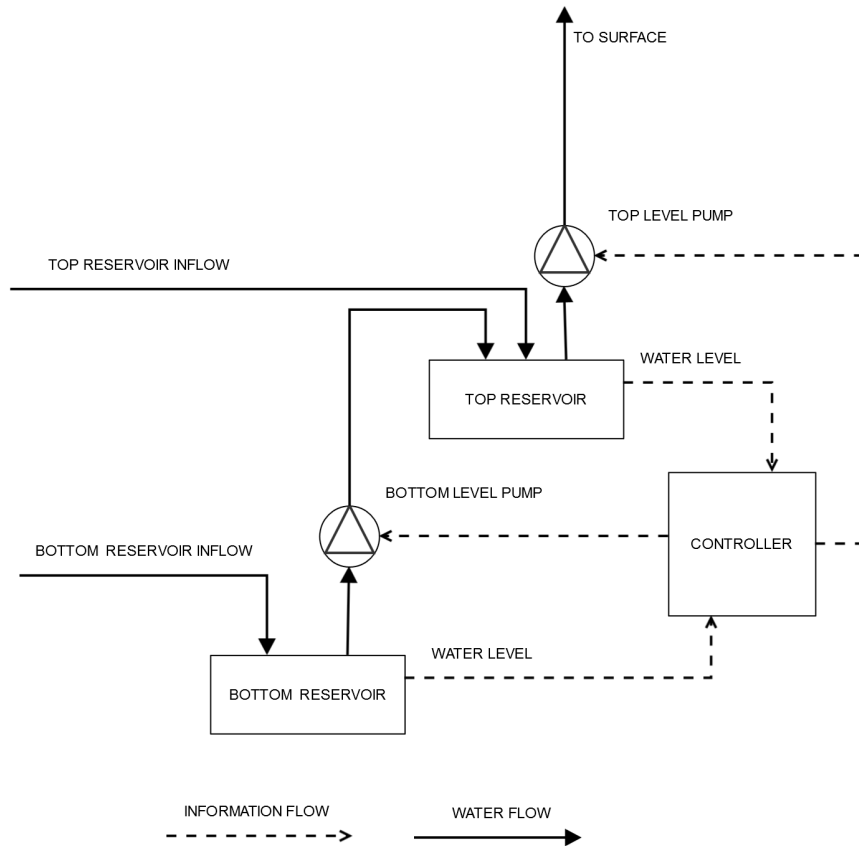


Figure 8-4 Centralized control scheme

A centralized control (Figure 8-4) assumes a complete knowledge of the whole system's state and centralized decision making. In all cases explored, the controllers received information about future hourly prices. The solution of the problem, if feasible, is the optimal pumping plan. This translates to achieving minimum operating costs, while respecting the constraints of maximum and minimum reservoir water levels and maximum and minimum discharge of each pump, if activated. As mentioned in previous sections, centralized control compromises the whole system in case of communication outage. Non-centralized approaches can enhance system control robustness or the ability of the whole system to safely operate even when each pump is behaving without knowledge of its neighbor's control objectives.

### 8.2.2.2 Distributed Model Predictive Control (DMPC)

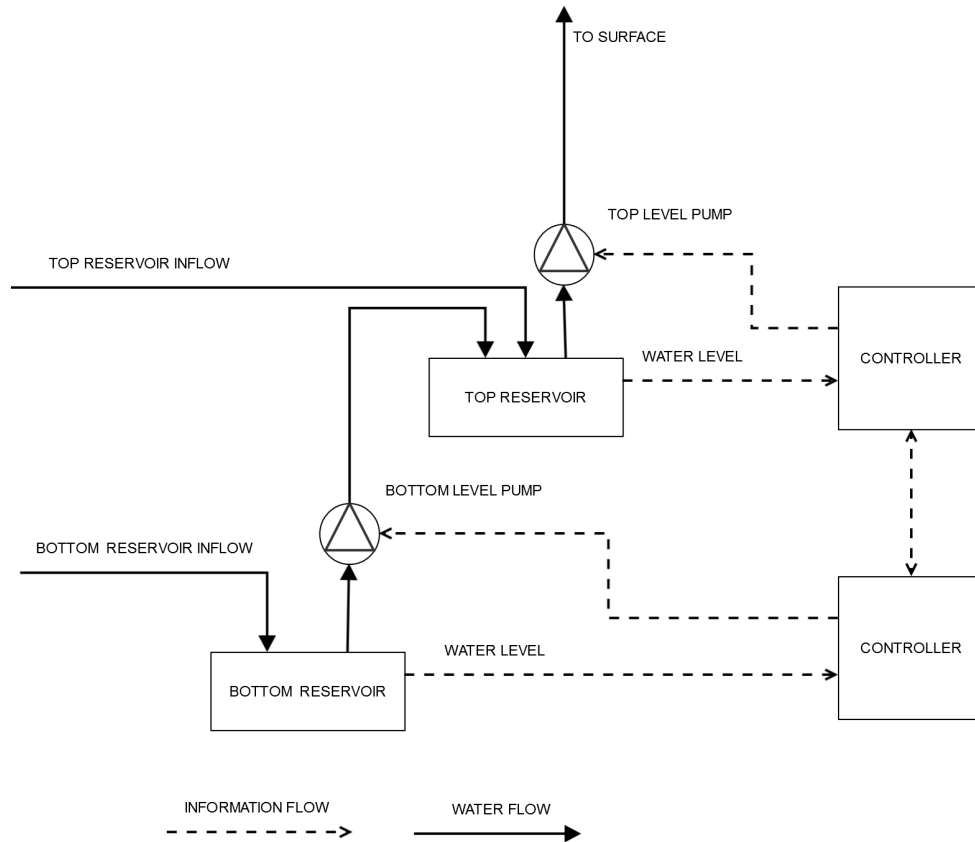


Figure 8-5 Distributed control scheme

The distributed model predictive control (DMPC) problem assumes perfect communication between the subsystems (agents), the “pump-reservoir” couples of each level and selfish decision making by each agent (Figure 8-5). The constraints of each subsystem are reservoir level and flow rate limits. The main consideration relates to the sequence of the optimization, the information shared and the possibility of recalculating the respective pumping plans as part of a type of bargain between the agents. For DMPC the present work assumes serial progressive optimization in which the bottoming subsystem optimizes its plan first based on its predicted inflows and electricity prices. Then, the upper subsystem optimizes its plan making use of the solution (pumping plan, including current pumping state) of the former, as well as its expected

water inflows and environmental electricity price. The overall solution obtained may not be equivalent to the optimal reservoir capacities and pumping plan of the centralized solution, but the DMPC sub-problems embody a practical simplification in sub-surface communications and a control robustness that is desirable in a mining context.

### 8.2.2.3 Decentralized Model Predictive Control (DcMPC)

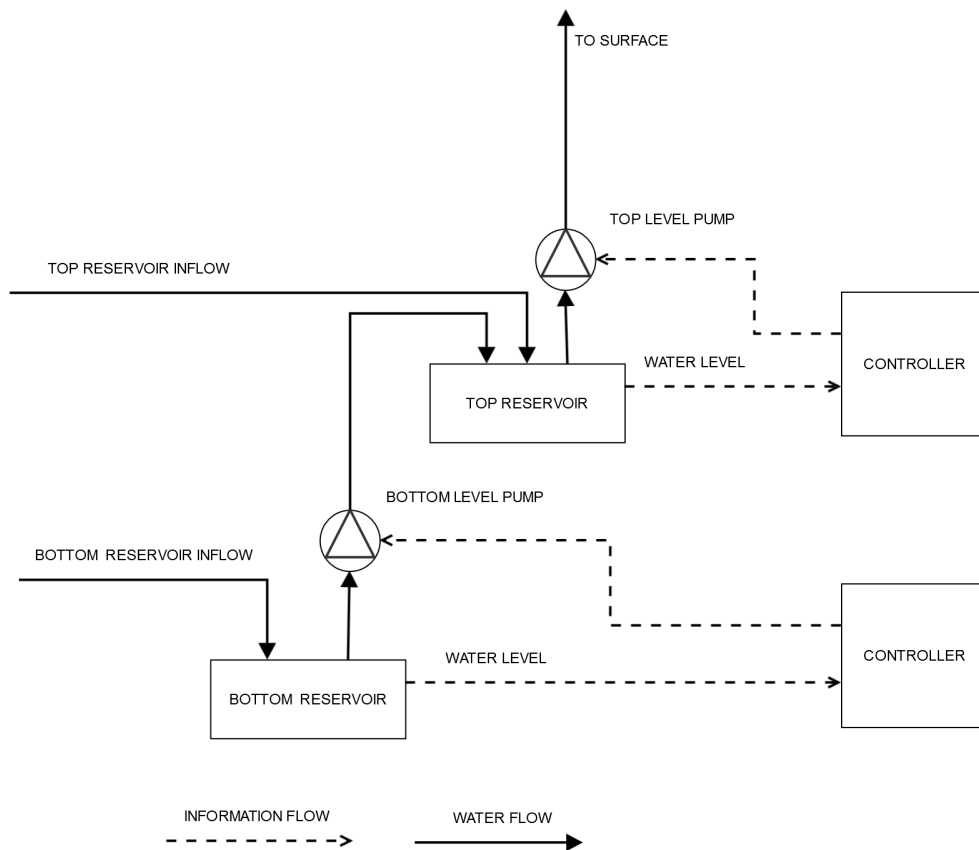


Figure 8-6 Decentralized control scheme

In the absence of communication between controllers (Figure 8-6) a so-called decentralized model predictive control (DcMPC) case arises which can be solved through adoption of one of a variety of control policy augmentations that are described in the literature (Christofides et al., 2013). Here it is solved by assuring that there is sufficient remaining storage capacity of an upper reservoir to accommodate flow discharged by a lower pump, sustained for a specified period of

time. A MPC system following a lower water level set point is implemented in the upper subsystem, which also considers that the expected flow from the lower tank is equal to that received from it during the time interval immediately prior to the current time interval of consideration. This assumption is valid due to the trend of the lower pump to maintain discharge flows, given that the ToU prices are broadly similar from one hour to the next.

The decentralized scheme can be compared with the traditional pumping operation based on high-low level driven operation. The architecture for traditional operation is illustrated in Figure 8-7. The controllers are reduced to few relay devices.

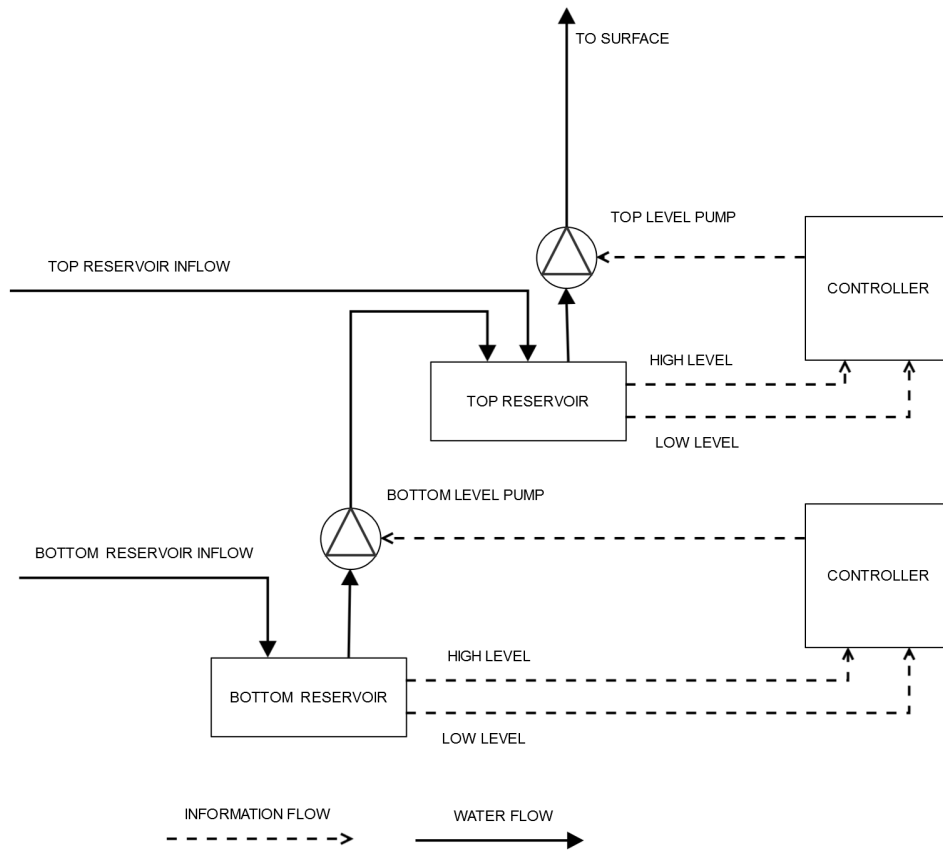


Figure 8-7 Traditional control scheme

## 8.3 Problem Formulation

### 8.3.1 Design Problem

The objective function of the design optimization problem can be expressed as follows

$$\text{Min } C_{tot} = C_{fix} + C_{var} \quad (8-1)$$

$C_{tot}$  is the total annual cost, while  $C_{fix}$  is the annuitized fixed cost (derived from dam's construction) and  $C_{var}$  is the annualized variable cost (pump electricity consumption and maintenance costs).

The annuitized fixed cost is expressed by Eq. 8-2. The variable cost integrates the operation along the 24 hours of each representative day of the year (here, a representative day applies for each month).

$$C_{fix} = k_{rf} \cdot (1 + k_{ic}) \cdot \sum_p c_{sto,DW,p} \cdot \Psi_{DW,p} \quad (8-2)$$

$$C_{var} = \sum_p \sum_i \sum_j p_{ij} \cdot \Phi_{EE,ij,p} \cdot t_{ij} + \sum_i GA_i \quad (8-3)$$

where  $k_{rf}$  is the capital recovery factor, also known as annuitization factor, and  $k_{ic}$  accounts for engineering and supervision expenses, etc;  $c_{sto,DW,p}$  is the cost of water storage per unit of volume and  $\Psi_{DW,p}$  is the respective reservoir capacity for  $p=1,2$ ;  $p_{ij}$  the cost of electricity in each hour of each representative day; and  $GA_i$  is the monthly payment for demand charges (implying that this case study applies to a mine in Ontario, where demand charges comprise the Global Adjustment payments).  $t_{ij}$  is the duration of the interval of time for the typical day  $i=1, \dots, 12$  (twelve typical days, one for each month) at the hour  $j=1, \dots, 24$ , and  $\Phi_{EE,ij,p}$  is the electricity consumed by the pump  $p=1,2$  at hour  $j$  within the day  $i$ . Water and electricity balance, across technology and utilities are defined by Equations 4-13 to 4-21. In addition to these

equations, the formulation also includes minimum and maximum pumps flow when these are operating. Thus, a binary variable has to be added expressing the state of each pump. Maximum and minimum values are expressed as a function of the nominal flow of the pump. Following Eq. 4-8, and using a similar approach when defining spinning reserve constraints (Section 4.2), flow constraints can be expressed as:

$$\Phi_{p,ij}^{pro} \leq \mu_{p,ij}^{op} \cdot P_{max,p} \quad (8-4)$$

$$\Phi_{p,ij}^{pro} \geq \mu_{p,ij}^{op} \cdot P_{min,p} \quad (8-5)$$

where  $\mu_{p,ij}^{op}$  is the activation state (binary variable) for each pump and time interval, and  $P_{max (min),p}$  the maximum (minimum) flow.

The model therefore defines a MILP problem, where, in addition to reservoirs' size, hourly pump states and flowrates are the decision variables. Thus, the solution of the design problem includes an optimal schedule of pump operation (that may or may not remain optimal depending on the real operating conditions: inflows and electricity prices), given schedules of inflows and electricity prices.

### 8.3.2 Control Problem

The operational optimization problem is defined with the same balance equations as the design problem, and solved every time interval in a rolling horizon of prices and inflows. The control problem objective function is therefore:

$$Min C_{tot} = C_{var} \quad (8-6)$$

$$C_{var} = \sum_p \sum_j (p_j + \Delta p_j) \cdot \Phi_{EE,j,p} \cdot t_j + \sum_p C_{N,p} \cdot (L_{ref} - L_{N,p})^2 \quad (8-7)$$

The objective function defined by Eqs. 8-6 and 8-7 does not include fixed costs, but instead, Eq. 8-7 includes a ‘quadratic’ cost function of the level of the reservoir at a certain time interval,  $L_{N,p}$ , which is taken to be the last time interval of the rolling horizon. This term is used only in DMPC and DcMPC cases, where access to other controller’s information may be partial or impossible. The term implements a localised control policy that aims to ensure the current reservoir water level is attracted to a reference level,  $L_{ref}$ , driven by a virtual cost. The coefficient  $C_{N,p}$  is tuned to the specific case, depending on the electricity costs and the tolerated terminal difference  $L_{ref} - L_{N,p}$ . In other words, it has to be selected so to reach at least the same order of magnitude than the electricity cost within the control horizon. This term makes no contribution to the actual annual cost of operating the system, it merely ‘points the system’ toward a given attracting state. The aim of the present work is not to perform a detailed analysis of the stability of the system, and  $C_{N,p}$  will be selected to ensure feasibility for the decentralized problems, where the lack of communication between agents may cause infeasible operation for some of the subsystems controlled.

The actual operating cost is the first term in the right hand side of Eq. 8-7, and is calculated using electricity prices and energy consumed,  $\Phi_{EE,j,p}$ . For the MPC problem,  $C_{var}$  is calculated as the sum of the interval costs within the control horizon ( $H$ ), ( $H: j=1, \dots, N$ ). In general,  $N$  is equal to 24 hours, or less if system stability requires. In comparison with Eq. 8-3, in Eq. 8-7 the DC term is removed and  $\Delta p_j$  is included. The latter is an additional electricity cost, added to  $p_j$ , that will apply only to the hours where expected demand charges have the influence (i.e., summer afternoon hours, from 12 PM to 6 PM). This price increment  $\Delta p_j$  is set as to discourage pumping in those hours, normally considering that  $\Delta p_j \gg p_j$ .

As mentioned in Section 5.2, OMSES balance equations described in Chapter 3 and 4 apply equally to the control problem. Water storage efficiencies are considered equal to 1 (for both design and control problem). For the operational problem, the requirement of equal water levels at the beginning and the end of the control horizon (terminal constraint) is removed from the equations. This is an unnecessary constraint for MPC compared with OMSES, but it should be noted that, in absence of terminal penalty and constraint the control plan involve full reservoirs at the end of the control horizon.

Equation 8-7 is formulated for  $p=1, 2$  in the case of the centralized problem. In the distributed and decentralized cases this subscript is unnecessary, because the problems are solved for each subsystem, but while the lower reservoir receives an inflow only from the mine, the upper reservoir receives also the pumped water from the lower one. Although reservoir sizes are input variables, the problem is still defined as a MILP because hourly pump activation states are binary variables.

Regarding the information needs of this formulation, it quickly becomes clear that the optimal design solution can only be really considered as optimal for the given schedules of inflows and prices, which can only be known certainly historically, even if probabilistic approaches can be taken to characterize the inflows and pricing time series. This chapter does not address the effect of uncertain inflows, but that of price of electricity. The reader can find an example of the former in Maestre et al. (2013).

#### **8.4 Framework for Assessment**

The case study adopted to illustrate the approach to optimal design is the dewatering system of an underground mine in Ontario. Firstly, the optimal design is calculated using mathematical

programming technique subject to the expected electricity prices and inflows and technical constraints. Subsequently the resulting system is simulated under MPC, seeking minimum cost operation. All outcomes of optimal design and optimal control are compared with results of a system that faithfully represent traditional design and control practice of dewatering systems in mines currently applied.

The ensuing discussion sets out by describing the characterization of the economic environment and the tariff environment faced by the system and continues by describing how pump duty is modulated within the model. Next the various cases and scenarios explored are described. These aim to elicit the merits or relative demerits of each case explored, where the principal variable is the type of MPC assumed adopted. This section sets out the framework for assessment of these mine dewatering system optimization schemes.

#### **8.4.1 Economic Environment**

For the design stage, hourly price profiles have been established for representative days of each of the twelve months, using 2011 electricity prices in Ontario, Canada. Demand charges, also representative of the Ontario system are calculated based upon the consumption for the representative day of July, where peak grid demand is expected.

This averaged ToU profile may underestimate savings from load shifting actions in design optimization, because the averaging process involved in establishing the price profiles reduces variance in the prices for the representative day. When considering real time hourly prices, as is the case with the operational optimization problem that follows, the enhanced potential savings will be recognized under MPC. To illustrate this point, Figure 8-8 compares the average price and the real time price for three consecutive days.

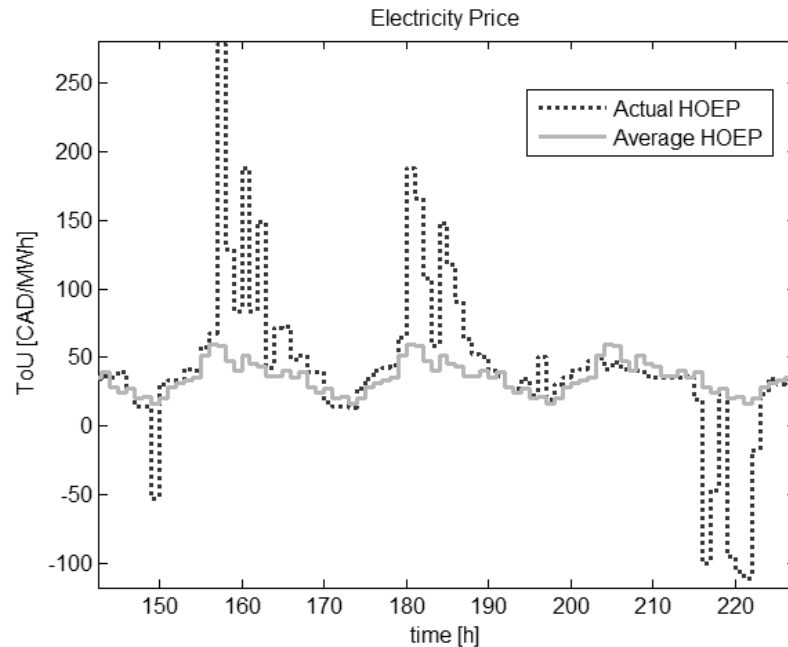


Figure 8-8 HOEP June 2011; Actual (dotted line) Vs average (continuous line) hourly profile

For the operational optimization, or control problem, the predicted price of electricity is assumed to be perfectly known. This is generally false, but what is available 24 hours (on a rolling basis) in advance is a predicted price. These prices are known to be volatile during already high price periods, exemplified by the Ontario network (IESO, 2014), and such circumstances clearly identify the need for adaptive responses in the pumping plan of a system already optimized for design.

Reservoir capacities may be constrained by an upper limit during optimal design of the dewatering system. There will always be space limitations for this kind of infrastructure (perhaps geotechnically constrained at depth), but here it is considered that it is always possible to excavate and build a proper dam or sump in the mine. This assumption does not affect an estimated cost of construction of the reservoirs, which is assumed to be proportional to reservoir volume.

### 8.4.2 Water Inflow

For each reservoir, the inflow can be approximated by considering a water flow term dependent on production (drilling, washing, etc) and a term dependent on infiltration from the water table, aquifers, rain, snow, etc. The former may have a daily pattern; the latter could be relatively constant throughout days representative of each month, but with seasonal variations month to month (or representative day to representative day).

The inflows adopted (**Error! Reference source not found.**) are used for both the design and the control optimization problems. Infiltration is considered as a constant flow rate while production associated flows follow the same hourly pattern for every representative day of the year. The sum of seepage and production associated inflow yields an inflow for each hour of the day for each reservoir. The upper sump does not receive water other than from seepage and the lower reservoir. While the design problem uses the typical daily inflow pattern, the control problem repeats the same daily inflow pattern for each day of the considered month. In the case of more accurate knowledge of mining operations or infiltration behavior being available, the predicted inflows for the control horizon will be improved with improved estimates of savings.

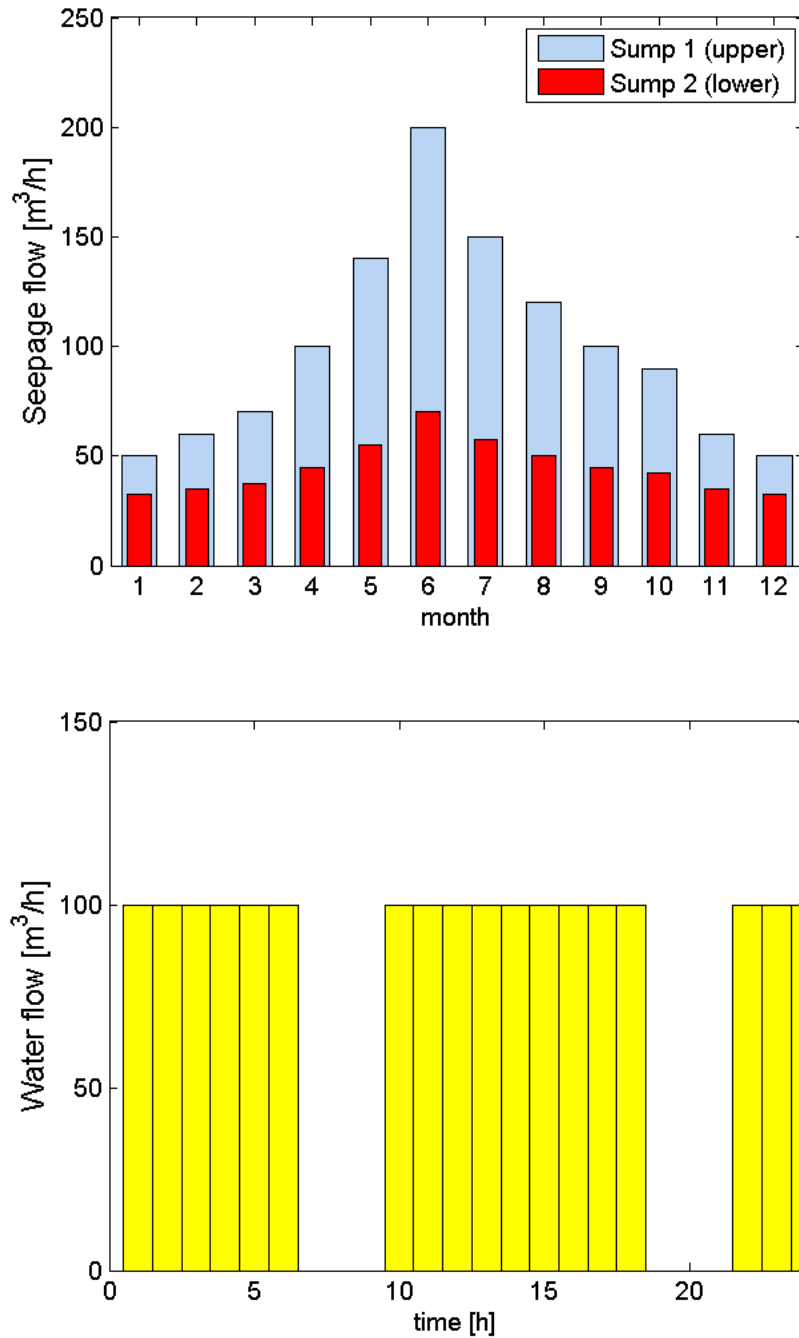
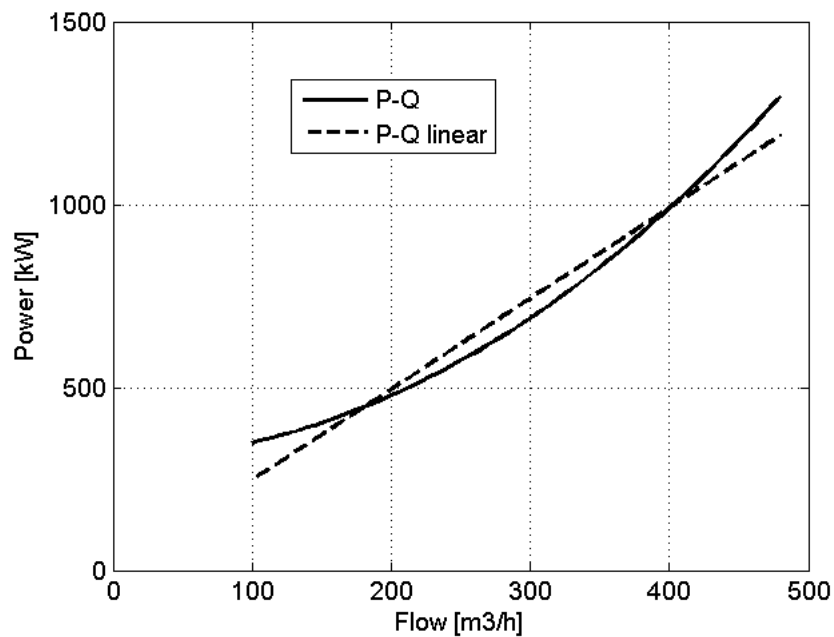


Figure 8-9 Water inflows; Top: Monthly infiltration inflows (constant flow) for each reservoir; Bottom: water inflow associated with mine production activities into the lower reservoir

### 8.4.3 Variable Speed Pump Implementation

The performance of a pump is defined by the flow that is able to deliver when connected to a pipework system, as it consumes a certain amount of power. This eventually defines the ToU

costs. The methodology chosen for both problems (design and control) is based on the characterization of the couple formed by a pump and the system to which it is installed. Given a pump with variable rotational speed and a fixed system arrangement (fixed static head, valves, etc) the power that a variable speed drive will consume as a function of the flowrate delivered by the pump can be analytically characterized by a series of interpolations and substitutions of the actual curves of both the pump and the system, as well as the affinity laws (H. Zhang, 2011).



**Figure 8-10 Example of power-flow curves for a variable speed pump: cubic (continuous line) and linear (dashed line) approximations**

Here the resulting cubic expression for the power-flowrate curve following (H. Zhang, 2011) is replaced by a linear approximation, as illustrated in Figure 8-10. The cubic expression, drawn in Figure 8-10 as a continuous line, is across data from an actual pump and a known system. This precise definition may not be necessary if we are interested in the performance of the pump in a narrower range of operation, and a lower order function (i.e., linear, dashed line in Figure 8-10) could reduce simulation and optimization time of both the design and control problem. If this is

the case, the emphasis when linearizing the power-flow function has to be placed in establishing the range where the system will be practically operated.

#### **8.4.4 Design and Control Cases Explored**

Figure 8-11 presents a structured listing of the individual situations that are considered in this case study example that aims to elucidate the various considerations articulated. The individual cases are given abbreviated names, and for each case, the effects of two DC scenarios are simulated: i) maintain an unavoidable and thus fixed DC and ii) minimize the DC. The benchmark case (TD) adopts the traditional design method for determination of reservoir capacity and considers maximum and minimum level switch control with constant speed pumps (when they are in operation). For a given reservoir, its volume is calculated by totalling eight (8) hours of mine inflows, including any flow rate arriving from other pumps. Practically, this amounts to 8 times the mean inflows for each representative day. This type of control offers no sensitivity to ToU electricity prices or DC.

In the remaining scenarios, having obtained the optimum design, the MPC simulations aim to permit assessment of the robustness of optimality in the face of unexpected changes in the environment, which in this case could be for either the tariff environment or the physical environment. Consequently, upon the tariff time series for electricity price and DC used in design optimization, an additional electricity ‘price hike’ is superimposed to reflect times of peak system demand; the hourly price that the controller senses is deliberately increased ( $\Delta p_j = 600$  CAD/MWh for these trials, for  $j=12, \dots, 18$  hours). Therefore, although this perceived price only is used by the controller, the desired outcome of reducing DC is possible even when ToU charges significantly increase.

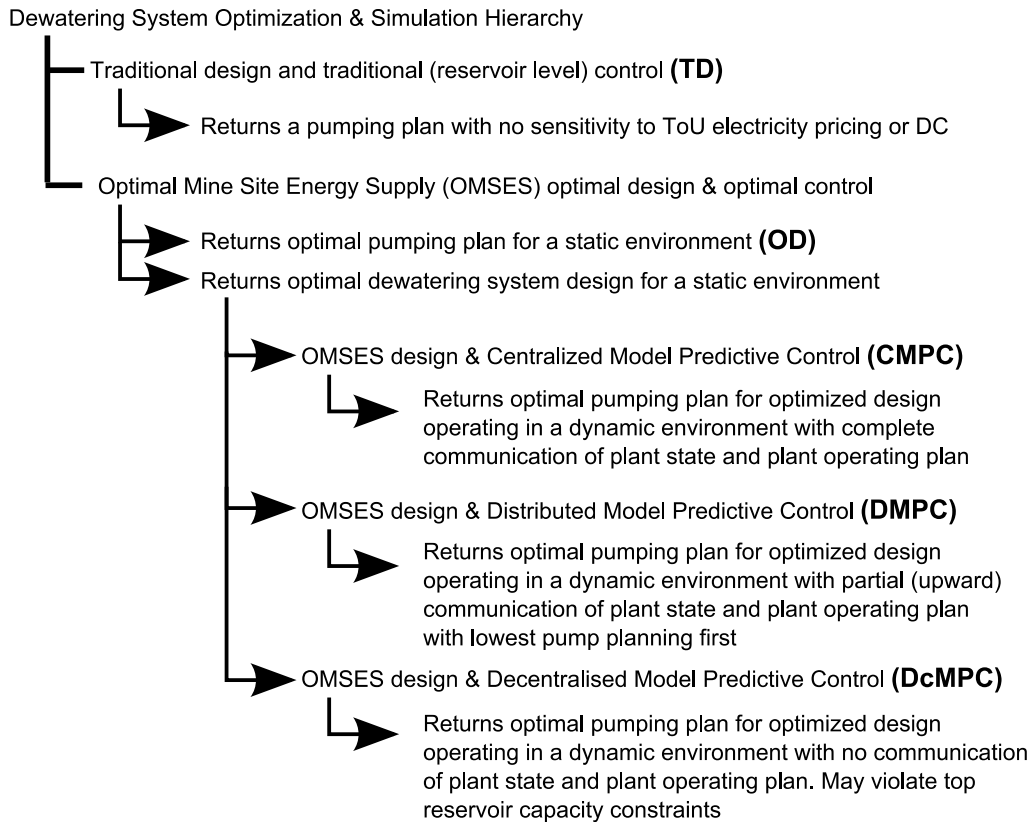


Figure 8-11 Dewatering system optimization & control simulation hierarchical summary, illustrating design, optimization and simulation cases considered (cases abbreviated with emboldened letters).

For DMPC the pump in the lower mine level first optimizes its control actions for the given planning horizon; a 24 hour long planning horizon is adopted. Information of the plan is sent to the controller at the upper level, which optimizes its plan in accordance with this information and its forecasted mine inflows and electricity price. In addition to the linear cost, the quadratic function term in Eq. 8-5 is activated to maintain the water level around a set point that assures sufficient reservoir volume to deal with high flowrate from the pump of the lower level. The DMPC implementation adopted has unidirectional information flow which can lead to shortcomings of DMPC as some controllers may not be able to sense plans for other parts of the system that may be material. The upper subsystem has a control horizon and prediction of 5 hours that, as it will be discussed, is enough in this problem. The referred set-point is selected once the design volumes have been obtained.

In DcMPC, there is no information exchange between controllers. The upper agent deals with this situation by assuming that, for a given interval, the current discharge from the lower pump is to be sustained during several hours. Practically, rather than in these exploratory simulations, this duration may be established heuristically based upon historical pump operation. DcMPC systems generally achieve inferior results than DMPC systems, especially when the latter may exchange information bi-directionally and iteratively.

The problem of overflow becomes more complicated in DcMPC, that is, pumping plans may violate constraints that were in fact embedded in the design problem. Some of the actions that render the feasibility of the top system (upper reservoir) are:

- Limit a lower subsystem's pump speed. The immediate consequence is a lower flowrate that provides more time to react, especially in the case we consider, where system measure and control actions are applied each hour.
- Adjust the terminal cost. The lower the reference level  $L_{ref}$  for the quadratic term in the cost function, the higher penalty factor ( $C_{N,p}$ ), or the closer the terminal interval  $N'$  considered (i.e.,  $N' < N$ ) to the initial interval ( $j=1$ ), the more room for inflow water will be in the reservoir to deal with unexpected circumstances. However, this reduces the actual cost optimization (CAD).
- Increase upper reservoir capacity. This action is related to the initial design, not to the controller itself. Increased capacity helps when the subsystem has not enough pump capacity in case of a high flow rates during several hours,

For the example problem considered, it was necessary to adopt all of these actions in combination in order to return solutions that were feasible. The approach followed is to maintain upper reservoir's water level as low as possible. June is the month with higher inflow conditions, and therefore the controllers are more stressed. The values used for the optimization problem are given in Table 8-1.

**Table 8-1 Inputs for design problem**

	Units	Value
<i>Pump performance</i>		
Pump capacity (Q)	[m <sup>3</sup> /h]	400
Range (Q)		
maximum	[-]	120%
minimum	[-]	80%
Nominal head	[m]	440
Nominal power	[kW]	800
<i>Bottom level (L1)</i>		
Pumps number	[-]	1
Max size reservoir	[m <sup>3</sup> ]	3000
<i>Top level (L2)</i>		
Pumps number	[-]	1
Max size reservoir	[m <sup>3</sup> ]	3000
<i>Other inputs</i>		
Interest rate (i)	[-]	0.1
Life (y)	[year]	20
Capital Recovery Factor ( $k_{rf}$ )	[-]	0.12
Reservoir construction costs ( $C_{DW}$ )	[CAD/m <sup>3</sup> ]	100
Installation cost factor ( $k_{ic}$ )	[-]	1.15

Flow and power data shown in Table 8-1 can be used to derive the conversion coefficients necessary for OMSES formulation and its MPC extension. For each pump, and given that the technology main utility is dewatering flow (DW),  $K_{p,EE} = 800 \text{ kW}/(400 \text{ m}^3/\text{h}) = 2 \text{ [kWh/m}^3\text{]}$ , and  $K_{p,DW} = 1 \text{ [-]}$ .

<b>PROBLEM: DEWATERING OF AN UNDERGROUND MINE ILLUSTRATION OF CMPC, DMPC AND DCMPC</b>		
<b>MINIMIZE</b>	<b>Equation</b>	<b>Inputs</b>
Total annual cost = Investment Cost + Variable Cost	(8-2) (8-3)	Table 8-1 Section 8.4.4 TD OMSES TD OMSES CMPC/ DMPC/DcMPC
+ Demand Charges + Penalties	(3-23) (8-7)	Figure 3-3 MPC Table 8-5
<b>SUBJECT TO</b>		
Utility Energy Balance	(3-12,13,14) (4-14) storage	Figure 8-9
Equipment performance:		Figure 9-10 Section 8.4.4 Table 8-1
- Conversion coefficients	(3-11)	
- Production limits	(3-9)	
o Maximum load	(8-4)	
o Minimum load	(8-5)	
<del>Infrastructure Constraints</del>	<del>(3-17,18)</del>	
Storage Balance		
- Hourly	(4-15) to (4-23)	
<del>— Monthly</del>	<del>(4-22,23)</del>	
Scenario Based:		
<del>— Resource Availability</del>		
o <del>Wind</del>	<del>(4-5) (4-6)</del>	
o <del>Biomass</del>	<del>(3-15,16)</del>	
<del>— Spinning Reserve</del>	<del>(4-7) to (4-11)</del>	
<del>— Storage Charging/Discharging</del>		
- Demand Charge		OMSES C/D/Dc/MPC1 C/D/Dc/MPC2
o Fixed		
o Free		
- Terminal constraint on storage		OMSES C/D/Dc/MPC
o Applied		
o Not applied		
<b>DECISION VARIABLES</b>		
<del>Technologies Available</del>		
<del>Equipment Units</del>		
- OMSES		
- MPC-OMSES		
- LT-OMSES		
Storage Size		
<del>Grid Capacity</del>		
Energy/Mass Flows		
- Typical days		OMSES
- Rolling horizon		MPC
<del>Incremental Equipment units</del>	<del>(5-6)</del>	

## 8.5 Results

Table 8-2 shows the results of system design using traditional design methods and OMSES methodology, expressed as the discounted annual cost of dewatering, with discount rate of 10% and 20 year system's life. R1 refers to the bottom reservoir, while R2 does for the top level reservoir. The results for the operating costs for the traditional design, both ToU and DC, have been obtained from simulation of the high and low level trigger control.

Table 8-2 shows that traditional design involves higher investment in reservoirs. Total investment cost is lower in both OD1 (optimal design without DC minimization) and OD2 (optimal design with DC minimization) compared with TD case. The optimized designs assign more capacity to the lower reservoir,  $R1 > R2$  in comparison with TD, where  $R2 > R1$ . The savings obtained are clearly favorable to optimized solutions, but the control problem will reveal if these idealized amounts are reasonable or not.

**Table 8-2 Results Design optimization**

		TD	OD1	OD2
Reservoir size				
R1	[m <sup>3</sup> ]	1560	1222	2469
R2	[m <sup>3</sup> ]	3560	556	1050
Costs				
ToU Cost	[CAD/yr]	258,516	234,080	226,921
Demand Charges	[CAD/yr]	382,677	432,790	77,866
Investment (Annuitized)	[CAD/yr]	69,160	24,017	47,534
Discounted annual cost of dewatering		710,353	690,886	352,321
Cost savings (relative to traditional)			-3%	-50%

**Table 8-3 Summary of optimized operation using CMPC**

		TD	CMPC1	CMPC2
<b>Reservoir Size</b>				
R1	[m <sup>3</sup> ]	1560	2469	2469
R2	[m <sup>3</sup> ]	3560	1050	1050
<b>Costs</b>				
ToU	[CAD/yr]	258,516	188,631	190,883
Demand Charges	[CAD/yr]	382,677	145,782	0
Peaks:	July 4pm	1.92	0	0
	July 4pm	1.92	0.96	0
	July 5pm	1.92	0.64	0
	July 2pm	0.96	0.96	0
Average Power*	[MW]	1.68	0.64	0
Investment (Annuitized)	[CAD/yr]	69,160	47,534	47,534
Discounted annual cost of dewatering		710,353	381,950	238,417
Cost savings (relative to traditional)			-46%	-66%

\* Power demanded in the reference hours; DC is calculated as the average of five reference hours (2011 peak demands in Ontario). In order to simplify the calculations, only reference hours of July were used for the average, which is consistent with the approach of the design problem.

Table 8-3 shows the results of the operational problem. DMPC and DcMPC results are not shown, for they produced infeasible control problems with the same simulation conditions as the CMPC case (24 hours control and prediction horizon, OD2 design). CMPC1, DMPC1 and DcMPC1 refer to control without DC minimization, while CMPC2, DMPC2 and DcMPC2 do minimize DC. Robust non-centralized controllers were not possible to realize unless the upper reservoir capacity or upper pump maximum flowrate were increased.

In order to ensure the feasibility of non-centralized approaches, the capacity of the upper reservoir obtained with OMSES was increased 2.5 times. With such increase the investment costs become of the same order as for the TD case and thus one can focus on the operational results. This increase also ensures that the DMPC and DcMPC solutions became feasible. To permit comparison with the distributed and decentralized control cases, the feasible solutions of CMPC1 and CMPC2 of Table 8-3 were recalculated with increased reservoir capacities to produce the results presented as CMPC1' and CMPC2' of Table 8-4.

**Table 8-4 MPC comparison with increased systems design robustness**

		CMPC1'	CMPC2'	DMPC1	DMPC2	DcMPC1	DcMPC2
Size							
R1	[m3]	2469	2469	2469	2469	2469	2469
R2	[m3]	2625	2625	2625	2625	2625	2625
Costs							
ToU	[CAD/yr]	198,885	201,918	221,340	222,526	232,046	230,164
Demand Charges	[CAD/yr]	145,782	0	118,698	0	100,225	44,976
Peaks:	July 4pm	0	0	0	0	0.80	0.79
	July 4pm	0.96	0	0.72	0	0.96	0
	July 5pm	0.64	0	0.64	0	0	0
	July 2pm	0.96	0	0.7256	0	0	0
Average Power	[MW]	0.64	0	0.52	0	0.44	0.20
Investment (annuitized)	[CAD/yr]	68,809	68,809	68,809	68,809	68,809	68,809
Discounted annual cost of dewatering		413,476	270,727	408,850	291,335	401,082	343,950
Cost Savings (relative to traditional)		-42%	-62%	-42%	-59%	-44%	-52%

For completeness for any reader who may wish to confirm the results of the simulations, a summary of the control setup for distributed and decentralized MPC, used to obtain the feasible solutions, is shown in Table 8-5.

**Table 8-5 Non centralized controllers setup**

Parameter	Units	DMPC	DcMPC
$C_N$	[CAD]	0.01	1
$L_{ref}$	[m <sup>3</sup> ]	500	300
$N$	[-]	5	2
$Q_{I,max}$	[%]	120	100

The results superficially indicate that:

1. MPC results are superior to TD for feasible solutions
2. CMPC results are superior to DMPC and DcMPC
3. DMPC and DcMPC became feasible only when the optimum design using OMSES is ignored and an intervention is exercised.

## 8.6 Discussion

The work presented represents an approach that puts together two currently prevalent approaches to energy systems optimization. The first of these is the energy system design optimization, based on expected operating conditions, which has been shown to be successful in identifying energy savings. A second approach is MPC applied to energy systems operational optimization. The link that makes it possible to obtain results for the design optimization that are comparable with the operational optimization is that the simulation model is the same system model, the definition of the problem as a mathematical programming problem and a sufficient knowledge of the operating conditions exist, at least for OMSES and CMPC combined. MPC can use system models obtained from design optimization. We have made comparisons between MPC and OMSES. These reveal the advantages and the deficiencies of an optimal system design discussed in the following.

The average price used to calculate the optimal design may not show the real potential of load shifting strategies but it will give enough information to achieve the optimal design. For CMPC, comparison between Table 8-3 and Table 8-4 reveal how increasing reservoir size (R2 in this case) gives lower annual cost savings. Any operational cost reduction is countered by the increase of investment costs, thus demonstrating that, for the conditions simulated, design remains optimal even subject to price variability and uncertainty.

Given the choice, lower savings for the DMPC or DcMPC mean that they are undesirable in comparison to a centralized controller. This is a result of the reduced level of communication that exists with the non-centralized systems. How would this reduced level of communication occur? It would not be ‘designed in’ through selection of, say, DMPC over CMPC, rather the

communication system for CMPC could fail. Table 8-4 illustrates the effect one of many types of intervention that could mitigate the effect of partial communications failure with the decentralized MPC system reflecting a more serious failure.

Such interventions override optimal design parameters and potentially call the usefulness of OMSES into question. However using either OMSES or CMPC on their own for design (for the interventions imply a return to design), or using them together, leads to dramatic savings improvements, but using them together increases savings so one would always opt for this combined approach.

DMPC and DcMPC approaches, even with artificially increased upper reservoir size for reliability reasons, substantially improved upon TD. Better performance of DcMPC compared with CMPC and DMPC, for non-minimized DC, is due to a random casual improvement regarding power consumption in July which affects DC. As expected, if DC is minimized, then the CMPC approach is the best, followed by DMPC and finally DcMPC.

If the demand charge is not-deterministically defined (as is the case explored herein because Ontario demand charges cannot be calculated deterministically in advance, because it is not possible to determine the date of the peaks of provincial power demand, in any given year) design optimization can be improved using previous year's data for the occurrence of the peaks, to estimate occurrence in the current year, statistically. Operations optimization through improved control can be applied in the same fashion, in this case penalizing energy consumption by artificially increasing electricity price, which creates a perceived higher price during the undesirable hours.

It is clear that if a high unpredicted inflow happens, any controller designed here (re-optimizing every hour) may not be able to pump out the water fast enough to prevent overflow, especially when the reservoir is near capacity and for non-centralized control. In mining, safety is always a priority, and will be prioritized before any energy cost saving strategy. The choice of whether one adopts TD or CMPC depends upon the relative resilience of each design and control system to extreme environmental events. While we have considered how resilient a CMPC system is, through its degradation to DMPC and subsequently DcMPC, we have not established how well a TD system would behave in the same circumstances. The reason for this is that such a determination is strongly dependent on the state of the system when the extreme event occurs. The results of such analyses, which are through necessity, computationally comprehensive, will be reported elsewhere, in future.

Even without a more precise simulation that will reveal model inaccuracies regarding real power consumption, costs savings remain of the same order. For example: it has been determined that the dewatering simulation model would consume up to 10% more energy using the cubic expression, compared with the linear, (Figure 8-10) when the flow rate is at 120% the nominal value. A 10% increase in the energy cost is still absorbed by load shifting, the investment savings and the DC minimization, depending on the MPC case we focus on.

If the number of pumps is included as a decision variable, an increase of the number of pumps is expected. The optimal number of pumps will depend on several variables: specific cost of the pumps (CAD per kW or per m<sup>3</sup>/h), cost of the reservoirs, inflows and electricity prices (ToU and DC). If more pumps are installed, more economic advantage can be taken of the load shifting opportunities.

## 8.7 Conclusions

Cost minimization strategies such as load shifting, whether it is related to time of use or demand charges, requires understanding of the system dynamics, the environment in which it performs, and the consequences of applying the resulting control actions.

In this chapter, an optimization strategy has been applied to a mine dewatering system in order to minimize its total annual cost, defined by the investment costs and the operation costs.

Using expected flowrate and electric tariff data, an optimized design was obtained by means of mathematical programming. This design is significantly different from the traditional approach where, at each mine level, the size of water dams or reservoirs depend upon its own expected inflow.

In order to evaluate the effectiveness of this optimal design solution, model predictive control was applied to a model based simulation. Centralized and non centralized control were tested and compared. For the environmental conditions used (inflows and prices), the centralized MPC was the only control approach that ensured feasibility for the particular problem here solved, i.e., it perfectly avoided overflow. CMPC was used to test the optimality of the optimal design. Increased size of the upper reservoir did not lead to higher savings, which proves the optimality of the design.

In a later analysis with improved reliability of the controllers and the system (upper reservoir size), the three of them got similar performance when DC was not subject to minimization, otherwise centralized MPC got better results than the distributed and decentralized. These also largely improved the annual costs of the traditional design and its usual mode of operation based on switching triggers (High level/Low level).

The distributed problem, as well as the decentralized, revealed the shortcomings of having two constrained, coupled optimization problems with insufficient communication, a shortcoming well known in non-centralized problems (Negenborn, 2007). Upper reservoir overflow was overcome by introducing a quadratic terminal cost to maintain the water level close to a feasible and safe operating point, as well as by system's design modification. For the decentralized problem it was necessary also to reduce lower pump maximum flowrate.

The demand charges minimization strategy applied to MPC demonstrated its validity but it had to be adapted to achieve the objective of the optimal design.

Further analyses should be executed regarding inflow perturbations, as well as model inaccuracies impact. Different communication options and bargain strategies between the controllers should also be explored in order to improve distributed solution.

The present work is the preliminary step towards the generalization of MPC application to energy systems design optimization, especially for OMSES, which is the theme of Chapter 9 and 10.

# Chapter 9

## 9 Remote Mining and Wind Power

This chapter illustrates the generalization of the MPC approach to the complete mine energy supply system (ESS). In addition to water and heat storage, the problem includes wind energy as a renewable energy source and the use of diesel generator-based spinning reserve to mitigate the variability of wind power. The optimal design solution produced by OMSES is compared with the conventional design, which relies exclusively on diesel to meet all energy demands. Data from a real mine with a hybrid wind-diesel ESS was used to validate the results from the optimization process, which included simulation and optimal control of the energy system through MPC under uncertain wind power output forecasts.

Part of the content of this chapter was first published in (Romero et al., 2015a).

### 9.1 Mine Description

The mine considered in this case study is Diavik Diamond Mine (64.49°N, 110.28°W), a remote underground facility located in the Northwest Territories, Canada. The mine is only accessible several weeks per year through a winter road. Demands of electricity, mechanical work, dewatering, and some heating and ventilation are calculated based on data accessed online from different sources (Rio Tinto, 2012; Rio Tinto, 2009; Judd, 2014). The remoteness of the actual mine precluded the investment in a transmission line through which to import electricity. A complementary assessment of the cost-effectiveness of building a transmission line for different fuel price scenarios has been included in Appendix 4.



Figure 9-1 Environmental data sources (Google 2014)

### 9.1.1 Mine Utility Demands

Surface and underground diesel trucks, loaders, and other vehicles are used in Diavik. The operation of surface trucks does not interfere with other equipment in terms of energy, so the diesel required to operate them is treated as a final utility demand. In contrast, underground diesel plants interact with other technologies, such as those related to the ventilation systems, i.e., fans. Diesel consumed by underground mobile equipment is conveniently transformed into mechanical work. Electricity demands mainly include systems such as dewatering, ventilation, compressed air, lights, crushers, mills, backfill plants, and general services for workers.

The calculation of utility demands is based on ore production (tonnes). For example, total electricity consumption is calculated at 100 kWh per tonne of ore, while diesel consumption is estimated by 4 liters per tonne of ore, for underground and surface operations (1 liters/tonne

moved and a waste to-ore-ratio of 3) (Darling, 2011). The average daily ore production is 5,500 tonnes, which yields, assuming as a first approximation 24/7 operation during the 356 days of the year, an average of 22.92 MW in power demand. As ventilation and dewatering were accounted for separately, the figure of 100 kWh per tonne was reduced to 85 kWh per tonne.

Constant daily production throughout the year and a normalized daily profile were assumed. Historical values of hourly electricity consumption of a typical underground mine with two working shifts have been used to produce these normalized profiles, which define, for every hour of the year, the fraction of the electricity consumed daily. Figure 9-2 shows the normalized hourly values of the electric demand. To obtain the electric demand at a certain hour, the daily electric demand is multiplied by the value of the normalized profile at that hour. This profile equally applies to every month considered.

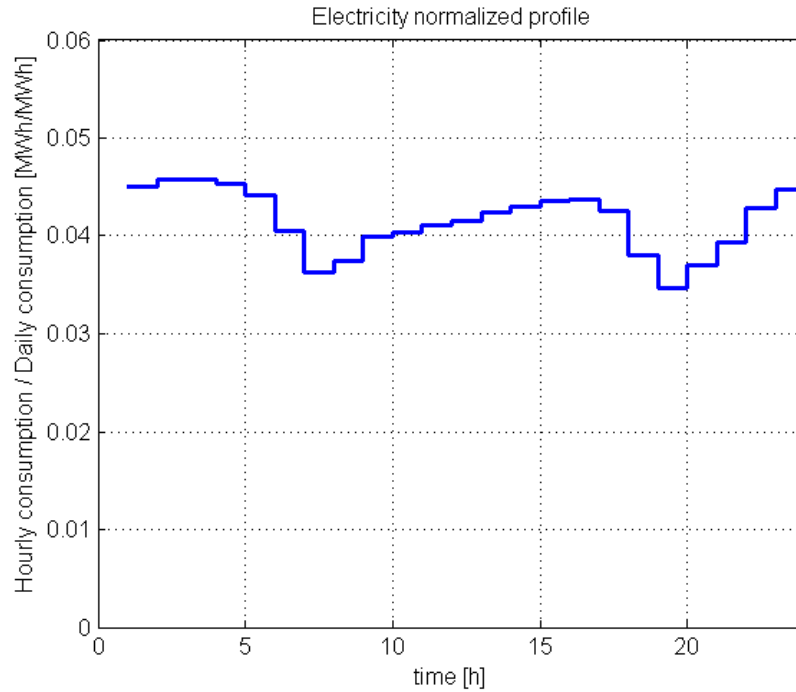


Figure 9-2 Normalized electricity demand profile

Dewatering needs are calculated using a water infiltration rate that, combined with the process water used underground (Romero et al., 2015c), totals 170 m<sup>3</sup>/h of water to be collected and pumped. The dewatering system is subject to optimization, specifically regarding the number of pumps and water storage capacity. This provides the mine with a dispatchable load, thus the pumps are run when it is more cost effective subject to assuring the safe management of the water underground (i.e., avoiding overflow of the reservoirs). The dewatering system is simplified into a set of pumps and one reservoir. Linearity is assumed for the power-capacity relationship and for parallel performance. A linear relationship of 3 kW electric per m<sup>3</sup>/h pumped (or 3 kWh/m<sup>3</sup>; in Chapter 8, the installed capacity amounted 4 kWh/m<sup>3</sup>) is considered.

In underground mines, the ventilation system's electric demand accounts for several megawatts. This power consumption is shared by surface fans and underground fans. It is assumed that the installation consumes 2.5 MW per million cubic meter of air per hour (Mm<sup>3</sup>/h). It is assumed that

the volumetric air flowrate is constant whenever ventilation is required underground. The flow-power relationship can be adjusted if the system components are known (fans, louvers, drifts, ducts, etc.) or can at least be estimated from more detailed ventilation models (e.g., Ventsim, VnetPC). As in the case of dewatering, linearization of the power-flow curve can be safely applied (Romero et al., 2015c).

Mechanical work demand is calculated using estimated diesel consumption. Diesel consumed by vehicles and diverse underground equipment is normally expressed in litres of fuel per tonne of ore moved or hauled. The demanded work output is calculated by multiplying the fuel consumption and the average thermal efficiency, which is considered 30% in a full duty cycle for the average underground equipment. A two-shift operation with an average of three hours' pause in mechanical work between shifts is assumed. During work breaks, a certain amount of ventilation is needed, especially for gases and dust clearance if blasting operations take place – during these breaks, a ventilation demand of 1.08 Mm<sup>3</sup>/h is considered in this work. For the remaining time, ventilation is a function of the applied regulation or dilution criteria 0.06 m<sup>3</sup>/s of air per kW of diesel power equipment in Ontario mines (Bétournay et al., 2005). Diesel demand for surface equipment (mainly hauling trucks) is considered constant throughout the year.

### **9.1.2 Economic Data**

The available technologies for the mine operation, their costs and coefficient matrix (Chapter 3), are shown in Table 9-1.

**Table 9-1 Equipment and matrix of production coefficients**

Equipment	Nominal Power [MW]*	Capital Cost (10 <sup>3</sup> CAD)	O&M Cost (CAD/MWh)	Electricity (EE)	Diesel (DI)	Steam (VA)	Hot Water (HW)	Cooling Water (CW)	Chilled Water (RW)	Ambient Air (AA)	Dewatering (DW)	Ventilation (AV)	Mech. Work (MW)
Diesel Engine	4.4	4400	5.0	<b>1</b>	2.27		0.80	0.20					
Electric Boiler	3.5	144	1.0	1.11			<b>1</b>						
Diesel Boiler	3.0	130	1.0		1.15		<b>1</b>						
Mech. Chiller	2.7	185	2.0	0.21				1.21	<b>1</b>				
Cooling Tower	5.0	82	5.0	0.02				1		<b>1</b>			
HW-CW HX	5.0	35	1.0				1.1	<b>1</b>					
Mobile Plant**	0.2	1000	150		3.33							0.46	<b>1</b>
Pump	30	60	0.1	.003							<b>1</b>		
Fan	.35	30	0.1	2.5				$\beta$	$\beta$			<b>1</b>	

\* Nominal installed capacity is in [MW] units except for pumps [m<sup>3</sup>/h] and fans [Mm<sup>3</sup>/h]

\*\* Technology included in order accounting for the interaction of mobile work and thermal loads through ventilation

Heat storage is considered at 18,500 CAD/MWh. The cost for water storage is 100 CAD/m<sup>3</sup> (Romero et al., 2015c). Installation, procurement, engineering, and other costs are added as 25% of equipment costs (Table 9-1). The energy system’s capital cost is annuitized using a capital recovery factor, with a 10-year life<sup>1</sup> of equipment and operations, and a 10% discount rate. Diesel is acquired in the market (delivered at the mine) at an equivalent cost of 130 CAD/MWh.

### 9.1.3 Environmental Data at the Mine Site

Local weather and wind speed was obtained from Inner Whaleback’s weather station (Environment Canada, 2014) and validated with data from several mine reports (Rio Tinto, 2012; Judd, 2014). Following the method described in Chapter 4 (Section 4.1.2), normalized wind

<sup>1</sup> At design time, mines are frequently assigned 10 year operating lives because ore bodies are drilled to prove around 10 years worth of ore before the mine development team approaches capital markets to raise finance to build the mine

profiles for characteristic days were calculated and used in the design problem. Also for the design problem, typical 24-hour temperature profiles were calculated using the method developed by (Erbs et al., (1983) and monthly average temperatures. For the simulation problem, actual hourly data was used (Environment Canada, 2014).

#### **9.1.4 Mine's Actual Wind Farm**

Diavik Diamond Mine installed wind power to reduce its diesel imports (Rio Tinto, 2012; Rio Tinto, 2009). The penetration factor (PF) is defined as the energy generated by the wind farm divided by total energy demanded. The mine declares, for its four-turbine wind farm, a 10% average penetration factor, offsetting approximately 10% of the diesel demand for power generation (Judd, 2014). The peak output of the wind farm is 52% of the mine electric baseload. Annual penetration thus equals the percentage of conventional energy displaced annually. For the mine, the wind farm project has a payback period of 8 years. Neither the discount rate nor the operating costs of the wind farm are declared, although total cost of the wind farm reported by the company is CAD 31 million (Mathisen, 2014).

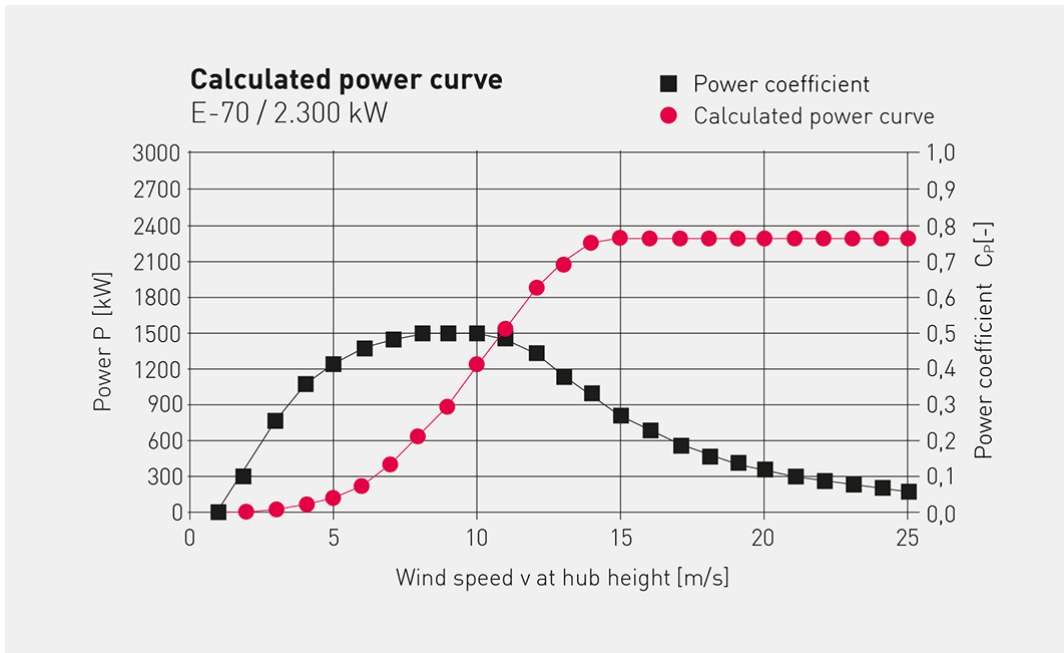


Figure 9-3 Enercon E-70 Wind turbine curves (Enercon website, 2015) ( $\rho_{\text{air}} = 1.225 \text{ kg/m}^3$ ) -  $P_{\text{nom}}$  is the turbine power output;  $C_p$  is the power coefficient

Each E-70 Enercon wind turbine has a nominal output of 2.3 MW between 15 and 25 m/s (cut-off speed 28-34 m/s, air density at standard conditions), and a 71m rotor diameter, with the hub located at 63m (Enercon website, 2015). A conservative reduction of 10% in the nominal output was applied to account for auxiliary equipment for special Arctic conditions (Figure 9-3). Wind farm losses (wake effect, availability, electrical efficiency, turbine performance) were taken as 20% of the gross generation, as a conservative value following the estimations from the European Wind Energy Association (2009). The wind turbine unit cost is considered as 3300 CAD/kW. A summary of the parameters that define the considered mine is shown in Table 9-2.

**Table 9-2 Problem inputs**

Mine	Diavik Diamond Mine		
Company	Rio Tinto		
Type	Underground		
Product	Diamonds		
Production	Year	2.0e6	tonne ore
	Day	5.5e3	tonne ore
Electricity*	Energy intensity**	85	kWh/tonne
	Mean power (all consumers)	23	MW
Mobile	Diesel intensity UG	4	liter/tonne ore
	Diesel intensity Surface	4	liter/tonne ore
	Average efficiency	30%	
	Diesel energy density	10	kWh/liter
	Operation time	18	hours/day
	Mean power	3.65	MW
	Engine shaft work intensity	12	kWh/tonne ore
Ventilation and Diesel	Regulated requirement	0.06	m <sup>3</sup> /s/ kW
	Operational safety factor	2	
	Total	0.12	m <sup>3</sup> /s /kW
Ventilation Electricity	Surface	0.5	MW/ (Mm <sup>3</sup> /h)
	UG	2	MW/ (Mm <sup>3</sup> /h)
	Total	2.5	MW/ (Mm <sup>3</sup> /h)
Wind	Mean speed	6.68	m/s
	V <sub>rnc</sub>	7.9	m/s
	P <sub>rnc</sub>	1479	kW
	WPADF <sub>rnc</sub> (2012)***	1.056	
Temperature	Annual mean	-4.57	°C
	January mean	-26.8	°C
	July mean	16.8	°C
	T <sub>set</sub> comfort level (Ventilation/Building)	15/20	°C
Dewatering	UA (buildings)	0.1	MW/°C
	Hourly average	170	m <sup>3</sup> /h

\*At Diavik there is an ore processing plant and a backfill plant

\*\*Not including utility consumers: ventilation, dewatering, cooling, or heating

\*\*\* Wind power air density factor (WPADF), due to temperature effect in ambient air density

## 9.2 Scenarios Investigated

Several scenarios were investigated using OMSES, and are presented in the following section. In order to reduce the scope of the optimal design analysis, and considering that Diavik does not have any electrical storage installed, the storage for this utility was not allowed to take part in the solutions of the scenarios considered, although later in the Chapter electricity storage is

permitted to enter the solution to explore the potential benefits for the mine operator. These scenarios are:

- Scenario I: No heat recovery, no wind turbines;
- Scenario II (*BAU*): Heat recovery, no wind turbines. Conservative design imposed for diesel generators (10 units) and boilers (9 units) for this and the following scenarios;
- Scenario III: Wind turbines allowed, no spinning reserve logic;
- Scenario IV: Wind turbines from solution of scenario III, spinning reserve logic included (Section 4.2);
- Scenario V: Wind turbines allowed, spinning reserve logic included;
- Scenario VI: Four wind turbines imposed, spinning reserve logic included.

Once the optimal design for each scenario was obtained, the formulation from Chapter 5 was applied, using MPC to optimize the operation of the resulting designs. Several considerations regarding the simulations set up should be made. All simulations were performed in a discretized time horizon using a state space representation of the system. A rolling horizon, typical of MPC, was used for the control of the system, whose operation is iteratively optimized. The state variables (mass and energy storage) are linked with the conservation equations (mass and energy) in the same manner as design problem (OMSES). However, in the simulation, there is no need to link the last interval with the initial, for the cyclical nature of demands and environmental conditions is not assured – the so-called relaxation of the model.

Utility demands are assumed to be perfectly known for every time step for future time intervals defined by the control horizon. Mines work with weekly, daily, and hourly task schedules that determine the energy required at each instant. Wind speed, however, is more variable and

difficult to predict. Whether for a sudden decrease in speed or because of strong gusts, wind turbine power output may decrease drastically. Short term forecast can be available through more or less sophisticated tools, but it is not unusual to use simple persistence models for wind forecast.

In this work, different forecast profiles and horizons are investigated. The OMSES approach followed here to characterize the daily wind profile is checked in the simulation problem, where the optimal or near-optimal operation plan can only be found with benign wind forecasts. Four different forecasting methods were performed to validate the methodology:

- Persistent wind
- Last hour + normalized 24-hour profile forecast
- Current + two-hour perfect forecast + normalized 24-hour profile forecast
- Perfect 24-hour forecast

Spinning reserve constraints apply through the whole control horizon (24 hours), which has the same length as the prediction horizon. However, in practice, the spinning reserve equations do not necessarily have to apply throughout the 24-hour control horizon. They can be limited to a shorter or extended to a longer period to ensure, for example, that there is enough energy storage to substitute idle engines. This is particularly interesting in the case of variable wind power, for which energy stored *today* may be useful and cost-effective *tomorrow*. A value of 0.2 was chosen for the turbulence intensity and 2 standard deviations were used to calculate wind speed swings during each hour. Figure 9-4 shows the representation of the conservative superstructure, where all the technologies are present from which OMSES selects the optimal combination.

PROBLEM: REMOTE UG MINE IN NWT + WIND POWER ILLUSTRATION MPC-OMSES FOR CONTROL		
	Equation	Inputs
<b>MINIMIZE</b>		Table 9-1
Total annual cost = Investment Cost	(3-4) (3-5) (3-6)	
+ Variable Cost	(4-12,13) storage	
+ Demand Charges	(3-7) (3-8)	
+ Support Revenues	<del>(3-23)</del>	
+ Penalties		
<b>SUBJECT TO</b>		
Utility Energy Balance	(3-12,13,14)	Figure 9-2
	(4-14) storage	Table 9-2
Equipment performance:		
- Conversion coefficients	(3-11)	Table 9-1
- Production limits	(3-9)	
o Maximum load	(3-10)	Table 9-1
o <del>Minimum load</del>		
<del>Infrastructure Constraints</del>	<del>(3-17,18)</del>	
Storage Balance		
- Hourly	(4-15) to (4-23)	
<del>Monthly</del>	<del>(4-22,23)</del>	
Scenario Based:		
- Resource Availability		
o Wind	(4-5) (4-6)	Figure 9-3
o <del>Biomass</del>	<del>(3-15,16)</del>	
- Spinning Reserve	(4-7) to (4-11)	S VI,V,VI
<del>Storage Charging/Discharging</del>		
- Demand Charge		
o Fixed		
o <del>Free</del>		
- Terminal constraint on storage		
o Applied		OMSES
o Not applied		MPC
<b>DECISION VARIABLES</b>		
Technologies Available		S I,II e.g. 0 WT
Equipment Units		S VI – 4WT
- OMSES		
- MPC-OMSES		
<del>LT-OMSES</del>		
Storage Size		
Grid Capacity		Appendix 4
Energy/Mass Flows		
- Typical days		OMSES
- Rolling horizon		MPC
Incremental Equipment units	(5-6)	See Chapter 10

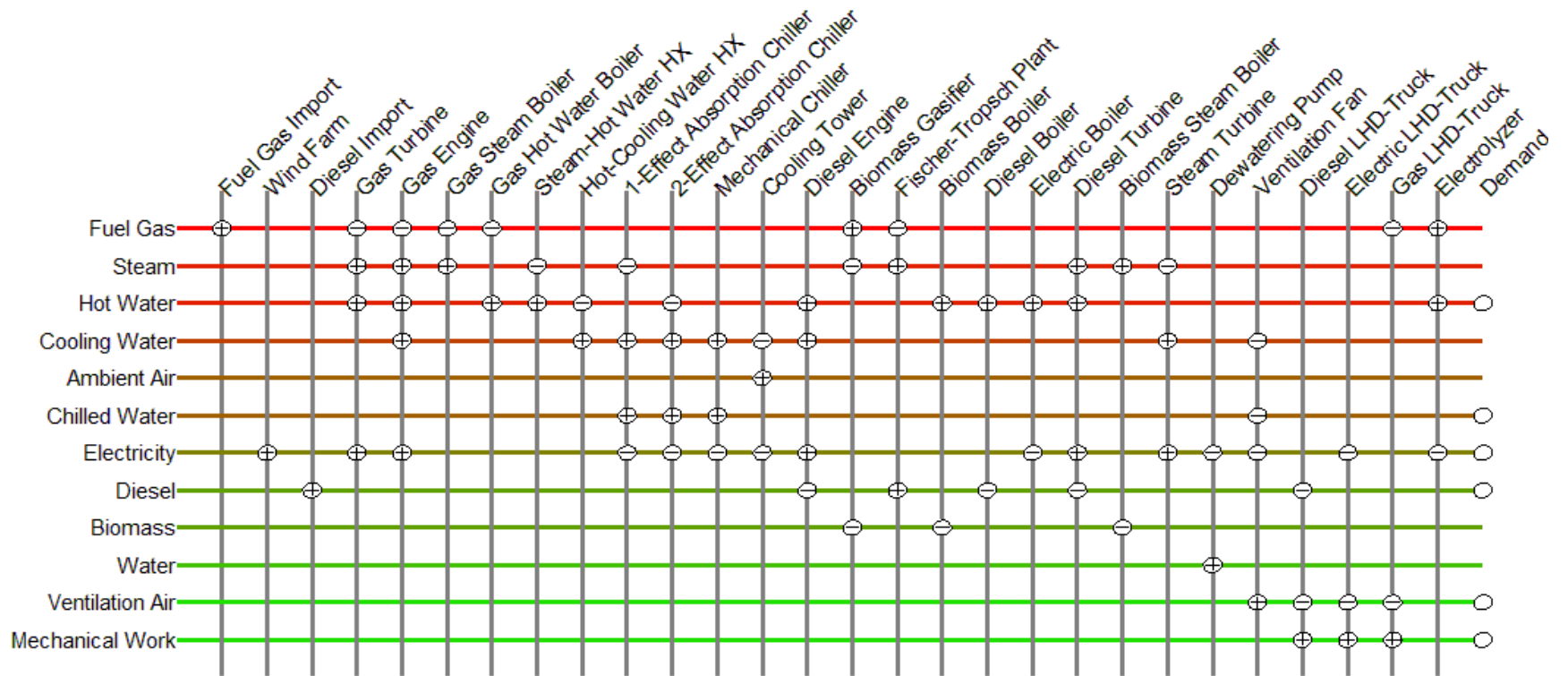


Figure 9-4 Conservative superstructure for an underground mine

## 9.3 Design Results Using OMSES

### 9.3.1 Wind Analysis Results

Inner Whaleback's weather station, located on a small island at Great Slave Lake (Environment Canada website, 2014), measures the wind speed free of obstacles and at a height that must be considered a good approximation of the conditions at the Diavik mine in the absence of closer and higher wind speed observations. The anemometer measures the wind speed free of obstacles, at 10 m from the ground and approximately 20 m from the surface of the lake (Oswald and Rouse, 2004). Ground roughness can be considered very small, making the station data a conservative but reliable estimation. Both Weibull and Rayleigh frequency distribution functions ( $h$ ), were calculated using the Generalized Reduced Gradient (GRG2) nonlinear optimization code from Microsoft Office Excel Solver tools (Microsoft website, 2007), which fitted  $c$  and  $k$  parameters based on the least square method. Subsequently, the Weibull distribution (shape parameter=2.364, scale parameter= 7.425) was used to calculate the power produced at each speed by the wind turbine.

Table 9-3 shows an estimation of the power that can be produced on-site using the selected wind turbine. For example, using the number of wind turbines installed at Diavik (four), an equivalent wind farm with the weather conditions of Inner Whaleback would yield (including all losses) 15.85 GWh annually. When the air density is corrected using the  $WPADF_{rnc}$ , the value reaches 16.74 GWh. These values correspond to a 27.3% capacity factor over 8760 hours of operation.

**Table 9-3 Wind speed data and wind turbine output (Inner Whaleback year 2012)**

Magnitude	Value	Units
Mean speed	6.68	m/s
$Power _{mean}$	0.40	kW
Root mean cube ( <i>rmc</i> ) speed	7.90	m/s
$Power _{rmc}$	0.60	kW
Expected annual production E-70 ( $\rho_{air}=1.225 \text{ kg/m}^3$ )	5.50	GWh

Assuming that all the energy produced can be integrated in the local grid without energy storage, the aerodynamic, electrical, and mechanical losses will reduce the energy harvested and the capacity factor. Considering that after distribution losses 80% of the wind farm electrical power can be used in the mine (EWEA, 2009), including the energy required to heat the blades (in case of ice formation) and the electronic components, the wind farm would yield 16.02 GWh with a capacity factor of 21%. Rio Tinto reports a characteristic wind speed of 7.22 m/s at a height of 60m, with an expected annual yield for the wind farm between 15 and 17 GWh (21-26% capacity factor) depending on the losses considered. The company also reports an average wind speed of 6.3 m/s (), a value close to the 6.68m/s at Inner Whaleback.

Wind speed data from the Inner Whaleback station was used to calculate the *root mean cube* speed values for each month during 2012, as well as the annual value (Figure 9-5). These monthly values were used together with the normalized hourly profiles for each month (Chapter 4), to compute the characteristic wind speed profiles used in the design problem.

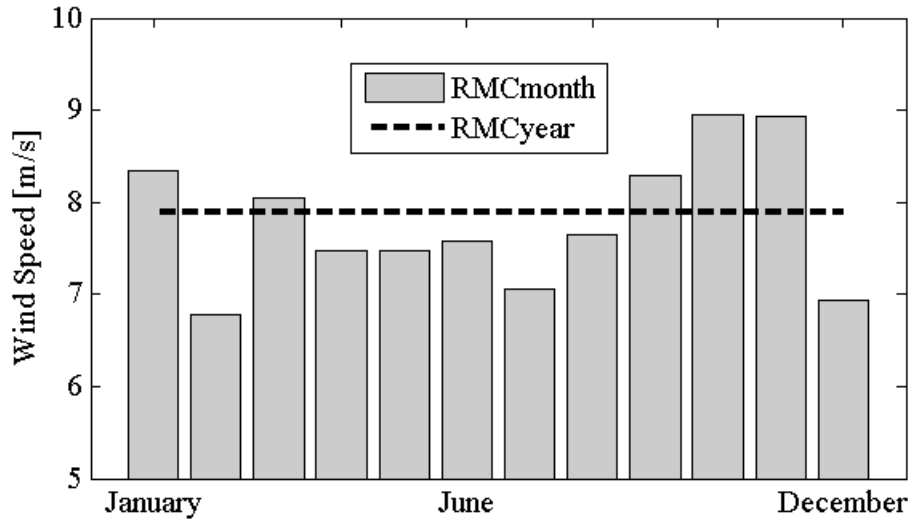


Figure 9-5 Root mean cubic (rmc) speed for the months of the year considered (2012) measured at the Inner Whaleback weather station

### 9.3.2 Optimal Design for the Scenarios Considered

Figure 9-6 shows the graphical result of the technologies included in the superstructure solution of the design problem, for all scenarios considered. Heat storage, although part of the optimal solution of several scenarios (II to VI), was not represented in order to reduce the complexity of the representation. Table 9-4 summarizes the results of six scenarios, and compares each with scenario II (*BAU*). Although the solutions of scenarios III to VI differ significantly in variable cost savings (primarily diesel cost), their total annual cost varies marginally when they are compared to scenario II. Therefore, no definitive conclusion can be drawn from the results regarding which may be the optimal solution in practice.

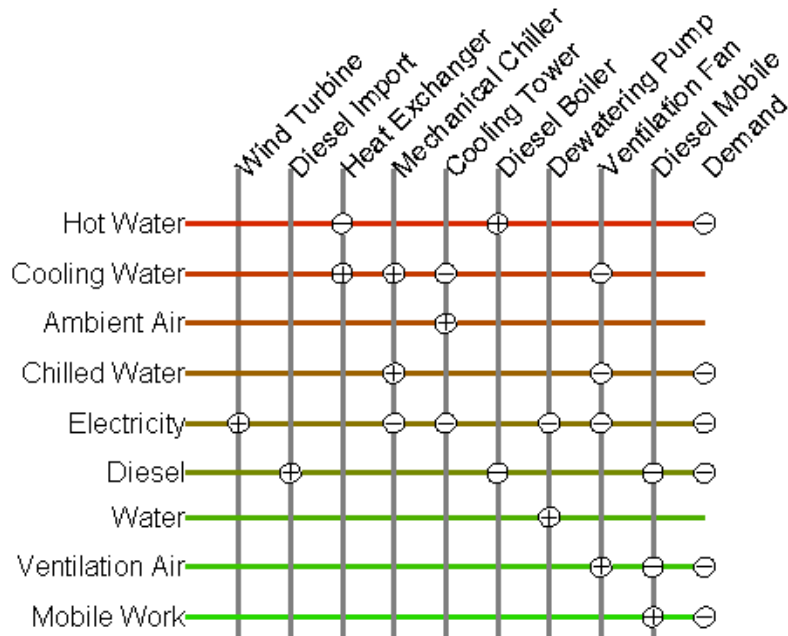


Figure 9-6 OMSES result superstructure with the installed technologies

Additional parameters to evaluate the risk of each option (2, 4, or 8 wind turbines) should be considered. For example, scenarios V and VI have total annual cost savings of the same order (0.07% and 0.02%). Differences between total annual cost savings amongst scenarios are swamped by the high annuitization factors associated with 10 year mine lives. Differences of 0.07% are nonetheless valuable in guiding decision making as operating cost savings are still substantial. Thus, scenario V can be considered a more attractive solution because its lower investment cost results in a lower financial risk. However, should the diesel consumption need to be reduced further, scenario VI or even IV can be considered better options.

Wind turbine capacity factors (CF) (Table 9-4) are in agreement with those reported for the actual wind farm (Judd, 2014). From the total annual cost values, it can be stated that wind turbines, with the cost considered, break even at a discount rate of 10% and 10 years project life, which agrees with the information reported by the operators of the actual wind farm.

**Table 9-4 Scenario results from the design optimization problem (mine life 10 years)**

	Units	Scenarios					
		I	II	III	IV	V	VI
Diesel Engine	-	6	10	10	10	10	10
Electric Boiler	-	0	0	0	0	0	0
Diesel Boiler	-	9	9	9	9	9	9
Single Effect Abs. Chiller	-	0	0	0	0	0	0
Mechanical Chiller	-	2	2	2	2	2	2
Cooling Tower	-	1	2	2	2	2	2
VA-HW HX	-	0	0	0	0	0	0
HW-WR HX	-	4	4	4	4	4	4
Pump	-	6	6	6	6	9	15
Fan	-	5	5	5	5	5	5
Diesel Mobile Plants	-	19	19	19	19	19	19
Electric Mobile Plants	-	0	0	0	0	0	0
Wind Turbines	-	0	0	8	8	2	4
Electric Storage	MWh	0.0	0.0	0.0	0.0	0.0	0.0
Heat Storage	MWh	0.0	8.1	12.8	12.8	10.1	9.0
Water Storage	m <sup>3</sup>	0.0	0.0	0.0	0.0	1000.0	984.2
Investment In Equipment	MCAD	55	76	138	138	91	107
Total Annual Cost	MCAD/year	112	102	102	103	102	102
Annuitized Fixed Cost	MCAD/year	9	12	22	22	15	17
Variable Cost	MCAD/year	103	90	80	81	87	85
BAU Variation	Investment	-27.15%		82.23%	82.23%	21.00%	42.05%
	Total annual	9.63%		-0.37%	0.67%	-0.07%	-0.02%
	Variable	14.65%		-11.63%	-10.45%	-2.94%	-5.76%
Imported Diesel	GWh	756.86	655.93	576.62	577.08	635.74	615.99
	-	15.4%		-12.1%	-12.0%	-3.1%	-6.1%
Wind Performance	Penetration	0		17.10%	16.99%	4.20%	8.45%
	CF	0		24.21%	24.06%	23.80%	23.93%

## 9.4 Further Parametrical Analysis Using OMSES

### 9.4.1 Total Annual Savings as a Function of Wind Turbines Installed

A parametrical analysis was conducted, flexing the number of wind turbines installed (as an additional constraint of the design problem). The savings obtained (Figure 9-7) are in agreement with Table 9-4. It was also assumed that electric storage is not allowed and spinning reserve is required. The optimal solution includes 2 wind turbines (in agreement with scenario V, Table

9-4), although 1 and 3 turbines yield similar results and even 4 generate savings in total annual costs. It should be noted that the use of a continuous line style to present the results in Figures 9-7 to 9-9 is to assist in interpreting trends; this does not imply that anything other than an integer number of turbines can be selected.

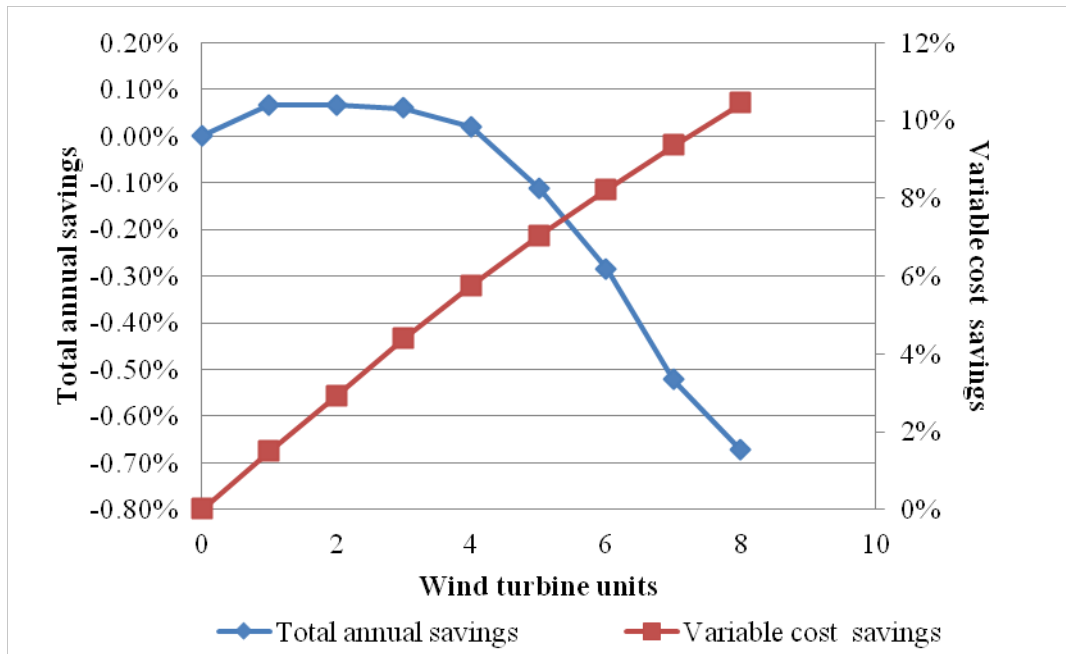


Figure 9-7 Optimal wind turbine units influence total annual cost and variable cost savings

### 9.4.2 Electricity Storage Influence in the Optimal Design

The scenarios presented previously precluded the selection of electrical storage system because Diavik does not have any. However, installing some storage capacity could be beneficial to the mine operator by reducing the TAC. This is explored in this section and revisited in Section 9-6.

Figure 9-8 shows the results of the same parametric analysis, but permitting electrical storage, whose results are also plotted. The curves show different optima: 2 and 4 wind turbines, respectively. It should be noted that the wind speed values used in the design problem

overestimate the spinning reserve that, in general, the wind farm will require from the microgrid. In practice (actual wind conditions), wind speed will remain high enough to stay away from the transition speeds, compared to the typical wind profiles which are somewhat flat due to the averaging process (Chapter 4, Section 4.1.2). This transition area is defined between the cut in speed and the minimal speed that provides the nominal power. When the wind blows within this range (Figure 9-3), higher drops and surges of power generation occur, and therefore more spinning reserve is required. Consequently, the optimal size of the wind farm, if cost-effective, is likely to change in practice. The optimal design will have a superior limit solution when spinning reserve is not a constraint of the problem (i.e., scenario III).

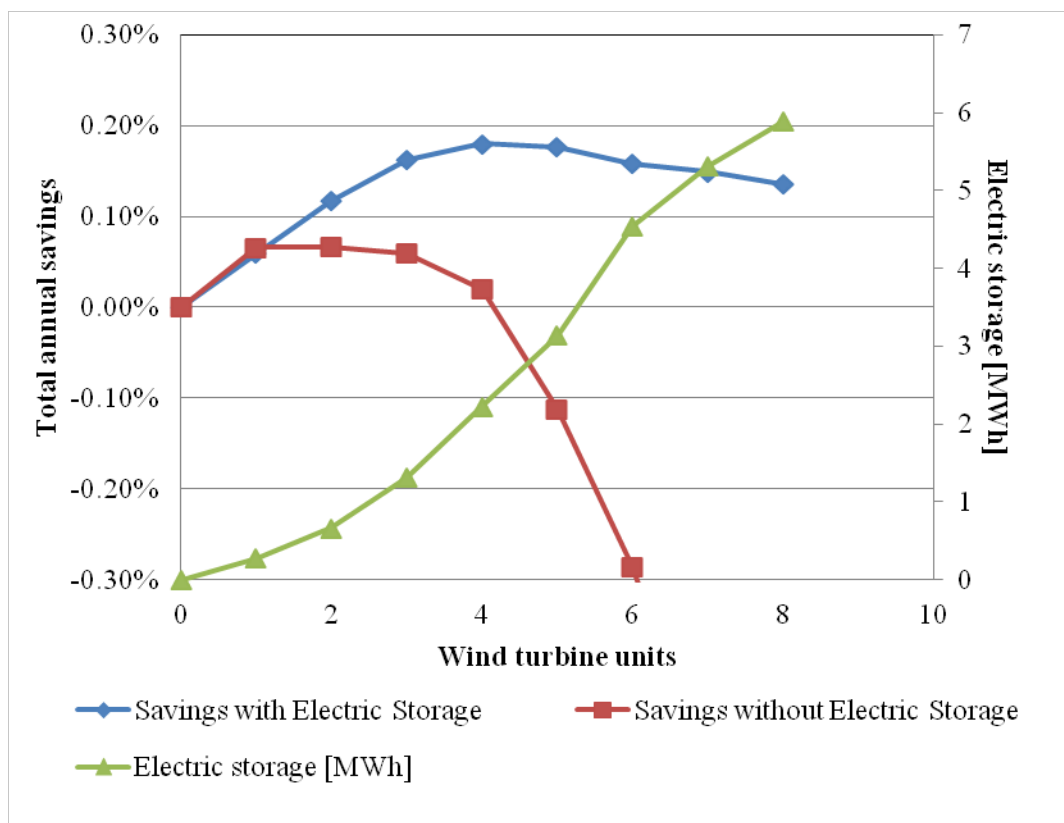


Figure 9-8 Electric storage influence optimal number of wind turbine units

Diminishing returns are observed in the installation of electrical storage (Figure 9-8). The maximum total annual cost savings, when electric storage is allowed, coincides with the inflection point of the corresponding curve (Figure 9-8).

### 9.4.3 Total Annual Savings as a Function of the Mine's Life and the Number of Wind Turbines

Assuming spinning reserve was not necessary, and with only dispatchable pumps as an electric storage, a sensitivity analysis of OMSES' optimal design was carried out regarding the life of the project. This affects the capital recovery factor. Figure 9-9 shows increased turbine installation with a longer mine life, and greater savings relative to BAU. But curves shown in Figure 9-9 should be regarded as upper bounds of the more complex problem that requires spinning reserve and allows electric storage in the form of electric batteries. Diminishing returns appeared when manipulating the number of wind turbines installed, illustrated by the different curves' maxima.

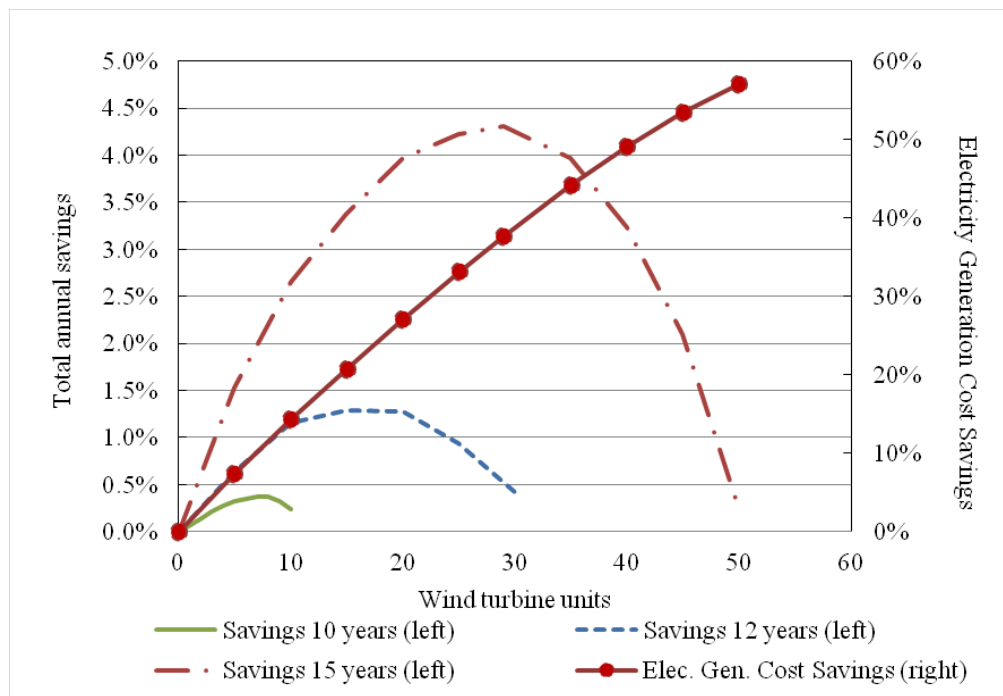


Figure 9-9 Project life influence on optimal wind turbine units and variable costs (without spinning reserve nor electric storage)

## 9.5 Simulation Results

### 9.5.1 Optimal Operation of Scenario VI Design

Before providing simulation results, it should be noted that the discussion focuses on the solution that includes four wind turbines. The reason for this selection is that the actual mine modeled has four turbines installed, which have been running since September 2012; their operation confirms the expected wind farm power output from the feasibility stages and herein calculated.

As expected, the use of average environmental conditions limits the ability of the optimal design to cope with practical demands. Simulations during the summer season revealed a shortage of chillers and cooling tower capacity. It was acknowledged that the actual summer temperature can vary from the average profile, which OMSES uses in the design stage. In winter months, because the system was designed with spare heating capacity (9 boilers), operating constraints were satisfied at each interval. When the system was simulated during the summer months, however, the problem became unfeasible for the design considered (IV). This indicated potential undercapacity of the installed equipment needed in summer – mechanical chillers and perhaps cooling towers and heat exchangers. The numbers of units installed of these technologies was increased until the problem became feasible. 2 and 3 additional units were required of mechanical chillers and cooling towers, respectively. A systematic approach to adjustments of the design of the ESS (such as these) is discussed in detailed in Chapter 10.

Table 9-5 illustrates the differences between the expected performance of the energy system in the design problem and in the simulation. Two scenarios were compared: the conventional system (scenario II) and the system with 4 wind turbines (scenario VI). The values shown are energy consumption (MWh) of diesel per day to generate electricity. For the simulation, the wind

turbine speed was calculated considering a perfect forecast for the first three hours, while for the remaining 21 hours using the normalized profile and the weighted average speed of the first three hours. Results shown in Table 9-5 do not consider wind power correction due to air density variations.

**Table 9-5 Average diesel used for electricity generation [MWh/day]**

Scenario	Design		Simulation	
	II	VI	II	VI
January	1354.4	1217.7	1354.3	1236.3
February	1354.4	1279.9	1354.3	1284.7
March	1354.4	1232.3	1354.3	1250.2
April	1354.4	1255.5	1354.3	1262.5
May	1355.2	1256.0	1355.1	1264.3
June	1361.7	1256.1	1356.5	1210.8
July	1373.0	1288.2	1373.8	1256.0
August	1364.5	1256.5	1383.1	1300.5
September	1355.9	1220.5	1367.1	1247.9
October	1354.4	1187.7	1354.7	1261.4
November	1354.4	1190.8	1354.3	1259.2
December	1354.4	1274.3	1354.3	1250.2
Average	1357.6	1243.0	1359.7	1257.0
RD		-8.45%		-7.87%

The relative difference, *RD* (Table 9-5), represents the reduction of diesel consumption to generate electricity in scenario VI, relative to scenario II. This value indicates the diesel offset or the average penetration factor of the wind farm. If the air density is corrected, the relative difference becomes -8.01%. Diesel savings from Table 9-5 are in agreement with the penetration ratio of Table 9-4 (VI column).

In contrast, when scenario IV with corrected air density is simulated, the relative difference with respect to scenario II yields -15.96%, in agreement with the Table 9-4 penetration ratio (16.99%). Simulation of both case VI and II meet the design results in terms of diesel used. There is no practical difference between the optimal solutions of the scenarios studied.

Simulation results in Table 9-5 are given as daily averages for each month, in order to facilitate the comparison with the design results. The results shown do not include the amount of diesel consumed to operate the engines acting as spinning reserve; here, this amount is low enough that it can be neglected without affecting the conclusions drawn. In the case of bigger wind farms with higher penetration factors, this assumption would not be valid.

Table 9-6 illustrates the difference in variable cost savings between scenarios IV-VI and scenario II (or *BAU*), for both design and simulation problems. The MPC-based simulation includes the spinning reserve and air density correction and, apart from the dewatering pumps which are effectively dispatchable loads, does not include electrical storage. In both the design optimization and the MPC simulation formulation, spinning reserve ( $\mu_{PM,ij}^{SR}$ ) can be decreased by shifting load demand (dewatering). This reduces the load ( $\Phi_{PM,ij}^{pro}$ ) of the active diesel generators ( $\mu_{PM,ij}^{op}$ ), which then reduces the need for engines in spinning reserve. As stated previously, the use of spinning reserve for the calculations in the design stage significantly overestimates the diesel consumed for the reserve engines. It should be remembered that the design problem uses *rmc* speed values to calculate wind power, and although these are valid to calculate monthly and annual wind energy harvested, they poorly represent what happens on individual days.

**Table 9-6 Variable costs savings (relative to Scenario II)**

	Scenario V (2 WT)	Scenario VI (4 WT)	Scenario IV (8 WT)
Design (Table 4)	2.93%	5.76%	10.45%
MPC Simulation	2.76%	5.65%	11.26%

### 9.5.2 Wind Forecast Analysis

The influence of the precision of wind speed forecast was investigated. Using the optimal design for scenario VI, different forecast cases in accordance to Section 9.1.4 were simulated. January

demands and environmental conditions (temperature and wind speed) were selected for illustration. Air density correction was included in the calculation of wind power. Table 9-7 shows how the goodness of the forecast affects the efficiency in which heat storage can be managed to reduce the heat produced by auxiliary boilers. It should be noted that this additional heat is small compared to the fuel used by the generators, but this might be different in mines with higher heating demands.

**Table 9-7 Wind speed forecast influence on diesel consumption**

Diesel	Electricity [MWh]	Heating [MWh]	Heating Variation from Persistent Wind
Persistent wind	1220.3	37.0	
1 hour extrapolation	1220.3	39.0	5.49%
3 hour extrapolation	1220.3	35.7	-3.58%
Perfect 24h forecast	1220.6	31.3	-15.26%

### 9.5.3 Wind Penetration, Spinning Reserve and Curtailment Analysis

Figure 9-10 illustrates the performance of the wind farm and the total spinning reserve needed, i.e., the number of synchronized engines ( $\mu_{PM,ij}^{SR}$ ). The data represents several hours of January from the MPC simulation, after OMSES' optimal design calculation, and reflects the power per wind turbine (in MW). The *power generated* by the wind farm (dashed line) is always equal to or lower than the total *available power* (solid line). The penetration ratio (*PR*) is calculated as the power generated by the wind farm (losses included) divided by the total power consumed in the mine. The curtailment (difference between available WT power and actual delivered) appears for significantly different penetration ratios, i.e., at t=410 (*PR*=14.0%) or at t=417 (*PR*=40.0%). The methodology is sensitive to the cost of operating an additional engine for spinning reserve. The maximum *PR* in January (scenario VI with air density correction) was 46.7% (t=428), requiring two generators in spinning reserve.

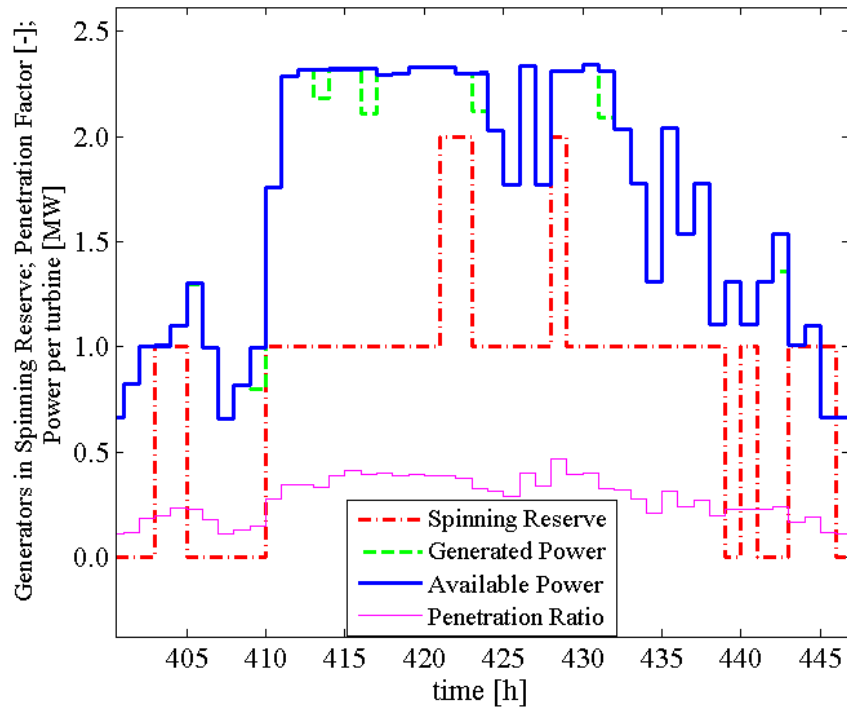


Figure 9-10 Spinning reserve and wind power curtailment during January

## 9.6 Discussion

In the previous section, results demonstrated that the optimal solution obtained using characteristic days was an adequate starting point for energy systems' design including wind energy. By simulation under more realistic operating conditions, it was possible to identify the deficiencies of that no-longer optimal design. In general, once these issues are solved, the resulting design for a particular scenario can be analyzed from the point of view of their performance under more realistic conditions. Further design modifications can be applied to investigate to what extent the approach used appropriately deals with the challenge of integrating renewable energy sources.

The aim of this section is to investigate the performance of the optimal design from scenario IV. The optimal design according to OMSES (Table 9-4) includes 2 wind turbines. However,

through simulation of the system was observed that the practical optimum is more likely to be found with 8 wind turbines (scenario III, Table 9-6). It is reminded that scenario III solution is the optimal when spinning reserve is not imposed. Furthermore, in order to investigate the usefulness of electricity storage, a simulation was conducted using scenario IV design results completed with 10 MWh of electricity storage. The described energy system was simulated throughout a complete year, and the results are discussed hereafter.

Using a control horizon of 24 hours and a three hour perfect forecast of wind speed (with *SR*) during the month of January, the overall diesel savings related to electricity generation, including that used for the spinning reserve idling generators, achieved 1% compared to the same design but without electricity storage. These savings, which are a function of the diesel that an idle engine consumes, may or may not offset the investment cost in electricity storage. Assuming annual savings in diesel for electricity of 1%, the electricity storage in the configuration selected (modified scenario IV) is paid in 3.5 years. It should be reiterated that, because of the inter-day limitation of the present design approach (OMSES, but also MPC with  $H_c=24$  hours), it is difficult to assess the cost-effectiveness of energy storage beyond its use for spinning reserve. However, using longer control and prediction horizons than those used here, the benefits of higher energy storage capacity may be identified.

The effect of electricity storage on spinning reserve was explored at operational level, and the results are shown in Figure 9-11 and Figure 9-12. In absence of electrical storage (Figure 9-11), there were as many as three engines in spinning reserve during some hours of January. This figure can be compared with Figure 9-10, where only two generators were required for a wind farm with 4 wind turbines.

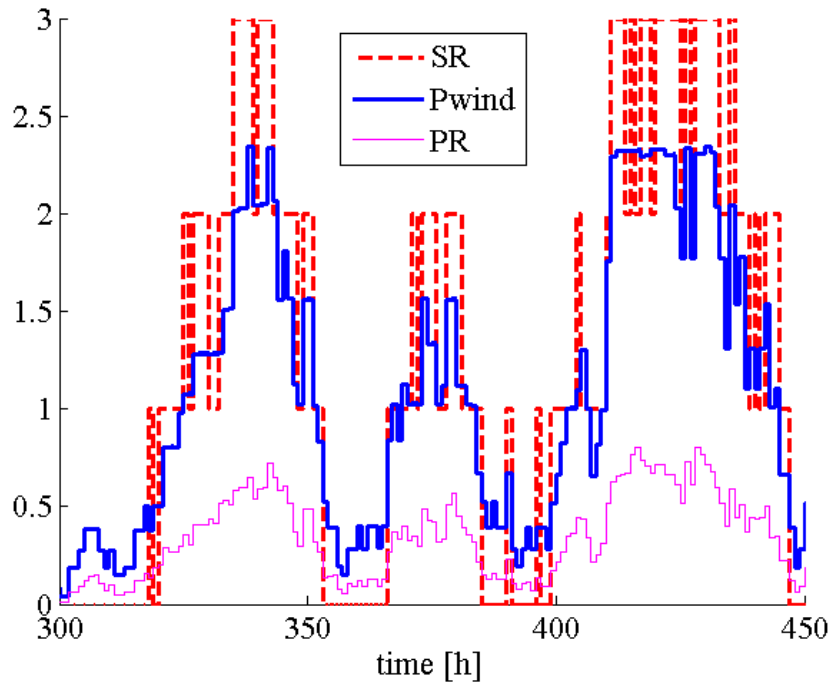
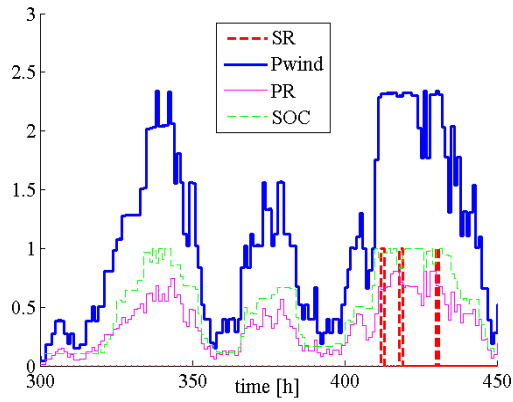
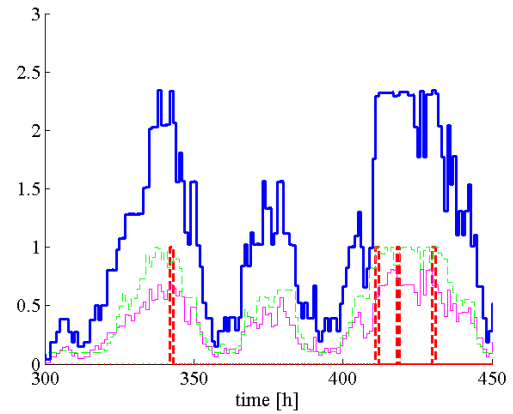


Figure 9-11 Spinning reserve in absence of electric storage.  $P_{wind}$  is the power produced by each turbine, in MW, SR is the spinning reserve, and PR is the penetration ratio.

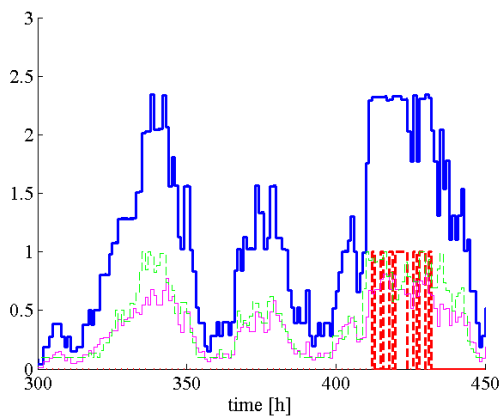
As shown in Section 9.4.2, electrical storage revealed cost-effective when the problem constraints were relaxed, increasing the optimal number of wind turbines (Figure 9-8). Figure 9-12 shows the influence of the control horizon on the spinning reserve and the schedule of electric storage, now present. This influence is illustrated by the evolution of the state of charge (SOC). For this analysis, the prediction horizon is equal to the control horizon. The values for the horizon were 3, 6, 12, and 24 hours, and the simulations were again performed for the month of January.



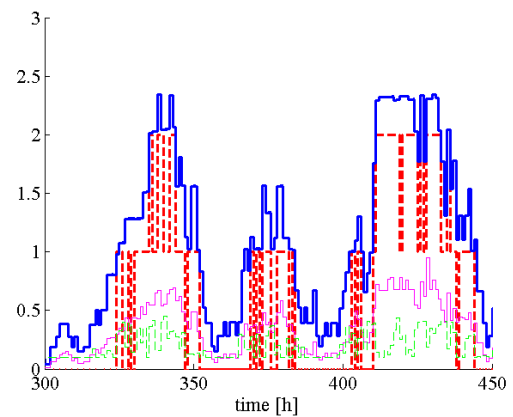
a.  $H_c=24$



b.  $H_c=12$



b.  $H_c=6$



b.  $H_c=3$

**Figure 9-12 Influence of control horizon on the electric storage and the spinning reserve**

It was found that the relatively low average penetration ratio (17%, Table 9-4) makes it useless to accumulate energy in the long term (i.e., for successive days). Figure 9-13 illustrates the relationship between the penetration ratio and the considered optimal *SOC*. Represented in this figure is the data from the simulation (blue circles) and the theoretical *SOC* (black lines) needed to displace all the engines used for spinning reserve. This latter can be easily calculated using the equations in Chapter 4 for spinning reserve and considering the average power demand from the mine (around 22 MW). Furthermore, the theoretical relationship (between penetration ratio and state of charge) was calculated for different values of the turbulence intensity (*TI*) (Figure 9-13).

As expected, an increase in  $TI$  requires a higher  $SOC$  to reduce the use of the generators as spinning reserve. The energy used for charging the electrical storage during periods of wind power generation is used up later, as Figure 9-12 indicates. The simulation assumes that  $TI$  is constant, although the actual wind variability provides periods with higher and lower wind speed around the mean value, and the  $SOC$  could therefore be maintained around the level determined by the MPC algorithm.

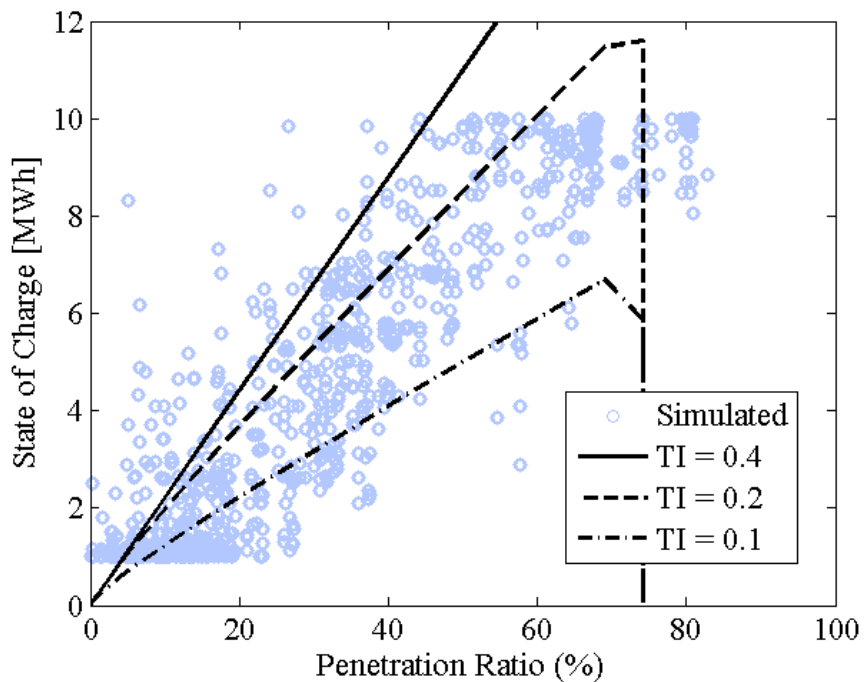


Figure 9-13 State of charge and penetration ratio relationship for different turbulence intensity levels ( $TI$ )

## 9.7 Conclusions

The present chapter investigated two aspects related to optimal energy supply systems: the consideration of wind power, using  $r_{mc}$  wind speed to characterize the resource within the

problem of optimal design, and the robustness of the optimal design previously determined under a more realistic, uncertain operating environment, i.e., through simulation.

The case of a remote underground mine was considered. Its demands were calculated based on data from an existing operation – Diavik Diamond Mine. The ESS of this mine is an actual hybrid microgrid, integrating diesel generators and wind turbines. The usefulness of the wind data obtained from a nearby location was assessed by comparison with the reported energy production declared by the operators of the existing wind farm at Diavik.

Six scenarios with different constraints were considered in the design stage. In all scenarios, the wind farm was found to be cost-effective, although the optimal number of wind turbines differed. For instance, when the formulation included constraints regarding spinning reserve, the optimal design included two wind turbines. Conversely, for the design problem where spinning reserve was unconstrained, the optimal solution included eight turbines. For the real mine, Rio Tinto reports a payback period of less than eight years for Diavik’s wind farm, demonstrating the cost-effectiveness of such an investment, which is in agreement with the results obtained.

Further investigations on the optimal design were addressed regarding the life of the mine. The main conclusion after running a series of parametrical analyses was that the size of the wind farm experiments eventually yielded diminishing returns, even if the technology is cost-effective under the economic environment defining a particular problem.

The limitation of the design problem to generate practical solutions was subsequently investigated. In order for it to meet the mine’s demands throughout the whole simulation interval (one year), the design was corrected by trial and error regarding the number mechanical chillers

and cooling towers. However, this approach can be substituted by a relaxation of the constraints of the simulation problem. This is investigated in Chapter 10.

The results from the simulation stage validated the design approach regarding the use of *rmc* wind speed to characterize this renewable energy resource, as well as the methodology to ensure proper spinning reserve to deal with wind variability.

An MPC approach for simulation and operation optimization was confirmed as necessary to evaluate not only OMSES' optimality, but also feasibility. OMSES, however, proved to be robust and reliable enough to assess the cost-effectiveness of renewable, naturally variable energy resources in mine energy systems in remote locations.

For validation purposes the same case study has been analyzed using the commercial, well established computer software HOMER. The results of the optimization process using this tool have been included and discussed in Appendix 5.

# Chapter 10

## 10 Applications of MPC to Mitigate OMSES Model Inaccuracies

This chapter explores the use of MPC to mitigate the effect of model inaccuracies on the control of optimal ESS, in particular for mine sites. To this end, and for illustration, a more detailed model of the heat storage system is developed that captures the dynamics of the thermal system present in the optimal solution for the previous case study (Chapter 9). This model is used in combination with a zero order dynamic model, which supports MPC in establishing the optimal operating plan in a receding horizon. This is possible given that MPC relies on the feedback information obtained, in this case, from the detailed model formulated.

In addition, MPC is used in this chapter to identify and eliminate the infeasibilities arising in OMSES design results that appear when the operating conditions deviate from the typical values. The process of demand averaging makes it difficult to achieve reliable system designs that can operate in peak demand conditions. MPC is applied to control the energy system of a mine, dealing with power shortages in some technologies, and leads to increased capacity for those technologies that economically make sense to install. This approach is compared with a more detailed OMSES development that considers a typical year with energy demands and environmental conditions defined through 8760 hours.

The cases explored in this chapter use the model of the mine described in Chapter 9. Emphasis is placed on the interaction between the cogeneration plant, the heat recovery loop from the diesel generators, the heat storage, and the wind power production.

## 10.1 Introduction

Thermal engines can be used to meet simultaneous demand for electricity and heat in the so-called cogeneration mode. When this happens, the engines require a different, more demanding control approach than for those only supplying electricity. In this case, the coproduced heat is released into the surrounding environment, while in cogeneration mode, all or part of the heat is consumed instantly or stored for a later use.

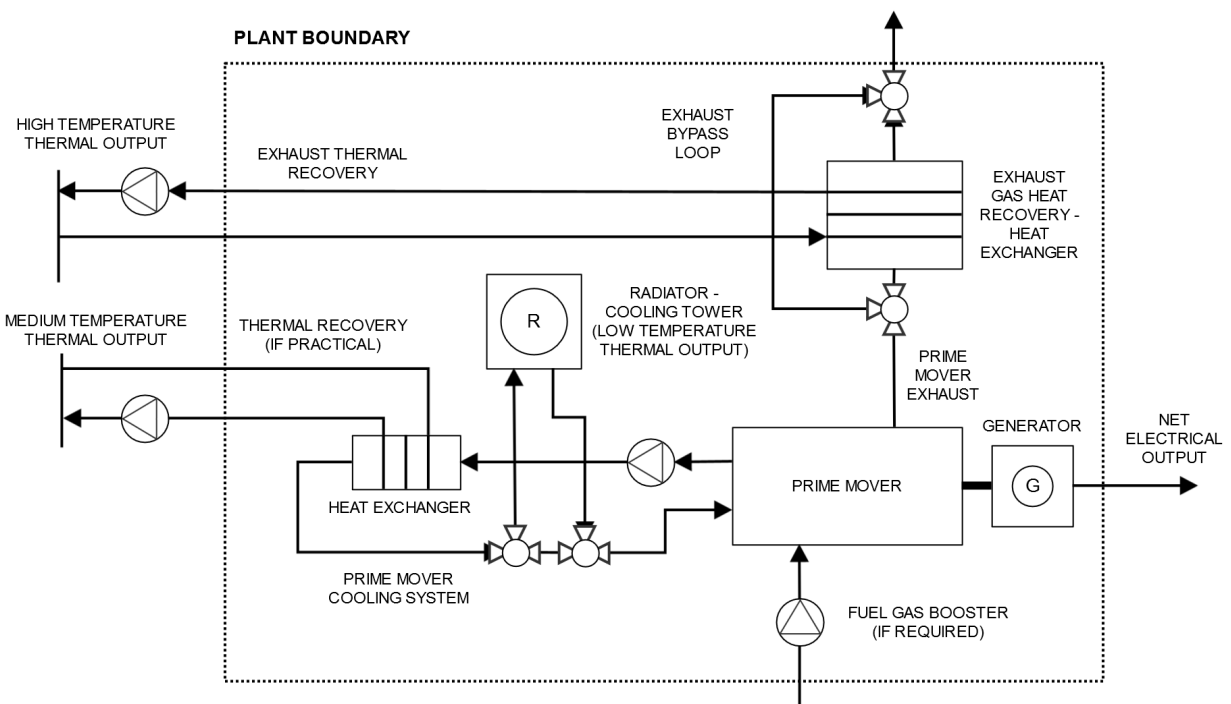


Figure 10-1 Cogeneration plant schematic, adapted from ASHRAE (2012)

When reciprocating internal combustion engines (ICE) are used, the cogenerated heat can be divided by temperature levels (usually two): high temperature from the exhaust gases (300-600 °C) and medium temperature from the engine block cooling system and the lubricating (oil) circuit (70 to 100°C). The medium grade heat is normally removed from the engine through an auxiliary cooling system, involving a secondary transfer fluid that, when this heat is not

consumed, releases it to the environment in cooling towers providing a heat sink at a lower temperature level.

Heat from the exhaust gases is recovered through heat recovery systems – heat exchangers that transfer energy from the gases to other fluids, such as water. When heat from the gases is not either consumed or stored, it is normally bypassed using an auxiliary stack system connected through diverters upstream of the heat recovery system.

## **10.2 Detailed Modeling of the Heat Storage System for Improved MPC-Based ESS Operation**

### **10.2.1 Heat Storage Modeling**

In this section, a model of the heat storage system (Figure 10-3) is developed. The arrows in and out of the storage can be considered as the charging and discharging loops that connect it with the rest of the cogeneration plant. The model described responds to a first order differential equation, intending to capture the heat transfer processes of charging the storage, as well as the heat losses as a consequence of a temperature gradient from the storage system and the surrounding environment.

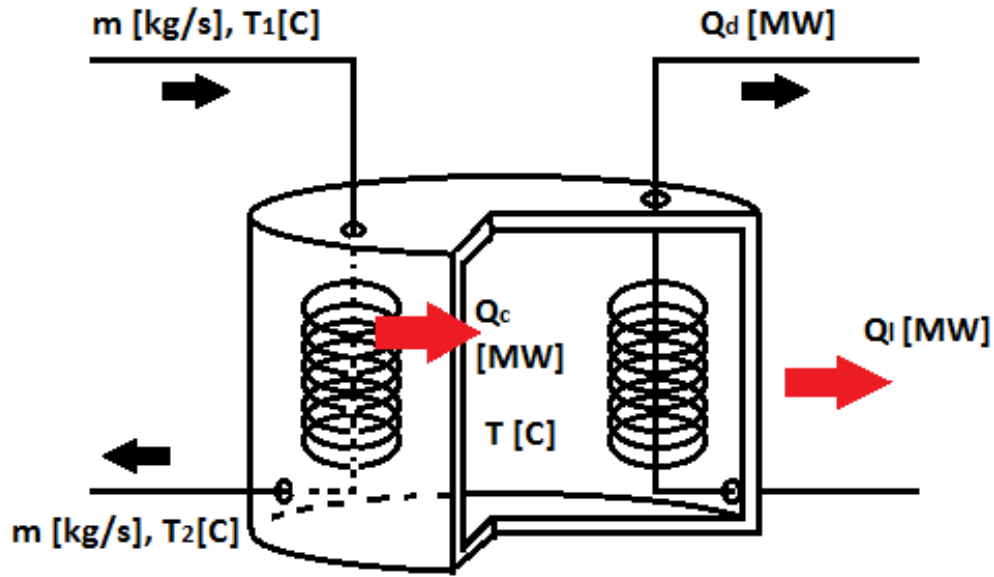


Figure 10-2 Thermal model of the heat storage system

Equations 10-1 through 10-8 define the thermal dynamic behavior of the heat storage system (Figure 10-2), and have been developed from several sources (Kim et al., 2000; Romero et al., 2015b).  $Q_d$  is the discharge heat flow, which is determined by the centralized controller. In addition,  $Q_c$ , the charge heat flow, is calculated by the control algorithm, but it is translated into a mass flow rate by means of Eq. 10-8, which uses the nominal values of the heat exchange process. The detailed model, which more accurately represents the dynamics of the storage than the MPC internal linear model does, is defined by a first order differential equation, Eq. 10-6.

$$Q_l = UA_{ext} \cdot (T - T_{amb}) \quad (10-1)$$

$$Q_c = UA_{int} \cdot (\bar{T} - T) \quad (10-2)$$

$$Q_c = \dot{m} \cdot C_p \cdot (T_1 - T_2) \quad (10-3)$$

$$\bar{T} = (T_1 + T_2)/2 \quad (10-4)$$

$$Q_c = UA_{int} \cdot (T_1 - T) / [1 + \frac{UA_{int}}{2 \cdot \dot{m} \cdot C_p}] \quad (10-5)$$

$$M_{STH} \cdot C_{p,STH} \cdot \frac{dT}{dt} = Q_c - Q_d - Q_l \quad (10-6)$$

$$M_{STH} \cdot C_{p,STH} \cdot \frac{dT}{dt} = UA_{int} \cdot \frac{T_1 - T}{1 + \frac{UA_{int}}{2 \cdot \dot{m} \cdot C_p}} - Q_d - UA_{ext} \cdot (T - T_{amb}) \quad (10-7)$$

$$\dot{m} \cdot C_p = \frac{\dot{m}_d \cdot C_p}{Q_{c,d}} \cdot Q_c^{MPC} = \frac{Q_c^{MPC}}{(T_1 - T_{2,d})} \quad (10-8)$$

The overall heat transfer parameter,  $UA$ , measured in W/K, has to be selected to adequately represent the thermal behavior of the actual system. In our case, the values for  $UA_{int}$  and  $UA_{ext}$  are 300,000 and 1,000 W/K respectively. The mass of the reservoir ( $M_{STH}$ ) is 215000 kg and the specific heat for the reservoir fluid and the charging fluid ( $C_p, C_{p,STH}$ ) are assumed to be the same (4200 J/kg-K). The remaining variables include the heat losses against the environment ( $Q_l$ ), the mass flow rate of the charging fluid ( $\dot{m}$ ), and the inlet and outlet temperatures ( $T_1, T_2$ ). The outlet temperature of the charging flux under design conditions,  $T_{2,d}$ , is taken as 50°C. The subscript  $d$  is used to refer to design conditions.

### 10.2.2 Model Predictive Control Layout

Figure 10-3 updates the schematic of a cogeneration plant to include heat storage (at medium temperature). In this section, a dynamic model of the heat storage system is developed to serve as a support for the controller during the simulation of the cogeneration plant that produces electricity and heat to meet the mine's demands. Auxiliary boilers can be placed in different locations, in a trade-off between design cost reduction and heat losses throughout the distribution system.

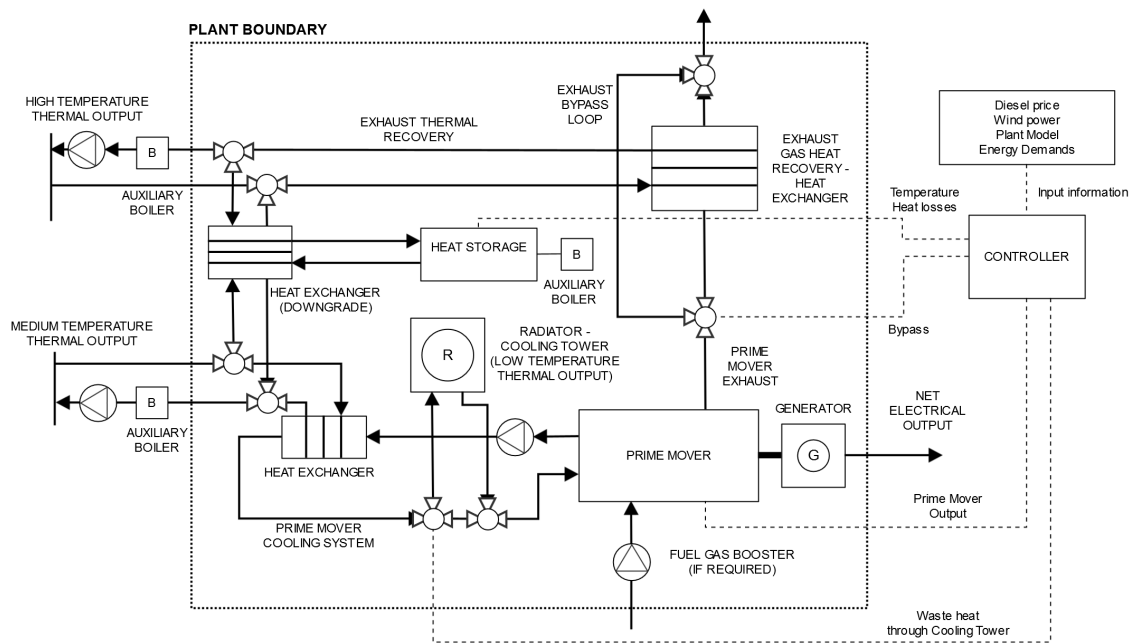


Figure 10-3 Cogeneration plant with heat storage and high-to-medium temperature heat exchange, adapted from (ASHRAE, 2012)

The aim of the controller is to decide and apply the actions that minimize the operating costs, supplying the energy required (electricity and heating in this case), and respecting all the constraints, which mainly consist of energy balances across the plant design.

The controller has information about the ESS through the mathematical descriptions of the technologies (Chapter 3) and the possible interactions between them. It knows the forecasted energy demands and available power from renewable sources, such as wind. The controller also has information about fuel price and O&M costs.

Regarding the cogeneration module, the controller decides about the management of the heat storage (charging and discharging heat flows), the prime mover output, heat recovery bypass, and the waste heat flow, which is removed from the system through the cooling towers.

In addition, the controller is assumed to have complete information about the remaining subsystems, such as ventilation, dewatering, and refrigeration systems, and has access to the actual state of charge of the heat storage and the heat losses or, alternatively, to the temperature and heat losses of a more detailed model.

### 10.2.3 Results

A preliminary assessment of the model was carried out, involving different constraints and control options: with and without information feedback of the system's thermal losses, and with and without feedback of the storage system's temperature. Simulations were run for a complete month. Every hour, a clock-wise model predictive controller optimized the actions of the mine's energy supply system, including those of the heat storage system, for the next 24 hours (control and prediction horizon selected).

Information feedback includes the actual temperature of the storage, more realistically obtained with the dynamic model. This dynamic model is simulated using Matlab *ode23* function, an ordinary differential equation solver (equations and flowchart included in Appendix 8). Heat losses to the surrounding environment are as well considered. At the end of every hour, the past losses are used to estimate those that would occur within the control horizon for which the predictive controller optimizes the operational plan.

For the simulation, it was assumed that  $T_1 = 90^\circ\text{C}$ , and that all the heat from the diesel generators has to be consumed, i.e., exhaust gas bypass was not allowed; Chapter 9 considered that the excess of heat from the cogeneration plant was dissipated through the cooling towers. This assumption will be investigated in the next section

Figure 10-4 and Figure 10-5 show simulation results for the temperature and the corresponding energy state of the storage. These simulations correspond to the first month (January), in which heat storage management is more demanding due to high heat demand and relatively high wind speeds (Chapter 9).

As expected, the maximum temperature of the storage system tends to be that of the charging fluid, i.e., 90°C.

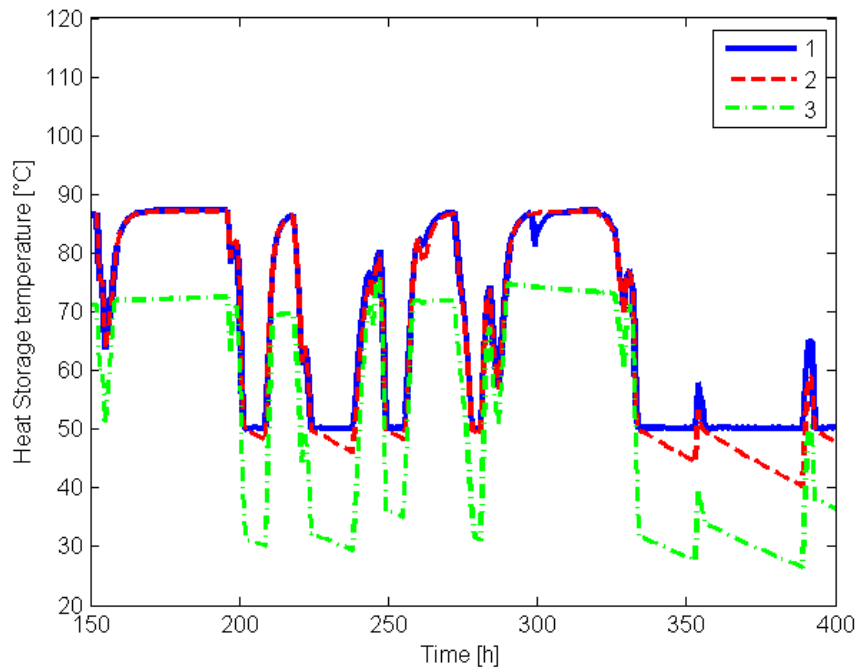


**Figure 10-4 Heat storage temperature with three feedback alternatives: 1) feedback in temperature of the reservoir and heat losses to the ambient; 2) only feedback in temperature; 3) no feedback**

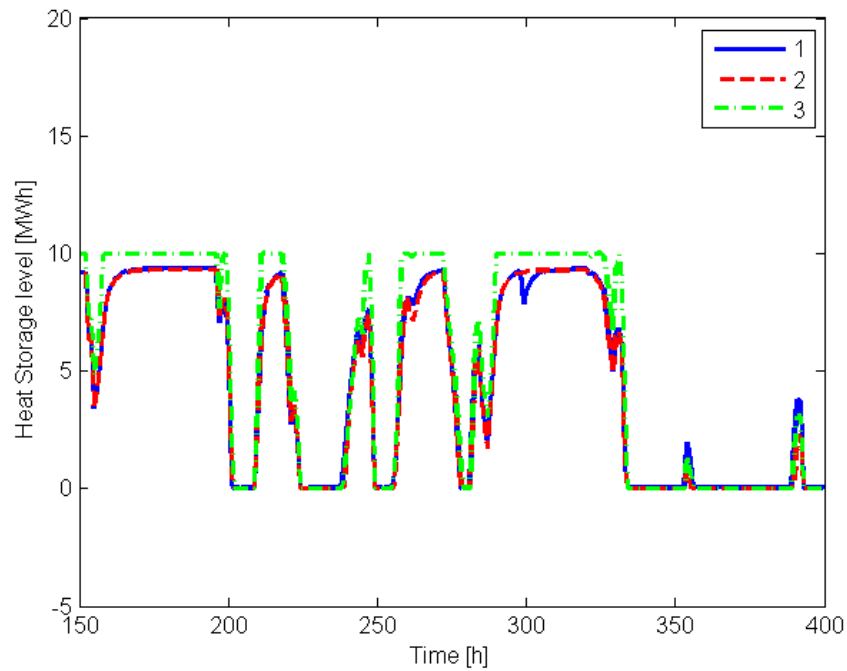


Figure 10-5 Heat storage level with three feedback alternatives: 1) feedback in temperature of the reservoir and heat losses to the ambient; 2) only feedback in temperature; 3) no feedback

In absence of information feedback from the actual plant (here a more realistic model), storage temperature decreases to the point that heat supply to the mine could be compromised; the temperature of the fluid that distributes heating throughout the mine may be lower than required at the consumption point, or return temperatures may drop below the freezing point.

Figure 10-4 illustrates how increasing information feedback of the state of the system and the actual heat losses makes it possible to use first order state space models to optimally control more complex dynamic systems. Without this information, the controller knowledge about the energy stored is close to what could be expected with the feedback loop (Figure 10-5). This is because the controller expects the level (energy) to be greater than or equal to the minimum defined beforehand. The controller always produces feasible plants according to the basic model (zero order dynamic). The lack of accurate information causes the progressive decline in the actual temperature of the system. It can be seen from Figure 10-4, that when heat losses are not

fed into the controller, a long period of underuse of the heat storage system may lead to critically low temperatures.

## **10.3 Analysis of Diesel Generators Waste Heat Bypass in Stand-Alone Systems with Renewable Energy**

### **10.3.1 Cogeneration and Heat Recovery Bypass Modeling Options**

Combined heat and power plants usually include exhaust gas bypass. However, such is not possible in some instances, and any excess in heat production must be transferred to the environment through the auxiliary cooling system, which is also in charge of the adequate cooling of the engine. An assessment of the optimal operation of the ESS of a mine using different heat bypass options in the cogeneration plant, as well as the MPC heat storage feedback loop, is included in this section. In addition, two different time series were used when solving the OMSES problem: typical days (288 hours long) and full year (8760 hours) models. In the second, the storage across days and weeks implies a more realistic energy operation and storage management, but offers a reference optimal operation against which to compare the results from the optimal control.

Before defining the simulated scenarios, a clarification must be made regarding the approach hitherto used for wasted energy in OMSES. In addition to the inherent losses of each technology, illustrated as not necessarily balanced energy exchanges, a utility could be dispersed into the environment if waste was allowed for it ( $\Phi_{uij}^{was} \geq 0$ ). In the case of an ESS where the only source of high grade heat (e.g., *hot water, steam utility*) is a cogeneration plant, hot gas bypass can be thought as the ability of the ESS to waste *hot water* utility (Chapter 3). This assumption is valid even when auxiliary boilers (producing such utilities) are present, in so far as the algorithm

is solved with perfect knowledge of the complete horizon, which is different for both models (typical days and full year). When solving OMSES for an ESS such as the one contemplated in Chapter 9, the following characteristics validate the assumption:

1. Hot water from the auxiliary diesel boiler must not be dumped, otherwise the solution is not optimal;
2. Hot water produced by electric boilers only happens when these are fed by renewable electricity, having zero marginal cost. The energy will only be stored if it is to be used later, otherwise it would result in over sizing the storage;
3. Hot water from the engine is used, stored or dumped. The same can be said for diesel or electric boilers. The difference is that the hot water from the diesel generators has to be produced, as it is a coproduced energy flow when generating electricity, while wind turbines can be curtailed and produce only electricity.

In stand-alone designs where instantaneous renewable penetration is below 100% of the electrical demand, renewable power will not be used to cover any heating demand by means of electric boilers. The exergoeconomic criterion prevails, unless other factors (e.g., power quality control) apply.

Therefore, when waste of *hot water* is considered, the candidate most likely to be dumped (because otherwise the solution is not optimal) is that produced by the diesel generators. Having considered in Chapter 9 that generators can bypass the heat from the hot exhaust gases to the environment, as is generally the case, the following question arises: what happens to the optimal solution given by OMSES when the bypass is not considered? This question is answered later in this chapter, simulating the corresponding scenarios, with and without bypass.

The importance of hot gas bypass in the heat recovery process in cogeneration plants depends on the relationship between heat and electricity simultaneous and average demands, the existence of storage (or the existence of dispatchable loads), and most importantly, the required flexibility of the plant (ASHRAE, 2012). When heat storage is not present, gas bypass through the corresponding diverter eliminates or at least reduces the need for auxiliary cooling systems for the fluid heated in the otherwise rigid waste heat recovery system.

### **10.3.2 Heat Storage Management**

In addition to the bypass treatment discussion, which affects both the outcome of the optimal design as well as the control of the plant, attention is given to the heat storage system. Its management is linked to the dispatch problem of the ESS that includes the operation of the diesel generators and the renewable energy sources. The management of heat bypass and the heat storage system becomes an interesting problem, especially when considering two sources of uncertainty: wind power and storage model inaccuracies, described in the previous section.

### **10.3.3 Investigated Scenarios**

The influence of heat recovery bypass was addressed first. OMSES was solved using the same constraints as in Scenario VI in Chapter 9, considering two cases, depending on whether *hot water* utility could be wasted.

In order to investigate this intricate problem of optimal management of storage with and without bypass under uncertainty, a series of simulations were run also considering the optimal design achieved by OMSES. For the simulations in this section, the optimal solution of Scenario VI (Chapter 9) was used, considering 10 MWh of storage. It should be remembered that only auxiliary diesel boilers were present. January was the selected month because of the high wind

speed and heating demand. The possibility to waste heat from the diesel generators exhaust and cooling system (*hot water* utility in this case, as nothing is recovered as *steam*), as well as the availability of a feedback loop regarding the heat storage system (with the same information as the previous section of this chapter), are considered in the following scenarios:

1. Without heat recovery gas bypass, without information feedback (in both temperature and heat losses of the heat storage);
2. Without bypass, with feedback;
3. With bypass, without feedback;
4. And with bypass, with feedback.

Regarding the simulations run, the MPC was implemented following these steps:

1. Set the initial conditions of the heat storage system (Equations 10-1 through 10-8);
2. Calculate forecasted demands and environmental conditions (temperature and wind);
3. Run OMSES using fixed equipment and 24 hours prediction and control horizon;
4. Use the first hour heat flows of the heat storage system to run one-hour simulation of the heat storage system;
5. Depending on the scenario, get the final temperature-state of the heat storage system and return to step 1.

The optimization and the simulation stages were carried out with Lingo (Lindo Systems) and Matlab® (Mathworks), respectively. Flow charts and programs are provided in the first part of Appendix 8.

## 10.3.4 Results

### 10.3.4.1 Design Results Considering Bypass Alternatives

The respective constraints for each alternative design problem influence the capacity of the system to dissipate the heat not consumed within the ESS. Thus, the technologies affected are the cooling towers and the heat exchangers that conveniently degrade the heat flow down to the ambient temperature.

When the waste of the heat from the engines is allowed (bypass allowed), the number of cooling towers installed is 2 (two) (see Chapter 9). In contrast, one unit more is installed when the bypass is not allowed. In reality, the bypass system will entail an additional cost that must be compared with the cost of additional cooling tower capacity. Furthermore, if heat and electricity demands are not simultaneous, heat storage becomes part of the trade-off combination.

The heat recovery bypass option should also be analyzed as a means to increase flexibility of operation, which can extend the life of the heat exchangers by reducing their exposure to high exhaust temperatures during low heat demand seasons, partial load, and start up operations.

### 10.3.4.2 Simulation Results

A summary of the cases simulated, illustrating what happens in January, is shown in Table 10-1.

**Table 10-1 Diesel consumption in January to maintain the storage temperature above 50°C**

Bypass	Feedback	Auxiliary Heating [MWh] (cost in CAD*)
No	No	101 (13,130.00)
No	Yes	0
Yes	No	240 (31,200.00)
Yes	Yes	0

\* Assuming 130 CAD/MWh of diesel burned in a diesel boiler

Table 10-1 shows the advantages of controlling the system with information feedback, as well as with a bypass system. The economic advantage is illustrated by the cost of the extra fuel consumed at the mine site, in this case for heating purposes, and for January. The auxiliary heating corresponds to diesel burned in the corresponding boiler to keep the temperature level of the heat storage system above the minimum temperature ( $50^{\circ}\text{C}$ ).

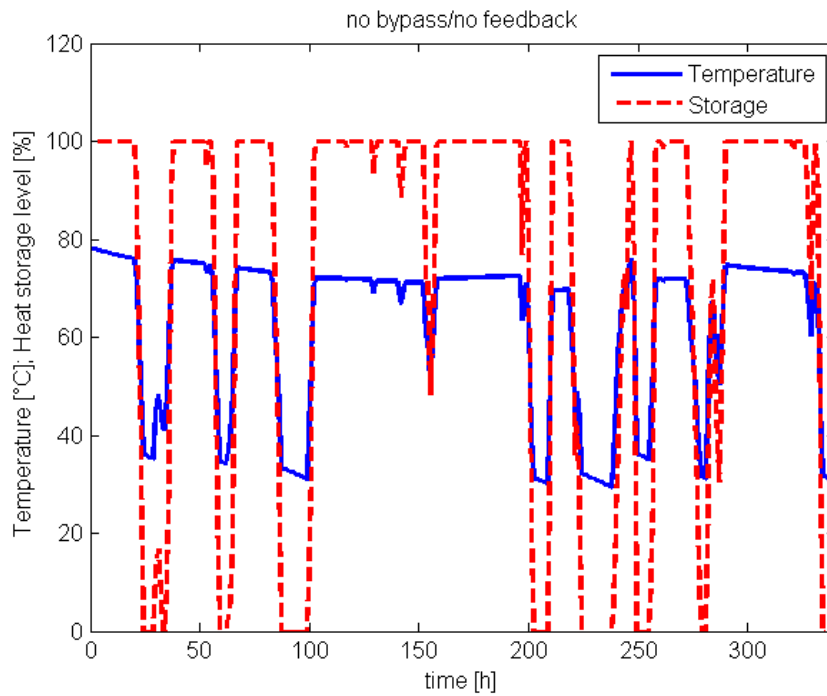


**Figure 10-6 Temperature and heat level of the heat storage system in January, no heat recovery bypass, no information feedback**

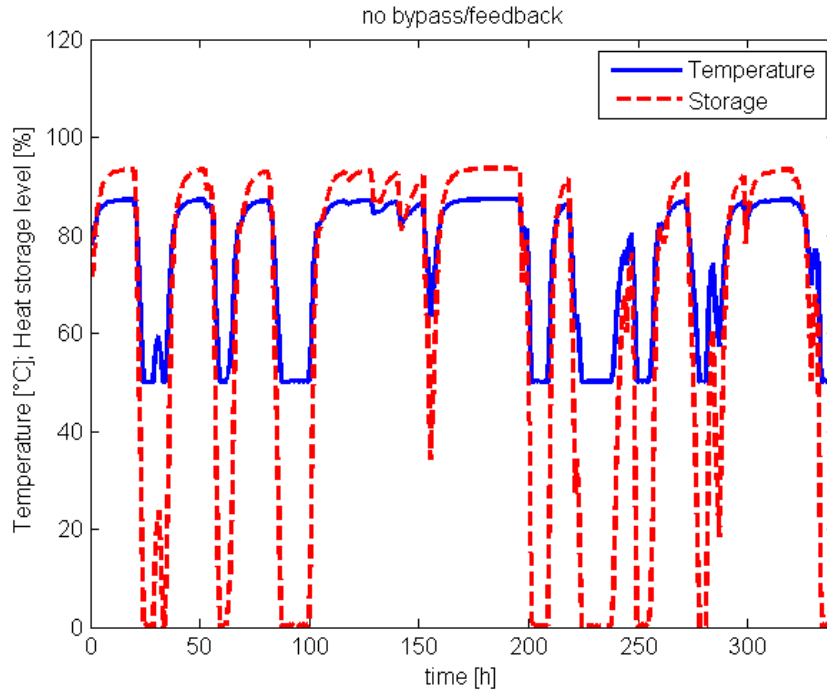


Figure 10-7 Temperature and heat level of the heat storage system in January, no heat recovery bypass, with information feedback

Figure 10-6 and Figure 10-7 show a portion of the simulation results of the heat storage evolution during the first half of January, without and with information feedback, respectively. In both cases, the exhaust bypass is not possible. Following the economic criteria, this heat can be stored at a lower cost than wasting it to the environment via the cooling tower, which consumes a certain amount of electricity. Thus, the level of storage, and therefore the temperature, remains high in both cases. When the controller has information about the storage losses, it can deal with them so that the temperature and the energy remain at or above the minimum level (50°C and 0 MWh, respectively), and below the inlet temperature of the heating fluid, considered 90°C. In the absence of this information, the temperature drops progressively, although this effect is counteracted by the economic criteria mentioned, by which the heat from the hot gases is always stored, stabilizing the actual (simulated) temperature between 30°C and 75°C (Figure 10-6).

For temperatures below the minimum, which involves negative energy states of the storage according to the model equations, the algorithm finds unfeasible states that need to be modified to make it possible to achieve feasible solutions for the control problem. Therefore, when the system's temperature drops below the minimum value, the storage level fed into the state equations for the following interval is set as 0 MWh. This mechanism is simple, but contains the essence of systems modelling, by which the model can only represent the real system within a certain range of operation. This consideration equally applies with and without information feedback. Thus, the algorithm will always believe that the starting point is, at least, 0 MWh, which may not be accurate. Because of the heat transfer model, the maximum level of energy stored will never be surpassed.

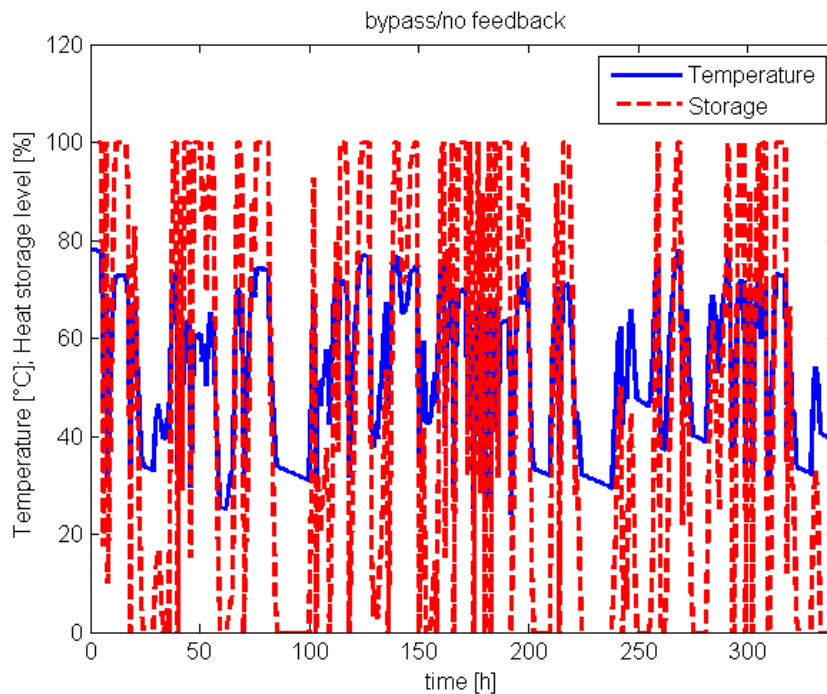
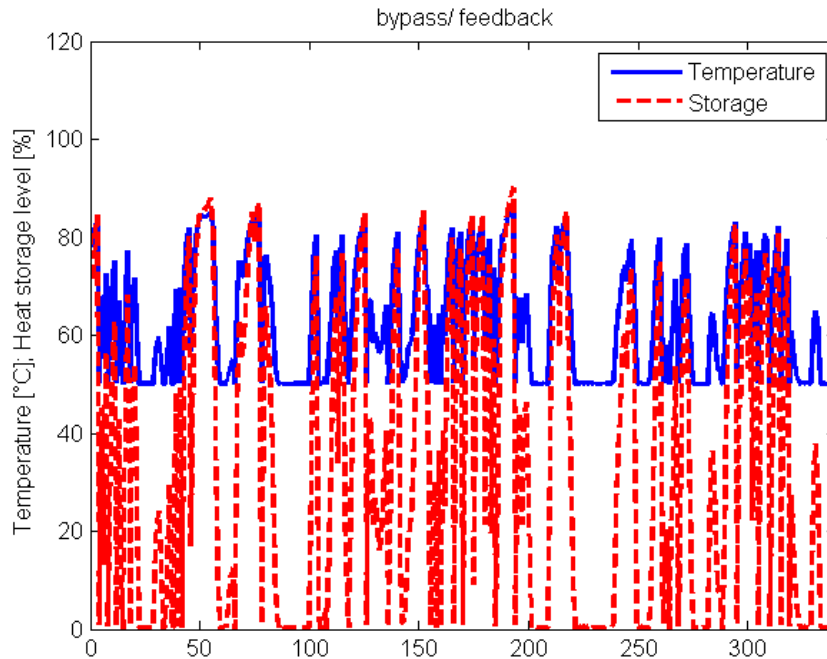


Figure 10-8 Temperature and heat level of the heat storage system in January, with heat recovery bypass, no feedback information



**Figure 10-9 Temperature and heat level of the heat storage system in January, with heat recovery bypass, and feedback information**

The opposite cases take place when bypassing the hot gases from the engine is possible. The alternatives, with and without information feedback, are shown in Figure 10-8 and Figure 10-9 respectively. In both cases, the economic criteria allows the system to store just as much heat as may be needed for the following 24 hours (control and prediction horizon). This penalizes the potential to store excess energy for subsequent days. This effect is more severe in the case of no information feedback, when the controller loses complete track of what is happening to the storage. Storage temperature drops below 30°C.

The compensation through temperature feedback, that allows the controller to recognize the initial temperature, as well as heat losses, maintains again the temperature of the storage at any time above the minimum setpoint. It is worth remembering that this minimum temperature is associated with the model design, which further corresponds to the nominal operating conditions

(50°C) required for the actual storage system. The heat storage is normally required to remain above a minimum temperature that would ensure the delivery of heat in the quality required for each of the consumers. Finally, it can be observed that the effect of system losses, even when the information feedback loop is present, precludes the actual storage (simulated) from reaching the maximum temperature (90°C) and storage level (10MWh).

## **10.4 MPC to Improve the Design**

It has already been mentioned that one of the main drawbacks of OMSES is its inability to produce reliable systems in uncertain and off-design operating conditions. Here, the concepts introduced in Section 5.5 to deal with system undercapacity are applied to control and redesign an optimal ESS previously calculated with OMSES. Results of the dynamic redesign are compared with those in which a more detailed definition of the demands for the whole year, with demands information with 1 hour resolution, considered the optimal with real demands but unrealistic perfect information.

### **10.4.1 Case Study**

It was found in Chapter 9 how the optimal solution given by OMSES became infeasible when used for simulation, due to shortages in installed capacity of certain technologies. This was the case for cooling capacity during high ambient temperature hours, in particular during July. During simulations, the approach taken to bring the model to feasible conditions was to increase progressively, through trial and error, the different technologies involved. Mechanical chillers and cooling towers as well as other technologies such as boilers and heat exchangers were increased until the specific source of infeasibility was found (cooling capacity shortage).

In order to improve this trial and error approach, the method explained in this section and Chapter 5 is applied to the same case study, running the simulation in July, and relaxing the OMSES design to deal with infeasible situations. The redesigned solution obtained at the end of the simulation was compared with the optimal solution obtained for the same mine using the full year model (8760 hours), whose results are presented in the next sub section.

Four scenarios were investigated to illustrate the benefits of the dynamic redesign using MPC. These are summarized in Table 10-2. Following the discussion on generators' heat recovery bypass, two alternatives were considered: with and without bypass. Additionally, the effect on the optimal solution and the redesign of different ventilation temperature setpoints was assessed (in bold, the conditions used in Chapter 9). Ambient temperature and wind speed evolution are shown in Figure 10-10.

**Table 10-2 Summary of scenarios for the evaluation of MPC redesign**

Heat Recovery Bypass	T <sub>set</sub>	
	10°C	15°C
Yes	S11	<b>S12</b>
No	S21	S22

The starting point for each of the four simulations was the optimal solution defined by the corresponding scenarios of bypass and the same temperature setpoint (15°C) using the OMSES method. Then, the simulation was run and the evolution of the equipment regarding chilling and cooling capacity was obtained, which is next addressed.

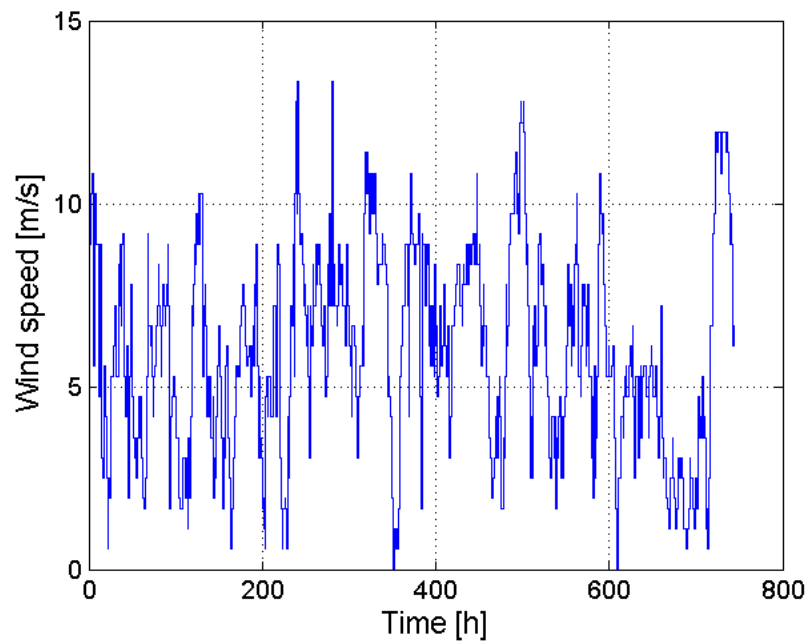
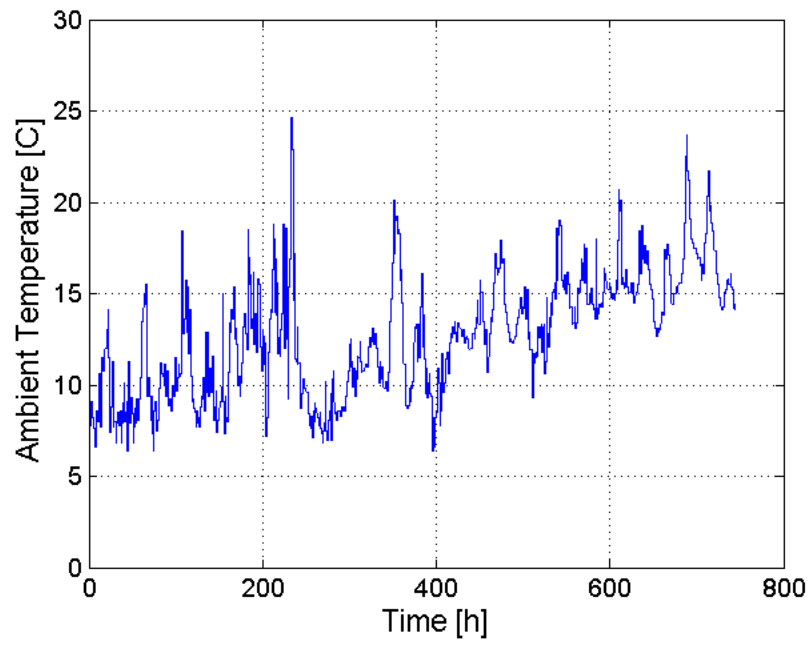


Figure 10-10 July ambient temperature evolution (top), and wind speed (bottom)

**PROBLEM: REMOTE UG MINE IN NWT + WIND POWER  
ILLUSTRATION MPC-OMSES FOR RESILIENT DESIGN**

MINIMIZE	Equation	Inputs
<p>Total annual cost = Investment Cost</p> <p style="padding-left: 40px;">+ Variable Cost</p> <p style="padding-left: 40px;">+ Demand Charges</p> <p style="padding-left: 40px;"><del>+ Penalties</del></p>	<p>(3-4) (3-5) (3-6)</p> <p>(4-12,13) storage</p> <p>(3-7) (3-8)</p> <p>(3-23)</p>	<p>Table 10-12</p> <p>Table 9-1</p> <p>Chapter 9</p>
<b>SUBJECT TO</b>		
Utility Energy Balance	(3-12,13,14) (4-14) storage	Table 10-12 Table 9-2, Fig. 9-2
Equipment performance:		
- Conversion coefficients	(3-11)	Table 9-1
- Production limits	(3-9)	
o Maximum load	(3-10)	Table 9-1
<del>o Minimum load</del>		
<del>Infrastructure Constraints</del>	<del>(3-17,18)</del>	
Storage Balance		
- Hourly	(4-15) to (4-23)	
<del>Monthly</del>	<del>(4-22,23)</del>	
Scenario Based:		
- Resource Availability		
o Wind	(4-5) (4-6)	
o Biomass	(3-15,16)	
- Spinning Reserve	(4-7) to (4-11)	
<del>Storage Charging/Discharging</del>		
<del>Demand Charge</del>		
<del>o Fixed</del>		
<del>o Free</del>		
- Terminal constraint on storage		
o Applied		
<del>o Not applied</del>		
<b>DECISION VARIABLES</b>		
<del>Technologies Available</del>		
Equipment Units		
- OMSES		
- MPC-OMSES		
<del>LT-OMSES</del>		
<del>Storage Size</del>		
<del>Grid Capacity</del>		
Energy/Mass Flows		
<del>Typical days</del>		
- Rolling horizon		
Incremental Equipment units	(5-6)	
<b>ORDINARY DIFFERENTIAL EQUATION</b>		
Heat storage model	(10-1) to (10-8)	Section 10.2.1

### 10.4.2 Results

The first two simulated scenarios considered a temperature setpoint ( $T_{set}$ ) for ventilation air of 10°C. The increase in units of mechanical chillers and cooling towers proceeds until the worst environmental condition takes place (Figure 10-10). This is case specific, for it depends on the existing equipment (installed) and the simultaneous combination of wind speed, heating, chilling, and electric demand.

Figure 10-11 represent a more restrictive case (S11), where bypass is not allowed, forcing the system to release the excess heat through the cooling tower. The second scenario (S12) considers the OMSES result for the same summer ventilation temperature setpoint as the starting point for the simulation. This requires additional capacity than that reflected in OMSES' optimal solution at the beginning of the simulation ( $t=0$ ). Again, the ambient temperature drives the increase in capacity. However, by the end of the simulation, an extra cooling tower is installed, due to a combination of sustained high temperatures and low wind speed (Figure 10-10) which results in the start up of the generators in spinning reserve, which produce an amount of waste heat that cannot be released into the atmosphere from the system with the current capacity of installed cooling towers.

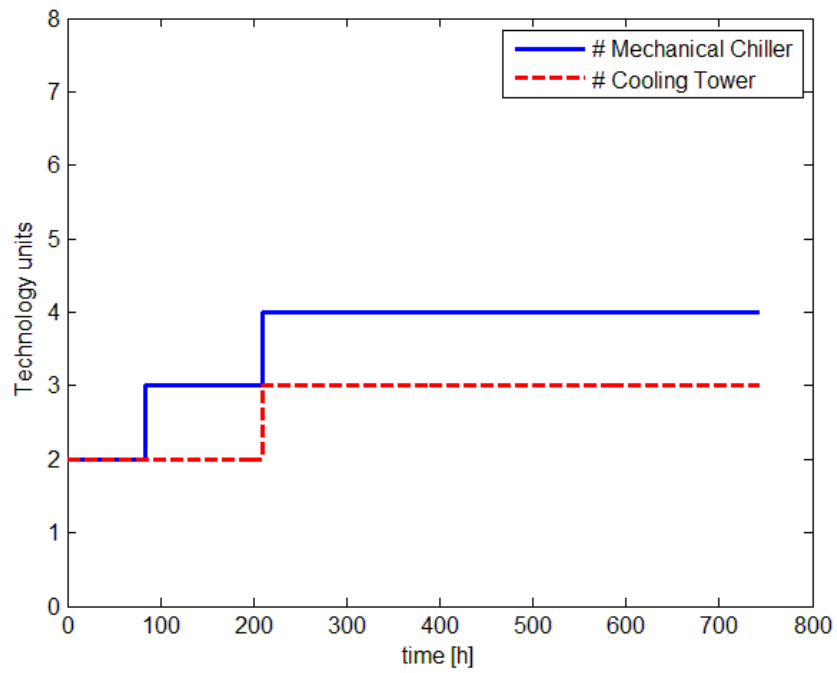


Figure 10-11 Scenario 11 Mechanical chiller and cooling tower evolution; engine exhaust bypass,  $T_{set} = 10^{\circ}\text{C}$

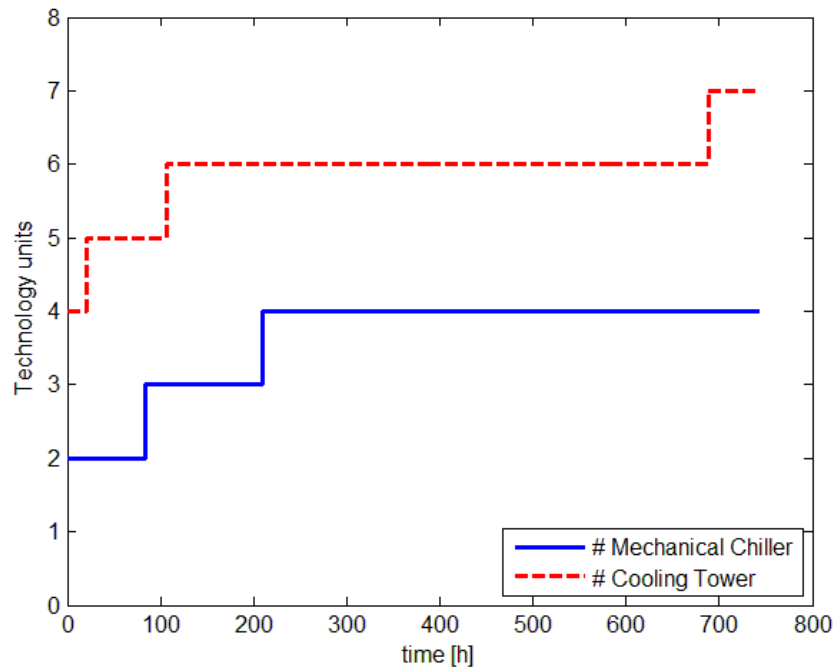


Figure 10-12 Scenario 12 Mechanical chiller and cooling tower evolution; No engine exhaust bypass,  $T_{set} = 10^{\circ}\text{C}$

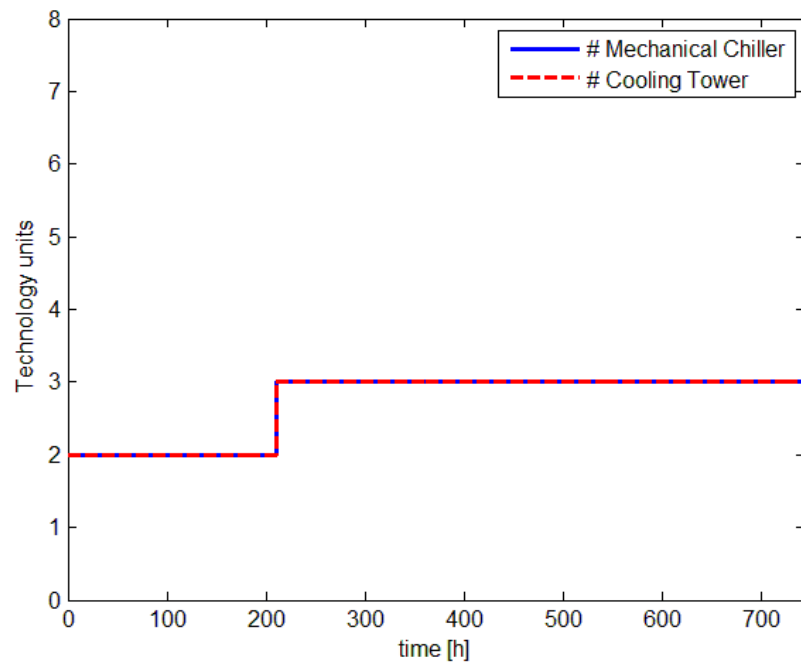


Figure 10-13 Scenario 21 Mechanical chiller and cooling tower evolution; engine exhaust bypass,  $T_{set} = 15^{\circ}\text{C}$

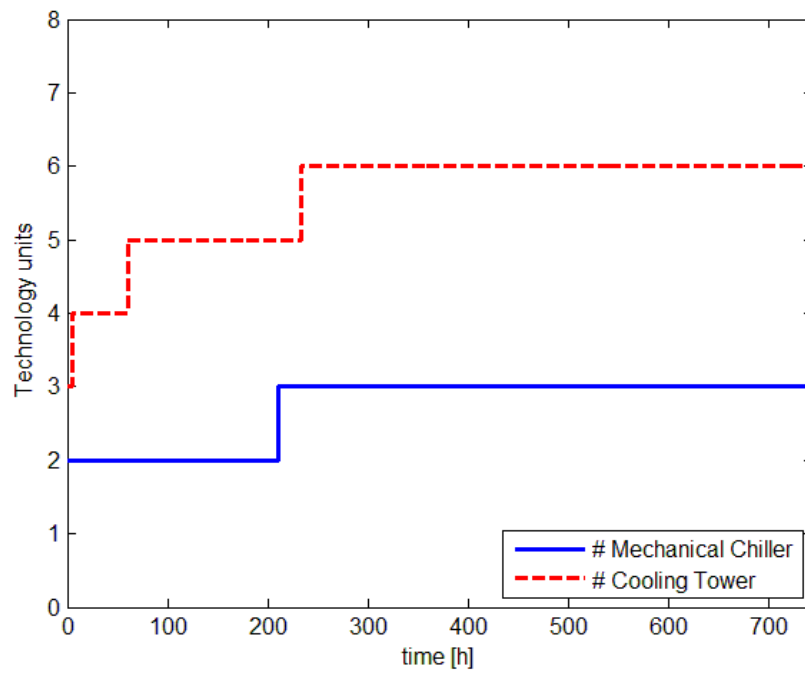


Figure 10-14 Scenario 22 Mechanical chiller and cooling tower evolution; No engine exhaust bypass,  $T_{set} = 15^{\circ}\text{C}$

The common feature between Figure 10-13 and Figure 10-14 is the temperature setpoint, 15°C, which is lower than the previous cases, and therefore the need for additional capacity of mechanical chillers will be lower. In the case of heat recovery bypass (Figure 10-13), both technologies increase by one unit at the worst temperature conditions in the month. When bypass is not considered (Figure 10-14), the need for extra cooling towers appears early (due to low wind conditions) while, as in the opposite case, chilling capacity increases by just one unit.

In order to verify the effectiveness of the MPC-OMSES method, one can compare the ESS operation with an ideal case that eliminates uncertainty of demand. Such an ideal case is offered by treating the demands used in the OMSES solution alone as perfectly known future demands. However the typical days data set effectively contains temporal discontinuities at the end of each day of the year and at the end of each month of the year, and has wind resource characterization that matches typical days, all of which is incompatible for comparison with the performance of the MPC-OMSES optimal re-design process. Consequently, the typical days data set must be dropped and annual demands and annual wind resources must be described on an hour-by-hour basis throughout the 8760 hours of the year. This option is referred to as the detailed demand model (Section 4.5.3). For further information regarding the use of the detailed demand model, see Appendix 7.

The optimization results using the detailed demand model for the same previous four scenarios are presented here. The constraints applied included the installation of 4 wind turbines, 10 diesel generators, 9 boilers, and 10 MWh of heat storage, approximately the configuration of Scenarios VI in Chapter 9.

Table 10-3 summarizes the results regarding the mechanical chiller and cooling tower units, including OMSES' typical days results for the same temperature setpoint. In general, it can be stated that perfect knowledge of the optimization horizon results in reduced installed capacity.

**Table 10-3 Detailed model and dynamic redesign results**

Heat Recovery Bypass	Dynamic Redesign		Detailed Demand Model	
	T <sub>set</sub> = 10°C	T <sub>set</sub> = 15°C	T <sub>set</sub> = 10°C	T <sub>set</sub> = 15°C
Yes	4/3*	3/3	4/3	3/2
No	4/7	3/6	4/6	3/5

\* Mechanical Chillers/Cooling Towers

In order to illustrate the influence of the heat recovery bypass system, the operational results of the optimization problem with detailed demands was plotted (Figure 10-15). As indicated in Table 10-3, in presence of bypass, two (2) cooling towers were selected for 15°C summer temperature setpoint. In absence of bypass, this capacity is insufficient, for the amount of cogenerated heat not used plus the condenser heat from the mechanical chillers (this sum equals the cooling tower load, in blue dashed thick line in Figure 10-15), requires more than five (5) cooling towers (red thick horizontal line), i.e., more than 25 MW.

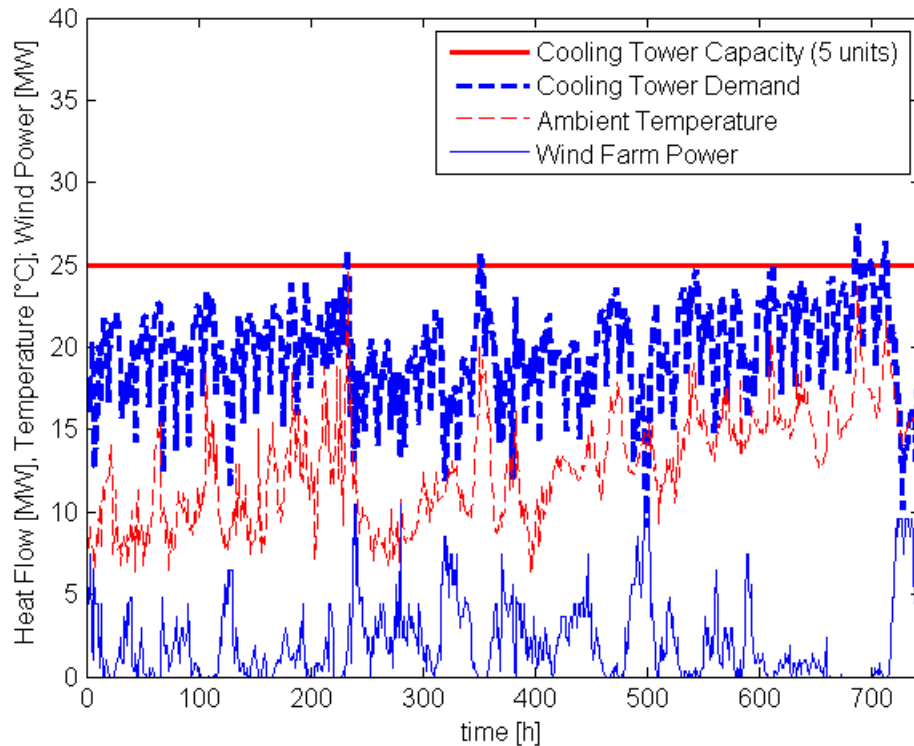


Figure 10-15 July optimal operation results for the detailed demand model with summer  $T_{set} = 15^{\circ}\text{C}$  and bypass allowed

The periods of higher cooling capacity demand are related with low wind speed and higher ambient temperatures, both atmospheric phenomena interrelated in certain climatic regions. Figure 10-16 suggests that such a correlation may exist in the current case, but the degree of scatter between the variables would present a challenge to any regression analysis. The materiality of this possible correlation is illustrated in the following. High speed winds are associated with cold air streams from the Arctic. Low wind speeds require higher diesel generator output, which increases the cogenerated heat, seldom in demand during summer. Simultaneously, high temperatures increase the demand for cooling which, although not great in this case, significantly contributes to the peak demand for the cooling tower capacity in absence of bypass. Even though capacity shortages may take place (Figure 10-15), it does not necessarily mean infeasible operational constraints. Energy storage can consume part of the heat to be

wasted through the cooling tower system, and release the heat when some capacity has been liberated due to higher wind or lower ambient temperature.

Finally, it should be remembered that the detailed model unrealistically foresees the operating conditions (energy demands, ambient temperature, wind speed) that allow it to optimally select the equipment, which will likely be insufficient (Table 10-3) with usual operation forecast conditions, e.g., with hourly or daily forecasts for wind and weekly forecast/scheduling for energy demands, such as electricity, heating, or cooling.

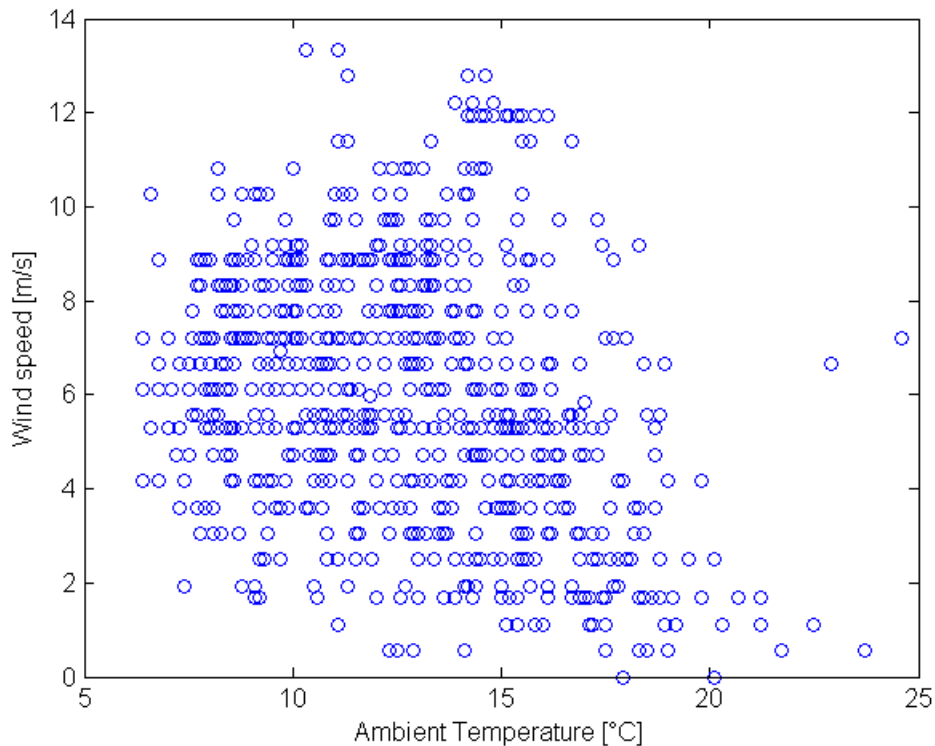


Figure 10-16 Local wind speed and ambient temperature

## 10.5 Conclusions

A more realistic model of the heat recovery loop and the heat storage was developed and used in conjunction with MPC. A first order dynamic model was implemented, assuming only sensible heat storage with no stratification (perfect mix).

In absence of feedback information, the controller ignores the actual state of the storage, represented by the homogeneous temperature, which falls below the design conditions necessary for a proper heat distribution throughout the mine. Successive improvements were achieved when: 1) the losses calculated within the dynamic model and 2) the actual temperature of the storage, were passed to the controller. The past losses were used to estimate those that would occur within the control horizon.

These first simulations, during the month of January, considered complete restriction of heat recovery bypass (hot exhaust gases from the generators). Subsequent simulations with bypass were run to investigate the benefits, quantitatively and qualitatively, of each option. It was found that MPC feedback succeeded in optimally controlling the system in either case. The diesel consumed in January by the cogeneration plant and the auxiliary diesel boiler in the 8760-hour model was 38313 MWh, lower than the best value achieved with the MPC approach (with feedback and without hot gas bypass), 38348 MWh. In case of hot gas bypass and no feedback, an additional 240 MWh (or CAD31,200.00) of diesel is required to avoid inadmissible low level heat storage (here considered 50°C) (Table 10-1). It was thus demonstrated that the centralized predictive controller was able to maintain the whole energy supply system's feasibility and optimality, even in the presence of wind power's uncertain output.

Subsequently, the concept of dynamic redesign was applied on an infeasible system's design produced by OMSES, which presented capacity shortages of mechanical chillers and cooling tower technologies during summer. This was found in Chapter 9, when simulating the whole year. Several simulations with MPC relaxed formulation (Chapter 6) were run for July, varying hot gases bypass and ventilation air conditioning temperature setpoint. This formulation was able to bring the system's design to the feasibility region, which resulted close to the optimal calculated with the detailed demand model (8760 hours).

The interaction between heat storage, bypass systems, cooling tower systems, and renewable energy produced an unexpected but interesting outcome. In summary, renewable penetration offsets electricity produced by generators, which results in lower cogenerated heat. This should be stored considering temperature and wind speed forecasts and the capacity to dissipate the stored heat in case of limited capacity of the cooling tower system and no hot gases bypass.

Finally, it is worth noting that the OMSES distinction between steam, hot water, and cooling water responds to the exergy level of each of the heat flows, which later allows OMSES to consider valid energy transformations respecting the second law of thermodynamics. When Chapter 7 and Chapter 9 considered that diesel engines produced only two levels of cogenerated heat (hot water and cooling water), this made it difficult to admit the possibility of bypassing the exhaust gases from the heat recovery system, for it was assumed that the heat of the gases was recovered as hot water. As Figure 10-2 illustrates, the medium temperature cogenerated heat (OMSES' hot water utility) is generally obtained from the engine cooling system.

The strict interpretation of the typical scheme of a cogeneration plant, illustrated in Figure 10-1 or Figure 10-2, eliminates the *cooling water* as a utility produced by the diesel generator. The

excess of heat in the form of *hot water*, i.e., not consumed within the system nor demanded, must nevertheless be degraded in *cooling water* through respective heat exchanger. In practice, the management of the plant is more complex and the levels of heat generated are not as differentiated. Thus the approach in modeling of diesel generators for OMSES (Carvalho and Millar, 2012) may be used under very specific, plant dependent circumstances.

Overall, the objective pursued with MPC, beyond a mere dynamic planning of the energy system's operation, was satisfied in all the expected dimensions: the optimal control of non-linear systems under uncertainty, and the dynamic improvement of OMSES solutions in the sense of feasibility. While the first of these has previously been extensively addressed in the literature (Chapters 1 and 5), it should be noted that the scope of the energy system treated, including multiple energy demands, material, and energy storage and renewable energy subject to uncertainty, makes this case of particular interest. Furthermore, and regarding the second dimension, this original contribution in the field of energy systems does not only alleviate the deficiencies of OMSES design optimization, but also results in a more realistic strategy to produce more robust solutions, given that it embeds the uncertainty associated with renewable sources such as wind, because it does not assume a perfect knowledge of demands and sources in unrealistic long control horizons, which is the case of the alternative strategy based on detailed energy demands, e.g., with 8760 consecutive intervals.

# Chapter 11

## 11 Electrical Vehicles in Underground Mines

This chapter uses the extended OMSES formulation introduced in Chapter 4 concerning material utilities and mobile technologies to assess: i) different vehicle technologies used in underground mines, and ii) how techno-economic and climatic environmental parameters may affect the choice equipment. The case study presented in herein involves the optimization of the ESS of an underground mine. In this case, as opposed to that presented in Chapter 9, two different underground vehicle technology alternatives are compared using OMSES: Diesel and Electric (battery powered). The main objective is to determine whether the expected energy savings achieved through the use of electric vehicles, due to their potentially lower ventilation requirement, offset their higher investment cost.

### 11.1 Mine Description

Musselwhite Mine, a gold mine with enough available information, is selected for the present study. The site's actual ore production (Lawson and Faubert, 2010) is used for the basis for the calculation of the mine's energy demands. The reference facility is located in Northern Ontario (52.61°N, 90.37°W), Canada (Figure 11-1). There is a 200 km all-season road connecting the mine with Pickle Lake, which provides the mine with power for the operations with a transmission line. The mine's operations includes underground mining and a surface processing plant. The existing on-site diesel generators which once provided up to 4.5 MW of electric power, are now used only in case of grid outages (Goldcorp, 2015).

In addition to diesel for the underground equipment and the electricity imported, Musselwhite Mine also trucks in propane for air conditioning, in particular for underground mine ventilation, burned directly within the air stream.

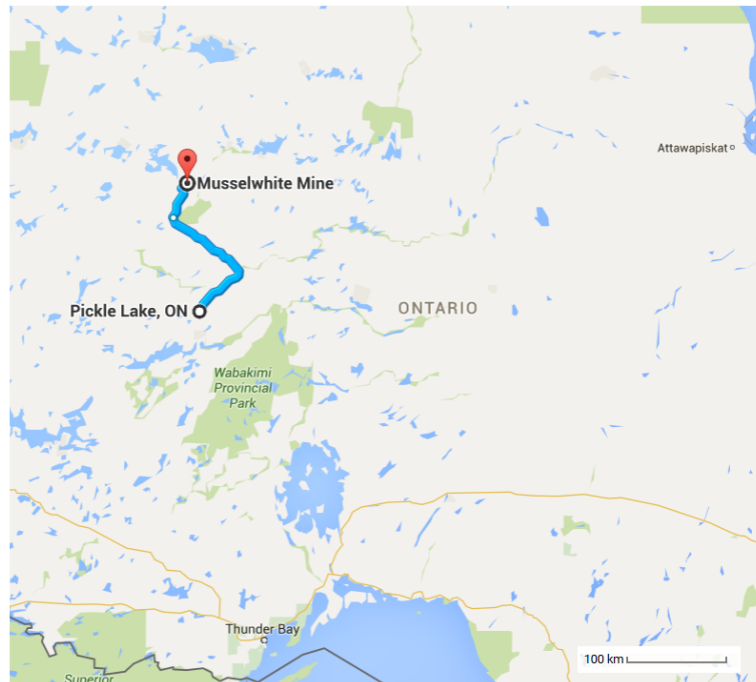


Figure 11-1 Musselwhite Mine location

### 11.1.1 Mine Utility Demands

The amount of rock mined per year is taken as 1.2 million tonnes (Lawson and Faubert, 2010). This value is used to calculate the daily rate and the subsequent energy demands. Although the rate can be higher in some months than others in the actual mine, especially compared with those where major maintenance tasks are scheduled, the case study assumes constant production throughout the year.

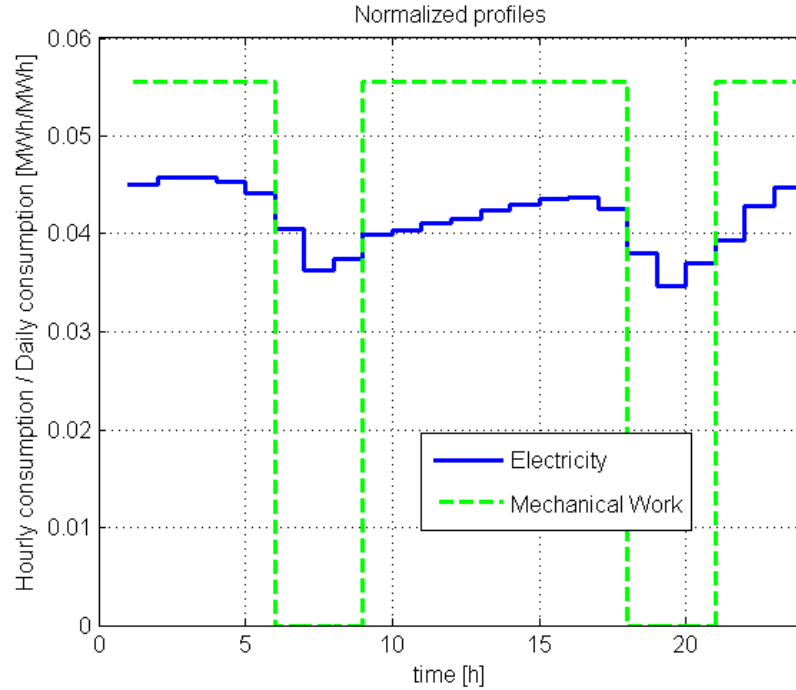


Figure 11-2 Normalized profiles for electricity and mechanical work

Using generic normalized profiles to represent the daily demand variation (Figure 11-2), the conversion to hourly production rates (tonnes/hour) is obtained by multiplying the profiles and the daily production (tonnes/day). Further conversion into energy demands is achieved assuming that the specific energy term is known, such as [kWh/tonne] for electricity, or [l/tonne] for diesel. These terms are called *Beta* factors (Eq. 11-1, 2):

$$\beta_{MW} = LHV_{DI} \cdot \beta_{DI} \cdot \eta_{MW} \quad (11-1)$$

$$\beta_{EE} = \alpha \cdot \beta_{EE,0} \quad (11-2)$$

The coefficient  $\alpha$  represents the fraction of the total electricity specific use ( $\beta_{EE,0}$ ) that does not come from the dewatering, ventilation, and cooling systems. The mechanical work demand is calculated assuming that the rate of conversion from diesel energy to mechanical work ( $\eta_{MW}$ ) is known, at least averaged within every hour.  $\beta_{DI}$  [l/ton] and  $\beta_{EE,0}$  [kWh/ton] are generally provided by the mining companies in their sustainability reports or can be deduced from indirect

information. The assumed values for these variables are:  $\alpha=0.65$ ,  $\beta_{EE,0}=90$  [kWh/ton],  $\beta_{DI}=2$  [l/ton],  $\eta_{MW}=0.25$ . Diesel lower calorific value,  $LHV_{DI}$ , has units of [kWh<sub>thermal</sub>/litre]. The conversion efficiency for the parameter  $\eta_{MW}$  is taken from experience in conventional diesel-fueled mobile plants.

The hourly demands for electricity and mechanical work depend on the ore tonnage and the total rock tonnage, respectively. The latter includes ore and waste rock, which are related through the waste to ore ratio. The ore extracted can be obtained from the company's public information, such as annual sustainability reports (Lawson and Faubert, 2010).

Additional demands are calculated for the remaining utilities, such as dewatering and ventilation. For the latter, in addition to the ventilation associated with the requirements for air quality during the shifts, blasting operations between the shifts will generate a demand for ventilation. A mine's dewatering needs are equivalent to a constant flow entering its underground dams and water reservoirs, which eventually has to be pumped out of the mine. Conversely, dewatering can be regarded as a supplied flow, or inflow at no cost, as seen in Chapter 8. Therefore, the constraint is on the supply side as opposed to the demand side.

Cooling and heating are calculated as functions of the ambient temperature. For this purpose, heat coefficients ( $UA$  and  $mC_p$ ) are used for both final demands and intermediate consumption (interactions among technologies) (see Section 4.7.4).

The use of underground equipment generates a local demand for cooling. It is assumed that the remaining heat loads underground are removed by thermal treatment of the ventilation air. In the present work, underground cooling demand is assumed to be fulfilled through the same technology used for ventilation air cooling, although other concepts can be used, such as ice

stopes or ice slurry (Ramsden et al., 2014). The waste heat from the refrigeration plants will be considered as a potential source for bulk air heating in one scenario.

**Table 11-1 Mine information**

Mine	Musselwhite Mine		
Company	Goldcorp		
Type	Underground (UG)		
Product	Gold		
Production	Annual	1.2x10 <sup>6</sup>	tonnes ore
	Day (365 days/year)	3,287	tonnes ore
	Daily shifts	2	
	Waste to ore ratio	1	
Electricity*	Energy Intensity**	58.5	kWh/tonnes ore
	Mean power (all consumers)	23	MW
Mobile	Diesel intensity UG***	2	liter/tonnes
	Diesel energy density	10	kWh/liter
	Diesel average efficiency	30%	
	Electric average efficiency	78%	
Ventilation	Operation time	18	hours/day
	Operational safety factor	2	
Diesel equipment	Regulated requirement	0.060	m <sup>3</sup> /s/ kW
	With safety factor	0.460	Mm <sup>3</sup> /h /MW
Electric equipment	Estimated (20% of diesel mobile)	0.012	m <sup>3</sup> /s/ kW
	Total	0.100	Mm <sup>3</sup> /h /MW
Between shifts	Total	1.080	Mm <sup>3</sup> /h
Ventilation Electricity	Surface fans	0.5	MW/ (Mm <sup>3</sup> /h)
	UG fans	2.0	MW/ (Mm <sup>3</sup> /h)
	Total	2.5	MW/ (Mm <sup>3</sup> /h)
Temperature	Annual mean	0.5	°C
	January mean	-19.3	°C
	July mean	17.6	°C
	T <sub>set</sub> (Vent heat/Vent cool/Building)	2/15/20	°C
Dewatering	UA (buildings)	0.1	MW/°C
	Hourly average	170	m <sup>3</sup> /h

\*At Musselwhite there is an ore processing plant and a backfill plant

\*\*Not including utility consumers: ventilation, dewatering, cooling, or heating, and consumer technologies

\*\*\* (Lawson and Faubert, 2010)

It is considered that UG mobile plants include different equipment: from drilling rigs, loaders, trucks, to utility vehicles used for worker transportation. However, the mining method considered is based on rock mucked, loaded, and hoisted to the surface, and thus the main plants

considered are loaders. Two shifts per day of ore mucking are considered; in the case of electric vehicles, each of these is divided into three subshifts in which a different battery pack is used (Ewing, 2015).

### 11.1.2 Economic Data

**Table 11-2 Equipment information considered in the conservative superstructure**

Equipment	Nominal Power *	Capital Cost (10 <sup>3</sup> CAD)	O&M Cost (CAD/MWh)	Electricity (EE)	Diesel (DI)	Steam (VA)	Hot Water (HW)	Cooling Water (CW)	Chilled Water (RW)	Ambient Air (AA)	Dewatering (DW)	Ventilation (AV)	Mech. Work (MW)	Propane (PR)
Diesel Engine	4.4	4400	5.0	<b>1</b>	2.27		0.80	0.20						
Electric Boiler	3.5	144	1.0	1.11			<b>1</b>							
Diesel Boiler	3.0	130	1.0		1.15		<b>1</b>							
Mech. Chiller	1.85	270	2.0	0.25				1.25	<b>1</b>					
Cooling Tower	5.0	82	5.0	0.02				1		<b>1</b>				
Heat Exchanger	5.0	35	1.0				1.10	<b>1</b>						
Mobile Diesel	0.05	500	150		3.33				<b>A</b>			0.46	<b>1</b>	
Mobile Electric	0.05	645	150	1.28					<b>A</b>			0.10	<b>1</b>	
Propane Boiler	3.9	150	1.0				<b>1</b>							1.22
Pump [m <sup>3</sup> /h]	30	60	0.1	.003							<b>1</b>			
Fan [Mm <sup>3</sup> /h]	.35	30	0.1	2.50				<b>B</b>	<b>B</b>			<b>1</b>		

\* Nominal installed capacity is in [MW] units except for pumps [m<sup>3</sup>/h] and fans [Mm<sup>3</sup>/h]

Table 11-2 presents the necessary description of the technologies included in the superstructure from which OMSES starts the optimization process. The coefficients A and B represent, respectively, the amount of cooling required underground to counteract the heat released by the mobile equipment, and the demand for heating and cooling for the fresh air, which depends on the ambient conditions, taken from the nearby Pickle Lake's weather station (Environment Canada, 2014)).

The nominal power of both Mobile Diesel and Electric equipment (50 kW for both technologies), has been calculated assuming a 40% load factor of the actual equipment, i.e., 125 kW. This modification is needed because OMSES considers hourly periods of constant flows, while these types of equipment vary their load continuously during their activities. The load factor has been estimated following Moore (2015). Notwithstanding, the coefficients linking mobile work and ventilation consumption are calculated based on the rated power of the vehicles (125 kW).

The cost of the different mobile equipment has been obtained as follows. First, it has been assumed that the conventional diesel unit, the one that characterizes the mobile equipment in the considered underground mine, is a 3-6 m<sup>3</sup> capacity scoop-tram. The cost is given by Stebbins (2011) as 500,000 USD (average for different daily ore production). The total cost of the electric units results from the sum of the vehicle itself, and the batteries. These are considered separately following OMSES' storage formulation. The battery installed is split in three packs following the formulation described in Chapter 4.

A relatively low price for the batteries (LiFePO<sub>4</sub> chemistry) have been assumed, 190 CAD/kWh, compared to other works (Lajunen, 2014; Paraszcak et al., 2014), but closer to the estimations based on production targets for automotive Lithium based batteries (Redelbach et al., 2014). This assumption will be verified when evaluating the cost of the electric vehicle including the batteries, estimated a 30% higher than the diesel counterpart (Moore, 2015). Battery packs charge and discharge power (MW) is constrained, respectively, to 50% and 25% of the battery capacity in MWh (e.g., charging time = 1 MWh/ 0.5 MW = 2 hours).

The cost and characteristic values for the electric storage, as well as for other storage technologies, is presented in Table 11-3. No losses are considered for the storage of heat, propane, and water storage. Propane storage is modeled using the monthly seasonal balance formulation (Chapter 4), with refueling constrained to the seventh month or characteristic day. Electric transmission line costs have been taken from Chapter 7.

The cost for water storage is 100 CAD/m<sup>3</sup> (Romero et al., 2015c). Installation, procurement, engineering, and other costs are added as 15% of equipment costs. The energy system's capital cost is annuitized using a capital recovery factor, with a 10 year life of equipment and operations and a 10% discount rate. Diesel is acquired in the market and delivered at the mine at an equivalent cost of 130 CAD/MWh. Propane is purchased at 80 CAD/MWh, although the import period is assumed to be limited to August. When assumed constant, electricity is also purchased at 80 CAD/MWh; this amount includes fixed demand charges, with the price based on 2014 data (IESO, 2015). Otherwise, the same approach to deal with variable demand charges as Chapter 7 is assumed. Power infrastructure costs are considered the same as that of Chapter 7.

**Table 11-3 Storage technologies information**

Parameter	Value	units
Electric storage		
Charge efficiency	90	%
Discharge efficiency	100	%
Decay losses	0	%
Maximum charge rate	50	%
Maximum discharge rate	25	%
Energy density	9	kg/kWh
Cost of storage		
Electricity	190 000	CAD/MWh
Heat	18 500	CAD/MWh
Propane	100	CAD/MWh
Water	100	CAD/m <sup>3</sup>

### 11.1.3 Scenarios Investigated

The scenarios considered are illustrated in **Error! Reference source not found.** Scenarios 11, 12, and 13 do not consider cooling demand to remove the excess of heat from underground mobile equipment. It is thus assumed that thermally treated ventilation air at the surface is enough to keep underground conditions at the required comfort level for both temperature and humidity. Scenarios 21, 22, and 23 require cooling, and the low grade or residual heat (CW, Table 11-2) cannot be used to heat the ventilation air. Finally, Scenarios 31, 32, and 33 do include underground cooling consumption, as well as the possibility of using CW as heating flow, which otherwise would be wasted and dissipated to the environment through the cooling water. For the last six scenarios, the coefficient A is defined, for diesel and for electric vehicles respectively, as 2.38 and 0.28 MWh of chilled water per MWh of mechanical work developed (energy not converted into mechanical work that goes into heat); for scenarios 11, 12 and 13, and both technologies,  $A = 0$ .

Diesel generators are not taken into account for the optimal solutions of each of these scenarios. Scenario 4 is used to evaluate the potential of diesel for electricity generation onsite in cogeneration mode, under conditions of underground cooling and residual heat used for ventilation heating. In this scenario, demand charges (Global Adjustment, Chapter 3) can be offset by generating power and reducing the imports from the grid at specific times during the year. In 2014, the maximum provincial demand, used to calculate Class A consumer's demand charges, took place in winter. This event took place due to the previous mild summer that limited power demand (Appendix 3). The low probability of this situation, especially considering the low elasticity of Ontario's demand, supports the use of the same approach as in Chapter 7. Scenario 4 is then divided into two: 4a) when self-generation is not allowed, and 4b) when the

mine can generate power on-site; this way, it is possible to assess the benefits of purchased power reduction to avoid demand charges. In all scenarios except for 4b, demand charges are considered constant (included in the purchasing price).

**Table 11-4 Allowed mobile technologies for the different scenarios**

Scenarios	Without UG cooling			With UG cooling CW wasted			With UG cooling CW used			
	11	12	13	21	22	23	31	32	33	4a,4b
Diesel	√	√		√	√		√	√		√
Electric		√	√		√	√		√	√	√

**PROBLEM: REMOTE UG MINE IN NORTHERN ONTARIO + EV ILLUSTRATION  
OF OMSES WITH SEASONAL STORAGE**

MINIMIZE	Equation	Inputs
<p>Total annual cost = Investment Cost</p> <p>+ Variable Cost</p> <p>+ Demand Charges</p> <p>+ Penalties</p>	<p>(3-4) (3-5) (3-6) (4-12,13) storage</p> <p>(3-7) (3-8)</p> <p>(3-23)</p>	<p>Table 11-2 Table 11-3 Section 11.1.2</p> <p>Scenario 4a,b</p>
<b>SUBJECT TO</b>		
<p>Utility Energy Balance</p>	<p>(3-12,13,14) (4-14) storage</p>	<p>Figure 11-2 Table 11-1</p>
<p>Equipment performance:</p> <ul style="list-style-type: none"> <li>- Conversion coefficients</li> <li>- Production limits <ul style="list-style-type: none"> <li>o Maximum load</li> <li>o Minimum load</li> </ul> </li> </ul>	<p>(3-11)</p> <p>(3-9) (3-10)</p>	<p>Table 11-2 Scenario based</p> <p>Table 11-2</p>
<del>Infrastructure Constraints</del>	<del>(3-17,18)</del>	
<p>Storage Balance</p> <ul style="list-style-type: none"> <li>- Hourly</li> <li>- Monthly</li> </ul>	<p>(4-15) to (4-23) (4-22,23)</p>	<p>Table 11-3 Electricity Propane Section 11.1.3</p>
<p>Scenario Based:</p> <ul style="list-style-type: none"> <li><del>Resource Availability</del> <ul style="list-style-type: none"> <li>o Wind</li> <li>o Biomass</li> </ul> </li> <li><del>Spinning Reserve</del></li> <li>- Storage Charging/Discharging</li> <li>- Demand Charge <ul style="list-style-type: none"> <li>o Fixed</li> <li>o Free</li> </ul> </li> <li>- Terminal constraint on storage <ul style="list-style-type: none"> <li>o Applied</li> <li>o Not applied</li> </ul> </li> </ul>	<p><del>(4-5) (4-6)</del> <del>(3-15,16)</del> <del>(4-7) to (4-11)</del></p>	<p>Figure 4-11</p> <p>Scenario 11 to 33 Scenario 4a,b</p>
<b>DECISION VARIABLES</b>		
<p>Technologies Available</p>		
<p>Equipment Units</p> <ul style="list-style-type: none"> <li>- OMSES</li> <li><del>MPC OMSES</del></li> <li><del>LT OMSES</del></li> </ul>		
<p>Storage Size</p>		
<p>Grid Capacity</p>		
<p>Energy/Mass Flows</p> <ul style="list-style-type: none"> <li>- Typical days</li> <li><del>Rolling horizon</del></li> </ul>		
<del>Incremental Equipment units</del>	<del>(5-6)</del>	

## **11.2 Results**

### **11.2.1 Summary of the Results**

Table 11-5 includes a summary of the results for each scenario considered in this case study. It contains the technologies installed, information regarding energy storage systems and infrastructure, and a summary of the most representative cost figures. The total installed capacity can be obtained using Table 11-2.

**Table 11-5 Summary of scenarios**

<b>Scenarios</b>		11	12	13	21	22	23	31	32	33	4a	4b
<b>Equipment installed</b>												
Diesel engine		0	0	0	0	0	0	0	0	0	0	2
Electric boiler		1	0	0	1	0	0	1	0	0	1	1
Propane boiler		3	3	3	3	3	3	3	3	3	2	2
Mechanical Chiller		2	2	2	4	2	2	4	2	2	2	2
Cooling Tower		1	1	1	2	1	1	2	1	1	1	2
Heat exchanger		0	0	0	0	0	0	2	2	2	2	2
Pump		7	6	6	9	6	6	9	6	6	8	8
FAN		4	4	4	4	4	4	4	4	4	4	4
Diesel mobile		37	1	0	37	0	0	37	1	0	0	0
Electric mobile		0	36	37	0	37	37	0	36	37	37	37
<b>Infrastructure and storage</b>												
Electricity connection capacity	MW	10.76	12.66	12.73	11.55	12.83	12.83	11.55	12.79	12.83	14.38	14.16
Electricity storage (per pack)	MWh	0.00	0.256	0.253	0.00	0.253	0.253	0.00	0.256	0.253	0.253	0.253
Hot Water Storage	MWh	0.28	0.74	0.74	0.87	0.74	0.74	0.87	2.84	2.84	4.19	3.77
UG Water storage	m3	261.90	0.00	0.00	646.74	0.00	0.00	646.74	0.00	0.00	1191.49	1191.49
Propane storage	MWh	33524.08	28955.67	28818.77	34173.49	28818.77	28818.77	22597.52	27436.81	27477.25	15664.41	16858.43
EV Batteries weight per pack	kg/pack	-	2304.00	2274.73	-	2274.73	2274.73	-	2304.00	2274.73	2274.73	2274.73
<b>Costs</b>												
Initial investment in equipment*	M CAD	27.19	38.66	38.90	28.17	38.90	38.90	26.92	38.61	38.87	37.81	48.15
Total Annual Cost	M CAD	27.34	26.27	26.28	28.75	26.44	26.44	27.57	26.31	26.32	25.38	24.81
Fixed cost	M CAD	9.78	12.60	12.67	10.33	12.72	12.72	10.13	12.65	12.72	13.31	14.89
Variable cost	M CAD	17.55	13.68	13.62	18.42	13.72	13.72	17.44	13.66	13.60	12.07	9.92
O&M cost	M CAD	1.99	2.21	2.22	2.22	2.25	2.25	2.17	2.24	2.24	2.24	2.27
Transmission line cost	M CAD	32.29	37.99	38.18	34.64	38.50	38.50	34.64	38.37	38.50	43.13	42.47
Annual cost of electricity	M CAD	7.67	9.04	9.07	8.25	9.15	9.15	8.25	9.12	9.14	8.55	5.46
Annual cost of diesel	M CAD	5.19	0.08	0.00	5.19	0.00	0.00	5.19	0.08	0.00	0.00	0.84
Annual cost of propane	M CAD	2.69	2.34	2.33	2.74	2.33	2.33	1.82	2.22	2.22	1.27	1.35

\* Connection cost not included

### 11.2.2 Seasonal Storage of Propane

Propane is purchased and stored to provide the fuel for heating, although some electricity is purchased to that effect in Scenarios 11, 21, 31, and 4 (both a and b). When electricity prices are considered constant and electric mobile equipment is not allowed, electricity is also consumed for heating (electric boilers). These are competitive with propane in terms of price as an energy source, but more expensive in capital when comparing the cost of storage and the transmission line. Because the electric line is designed for the most demanding situation, i.e., summer peak electricity demand, in winter there is available capacity for the electric boilers. In the case of variable price of electricity, both TOU and DC, electricity is consumed off-peak and stored in the form of heat, as the results for heat storage show in Table 11-5. Figure 11-3 illustrates the profile of propane storage in Scenario 11, which remains approximately the same for the remaining scenarios.

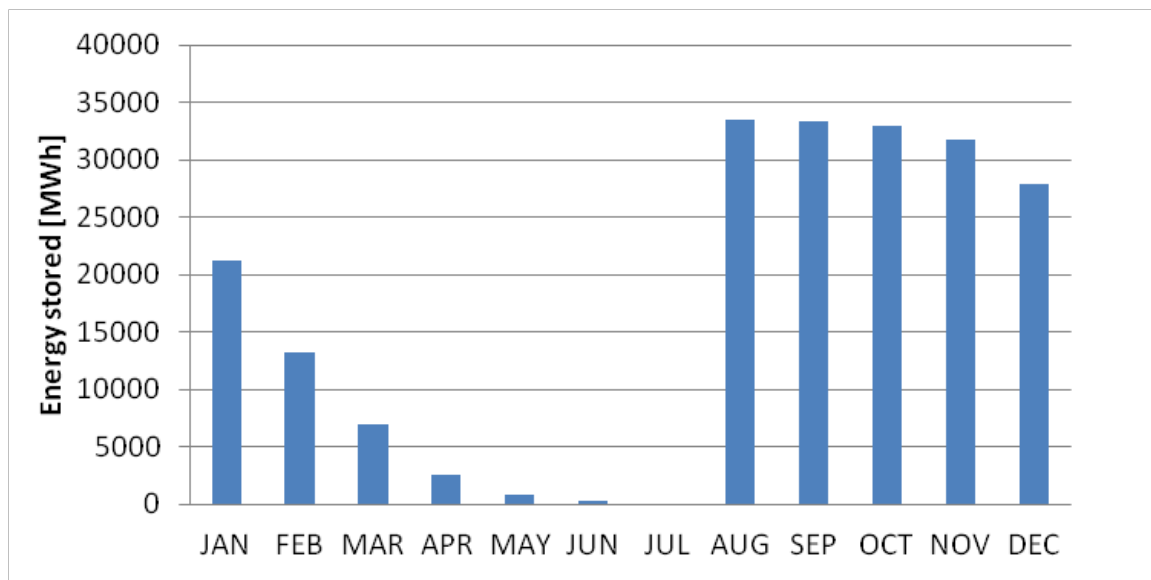


Figure 11-3 Scenario 11 Propane storage level

### 11.2.3 Reduction of Demand Charges

Figure 11-4 and Figure 11-5 illustrate the effect of allowing the system to reduce the electricity bill by minimizing the demand charges, which, as explained in Chapter 3, may be a function of what the consumer purchases (imports) during certain hourly intervals within each year.

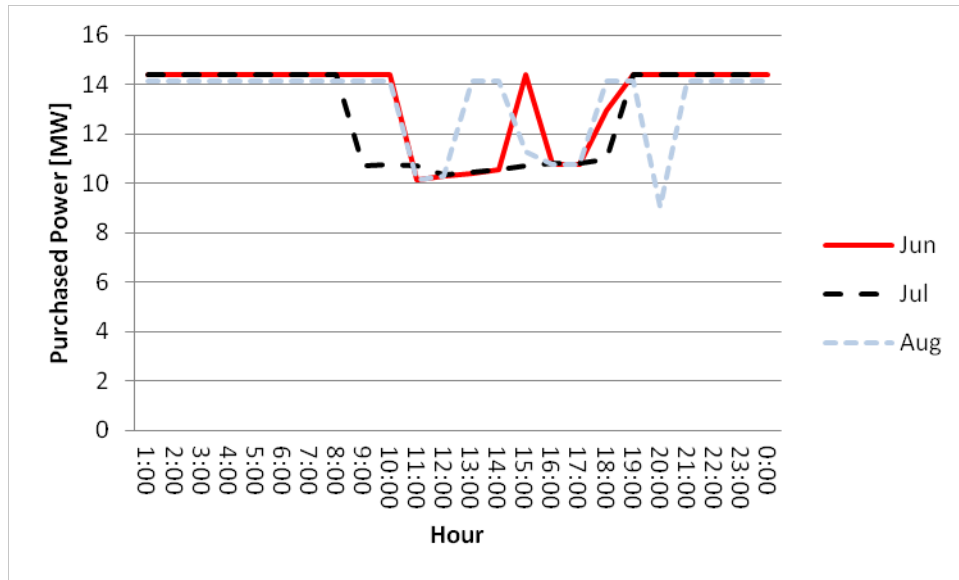


Figure 11-4 Purchased electricity in Scenario 4a

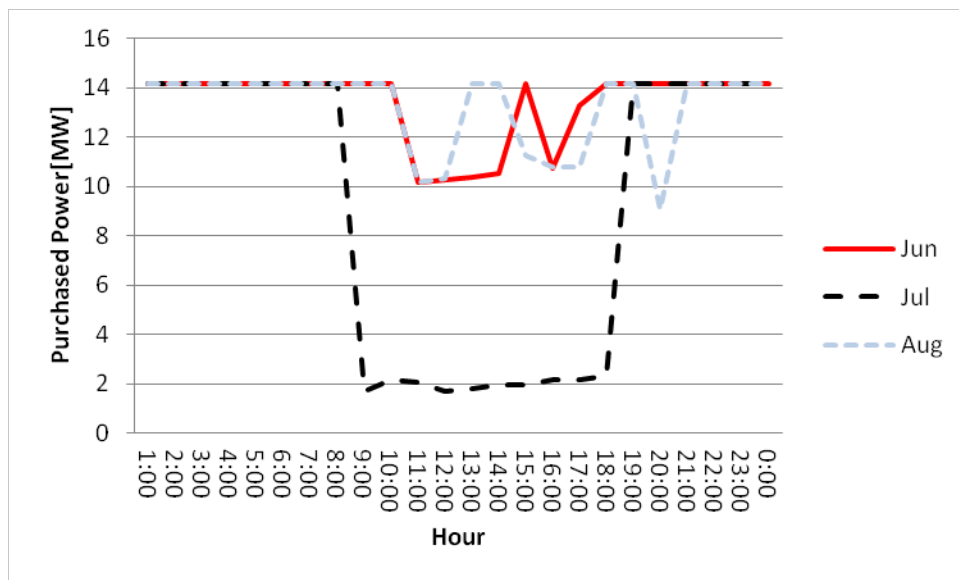


Figure 11-5 Purchased electricity in Scenario 4b

The figures correspond respectively to Scenarios 4a and 4b, where both TOU and DC vary with time and power imported. Diesel equipment for electricity generation is installed in Scenario 4b (Table 11-5) to dramatically reduce imports when needed (July central hours of the day). It is found that in the remaining days, on-site electricity generation cannot economically compete against imports, even with the generators already installed. This result agrees with those obtained in Chapter 7. This results from the elimination of a substantial part of the Global Adjustment (GA), that dramatically lowers the cost of the purchased electricity from 40 CAD/MWh consuming 11 MW (Figure 11-4), to 7 CAD/MWh consuming 2 MW in the central hours (9AM to 6PM) of July (Figure 11-5).

#### **11.2.4 Battery Management**

In Scenario 4b, it is possible to install diesel generators on-site to reduce electricity imports to lower DC, while in Scenario 4a, the only way of reducing the imports depends on how much load can be deferred (load shedding). In both scenarios, the maximum viable water storage capacity for the dewatering system, which is a function of the daily inflow, is installed (Table 11-5). The charge of the electric mobile equipment, present in both scenarios as optimal choices, is managed optimally so that the least amount of electricity is consumed for charging during the central hours of July. This management is more demanding in Scenario 4a, where no electricity can be generated on site.

The impact of DC in the management for several months, as well as that of TOU intraday variations, can be appreciated in Figure 11-6 through Figure 11-8. In July, and for the three battery packs, the optimal management strategy avoids charging from 8AM to 7PM. For the remaining months, the charging strategy is based exclusively on the HOEP and the mobile work

demand. These results are in agreement with those obtained in the previous section, as well as in Chapter 7.

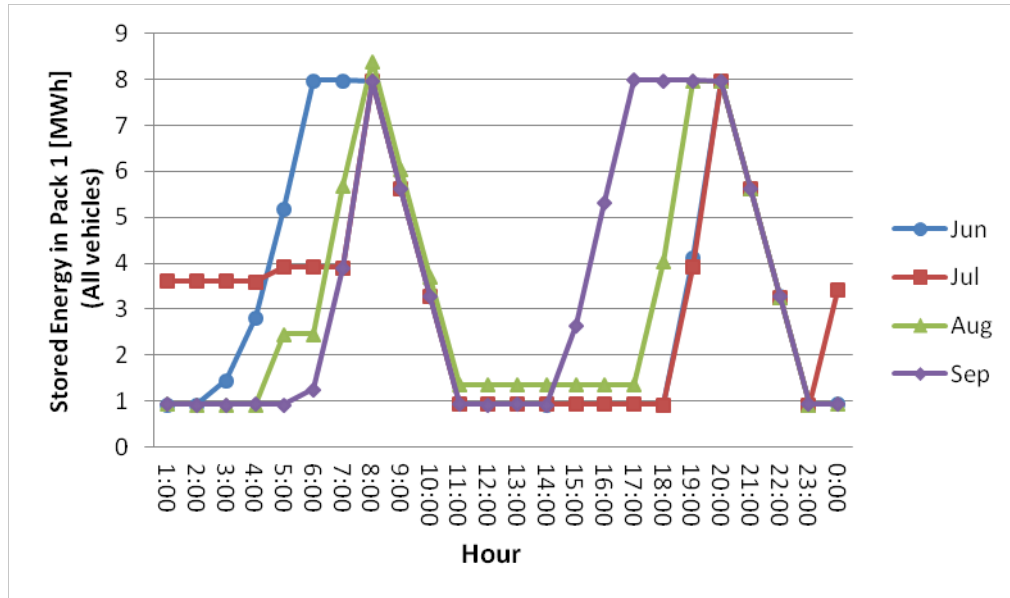


Figure 11-6 Scenario 4a Battery pack 1

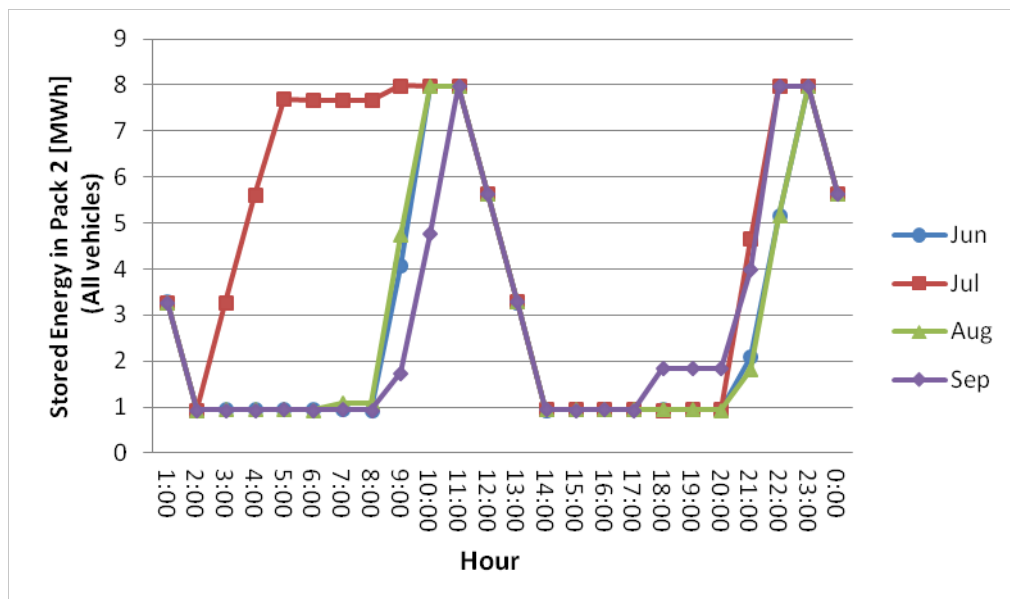


Figure 11-7 Scenario 4a Battery pack 2

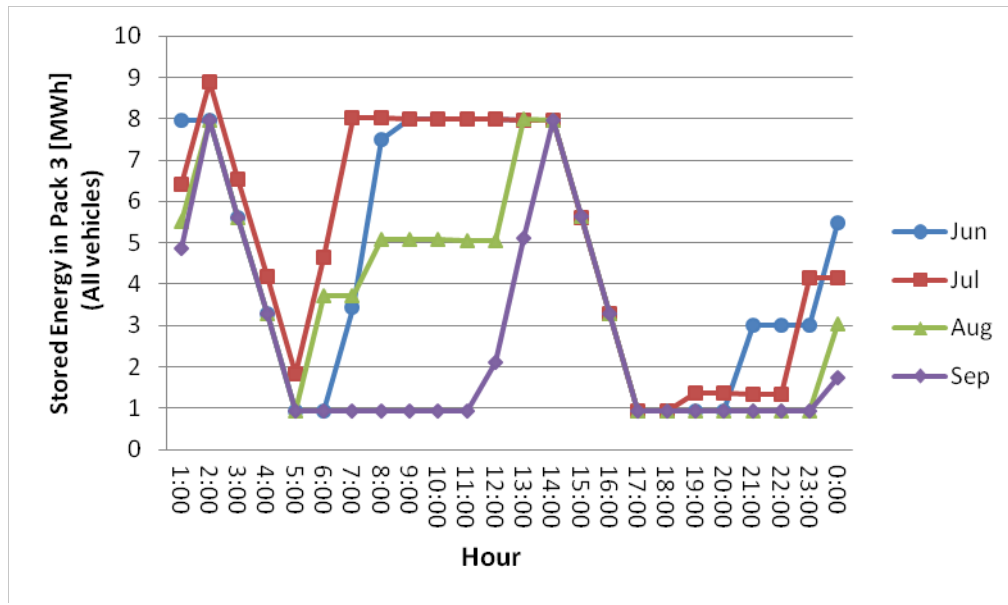


Figure 11-8 Scenario 4a Battery pack 3

### 11.3 Discussion

Figure 11-9 summarizes the total annual cost for the different scenarios. From this figure, several conclusions can be drawn. Note that the vertical axis is not zero-plotted. Scenario 11 is considered “business as usual” and thus is used for comparison. When underground cooling needs are considered, the maximum total annual cost savings from Scenario 11 to Scenario 4b are of 14% or CAD 4 Million.

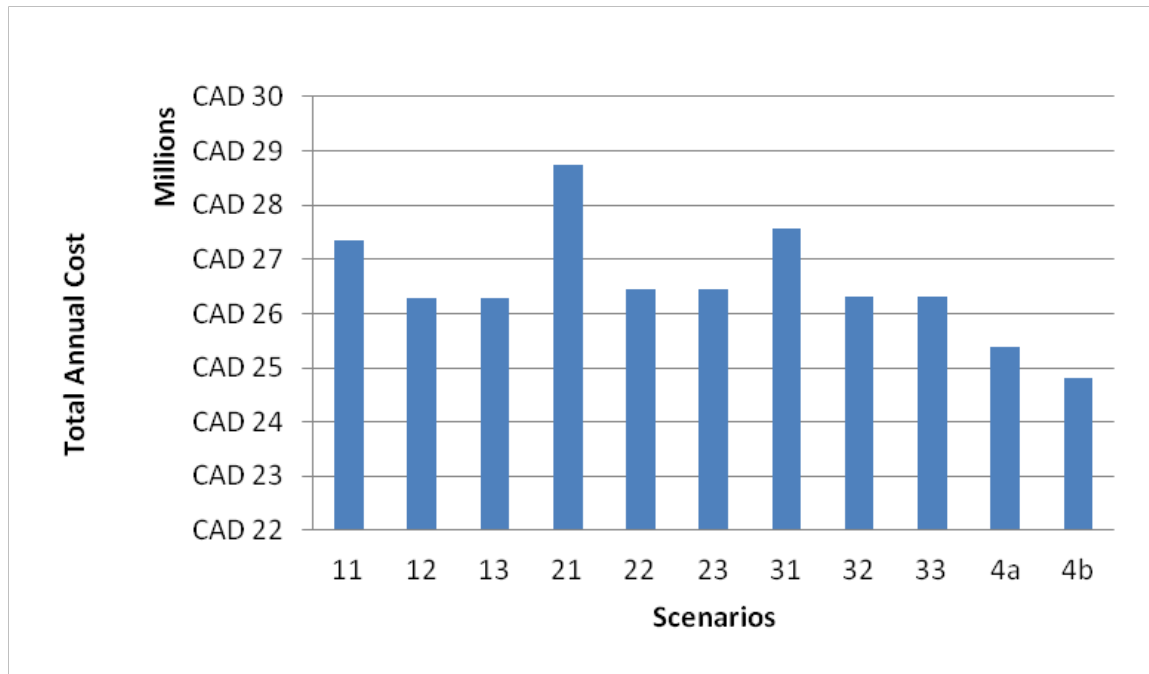


Figure 11-9 Total annual cost for the different scenarios depicted in Table 11-4

It can be seen from Figure 11-9 that the use of electric mobile plants instead of their diesel counterparts reduces the total annual cost. From the same figure, it can also be said that using low grade heat for ventilation entails less savings when electric vehicles are selected instead of diesel vehicles - the same results are found in scenarios 32 and 33 compared respectively to 22 and 23.

When the mine manages the operation of the energy system with careful attention to hourly prices significant savings can be achieved, especially when demand charges can also be minimized by on-site self-generation of electricity (Scenarios 4a and 4b).

Additional replacement costs may have to be considered, however, for the batteries. Given that the life of the mine has been limited to 10 years, total charging cycles amount 7300 (twice a day per pack). With today's state of development, battery packs are expected to be replaced at least

once. Considering 28 MWh of total battery storage capacity (Table 11-5), the annuitized cost of the replaced batteries amounts 1.01 million CAD. There is, though, a residual value on used batteries, and the replacement cost could be significantly reduced.

The cost of each three-pack of batteries assigned to each vehicle can be calculated assuming 252 kWh per pack and 190 CAD/kWh. The result is CAD 143,640 added to each vehicle, which is 28.7% of the cost of the diesel vehicle, in agreement with Moore (2015). The conservative assumption of 30% cost increase for the electric vehicle (without batteries) could then be relaxed, although the uncertainty of the actual cost of the batteries and maximum life cycles discourages this relaxation.

In addition to the results here presented (Table 11-5), the same scenarios were investigated with battery costs at 988 CAD/MWh (760 US\$/kWh considering 1.3CAD/US\$) (Lajunen, 2014; Paraszczak et al., 2014), a more, perhaps too conservative cost at present. This worsens the cost-effectiveness of the electric mobile option, which are not selected in any of the scenarios but remain closely competitive with the diesel counterpart in Scenarios 4a and 4b.

## **11.4 Conclusions**

This chapter exemplified the inclusion of mobile work as an energy demand in an underground mine in the context of OMSES. It also considered the use of seasonal energy storage for imported fuels using the formulation described in Chapter 4 for monthly storage balance.

The results obtained showed consistency with the data reported from different sources (Moore, 2015; Ewing, 2015; Lawson and Faubert, 2010). Using OMSES, it has been shown that electric vehicles are currently a competitive option to reduce energy costs and improve air quality in underground mines, in particular for those placed in regions where ventilation air has to be

thermally treated before it is delivered to the working areas. Increasing mining depth and remoteness of mines' regions will increase the advantage of using electricity as a fuel for mobile equipment, despite the high cost of electricity in certain areas. Even in this case, the cost reduction due to lowered ventilation demand (Table 11-2), as well as the fuel required to treat it, may offset any increase in electricity consumption from the electric mobile plants and its more expensive investment cost.

# Chapter 12

## 12 An Example Application of Long Term OMSES

This chapter presents the final case study of the thesis, which illustrates the difficulties and benefits of meeting varying energy demands for different years of the mine's life span. The economic benefit of considering production ramp up in mines when addressing the OMSES problem is demonstrated. This is carried out with a case study where the investment in high cost renewable energy is done progressively, taking advantage of the lower energy demands in the first years of the mine's operation. The conceptual challenge in trying to address this problem is to provide sufficiently well characterized demands and resources over a much extended time horizon without rendering the OMSES problem size so large that it cannot be solved in practical times with the current level of computing power. Compromises have to be made. In the same way that the typical days approach of using 288 hours of demand data to represent a complete year of 8760 hours is the approach advocated for the basic OMSES formulation, here, the cardinality of the set of typical days used to represent the year is reduced further, so that multiple years can be considered with approximately the same computer runtime.

### 12.1 Mine Description

Generally, open pit and underground mines deepen progressively throughout their operation. In addition, an initial phase of development takes place before actual extraction of the useful mineral begins. Finally, even production output can vary in what is called *ramp up* production, taking place during the first months or even years. Therefore, it is convenient to consider the ESS

of mines as something dynamic, i.e., a system that evolves in time, whose design configuration changes, as a series of planned investments takes place.

### 12.1.1 Mine Utility Demands

In Chapter 6, the foundations of a long term OMSES were set, making use of and adapting other existing optimization tools, such as TURN (Samsatli and Jennings, 2013) to the mining problem. The case study upon which this section rests is Victor Mine, the open pit mine studied in detail in Chapter 7. Scenario 2 from Chapter 7 has been selected, which considered off-grid conditions and a limitation on the amount of diesel and biomass imported. The latter, however, has been increased to 450,000 MWh annually; as explained in Chapter 7, the off-grid mine exhausted biomass import constraint (then 400,000 MWh only) to meet the electricity demand.

In order to reduce the size of the mathematical problem for a multiyear problem, the energy demand profiles throughout the life of the mine has been discretized into 432 time intervals. These represent 3 different set of years, which are composed of 6 typical days that capture seasonal variations, being each day divided into 24 periods of 1 hour duration. Here, a ramp up production is considered, consisting of three periods of 5, 5, and 10 years respectively, each with the same normalized demand profiles. The production rate for the three typical years, compared to full production, is 50%, 75%, and 100% respectively. Thus, multiplying these percentages by the demands detailed in Appendix 2, the typical year demands are obtained.

### 12.1.2 Economic Data

The rate of degradation from the installation year ( $k_{O\&M,\hat{y}}$ ) was defined (Section 6.2.2) as a multiplier applied on the operating and maintenance costs;  $k_{O\&M,\hat{y}}$  takes the illustrative values of 1, 2, and 3 for the consecutive typical years ( $\hat{y}$ ) since the installation. In this study, the

degradation applies with the same rate to all technologies, although it can accommodate variable values. The values for the discount rate ( $i_d$ ), general inflation ( $j_r$ ), and fuel inflation ( $j_e$ ) are 10%, 5%, and 8% respectively (Haberl, 1993).

The total annual cost has been calculated using the methodology described in Chapter 6, which differs from the expression used elsewhere in this thesis, which is defined in Chapter 3. The reason for such a difference is the existence of different and subsequent investment instances; there are as many as there are typical years of operation. The respective investment is assumed to take place at the beginning of each typical year, although this should be regarded as the moment in which the cost is accounted for, as opposed to when the equipment is installed, which can span several months in either the current and/or the past typical year.

### **12.1.3 Scenarios Investigated**

In total, seven scenarios were investigated in order to briefly demonstrate the advantages of using what is called Long Term Optimal Mine Site Energy Supply or simply LTOMSES.

The scenarios are grouped into three categories. The first category (comprising Scenarios 1, 2 and, 3) is used to compare the effect of inflation and variable operation and equipment ageing. Scenario 1 is the most benign scenario, with null inflation and no degradation of the equipment (constant operation and maintenance costs). Scenario 2 contemplates the case when inflation is considered, and no equipment degradation takes place. Scenario 3 modifies the former by also considering the degradation of the equipment installed (increase in O&M costs).

The second category is used to investigate the advantages of considering mine production ramp-up, as well as inflation and equipment ageing. In order to illustrate the advantages of the optimal

investment plan, this scenario category was solved twice: first, with free selection of equipment (Scenario 4a), and second, imposing the investment plan obtained in Scenario 1 (Scenario 4b).

The third group also considers two scenarios (5a and 5b), and only differs from the second category in that the effect of inflation is removed from the calculation.

The programmed code to solve for the optimal operation plan is provided in the second part of Appendix 8. The flow chart includes the possibility to solve the optimization problem dynamically in a receding horizon, but here only one-step optimization is applied to calculate the minimum cost investment plan and operation schedule.

**PROBLEM: REMOTE OPEN PIT MINE IN NORTHERN ONTARIO ILLUSTRATION OF LT-OMSES**

MINIMIZE	Equation	Inputs
<p>Total annual cost = Investment Cost</p> <p style="padding-left: 40px;">+ Variable Cost</p> <p style="padding-left: 80px;"><del>+ Demand Charges</del></p> <p style="padding-left: 80px;"><del>+ Penalties</del></p>	<p>(6-3) to (6-6) (4-12,13) storage (6-7) to (6-13)</p> <p><del>(3-23)</del></p>	<p>Section 7-2 Section 12.1.3 Section 7-2 Section 12.1.3</p>
<b>SUBJECT TO</b>		
<p>Utility Energy Balance</p> <p>Equipment performance:</p> <ul style="list-style-type: none"> <li>- Conversion coefficients</li> <li>- Production limits <ul style="list-style-type: none"> <li>o Maximum load</li> <li><del>o Minimum load</del></li> </ul> </li> </ul>	<p>(3-12,13,14) (4-14) storage Extended for years</p> <p>(3-11) (3-9) (3-10)</p>	<p>Section 12.1.1 Appendix 2 Table 7-1</p> <p>Table 7-2 Table 7-2</p>
<p>Infrastructure Constraints</p> <p><del>Storage Balance</del></p> <ul style="list-style-type: none"> <li><del>—Hourly</del></li> <li><del>—Monthly</del></li> </ul> <p>Scenario Based:</p> <ul style="list-style-type: none"> <li>- Resource Availability <ul style="list-style-type: none"> <li><del>o Wind</del></li> <li>o Biomass</li> <li><del>—Spinning Reserve</del></li> <li><del>—Storage Charging/Discharging</del></li> <li><del>—Demand Charge</del> <ul style="list-style-type: none"> <li><del>o Fixed</del></li> <li><del>o Free</del></li> </ul> </li> <li><del>—Terminal constraint on storage</del> <ul style="list-style-type: none"> <li><del>o Applied</del></li> <li><del>o Not applied</del></li> </ul> </li> </ul> </li> </ul>	<p>(3-17,18)</p> <p><del>(4-15) to (4-23)</del> <del>(4-22,23)</del></p> <p><del>(4-5) (4-6)</del> (3-15,16) <del>(4-7) to (4-11)</del></p>	<p>Off grid</p> <p>Section 12.1.1</p>
<b>DECISION VARIABLES</b>		
<p>Technologies Available</p> <p>Equipment Units</p> <ul style="list-style-type: none"> <li><del>—OMSES</del></li> <li><del>—MPC-OMSES</del></li> <li>- LT-OMSES</li> </ul> <p><del>Storage Size</del></p> <p><del>Grid Capacity</del></p> <p>Energy/Mass Flows</p> <ul style="list-style-type: none"> <li>- Typical days</li> <li><del>—Rolling horizon</del></li> </ul> <p><del>Incremental Equipment units</del></p>	<p><del>(5-6)</del></p>	

## 12.2 Results

The summary of the results of the seven scenarios is shown in Table 12-1. It can be observed that, as expected, that inflation, equipment degradation, and production ramp-up significantly affect the optimal investment plan and the total annual cost of the ESS. A more in-detail analysis is presented in the next section.

**Table 12-1 Scenario results for a mine with different demands throughout its life and different economic environment**

	Category 1 Scenarios									Category 2 Scenarios									Category 3 Scenarios					
	1			2			3			4a			4b			5a			5b					
Discount rate (id)	0.1			0.1			0.1			0.1			0.1			0.1			0.1					
Inflation (jr)	0			0.05			0.05			0.05			0.05			0			0					
Energy inflation (je)	0			0.08			0.08			0.08			0.08			0			0					
Year period (y)	1	2	3	1	2	3	1	2	3	1	2	3	1	2	3	1	2	3	1	2	3			
Period span (years) (ny)	5	5	10	5	5	10	5	5	10	5	5	10	5	5	10	5	5	10	5	5	10			
Production ramp	1	1	1	1	1	1	1	1	1	0.5	0.75	1	0.5	0.75	1	0.5	0.75	1	0.5	0.75	1			
O&M factor (fov)	1	1	1	1	1	1	1	2	3	1	2	3	1	2	3	1	2	3	1	2	3			
Gas Turbine	0	0	0	0	0	0	0	0	0	0	0	0	0	0	0	0	0	0	0	0	0			
Gas Engine	3	0	0	4	0	0	3	3	0	3	2	0	3	0	0	2	1	0	3	0	0			
Steam Boiler	1	0	0	0	0	0	1	0	0	0	0	0	1	0	0	0	0	1	1	0	0			
Hot Water Boiler	0	0	0	0	0	0	0	0	0	0	0	0	0	0	0	0	0	0	0	0	0			
HX Steam-Water	0	0	0	0	0	0	0	0	0	0	0	0	0	0	0	0	0	0	0	0	0			
HX Hot-Warm	1	0	0	1	0	0	1	1	0	1	1	0	1	0	0	1	1	0	1	0	0			
2 Abs Chiller	0	0	0	0	0	0	0	0	0	0	0	0	0	0	0	0	0	0	0	0	0			
1 Abs Chiller	1	0	0	1	0	0	1	0	0	1	0	0	1	0	0	1	0	0	1	0	0			
Mechanical Chiller	0	0	0	0	0	0	0	0	0	0	0	0	0	0	0	0	0	0	0	0	0			
Cooling Tower	3	2	0	2	2	0	3	2	2	2	2	2	3	2	0	2	2	2	3	2	0			
Diesel Engine	0	0	0	0	0	0	0	0	0	0	0	0	0	0	0	0	0	0	0	0	0			
Gasifier	9	0	0	12	1	0	9	2	0	5	6	0	9	0	0	5	3	1	9	0	0			
Fischer-Tropsch	0	0	0	2	1	0	0	1	0	0	2	0	0	0	0	0	0	0	0	0	0			
Biomass Steam Boiler	3	0	0	0	0	0	3	0	0	1	0	0	3	0	0	1	0	2	3	0	0			
Diesel Boiler	0	0	0	0	0	0	0	0	0	0	0	0	0	0	0	0	0	0	0	0	0			
Electric Boiler	0	0	0	0	0	0	0	0	0	0	0	0	0	0	0	0	0	0	0	0	0			
Steam Turbine	1	0	0	1	0	0	1	0	0	1	0	0	1	0	0	1	0	0	1	0	0			
Propane Engine	0	0	0	0	0	0	0	0	0	0	0	0	0	0	0	0	0	0	0	0	0			
Propane Boiler	0	0	0	0	0	0	0	0	0	0	0	0	0	0	0	0	0	0	0	0	0			
Total annual cost(CAD) x10 <sup>8</sup>	3.9			6.6			6.9			5.5			5.6			2.9			3.1					
Increase* (%)													2.5						4.0					

\* Increase in cost from 4a to 4b, and from 5a to 5b, respectively

### 12.3 Discussion

When production rate does not change, the most significant impact is observed when inflation is added (Table 12-1). Inflation of both value of money and cost of fuels increases the total annual cost by 70% and 77% for Scenario 2 and 3 respectively, in comparison with Scenario 1. It should be remembered that the mine operates for 20 years, which under the inflation parameters considered, significantly increases the cost of the energy procured. Furthermore, if the *business as usual* approach had been taken for the ESS (e.g., import electricity and diesel, or import diesel with electricity generation on-site), the effect of inflation would have been worse, as the share of variable cost in the total annual cost grows. This is consistent with Scenario 2's investment in additional gasification capacity, in comparison with Scenario 1.

To consider equipment degradation precludes, in general, the investment in more equipment when this investment seeks to reduce operation costs. Thus, a trade-off appears when inflation and degradation are considered simultaneously, which is evident when comparing Scenario 3 with the earlier; and so, investment is more dispersed in time in Scenario 3 than previously. The total number of units installed is comparable to Scenario 2, but higher than Scenario 1. In Scenario 3, the additional equipment is installed to overcome the degradation of the previously installed equipment.

It is interesting to observe the case of syndiesel production capacity (FT units). Scenario 1 does not consider the synthesis of biomass into synthetic diesel to be cost-effective, which was already discussed in Chapter 7. With the addition of inflation, however, it becomes very cost-effective. It should be remembered that to nearly eliminate diesel imports, four (4) FT units were needed (Scenario 1a, Chapter 7). In contrast, when equipment degradation is considered, the FT

capacity is reduced and postponed until the second annual interval, which demonstrates again the trade-off between inflation and degradation.

Regarding the production of syndiesel, it must be remembered that, because on the maximum import capacity for biomass and the off-grid constraint, most of the biomass purchased was converted into electricity. The rest of the biomass, which in this chapter is 50,000 MWh, can be converted into syndiesel with a conversion factor of approximately 70%, given the technology's conversion factors. This compares with the conversion pathways in Sterner (2009), which were estimated between 33% to 66%. Thus, 50,000 MWh of biomass energy can be converted into around 34,000 MWh of syndiesel, or 34% of the total diesel demand at the mine site.

The first three scenarios complement the analysis of Chapter 7, in which production was considered constant for the 20 years of the mine's life. However, the subsequent scenarios (4a, 4b, 5a, and 5b) cannot be directly compared, because the total production of the mine at the end of its life is reduced significantly, particularly when compared to the first ten years.

However, there are several comparisons possible, for example observing the FT units installed in Scenarios 4a and 3. When the ramp-up is considered during the first 10 years, there is enough biomass import capacity to allow for more FT units than in previous scenarios. One should not forget that for these two scenarios, inflation and equipment degradation are considered. More FT units were installed in Scenario 2, but in this case inflation without degradation lead to this outcome despite a lower utilization rate (load factor) than Scenario 4a, due to tighter biomass constraints in Scenario 2.

Scenario 4b imposed the investment plan from Scenario 1, in order to understand the economic consequences of postponing investment as much as possible, while meeting mine utility

demands. As illustrated in Table 12-1, the savings achieved are of 2.55% of the total annual cost. This significant but modest reduction is less important than the benefits of not having to install all the equipment at once, which is of particular interest in an ESS that would like to see a reduction in operating costs by the use of expensive renewable energy technologies.

Finally, Scenarios 5a and 5b were used to better understand the effects of inflation. Like Scenarios 4a and 4b, production ramp-up and degradation were considered. Removing inflation has two main effects: spanning the installation of equipment, and reducing the total number of units installed. These effects can be found in Table 12-1 and are next explained. When inflation on energy is removed, the price in the future does not vary, which precludes any investment oriented to reduce the operating costs in exchange of an increase in capital expenditure. This is the case with the use of FT units to reduce diesel imports – Scenario 5a does not install a single unit, in contrast with the two (2) units in Scenario 4a. Inflation of the value of currency has a different effect: when zero inflation is considered, the present cost of a future investment is lower (Chapter 6, Equations 6-3 through 6-6), and therefore the investment is encouraged. This is reinforced with Scenario 5a, where there are the same number of gas engines, gasifiers, and biomass boilers, but their installation is distributed over a longer period of time. Savings achieved in Scenario 5a compared with Scenario 5b, which again applies the investment plan of Scenario 1, are 4% of the total annual cost, but here the more evenly distributed investment reduces the risk derived from installing too many pieces of equipment without the absolute certainty that the mine will operate for the remainder of its lifetime.

## 12.4 Conclusions

Through a case study, this chapter has illustrated how the methodology developed in Chapter 6 improves OMSES' original formulation, which considered constant energy demands throughout the life of the mine.

This chapter has shown that the progressive increase in energy demands can be an opportunity if these can be estimated beforehand as a function of, for instance, mine development stage requirements and influence of depth in energy intensity. The relationships between energy demand and both depth and ore grade are well known (Chapman and Roberts, 1983; Northey et al., 2014; Levesque et al., 2014). As such, knowledge of the mining schedule (i.e., the pathway that indicates which areas of the mineral deposit are mined first) can be used to calculate the optimal series of investments regarding the ESS.

Given that both energy intensity and energy cost in mining are increasing (Levesque et al., 2014), schedule optimization and ESS optimization could be obtained simultaneously, which may result in a lower cost solution compared to the previous sequential optimization, in which first the schedule, and later the ESS, are optimized.

This chapter has presented the influence of inflation (value of money and energy) and equipment mechanical degradation, using an off-grid remote mine to illustrate such influences. In general, energy inflation promotes capital-intensive energy supply systems that can reduce operating costs, such as those including renewable energy technologies, illustrated here with biomass gasification and the Fischer-Tropsch process. With general inflation, which applies to the

investment in equipment, the present cost of a future investment is higher, which, all things being equal, brings to the present any future scheduled investment.

The consideration of equipment degradation was revealed to be of importance. Technologies which are subject to degradation, and thus that increase O&M costs, may lose their cost-effectiveness after several years of operation. This has been illustrated for some technologies included in this chapter (gasifiers and FT plants); the cost-effectiveness of FT to produce syndiesel on site was reduced.

However, determining the operational degradation as a function of the hours used and the date of installation presents a particular challenge. It has been assumed here that degradation takes place regardless of the hours operated, which is recognized as a poor assumption in certain cases, in particular for technologies operating few hours per year. In this latter case, though, is not expected to be a weak assumption, unless OMSES finds a great economic advantage when installing any technology (Chapter 7, demand charges effect). Nevertheless, the effects of that assumption should be analyzed for each piece of equipment and its resulting operating hours.

Finally, this chapter set the basis of a methodology for a less explored field, which includes dynamic design in a receding horizon, as illustrated in Chapter 6. The remaining work, hopefully investigated in the future by the author of this thesis, will entail the use of MPC and variable horizon discretization as proposed by Goodwin et al. (2008) for mine scheduling, applied to the ESS dynamic design.

# Chapter 13

## 13 Contributions and Future Work

Most of the chapters of this thesis have included a conclusion section. Thus, in order to avoid repetition, the present chapter summarizes the most significant contributions of this thesis supported by the results obtained. Some of these contributions should, however, be taken as novel applications of existing concepts in energy systems and model predictive control in the field of mining. This final chapter also recommends some specific topics worth being studied in the future.

### 13.1 Contributions to the Current State of Knowledge

Using the same structure as the key research questions in Section 1.4, the conclusions can be summarized as follows.

- What kind of uncertainties can and should be addressed, and how? Example: mine life, production uncertainty, wind and solar variability, future costs...

The energy demands' variability as a function of changing environmental conditions was studied, demonstrating the limitations of the optimal design obtained with OMSES' typical day's formulation. Other sources of uncertainty were not addressed, but sensitivity analyses were conducted regarding the life of the mine (Appendix 7), the price of energy sources and the connection distance (Chapter 7), or a combination of several factors (Appendices 4 and 5).

Production uncertainty, resulting from adjustments for commodity price fluctuations, was not addressed here, but the basis of the relationships between energy demands and production (i.e., ore extracted) was established in Chapter 6.

OMSES methodology remains valid as an approach to evaluate the economic potential of ESS solutions involving polygeneration, energy storage and renewable energy. OMSES, nevertheless, must be considered at the pre-feasibility level, never as the ultimate decision tool, for there are aspects of the system that the mathematical formulation does not capture, such as part load operation of equipment, reactive power or power quality (voltage and frequency) constraints.

- How can renewable energy sources with output that can vary over very short time scales be integrated with in OMSES' typical day formulations while keeping problem sizes small?

The use of OMSES typical day's (or other typical time interval) formulation should be thus limited to problems with low uncertainty and variability in demand profiles or in the renewable resources output. As large consumers, mines generally present flat and predictable demands. When integrating sources of energy such as solar or wind, precautions must be taken, even with low penetration solutions. These include, for instance, constraints in the maximum instantaneous penetration, spinning reserve, the use of renewable adjusted profiles to account for zero output, or a constraint so that a conventional supply system is always installed in any case.

- Can MPC be used to evaluate the robustness and resilience of optimal polygeneration design and, when possible, improve it? If so, how?

Many recent studies have addressed the topic of ESS optimal design and the difficulties involved (Section 2.3). ESS optimal solutions should be strengthened, tested in more realistic operating conditions, to evaluate whether or not the designs and the schedules remain, not only optimal, but also feasible. The process to obtain more robust solutions to ensure these two last aspects, had been accomplished previously by simulation of a large number of configurations, or re-optimizing designs and operation plans in more realistic or constrained environments.

In this thesis the use of MPC-based simulations has been proposed. This approach integrates, in addition to the feasibility check, the capacity to account for the uncertainty present in more realistic operating conditions. The simulation approach in combination with forecast capability provides flexibility on the control strategies, which are not possible when the system is optimized (design and operation) at once even when a large data set of historical demands is available. The dynamic approach, a methodological contribution of the present thesis to obtain robust, near optimal designs integrates, in contrast to other methods, the uncertainty typical of systems that rely on limited forecasts of ambient temperatures, for instance, to determine heating and cooling loads, or the power output from a wind farm. Chapter 10 demonstrated that even with highly detailed demand profiles, OMSES may yield unfeasible designs under uncertain operational conditions, dependent on variable wind speed or ambient temperature. Nevertheless, the optimal solution of the detailed OMSES problem offers a convenient reference (ideal case) for the typical days OMSES, and its improved design through MPC.

Using the typical days approach to define the mine's energy demands constrained the validity of OMSES' solution, but it is a widely accepted approach in the field of energy systems optimization. However, when considering variable renewable energy sources, the validity is

further limited to the case of low renewable penetration, providing that the formulation includes the need for enough backup generation for the periods in which there is no renewable generation. Chapters 9 and 10 introduced this problem, and Appendix 7 extended the assessment to seasonal energy storage, which stressed the need for inter-day and inter-season energy balance analysis, which can hardly be assessed using typical days.

- Is it possible to use material or energy storage for Demand Side Management (DSM) strategies and integrate these into a polygeneration system optimization for mine sites?

The advantages of considering material flows in the ESS included the adaptation of demand-side management techniques (Chapter 8) and the potential use of alternative technologies for the same demand of material handling (Chapter 11). Polygeneration, as described in Chapter 1, can potentially include material flows, but few examples are found in the literature in this regard, dealing mainly with desalination plants, whose product is measured in volume units of fresh water. In this thesis, mining has been identified as an energy consumer for which material flows interact intensively with energy flows, therefore increasing the opportunities for alternative technologies that would otherwise not participate in the ESS design problem.

- Can polygeneration systems' optimization be extended to accommodate mobile equipment, which is so important in the mine production processes?

Although material flows within ESS does itself not present an original methodological contribution, it has been shown how the mining industry is different from consumers considered in other works, in the sense that it combines in the same site stationary and mobile systems, constant and dispatchable demands, and the remoteness aspect. Thus, the work in this thesis is original for the consideration of optimal design and control of polygeneration systems, energy

storage, mobile plants and material flows, to name a few features included through the chapters, in a systematic manner. Accordingly, OMSES formulation and its MPC-based extension meet the needs of other industries, such as farming or forestry, as well as ESS for small communities or even nations.

- What happens with the period in which the mine still does not produce ore (just development)?

Finally, the case of a mine with inter-annual energy demand variation was addressed in Chapter 12. This case considered a mine that increases its energy demands through its life due to production ramp-up and extraction deepening. It was shown that, for the case considered, when a more detailed picture of the energy consumed in the mine over the years is considered, the progressive installation of elements of the ESS results in a lower cost than when installing all the equipment at the beginning of the life of the mine. Whether this holds generally, was not explored in Chapter 12, it being considered that when the OMSES methodology is applied for real design purposes, the designer will explore the longer term options following the LT-OMSES methodology. Furthermore, depending on such parameters selection, the optimal investment plan varies in quality (when the elements are installed) and quantity (how many of them there are). This approach is of particular interest in projects where renewable energy results are cost-effective in the long term and the risk derived from its high investment cost is to be reduced.

The contributions of this thesis are summarized as follows:

1. Derive the formulation for demand charges minimization, as well as the OMSES extension to include investment in transmission lines and pipelines for remote mines;

2. Develop a formulation for the dynamic redesign of energy supply systems under uncertainty based on the preselection of near-optimal solutions through OMSES;
3. Integrate in the optimization problem different alternatives for mobile work technologies;
4. Formulate the problem for long term optimization of energy systems with limited life and variable demand.

Other contributions of this thesis include:

1. Development of a graphical tool in Matlab for OMSES superstructure representation of the stated design problem, as well as the design and operation solutions;
2. Assessment of MPC degree of decentralization importance in mine dewatering systems;
3. Assessment of electrification of mobile plant opportunities in deep underground mines;
4. Assessment of the effectiveness of Ontario's support programs for the implementation of clean energy technologies (cogeneration), illustrated with a real case study;

The following key research questions were also addressed in several chapters:

- Can seasonal energy storage be integrated in OMSES? This was addressed in Chapters 4 and 11
- Can a typical day approach accommodate seasonal storage, or is a more detailed definition of the time frame required? This was addressed in Appendix 7

## 13.2 Future work

Chapters 5 and 6 introduced some of the ideas envisioned for future work. These include the use of MPC for a short-to-medium term control optimization with variable time discretization of the control and prediction horizons. MPC enables the capture of the uncertainty inherent in mining production, with a continuous deviation from the initial schedule that significantly affects the energy demands, in addition to, for instance, renewable sources' output variability.

This, in combination with the dynamic improvement of the design and the long term OMSES formulation will hopefully reduce the energy costs, the risk associated with the installation of expensive technologies, and increase the robustness of the design under uncertain environmental conditions, while integrating the mine's production plan as a variable of the problem. Such a scheme could be used to inform the managers of the potential economic advantages of varying the production schedule to achieve energy cost savings.

Regarding the use of MPC exclusively for operational control of the ESS, there is still room for further research on stand-alone systems analysis where the consumer's objectives may include several factors, such as production, energy costs, and emissions. Multi-objective optimization in mining would be enriched when both production output and emissions are considered.

Finally, further research is recommended regarding the objective of 100% renewable energy supply. Considering the limitations of this theoretical framework, which does not include detailed engineering aspects, it was found that such achievement (100% renewable) is technically possible, but is far from being economical under the typical parameters of investment costs and mine life. However, and in agreement with other works, it was shown that

a considerable reduction (up to 50%) in conventional energy use was cost-effective, even for the typical project life estimations of 10 years. Following the interest on energy storage in the form of hydrogen, this work concluded that internal combustion engines are still more cost effective than fuel cells for remote applications in which heating demand is significant. This work assessed whether a mine can be supplied solely with energy from renewable sources (Appendix 7), but not including the fuel for the mobile equipment, which is left for future work.

Throughout history, miners have shown that even in the most challenging environments it is possible to ensure an adequate energy supply. Considering the progressive depletion of high-quality conventional energy sources upon which most mines so intensely rely, the profitability of this extractive industry in the future might be determined by the use of local and renewable sources of energy to mine lower grade, higher depth mineral deposits in less geographically accessible areas.

## 14 References

- Abaravičius, J., and Pyrko, J. 2006. Load Management from an Environmental Perspective. *Energy and Environment*, 17 (4) pp. 583–601.
- Aboriginal Affairs and Northern Development Canada website. 2015. *Fort Severn - First Nation Detail*. [online] Available at [http://pse5-esd5.ainc-inac.gc.ca/fnp/Main/Search/FNMain.aspx?BAND\\_NUMBER=215&lang=eng](http://pse5-esd5.ainc-inac.gc.ca/fnp/Main/Search/FNMain.aspx?BAND_NUMBER=215&lang=eng) [Accessed May 20, 2011].
- Aggarwal, S.K. 2013. Simulations of Combustion and Emissions Characteristics of Biomass-Derived Fuels. In *Technologies for Converting Biomass to Useful Energy: Combustion, Gasification, Pyrolysis, Torrefaction and Fermentation*. Boca Raton, FL, Dahlquist (Ed.), CRC press, pp. 5–33.
- Al-gwiaz, M.M., Aseeri, A., and Noureldin, M.B.M. 2008. Pump Load Management via Repeated Simulation. In *Proceedings of Spring Meeting & 4th Global Congress on Process Safety*. New Orleans, LA, American Institute of Chemical Engineering,.
- Alkano, D., Nefkens, W.J., Scherpen, J.M.A., and Volkerts, M. 2014. Optimal Control in a Micro Gas Grid of Prosumers Using Model Predictive Control. In *Proceedings of 21st International Symposium on Mathematical Theory of Networks and Systems, July 7-11*. Groningen, The Netherlands, pp. 592–98.
- Alvarado, I., Limon, D., Muñoz De La Peña, D., Maestre, J.M., Ridao, M. a., Scheu, H., Marquardt, W., et al. 2011. A Comparative Analysis of Distributed MPC Techniques Applied to the HD-MPC Four-Tank Benchmark. *Journal of Process Control*, 21 (5) pp. 800–815. doi:10.1016/j.jprocont.2011.03.003.
- Arriaga, M., Canizares, C., and Kazerani, M. 2013. Renewable Energy Alternatives for Remote Communities in Northern Ontario, Canada. *JOUR. IEEE Transactions on Sustainable Energy*, 4 (3) pp. 661–70.
- ASHRAE. 2012. Combined Heat and Power Systems. In *ASHRAE Handbook: Heating, Ventilating & Air-Conditioning Systems*. Atlanta, GA, American Society of Heating, Refrigeration and Air Conditioning Engineers, Inc.,.
- Avcı, M., Erkoç, M., Rahmani, A., and Asfour, S. 2013. Model Predictive HVAC Load Control in Buildings Using Real-Time Electricity Pricing. *JOUR. Energy and Buildings*, 60 pp. 199–209.
- Basu, P. 2010. *Biomass Gasification and Pyrolysis: Practical Design and Theory*. BOOK. Burlington, MA: Academic press.
- Bentley Software website. 2014. *WaterCAD: Water Distribution Modeling and Analysis Software*. [online] Available at <http://www.bentley.com/en-US/Products/WaterCAD/> [Accessed May 18, 2016].

- Bétournay, M., Gangal, M., Rubeli, B., Laliberté, P., Zaghib, K., and Tchouvelev, A. 2011. Consideration of Clean Diesel and Alternative Energies for Underground Production Vehicles. CONF. *In Proceedings of CIM-ICM Conferences & Exhibitions*. Montreal, Canada.
- Bétournay, M., Laliberté, P., Lacroix, R., Kocsis, C., Hardcastle, S., Desrivières, G., Mousset-jones, P., and Righettini, G. 2005. Fuel Cell versus Diesel Loader Operation: Cost-Benefit Analysis Study. *CIM Bulletin*, May.
- Bizzarri, G., and Morini, G.L. 2004. Greenhouse Gas Reduction and Primary Energy Savings via Adoption of a Fuel Cell Hybrid Plant in a Hospital. JOUR. *Applied Thermal Engineering*, 24 (2) pp. 383–400.
- BizzEE Software website. 2012. *Custom Degree Day data*. [online] Available at <http://www.degreedays.net> [Accessed November 5, 2012].
- Brinkhaus, M., Jarosch, D., and Kapischke, J. 2011. All Year Power Supply with off-Grid Photovoltaic System and Clean Seasonal Power Storage. JOUR. *Solar Energy*, 85 (10) pp. 2488–96.
- Bungener, S.L., Marechal, F., Eetvelde, G. Van, and Descales, B. 2015. Optimisation of Unit Investment and Load Sheeding in a Steam Network Facing Undercapacity. Inproceedings. *In Proceedings of 28th International Conferente on Efficiency, Cost, Optimization and Simulation*. Pau, France.
- Buoro, D., Casisi, M., Pinamonti, P., and Reini, M. 2012. Optimal Synthesis and Operation of Advanced Energy Supply Systems for Standard and Domotic Home. JOUR. *Energy Conversion and Management*, 60 pp. 96–105.
- Çakir, U., Çomakli, K., and Yüksel, F. 2012. The Role of Cogeneration Systems in Sustainability of Energy. JOUR. *Energy Conversion and Management*, 63 pp. 196–202.
- Camacho, E.F., and Bordons, C. 2004. *Model Predictive Control*. Berlin, Germany: Springer Verlag.
- Carvalho, M. 2011. Thermoeconomic and Environmental Analyses for the Synthesis of Polygeneration Systems in the Residential-Commercial Sector. *University of Zaragoza, PhD Thesis*.
- Carvalho, M., Lozano, M.A., and Serra, L.M. 2012. Multicriteria Synthesis of Trigeneration Systems Considering Economic and Environmental Aspects. JOUR. *Applied Energy*, 91 (1) pp. 245–54.
- Carvalho, M., and Millar, D.L. 2012. Concept Development of Optimal Mine Site Energy Supply. JOUR. *Energies*, 5 (11) pp. 4726–45.
- Carvalho, M., Romero, A., and Millar, D. 2014a. Biomassa E Energia Solar Térmica Na Síntese E Otimizaçãode Um Sistema de Poligeração. CONF. *In Proceedings of V Congresso Brasileiro de Energia Solar*. Recife, Brasil.

- Carvalho, M., Romero, A., Shields, G., and Millar, D. 2014b. Optimal Synthesis of Energy Supply Systems for Remote Open Pit Mines. JOUR. *Applied Thermal Engineering*, 64 (1) pp. 315–30. doi:<http://dx.doi.org/10.1016/j.applthermaleng.2013.12.040>.
- Carvalho, M., Serra, L.M., and Lozano, M.A. 2011. Geographic Evaluation of Trigeneration Systems in the Tertiary Sector. Effect of Climatic and Electricity Supply Conditions. JOUR. *Energy*, 36 (4) pp. 1931–39.
- Chapman, P.F., and Roberts, F. 1983. *Metal Resources and Energy*. BOOK. London: Butterworths.
- Chen, Y.C., and Coulbeck, B. 1991. Optimized Operation of Water Supply Systems Containing a Mixture of Fixed and Variable Speed Pumps. Inproceedings. In *Proceedings of International Conference on Control 91*, pp. 1200–1205.
- Chicco, G., and Mancarella, P. 2009. Distributed Multi-Generation: A Comprehensive View. JOUR. *Renewable and Sustainable Energy Reviews*, 13 (3) pp. 535–51.
- Christofides, P.D., Scattolini, R., Muñoz de la Peña, D., and Liu, J. 2013. Distributed Model Predictive Control: A Tutorial Review and Future Research Directions. *Computers and Chemical Engineering*, 51 pp. 21–41. doi:10.1016/j.compchemeng.2012.05.011.
- Collazos, A., Maréchal, F., and Gähler, C. 2009. Predictive Optimal Management Method for the Control of Polygeneration Systems. JOUR. *Computers & Chemical Engineering*, 33 (10) pp. 1584–92.
- Crowson, P.C.F. 2011. Economics of the Minerals Industry. Incollection. In *SME Mining Handbook*. Englewood, Colo., Darling (Ed.), Society for Mining, Metallurgy, and Exploration Inc., 3rd ed., pp. 39–47.
- Dahlquist, E. 2013. An Overview of Thermal Biomass Conversion Technologies. In *Technologies for Converting Biomass to Useful Energy: Combustion, Gasification, Pyrolysis, Torrefaction and Fermentation*. Boca Raton, FL, Dahlquist (Ed.), CRC Press, pp. 1–3.
- Dantzig, G.B. 1948. *A Procedure for Maximizing a Linear Function Subject to Linear Inequalities*. Article. Washington: US Air Force Comptroller.
- Dantzig, G.B. 1963. *Linear Programming*. Misc. Princeton, NJ: Princeton University Press.
- Dantzig, G.B., Orden, A., and Wolfe, P. 1955. The Generalized Simplex Method for Minimizing a Linear Form under Linear Inequality Restraints. *Pacific Journal of Mathematics*, 5 (2) pp. 183–95.
- Dantzig, G.B., and Thapa, M.N. 1997. *Linear Programming: 2: Theory and Extensions*. Article. Glynn and Robinson (Eds.). New York, NY: Springer-Verlag.
- Darling, P. 2011. *SME Mining Engineering Handbook*. BOOK. Vol. 3. Englewood, Colo.: Society for Mining, Metallurgy, and Exploration.

- De Beers. 2010. 2010 Report to Society Canada. [online] Available at <http://www.angloamerican.com/~media/Files/A/Anglo-American-PLC-V2/investors/reports/csreports/2011br/de-beers2010-reporttosociety.pdf> [Accessed April 4, 2016].
- De Beers. 2014. Victor Mine Socio-Economic Assessment Toolbox (SEAT) Report. [online] Available at [http://www.debeersgroup.com/content/dam/de-beers/canada/documents/Reports/2013Victor Mine SEAT Report \(web ready\).pdf](http://www.debeersgroup.com/content/dam/de-beers/canada/documents/Reports/2013Victor%20Mine%20SEAT%20Report%20(web%20ready).pdf) [Accessed April 4, 2016].
- de la Vergne, J. 2003. *Hard Rock Miner's Handbook*. Andersen (Ed.). 3rded. North Bay, Ontario: McIntosh Engineering.
- de Souza, E. 2015. Cost Savings Strategies in Mine Ventilation. *In Proceedings of The CIM Conference and Exhibition*. Montreal.
- del Real, A.J., Arce, A., and Bordons, C. 2014. Combined Environmental and Economic Dispatch of Smart Grids Using Distributed Model Predictive Control. *JOUR. International Journal of Electrical Power & Energy Systems*, 54 pp. 65–76.
- Dincer, I., and Zamfirescu, C. 2014. *Advanced Power Generation Systems*. Book. Amsterdam: Elsevier.
- Directive 2004/8/EC on the Promotion of Cogeneration Based on a Useful Heat Demand. 2004.
- du Plessis, G.E., Liebenberg, L., and Mathews, E.H. 2013. Case Study: The Effects of a Variable Flow Energy Saving Strategy on a Deep-Mine Cooling System. *Applied Energy*, 102 pp. 700–709. doi:10.1016/j.apenergy.2012.08.024.
- Dube, R. 2015. *Chile mines turn to renewable energy*. *Wall Street Journal*. [online] Available at <http://www.wsj.com/articles/chile-mines-turn-to-renewable-energy-1439337896> [Accessed April 4, 2016].
- Enercon website. 2015. *Enercon Wind Turbine E-70*. [online] Available at <http://www.enercon.de/en/products/ep-2/e-70/> [Accessed May 20, 2009].
- Energy and Mines website. 2015a. *Industry Q&A: RIJN Capital Chile - Exploring the benefits of the mining-solar collaboration in Chile*. [online] Available at [www.energyandmines.com/chile](http://www.energyandmines.com/chile) [Accessed April 20, 2016].
- Energy and Mines website. 2015b. *Industry Q&A: SOLARRESERVE - Solar for mines: providing baseload solutions*. [online] Available at <http://energyandmines.com/wp-content/uploads/2015/03/EM-QA-Booklet-SolarReserve-web-opt.pdf>. [Accessed April 20, 2016].
- Engica Technology Systems International website. 2015. *Integrated Enterprise Asset Management (EAM)*. [online] Available at <http://www.engica.com/EAM-Enterprise-Asset-Management.aspx?gclid=CJP97M6mhsYCFRCqaQodnGUA2Q> [Accessed June 10, 2015].

Environment Canada. 1983. Principal Station Data – PSD/DPS 27. Sudbury A. RPRT. [online] Available at [ftp://ftp.tor.ec.gc.ca/Pub/Historical\\_Publications/Principal\\_station\\_data/Sudbury A.pdf](ftp://ftp.tor.ec.gc.ca/Pub/Historical_Publications/Principal_station_data/Sudbury_A.pdf).

Environment Canada website. 2014. *Hourly Data*. ICOMM. [online] Available at <http://climate.weather.gc.ca> [Accessed September 1, 2014].

Erbs, D.G., Beckman, W.A., and Klein, S.A. 1983. Estimation of Degree-Days and Ambient Temperature Bin Data from Monthly-Average Temperatures. *JOUR. ASHRAE Journal*, 25 (6) pp. 60–65.

Espirito Santo, D.B. 2012. Energy and Exergy Efficiency of a Building Internal Combustion Engine Trigeneration System under Two Different Operational Strategies. *JOUR. Energy and Buildings*, 53 pp. 28–38.

EWEA. 2009. Wind Energy–The Facts. A Guide to the Technology, Economics and Future of Wind Power. *JOUR. Earthscan, London, UK*.

Ewing, I. 2015. *Kirkland Lake Gold finds its feet again*. MGZN. *CIM Magazine*. [online] Available at <https://magazine.cim.org/en/2015/March-April/project-profile/Excellent-recovery.aspx> [Accessed April 5, 2016].

Fabrizio, E. 2011. Feasibility of Polygeneration in Energy Supply Systems for Health-Care Facilities under the Italian Climate and Boundary Conditions. *JOUR. Energy for Sustainable Development*, 15 (1) pp. 92–103.

Five Nations Energy Inc. website. 2015. *History of Five Nations Energy Inc.* [online] Available at <http://www.fivenations.ca> [Accessed September 16, 2015].

Funatsu, T., Dohzono, Y., and Fukuda, M. 1999. Startup Analysis of an H<sub>2</sub>-O<sub>2</sub> - Fired Gas Turbine Cycle. *Electrical Engineering in Japan*, 128 (1) pp. 9–16.

General Electric Transportation website. 2015. *GE Fairchild Battery Powered Load Haul Dump*. ICOMM. [online] Available at <http://www.getransportation.com/mining/ge-fairchild-battery-powered-load-haul-dump> [Accessed June 10, 2015].

Georgiou, P.N. 2015. A Bottom-up Optimization Model for the Long-Term Energy Planning of the Greek Power Supply Sector Integrating Mainland and Insular Electric Systems. *Computers & Operations Research*, no. 60 pp. 1–21. doi:10.1016/j.cor.2015.02.015.

Gleeson, J., Zeller, A., and McLaughlin, J.W. 2006. *Peat as a Fuel Source in Ontario: A Preliminary Literature Review*. *Forest Research Information Paper no.161*. Sault Ste. Marie, ON: Ontario Forest Research Institute.

Goldcorp. 2015. Core Strengths - Sustainability Report 2014. . Vancouver. [online] Available at [http://csr.goldcorp.com/2014/\\_pdf2print/pdfs/0\\_0\\_goldcorp\\_csr\\_2014\\_full.pdf](http://csr.goldcorp.com/2014/_pdf2print/pdfs/0_0_goldcorp_csr_2014_full.pdf) [Accessed April 4, 2016].

Gomatom, P., and Jewell, W. 2002. Feasibility Evaluation of Distributed Energy Generation and

Storage for Cost And Reliability Using the“ Worth Factor” Criterion. CONF. *In Proceedings of Frontiers of Power Conference*. Stillwater, OK, Engineering Energy Laboratory, Oklahoma State University,.

Goodwin, G.C., Seron, M.M., and Mayne, D.Q. 2008. Optimization Opportunities in Mining, Metal and Mineral Processing. *Annual Reviews in Control*, 32 (1) pp. 17–32. doi:10.1016/j.arcontrol.2008.02.002.

Goodwin, G.C., Seron, M.M., Middleton, R.H., Zhang, M., Hennessy, B.F., Stone, P.M., and Menabde, M. 2006. Receding Horizon Control Applied to Optimal Mine Planning. *Automatica*, 42 (8) pp. 1337–42. doi:10.1016/j.automatica.2006.01.016.

Government of Canada website. 2015. *Fort Severn - Connectivity Profile*. [online] Available at <https://www.aadnc-aandc.gc.ca/eng/1357840942062/1360163858881> [Accessed May 20, 2011].

Government Ontario website. 2010. *Ontario Regulation 398/10*. GEN. [online] Available at <http://www.ontario.ca/laws/regulation/r10398> [Accessed April 5, 2016].

Grünbaum, R., and Willemsen, N. 2013. Facts for Voltage Stability and Power Quality Improvement in Mining. *In Proceedings of 22nd International Conference on Electricity Distribution (CIRED)*. Stockholm.

Haberl, J.S. 1993. Economic Calculations for ASHRAE Handbook. Article. *Energy Systems Laboratory Report EST-TR-93/04-07*, College Station, TX: Texas A&M University.

Halvgaard, R., Bacher, P., Perers, B., Andersen, E., Furbo, S., Jørgensen, J.B., Poulsen, N.K., and Madsen, H. 2012. Model Predictive Control for a Smart Solar Tank Based on Weather and Consumption Forecasts. *Energy Procedia*, 30 pp. 270–78. doi:10.1016/j.egypro.2012.11.032.

Henning, H.M., and Palzer, A. 2014. A Comprehensive Model for the German Electricity and Heat Sector in a Future Energy System with a Dominant Contribution from Renewable Energy technologies—Part I: Methodology. *JOUR. Renewable and Sustainable Energy Reviews*, 30 pp. 1003–18.

Hunter, R., Friis Pedersen, T., Dunbabin, P., Antoniou, I., Frandsen, S.T., Klug, H., Albers, A., and Lee, W.K. 2001. *European Wind Turbine Testing Procedure Developments. Task 1: Measurement Method to Verify Wind Turbine Performance Characteristics*. RPRT. Vol. R-1209(EN). Roskilde, Denmark: Risø National Laboratory.

IESO. 2011a. *Global Adjustment*. ICOMM. [online] Available at <http://www.ieso.ca/Pages/Ontario's-Power-System/Electricity-Pricing-in-Ontario/Global-Adjustment.aspx> [Accessed April 26, 2016].

IESO. 2011b. *Global Adjustment*. ICOMM. [online] Available at <http://www.ieso.ca/Pages/Ontario's-Power-System/Electricity-Pricing-in-Ontario/Global-Adjustment.aspx> [Accessed April 26, 2016].

IESO. 2011c. *Market reports*. ICOMM. [online] Available at <http://www.ieso.ca/Pages/Power-Data/Market-Summaries-Archive.aspx#> [Accessed April 26, 2016].

- IESO. 2012a. *Global Adjustment Archive*. ICOMM. [online] Available at <http://www.ieso.ca/Pages/Ontario's-Power-System/Electricity-Pricing-in-Ontario/Global-Adjustment.aspx> [Accessed April 26, 2016].
- IESO. 2012b. *Market reports*. ICOMM. [online] Available at <http://www.ieso.ca/Pages/Power-Data/Market-Summaries-Archive.aspx#> [Accessed April 26, 2016].
- IESO. 2014. *Changes to the Global Adjustment*. [online] Available at <http://www.ieso.ca/Pages/Participate/Settlements/Changes to Class A Eligibility.aspx> [Accessed April 26, 2016].
- IESO. 2015. *Hourly Ontario Electricity Price*. [online] Available at [www.ieso.ca](http://www.ieso.ca).
- Ilic, D.D., Dotzauer, E., and Trygg, L. 2012. District Heating and Ethanol Production through Polygeneration in Stockholm. *JOUR. Applied Energy*, 91 (1) pp. 214–21.
- Jacobsen, J. 2015. A New Way to Power Mining Projects. *Mining Magazine*, June. [Accessed May 18, 2016] Available at <http://www.miningmagazine.com/management/water-environment/a-new-way-to-power-mining-projects/>.
- Jefferson, J. 2006. Energy Efficiency Opportunities in Ontario Hospitals. *JOUR. Burlington (ON), Canada*. [online] Available at <http://www.oha.com/CurrentIssues/keyinitiatives/eHealth/Documents/EnergyEfficiencyOpportunitiesfeb28.pdf> [Accessed June 20, 2004].
- Judd, E. 2014. *Building a wind farm in Arctic conditions: Rio Tinto's Diavik Mine*. *GEN*. [online] Available at <http://energyandmines.com/2014/04/rio-tinto-diavik-mine-wind-powering-diamond-mine-in-the-arctic/> [Accessed April 20, 2016].
- Judd, E. 2015a. *Market Spotlight: Chile - Renewables getting better at customizing PPAs for mines but more dialogue is necessary*. [online] Available at [http://energyandmines.com/wp-content/uploads/2015/03/EM-Market-Spotlight-Chile\\_opt.pdf](http://energyandmines.com/wp-content/uploads/2015/03/EM-Market-Spotlight-Chile_opt.pdf) [Accessed April 6, 2016].
- Judd, E. 2015b. The Appetite for Renewables. *Mining Magazine*, June. [Accessed June 20, 2005] Available at <http://www.miningmagazine.com/management/water-environment/the-appetite-for-renewables/>.
- Kauranen, P.S., Lund, P.D., and Vanhanen, J.P. 1994. Development of a Self-Sufficient Solar-Hydrogen Energy System. *JOUR. International Journal of Hydrogen Energy*, 19 (1) pp. 99–106.
- Kelly, N. a., Gibson, T.L., and Ouwerkerk, D.B. 2011. Generation of High-Pressure Hydrogen for Fuel Cell Electric Vehicles Using Photovoltaic-Powered Water Electrolysis. *International Journal of Hydrogen Energy*, 36 (24) pp. 15803–25. doi:10.1016/j.ijhydene.2011.08.058.
- Kim, T.S., Lee, D.K., and Ro, S.T. 2000. Analysis of Thermal Stress Evolution in the Steam Drum during Start-up of a Heat Recovery Steam Generator. *JOUR. Applied Thermal Engineering*, 20 (11) pp. 977–92. doi:[http://dx.doi.org/10.1016/S1359-4311\(99\)00081-2](http://dx.doi.org/10.1016/S1359-4311(99)00081-2).

Kjaer, C., Douglas, B., Bianchin, R., and Sander, E., eds. 2009. *Wind Energy-the Facts: A Guide to the Technology, Economics and Future of Wind Power*. Book. London: Earthscan.

Koltsaklis, N.E., Liu, P., and Georgiadis, M.C. 2015. An Integrated Stochastic Multi-Regional Long-Term Energy Planning Model Incorporating Autonomous Power Systems and Demand Response. *Energy*, 82 pp. 865–88. doi:10.1016/j.energy.2015.01.097.

Kookos, I.K., and Perkins, J.D. 2001. An Algorithm for Simultaneous Process Design and Control. *Industrial & Engineering Chemistry Research*, 40 (19) pp. 4079–88. doi:10.1021/ie000622t.

Kurek, W., and Ostfeld, A. 2013. Multi-Objective Optimization of Water Quality, Pumps Operation, and Storage Sizing of Water Distribution Systems. *Journal of Environmental Management*, 115 pp. 189–97. doi:10.1016/j.jenvman.2012.11.030.

Kyriakarakos, G., Dounis, A.I., Rozakis, S., Arvanitis, K.G., and Papadakis, G. 2011. Polygeneration Microgrids: A Viable Solution in Remote Areas for Supplying Power, Potable Water and Hydrogen as Transportation Fuel. *JOUR. Applied Energy*, 88 (12) pp. 4517–26.

Lajunen, A. 2014. Energy Consumption and Cost-Benefit Analysis of Hybrid and Electric City Buses. *Transportation Research Part C: Emerging Technologies*, 38 pp. 1–15. doi:10.1016/j.trc.2013.10.008.

Lambert, T., Gilman, P., and Lilienthal, P. 2006. Micropower System Modeling with Homer. *JOUR. In Integration of Alternative Sources of Energy*, Farret and Simões (Eds.), John Wiley & Sons, pp. 379–418. doi:10.1002/0471755621.ch15.

Landberg, L., Giebel, G., Nielsen, H.A., Nielsen, T., and Madsen, H. 2003. Short-Term Prediction - An Overview. *Wind Energy*, 6 (3) pp. 273–80. doi:10.1002/we.96.

Langreder, W., and Bade, P. 2012. The Wind. Book. In *Wind Power Plants - Fundamentals, Design, Construction and Operation*. Berlin, Germany, Gasch and Tewe (Eds.), Springer Science & Business Media, 2nded., pp. 114–64.

Lawson, G., and Faubert, A. 2010. Musselwhite Mine Sustainability Report 2008-2009. . Thunder Bay. [online] Available at [http://csr.goldcorp.com/2010/docs/2009\\_musselwhite.pdf](http://csr.goldcorp.com/2010/docs/2009_musselwhite.pdf) [Accessed April 6, 2016].

Levesque, M., Millar, D., and Paraszczak, J. 2014. Energy and Mining – the Home Truths. *JOUR. Journal of Cleaner Production*, 84 (December) pp. 233–55. doi:http://dx.doi.org/10.1016/j.jclepro.2013.12.088.

Li, C.Z., Shi, Y.M., and Huang, X.H. 2008. Sensitivity Analysis of Energy Demands on Performance of CCHP System. *JOUR. Energy Conversion and Management*, 49 (12) pp. 3491–97.

Lindo Systems website. 2007. *LINGO 15.0 - Optimization Modeling Software for Linear, Nonlinear, and Integer Programming*. GEN. [online] Available at [http://www.lindo.com/index.php?option=com\\_content&view=article&id=2&Itemid=10](http://www.lindo.com/index.php?option=com_content&view=article&id=2&Itemid=10)

[Accessed April 19, 2016].

Liu, P., Georgiadis, M.C., and Pistikopoulos, E.N. 2011. Advances in Energy Systems Engineering. JOUR. *Industrial & Engineering Chemistry Research*, 50 (9) pp. 4915–26.

Lozano, M.A., Ramos, J.C., Carvalho, M., and Serra, L.M. 2009. Structure Optimization of Energy Supply Systems in Tertiary Sector Buildings. JOUR. *Energy and Buildings*, 41 (10) pp. 1063–75.

Lozano, M.A., and Valero, A. 1993. Theory of the Exergetic Cost. Article. *Energy*, 18 (9) pp. 939–60.

Lozano, M.A., Valero, A., and Serra, L. 1993. Theory of Exergetic Cost and Thermo-economic Optimization. Inproceedings. *In Proceedings of The International Symposium ENSEC'93*. Cracow, Poland.

Maciejowski, J.M. 2002. *Predictive Control: With Constraints*. Book. London: Pearson Education Limited, Prentice Hall.

Maestre, J.M., and Negenborn, R.R. 2014. *Distributed Model Predictive Control Made Easy*. Book. Dordrecht, The Netherlands: Springer.

Maestre, J.M., Raso, L., van Overloop, P.J., and De Schutter, B. 2013. Distributed Tree-Based Model Predictive Control on a Drainage Water System. *Journal of Hydroinformatics*, 15 (2) pp. 335. doi:10.2166/hydro.2012.125.

Majewski, D.E., Voll, P., and Bardow, A. 2015. Strictly Robust Optimal Design of Decentralized Energy Systems. *In Proceedings of 28th International Conference on Efficiency, Cost, Optimization and Simulation*. Pau, France.

Mancarella, P. 2014. MES (Multi-Energy Systems): An Overview of Concepts and Evaluation Models. JOUR. *Energy*, 65 (0) pp. 1–17. doi:http://dx.doi.org/10.1016/j.energy.2013.10.041.

Manfren, M., Caputo, P., and Costa, G. 2011. Paradigm Shift in Urban Energy Systems through Distributed Generation: Methods and Models. JOUR. *Applied Energy*, 88 (4) pp. 1032–48.

Manwell, J.F., McGowan, J.G., and Rogers, A.L. 2009. *Wind Energy Explained: Theory, Design and Application*. Book. Chichester, UK: John Wiley & Sons.

Mason, T., Curry, T., and Wilson, D. 2012. Capital Costs for Transmission and Substations: Recommendations for WECC Transmission Expansion Planning. JOUR. *Black & Veatch Project No. 181374*.

Massé, P., and Gibrat, R. 1957. Application of Linear Programming to Investments in the Electric Power Industry. Article. *Management Science*, 3 (2) pp. 149–66. doi:10.1287/mnsc.3.2.149.

Mathisen, H. 2014. In to the Wind. MGZN. *CIM Magazine*, 8 pp. 60–63.

Mayhorn, E., Kalsi, K., Elizondo, M., Zhang, W., Lu, S., Samaan, N., and Butler-Purry, K.

2012. Optimal Control of Distributed Energy Resources Using Model Predictive Control. CONF. *In Proceedings of IEEE Power and Energy Society General Meeting*, IEEE, pp. 1–8.
- Mayhorn, E., Kalsi, K., Lian, J., and Elizondo, M. 2013. Model Predictive Control-Based Optimal Coordination of Distributed Energy Resources. CONF. *In Proceedings of 46th Hawaii International Conference on System Sciences (HICSS)*, IEEE, pp. 2237–44.
- McCormick, G., and Powell, R.S. 2003. Derivation of near-Optimal Pump Schedules for Water Distribution by Simulated Annealing. *Journal of the Operational Research Society*, no. 0 pp. 1–9.
- McIlveen-Wright, D.R., McMullan, J.T., and Guiney, D.J. 2003. Wood-Fired Fuel Cells in Selected Buildings. JOUR. *Journal of Power Sources*, 118 (1) pp. 393–404.
- McMillan, B. 2013. GSU Greater Sudbury Hydro Inc. (Personal Communication). PCOMM.
- Mendes, G., Ioakimidis, C., and Ferrão, P. 2011. On the Planning and Analysis of Integrated Community Energy Systems: A Review and Survey of Available Tools. JOUR. *Renewable and Sustainable Energy Reviews*, 15 (9) pp. 4836–54.  
doi:<http://dx.doi.org/10.1016/j.rser.2011.07.067>.
- Menon, R.P., Paolone, M., and Maréchal, F. 2013. Study of Optimal Design of Polygeneration Systems in Optimal Control Strategies. JOUR. *Energy*, 55 pp. 134–41.
- Meyer, H.S., Hill, V.L., Flowers, A., Happel, J., and Hnatow, M.A. 1982. Direct methanation—A New Method of Converting Synthesis Gas to Substitute Natural Gas. Article. *Preprint Papers-American Chemical Society. Division of Fuel Chemistry*, 27 (1) pp. 109–15.
- MHSA website. 2015. *Heat Stress in Mining*. [online] Available at <http://www.msha.gov/s&hinfo/heatstress/manual/heatmanual.htm> [Accessed September 1, 2015].
- Microsoft website. 2007. *Microsoft Excel*. [online] Available at <https://products.office.com/en-us/excel> [Accessed April 5, 2016].
- Middelberg, A., Zhang, J., and Xia, X. 2009. An Optimal Control Model for Load Shifting—with Application in the Energy Management of a Colliery. JOUR. *Applied Energy*, 86 (7) pp. 1266–73.
- Miller, A.R., van den Berg, G., Barnes, D.L., Eisele, R.I., Tanner, D.M., Vallely, J.M., and Lassiter, D.A. 2012. Fuel Cell Technology in Underground Mining. *In Proceedings of 5th International Platinum Conference, 18–20 September*. Sun City, South Africa, The Southern African Institute of Mining and Metallurgy, pp. 533–46.
- Moore, E. 2015. Battery-Powered LHDs Offer Miners Cleaner, Cooler and Quieter Alternatives to Diesel. *CIM Magazine*, May. [Accessed April 5, 2016] Available at <http://www.cim.org/en/Publications-and-Technical-Resources/Publications/CIM-Magazine/2015/May/technology/Charged-up.aspx>.

- Mudd, G.M. 2007. Global Trends in Gold Mining: Towards Quantifying Environmental and Resource Sustainability. *JOUR. Resources Policy*, 32 (1) pp. 42–56.
- Negenborn, R.R. 2007. Multi-Agent Model Predictive Control with Applications to Power Networks. *Delft University of Technology, PhD Thesis*.
- Norgate, T., and Haque, N. 2010. Energy and Greenhouse Gas Impacts of Mining and Mineral Processing Operations. *JOUR. Journal of Cleaner Production*, 18 (3) pp. 266–74.
- Northey, S., Mohr, S., Mudd, G.M., Weng, Z., and Giurco, D. 2014. Modelling Future Copper Ore Grade Decline Based on a Detailed Assessment of Copper Resources and Mining. *JOUR. Resources, Conservation and Recycling*, 83 (0) pp. 190–201.  
doi:<http://dx.doi.org/10.1016/j.resconrec.2013.10.005>.
- Northwest Territories Power Corporation website. 2015. *Northwest Territories Business Electrical Rates*. [online] Available at <https://www.ntpc.com/customer-service/business-service/business-rates> [Accessed November 1, 2015].
- NRCan. 2001. Health Care Energy Survey: Comparing Energy Management in Canadian Health Care Facilities. RPRT. [online] Available at <http://oee.nrcan.gc.ca/publications/commercial/1388> [Accessed June 20, 2005].
- NRCan. 2008. Commercial and Institutional Consumption of Energy Survey. RPRT. [online] Available at <http://oee.nrcan.gc.ca/publications/statistics/cices08/pdf/cices08.pdf> [Accessed June 20, 2005].
- NRCan website. 2011a. *ecoENERGY Efficiency for Buildings*. RPRT. [online] Available at <http://www.nrcan.gc.ca/corporate/5693> [Accessed April 20, 2016].
- NRCan website. 2011b. *Frequently asked questions about natural gas prices*. ICOMM. [online] Available at <http://www.nrcan.gc.ca/energy/sources/natural-gas/1239> [Accessed December 24, 2012].
- Nyboer, J., and Groves, S. 2012. A Review of Existing Cogeneration Facilities In Canada. RPRT. Burnaby, BC. [online] Available at [www2.cieedac.sfu.ca/media/publications/Cogeneration\\_Report\\_2012\\_Final.pdf](http://www2.cieedac.sfu.ca/media/publications/Cogeneration_Report_2012_Final.pdf) [Accessed June 20, 2005].
- Ochs, F., Heidemann, W., Müller-Steinhagen, H., and Kock, H. 2006. Soil-Water Pit Heat Store with Direct Charging System. *In Proceedings of Ecostock 2006, Richard Stockton College of New Jersey*. New Jersey.
- Oh, S.D., Lee, H.J., Jung, J.Y., and Kwak, H.Y. 2007. Optimal Planning and Economic Evaluation of Cogeneration System. *JOUR. Energy*, 32 (5) pp. 760–71.
- Ontario Power Authority website. 2011a. *OPA - Ontario Power Authority, “Clean Energy Standard Offer Program (CESOP).”* ICOMM.
- Ontario Power Authority website. 2011b. *OPA - Ontario Power Authority, “Combined Heat and*

*Power Standard Offer Program (CHPSOP).*” ICOMM.

Oo, A., Kelly, J., and Lalonde, C. 2012. Assessment of Business Case for Purpose-Grown Biomass in Ontario. Article. . Sarnia, ON.

Österreicher, D., and Pol, O. 2007. Concerto Initiative and Polygeneration. *In Proceedings of 1st European Conference on Polygeneration. Technologies and Applications*. Tarragona, Coronas (Ed.), Universitat Rovira i Virgili, pp. 39–54.

Oswald, C.J., and Rouse, W.R. 2004. Thermal Characteristics and Energy Balance of Various-Size Canadian Shield Lakes in the Mackenzie River Basin. *Journal of Hydrometeorology*, 5 (1) pp. 129–44. doi:10.1175/1525-7541(2004)005<0129:TCAEBO>2.0.CO;2.

Pairaudeau, F. 2009. Saving Healthcare Dollars through Efficiency. JOUR. [online] Available at <http://thecesh.com/> [Accessed April 5, 2016].

Palzer, A., and Henning, H.M. 2014a. A Comprehensive Model for the German Electricity and Heat Sector in a Future Energy System with a Dominant Contribution from Renewable Energy technologies–Part II: Results. JOUR. *Renewable and Sustainable Energy Reviews*, 30 pp. 1019–34.

Palzer, A., and Henning, H.M. 2014b. A Future German Energy System with a Dominating Contribution from Renewable Energies: A Holistic Model Based on Hourly Simulation. JOUR. *Energy Technology*, 2 (1) pp. 13–28.

Paraszczak, J., Svedlund, E., Fytas, K., and Laflamme, M. 2014. Electrification of Loaders and Trucks – A Step Towards More Sustainable Underground Mining. *Renewable Energy and Power Quality Journal*. Cordoba, Spain, no. 12.

Patel, M.R. 2005. *Wind and Solar Power Systems: Design, Analysis, and Operation*. BOOK. Boca Raton, FL: CRC press.

Pereira, M., Limon, D., Alamo, T., Valverde, L., and Bordons, C. 2013. Economic Model Predictive Control of a Smartgrid with Hydrogen Storage and PEM Fuel Cell. CONF. *In Proceedings of Industrial Electronics Society, IECON 2013-39th Annual Conference of the IEEE*, IEEE, pp. 7920–25.

Petruschke, P., Gasparovic, G., Voll, P., Krajačić, G., Duić, N., and Bardow, A. 2014. A Hybrid Approach for the Efficient Synthesis of Renewable Energy Systems. *Applied Energy*, 135 pp. 625–33. doi:10.1016/j.apenergy.2014.03.051.

Piacentino, A., and Cardona, F. 2008. EABOT–energetic Analysis as a Basis for Robust Optimization of Trigeneration Systems by Linear Programming. JOUR. *Energy Conversion and Management*, 49 (11) pp. 3006–16.

Pichler, M.F., Lerch, W., Heinz, A., Goertler, G., Schranzhofer, H., and Rieberer, R. 2014. A Novel Linear Predictive Control Approach for Auxiliary Energy Supply to a Solar Thermal Combustion. *Solar Energy*, 101 pp. 203–19. doi:10.1016/j.solener.2013.12.015.

- Pilavachi, P.A., Stephanidis, S.D., Pappas, V.A., and Afgan, N.H. 2009. Multi-Criteria Evaluation of Hydrogen and Natural Gas Fuelled Power Plant Technologies. *Applied Thermal Engineering*, 29 (11–12) pp. 2228–34. doi:10.1016/j.applthermaleng.2008.11.014.
- Postels, S., Assen, N. Von Der, Voll, P., and Bardow, A. 2015. Reducing Dimensionality in Multi-Objective LCA-Based Optimization of Energy Systems – The Impact of Normalization Variants and Weighting Factors. *In Proceedings of 28th International Conferente on Efficiency, Cost, Optimization and Simulation*. Pau, France.
- Powertel website. 2015. *De Beers Victor Mine Substation*. [online] Available at <http://www.powertel.ca/debeers-victor-mine-substation.shtml> [Accessed September 16, 2015].
- Pulido-Calvo, I., Gutiérrez-Estrada, J.C., and Asensio-Fernández, R. 2006. Optimal Design of Pumping Stations of Inland Intensive Fishfarms. *Aquacultural Engineering*, 35 (3) pp. 283–91. doi:10.1016/j.aquaeng.2006.03.004.
- Ramsden, R., Allen, C., Millar, D.L., and Guse, T. 2014. The Use of Natural Cooling to Delay and Reduce Refrigeration Requirements. *In Proceedings of 10th International Mine Ventilation Congress*. Sun City, South Africa, von Glehn and Biffi (Eds.), The Mine Ventilation Society of South Africa, pp. 27–32.
- RDH website. 2015. *RDH Mining Equipment: MUCKMASTER 300EB*. ICOMM. [online] Available at <http://www.rdhminingequipment.com/product/muckmaster-300eb/> [Accessed June 10, 2015].
- Redelbach, M., Özdemir, E.D., and Friedrich, H.E. 2014. Optimizing Battery Sizes of Plug-in Hybrid and Extended Range Electric Vehicles for Different User Types. *Energy Policy*, 73 pp. 158–68. doi:10.1016/j.enpol.2014.05.052.
- Ren, H., and Gao, W. 2010. A MILP Model for Integrated Plan and Evaluation of Distributed Energy Systems. *JOUR. Applied Energy*, 87 (3) pp. 1001–14.
- Rio Tinto. 2009. *Diavik Diamond Mine - Fact Book*. RPRT. . Yellowknife, NT, Canada. [online] Available at <http://www.diavik.ca/documents/DiavikFactBook.pdf>.
- Rio Tinto. 2012. *Diavik Diamond Mine - Sustainable Development Report 2011*. RPRT. . Yellowknife, NT, Canada. [online] Available at [http://www.riotinto.com/documents/Diavik\\_2011\\_SD\\_report.pdf](http://www.riotinto.com/documents/Diavik_2011_SD_report.pdf) [Accessed June 20, 2005].
- Robertson, A.C. 1985. Current and Future Developments in Truck Haulage Systems for Underground Mines. *In Proceedings of Underground Operator's Conference*. Kalgoorlie, Australia, Australasian Institute of Mining and Metallurgy, pp. 185–96.
- Romero, A., Carvalho, M., and Millar, D. 2015a. Optimal Design and Control of Wind-Diesel Hybrid Energy Systems for Remote Arctic Mines. *In Proceedings of 28 Th International Conferente on Efficiency, Cost, Optimization and Simulation*. Pau, France.
- Romero, A., Carvalho, M., and Millar, D.L. 2014. Application of a Polygeneration Optimization Technique for a Hospital in Northern Ontario. *JOUR. Transactions of the Canadian Society for*

*Mechanical Engineering*, 38 (1) pp. 45–62.

Romero, A., Chacartegui, R., Becerra, J.A., Carvalho, M., and Millar, D.L. 2015b. Analysis of the Start-up and Variable Load Operation of a Combined Cycle Power Plant for off-Grid Mines. *In Proceedings of Global Conference in Global Warming, Athens, May 24 -27, 2015*. Athens.

Romero, A., Millar, D., Carvalho, M., Maestre, J.M., and Camacho, E.F. 2015c. A Comparison of the Economic Benefits of Centralized and Distributed Model Predictive Control Strategies for Optimal and Sub-Optimal Mine Dewatering System Designs. *JOUR. Applied Thermal Engineering*, 90 pp. 1172–83. doi:<http://dx.doi.org/10.1016/j.applthermaleng.2015.01.031>.

Rossiter, J.A. 2004. *Model-Based Predictive Control - A Practical Approach*. Boca Raton, FL: CRC Press.

Rossman, L.A. 2000. EPANET User Manual. [Accessed June 11, 2015] Available at <http://www2.epa.gov/water-research/epanet>.

Rubio-Maya, C., Uche-Marcuello, J., and Martínez-Gracia, A. 2011a. Sequential Optimization of a Polygeneration Plant. *JOUR. Energy Conversion and Management*, 52 (8) pp. 2861–69.

Rubio-Maya, C., Uche-Marcuello, J., Martínez-Gracia, A., and Bayod-Rújula, A.A. 2011b. Design Optimization of a Polygeneration Plant Fuelled by Natural Gas and Renewable Energy Sources. *JOUR. Applied Energy*, 88 (2) pp. 449–57.

Salsbury, T., Mhaskar, P., and Qin, S.J. 2013. Predictive Control Methods to Improve Energy Efficiency and Reduce Demand in Buildings. *Computers and Chemical Engineering*, 51 pp. 77–85. doi:[10.1016/j.compchemeng.2012.08.003](https://doi.org/10.1016/j.compchemeng.2012.08.003).

Samsatli, N., and Jennings, M.G. 2013. Optimization and Systems Integration. In *Urban Energy Systems. An Integrated Approach*. Abingdon, Keirstead and Shah (Eds.), Routledge, pp. 312.

Sanchez, S. 2003. Optimal Design of Trigeration Systems with Reciprocating Internal Combustion Engines for the Residential-Commercial Sector. In Spanish. *University of Zaragoza, PhD Thesis*.

Schafrik, S. 2014. The Use of Packed Sphere Modelling for Airflow and Heat Exchange Analysis in Broken or Fragmented Rock. . Sudbury, Ont. *Laurentian University, Faculty of Graduate Studies*. Available at <https://zone.biblio.laurentian.ca/dspace/handle/10219/2309>.

Scott, D.S. 2005. Conventional Wisdom. *International Journal of Hydrogen Energy*, 30 (6) pp. 569–77. doi:[10.1016/j.ijhydene.2004.09.009](https://doi.org/10.1016/j.ijhydene.2004.09.009).

Serra, L.M., Lozano, M.A., Ramos, J., Ensinas, A. V., and Nebra, S. a. 2009. Polygeneration and Efficient Use of Natural Resources. *Energy*, 34 (5) pp. 575–86. doi:[10.1016/j.energy.2008.08.013](https://doi.org/10.1016/j.energy.2008.08.013).

Shi, J., Kelkar, A.G., and Soloway, D. 2005. Stable Reconfigurable Generalized Predictive Control With Application to Flight Control. *JOUR. Journal of Dynamic Systems, Measurement, and Control*, 128 (2) pp. 371–78. Available at <http://dx.doi.org/10.1115/1.2194076>.

- Shields, G. 2013. De Beers (Personal Communication). Personal communication.
- Simon, B. 2014. Transforming Wind into Fuel. *CIM Magazine*, October.
- Stachulak, J. 1989. Ventilation Strategy and Unique Air Conditioning at Inco Ltd. *In Proceedings of 4th US Mine Ventilation Symposium*. Berkley, USA.
- Stadler, M., Marnay, C., Siddiqui, A., Lai, J., Coffey, B., and Aki, H. 2008. Effect of Heat and Electricity Storage and Reliability on Microgrid Viability: A Study of Commercial Buildings in California and New York States. RPRT. . Berkeley, CA. Vol. LBNL-1334E.
- Stebbins, S.A. 2011. Cost Estimating for Underground Mining. Incollection. In *SME Mining Handbook*. Englewood, Colo., Darling (Ed.), Society for Mining, Metallurgy, and Exploration Inc., 3rd ed., pp. 263–79.
- Sterner, M. 2009. Bioenergy and Renewable Power Methane in Integrated 100% Renewable Energy Systems: Limiting Global Warming by Transforming Energy Systems. . Kassel, Germany. *Kassel University, PhD Thesis*.
- Strashok, C., Dale, A., Herbert, Y., and Foon, R. 2010. *Greening Canadian Hospitals*. JOUR. *Community Research Connections Discussion Paper Series No. 7*. [online] Available at [https://crrresearch.org/files-crrresearch\\_v2/File/Discussion\\_Paper-7\\_Greening\\_Canadian\\_Hospitals.pdf](https://crrresearch.org/files-crrresearch_v2/File/Discussion_Paper-7_Greening_Canadian_Hospitals.pdf) [Accessed April 6, 2016].
- Tan, Y., Meegahapola, L., and Muttaqi, K.M. 2014. A Review of Technical Challenges in Planning and Operation of Remote Area Power Supply Systems. JOUR. *Renewable and Sustainable Energy Reviews*, 38 pp. 876–89.
- Telford, P.G. 2009. Peat Fuel—a Sustainable Bioenergy Resource. *In Proceedings of IASTED International Conference on Environmental Management and Engineering*, pp. 6–8.
- The CHP Site Assessment Tool*. 2012. ICOMM. [online] Available at [http://chp.decc.gov.uk/CHPAssessment/\(S\(svoplow24plf3w5dey50m4mj\)\)/Default.aspx](http://chp.decc.gov.uk/CHPAssessment/(S(svoplow24plf3w5dey50m4mj))/Default.aspx) [Accessed November 5, 2012].
- The Weather Network website. 2012. *Statistics: Sudbury A (ON) Canada*. [online] Available at <http://www.theweathernetwork.com/statistics/degreedays/cl6068150> [Accessed August 16, 2012].
- Thomae, F.A.W. 1933. *Power Plants on Metal Mines*. BOOK. London: Mining Publications.
- Tonnos, A.M., and Allen, C. 2008. Technology Convergence for Sustainable Underground Mine Ventilation System Control. *In Proceedings of 12th U.S. North American Mine Ventilation Symposium*, Wallace (Ed.), pp. 37–40. Available at <http://www.smenet.org/uvc/mineventpapers/pdf/005.pdf>.
- Torreglosa, J.P., García, P., Fernández, L.M., and Jurado, F. 2015. Energy Dispatching Based on Predictive Controller of an off-Grid Wind Turbine/photovoltaic/hydrogen/battery Hybrid System. JOUR. *Renewable Energy*, 74 pp. 326–36.

- Trapani, K., and Millar, D.L. 2013. Proposing Offshore Photovoltaic (PV) Technology to the Energy Mix of the Maltese Islands. *Energy Conversion and Management*, 67 pp. 18–26. doi:10.1016/j.enconman.2012.10.022.
- Ulleberg, Ø. 2004. The Importance of Control Strategies in PV–hydrogen Systems. JOUR. *Solar Energy*, 76 (1) pp. 323–29.
- Ulleberg, Ø., Nakken, T., and Eté, A. 2010. The Wind/hydrogen Demonstration System at Utsira in Norway: Evaluation of System Performance Using Operational Data and Updated Hydrogen Energy System Modeling Tools. *International Journal of Hydrogen Energy*, 35 (5) pp. 1841–52. doi:10.1016/j.ijhydene.2009.10.077.
- US Energy Information Agency website. 2015. *Commercial Buildings Energy Consumption Survey (CBECS). 2012*. [online] Available at <http://www.eia.gov/consumption/commercial/#consumexpen03> [Accessed November 5, 2015].
- Valero, A., Lozano, M.A., and Muñoz, M. 1986. A General Theory of Exergy Saving. I. On the Exergetic Cost. Article. In *Computer-Aided Engineering and Energy Systems, Vol. 3 Second Law Analysis and Modelling*. New York, NY, Gaggioli (Ed.), ASME,.
- Van Staden, A.J., Zhang, J., and Xia, X. 2011. A Model Predictive Control Strategy for Load Shifting in a Water Pumping Scheme with Maximum Demand Charges. JOUR. *Applied Energy*, 88 (12) pp. 4785–94.
- Verhelst, S., and Wallner, T. 2009. Hydrogen-Fueled Internal Combustion Engines. *Progress in Energy and Combustion Science*, 35 (6) pp. 490–527. doi:10.1016/j.pecs.2009.08.001.
- Voll, P., Hennen, M., Klaffke, C., Lampe, M., and Bardow, A. 2013. Exploring the near-Optimal Solution Space for the Synthesis of Distributed Energy Supply Systems. *Chemical Engineering Transactions*, 35 pp. 277–82. doi:10.3303/CET1335046.
- Vosen, S.R., and Keller, J.O. 1999. Hybrid Energy Storage Systems for Stand-Alone Electric Power Systems: Optimization of System Performance and Cost through Control Strategies. JOUR. *International Journal of Hydrogen Energy*, 24 (12) pp. 1139–56.
- Vosloo, J., Liebenberg, L., and Velleman, D. 2012. Case Study: Energy Savings for a Deep-Mine Water Reticulation System. JOUR. *Applied Energy*, 92 pp. 328–35.
- Voss, K., Goetzberger, A., Bopp, G., Häberle, A., Heinzl, A., and Lehmberg, H. 1996. The Self-Sufficient Solar House in Freiburg—Results of 3 Years of Operation. JOUR. *Solar Energy; Selected Proceedings of ISES 1995: Solar World Congress. Part I*, 58 (1) pp. 17–23. doi:[http://dx.doi.org/10.1016/0038-092X\(96\)00046-1](http://dx.doi.org/10.1016/0038-092X(96)00046-1).
- Wang, L. 2009. *Model Predictive Control System Design and Implementation Using MATLAB*. Book. London: Springer Science & Business Media.
- Weber, C., Maréchal, F., Favrat, D., and Kraines, S. 2006. Optimization of an SOFC-Based Decentralized Polygeneration System for Providing Energy Services in an Office-Building in Tōkyō. JOUR. *Applied Thermal Engineering*, 26 (13) pp. 1409–19.

- Weron, R. 2007. *Modeling and Forecasting Electricity Loads and Prices: A Statistical Approach*. Book. Chichester, UK: John Wiley & Sons, Ltd. Available at <https://books.google.ca/books?id=cXcWdMgovvoC>.
- Xenos, D.P., Kopanos, G.M., Ciccioiti, M., and Thornhill, N.F. 2016. Operational Optimization of Networks of Compressors Considering Condition-Based Maintenance. *Computers & Chemical Engineering*, 84 pp. 117–31. doi:10.1016/j.compchemeng.2015.08.008.
- Yang, Z., and Børsting, H. 2010. Energy Efficient Control of a Boosting System with Multiple Variable-Speed Pumps in Parallel. *In Proceedings of 49th IEEE Conference on Decision and Control*. Atlanta, GA, pp. 2198–2203. doi:10.1109/CDC.2010.5717312.
- Yokoyama, R., Hasegawa, Y., and Ito, K. 2002. A MILP Decomposition Approach to Large Scale Optimization in Structural Design of Energy Supply Systems. *JOUR. Energy Conversion and Management*, 43 (6) pp. 771–90.
- Yoshida, S., Ito, K., and Yokoyama, R. 2007. Sensitivity Analysis in Structure Optimization of Energy Supply Systems for a Hospital. *JOUR. Energy Conversion and Management*, 48 (11) pp. 2836–43.
- Zakeri, B., and Syri, S. 2015. Electrical Energy Storage Systems: A Comparative Life Cycle Cost Analysis. *JOUR. Renewable and Sustainable Energy Reviews*, 42 (0) pp. 569–96. doi:<http://dx.doi.org/10.1016/j.rser.2014.10.011>.
- Zhang, H. 2011. Optimal Sizing and Operation of Pumping Systems to Achieve Energy Efficiency and Load Shifting. *University of Pretoria, Master Thesis*.
- Zhang, H., Xia, X., and Zhang, J. 2012. Optimal Sizing and Operation of Pumping Systems to Achieve Energy Efficiency and Load Shifting. *JOUR. Electric Power Systems Research*, 86 pp. 41–50.
- Zhang, J., and Xia, X. 2011. A Model Predictive Control Approach to the Periodic Implementation of the Solutions of the Optimal Dynamic Resource Allocation Problem. *Automatica*, 47 (2) pp. 358–62. doi:10.1016/j.automatica.2010.10.049.
- Zhou, Z., Liu, P., Li, Z., and Ni, W. 2013. Economic Assessment of a Distributed Energy System in a New Residential Area with Existing Grid Coverage in China. *Computers and Chemical Engineering*, 48 pp. 165–74. doi:10.1016/j.compchemeng.2012.08.013.
- Zhuan, X., and Xia, X. 2013. Optimal Operation Scheduling of a Pumping Station with Multiple Pumps. *Applied Energy*, 104 pp. 250–57. doi:10.1016/j.apenergy.2012.10.028.
- Zong, Y., Mihet-Popa, L., Kullmann, D., Thavlov, A., Gehrke, O., and Bindner, H.W. 2012. Model Predictive Controller for Active Demand Side Management with PV Self-Consumption in an Intelligent Building. *CONF. In Proceedings of 3rd IEEE PES International Conference and Exhibition on Innovative Smart Grid Technologies (ISGT Europe)*, IEEE,.
- Zoulias, E.I., and Lymberopoulos, N. 2007. Techno-Economic Analysis of the Integration of Hydrogen Energy Technologies in Renewable Energy-Based Stand-Alone Power Systems.

JOUR. *Renewable Energy*, 32 (4) pp. 680–96.

## Appendices

## **A1. Polygeneration in a hospital in Northern Ontario**

This chapter demonstrates the use of the formulation described in Chapter 3 to optimize energy supply systems, given the consumer's demands under a certain economic environment. The energy consumer selected is a hospital in Northern Ontario, Canada, whose energy demands have been calculated indirectly and compared with real data from an actual hospital in the same environment, both climatic and economic. OMSES is used to calculate the optimal ESS configuration and the optimal operation plan for the considered demands and energy prices. Results of different scenarios are presented and discussed, including varying electric grid connection constraints, as well as different support programs for clean energy in the considered jurisdiction.

The content of this chapter was first published in (Romero et al., 2014).

### **A1.1. Introducing Energy Systems Optimization in Northern Ontario**

Hospitals are good candidates for polygeneration systems due to their sustained and relatively high energy requirements (heat, steam, cooling, and electricity) as well as their need for high power quality and reliability (Carvalho et al., 2012). With over 3,000 hospitals, medical facilities, and surgery centers across Canada, these facilities have a significant impact on the health of individuals and on the ecological, social, and economic health of communities (Strashok et al., 2010).

Canadian hospitals typically use more energy than hospitals in other countries due to a colder climate and lower historical energy costs (Jefferson, 2006). However, with rising energy costs, several Canadian hospitals are now trying to improve their energy efficiency. Nordic countries

are world leaders in energy reduction. On a floor area basis, Norwegian hospitals use approximately half the amount of energy consumed by their US and Canadian counterparts, and Swedish hospitals only consume one third as much (Pairaudeau, 2009).

In 2001, Natural Resources Canada evaluated energy management in Canadian health care facilities, and stated that hospitals could become far more proactive in lowering their costs and reducing harmful greenhouse gas emissions through energy improvements (NRCan, 2001). However, it was not until 2011 that Canada was placed on a comparable footing with countries that lead the world in energy efficient building construction. The National Energy Code for Buildings 2011 required an overall 25% improvement in energy efficiency over the previous code and indicated the minimum requirements for energy efficiency in new buildings (NRCan website, 2011a).

Several studies have been carried out on the optimization of energy systems in hospital environments, the development of methods and models that combine principles from thermal sciences (thermodynamics, heat transfer, and fluid mechanics) with economic engineering to aid in decision making, and the design and operation of rational energy systems (Carvalho et al., 2012; Yoshida et al., 2007; Piacentino and Cardona, 2008; Fabrizio, 2011). Although rational and efficient use of energy through adoption of polygeneration systems has been in the spotlight in recent years, the implementation of polygeneration systems in hospitals has achieved only limited penetration; according to the Canadian Industrial Energy End-use Data and Analysis Center database, only ~103 MW<sub>e</sub> of the total combined heat and power operating capacity of 6.5 GW<sub>e</sub> is installed in hospitals (Nyboer and Groves, 2012).

The present work adapted the optimization methodology set out in Carvalho et al. (2012), Lozano et al. (2009), Carvalho et al. (2011), and Carvalho (2011), based on Mixed Integer Linear Programming (MILP), which has been used extensively in the optimization of energy supply systems (Buoro et al., 2012; Ren and Gao, 2010; Yokoyama et al., 2002). The aforementioned methodology, which was originally developed for Mediterranean buildings, was adapted to a 454-bed hospital located in Sudbury, Ontario, Canada. Real energy consumption data were available, steam was added as an additional utility (for laundry and sterilization), and particularities of the system's operation were also considered in the optimization model.

## **A1.2. Estimation of Utility Demand Curves**

This study analyzed a 454-bed hospital, located in Sudbury (ON), with the following energy services: electricity, steam, heat and cooling. The heat load included heat for Sanitary Hot Water (SHW) and for space heating. The study considered one operational year, divided into 8 representative days (two days per season: one weekday and one weekend day), and subdivided into 24 intervals of one hour.

Representative energy demands were calculated using degree-day data (“BizzEE Software - Custom Degree Day Data” 2012; “Principal Station Data – PSD/DPS 27. Sudbury A. ” 1983; “The Weather Network - Statistics: Sudbury A, ON, Canada” 2012) and energy intensity coefficients were obtained from energy surveys and audits (US Energy Information Agency website, 2015; NRCAN, 2008). The latter provide reliable data on energy consumption as a function of building floor area and climate zone. The total area of the building is thus a key parameter for estimating annual demands. With an occupied floor area of  $\approx 93,000 \text{ m}^2$ , the

Sudbury hospital has the following annual energy demands: electricity 27,086 MWh, heat (SHW + space heating) 28,739 MWh, steam 6,778 MWh, and cooling 9,908 MWh.

Monthly-average ambient temperatures along with degree-days were used to distribute the annual energy demands across the seasons and days, adopting procedures established by Erbs et al. (1983) and Sanchez (2003). The supplied data indicated that SHW and electricity daily demands were different for weekdays and weekends. The relationship between these representative days was established in accordance with known demands for hospitals (Bizzarri and Morini, 2004; Çakir et al., 2012; Oh et al., 2007), energy profile generators (*The CHP Site Assessment Tool*, 2012), and published research (Li et al., 2008; McIlveen-Wright et al., 2003; Espirito Santo, 2012).

Electricity consumption is directly related to the schedule of operation, which is fixed by the hospital management, and so electricity consumption follows a predetermined pattern (as do steam and SHW consumption). Lighting, ventilation, elevators, pumps, computers, and medical equipment contribute to the entire electrical demand in this way. However, air conditioning services (heating, cooling, and ventilation) also follow weather behavior. Production of cooling follows the outside ambient temperature profile, with peak demand in the warmest hour of the day in summer. Medical refrigeration, ventilation, and lighting constitute the base load of the daily electricity demand, as they are uninterruptible services for the proper operation of the hospital.

For each month, the predicted electricity consumption was compared with the real consumption data (Figure A1-1). The estimation is in good accordance with the real data, with a maximum relative error  $\varepsilon = 0.09$  (which occurs in June). The dotted line shows the electricity pattern used

in this case study, which defines four main operational seasons (three month each), thus reducing the computational effort of the optimization problem.

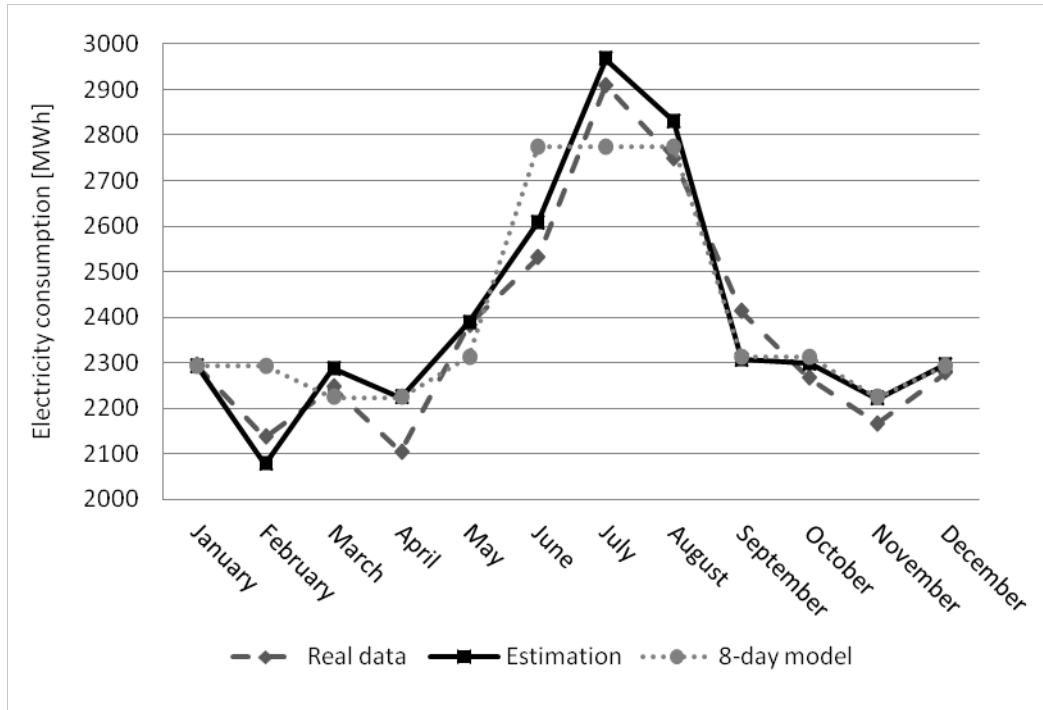


Figure A1-1 Comparison between real electricity data, estimation and an 8-day model

Table A1-1 Hospital heat, cooling, steam, and electricity demands

Season Day Type	$n_i^1$	Heat		Cooling		Steam		Electricity	
		Total kWh/day	Peak kW						
Winter Wd <sup>2</sup>	60	162,915	9361	0	0	28,242	7060	75,039	3465
Winter Wn <sup>3</sup>	32	128,678	7534	0	0	0	0	72,038	3081
Spring Wd	60	49,323	3176	13,917	1229	28,242	7060	75,039	3465
Spring Wn	30	41,893	2780	10,633	939	0	0	72,038	3081
Summer Wd	60	16,348	1186	102,733	9073	28,242	7060	75,039	3465
Summer Wn	33	15,029	1116	78,488	6932	0	0	72,038	3081
Autumn Wd	60	107,314	6334	0	0	28,242	7060	75,039	3465
Autumn Wn	30	86,198	5207	0	0	0	0	72,038	3081
		MWh/yr	kW	MWh/yr	kW	MWh/yr	kW	MWh/yr	kW
Year	365	28,739	9361	9908	9073	6778	2172	27,086	3465

<sup>1</sup> (days/yr)

<sup>2</sup> working days

<sup>3</sup> weekends

A summary of the energy and peak power demands for selected periods is described in Table A1-1. The daily distribution of hourly power consumption is shown for winter in Figure A1-2

and for summer in Figure A1-3. These curves result from multiplying the specific consumption in MWh/year by normalized daily profiles.

For the electric demand, it can be assumed that the profile is the same throughout the year (Sanchez, 2003), for it does not include heating and cooling equipment consuming electricity. Space heating and cooling annual demands (MWh/year) can be distributed for each month using weather information, distributing the energy in proportion to the monthly heating and cooling degree-days, respectively. It also has to be considered that demands in the hospital vary between weekdays and weekends. In this work, a factor of 0.764 has been used to calculate the ratio of weekend to weekday demand for heating and cooling: 0.83 for electricity, and 1 for sanitary hot water (Carvalho, 2011). SHW demand in June, July, August, and September is assumed to be 60% of the demand in the remaining months to account for seasonal consumption patterns (Carvalho, 2011). Final heat demand is calculated as the sum of heating and SHW demands. Steam demand was considered to be constant during the operating hours of the laundry and sterilization facilities (9h to 21h), and throughout the year's typical days. The normalized profiles for each typical day and demand are shown in Table A1-2.

Conventional approaches use the peak demand as a key design constraint, where system size is based on a peak condition that accounts for climate-related loads and internal loads from occupants, lighting, and equipment. For some of these parameters, there are well-established criteria for peak conditions (e.g., degree days for climate), whereas for others, the designer has to use context-specific information (e.g., load diversity) and engineering judgment to determine the peak load.

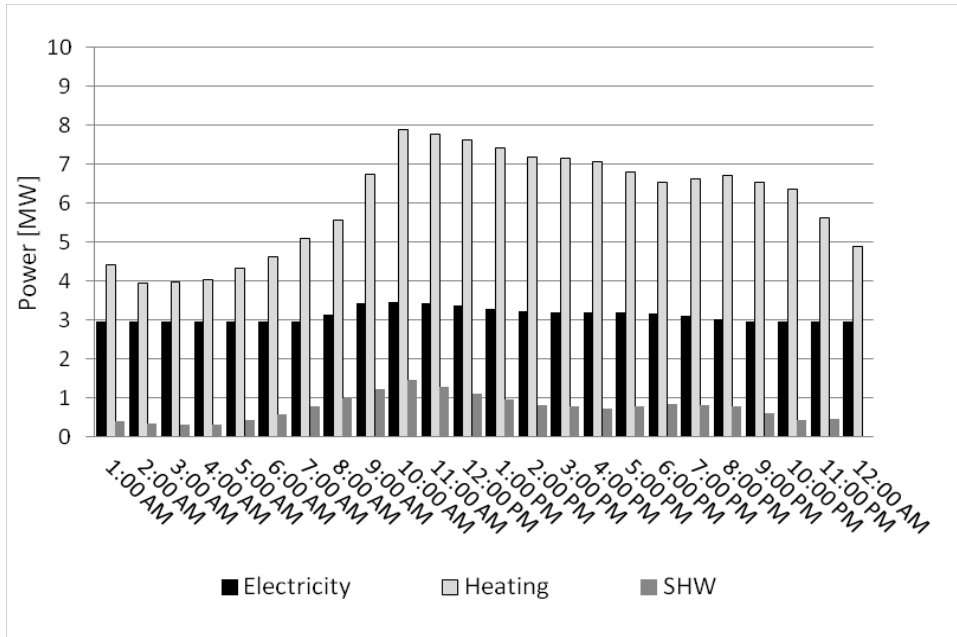


Figure A1-2 Hourly demands for a typical working day in winter

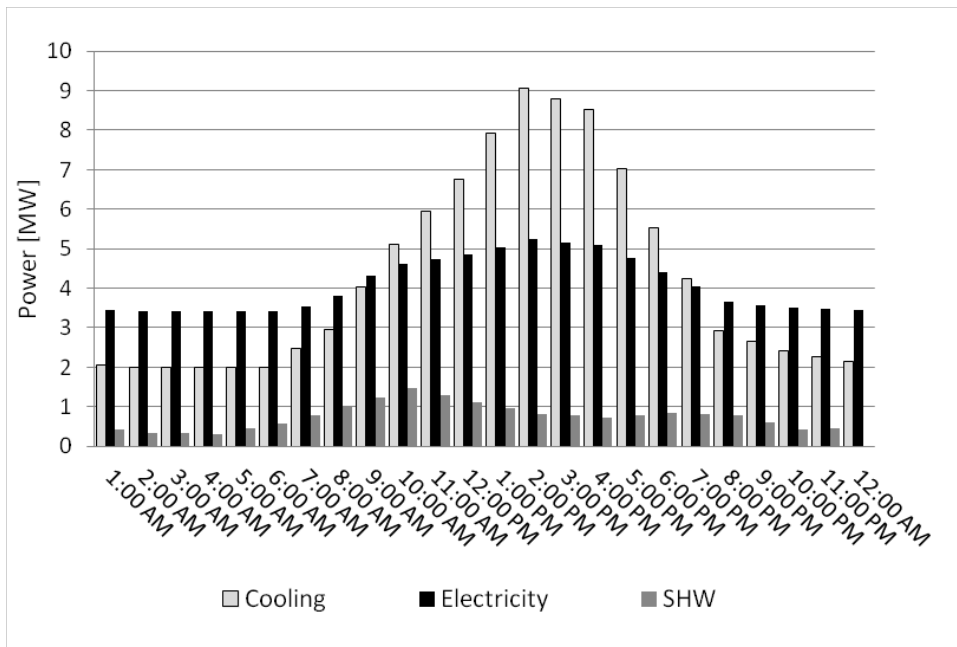


Figure A1-3 Hourly demands for a typical working day in summer electricity demand includes, for illustration purposes, the theoretic consumption of a mechanical chiller supplying the cooling demand with COP = 4.5)

**Table A1-3 Hourly normalized profiles**

Period	Heat Demand		Sanitary Hot Water		Cooling		Electricity	
	Weekday	Weekend	Weekday	Weekend	Weekday	Weekend	Weekday	Weekend
0 – 1h	0.031	0.037	0.023	0.023	0.020	0.020	0.040	0.041
1 – 2h	0.027	0.037	0.019	0.019	0.019	0.019	0.040	0.041
2 – 3h	0.028	0.036	0.018	0.018	0.019	0.019	0.040	0.041
3 – 4h	0.028	0.036	0.017	0.017	0.019	0.019	0.040	0.041
4 – 5h	0.030	0.036	0.025	0.025	0.019	0.019	0.040	0.041
5 – 6h	0.032	0.036	0.033	0.033	0.019	0.019	0.040	0.041
6 – 7h	0.035	0.039	0.044	0.044	0.024	0.024	0.040	0.041
7 – 8h	0.038	0.041	0.056	0.056	0.029	0.029	0.042	0.042
8 – 9h	0.046	0.048	0.069	0.069	0.039	0.039	0.046	0.043
9 – 10h	0.054	0.055	0.082	0.082	0.050	0.050	0.046	0.043
10 – 11h	0.054	0.052	0.072	0.072	0.058	0.058	0.046	0.043
11 – 12h	0.053	0.050	0.062	0.062	0.066	0.066	0.045	0.042
12 – 13h	0.051	0.049	0.054	0.054	0.077	0.077	0.044	0.042
13 – 14h	0.050	0.048	0.046	0.046	0.088	0.088	0.043	0.042
14 – 15h	0.049	0.044	0.044	0.044	0.086	0.086	0.042	0.042
15 – 16h	0.049	0.041	0.041	0.041	0.083	0.083	0.043	0.042
16 – 17h	0.047	0.041	0.045	0.045	0.068	0.068	0.043	0.042
17 – 18h	0.045	0.041	0.048	0.048	0.054	0.054	0.042	0.042
18 – 19h	0.046	0.040	0.046	0.046	0.041	0.041	0.042	0.042
19 – 20h	0.046	0.039	0.044	0.044	0.028	0.028	0.040	0.041
20 – 21h	0.045	0.039	0.034	0.034	0.026	0.026	0.040	0.041
21 – 22h	0.044	0.039	0.024	0.024	0.023	0.023	0.040	0.041
22 – 23h	0.039	0.039	0.026	0.026	0.022	0.022	0.040	0.041
23 – 24h	0.034	0.038	0.028	0.028	0.021	0.021	0.040	0.041

### A1.3. Description of Polygeneration Superstructure for the Problem

The energy superstructure for this hospital polygeneration problem is shown in Figure A1-4. The problem with defining the optimal configuration for polygeneration is to determine the best technologies and linkages in the superstructure network. In addition, the optimization process determines the best mode of operation of these technologies for each representative period, as the energy flows associated with the best technologies and linkages need to be quantified to establish, and minimize, the total annual cost.

Site loads (extreme right hand side) comprise electricity, steam, heat, and cooling. Utilities for the hospital are supplied from the utility distribution systems, including energy conversion technologies that convert the utility imported into another form in which is required.

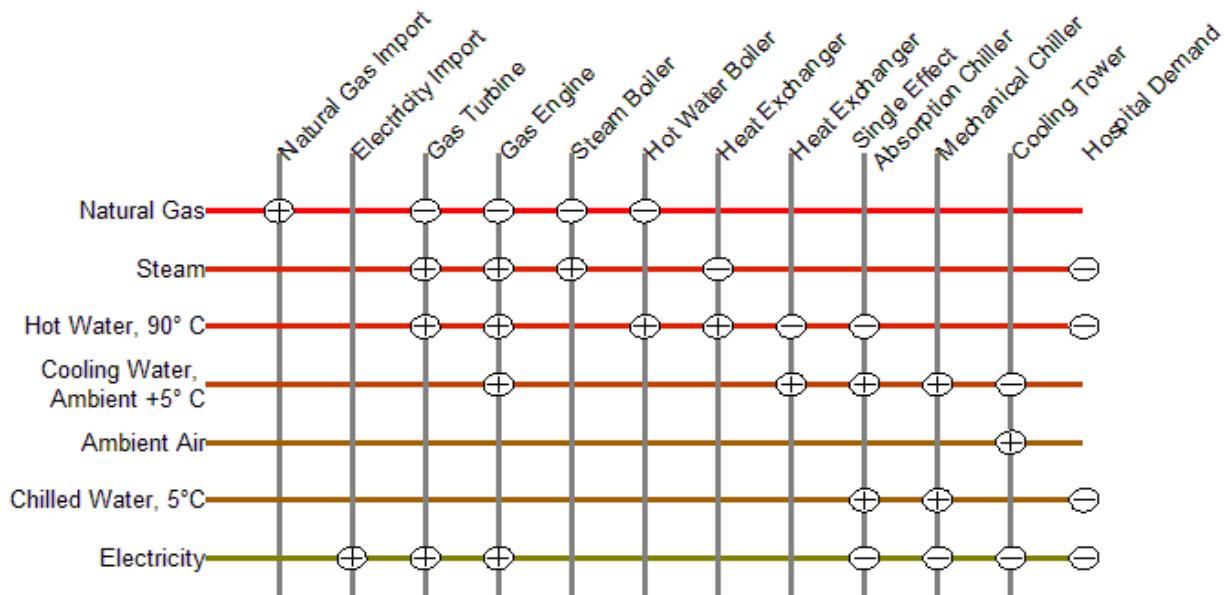


Figure A1-4 Superstructure for energy distribution and conversion system for a hospital polygeneration system

Figure A1-4 indicates that for this hospital case, the energy superstructure includes the possibility to import natural gas and electricity from external distribution grids (Top, left hand side of Figure A1-4). The equipment available for possible installation is listed along the top of the diagram and the energy conversion pathways can be traced by moving from node to node in the superstructure. There can be multiple units of each technology. Double-effect absorption chillers were not considered because the consulted manufacturers had not obtained Canadian Registration Numbers, indicating approval for these high-pressure vessels. Steam/hot water heat exchangers are referred to as ST/HW HX and hot water/cooling water heat exchangers are referred to as HW/CW HX.

#### A1.4. Technology Considered in the Superstructure

A detailed survey of technologies, including the review of manufacturer catalogues and consultations with sales representatives, was carried out. A database of the models of the potentially installable equipment was compiled, with sufficient fields to record the investment costs, operating costs and characterization of operation. Commercially available equipment in Canada was considered (Table A1-3).

**Table A1-3 Selected equipment and matrix of production coefficients (normalized to the primary utility output).**

Equipment <sup>1</sup>	Capital Cost [10 <sup>3</sup> CAD]	O&M Costs [CAD/MWh]	Nominal Power [MW]	Electricity	Natural Gas	Steam	Hot Water	Cooling Water	Chilled Water	Ambient Air
Gas Turbine	4000	5	3.6	<b>1</b>	- 3.03	0.59	0.66			
Gas Engine	3600	5	3.6	<b>1</b>	- 2.44	0.70	0.41	0.23		
Steam Boiler	144	3	3.0		- 1.18	<b>1</b>				
Hot Water Boiler	150	3	3.9		- 1.22		<b>1</b>			
ST/HW HX	10	1	1.0			-1	<b>1</b>			
HW/CW HX	7	1	1.0				-1	<b>1</b>		
Absorption Chiller	280	5	1.5	- 0.01			- 1.36	2.36	<b>1</b>	
Mechanical Chiller	270	2	1.8	- 0.17				1.17	<b>1</b>	
Cooling Tower	82	5	5.0	- 0.01				1		<b>1</b>

<sup>1</sup>Solar turbines, *Caterpillar* gas engines, *SMART* electrical chillers, *York* hot water absorption chillers, *Cleaver Brooks* hot water boilers, *Vapour Power* steam boilers and *Marley* cooling towers

The right hand side of Table A1-3 displays the production coefficients of the equipment selected for inclusion in the polygeneration superstructure, normalized to the main energy utility supplied by the equipment (indicated in bold). A positive coefficient indicates that a utility is produced, whereas a negative coefficient indicates the consumption of a utility. The capital costs of the

equipment, nominal power, as well as operation and maintenance costs, are also included in Table A1-3 on the left.

Capital cost included transportation and installation of the equipment. Non-recurring fixed costs were multiplied by an annuitization factor to convert these costs into a series of equal annual payments over the project horizon, at a given discount rate. The lifetime of the system was considered to be 20 years and the discount rate used was 10%, yielding  $k_{rf} = 0.12 \text{ year}^{-1}$ . For  $k_{ic}$ , 15% was assumed. In all scenarios considered, waste flow ( $\Phi_{uij}^{was}$ ) is possible only for the *ambient air* utility.

A cogeneration plant has already been installed at the hospital, a rendering of which is shown in Figure A1-5, but in this study a retrospective analysis approach is adopted that also considers direct connection of the hospital to the electricity and gas distribution grids only, as well as other intermediate connection options.



Figure A1-5 Cogeneration system installed at the hospital in Sudbury (Courtesy of Toromont Energy Ltd. Used with permission)

## A1.5. Mathematical Model

OMSES is essentially a MILP problem defined upon the mathematical representation of all possible ESS capable of meeting the consumers' demands. Here, OMSES was implemented in LINGO (Lindo Systems website, 2007). The model represents the superstructure containing all configuration/operation alternatives and the conditions of demand, prices, etc. The optimization selects the best combination of technologies capable of satisfying the energy demands of the hospital, and establishes the operational mode for the installed technologies on an hourly basis, so that the total annual cost is minimized. The branch-and-bound method was applied, and the runtime to solve the different scenarios considered with an Intel i7 architecture based personal computer ranged from 2 to 10 seconds.

#### **A1.6. Price of Natural Gas**

The 1985 Agreement on Natural Gas Prices and Markets between the Federal government and Alberta, British Columbia, and Saskatchewan deregulated natural gas commodity prices in Canada. The result was an open and integrated North American market for natural gas (NRCan website, 2011b), and since then, consumers have been able to choose their natural gas supplier instead of having to purchase from a regulated utility.

Natural Gas has a market-driven price that is affected by climatic and logistic factors. As a primary fuel, it has a considerable influence on electricity prices. Usually, lower gas prices lead to lower electricity prices. Utilities across Canada use a variety of short- and long-term purchasing options to obtain their natural gas. The Ontario Provincial government typically reviews and approves rates less frequently, which tends to even out market prices over longer time periods.

The hospital has a fixed-price contract for natural gas for a specified time period, which is the option preferred by hospital management in order to facilitate budget decisions. Gas transportation and distribution costs have to be added to the contract price (IESO, 2012b) for an overall gas price ( $p_{NG}$ ) of CAD 15/MWh.

### **A1.7. Islanded Polygeneration OMSES Solution**

Several scenarios are explored in this and the next sections that illustrate how the framework presented in Chapter 3 is used. The first scenario presented constrains the optimal design solution on the side of the interactions with the external utility grids. In particular, the import of electricity is forbidden, equivalent in OMSES' formulation to  $Y_{EE}^{pur} = 0$ . Therefore, the ESS must generate the required electricity, both for the final demand and the consumers present in the solution (i.e., mechanical chillers and cooling towers). In addition,  $Y_{EE}^{pur} = 0$  is imposed as well, so that the polygeneration system is forced to work, in absence of any dump load, in electricity-tracking mode (Rubio-Maya et al., 2011b).

#### ***A1.7.1 Superstructure Solution and Annual Energy Flows***

The optimal solution can be represented using the superstructure, where the elements (technology or imports/exports) not present are plotted with a lighter color (Figure A1-6).

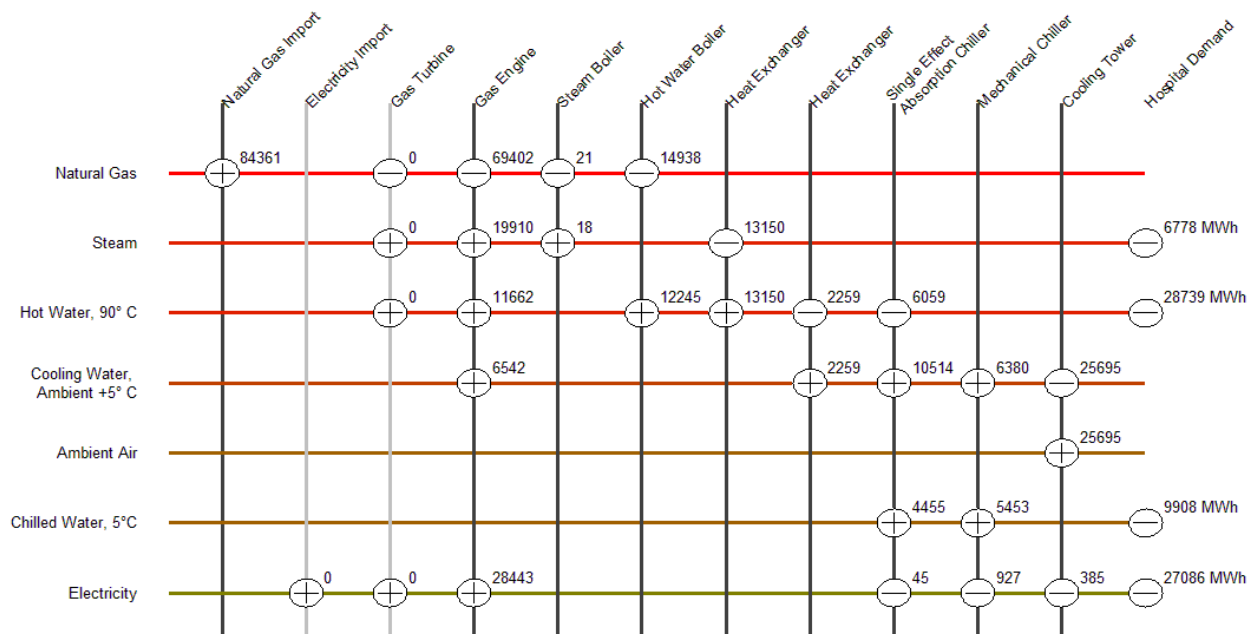


Figure A1-6 Optimal solution and annual energy flows (MWh) for the islanded scenario

Figure A1-6 offers a summary of the solution in several respects. The technologies present are denoted by dark vertical lines and non-zero energy exchanges beside the corresponding nodes (above and right side), which express the direction of the flow. These exchanges integrate the flows throughout the year. It can be observed how the balance of the terms across each horizontal line is zero, except for the *ambient air* utility, which can be wasted. The vertical balances are not necessarily conservative for the technologies, by definition in OMSES, as well as for the imports.

### A1.7.2 Detailed Design Solution – Technology Details and Costs

Table A1-4 presents a more granular description of the optimal design, as well as the detailed cost results of the islanded solution. In order to be self-sufficient, the ESS must include two (2) gas engines, which produce electricity to meet the final electricity demand and for the consumers in the ESS (mechanical chiller and cooling tower), heat for heating demands and for

the single effect absorption chiller (consumer), and the steam demand for the laundry facility. Auxiliary boilers are installed to operate when the engines cannot deliver enough cogenerated heat.

**Table A1-4 Design solution for the islanded polygeneration system**

System Composition	Number (Installed Power)
Gas turbines	0 (0 MW)
Gas engines	2 (7.2 MW)
Steam boilers	1 (3.0 MW)
Hot water boilers	2 (7.8 MW)
Heat exchangers (steam→hot water)	3 (3.0 MW)
Heat exchangers (hot water→cooling water)	2 (3.0 MW)
Single effect absorption chillers	2 (3.0 MW)
Vapor compression chillers	4 (7.4 MW)
Cooling towers	3 (15.0 MW)
Electricity connection capacity	---
Imported natural gas (MWh/year)	84,361
Imported electricity (MWh/year)	---
Exported electricity (MWh/year)	---
Capital cost of system (CAD)	11,010,100
Connection to the electric grid (CAD)	---
Annualized cost of natural gas (CAD)	1,265,418
Annualized cost of electricity (CAD)	---
Annualized profit (sale of electricity) (CAD)	---
Annuitized cost of equipment (CAD)	1,293,242
Annualized revenue: OPA support (CAD)	---
Annualized operation & maintenance (CAD)	356,068
Total annual cost (CAD)	2,914,729

### *A1.7.3 Optimal Operation Plan for the Typical Days*

Figure A1-7 illustrates the optimal operation plan for a typical summer day, both weekday and weekend day. The optimal output of the gas engines not only satisfies the electric demand of the hospital, but also produces the electricity consumed mainly by the mechanical chillers (4 units installed). The cooling demand can be either met by means of this technology or the single

effect absorption chillers (2 units installed). The optimal plan selects the combination that minimizes the consumption of natural gas, which, in periods of low demand (nights) results in the use of absorption chillers. In contrast, in periods of high electrical demand during weekdays, which are coincident with laundry hours, the cogenerated heat is used to meet the steam demand, and cooling is mostly supplied by the mechanical chillers. During weekends, the lack of steam demand generally results in a lower marginal operating cost of the absorption chillers. These swings in operating mode are caused by changes in marginal costs of the utilities flowing within the ESS, explained in detail in, for example, Carvalho (2011).

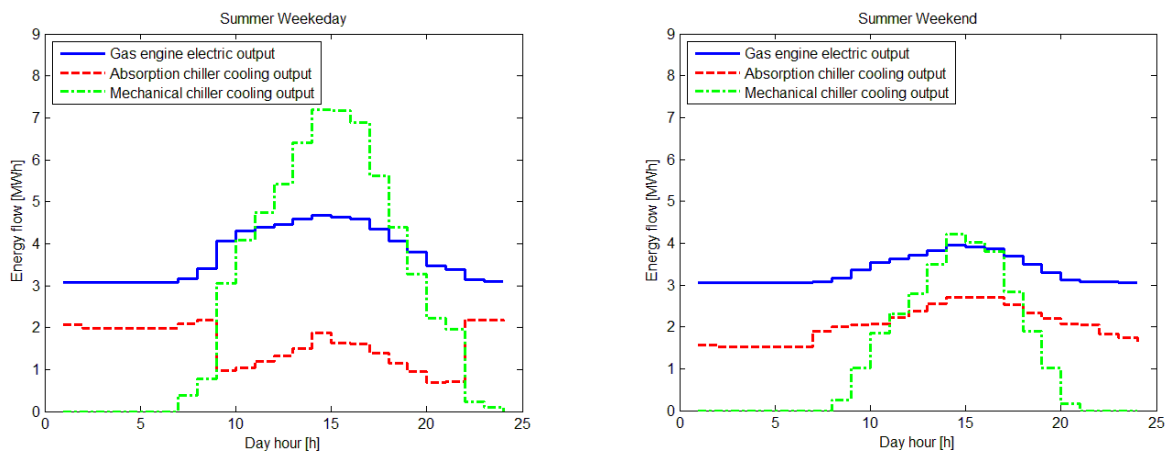


Figure A1-7 Optimal scheduled power output for selected technologies

## A1.8. Electricity Price

The remaining scenarios consider the possibility of establishing a connection with the local electricity grid. This way, the hospital's ESS can purchase electricity from (and potentially sell to) the local distributor. The Hourly Ontario Energy Price (HOEP) is the hourly competitive price that is charged to local distribution companies, self-scheduling generators, and non-dispatchable loads. This study considers a varying hourly competitive price for electricity

(IESO, 2011c) based on the HOEP, that is typical for large electricity consumers such as the hospital.

The IESO (IESO, 2011a; IESO, 2012a) establishes that every consumer must pay, in addition to the HOEP, the additional so called Global Adjustment (GA). On an annual basis, the GA can be up to 100% of the average competitive price (calculated from the HOEP time series), and even more. The rate is set to reflect the difference between the market price and: 1) the regulated rates paid to Ontario Power Generation's nuclear and hydroelectric base load generating stations; 2) payments made to suppliers that have been awarded contracts through the Ontario Power Authority, such as new gas-fired facilities, renewable energy facilities (e.g., wind farms), and demand response programs; and 3) contracted rates administered by the Ontario Electricity Financial Corporation that are paid to existing generators.

Table A1-5 shows the hourly electricity costs for each representative day used in the study, calculated as an average of the HOEP prices for each season. This assumption actually makes the methodology more suited for design purposes than for operational control, for prices actually fluctuate considerable around the mean values. Nevertheless, the model can be used for control purposes for price forecasts are normally available from the electric system operators. Control optimization using forecasts is discussed in Chapter 5 and implemented in Chapters 8, 9 and 10. Figure A1-8 shows the daily HOEP summer values used, along with their maximum and minimum values.

The GA currently (2014) differentiates between consumers with an average power demand lower than or equal to 5 MW (Class B) and over 5 MW (Class A). GA values for Class A consumers are based on the percentage that their peak demand contributes to overall system

demand during the five peak hours of a defined annual base period on five different days of the base period (Government Ontario website, 2010). According to Ontario Regulation 398/10, the hospital in Sudbury cannot be considered a Class A consumer because its average power demand does not exceed 5 MW.

Therefore, the hospital is a Class B consumer, and the corresponding GA values can be consulted in IESO (2011b). An average value of 40.84 CAD/MWh is used for the GA, based on 2011 values.

**Table A1-5 Purchase price of electricity assumed for this investigation, in CAD/MWh (excluding Global Adjustment)**

	Winter Weekda y	Winter Weeken d	Spring Weekda y	Spring Weeken d	Summer Weekda y	Summer Weeken d	Winter Weekda y	Winter Weeken d
0 –								
1h	34.9	30.6	17.5	17.0	33.8	30.2	26.7	22.5
1 –								
2h	31.8	30.2	15.6	20.1	31.1	28.5	25.6	25.2
2 –								
3h	31.0	30.7	14.4	12.5	30.2	24.7	27.3	22.1
3 –								
4h	29.1	31.2	11.8	12.1	27.0	23.3	24.5	19.6
4 –								
5h	28.2	29.5	15.0	11.3	27.0	20.3	19.7	15.9
5 –								
6h	30.3	26.9	23.4	10.6	24.5	17.1	23.8	23.4
6 –								
7h	33.9	29.0	23.5	13.7	27.3	22.7	32.8	24.8
7 –								
8h	37.7	28.3	26.2	21.2	30.7	28.3	29.6	27.6
8 –								
9h	35.8	29.5	26.7	31.8	34.4	30.5	31.2	22.1
9 –								
10								
h	35.5	31.3	30.3	33.1	38.8	35.3	30.8	27.9
10								
–								
11								
h	34.4	31.8	31.7	35.3	46.9	35.5	31.6	28.8

11								
-								
12								
h	34.1	32.5	31.3	33.7	48.2	38.5	30.9	30.9
12								
-								
13								
h	33.6	31.6	28.7	32.1	40.4	37.3	29.9	25.3
13								
-								
14								
h	33.9	30.9	28.4	28.3	43.5	35.9	29.9	24.1
14								
-								
15								
h	32.8	32.2	33.5	30.2	42.4	36.5	29.3	21.0
15								
-								
16								
h	32.0	32.0	56.0	32.6	44.6	38.5	29.6	25.3
16								
-								
17								
h	32.6	34.8	40.9	35.0	52.5	40.9	31.0	27.1
17								
-								
18								
h	34.8	38.8	29.6	33.5	47.2	39.6	44.0	33.6
18								
-								
19								
h	40.3	38.0	31.1	28.2	41.2	36.8	41.3	31.2
19								
-								
20								
h	42.4	35.2	30.6	37.5	37.8	36.4	36.0	31.0
20								
-								
21								
h	36.3	35.0	30.7	39.8	40.3	36.5	34.0	30.0
21								
-								
22								
h	34.2	31.5	22.8	30.7	36.0	34.1	32.1	28.9
22	32.4	30.3	24.3	26.8	35.2	32.5	28.5	23.8

—								
23								
h								
23								
—								
24								
h	31.9	30.4	20.7	23.2	31.9	30.5	28.4	20.3

It is important to note that Table A1-5 also shows the prices that operators get paid for electricity they supply to the grid. Consumers have to pay the Global Adjustment as well. This significant price differential indicates that conservation measures for the hospital should be self-financing.

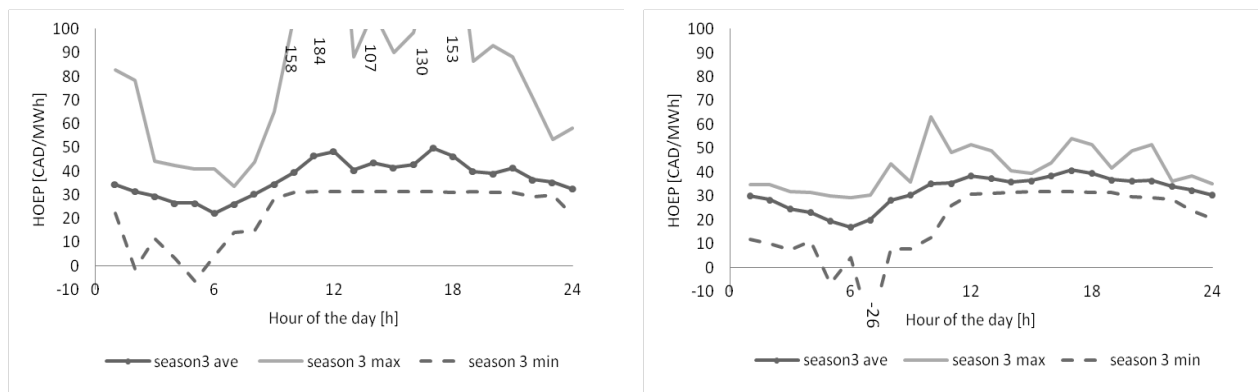


Figure A1-8 Daily HOEP Summer average, maximum and minimum values and annual averages: (left) weekday values, (right) weekend values

Grid-based electricity is available at the hospital location. However, connecting to the electric grid is a variable in the optimization procedure. Connection to the electric grid implies a connection cost,  $C_{inf,EE}$ , which comprises the cost of the underground line from the existing 12 kV system (the hospital is in a 12 kV service territory), to the vault space within the hospital site, transformer costs, and substation costs. According to various sources (Brian McMillan, personal communication, 2013; Mason et al., 2012; Gomatom and Jewell, 2002), underground lines are 166,000 CAD/(MW-km), a transformer costs between 75,000 100,000 CAD for

transformers in the  $\leq 3\text{MW}$  range, and the building cost of a substation is 102,000 CAD per MW of demand.

The connection distance between the nearest 12 kV line and the hospital site is considered 0.1 km. Based on the information above, values of 120,000 CAD/MW and CAD 166 CAD/MW-km are used for  $a_{inf,EE}$  and  $b_{inf,EE}$  respectively.

### A1.9. Grid-Connected Conventional Supply Solution

The conventional case study presents constraints in the selection of equipment that precludes the installation of cogeneration modules and absorption chillers. Electricity is purchased from the grid to meet electrical demand, including refrigeration demand (through mechanical chillers), while natural gas is purchased to meet heat demands by fuelling boilers. Figure A1-9 displays the system's structure and relevant annual energy flows for this ESS.

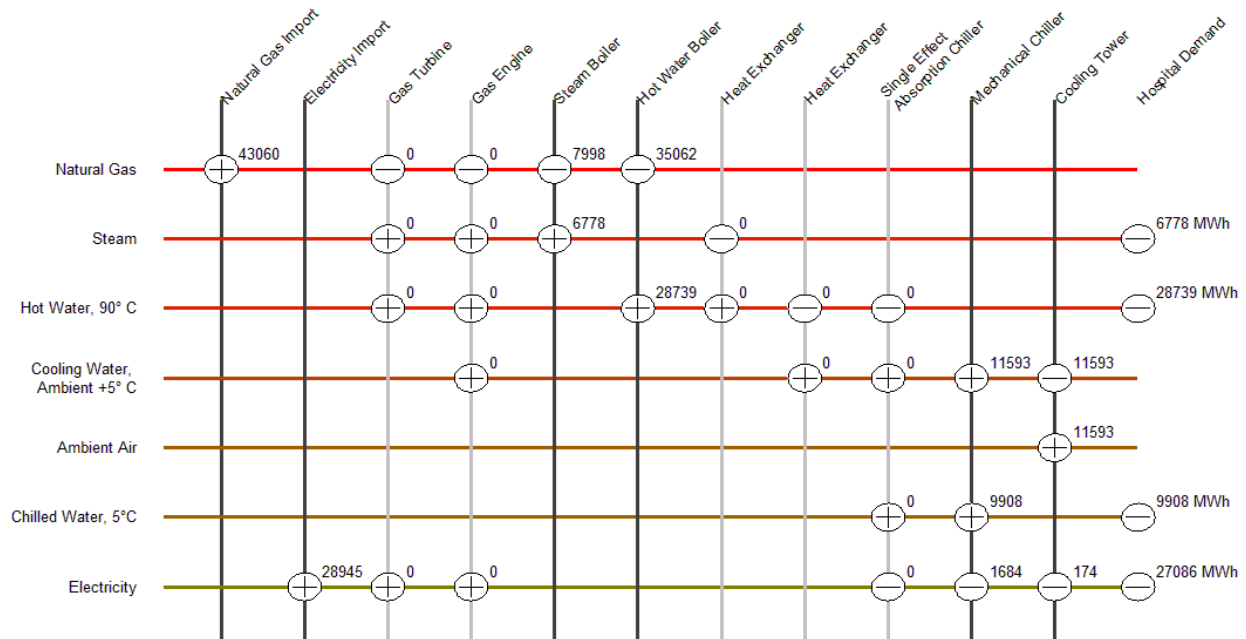


Figure A1-9 Optimal solution and annual energy flows (MWh) for the conventional scenario

Figure A1-9 shows how the new constraints effectively result in a grid-connected solution for both electricity and natural gas. In absence of absorption chillers, all the cooling demand is met by six (6) mechanical chillers, which increase the peak demand (including internal consumption) for electricity. The optimized connection capacity (active power) for electricity is 4.92 MW (Table A1-6), slightly higher than the previous islanded scenario (4.67 MW).

Table A1-6 summarizes the technological solution and its characteristic costs. It includes the separate share of the infrastructure (*Connection of the electric grid*), included in the *Capital cost of system* amount. This conventional solution requires a lower investment in equipment (technology), but additional infrastructure investment (electricity connection). In short, this solution, though more expensive in terms of total annual cost, has the advantage of being technologically less complex.

**Table A1-6 Design solution for the conventional system**

System Composition	Number (Installed Power)
Gas turbines	0 (0 MW)
Gas engines	0 (0 MW)
Steam boilers	1 (3.0 MW)
Hot water boilers	3 (11.4 MW)
Heat exchangers (steam→hot water)	0 (0 MW)
Heat exchangers (hot water→cooling water)	0 (0 MW)
Single effect absorption chillers	0 (0 MW)
Vapor compression chillers	6 (10.8MW)
Cooling towers	3 (15.0 MW)
Electricity connection capacity	(4.92 MW)
Imported natural gas (MWh/year)	43,060
Imported electricity (MWh/year)	28,944
Exported electricity (MWh/year)	---
Capital cost of system (CAD)	3,602,584
Connection to the electric grid (CAD)	672,682
Annualized cost of natural gas (CAD)	645,895
Annualized cost of electricity (CAD)	2,111,892
Annualized profit (sale of electricity) (CAD)	---

Annuitized cost of equipment (CAD)	423,158
Annualized revenue: OPA support (CAD)	---
Annualized operation & maintenance (CAD)	184,329
Total annual cost (CAD)	3,365,276

---

## **A1.10. Intermediate Polygeneration Scenarios with Export/Import Electricity Constraints**

### *A1.10.1 Connection for Electrical Import Only*

No constraints on the selection of technologies were imposed for this case. The minimum total annual cost was obtained by installing 1 gas engine, 1 steam boiler, 2 hot water boilers, 5 heat exchangers (3 ST/HW and 2 HW/CW), 1 absorption chiller, 5 vapor compression chillers, and 3 cooling towers. There are no restrictions on the operating hours of the polygeneration system. In this case, a low capacity electricity grid connection (1.14 MW) is installed, due to the lower requirements for imported electricity.

Figure A1-10 shows the annual energy flows and the selected technologies for the optimal solution under the constraints of this scenario.

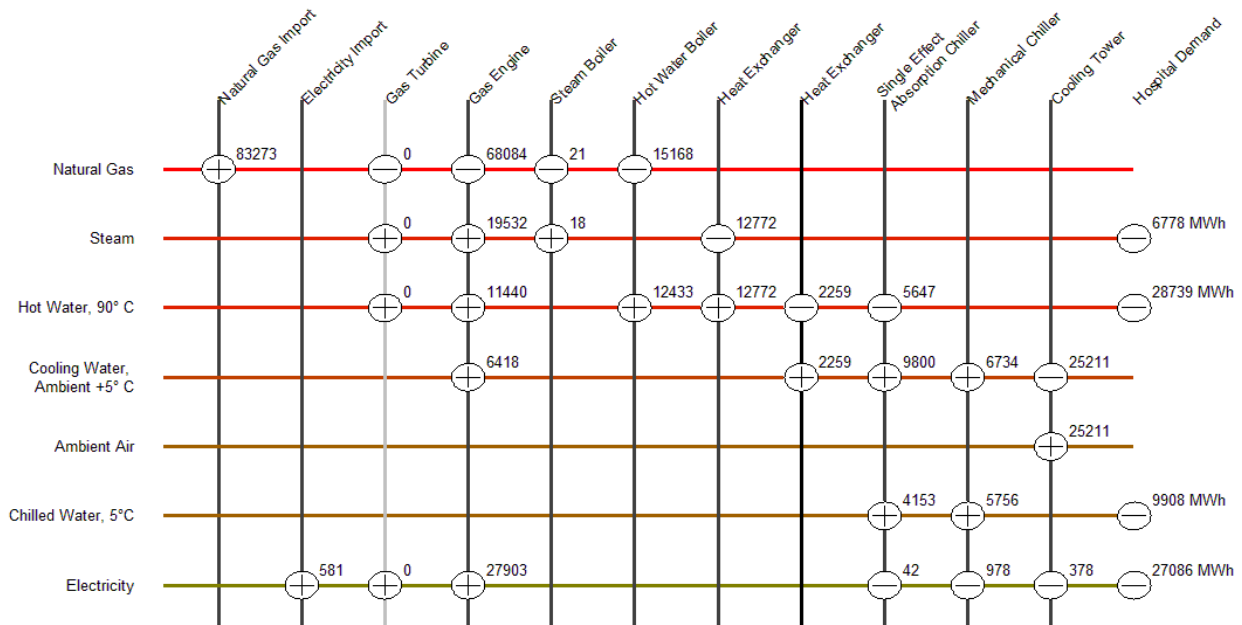


Figure A1-10 Optimal solution and annual energy flows (MWh) for the *import only* scenario

### A1.10.2 Connection for Electrical Import and Export

In this case, the hospital is connected to the electricity grid for importing and exporting electricity. All electricity generated must be sold to the electricity grid. There are no restrictions on the equipment. As it turns out, the optimal solution under those conditions is exactly the same as the conventional solution (Case A). When the system is allowed to sell electricity—and it must sell everything produced—the optimization procedure decides in favor of only importing electricity. It is not economically advantageous to generate and sell electricity.

## A1.11. Regulatory Background for the Sale of Electricity

The Ontario Power Authority (Ontario Power Authority website, 2011b) supports the efficient use of gas-fired electricity generating facilities that use combined heat and power (CHP, cogeneration) technology. In the last decade several support programs have been developed, including the Clean Energy Standard Offer Program Initiative (CESOP) (Ontario Power

Authority website, 2011a), which is now in force and facilitates the development of CHP facilities up to 20 MW. These CHP plants must be connected to an electricity distribution system in areas where this connection can be effectively accommodated, and must also fulfill some other constraints, depending on the support program.

The Combined Heat and Power Standard Offer Program (CHPSOP) (Ontario Power Authority website, 2011b) provides the supplier with a long-term financial benefit in the form of a monthly payment, which is based on the revenue requirements of a reference virtual power plant minus imputed market revenues derived from the operation of the virtual plant.

Following the OPA, CHPSOP electricity is sold to the grid on weekdays, between 7h and 23h, and the hospital would produce electricity when market prices (HOEP and natural gas) make it cost-effective to do so. The CHPSOP contract does not allow behind the meter generation (*i.e.*, all electricity must be sold to the grid), unless there are strong technical reasons for that type of configuration to be necessary. The Government rationale is that connecting behind the meter allows the host to avoid certain charges, which is a benefit that the CHPSOP price does not incorporate. If the OPA permitted behind the meter generation, the behind the meter benefits would be clawed back to ensure that the CHPSOP contract-holder is not overly enriched (at the expense of ratepayers). In the scenario where the sale of electricity is considered, all electricity generated is sold to the electricity grid, and the operation of the cogeneration modules is only allowed between 07h and 23h.

To be eligible to participate, a proposed generating facility must be located in an area of Ontario that has been designated as eligible for CESOP projects. However, regardless of eligibility, applications are subject to connection availability tests to assess whether the project can be

accommodated by the local distribution and transmission systems. Northern Ontario, where the hospital is located, is a notable exception to the eligible areas, but one of the study case scenarios will consider the financial benefit of participation in CHPSOP to verify the implications of extending the program province-wide.

#### *A1.11.1 Objective Function Including Incentives on Polygeneration*

The objective is to minimize the total annual cost ( $C_{tot}$ ), adapting Eq. 3-7 to include  $REV_{sup}$ , the support revenue for CHP systems ( $R_{sup} \geq 0$ ):

$$C_{var} = \sum_{ij} c_{e,ij} \cdot t_{ij} + \sum_{vij} c_{O\&M,v} \cdot \Pi_{vij} \cdot t_{ij} - REV_{sup} \quad (3-1)$$

The annual support revenue ( $REV_{sup}$ ) is defined as:

$$REV_{sup} = ACC \cdot \left[ NRSL \cdot n_m + \sum_{ij}^{n_{st}} p_{NG,ij} \cdot STG + \sum_{ij}^{n_{ih}} (p_{NG,ij} \cdot CHR + VOM - p_{EE,ij}) \right] \quad (3-2)$$

where, in accordance with OPA (2011a), ACC is the adjusted contract capacity (MW), NRSL is the net revenue support level (CAD/MW-month),  $n_m$  is the number of months per year in which the support is received (12), STG is the start-up fuel consumption (MWh/MW), CHR is the contract heat rate (MWh/MWh<sub>e</sub>), and VOM are the operation and maintenance costs (CAD/MWh).  $n_{ih}$ ,  $n_{st}$  are imputed operating hours and imputed start-up hours, defined with the criteria of the OPA for the CHPSOP (Ontario Power Authority website, 2011b), and calculated *a posteriori* with the HOEP instead of the pre-dispatch values.  $p_{NG,ij}$  (or  $p_{NG}$ , as it is constant) is the price of natural gas (CAD/MWh), and  $p_{EE,ij}$  is the Hourly Ontario Energy Price (HOEP) (CAD/MWh, shown in Table A1-5).

With the exception of the gas and the electricity prices ( $p_{NG}$  and  $p_{EE,ij}$ ), the remaining parameters of Eq. 3-2 are regulated and based on the behavior of a hypothetical Virtual Power Plant, as shown in Table A1-7. Assuming 20 start-ups per month and continuous operation during the allowed hours  $n_{ih}$ , the annual support remains at 1.1 million CAD per engine installed of 3.6 MW power.

**Table A1-7 Regulated parameters for Eq. 6 (OPA 2011b)**

Parameter	Value	Units
<i>NRSL</i>	28900	CAD/MW-month
<i>STG</i>	0.146	MWh/MW-start
<i>CHR</i>	1.758	MWh/MWh <sub>e</sub>
<i>VOM</i>	6	CAD/MWh

#### *A1.11.2 Results under Regulated Sale and Support Program*

The last study case considers support revenues from the regulated sale of electricity, under provincial programs that aim to promote gas cogeneration. There are no restrictions on the installation of equipment; however, the cogeneration modules have restricted operation between 07h and 23h, Monday to Friday. All cogenerated electricity must be sold to the electricity grid, and so the electricity demands of the building are covered by purchasing electricity from the grid. For the overall business, (i.e., hospital + cogeneration plant), the best results are achieved with this condition, although this solution involves the highest plant costs and is only available in designated areas (currently excluding the City of Greater Sudbury). The optimal solution configuration and energy flows are shown in Figure A1-11.

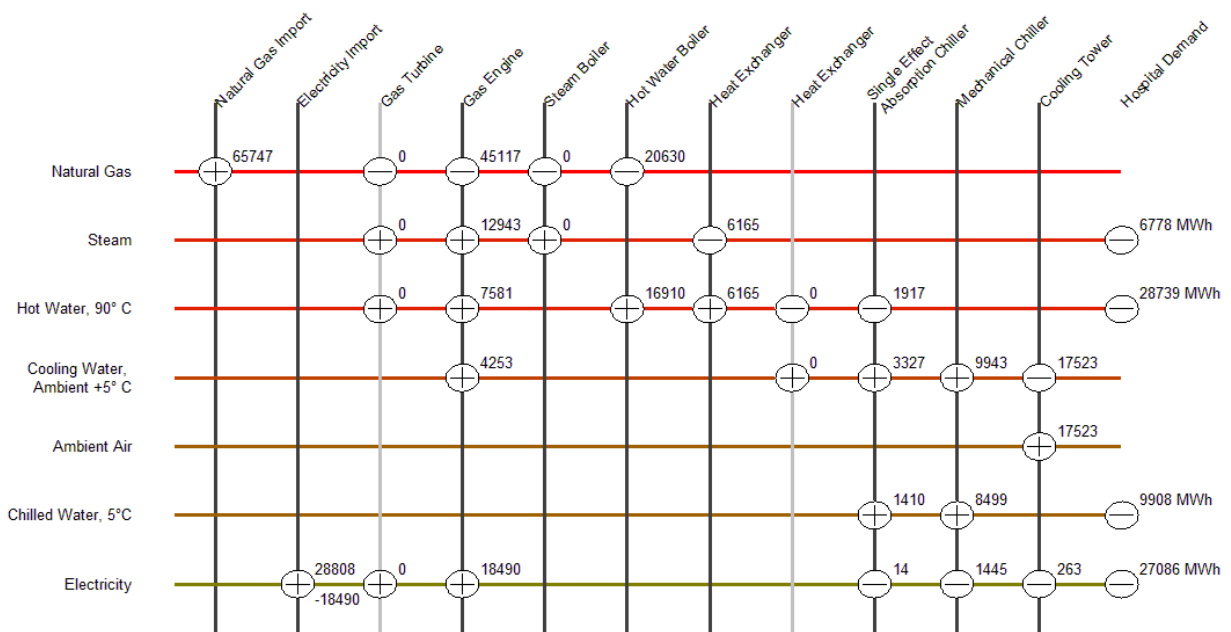


Figure A1-11 Optimal solution and annual energy flows (MWh) for the *regulated sale* scenario

As a result of the conservative property of energy for every utility, the net balance across utilities is zero (Figure A1-11). The graph includes now, in contrast with the previous scenarios, the electricity exported which, for coherency purposes, has been plotted with a negative sign, just below the imports value on the right hand side of the corresponding node. As the Figure A1- shows, the constraint regarding the generation of electricity, which forces the entire sale of the production, is rigorously met.

Table A1-8 contains the detailed design structure and the scenario's costs. Regarding the design, it is clear that the solution is almost identical to that of the *islanded* scenario, the difference being the heat exchangers installed. Furthermore, in the *regulated sale* scenario, a 6.40 MW electric grid connection infrastructure, the highest among all scenarios, is installed. The energy balances of both scenarios are radically different, which can be observed by comparing the resulting superstructure (Figure A1-11 and Figure A1-6).

Table A1-8 Design solution for the *regulated sale* system

System Composition	Number (Installed Power)
Gas turbines	0 (0 MW)
Gas engines	2 (7.2 MW)
Steam boilers	0 (0 MW)
Hot water boilers	2 (7.8 MW)
Heat exchangers (steam→hot water)	4 (4.0 MW)
Heat exchangers (hot water→cooling water)	0 (0 MW)
Single effect absorption chillers	2 (3.0 MW)
Vapor compression chillers	4 (7.4 MW)
Cooling towers	3 (15.0 MW)
Electricity connection capacity	(6.40 MW)
Imported natural gas (MWh/year)	65,746
Imported electricity (MWh/year)	28,807
Exported electricity (MWh/year)	18,490
Capital cost of system (CAD)	11,844,657
Connection to the electric grid (CAD)	873,702
Annualized cost of natural gas (CAD)	986,198
Annualized cost of electricity (CAD)	2,099,319
Annualized profit (sale of electricity) (CAD)	- 664,251
Annuitized cost of equipment (CAD)	1,391,269
Annualized revenue: OPA support (CAD)	-2,200,000
Annualized operation & maintenance (CAD)	261,005
Total annual cost (CAD)	1,873,541

The optimal operating plan for summer, weekday, and weekend, is shown in Figure A1-12. The constraints regarding the obligation to sell all the electricity produced, as well as the prohibition to generate outside the time window when receiving the support revenue  $REV_{sup}$ , can be observed in both weekdays and weekend days. The engines' operation plan depends mainly on the income from electricity sale at the HOEP (Figure A1-12), the benefits of on-site cogenerated heat for cooling purposes, and the steam demand. Furthermore, the operation of the engines is constrained by not having installed any HW/CW heat exchangers, which, at most, permit the polygeneration system to track the heat load and the necessary heat to operate the single absorption chillers. It can be observed that, in this scenario, operating absorption chillers remain more cost effective than the mechanical chillers, especially during weekends.

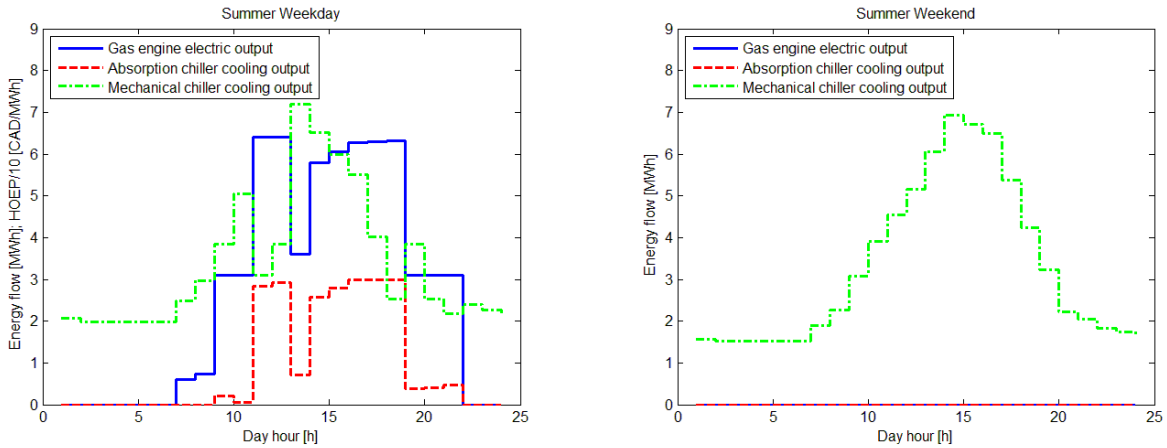
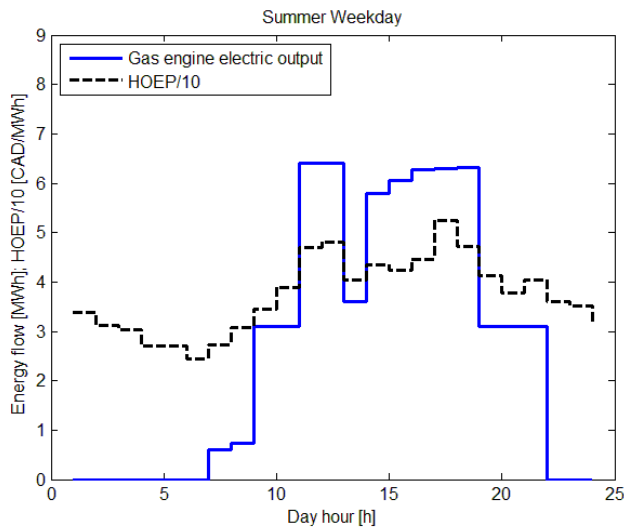


Figure A1-12 Optimal scheduled power output for selected technologies



Electricity produced and HOEP for a typical summer weekday, considering regulated electricity sale

## A1.12. Summary of the Scenarios

The site energy demands, together with the polygeneration superstructure, the technical coefficients, the imported energy prices, and the mathematical formulation, determine the optimal configuration of equipment and optimal mode of operating that equipment. Constraints and conditions imposed on the system effectively define scenarios that were investigated through repeated optimization processes. Five distinct scenarios were explored for the

polygeneration system at the hospital. Together, these were used to investigate the latter's ongoing suitability within contemporary energy, economic, and policy environments. Table A1-9 summarizes the results obtained for each case studied. The cases or scenarios have been categorized as follow:

- Case A (base). Conventional connect scenario
- Case B. Electricity islanded case
- Case C. Connection for electrical import only
- Case D. Connection for electrical import and export
- Case E. Regulated sale of electricity

**Table A1-9 System configuration and main energy flows for all study cases**

	A. Conventional	B. Islanded	C. Import only	D. Import & Export	E. Regulated sale
System Composition	Number (Installed Power)				
Gas turbines	0 (0 MW)				
Gas engines	0 (0 MW)	2 (7.2 MW)	1 (3.6 MW)	0 (0 MW)	2 (7.2 MW)
Steam boilers	1 (3.0 MW)	1 (3.0 MW)	1 (3.0 MW)	1 (3.0 MW)	0 (0 MW)
Hot water boilers	3 (11.4 MW)	2 (7.8 MW)	3 (7.8 MW)	3 (11.4 MW)	2 (7.8 MW)
Heat exchangers (steam→hot water)	0 (0 MW)	3 (3.0 MW)	2 (3.0 MW)	0 (0 MW)	4 (4.0 MW)
Heat exchangers (hot water→cooling water)	0 (0 MW)	2 (3.0 MW)	2 (2.0 MW)	0 (0 MW)	0 (0 MW)
Single effect absorption chillers	0 (0 MW)	2 (3.0 MW)	2 (1.5 MW)	0 (0 MW)	2 (3.0 MW)
Vapor compression chillers	6 (10.8MW)	4 (7.4 MW)	4 (9.25 MW)	6 (10.8MW)	4 (7.4 MW)
Cooling towers	3 (15.0 MW)				
Electricity connection capacity	(4.92 MW)	---	(1.07 MW)	(4.92 MW)	(6.40 MW)
Imported natural gas (MWh/year)	43,060	84,361	83,273	43,060	65,746
Imported electricity (MWh/year)	28,944	---	581	28,944	28,807
Exported electricity (MWh/year)	---	---	---	---	18,490
Capital cost of system (CAD)	3,602,584	11,010,100	7,038,287	3,602,584	11,844,657
Connection to the electric grid (CAD)	672,682	---	146,250	672,682	873,702
Annualized cost of natural gas (CAD)	645,895	1,265,418	1,249,099	645,895	986,198
Annualized cost of electricity (CAD)	2,111,892	---	49,291	2,111,892	2,099,319
Annualized profit (sale of electricity) (CAD)	---	---	---	---	- 664,251
Annuitized cost of equipment (CAD)	423,158	1,293,242	826,714	423,158	1,391,269
Annualized revenue: OPA support (CAD)	---	---	---	---	-2,200,000
Annualized operation & maintenance (CAD)	184,329	356,068	350,227	184,329	261,005
Total annual cost (CAD)	3,365,276	2,914,729	2,475,334	3,365,276	1,873,541

### A1.13. Discussion

Despite high efficiency and reliability, diesel engines were not considered as an option in the superstructure model for the problem. This was because the procurement price of diesel at 1.30 CAD/litre (91 CAD/MWh) (OME 2013) is much higher than that of natural gas at 0.156 CAD/m<sup>3</sup> (15 CAD/MWh) (OEB 2013), so that the optimization process would never favor a diesel-fuelled prime mover over a natural gas-fuelled prime mover.

Comparisons across the results of scenarios A to E of the previous section show that in cases B, C, and E, polygeneration returns the lowest annual cost of meeting site demand, even when a connection to the electrical grid is available within 100 meters of the site. As the computed annual costs include an annuitized portion for the capital expenditure, they reflect the discounted annual cost of all energy consumed.

Case D allowed for the installation of polygeneration equipment, but the additional export benefit includes the additional constraint that all generated electricity must be exported. This constraint annuls any benefit of auto-generation and self-consumption.

Outside the incentive area, cogeneration facilities may export electricity to the grid at a competitive price (Table A1-5, Figure A1-8). As all auto-generated electricity must be exported, the electrical demand of the facility is met by electricity imported from the grid (competitive price plus share of global adjustment—the latter can be significant, or at times, dominant).

The polygeneration solution with highest capital cost (Scenario B) presents a lower total annual cost than the straightforward electricity and gas connection (Scenario A). Despite the fact that the capital cost of Scenario B is three times that of Scenario A, the latter presents a heavy

contribution from global adjustment payments, which significantly increases the total annual cost for the hospital.

The solutions found in Table A1-9 are controlled by the electricity connection arrangements, and not by the combined heat and power economic factors (such as heat/cooling/power ratios), as would normally be expected.

If an electricity import connection is used with a polygeneration system, at a rating where the peak electrical demand is met from a supplementing grid supply, this allows for the installation of a lower capacity prime mover for the polygeneration system (Scenario C instead of Scenario B). With the lower generating capacity of Scenario C, the load factor of the system is higher and the capital and total annual costs are substantially lower.

Although Scenario C is technically obtainable in any area, in some jurisdictions electricity export may not be permissible or desirable, and this is why Scenario C was considered.

A modification in Scenario C to permit the export of surplus electricity (instead of 100% export) leads to a reduction in the annual operational cost of meeting all energy demands. This additional scenario is not included in Table A1-9.

Some jurisdictions occasionally insist that all electricity produced by on-site cogeneration systems must be exported to the electricity grid, and therefore the effects of this constraint were evaluated by Scenario D. Such a constraint applies to Ontario when a polygeneration system is installed within an incentive area, leading to additional revenues that compensate for the loss of benefit from auto-generation.

When connections to the electricity and natural gas distribution grids are available and the hospital fulfills the criteria for regulated sale (Scenario E, which means the system is located within an incentive area), the best option to achieve minimal annual cost is to operate the gas engines at full load to generate electricity (which must be sold to the electricity grid between 07h and 23h), and receive the Government support payments for CHP systems. There was an increase of approximately 60% in capital cost when compared to Scenario C, but a 20% lower annual cost was obtained (due to Government support). However, this option is not available everywhere. The Sudbury hospital is outside of any incentive area, so its best solution is installing cogeneration modules for auto-generation (and consequent self-consumption) with electricity imports to balance off the system (Scenario C).

An interesting alternative to be explored for Scenario E is to re-optimize in the face of lower average annual competitive price for electricity. The results suggest that it is not cost-effective to install a connection capacity equal to the total generating installed capacity. As the price of electricity drops, so does the optimal rating of the connection, to a limit of 4.9 MW, which is fixed by the imported demand.

Other significant findings were:

In Scenarios B, C, and E (Islanded, Import only, and Regulated Sale scenarios), gas engines were more cost-effective than gas turbines for this scale of consumer center. This could be attributed mainly to the lower electricity production efficiency of relatively small gas turbines. The results could change with an increase in heat demand, as turbines provide more steam and hot water when generating electricity than do gas engines.

In the case that Scenario E is a feasible option for a given location within Ontario, the optimal economic solution is more determined by a need to sell electricity to the grid, even when wasting appreciable cogenerated heat, rather than typical “heat demand following” or “electricity demand following” auto-generation and self-consumption stances that frequently guide cogeneration system design.

Inside an incentive area, increasing the global adjustment to 65 CAD/MWh and over will favor Scenario C over Scenario E.

If Sudbury was located within the region for government CHP subsidy, the decision to participate or not in the regulated sale depends on: 1) whether one actually has the cash for the higher capital expenditure; and 2) one’s assessment of risk of withdrawal of subsidy or underestimation of the level of difficulty of actually subscribing.

In the case of regulated sale (Scenario E), subscription to the revenue payment system strongly incentivizes the configuration of the system to install additional generation capacity (higher MW) than required for the on-site demand. For a public-sector building, like a hospital, it’s the taxpayer that indirectly pays the capital expenditure for higher installed capacity, even when ultimately the system is owned and operated by a private corporation. The subsidy associated with subscription comes from the Ontario electricity consumers, who pay part of the global adjustment.

#### **A1.14. Conclusions**

This paper studied the planning issue of determining the optimal configuration of an energy conversion and supply system to be installed in a hospital in Northern Ontario. The original methodology, developed for tertiary sector buildings in the Mediterranean, was extended for

Canada and Ontario in particular, so that peculiarities in the Ontario electricity market system could be explored.

The annual energy service demands of a Northern Ontario hospital were estimated, and were validated by actual data for a hospital in Sudbury. Two representative days per season were chosen to express, on an hourly basis, the energy demands of the hospital. A polygeneration superstructure for optimization of the energy supply system was created so that the energy demands of the consumer center could be met and different scenarios of constraints could be investigated. Energy prices were determined and conditions arising from the regulatory framework were introduced.

The results arising from a series of optimization scenarios, taken to be credible, practical options for new hospital facilities in Ontario, economically favored polygeneration approaches over straightforward electricity and gas connections, even when these were available very close to the site. In incentive areas, if the developer of the facility has sufficient capital, opting for CHPSOP to support polygeneration is economically attractive; however, it incentivizes developers to install substantially oversized equipment compared with that needed to meet on-site demand.

As well as illustrating the core OMSES methodology, the material of this chapter indicated that much depends on the external circumstances of the tariff environment and the various revenue support mechanisms available within the jurisdiction where the polygeneration system is or is to be installed.

## A2. Victor Mine demand series

All energy demands in MWh, for each typical day of the 12 months, for hour ending.

Table A2-1 Victor Mine energy demands

Month	Hour	Hot water	Chilled water	Electricity	Diesel
January	1:00 AM	0.3028	0	13.58	16.11
	2:00 AM	0.2657	0	14.67	16.11
	3:00 AM	0.2655	0	15.17	16.11
	4:00 AM	0.2647	0	14.88	16.11
	5:00 AM	0.3017	0	14.87	16.11
	6:00 AM	0.338	0	14.88	16.11
	7:00 AM	0.4929	0	15.27	16.11
	8:00 AM	0.5188	0	15.48	16.11
	9:00 AM	0.4332	0	15.58	16.11
	10:00 AM	0.476	0	15.19	16.11
	11:00 AM	0.474	0	15.38	16.11
	12:00 PM	0.4643	0	15.19	16.11
	1:00 PM	0.4479	0	15.47	16.11
	2:00 PM	0.6076	0	15.58	16.11
	3:00 PM	0.6046	0	15.18	16.11
	4:00 PM	0.4944	0	15.09	16.11
	5:00 PM	0.4887	0	15.57	16.11
	6:00 PM	0.4824	0	15.68	16.11
	7:00 PM	0.4822	0	15.78	16.11
	8:00 PM	0.4818	0	15.68	16.11
	9:00 PM	0.5714	0	15.97	16.11
	10:00 PM	0.5615	0	15.87	16.11
	11:00 PM	0.3752	0	15.86	16.11
	12:00 AM	0.3398	0	15.67	16.11
February	1:00 AM	0.2735	0	15.38	17.22
	2:00 AM	0.2391	0	15.39	17.22
	3:00 AM	0.2384	0	15.59	17.22
	4:00 AM	0.237	0	15.68	17.22
	5:00 AM	0.2737	0	15.59	17.22
	6:00 AM	0.3099	0	15.79	17.22
	7:00 AM	0.4747	0	15.78	17.22
	8:00 AM	0.4968	0	15.8	17.22
	9:00 AM	0.3858	0	15.8	17.22
	10:00 AM	0.417	0	15.71	17.22
	11:00 AM	0.4166	0	15.6	17.22
	12:00 PM	0.4077	0	15.01	17.22

Table A2-1 Victor Mine energy demands (continuation)

Month	Hour	Hot water	Chilled water	Electricity	Diesel
February	1:00 PM	0.3926	0	15.4	17.22
	2:00 PM	0.5724	0	15.2	17.22
	3:00 PM	0.5699	0	15.2	17.22
	4:00 PM	0.4487	0	15	17.22
	5:00 PM	0.4462	0	14.81	17.22
	6:00 PM	0.4431	0	15.4	17.22
	7:00 PM	0.4417	0	15.2	17.22
	8:00 PM	0.44	0	15	17.22
	9:00 PM	0.5416	0	15.39	17.22
	10:00 PM	0.5331	0	15.19	17.22
	11:00 PM	0.337	0	15.28	17.22
	12:00 AM	0.3079	0	15.29	17.22
March	1:00 AM	0.2672	0	14.46	12.45
	2:00 AM	0.234	0	14.36	12.45
	3:00 AM	0.2335	0	14.46	12.45
	4:00 AM	0.2324	0	14.66	12.45
	5:00 AM	0.267	0	14.46	12.45
	6:00 AM	0.3009	0	13.46	12.45
	7:00 AM	0.452	0	12.66	12.45
	8:00 AM	0.4741	0	12.67	12.45
	9:00 AM	0.3791	0	11.88	12.45
	10:00 AM	0.4126	0	11.88	12.45
	11:00 AM	0.4117	0	12.38	12.45
	12:00 PM	0.4031	0	12.08	12.45
	1:00 PM	0.3884	0	12.67	12.45
	2:00 PM	0.5498	0	12.57	12.45
	3:00 PM	0.5473	0	11.87	12.45
	4:00 PM	0.4376	0	12.37	12.45
	5:00 PM	0.4341	0	12.57	12.45
	6:00 PM	0.43	0	12.67	12.45
	7:00 PM	0.4291	0	13.27	12.45
	8:00 PM	0.428	0	13.56	12.45
	9:00 PM	0.5189	0	13.87	12.45
	10:00 PM	0.5105	0	13.96	12.45
	11:00 PM	0.33	0	14.06	12.45
	12:00 AM	0.3005	0	14.06	12.45

Table A2-1 Victor Mine energy demands (continuation)

Month	Hour	Hot water	Chilled water	Electricity	Diesel
April	1:00 AM	0.1812	0	13.17	9.87
	2:00 AM	0.1571	0	13.67	9.87
	3:00 AM	0.1557	0	13.56	9.87
	4:00 AM	0.1539	0	13.67	9.87
	5:00 AM	0.1831	0	13.86	9.87
	6:00 AM	0.212	0	13.76	9.87
	7:00 AM	0.3578	0	13.97	9.87
	8:00 AM	0.3704	0	14.07	9.87
	9:00 AM	0.2475	0	13.98	9.87
	10:00 AM	0.2572	0	13.79	9.87
	11:00 AM	0.2589	0	13.79	9.87
	12:00 PM	0.2529	0	13.69	9.87
	1:00 PM	0.2423	0	13.18	9.87
	2:00 PM	0.4139	0	13.38	9.87
	3:00 PM	0.4124	0	13.29	9.87
	4:00 PM	0.3004	0	13.58	9.87
	5:00 PM	0.3025	0	13.17	9.87
	6:00 PM	0.3042	0	13.27	9.87
	7:00 PM	0.3015	0	13.47	9.87
	8:00 PM	0.2985	0	13.56	9.87
	9:00 PM	0.3962	0	13.75	9.87
	10:00 PM	0.3913	0	13.66	9.87
	11:00 PM	0.2204	0	13.55	9.87
	12:00 AM	0.2054	0	13.66	9.87
May	1:00 AM	0.129	0	13.46	9.67
	2:00 AM	0.1106	0	13.55	9.67
	3:00 AM	0.1088	0	13.56	9.67
	4:00 AM	0.1067	0	13.36	9.67
	5:00 AM	0.1319	0	13.45	9.67
	6:00 AM	0.1568	0	13.65	9.67
	7:00 AM	0.2928	0	13.75	9.67
	8:00 AM	0.3001	0	13.87	9.67
	9:00 AM	0.1689	0	13.77	9.67
	10:00 AM	0.1662	0	13.17	9.67
	11:00 AM	0.1692	0	12.97	9.67
	12:00 PM	0.1648	0	12.27	9.67

Table A2-1 Victor Mine energy demands (continuation)

Month	Hour	Hot water	Chilled water	Electricity	Diesel
May	1:00 PM	0.1568	0	12.86	9.67
	2:00 PM	0.3251	0	12.25	9.67
	3:00 PM	0.3243	0	11.85	9.67
	4:00 PM	0.2165	0	11.94	9.67
	5:00 PM	0.2214	0	11.75	9.67
	6:00 PM	0.2259	0	11.73	9.67
	7:00 PM	0.2223	0	11.72	9.67
	8:00 PM	0.2185	0	12.42	9.67
	9:00 PM	0.3149	0	13.01	9.67
	10:00 PM	0.3121	0	13.1	9.67
	11:00 PM	0.1543	0	13.31	9.67
	12:00 AM	0.1474	0	13.01	9.67
June	1:00 AM	0.0992	0	12.33	8.84
	2:00 AM	0.0838	0	12.33	8.84
	3:00 AM	0.0817	0	11.73	8.84
	4:00 AM	0.0793	0	10.33	8.84
	5:00 AM	0.103	0	10.64	8.84
	6:00 AM	0.1265	0	11.03	8.84
	7:00 AM	0.2633	0	12.23	8.84
	8:00 AM	0.2672	0	12.15	8.84
	9:00 AM	0.1227	0	11.45	8.84
	10:00 AM	0.111	0.0205	10.26	8.84
	11:00 AM	0.115	0.1049	10.15	8.84
	12:00 PM	0.1115	0.1714	9.96	8.84
	1:00 PM	0.1049	0.2202	9.75	8.84
	2:00 PM	0.2805	0.2532	10.35	8.84
	3:00 PM	0.2801	0.2682	12.15	8.84
	4:00 PM	0.1692	0.2589	12.14	8.84
	5:00 PM	0.1763	0.2217	12.15	8.84
	6:00 PM	0.1832	0.1623	12.24	8.84
	7:00 PM	0.1788	0.0945	12.14	8.84
	8:00 PM	0.1742	0.0323	12.45	8.84
	9:00 PM	0.2751	0	12.32	8.84
	10:00 PM	0.2736	0	12.53	8.84
	11:00 PM	0.1161	0	12.73	8.84
	12:00 AM	0.1146	0	12.63	8.84

Table A2-1 Victor Mine energy demands (continuation)

Month	Hour	Hot water	Chilled water	Electricity	Diesel
July	1:00 AM	0.0792	0	12.12	9.34
	2:00 AM	0.0661	0	12.13	9.34
	3:00 AM	0.0639	0	11.93	9.34
	4:00 AM	0.0615	0	12.03	9.34
	5:00 AM	0.0833	0	12.42	9.34
	6:00 AM	0.1049	0	12.62	9.34
	7:00 AM	0.2355	0	12.82	9.34
	8:00 AM	0.2375	0.03	13.03	9.34
	9:00 AM	0.0933	0.13	12.64	9.34
	10:00 AM	0.0775	0.25	13.25	9.34
	11:00 AM	0.0819	0.35	12.84	9.34
	12:00 PM	0.079	0.44	12.75	9.34
	1:00 PM	0.0734	0.5	12.94	9.34
	2:00 PM	0.2442	0.54	12.74	9.34
	3:00 PM	0.244	0.56	12.75	9.34
	4:00 PM	0.1369	0.55	12.44	9.34
	5:00 PM	0.1448	0.5	11.04	9.34
	6:00 PM	0.1525	0.43	10.45	9.34
	7:00 PM	0.1479	0.34	11.64	9.34
	8:00 PM	0.1431	0.26	12.04	9.34
	9:00 PM	0.2415	0.2	12.42	9.34
	10:00 PM	0.2407	0.15	12.62	9.34
	11:00 PM	0.0911	0.11	12.83	9.34
	12:00 AM	0.0923	0.07	12.83	9.34
August	1:00 AM	0.0858	0	12.62	9.37
	2:00 AM	0.072	0	12.62	9.37
	3:00 AM	0.0699	0	12.52	9.37
	4:00 AM	0.0675	0	12.73	9.37
	5:00 AM	0.0898	0	12.42	9.37
	6:00 AM	0.1118	0	12.73	9.37
	7:00 AM	0.2431	0	12.72	9.37
	8:00 AM	0.2458	0	12.33	9.37
	9:00 AM	0.1033	0.0761	12.64	9.37
	10:00 AM	0.0893	0.1842	12.54	9.37
	11:00 AM	0.0935	0.2819	12.44	9.37
	12:00 PM	0.0904	0.3589	11.75	9.37

Table A2-1 Victor Mine energy demands (continuation)

Month	Hour	Hot water	Chilled water	Electricity	Diesel
August	1:00 PM	0.0845	0.4153	11.53	9.37
	2:00 PM	0.255	0.4535	11.34	9.37
	3:00 PM	0.2547	0.4709	10.75	9.37
	4:00 PM	0.1475	0.4601	11.64	9.37
	5:00 PM	0.155	0.4171	11.94	9.37
	6:00 PM	0.1623	0.3483	11.94	9.37
	7:00 PM	0.1578	0.2698	12.24	9.37
	8:00 PM	0.1532	0.1978	12.63	9.37
	9:00 PM	0.2512	0.1405	12.72	9.37
	10:00 PM	0.2502	0.0956	12.42	9.37
	11:00 PM	0.0995	0.0568	12.21	9.37
	12:00 AM	0.0997	0.0205	12.42	9.37
September	1:00 AM	0.1109	0	13.17	10.08
	2:00 AM	0.0942	0	13.67	10.08
	3:00 AM	0.0922	0	13.56	10.08
	4:00 AM	0.0899	0	13.67	10.08
	5:00 AM	0.1144	0	13.86	10.08
	6:00 AM	0.1387	0	13.76	10.08
	7:00 AM	0.2768	0	13.97	10.08
	8:00 AM	0.2819	0	14.07	10.08
	9:00 AM	0.1405	0	13.98	10.08
	10:00 AM	0.1318	0	13.79	10.08
	11:00 AM	0.1356	0	13.79	10.08
	12:00 PM	0.1317	0	13.69	10.08
	1:00 PM	0.1245	0	13.18	10.08
	2:00 PM	0.2995	0	13.38	10.08
	3:00 PM	0.2989	0	13.29	10.08
	4:00 PM	0.1879	0	13.58	10.08
	5:00 PM	0.1943	0	13.17	10.08
	6:00 PM	0.2004	0	13.27	10.08
	7:00 PM	0.1963	0	13.47	10.08
	8:00 PM	0.1919	0	13.56	10.08
	9:00 PM	0.2924	0	13.75	10.08
	10:00 PM	0.2904	0	13.66	10.08
	11:00 PM	0.131	0	13.55	10.08
	12:00 AM	0.1276	0	13.66	10.08

Table A2-1 Victor Mine energy demands (continuation)

Month	Hour	Hot water	Chilled water	Electricity	Diesel
October	1:00 AM	0.1443	0	14.46	10.4
	2:00 AM	0.1242	0	14.36	10.4
	3:00 AM	0.1226	0	14.46	10.4
	4:00 AM	0.1206	0	14.66	10.4
	5:00 AM	0.1469	0	14.46	10.4
	6:00 AM	0.1727	0	13.46	10.4
	7:00 AM	0.3104	0	12.66	10.4
	8:00 AM	0.3194	0	12.67	10.4
	9:00 AM	0.1922	0	11.88	10.4
	10:00 AM	0.1935	0	11.88	10.4
	11:00 AM	0.1961	0	12.38	10.4
	12:00 PM	0.1912	0	12.08	10.4
	1:00 PM	0.1824	0	12.67	10.4
	2:00 PM	0.35	0	12.57	10.4
	3:00 PM	0.349	0	11.87	10.4
	4:00 PM	0.241	0	12.37	10.4
	5:00 PM	0.245	0	12.57	10.4
	6:00 PM	0.2485	0	12.67	10.4
	7:00 PM	0.2452	0	13.27	10.4
	8:00 PM	0.2417	0	13.56	10.4
	9:00 PM	0.3375	0	13.87	10.4
	10:00 PM	0.3341	0	13.96	10.4
	11:00 PM	0.1738	0	14.06	10.4
	12:00 AM	0.1643	0	14.06	10.4
November	1:00 AM	0.2002	0	15.38	11.56
	2:00 AM	0.174	0	15.39	11.56
	3:00 AM	0.1727	0	15.59	11.56
	4:00 AM	0.1711	0	15.68	11.56
	5:00 AM	0.2016	0	15.59	11.56
	6:00 AM	0.2317	0	15.79	11.56
	7:00 AM	0.3796	0	15.78	11.56
	8:00 AM	0.3942	0	15.8	11.56
	9:00 AM	0.2762	0	15.8	11.56
	10:00 AM	0.2909	0	15.71	11.56
	11:00 AM	0.2921	0	15.6	11.56
	12:00 PM	0.2855	0	15.01	11.56

Table A2-1 Victor Mine energy demands (continuation)

Month	Hour	Hot water	Chilled water	Electricity	Diesel
November	1:00 PM	0.274	0	15.4	11.56
	2:00 PM	0.4446	0	15.2	11.56
	3:00 PM	0.4429	0	15.2	11.56
	4:00 PM	0.3306	0	15	11.56
	5:00 PM	0.3316	0	14.81	11.56
	6:00 PM	0.3322	0	15.4	11.56
	7:00 PM	0.3297	0	15.2	11.56
	8:00 PM	0.3271	0	15	11.56
	9:00 PM	0.4241	0	15.39	11.56
	10:00 PM	0.4185	0	15.19	11.56
	11:00 PM	0.2444	0	15.28	11.56
	12:00 AM	0.2264	0	15.29	11.56
December	1:00 AM	0.2649	0	13.58	16.05
	2:00 AM	0.2319	0	14.67	16.05
	3:00 AM	0.2314	0	15.17	16.05
	4:00 AM	0.2303	0	14.88	16.05
	5:00 AM	0.2647	0	14.87	16.05
	6:00 AM	0.2985	0	14.88	16.05
	7:00 AM	0.4493	0	15.27	16.05
	8:00 AM	0.4712	0	15.48	16.05
	9:00 AM	0.3756	0	15.58	16.05
	10:00 AM	0.4085	0	15.19	16.05
	11:00 AM	0.4076	0	15.38	16.05
	12:00 PM	0.3991	0	15.19	16.05
	1:00 PM	0.3845	0	15.47	16.05
	2:00 PM	0.5461	0	15.58	16.05
	3:00 PM	0.5435	0	15.18	16.05
	4:00 PM	0.4339	0	15.09	16.05
	5:00 PM	0.4305	0	15.57	16.05
	6:00 PM	0.4266	0	15.68	16.05
	7:00 PM	0.4256	0	15.78	16.05
	8:00 PM	0.4245	0	15.68	16.05
	9:00 PM	0.5155	0	15.97	16.05
	10:00 PM	0.5072	0	15.87	16.05
	11:00 PM	0.3271	0	15.86	16.05
	12:00 AM	0.2979	0	15.67	16.05

### **A3. Ontario Power demand, Humidex and Community Power Consumption**

This appendix describes how to calculate useful relationships between the aggregated electric energy consumed by a group of consumers and the environmental conditions. The mathematical formulae can be obtained for a town (or community) or a country, as it will be demonstrated. Expressing the relationships in terms of energy and not power eliminate noise and thus permits a clearer picture of both the predominant loads of the system, an approximate effort of the system to compensate for heating and cooling loads, and the behaviour of the users when facing extreme temperatures.

The methodology requires the knowledge of historical series of power demand, ambient temperature and, when possible, relative humidity. It is known that in some regions latent cooling loads can be comparable to the sensible load. When active, air conditioning systems and refrigeration plants do not necessarily consume more energy, but the activation threshold will be lower for more humid weather given the same dry bulb temperature. Thus, when possible and known significant, humidity should be considered as a driver of power demand, for example by using the *humidex* (or humidity index) (Weron, 2007) instead of simply the environmental dry bulb temperature.

In winter, the effect of humidity on heating loads is lower, for the content of latent heat in the air drops significantly for low temperatures. Wind has a significant impact on power demand (Weron, 2007) through the so called *wind chill* effect. The effect of wind is neglected, for here we are more interested in the daily and seasonal average relationship, rather than instantaneous values.

Given the time series (e.g., hourly data), daily averages of power demand (available through the system operator in the case of nation scale grids (IESO, 2015)) and environmental temperatures (or humidex, available from, i.e., environment or meteorology institutions) are calculated. Then, two main groups are distinguished – one including weekdays, and the other weekend days, statutory holidays, etc. This separation is reasonable in western countries with such labour regulation. More groups can be added, but for the case considered in this thesis, two seems enough. A plot of the average daily energy demanded as a function of the average daily temperature (humidex) indicates for each group a clear relationship, which a second order polynomial fits reasonably well in all but the extreme temperature zones in the graph (left and right ends).

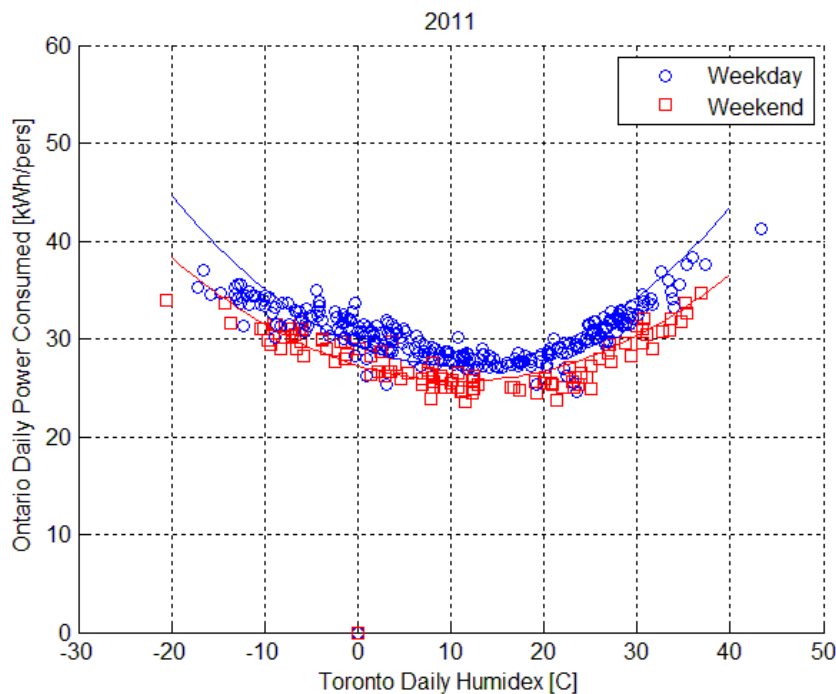
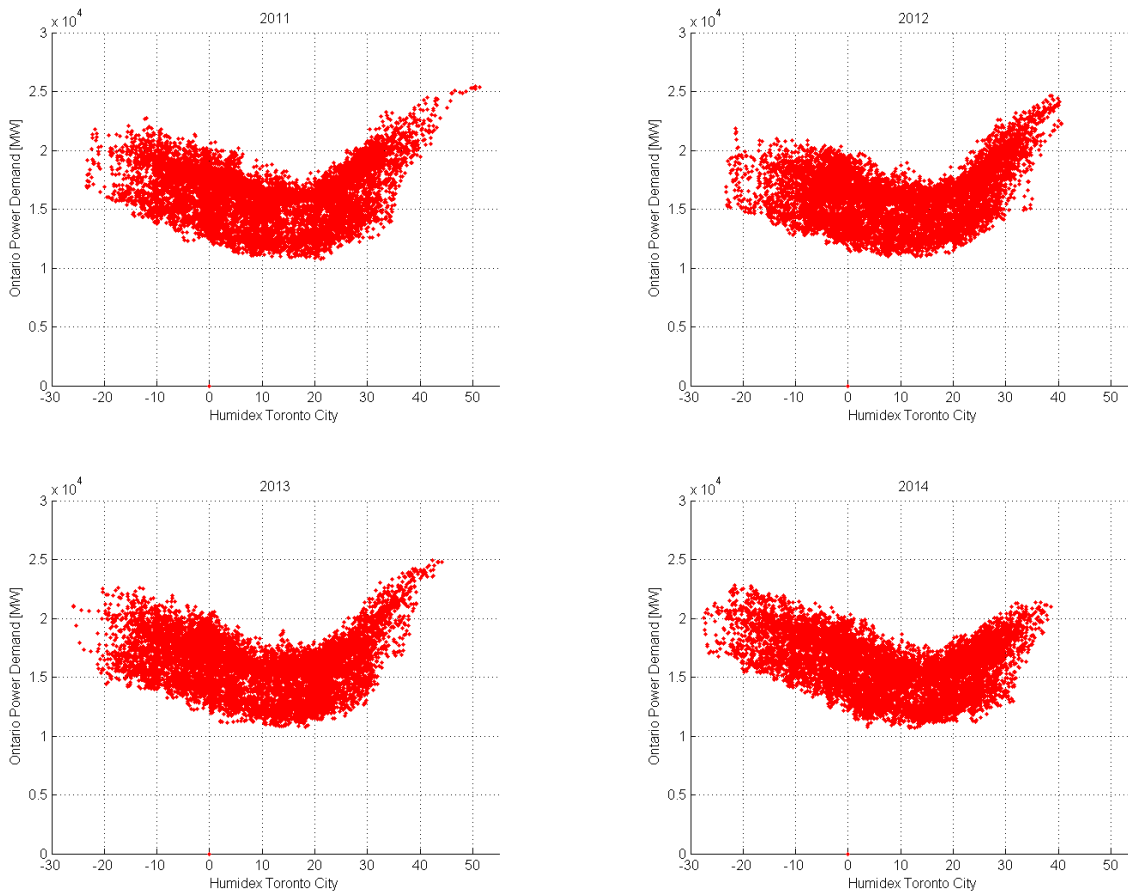


Figure A2-1 Energy-temperature relationship example

The figure above shows the limitations of the second order polynomial fitting, as well as the existence of some “outliers” (blue circles), that lie in the region of weekend-type demand days

(red squares), which may have been identified as provincial statutory holidays. The curve seems to fit the extreme hot days, but not the coldest ones, where a flattening appears. These considerations can be observed in the next figures, which illustrate the case of Ontario provincial power demand for four consecutive years. The first figures represent hourly plots, while the last four represent the daily averages.



**Figure A2-2 Ontario hourly power demand for several years**

The same bird-like shape is repeated every year. The structure of the loads, heating and cooling included, determine to a large extent the shape. Minimum and maximum daily average temperatures for each year can be read in the graph, in this case being humidex in Toronto City. This type of representation is useful regarding the maximum load of the system, which depends

on weather patterns, as well as socioeconomic development (i.e., access of the population to house air conditioning systems, predominant heating fuels, etc.).

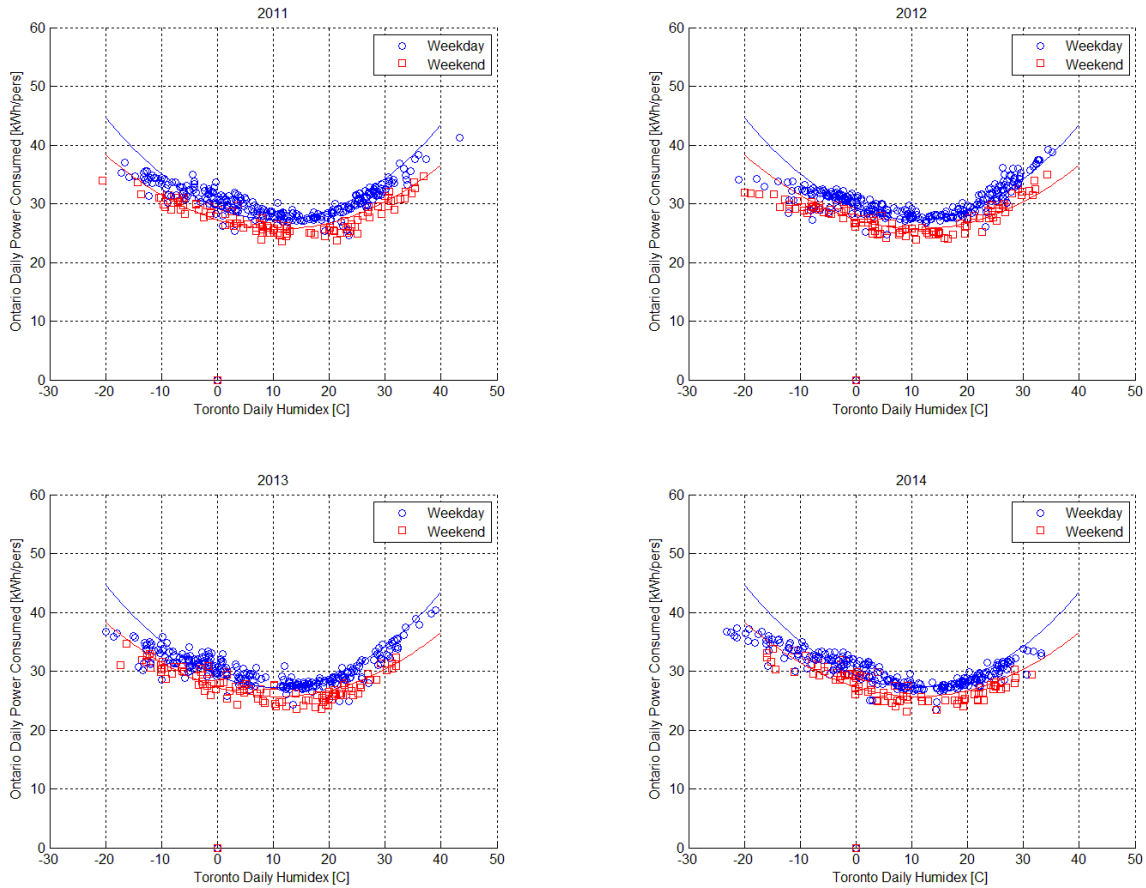


Figure A2-3 Ontario daily average electrical consumption per capita for several years

The figure above shows the energy-temperature relationship considering daily averages and per capita consumption. For all the years, the same curves (second order polynomial) are plotted fitted for weekdays and weekends of 2012. No quantitative difference is appreciated among the years. The per capita consumption flattens with colder temperatures, probably showing the effect of thermal inertia of the overall consumer system. The daily averaging process eliminates from the analysis the consumer effort in reducing the peak consumption as price (hourly tariff or demand charges) response – consumers will likely shift the loads to daily periods with a lower electricity price.

Finally, the same approach was used to represent the aggregated energy relationship with temperature for Fort Severn, a small community in Northern Ontario. Population number varies depending on the source, but a safe estimation lies between 400 (Aboriginal Affairs and Northern Development Canada website, 2015) to 490 (Government of Canada website, 2015) people living within the town.

Environmental temperature was obtained from (Environment Canada, 2014), while the power data was generously provided by the local grid operator. The results of daily electric energy consumed per capita (490 inhabitants considered) are shown together with Ontario results, both for the year 2011.

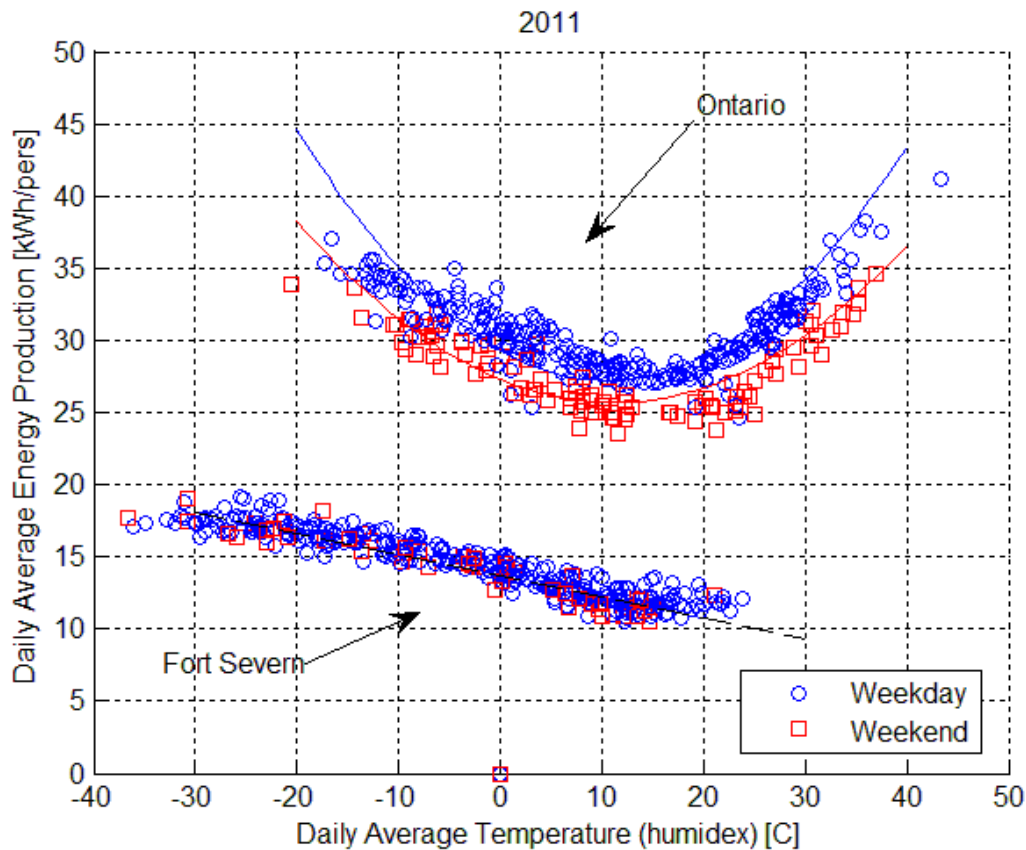


Figure A2-4 Fort Severn electricity production

Weekend and weekday differences are less evident regarding the community. Most importantly, the per capital energy production is significantly lower for the community. It was assumed that the consumption equals to the production, which may be reasonable for the community, but not for Ontario, where transportation losses will reduce the calculated consumption by 15% from the production level. This assumption, in addition to the fact that heating is mainly provided by oil stoves, as well as the lack of energy intensive industries on the site, causes the energy per capita gap between the community and the province.

Above 10°C the effect on power consumption flattens, while only over 20°C the power begins to rise again. These considerations apply to both the community and provincial cases. Although inversely correlated with sunlight available, which obviously correlates with environmental temperature, lighting electricity use can be probably neglected as electrical load when compared to heating loads, also present in many places where fuel boilers cannot be used, such as vehicle block heaters, pipelines heaters, etc. Assuming 15°C as comfort neutral temperature (no heating or cooling for human being comfort in the average indoor space), the same slope on both sides of the figures can be expected, and is indeed observed, which may indicate the lower influence of daylight time on lighting loads (in houses and offices, the lack of sufficient natural light causes the lights to be switched on irrespective to the outdoor situation).

#### **A4. Connection Capacity and Wind Power parametrical analysis**

A more detailed analysis of the supply alternatives for Chapter 9 Diavik Mine includes, evidently, the possibility to deploy a transmission line up to the mine site, with the corresponding investment cost involved.

In the region of interest, the Northwest Territories, electricity rates are higher than in Ontario. This might have been one of the many reasons why Diavik was actual energy supply system was conceived off-grid. Divided in geographical areas, consumers located in each of them pay different rates (Northwest Territories Power Corporation website, 2015), which reflect the characteristics of the infrastructure, as well as the generator type (hydropower or diesel mainly). In this analysis, the purchase cost of electricity is considered 155 CAD/MWh (in the neighborhood of the rates paid in Fort Resolution/Fort Smith area). The same cost for the transmission line as in Chapter 7 is considered in the present analysis.

The results shown in this appendix complements as well Chapter 12's. Accordingly, the number of diesel generators or boilers is not constrained as it was the case in Chapter 9. That is why the results in terms of the wind farm size shown in this appendix should agree with Chapter 12. In the same manner, diesel final demand was not included in order to have a clearer picture of the TAC evolution.

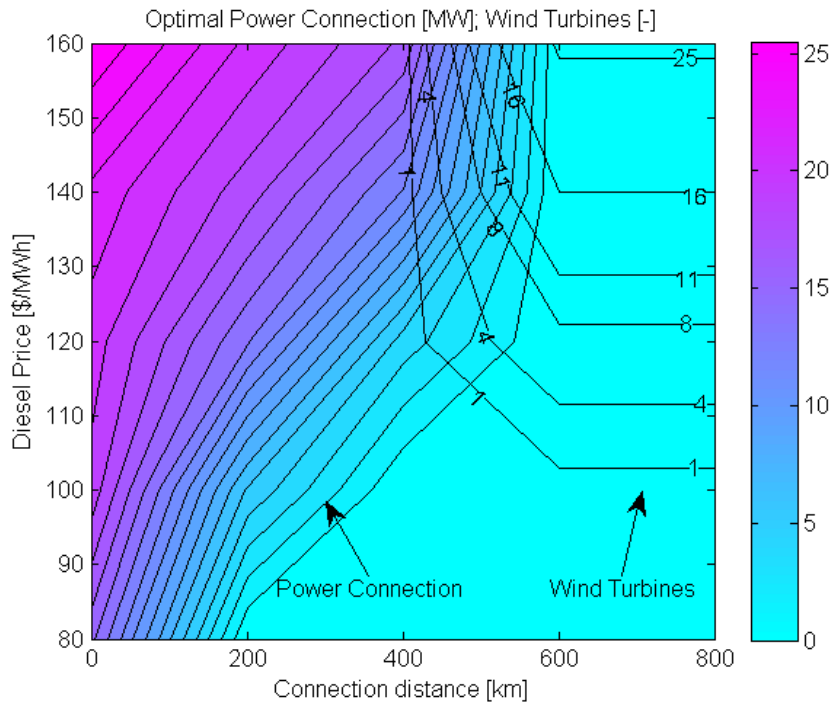


**Figure A4-1 Optimal grid connection and wind farm size**

Figure A4-1 shows the results for the optimal connection capacity and the optimal size of the wind farm for the corresponding scenario of diesel price and distance. Wind daily profile #3 used in the calculations, and the agreement regarding wind turbines (Figure A5-1) and total annual cost (Figure A4-2) can be observed for off-grid solutions.

Below 200 km the energy supply considers cost effective some grid connection capacity, this increasing as diesel price rises. The top-left triangular section is dominated by the transmission line as the main electricity supplier. However, above 400 km and 100 CAD/MWh diesel wind turbines becomes a cost effective power supplier. A transition region appears above 110CAD/MWh and between 400 and 600 km where the optimal energy supply is a mix between grid connection, diesel generators and wind turbine – a grid connected wind-diesel hybrid system.

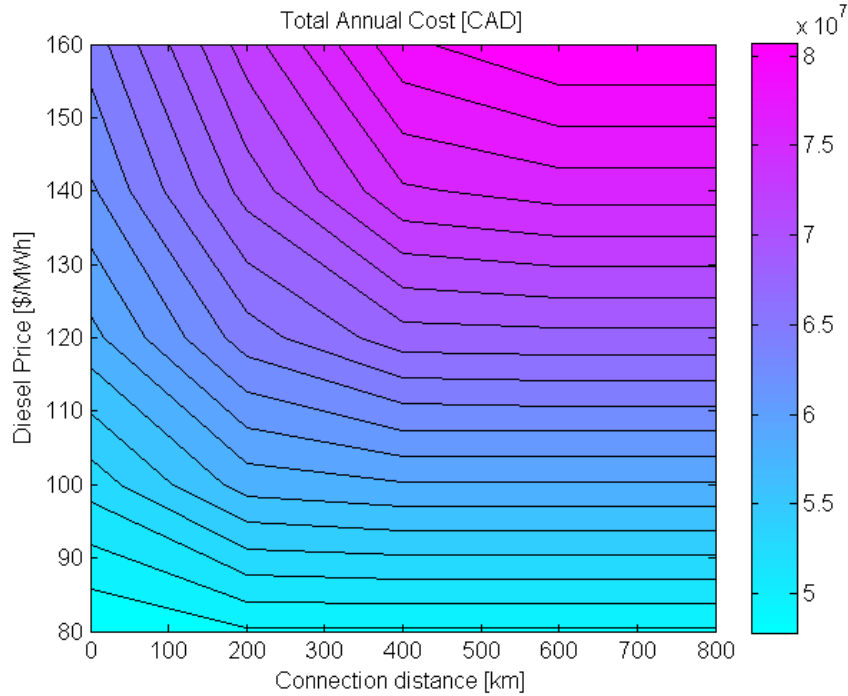


**Figure A4-2 Total annual cost**

Under the considered scenario, the TAC varies between 50 and 80 million CAD. From Figure A4-2 it can be seen that, under the characteristics of the model and the constraints used, the optimal energy supply system is more sensitive to the diesel price than to the connection distance regarding the TAC. However, the typology of the solutions varies significantly. Although grid connected solutions are attractive up to 600 km with typical (current) diesel price, the high investment required could be constrained by the ability to finance the investment given the high inherent risk of mining developments.

## **A5. Propane, Natural Gas, Diesel and Electricity Infrastructure options for a remote mine**

Its power market, climate and available infrastructure make of Northern Ontario a unique energy playfield. OMSES is the only computer tool that integrates energy demands, storage, and multiple potential energy infrastructures.

The approach taken including annuitized cost of energy infrastructure is a key factor when deciding which energy sources will be used at the mine site through its life. The following results complement the analysis of the mine described in Chapter 11. The difference with this, in addition to the variation in diesel price and connection distance, includes the possibility to develop a natural gas pipeline connection.

The analysis consists of flexing the purchase price of diesel (including truck-in constant costs) and the distance of the mine to the existing infrastructure, calculating with OMSES the optimal combination of technologies (infrastructure included) and the optimal operation schedule. The closest point of natural gas interconnection is considered to be at the same distance as for the electric grid interconnection. The cost of the pipeline is estimated at 1,110,000 CAD/km, to which 2% is added as O&M cost to be annuitized. Natural gas is available at 15 CAD/MWh. Natural gas boilers have been included in the conservative superstructure (Chapter 7 costs). A maximum storage capacity of 30,000 MWh of propane has been applied (in Chapter 11, 33,524.08 MWh was installed under the Scenario 11 constraints).

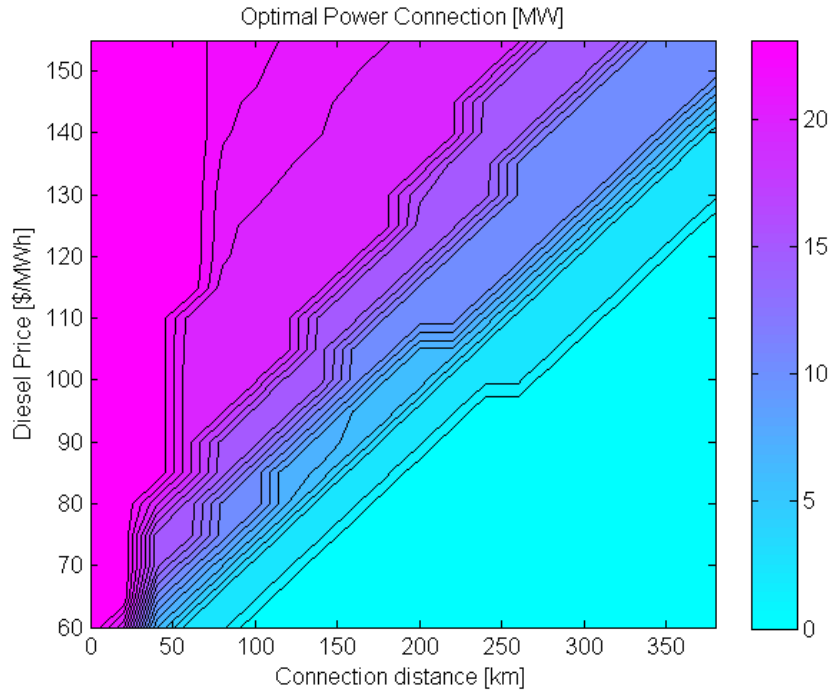


**Figure A5-1 Optimal power connection**

As expected, electricity costs are low enough to remain connected as long as diesel costs remain high, following a fairly linear relationship. As an example, diesel is used to generate all the electricity consumed on site for distances higher than 250 km and diesel below 100 CAD/MWh (~1.00 CAD/liter).

The optimal natural gas connection, expressed by the maximum energy rate (MWh/h) drawn as a result of OMSES solution, is shown in Figure A5-2. The available technologies in Chapter 11 were extended to include natural gas boilers. Because of this, natural gas use is limited to provide heating, and compete against propane, cogenerated heat from diesel generators and diesel boilers heat. Beyond certain distance, the sum of the annuitized pipeline investment and marginal natural gas energy cost results more expensive than the propane alternative. This is found in Figure A5-3, where it can also be seen that diesel generated heating becomes cost effective below 90 CAD/MWh.

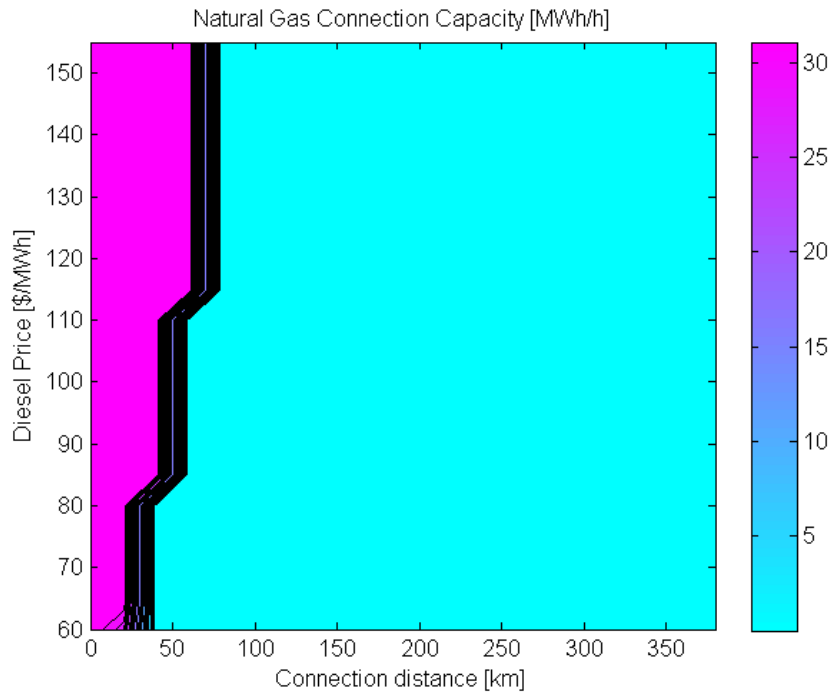


Figure A5-2 Optimal natural gas connection

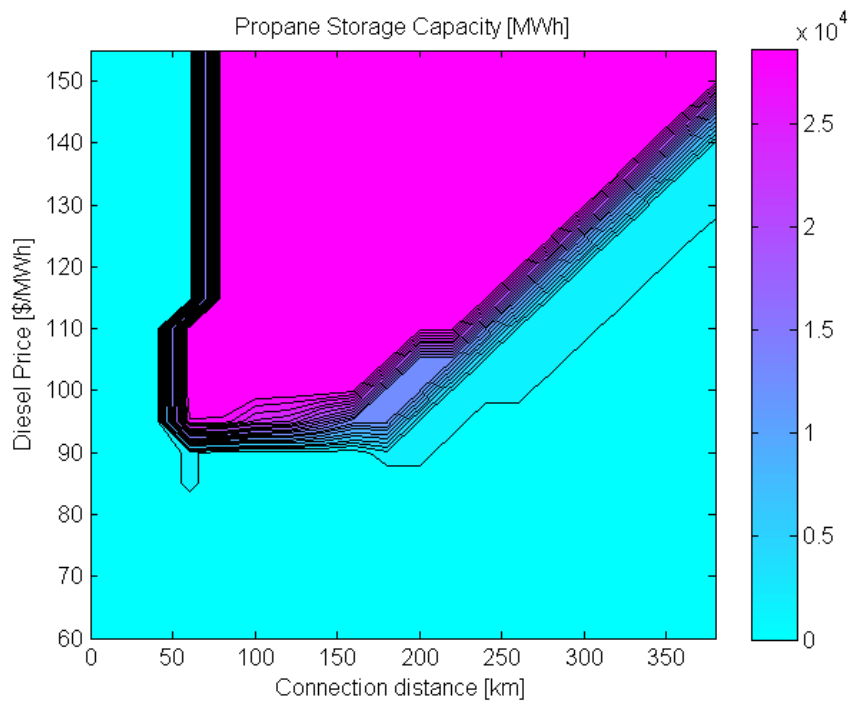
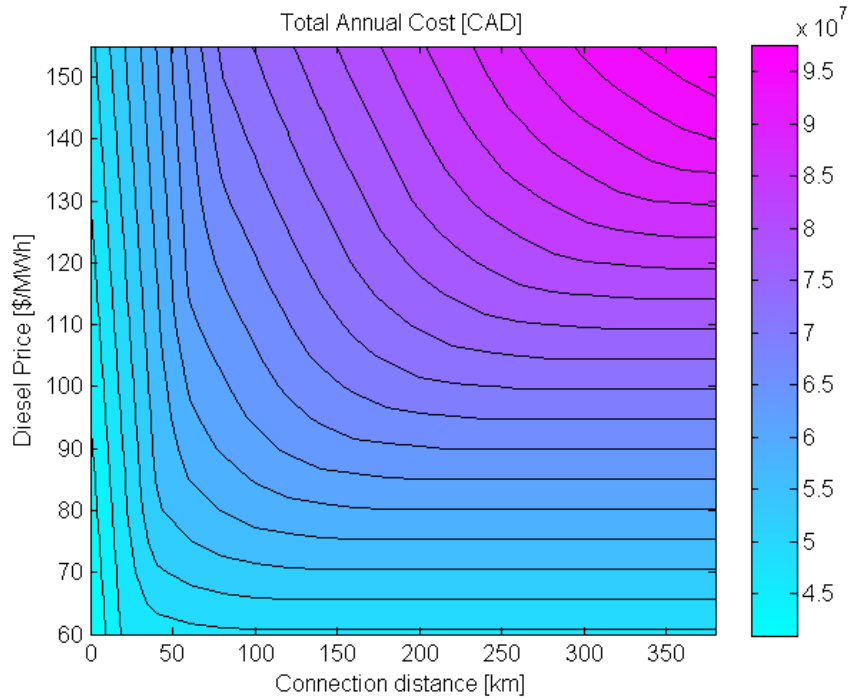


Figure A5-3 Optimal propane storage capacity

The bottom left triangular section of the previous figures indicates the economic and geographical environment (providing the same climate for any mine) where diesel engines are used to generate electricity and cogenerate heat



**Figure A5-4 Total annual costs**

Total annual cost (TAC) remains constant in the region of diesel generated electricity and heating (Figure A5-4). However, the minimization of the TAC does not include increasing price of diesel with distance (simplification valid for the considered range), and only without this consideration, constant TAC are expected when transmission lines or pipelines do not participate of the optimal solution.

## **A6. Comparison of OMSES and HOMER Results**

### **A6.1. Introduction**

*"The HOMER Micropower Optimization Model is a computer model developed by the U.S. National Renewable Energy Laboratory (NREL) to assist in the design of micropower systems and to facilitate the comparison of power generation technologies across a wide range of applications". (Lambert et al., 2006)*

One can immediately identify the main difference regarding the field of application between HOMER and OMSES. HOMER was developed for power systems exclusively, while OMSES model accommodates demands in other energy forms. It was after some versions that HOMER included heat loads and hydrogen fuel. Regarding the storage of energy, HOMER is limited to electricity, hydrogen and, indirectly, any deferrable load that may be assimilated as an electrical one. In contrast, OMSES was updated from its original conception to include storage in all possible energy forms, including, for instance, heat, cooling, electricity, fuels, etc. Heat storage and cooling loads is what allows OMSES to model and optimize all kinds of polygeneration systems, as opposed to HOMER.

This appendix is intended to compare the use of these two optimization tools for the case study correspondent to Chapter 9. The comparison adds discussion to the analysis presented in Appendix 4 for the same case study.

## A6.2. Case study adapted to HOMER

Using the Location Map, the site was selected to simulate the conditions existing at Diavik Mine (Figure A6-1). Wind resource was imported from Environment Canada, using hourly data collected at the weather station Inner Whalebacks for the year 2011.

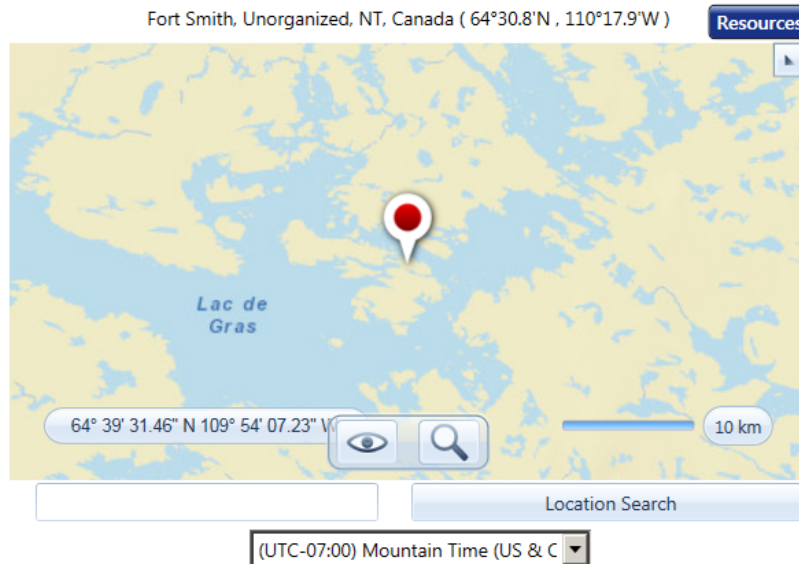


Figure A6-1 HOMER map indicating the location of the mine

### A6.2.1 Energy Demands

#### *Electricity demand*

The electrical demand considered for HOMER includes all the mine consumers, such as dewatering and ventilation. Dewatering demand could have been modeled independently as a deferrable load; however, this was discarded in order to be consistent with Chapter 12 and Appendix 4. A capture of the modeled demand is shown in Figure A6-2.

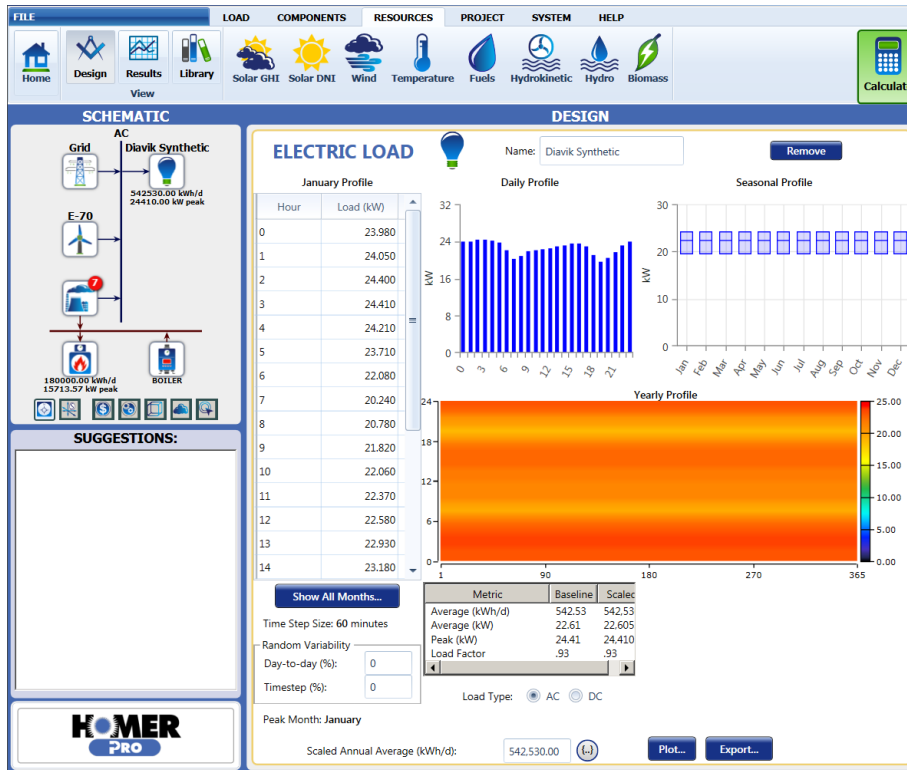


Figure A6-2 – Electrical load

### Heating demand

The same principles were considered when calculating HOMER heating demand. In this case, although the software capabilities to create the daily and seasonal profiles could have been used, this simplified option was discarded because of the significantly different seasonal profile, which modified the results outcome. Thus, the sum of low and medium temperature heating was calculated and introduced in HOMER (Figure A6-3).

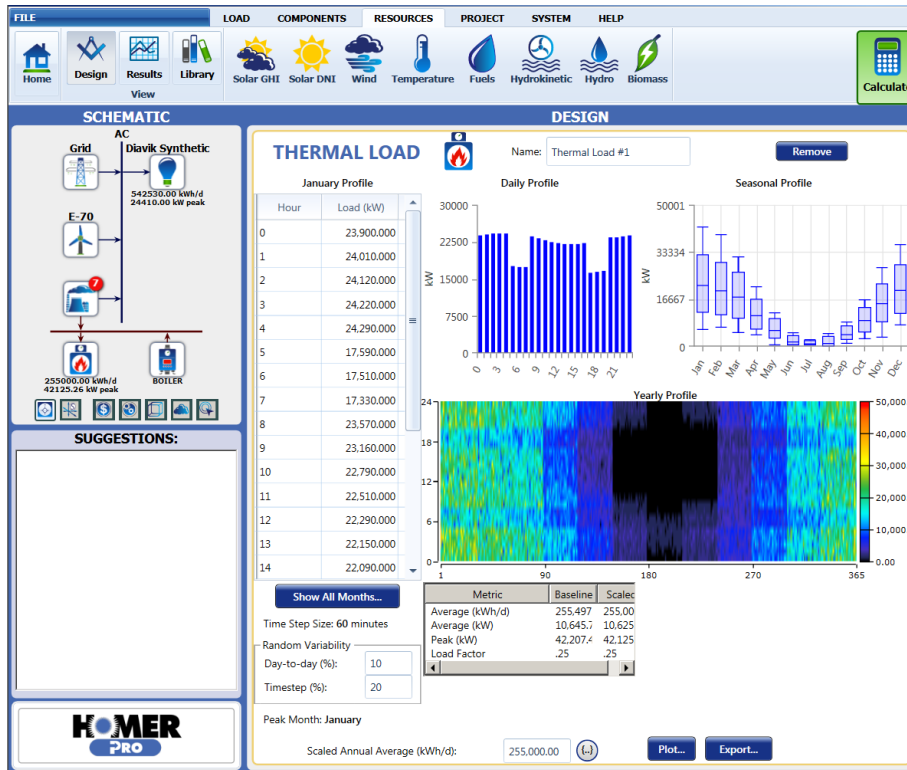


Figure A6-3 Heating load

### A6.2.2 Environmental conditions and renewable sources

HOMER offers the possibility to select the value of several parameters defining the wind resource, such as the average speed, the height of the station and the roughness factor. It is considered that the weather station registered the speed at the same height as the wind turbines, for the station is located in a small island, in the middle of the Great Slave Lake. This consideration is supported by Diavik documentation regarding the wind farm performance. The additional inputs regarding this renewable resource are shown in Table A6-1, and a capture of the software is presented in Figure A6-4.

**Table A6-1 Wind Resource parameters**

Parameter	Units	Value
Altitude above the sea level	[m]	0
Anemometer height	[m]	60
Wind speed profile		logarithmic
Surface roughness height	[m]	0.01
Weibull	[-]	2.4
1 hour autocorrelation factor	[-]	0.85
Diurnal pattern strength	[-]	0.25
Hour of peak wind speed	[h]	15

\*The actual elevation is 416 m, for which results are discussed later.



**Figure A6-4 Wind resource imported**

Ambient temperature values were obtained automatically for the location selected (Figure A6-5).

This compare reasonably well with the temperatures from Inner Whaleback (Figure A6-6)

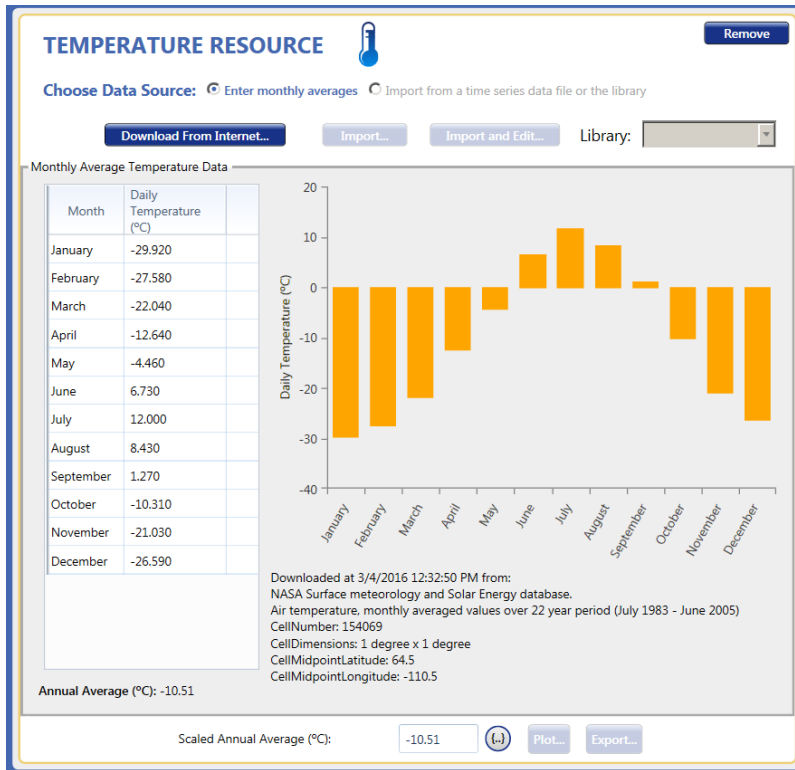


Figure A6-5 Ambient temperatures imported by HOMER

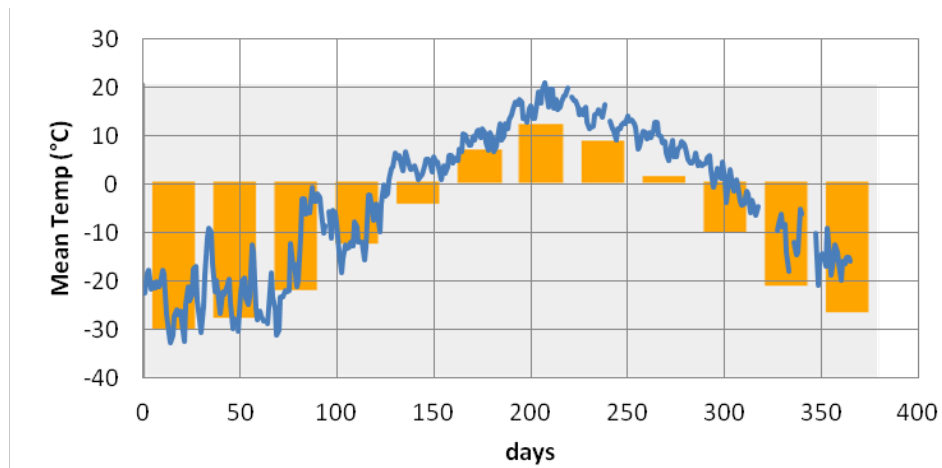


Figure A6-6 Ambient temperature: Inner Whalebacks 2011 (blue line), and HOMER averages (orange bars)

### A6.2.3 Conventional energy sources and energy infrastructure

Diesel can be purchased and imported at an equivalent cost of 130 CAD/MWh (approximately 1.3 CAD/liter). A possible grid extension was included in the scenarios simulated with HOMER. The option “Grid extension” available for the module “Advanced Grid” was selected, for which cost parameters must be introduced (Table 2).

**Table A6-2 Economic parameters for the grid extension**

Parameter	Units	Value
Capital cost	[CAD/km]	400,000
O&M cost	[CAD/yr/km]	8,000
Grid power price	[CAD/MWh]	155

#### *A6.2.4 Technologies available*

##### *Diesel engine*

Conventional diesel generators with heat recovery were modeled following as close as possible those described in Chapter 9 and used onwards. Minimum running time was selected as one hour, which, although it may be a generous assumption, it was the assumption used in OMSES’s simulation. (It may be nevertheless observed that this has a little impact with 9 diesel generators installed, as it is the case of Diavik, when the minimum running time is increased to 180 minutes.) Operating and maintenance costs are adjusted to reflect the cost per hour (Figure A6-7). Lifetime, expressed in hours, is chosen as if each of them were to be running 24/7 for 10 years. However, it is expected that the operation of the engines will include alternation of the units to balance their use and wearing, and thus the actual operating hours of each unit will be significantly lower than the lifetime considered.

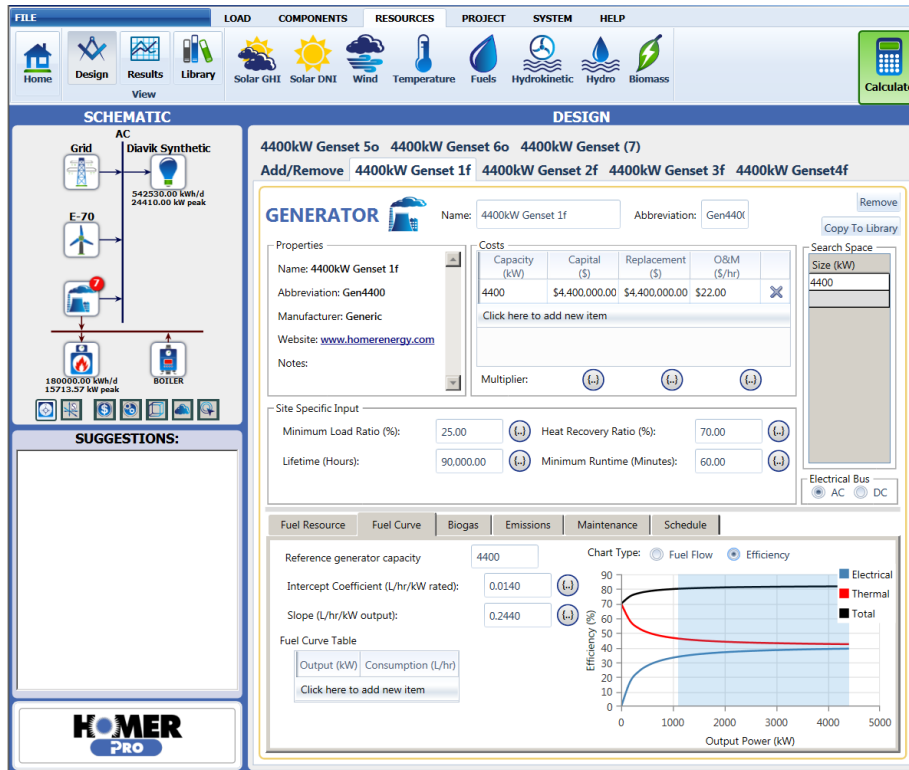


Figure A6-7 – Diesel engine model

### Wind Turbine

Using data from the manufacturer, the Enercon E-70 was modeled. OMSES assumed that the O&M costs of the turbine were embedded in the investment cost; considering 2% of the capital cost, O&M results in 138,000.00 \$ per year. Conservative estimates for the turbine losses were assumed, following Chapter 9. Thus, “Electrical losses” and “Other losses” were assumed to be 20% and 10% respectively. Heaters for the blades and the electronic components of the turbine adapted to Arctic conditions were assumed. A capture of the model is shown in Figure A6-8.

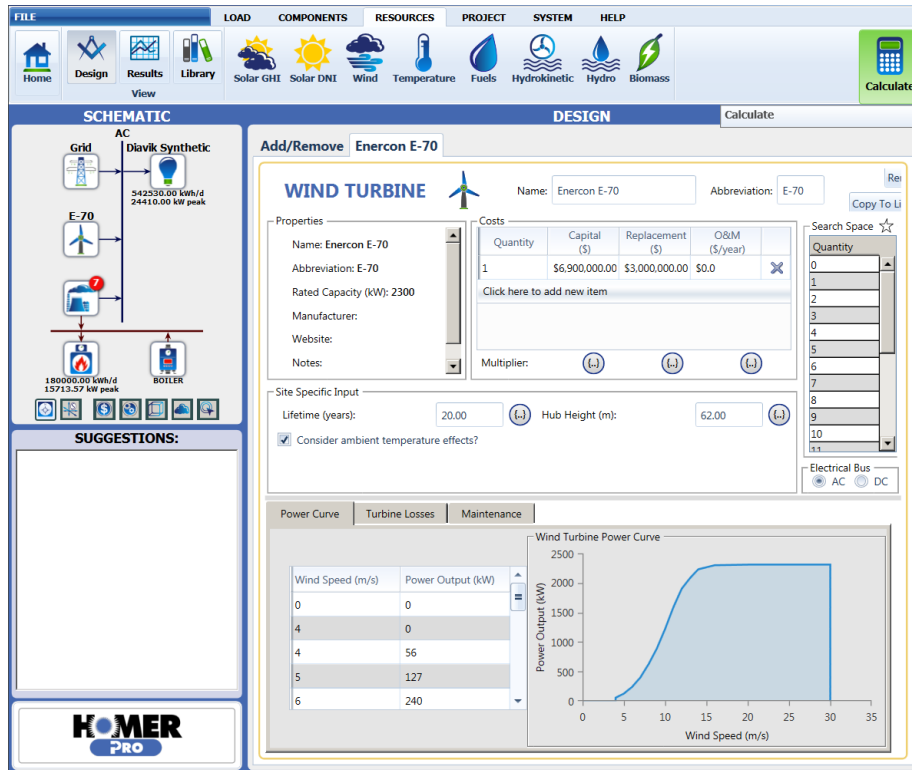


Figure A6-8 – Wind turbine data

### Boiler and thermal load controller

A standard diesel boiler with 80% thermal efficiency was modeled. The component “Thermal load controller” (TLC), which is equivalent to an electric boiler in OMSES, was added to the system selecting the option “Do not include the thermal load controller in the optimization”. This option models the thermal load controller with infinite capacity and no cost. This is justified due to the low installation costs of the electric boilers, which applies in general to fuel boilers, heat exchangers and cooling towers, compared with the diesel engines and wind turbines.

The TLC is also required to dump the excess of electricity produced, which is needed in case of high renewable power penetration. OMSES was designed to account for specific curtailment options, such as pitch control in the case of wind turbines, making it unnecessary resistive loads

to dissipate the excess of power produced, that would be otherwise not used to supply heating loads.

### *A6.2.5 General information*

The remaining economic parameters required to define the optimization problem are summarized in Table A6-3. The life of the project was reduced to 8 years in order to account for the 15% of increase of the capital costs due to engineering, procuring, installation, etc. A project life of 8 years yields a capital recovery factor equal to the product of 1.15 times the capital recovery factor for 10 years project life.

**Table A6-3 General economic parameters**

Parameter	Units	Value
Discount rate	%	10
Inflation rate	%	0
Annual capacity shortage	%	0
Project lifetime*	[year]	8

\*base case

### **A6.3. Scenarios investigated**

Several scenarios were prepared in order to compare the results obtained by OMSES, in particular the sensitivity analysis of Appendix 4. First, the optimal solution was calculated for the aforementioned economic environment. Second, a sensitivity analysis was conducted varying the price of diesel fuel from 0.8 to 1.6 dollars per liter in steps of 10 cents. In addition, the life of the project was progressively increased in order to study its impact in the optimal configuration. Third, and for each of the previous cases, the corresponding break-even grid extension distance was calculated.

For all the scenarios, 7 engines were added to the problem, 5 of them as a fixed part of the solution. Approximately 6 of them are needed to supply the peak power load when the wind does not blow.

## **A6.4. Results and discussion**

### *A6.4.1 Optimal solution*

The optimal solution included 5 wind turbines E-70 and 6 engines. This result agrees with the scenario M8760 in Appendix 7 (detailed demand problem, including 8760 periods, 1 hour long), where the optimal solution (4 wind turbines) when diesel purchase was not constrained. The typical days' models resulted in a minimum value of 8 and a maximum of 11, depending on the daily profile selected. However, as observed in Figure A6-9, the relationship between the number of wind turbines and the parameter "Cost of Energy" (COE) remains almost constant between 2 and 8 units at 294 CAD/MWh. This supports that even for constant daily wind profiles and typical day's models, OMSES yields useful results for low penetration systems, where renewable power does not

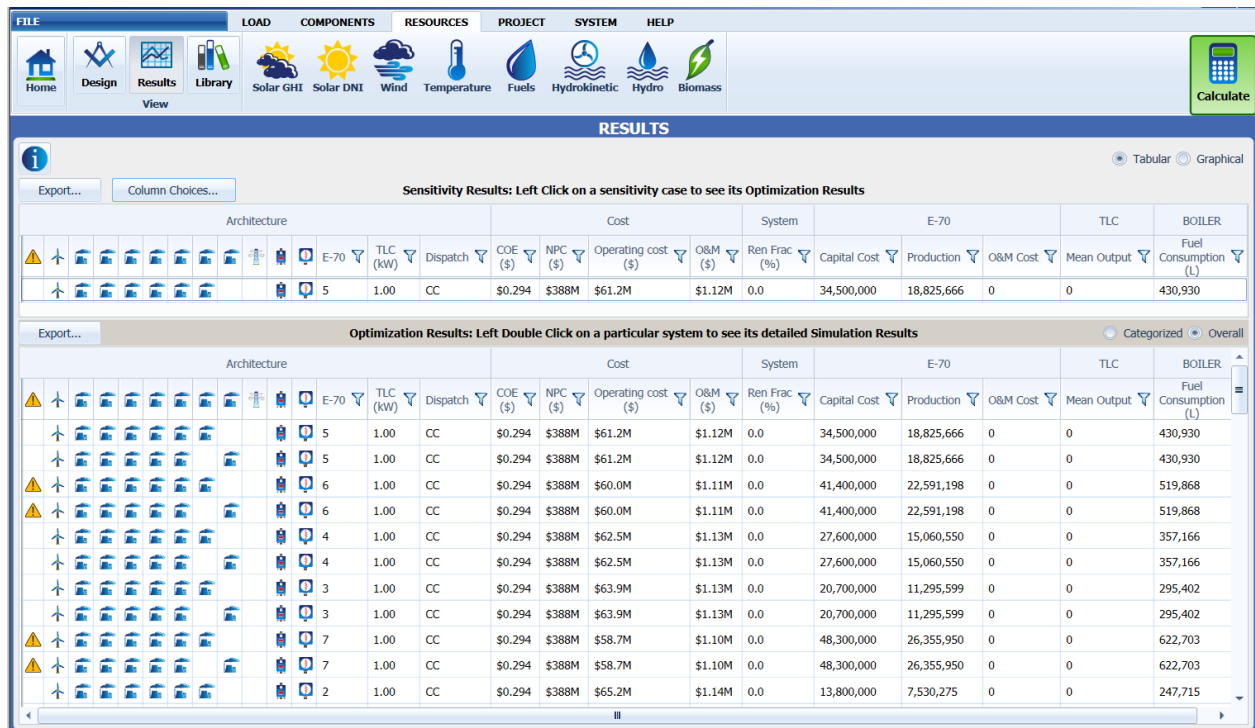


Figure A6-9 HOMER base case results (10 years, diesel @ 1.3 CAD/liter)

#### A6.4.2 Diesel price sensitivity analysis and project life sensitivity analysis

Table 4 summarizes the main outcome of the combined sensitivity analysis, showing the optimal number of wind turbines. This information is complemented with Fig. 8 for the specific case of 1.3 CAD/liter of diesel.

Table A6-4 HOMER optimal number of wind turbines for different values of diesel price and project life time

Diesel price [CAD/liter]	Project life [year]			
	10	15	20	40
0.8	0	2	2	2
0.9	2	2	2	3
1	2	2	7	9
1.1	2	2	11	12
1.2	2	8	12	14
1.3	5	11	14	16
1.4	9	13	16	18
1.5	11	14	18	20
1.6	13	16	20	23

The optimal number of wind turbines for 130 CAD/MWh appears in bold letters. These values should be compared with those same results contained in Chapter 9 and Chapter 12. These chapters considered, when optimizing the system for different project lifetime, an almost flat daily wind speed profile, and a sinusoidal one, respectively.

In Chapter 9 it was concluded that 8 and 29 the optimal number of wind turbines for 10 and 15 years projects when the need spinning reserve was not imposed. When this was the case, the optimal solution yielded 2 wind turbines. Nevertheless, the flat wind profile used overestimated the capacity of the system to integrate renewable energy beyond a certain level of power. Furthermore, the MPC-based simulation indicated that the savings in variable costs exceeded those obtained in the design problem using typical days.

Appendix 7 analysis resulted in 8, 15 and 16 wind turbines for 10, 20 and 40 years of project lifetime. Table A6-4 shows 5, 14 and 16 respectively. This compares with the result for OMSES model with 8760 hours (Appendix 7), for which the optimal number of wind turbines, assuming 10 years and 1.3 CAD/liter, was 4.

Figure A6-10 indicates that there exists diminishing returns in wind turbine additions and project life, so that for an infinite life, i.e., beyond 40 years for a mine with such demands and economical environment, no more than the greatest number of wind turbines to be installed economically lies around 20, with a maximum COE savings of 10%.

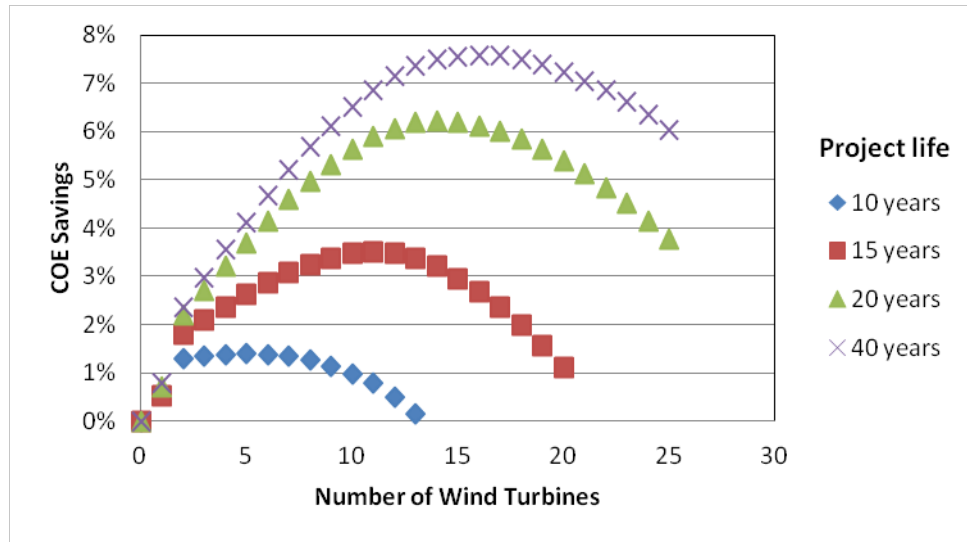


Figure A6-10 HOMER sensitivity analysis showing the savings in COE for different project life and wind turbines

It should be advised that the savings shown in Fig. 8 cannot be compared directly with those of Chapter 9 (Fig. 9-9), for these were calculated for a problem that included the costs of the final demand of diesel, as well as the investment cost in the vehicles for the underground operations.

#### A6.4.3 Grid connection analysis

HOMER’s “Advance Grid” module can calculate the maximum distance for which the installation of a grid results a more cost-effective option than the alternative calculated. Because of the structure of the costs for the hypothetical grid, and the possibility given by OMSES to optimize the connection capacity (Appendix 4), the break-even distances must differ. This can be graphically explained (Figure A6-11) where it can be observed that HOMER grid costs are selected to be as close as possible to OMSES in the range of 150 to 250 km. This means that, below 200 km, the HOMER grid costs are lower, and it will be cost effective to build a 30 MW transmission line, supplying all the power consumed every hour of the year by the mine at the considered grid cost (155 CAD/MWh).

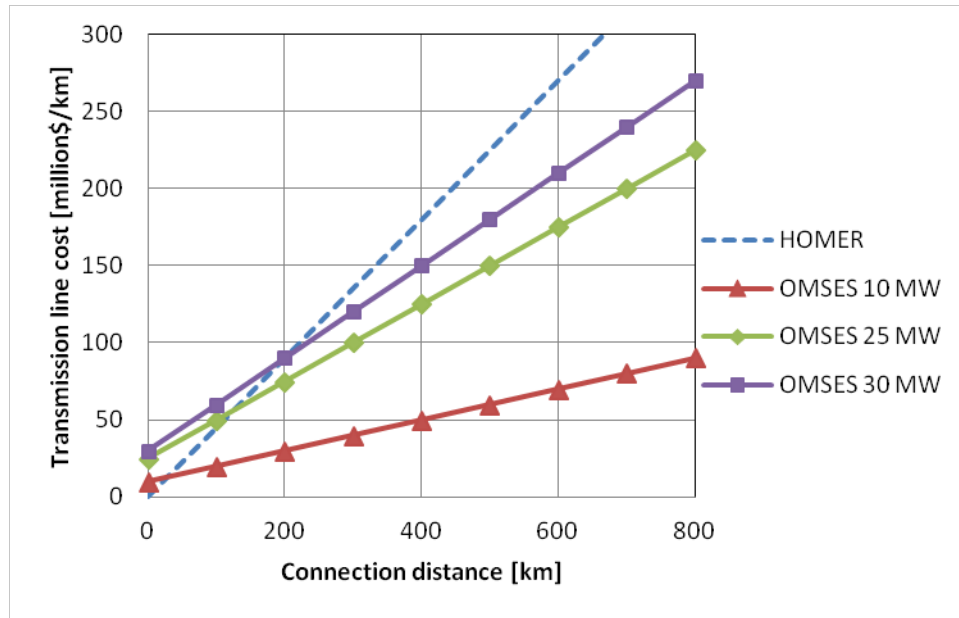


Figure A6-11 – Connection costs considered by HOMER and OMSES

Figure A6-11 shows the breakeven distance calculated by HOMER. In order to facilitate comparison, the background picture shows the results obtained with OMSES (Appendix 4). The influence of different project life was expected: higher life reduces the weight of the investments in the total costs function, and thus increases the breakeven distance. The maximum cost deviation in HOMER is +36% and +63% for a 30 and 25 MW transmission line respectively and a distance of 1000 km.

Nevertheless, results shown in Figure A6-12 indicates that at least qualitatively, the results obtained are agreement, and either way shows with good fidelity how the economic environment influences the decision of being or not off-grid.

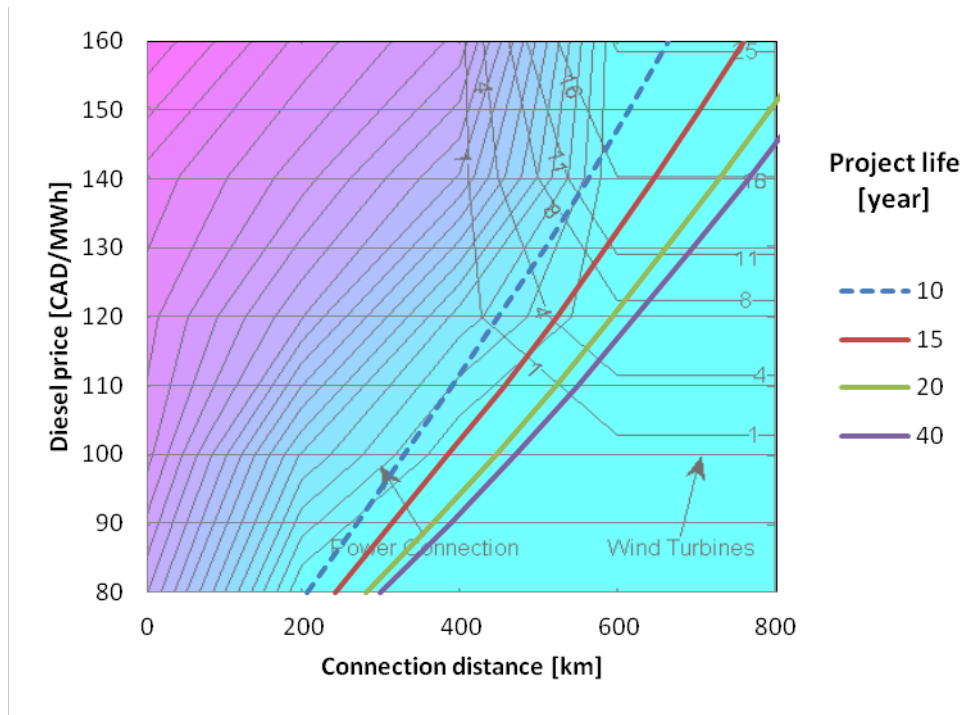


Figure A6-12 – HOMER Breakeven grid extension distance superimposed on OMSES results

Further discussion could follow regarding the optimal combinations of grid, diesel generators and wind turbine using HOMER, but this lies beyond the scope of the present work, and is left for future work.

## **A7. 100% Renewable supply of electricity, heat and cooling for a remote mine**

This work uses OMSES to investigate the potential of hydrogen as an energy carrier to store seasonal energy from wind power. Hydrogen is used later for electricity and heat generation. In the case study included in the present chapter, only electricity, cooling, and heating demands are considered. However, the analysis could be easily extended to include others, such as mobile work demand, as well as related conversion technologies such as hydrogen-fueled mobile equipment.

### **A7.1. Initial Considerations for a 100% Renewable Fueled Mine**

#### *Introduction*

The reasons to consider seasonal energy storage in mining can be summarized as follows. First of all, renewable energy sources, such as solar and wind, present significant output variability in the short (minutes to days) and the long term (months to seasons). However, this brings the opportunity to store potential excess of energy in certain periods for its use in a future time interval. Second, some forms of energy are seasonally available at a lower cost. This may be case of cooling during winter, and heating during summer, being the environment the supplier at a zero marginal cost. Other examples include natural gas and other fossil fuels whose price varies seasonally following customers' demand and grid capacity. Large seasonal thermal energy storage, taking advantage of the local climate, is presently used in Creighton Mine (Schafrik, 2014) and Stobie Mine (Stachulak, 1989), which encourages further research in other types of seasonal storage in the context of mines' ESS.

As of now, no mining facility that stores energy in the form of H<sub>2</sub> has been reported. There is, however, at least a demonstration plant projected on a reduced scale at Raglan Mine, in Quebec (Canada), which is not used for seasonal storage (Simon, 2014). If a mine is to be operated with energy supplied solely from renewable sources with daily and seasonal variability, some sort of long term, physical and chemically stable, energy storage is required. Electric batteries do not represent a practical and cost-effective solution for this objective.

The current trend in H<sub>2</sub> based energy systems is to rely on fuel cells for backup generation to producing when renewable energy is unavailable. Examples from the existing literature have been mentioned in Chapter 4, but it is worth mentioning a study conducted in which a hydrogen internal combustion engine (H<sub>2</sub>-ICE) is used (Ulleberg et al., 2010). The work highlights a trade-off situation involving the cost advantage of the combustion technology and the higher H<sub>2</sub>-to-electricity conversion efficiency of fuel cells. Economic assessment during the whole life of the system is thus necessary to determine the best option.

However, the current state of development of both alternatives makes it difficult to objectively determine the best option. While a significantly worse efficiency (chemical to mechanical energy conversion) is shown for the combustion engine compared with the fuel cell in Ulleberg et al. (2010), an extensive body of research proves that brake efficiencies of H<sub>2</sub>-ICE can even surpass 40% (Verhelst and Wallner, 2009). Furthermore, aspects other than electrical efficiency and cost must be considered. First, a system demanding heat and power may benefit, thermally and economically, from a poorer electrical efficiency in a cogeneration system. Second, contemporary internal combustion engines are more reliable than fuel cells, with a broader operating window of ambient temperature (Ulleberg et al., 2010). Third, the versatility of ICE to operate with different fuel blends is an advantageous feature from different points of view. Gas

engines (burning gasified biomass) that could operate with diesel are recommended by Thomae (1933) as a way of reducing downtime in case of labour strikes in mines. More importantly, some fuel blends are known to improve engine performance without compromising reliability (Verhelst and Wallner, 2009). Finally, it is worth mentioning that in combined cycle mode, where the waste heat gases are recovered in a Rankine cycle, the electric efficiency of gas engines (including those burning H<sub>2</sub>) can be extended up to 60%, or even further (Funatsu et al., 1999; Pilavachi et al., 2009).

### *Literature Review*

Hydrogen as a vector in energy systems has been exhaustively studied since the 1990s. Progress has been made, especially in conversion technologies (electrolyzers and fuel cells) and in systems integration, particularly islanded, with renewable energy sources and electric batteries. Numerous papers have since then studied the performance of such integrated systems, focusing on conversion efficiency (for each component and overall), reliability and control, and costs.

Technical feasibility of the concept was already proven in the early 1990s. The experimental test and computer simulation described in Kauranen et al. (1994) demonstrated that a 100% renewable energy system is possible in a Northern latitude and climate, using energy stored in summer, with a combination of photovoltaic (PV) modules, electrolyzer, fuel cell, hydrogen storage, and batteries. Regarding the system configuration, the authors emphasized the simplicity of their approach (no need for dc-dc converters due to appropriate voltage matching of elements connected in parallel), as well as the need for an adequate control to reduce life consumption of the batteries. Simulations with one-minute time intervals over the order of a few days and

experimental results were used to adjust the computer model parameters. These were used to simulate one-year operation with one-hour intervals.

A later paper described the design and its performance of a near zero energy demand household (Voss et al., 1996) over the course of approximately three years of operation. Consumer demands included power (lighting and appliances, including cooking), heating, and hot water. The nearly 100% solar energy system (a marginal amount of electricity was exchanged with the grid) was based on PV, thermal solar collectors, electrolyzer, fuel cell, and H<sub>2</sub> and O<sub>2</sub> storage. Transparent insulation for the building envelope and electrochemical batteries completed the design. This technical demonstration based its success in a significant demand reduction (through TI) and seasonal storage of high exergy hydrogen, maximizing the use of the annual solar radiation received. Battery aging and the need for state of charge (SOC) control was emphasized.

Another study analyzed the impact of the control strategy on the design of a hybrid seasonal energy storage system in Yuma, Arizona (US) (Vosen and Keller, 1999). Performance and costs were compared for different control strategies (SOC-based control against the use of neural net, NN), and for different storage configuration: single storage (hydrogen or battery) or hybrid (both). One-hour step simulations were run for a single household system case study. From the point of view of the component's efficiency, the inverter efficiency had the largest effect in the calculated levelized cost of energy (LCOE) to be paid by the users. Battery, PV, and H<sub>2</sub> storage (hybrid) costs showed the largest effect in LCOE from the point of sensitivity to components costs. Abundant solar radiation throughout the year permitted a very cost-effective and efficient system.

In Ulleberg (2004), the effects of different control settings on plant performance were again investigated by increasing the scale of the system. The energy system combined PV, H<sub>2</sub>, and batteries to supply power to an office building in Germany. The sizes of the elements were not subject to optimization. The investigation included one year simulations (1-hour intervals) that were used to evaluate the performance of controllers regarding SOC evolution and hydrogen storage production. No cost or overall system efficiency was reported.

An example of energy system optimization was presented in Zoulias and Lymberopoulos (2007). Combined simulation and optimization of standalone power systems (SAPS) was performed using HOMER (Lambert et al., 2006). System costs and performance were compared for three cases: a conventional PV-diesel-battery system and a PV-H<sub>2</sub>-battery with two cost scenarios - current (2007) and future (2020). The application was a small community including ten households located on a Greek island, not inhabited in winter and with peak loads in summer. The promising efficiency and cost values were mainly due to PV direct consumption, as well as the aggregation effect of the demand, which was concentrated during sunlight hours.

Experimental (in a demonstration plant) and simulation results were presented in Brinkhaus et al. (2011). The authors analyzed the results from a PV-H<sub>2</sub>-battery islanded energy system supplying power to a typical household (emulated demand) in the south of Germany. The emphasis of the discussion was again placed on the control of the battery state through frequency regulation of the AC side. Field tests presented included a summer and a winter typical days, and H<sub>2</sub>-battery interaction was discussed. Subsequently, results from one-year simulated operation were shown, for both PV-battery and PV-H<sub>2</sub>-battery systems, being the size of these elements not selected to minimize the LCOE. Over dimensioned PV and control issues were remarked in the former system.

Around the same time, a paper was published that investigated the wider problem of supplying power, fresh water, and fuel for transportation to two off-grid households located on a Greek island (Kyriakarakos et al., 2011). The energy system was optimized (using Particle Swarm Optimization, PSO) imposing 100% renewable energy supply based on a mix of PV-Wind-H<sub>2</sub>-desalination. A Monte Carlo simulation was carried out as well, to investigate the cost-effectiveness of such a combination under input cost uncertainty. Compared with the conventional approach, which entailed the purchase of diesel, gasoline, and fresh water - for power, mobility and domestic uses, respectively - the 100% renewable system was shown to be more economic, with 90% confidence considering current costs (2011), and with 100% confidence under future cost expectations. Seasonal storage of hydrogen and water produced were a key factor for the promising results, although at the expense of high investment costs.

A more recent energy system optimization regarding a single household was presented in Lacko et al. (2014). The optimal design was influenced by the decision to not include batteries for a simulated household power demand without a smooth profile (which may be more realistic than the previous works, though), where peak demand was an order of magnitude higher than the average, and almost two orders higher than the minimum. HOMER was used to calculate the optimal design for this household, located in Slovenia. Then, the design was scaled in size and time to match a pilot plant available that also included PV-Wind-H<sub>2</sub> technologies. Results from experimental and simulated tests were compared, showing comparable results, and thus validating the model. The poor wind resource and the absence of batteries, however, led to weaker results than other previous works here mentioned regarding the system's cost-effectiveness.

An ambitious study recently presented in several publications (Palzer and Henning, 2014b; Henning and Palzer, 2014; Palzer and Henning, 2014a) covered Germany's power demand and building heat demand in a single integrated energy system. The authors answered the question of whether Germany could rely completely on renewable energy for those two energy demands, and what would be the optimal configuration of such a system and its cost. The design optimization problem also included the possibility of a building retrofit (at a certain cost) to reduce systems demand for heating. Due to the magnitude of the problem, three cases were explored: a 100% RE system with no interaction across its boundaries; a RE system with the possibility of limited electricity cross-border exchanges; and a dual RE-fossil fuel system with fixed annual amounts of fossil natural gas consumed.

The outcome of this holistic approach on a national scale was that a system which is 100% based on renewable resources is technically feasible and economically competitive with the current model based mainly on fossil fuels and nuclear power. Special attention was given to the effect of building retrofiting, which offered a trade-off in optimal solutions with an inverse relation between system power capacity (RE and conversion technologies) and retrofit applied.

However, the problem was formulated slightly differently, for the long term energy vector was synthetic methane instead of hydrogen. This conversion pathway is based on research detailed in, Sterner (2009) for example, which relies on the existing natural gas network and associated, well-understood and developed technologies (natural gas boilers and gas turbines) to eliminate the uncertainties derived from large scale, widespread use of hydrogen (Henning and Palzer, 2014).

Currently, the main obstacle for the deployment of a standalone renewable energy system with hydrogen storage is the cost, which exceeds that of conventional (normally diesel fueled) solutions. Economic assessments reveal that, in marginal cases, this integrated approach is cost-effective only when the high investment cost can be assumed either at the beginning of the project or financed throughout part of its life.

Research in long and short term energy storage currently receives, and will continue to receive in future, the attention of many researchers and institutions. Relevant in this regard, though partially covering the problem, is the summarizing effort and cost analysis presented in Zakeri and Syri (2015), for it is well established that life-cycle costs influence the economical feasibility of the schemes presented. In the short and medium term, costs are likely to drive the success of such RE-based systems, ignoring the relevant fact that these are substantially if not completely free of emissions.

## **A7.2. Mine Description**

### *2.1 Mine Utility Demands*

The mine considered in this again Diavik Mine (Chapter 9). Here, the approach is to consider, in addition to the typical day demands profile, annual demands with hourly definition for all 365 days. The use of a greater number of time intervals leads to greater computational difficulty. In order to reduce computational effort, the discussion is centered on the basic demands for electricity, heating and cooling; the demand for mechanical work has not been considered in this chapter, although the effects that it has in terms of electricity, heating, and cooling through the ventilation system have been preserved. The same approach has been considered for the pumping

system, whose electricity consumption has not been discounted from the specific energy term (Section 11.1.1).

As explained in Chapter 3 and Chapter 9, energy intensity indicators regarding electricity, or even diesel, can be adjusted to exclude those final demands that can actually be met with other utilities. The most common example is the use of electricity or heat for cooling demands. In the present chapter, however, it is assumed that certain technologies are to be used, following with the results obtained in Chapter 9, i.e., mechanical chillers and diesel mobile equipment. Accordingly, the use of these technologies imposes certain demand flows, which can be taken into account operating with the coefficients that relate technologies and utilities (Section 3.3.2). As an illustration, the demands for heating and cooling for a known mechanical work demand are next deduced.

$$\dot{Q} = \rho \cdot \dot{q} \cdot C_p \cdot \Delta T = \rho \cdot C \cdot \dot{W} \cdot C_p \cdot \Delta T \quad (12-1)$$

Equation 12-1, expressed in terms of power, is used to calculate ventilation air conditioning loads ( $\dot{Q}$ ) both for summer and winter, as a function of  $\Delta T$ , the difference between the ambient temperature and the temperature setpoint. The variables  $\rho$ ,  $\dot{q}$ ,  $C$ ,  $\dot{W}$ , and  $C_p$  represent, respectively, the air density [ $\text{kg}/\text{m}^3$ ], the ventilation volumetric flowrate [ $\text{m}^3/\text{s}$ ], the ventilation requirement per unit of mechanical work [ $\text{m}^3/\text{s}/\text{MW}$ ], the mechanical work [ $\text{MW}$ ], and the specific heat of the air [ $\text{MJ}/\text{kg}/\text{K}$ ]. As in Chapter 9, it has been assumed that any heat released by underground mobile plants, which would in turn generate a demand for underground cooling, is cancelled by adjusting the setpoint temperature at the intake of the mine.

## 2.2 Economic Data

The selected technologies for this chapter are included in Table A7-1.

Table A7-1 Technologies

Equipment	Nominal Power (MW)	Capital Cost (103 CAD)	O&M Cost (CAD/MWh)	Electricity (EE)	Diesel (DI)	Steam (VA)	Hot Water (HW)	Cooling Water (CW)	Chilled Water (RW)	Ambient Air (AA)	Hydrogen (HY)
Diesel Engine	4.4	4400	5.0	1	2.27		0.80	0.20			
Electric Boiler	3.5	144	1.0	1.11			1				
Diesel Boiler	3.0	130	1.0		1.15		1				
Mech. Chiller	2.7	185	2.0	0.25				1.25	1		
Cooling Tower	5.0	82	5.0	0.02				1		1	
Heat Exchanger	5.0	35	1.0				1.10	1			
Fuel Cell	3.6	7200	10	1		1					2
H <sub>2</sub> ICE	3.6	3600	10	1		0.91	0.52	0.43			2.86
Electrolyzer	5	6500	10	1.47			0.38				1

Installation, procurement, engineering, and other costs are added as 15% of equipment costs. The energy system's capital cost is annuitized using a capital recovery factor, with a 10 year life of equipment and operations and a 10% discount rate, although 20 and 40 years have also been considered. Diesel is acquired in the market (delivered at the mine) at an equivalent cost of 130

CAD/MWh. The cost of the hydrogen storage (pressurized vessel) is considered as 6820 CAD/MWh, a 30% reduction from that of other studies for sizes around 1 MWh (Section 4.6.2). The reason for this is that the scale in the present work is higher (as indicated in the results), which allows for significant unit cost reduction. Heat storage cost is taken as 100 CAD/MWh, smaller than other similar works (Henning and Palzer, 2014), which accounts for the fact that construction of the storage is based on locally available materials and equipment (Ochs et al., 2006).

Wind is considered as the potential renewable source candidate to supply the energy required by the mine. The wind power output is obtained considering the power curve of the E-70 using the wind speed data of Inner Whaleback weather station (Environment Canada, 2014). The same costs and assumptions used in Chapter 9 apply in the present chapter.

### *2.3 Scenarios Investigated*

Regarding the problem of designing a seasonal storage system with OMSES, two options were considered: i) using the *typical days* formulation, and ii) using the more detailed definition of the 8760 consecutive hours of a typical year (Chapter 4). A model such as the latter allows for a better seasonal energy balance than that achieved with the monthly balance, for the wind speed varies from hour to hour, day to day, and between months and seasons. A model containing 8760 consecutive hours also allows for a better seasonal energy storage balance than that achieved with the monthly seasonal balance (Chapter 4).

In addition, typical profiles of wind speed were calculated using a different approach than that used in Chapter 9. Here, three different wind profiles (WP) have been used in as many systems' optimizations. Wind profiles WP1 and WP2 have been selected as truncated, sinusoidal curves

with different frequency and phase (Figure A7-1). WP3 was calculated following the procedure explained in Chapter 4, which yields a fairly constant profile. These three profiles have been normalized with the same *r<sub>mc</sub>* speed, differing only in shape, as shown in Figure A7-1. It is anticipated that the profile selection will have a significant impact on the typology of the optimal solution for high penetration ratios.

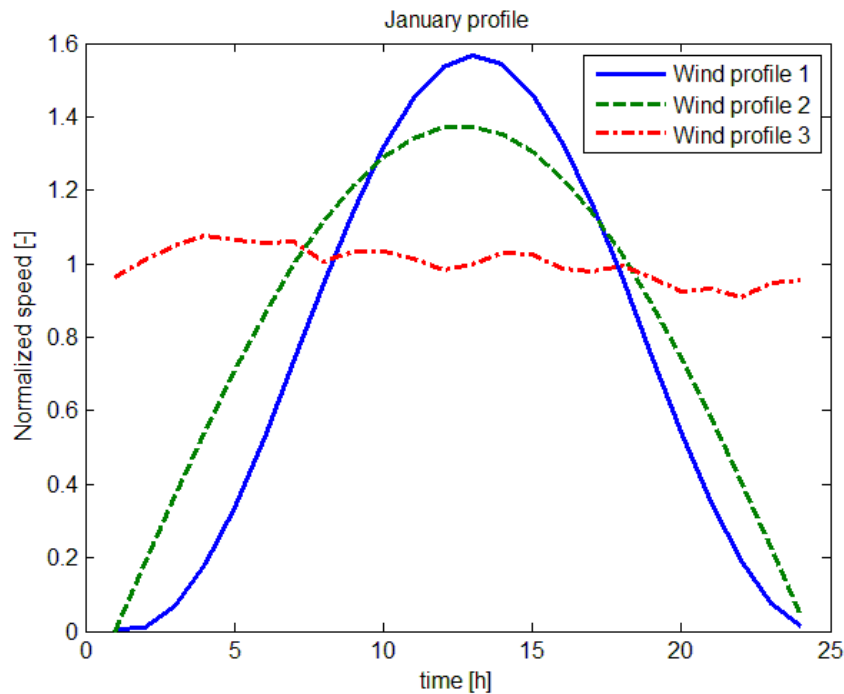


Figure A7-1 Different wind profiles used for January – Wind profiles are calculated according to: wind hourly averages throughout each month (WP1), and two different sinusoidal profiles (WP2 and WP3)

In the scenarios considered here, as opposed to Chapter 9, a fixed number of diesel generators and boilers have not been imposed. This decision was made in order to compare the results obtained with the two time models, with 288 and 8760 hours. In both cases, when WP1 or WP2 is selected, enough engines are installed to deal with periods in which the wind farm, in case of installation, does not produce power. Electricity storage is not considered unless specified. Spinning reserve has not been considered to reduce the computational effort.

In total, 10 scenarios have been investigated. In each of them, the amount of conventional energy source (diesel) has been progressively constrained: 100%, 80%, 60%, 40%, 20% and 0% of the total purchased in the conventional scenario or BAU. The 10 scenarios arise when combining three profiles, two time models, and three values for mine life expectancy – 10, 20 and 40 years. A summary is presented in Table A7-2. In these scenarios, fuel cells are considered as the technology to convert hydrogen into electricity (with a conversion efficiency of 50%). In the last part of the following section, the results comparing fuel cell and hydrogen internal combustion engine will be presented.

**Table A7-2 Summary of the scenarios considered (nomenclature)**

Life	10 years		20 years	40 years
Days	288	8760	288	288
WP1	M02881	M8760	20M02881	40M02881
WP2	M02882	-	20M02882	40M02882
WP3	M02883	-	20M02883	40M02883

### A7.3. Results

In any of the figures below, where the horizontal axis is labeled as *diesel allowance*, the reader should interpret this as a fraction of the diesel consumed in comparison with the conventional energy supply system based exclusively in diesel as the energy resource. In the mathematical formulation, this fraction is used in a constraint on the maximum amount of diesel that can be used in the solution.

#### 3.1 M0288: Optimal Solution for Different Wind Profiles

Figure A7-2 illustrates the trend in total annual costs (TAC) when increasingly flatter profiles are selected to represent the wind resource’s daily variation. The flatter the profile, the higher the load factor of the equipment installed, and therefore the lower the overall installed capacity. This

is reflected in the costs, influenced by the most expensive technologies related to renewable and seasonal storage: wind turbines (WT) and electrolyzers (EZ). Figure A7-3 shows the effect of flatter profiles in the selected equipment; scenario M02883, where almost no seasonal storage and electrolyzers are installed even in the most demanding case of diesel-free solution. The number of wind turbines, however, remains similar for the three profiles, as they keep the same rmc speed, which determines the total energy produced and therefore the installed capacity required to meet the mine's demands.

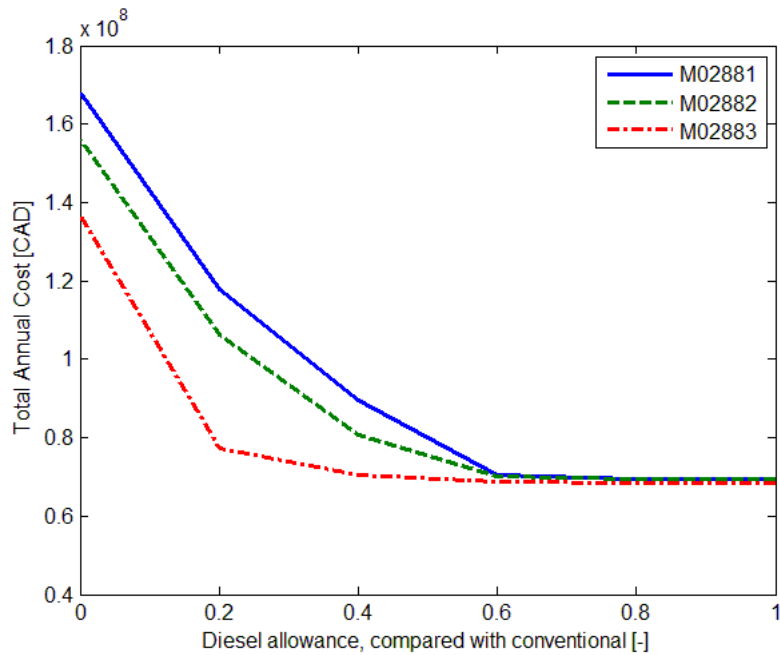


Figure A7-2 Total annual cost variation with diesel allowed, 3 profiles

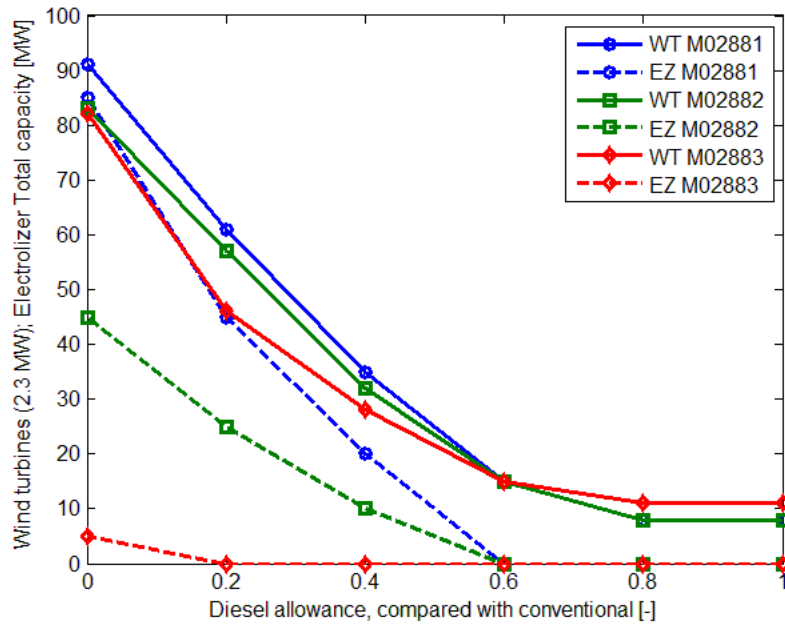


Figure A7-3 Variation of WT and EZ with diesel allowed, 3 profiles

### 3.2 Comparison between Different Time Models M0288 and M8760

Figure A7-4 and Figure A7-5 summarize the comparison between the optimal solution obtained for the energy supply system of the same mine using two time resolutions, one with 288 hours and the other with 8760 hours (models M0288 and M8760 respectively). All the typical days' models have been included in the comparison. It should be noted that in this comparison, batteries are not considered in order to facilitate scenario comparison, although the benefits obtained when those are included are later discussed.

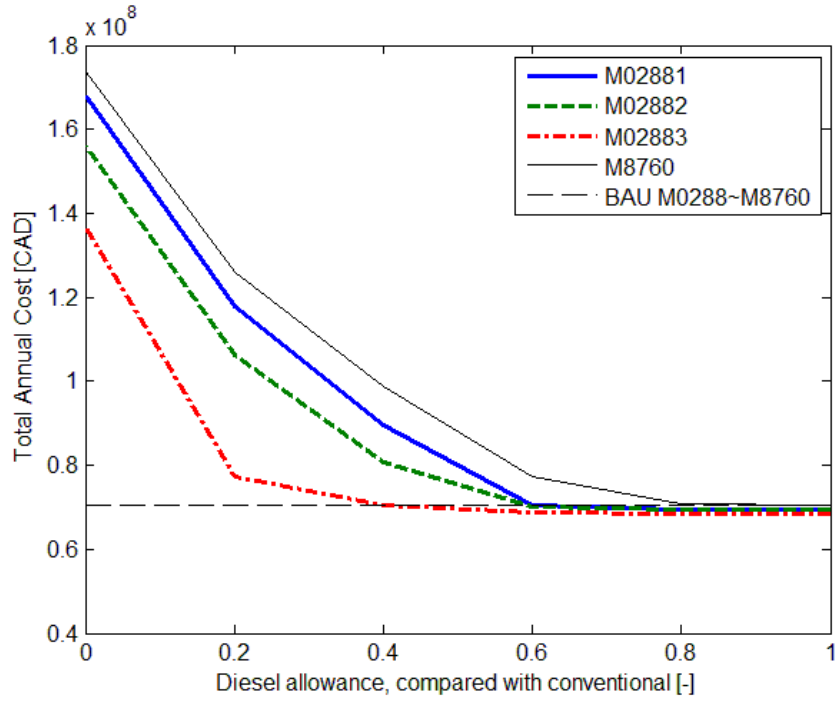


Figure A7-4 Total annual cost variation with diesel allowed. Comparison between 8760 and 288 models

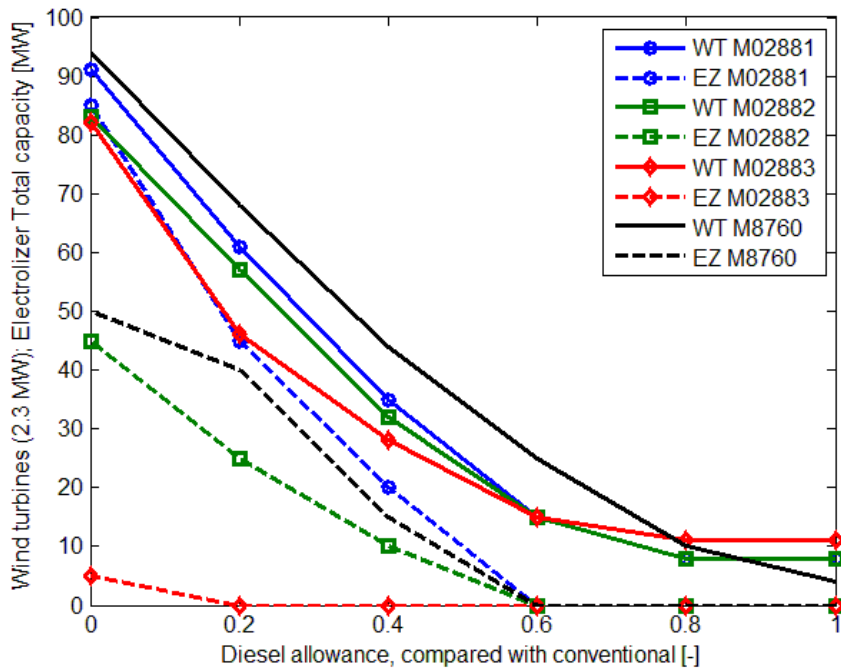


Figure A7-5 Variation of WT and EZ with diesel allowed, Comparison between 8760 and 288 models (Wind profile 1)

M8760 results appear as an upper boundary for the total annual costs, being the difference the lowest compared with M02881 (Figure A7-4). Observing the equipment installed (Figure A7-5), significant differences arise, and several conclusions can be drawn. First, the optimal solution in M8760 when diesel purchased is not constrained includes 4 wind turbines, which is less than the M0288 models. Thus, it can be said that beyond approximately 50% hourly penetration ratio, the returns in the investment decrease.

When constraints in diesel appear, the effort required to produce the same diesel reduction in absence of long term storage is greater for M8760. This leads to a need for more wind turbines (10 units) than M02881 and M02882 (8 units each) to meet 80% diesel allowance, but fewer than M02883 (11 units), which achieves further diesel offset with an additional wind turbine compared with M8760. The lower energy payback per wind turbine for M8760 is due, in general, to the intermittency (including inter-day variation) which is absent from the M02883 model and limited to few hours per day in M02881 and M02882.

A different trend is observed in the electrolysis capacity for the M8760 model, which can be explained by observing the results when, for 20% diesel allowance, electrolysis capacity is set at 30 MW (6 units compared with the previous 8). In this case, the new constrained scenario results in a 0.17% total annual cost increase, with two additional wind turbines and slightly less hydrogen storage capacity (2672 MWh compared with 2890 MWh, Table A7-3). This information and the results in Table A7-3 (M02881) make it clear that for every diesel allowance scenario, different sets of wind turbine, electrolysis, and storage capacity may present similar total annual costs. This offers flexibility for the designers, who could select a particular set under more arbitrary criteria.

[Table A7-3 Installed Hydrogen storage capacity \[MWh\]](#)

	Diesel allowance					
	100%	80%	60%	40%	20%	0%
M02881	0	0	0	539	439	12848
M02882	0	0	0	82	292	19893
M02883	0	0	0	0	0	19927
M8760	0	0	0	743	2890	16316

In both models, seasonal storage is required beyond 40% diesel purchase reduction (or below 60% diesel allowance). Electrolysis capacity for M8760 remains close to M02881 and M02882 up to 80% diesel reduction. In this interval of diesel constraint, hydrogen production is used mainly for intra-month storage, as can be seen in Figure A7-6 (M8760 with a diesel allowance of 20%). For the typical day's models, however, a different storage dynamic result from the fact that all days within each month present the same wind speed conditions, and thus the daily stored energy is consumed within the same day. Both storage mechanisms are fundamentally different; although they produce similar results in terms of the installed capacity of wind turbines and electrolyzers (because ultimately the user's energy demands do not change), they result in a significantly different storage capacity installed (Table A7-3). This is especially the case in scenario M02883, which benefits from an almost constant wind profile. This invalidates the solutions that the three typical days models (M02881, M02882 and M02883) obtain for such diesel allowance constraint.

Figure A7-7 compares the results regarding the annual variation of the hydrogen storage level for M8760 and M02882 when diesel purchase is not allowed. For the latter, the level shown is level for the beginning of each month. The storage capacity is different in both cases, although a similar trend can be observed. The main difference appears during months in which wind output is high enough to store energy for several days and even weeks, a circumstance that the M0288

model cannot register. In general, and as anticipated in Chapter 6, the higher the penetration imposed, the more drastic the difference between the problems aimed to be solved (Chapter 5).

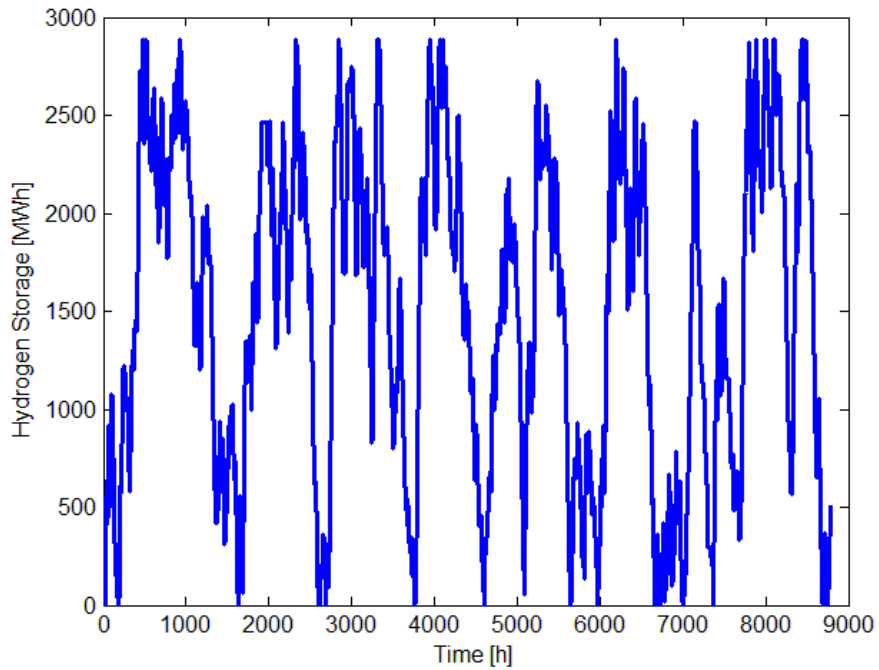


Figure A7-6 Hydrogen storage annual level variation for M8760 with diesel allowance of 20%

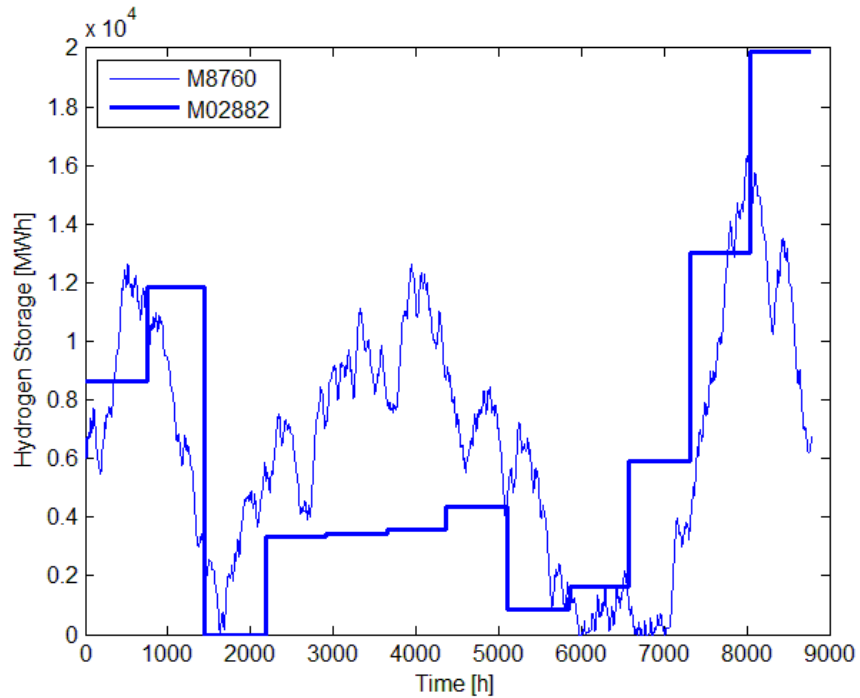


Figure A7-7 100% RE H<sub>2</sub> storage comparison for M8760 (capacity 16317 MWh) and M02882 (capacity 19892 MWh)

### 3.3 Optimal Solution for Different Project Life Using M02881

Figure A7- 8 shows the total annual cost results from the parametrical analysis carried out, in which the project life in the M02881 was manipulated. The longer the project life, the lower the annuitization factor (Chapter 3). The effect of extending the project life on the reduction of TAC is not linear, as it is shown in Figure A7-8. The lower limit of the capital recovery factor when the life increases indefinitely, is CAD 102.5 million. With today's investment costs and assuming a mine's life is between 10 and 20 years, an energy supply system with up to 50% renewable penetration would be cost effective. Further increases in penetration do not result beneficial from the economic point of view. This is valid for M02881, although observing Figure A7-4, at least 40% penetration can be obtained in a cost effective way using the realistic M8760.

Despite the validity of 288 hour models limited to low penetration, the total annual cost involved in the optimal solution may be used here as a first approximation of what the 8760 hours model could yield. As it has been shown, using either M02881 or M8760 results in similar annual costs and equipment installed.

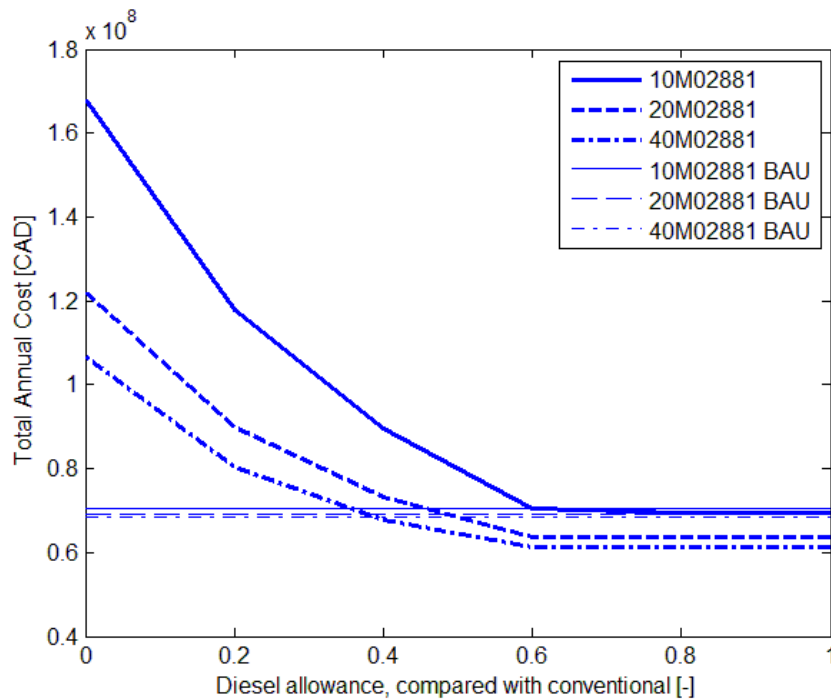


Figure A7-8 Life of the mine influence in TAC

### 3.4 Fuel Cell and Hydrogen Internal Combustion Engine Comparison

Table A7-9 illustrates how the alternative hydrogen technologies (FC and ICE) for mobile equipment compare. Above 40% diesel allowance, the need for seasonal storage is limited (Figure A7-5). Both technologies produce significant amounts of cogenerated heat, which the mine demands in significant amounts. The difference in efficiencies of the technologies, 50% and 35% for FC and H<sub>2</sub>-ICE respectively, can be appreciated in qualitative and quantitative

terms. Lower efficiency involves greater effort to produce and store hydrogen, which translates in higher total annual costs. In all cases, the number of units installed is higher, except for a diesel allowance of 40%, where the number of wind turbine does not increase. Lower efficiencies, however, result in more heat production, which may be advantageous in Arctic regions where there is a significant demand for heating.

**Table A7-9 Hydrogen-electricity conversion technologies comparison**

Diesel allowance	0%		20%		40%	
	FC	H2-ICE	FC	H2-ICE	FC	H2-ICE
Wind turbines [u.]	94	105	68	72	44	44
Electrolyzer [u.]	10	16	8	9	3	5
H <sub>2</sub> storage [MWh]	16316	17966	2890	3123	743	959
Heat storage [MWh]	1947	509	415	400	250	300
TAC [MCAD]	173.8	187.8	125.8	129.7	98.6	99.5

Furthermore, lower diesel allowance involves increasing investment to meet the demands, in agreement with the results previously presented. It is worth highlighting that a diesel allowance of 40% involves that a significant reduction of GHG emissions can be achieved, at approximately the same cost, with either fuel cells or conventional internal combustion engines. This may result in further cost reduction considering the possibility to use dual fuel (diesel, hydrogen) internal combustion engines (Thomae, 1933) and avoid the use of still immature fuel cell technologies, particularly in cold regions (Ulleberg et al., 2010).

#### **A7.4. Conclusions**

Results included in the present work have shown that it is technically feasible to supply electricity, heating, and cooling to a remote mine using exclusively a local renewable energy resource. The scale of the energy supply system makes such an option challenging in comparison with a fossil fuel based system. Unfortunately, still today, the investment costs entailed for a

project life of 10 years using a discount rate of 10% makes the solution uneconomic, more than doubling the total annual cost of the conventional solution based on diesel.

Results showed that a reduction of 80% of diesel reliance is possible and economical when reasonable hypotheses are assumed, such as a mine production plan of 20 years. Moreover, if the investment in the energy system is done progressively, with a gradual increase in the mine's production and therefore the mine's energy demand, the main drawback of high renewable energy penetration can be alleviated.

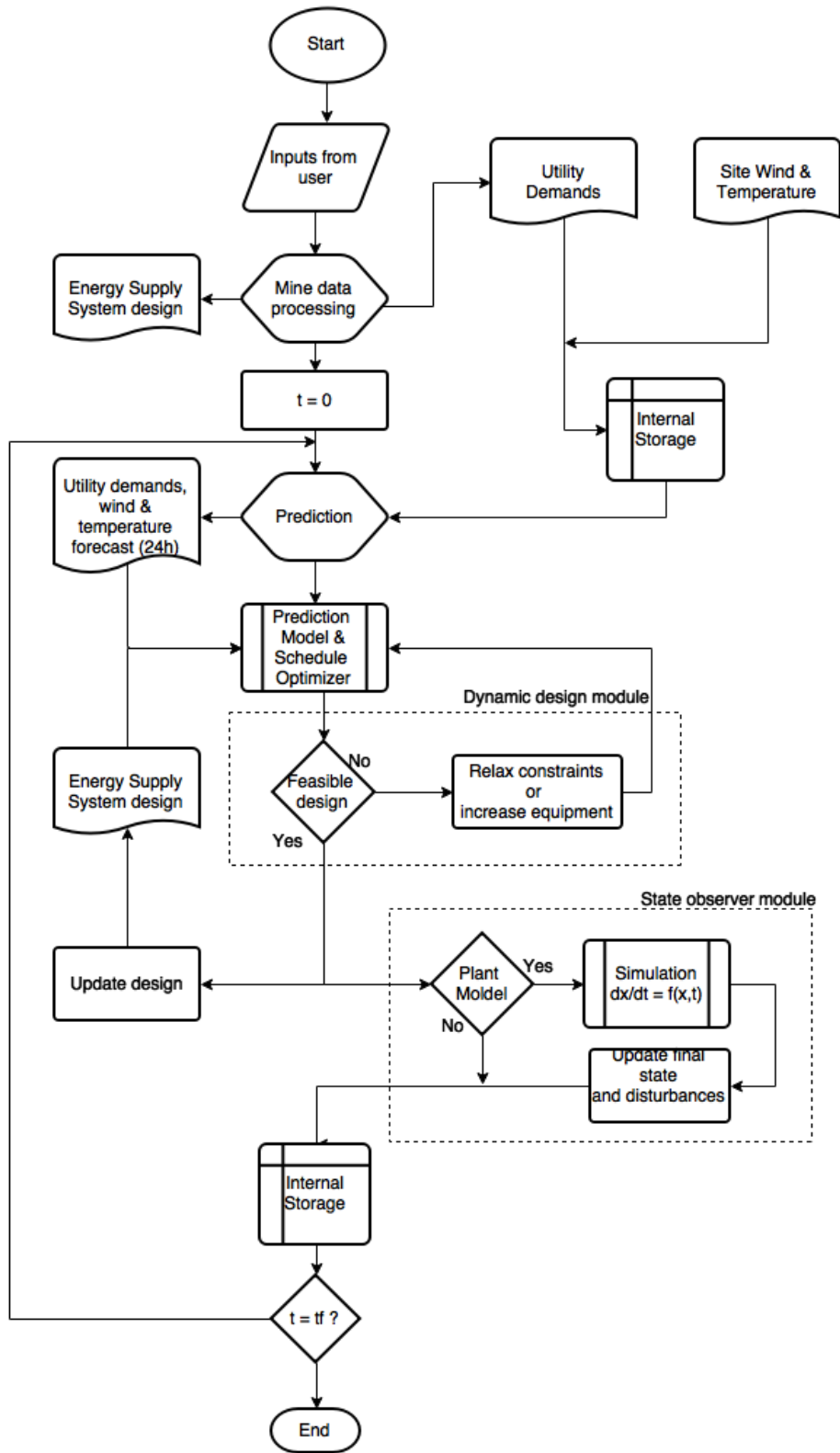
When comparing fuel cells and H<sub>2</sub> internal combustion engines, it was found that the use of the former is competitive between 60% and 40% diesel allowance (or reduction), especially considering that internal combustion engines capable of using fuel blends can be installed avoiding duplicity and reducing the spare parts at the mine site, and considering that fuel cells present reliability problems in cold environments (Ulleberg et al., 2010). When taking into account these fuel cell issues in Arctic regions, and up to 20% reduction in diesel allowance, the H<sub>2</sub>-ICE is still a more reliable and economical option.

This preliminary assessment of 100% RE ESS for a remote mine will require further analysis to account for uncertainty. Costs for certain equipment, including storage, may require the use of sensitivity analysis, because of the scale effects and the future cost trends in technologies not fully commercial. In addition, uncertainty during system operation should be addressed by, for instance, MPC-based simulation, following the concepts introduced in Chapter 5 and applied in Chapter 9 and Chapter 10.

**A8. Flowcharts and Algorithms for MPC and Long Term OMSES  
Implementation**

**A8.1. Model predictive control for optimal operation with dynamic design**

Flowchart



## Matlab main routine

```
%% Last Update 21 Jan 2016
%   Author: Alberto Romero
%   Title:  Operation optimization algorithm for a mine energy system
%   Features:
%       - Hybrid wind-diesel power plant
%       - Energy storage: gas fuel, heat, electricity
%       - Demand side management through dewatering system
%       - Heat storage dynamic model to emulate actual plant
%       - Wind and temperature forecast (24 hours)

function matlin
clc
clear all
format short g
global STHDISC STHCHAR T0 Tamb STHMAX heatloss

% Create object.
ExcelApp = actxserver('Excel.Application');
% Show window (optional).
ExcelApp.Visible = 0;
% Open input/output excel files
file = ExcelApp.Workbooks.Open(fullfile(pwd, 'modelinput.xlsx'));
file1 = ExcelApp.Workbooks.Open(fullfile(pwd, 'utilitydemands.xlsx'));
file2 = ExcelApp.Workbooks.Open(fullfile(pwd, 'PV.xlsx'));
file3 = ExcelApp.Workbooks.Open(fullfile(pwd, 'Results.xlsx'));
file4 = ExcelApp.Workbooks.Open(fullfile(pwd, 'HOEP.xlsx'));
file5 = ExcelApp.Workbooks.Open(fullfile(pwd, 'UD.xlsx'));
file6 = ExcelApp.Workbooks.Open(fullfile(pwd, 'actualwind.xlsx'));
file7 = ExcelApp.Workbooks.Open(fullfile(pwd, 'WIND.xlsx'));
file8 = ExcelApp.Workbooks.Open(fullfile(pwd, 'Windsud2012.xlsx'));
file9 = ExcelApp.Workbooks.Open(fullfile(pwd, 'temperature.xlsx'));

%% Build a whole year vectors
months=['001'   '024'
'025'   '048'
'049'   '072'
'073'   '096'
'097'   '120'
'121'   '144'
'145'   '168'
'169'   '192'
'193'   '216'
'217'   '240'
'241'   '264'
'265'   '288'];
days=[31 29 31 30 31 30 31 31 30 31 30 31]';

contador=0; % used for the dynamic model of the heat storage

%% Loop for the simulation and optimal control for every month "kk" to "kke"
kke=1;
for kk=1:kke
```

```

file1.Activate
UDa=[]; % Auxiliar vector of demands
% Loop for utility demands importing and annual vector generation
for i=1:12
    pickup2=strcat('A',months(i,1:3),' ','I',months(i,4:6));
    Activesheet = ExcelApp.Activesheet.get('Range',str2mat(pickup2)) ;
    UDb(1:24,:)=cell2mat(Activesheet.value);
    repmat(UDb,days(i),1);
    UDa=vertcat(UDa,repmat(UDb,days(i),1));
end

%% Actual wind hourly
windmulti=1; % multiplier to correct for different wind conditions
file6.Activate
Activesheet = ExcelApp.Activesheet.get('Range','A1:A8784');
WINDa(:, :) = windmulti*(cell2mat(Activesheet.value));

%% Actual temperature hourly
% The forecast of temperature is assumed perfect for the next 24 hours.
% What is actually imported is the coefficients that relate temperature
% and heat and cooling demands, as well as the demand for hot water
file9.Activate
Activesheet = ExcelApp.Activesheet.get('Range','K1:L8784');
FNCOEFa(:, :) = (cell2mat(Activesheet.value));
Activesheet = ExcelApp.Activesheet.get('Range','O1:O8784');
DWCHa(:, :) = (cell2mat(Activesheet.value));

%% If only a month is simulated the vectors are initialized to this month
UDa=circshift(UDa,[-24*sum(days(1:kk-1)) 0]); %Offset days
WINDa=circshift(WINDa,[-24*sum(days(1:kk-1)) 0]); %Offset days
FNCOEFa=circshift(FNCOEFa,[-24*sum(days(1:kk-1)) 0]); %Offset days
DWCHa=circshift(DWCHa,[-24*sum(days(1:kk-1)) 0]); %Offset days

%% Add this to include actual temperature influence by OMSES coefficients
% These coefficients relates the ventilation air requirements and the
% heating and cooling.
UDa(:,8:9)=FNCOEFa;
UDa(:,2)=DWCHa;

% Auxiliar vectors
UDaux=UDa(1:24,:);
WINDaux=WINDa(1:24*days(kk),1);
FNCOEFaux=FNCOEFa(1:24*days(kk),:);
DWCHaux=DWCHa(1:24*days(kk),:);

%% Dimension definitions
NET=zeros(24,1);
UD=zeros(24,9);
scenarios=24*days(kk);
RHC=zeros(scenarios,1);
PWIND=zeros(24,1);
PWINDLOW=zeros(24,1);
PWINDi=zeros(24*days(kk),1);

%% Utility Demands (UD) reading
UD(:,:)=UDaux; % this corresponds to the selected month kk

```

```

%% Wind vector set up
AW(1:24*days(kk),:)=WINDaux; % this corresponds to the selected month kk

% Forecast profiles:
% Jan.B Feb.C Mar.D Apr.E May.F Jun.G Jul.H Aug.I Sep.J Oct.K Nov.L Dec.M
wpmnth=['B' 'C' 'D' 'E' 'F' 'G' 'H' 'I' 'J' 'K' 'L' 'M'];
pickup3=strcat(wpmnth(kk),'1:',wpmnth(kk),'24');
%Activesheet = ExcelApp.Activesheet.get('Range',str2mat(pickup3));
Activesheet = ExcelApp.Activesheet.get('Range','B1:B24');
WP(:,1) = (cell2mat(Activesheet.value)); % 24H NORMALIZED WIND PROFILE
WF(:,1) = WP(:,1)*mean(AW(1:3,1)); % 24H FORCASTED WIND [m/s]

%% Energy prices (Not used, although could be sent to file 1 and file 4)
CDI=130; % Diesel [$/MWh]
CPR=80; % Propane [$/MWh]
CBM=30; % Biomass [$/MWh]
CCG=50; % Natural gas[$/MWh]

%% Wind turbine data
Prated=2.3; % [MW]
vmax=12; % [m/s]
vcin=2.5; % [m/s]
acoef=Prated/(vmax-vcin)^2; % [kW/(m2/s2)]
TI=0.2; % Turbulence Intensity
sigmamulti=2; % Sigma multiplier for TI application
NWT=4;

%% Initial equipment to run the dynamic optimization of the design
FMWR=2; % Mechanical chiller (units)
ICWR=2; % Cooling towers (units)
% Files update (for later Lingo reading)
file.Activate
Sheets = ExcelApp.ActiveWorkBook.Sheets;
sheet2 = get(Sheets, 'Item', 2);
invoke(sheet2, 'Activate');
Activesheet = ExcelApp.Activesheet;
eActivesheetRange = ExcelApp.Activesheet.get('Range', 'C10');
eActivesheetRange.Value = FMWR;
eActivesheetRange = ExcelApp.Activesheet.get('Range', 'C11');
eActivesheetRange.Value = ICWR;

%% Storage levels
% Total capacity
STEMAX=0; % [MWh]
STHMAX=10; % [MWh]
STWMAX=984; % [m^3]
STGMAX=0;
% Inital state
STE=STEMAX/2;
STH=STHMAX/2;
STW=STWMAX/2;
STG=0;
heatloss=0; % Heat storage losses, when considered
% Files update (for later Lingo reading)
file.Activate
eActivesheetRange = ExcelApp.Activesheet.get('Range', 'S30');
eActivesheetRange.Value = STEMAX;

```

```

eActivsheetRange = ExcelApp.Activesheet.get('Range', 'S31');
eActivsheetRange.Value = STHMAX;
eActivsheetRange = ExcelApp.Activesheet.get('Range', 'S32');
eActivsheetRange.Value = STWMAX;
eActivsheetRange = ExcelApp.Activesheet.get('Range', 'S33');
eActivsheetRange.Value = STGMAX;

%% Simulation Start
tic
for i=1:scenarios
    penalty=9940;    % This penalty applies to the final state of storage

    file.Activate
    Sheets = ExcelApp.ActiveWorkBook.Sheets;
    sheet1 = get(Sheets, 'Item', 1);
    invoke(sheet1, 'Activate');
    Activsheet = ExcelApp.Activesheet;
    eActivsheetRange = ExcelApp.Activesheet.get('Range', 'R30');
    eActivsheetRange.Value = STE;
    eActivsheetRange = ExcelApp.Activesheet.get('Range', 'R31');
    eActivsheetRange.Value = STH;
    eActivsheetRange = ExcelApp.Activesheet.get('Range', 'R32');
    eActivsheetRange.Value = STW;
    eActivsheetRange = ExcelApp.Activesheet.get('Range', 'R33');
    eActivsheetRange.Value = STG;
    eActivsheetRange = ExcelApp.Activesheet.get('Range', 'Q34');
    eActivsheetRange.Value = NWT;
    eActivsheetRange = ExcelApp.Activesheet.get('Range', 'Q35');
    eActivsheetRange.Value = penalty;
    eActivsheetRange = ExcelApp.Activesheet.get('Range', 'Q36');
    eActivsheetRange.Value = heatloss;

    file5.Activate
    eActivsheetRange = ExcelApp.Activesheet.get('Range', 'A1:I24');
    eActivsheetRange.Value = UD;

for j=1:24
    ror(j)=(1.2999-0.0048*(20-UD(j,2)/0.1))/1.225; % corrected density
    if WF(j)>vcin
        PWIND(j,1)=round(ror(j)*min(Prated,acoe*(WF(j)-vcin)^2)*1e3)/1e3;
        PWINDLOW(j,1)=round(ror(j)*min(Prated,acoe*(WF(j)*(1-2*TI)-...
            vcin)^2)*1e3)/1e3;
    else
        PWIND(j,1)=0;
        PWINDLOW(j,1)=0;
    end
    if PWIND(j,1)==0
        PWIND(j,1)=0;
    end
end
PWINDi(i)=PWIND(1,1);
PWINDilow(i)=PWIND(1,1);
% Files update (for later Lingo reading)
file7.Activate
eActivsheetRange = ExcelApp.Activesheet.get('Range', 'W1:W24');
eActivsheetRange.Value = PWIND;
eActivsheetRange = ExcelApp.Activesheet.get('Range', 'Y1:Y24');

```

```

eActivsheetRange.Value = PWINDOW;

%% Run Lingo (24 hours horizon optimization)
system('C:\LINGO11\RunLingo
C:\Users\aromero.CORP\Desktop\PhD\MPC\Lingo\P2H\matlin.ltf')
%%%%%%%%%%%%%%%%%%%%%%%%%%%%%%%%%%%%%%%%%%%%%%%%%%%%%%%%%%%%%%%%%%%%%%%%
%% Results from Lingo
file3.Activate
Activsheet = ExcelApp.Activesheet.get('Range', 'E41');
COST(i) = (Activsheet.value);
Activsheet = ExcelApp.Activesheet.get('Range', 'O42:O43');
EXTRA(:,1) = cell2mat(Activsheet.value);

%% OPTIONAL MODULE: Dynamic design loop with different options (with and
without while loop)
% while COST(i)<=0
    FMWR=FMWR+EXTRA(1,1)
    ICWR=ICWR+EXTRA(2,1)
    file.Activate
    Sheets = ExcelApp.ActiveWorkBook.Sheets;
    sheet2 = get(Sheets, 'Item', 2);
    invoke(sheet2, 'Activate');
    Activsheet = ExcelApp.Activesheet;
    eActivsheetRange = ExcelApp.Activesheet.get('Range', 'C10');
    eActivsheetRange.Value = FMWR;
    eActivsheetRange = ExcelApp.Activesheet.get('Range', 'C11');
    eActivsheetRange.Value = ICWR;
%
% system('C:\LINGO11\RunLingo
C:\Users\aromero.CORP\Desktop\PhD\MPC\Lingo\P2H\matlin.ltf')
% Activsheet = ExcelApp.Activesheet.get('Range', 'E41');
% COST(i) = (Activsheet.value);
% end
FMWRaux(i)=FMWR;
ICWRAux(i)=ICWR;
% Dynamic design loop end

file3.Activate
Activsheet = ExcelApp.Activesheet.get('Range', 'E2:E25');
NET(:,i) = round(cell2mat(Activsheet.value));
Activsheet = ExcelApp.Activesheet.get('Range', 'E41');
RHC(i) = (Activsheet.value);
Activsheet = ExcelApp.Activesheet.get('Range', 'O6');
GEN(i) = (Activsheet.value);
Activsheet = ExcelApp.Activesheet.get('Range', 'O12');
HEAT(i) = (Activsheet.value);
Activsheet = ExcelApp.Activesheet.get('Range', 'O14');
DIESEL(i) = (Activsheet.value);
Activsheet = ExcelApp.Activesheet.get('Range', 'O15');
NMDSR(i) = (Activsheet.value);
Activsheet = ExcelApp.Activesheet.get('Range', 'O7');
NMDS(i) = (Activsheet.value);
Activsheet = ExcelApp.Activesheet.get('Range', 'O13');
EWIND(i) = (Activsheet.value);
Activsheet = ExcelApp.Activesheet.get('Range', 'O16');
NWTS(i) = (Activsheet.value);
Activsheet = ExcelApp.Activesheet.get('Range', 'O17');
EENGH(i) = (Activsheet.value);

```

```

Activesheet = ExcelApp.Activesheet.get('Range','O8');
DIESELUG(i) = (Activesheet.value)/0.3;
DIESELSF(i) = UD(1,3);
Activesheet = ExcelApp.Activesheet.get('Range','E23');
QCD = (Activesheet.value);
file3.Activate
Activesheet = ExcelApp.Activesheet.get('Range','P2');
STE = (Activesheet.value);
Activesheet = ExcelApp.Activesheet.get('Range','P3');
STH = (Activesheet.value);
Activesheet = ExcelApp.Activesheet.get('Range','P4');
STW = (Activesheet.value);
Activesheet = ExcelApp.Activesheet.get('Range','P5');
STG = (Activesheet.value);
STEi(i)=STE;
STHi(i)=STH;
STWi(i)=STW;
STGi(i)=STG;

%% OPTIONAL MODULE: State observer model for heat storage using ODE
file9.Activate
pickup3=strcat('A',num2str(24*sum(days(1:kk-1))+i));
Activesheet = ExcelApp.Activesheet.get('Range',pickup3);
Tamb = (Activesheet.value);

file3.Activate
Activesheet = ExcelApp.Activesheet.get('Range','O40');
STHDISC = (Activesheet.value);
Activesheet = ExcelApp.Activesheet.get('Range','O39');
STHCHAR = (Activesheet.value);

STHDISCaux(i)=STHDISC;
STHCHARaux(i)=STHCHAR;

simtime=3600;%input('introduce tiempo de simulacion');
tincremento=1;
tsim=[0:tincremento:simtime];
if i==1
    initx=(90+50)/2;
    T0=(90+50)/2;
    Ttotal=T0;
    initx=T0;
else
    initx=T0;
end
[t x]=ode23('fSTH',tsim,initx);
T0 = x(simtime/tincremento+1);
Tfaux(i)=T0;
Ttotal=horzcat(Ttotal,x(2:simtime)');

% Feedback model update
%STH=215000*4.2/3.6*(T0-50)*1e-6,0;
if STH>=STHMAX || STH<=0
    STH=min(STHMAX,max(STH,0));
    contador=contador+1;
end

```

```

% Updating the ammount of heat required to maintain the level (optional)
%   if STHi(i)>=215000*4.2/3.6*(T0-50)*1e-6 && T0<50
%       HEATaux(i)= (STHi(i)-215000*4.2/3.6*(T0-50)*1e-6)*1.2;
%       T0=50;
%   end
%   STHi(i)=STH;
% Dynamic model for heat storage end

%% Update forecasts
UDa = circshift(UDa, [-1 0]); % Utility demands
UD=UDa(1:24,:);
WF = circshift(WF, [-1 0])*(AW(1,1)/WP(1,1)+...
    AW(2,1)/WP(2,1)+AW(3,1)/WP(3,1))/3; % Wind forecast 24h based on
three next hours
WP = circshift(WP, [-1 0]); % Wind profile monthly
AW = circshift(AW, [-1 0]); % Actual wind

% For other wind forecast options
% WF(:,1)= AW(1,1); % Persistent wind
% WF(1:3,1)= AW(1:3,1); % For perfect next 3 hour forecast
%%%%%%%%%%%%%%%%%%%%%%%%%%%%%%%%%%%%%%%%%%%%%%%%%%%%%%%%%%%%%%%%%%%%%%%%

[kk i STG] % Simulation progress command window

end
toc
%% End of simulation for the month kk

sumGEN(kk)=sum(GEN(1:24*days(kk)));
sumDIESEL(kk)=sum(DIESEL(1:24*days(kk)));
sumDIESELSR(kk)=sum(NMDSR(1:24*days(kk))/0.40048*0.1);
sumHEAT(kk)=sum(HEAT(1:24*days(kk))*1.15);
sumDIESELUG(kk)=sum(DIESELUG(1:24*days(kk)));
sumDIESELSF(kk)=sum(DIESELSF(1:24*days(kk)));

hold on

end

%% Close excel connections
file.Save;
file.Close;
file1.Save;
file1.Close;
file2.Save;
file2.Close;
file3.Save;
file3.Close;
file4.Save;
file4.Close;
file5.Save;
file5.Close;
file6.Save;
file6.Close;
file7.Save;
file7.Close;
file8.Save;

```

```
file8.Close;  
file9.Save;  
file9.Close;  
ExcelApp.Quit;  
ExcelApp.release;
```

### *Matlab dynamic model subroutine (differential equations)*

```
function xp=fSTH(t,x);
global STHDISC STHCHAR Tamb STHMAX heatloss
xp=zeros(1,1); % size of the ODE system dx/dt=f(x,t)
UAint=3e5; % Overall heat transfer coefficient for charge process[W/K]
UAamb=1e3; % Overall heat transfer coefficient for external losses[W/K]
M=215000; % Mass of the heat storage system (assuming water)[kg]
Cp=4200; % Specific heat for heat storage (assuming water)[J/kg-K]
Tc1=90; % Inlet temperature of the hot fluid (charging) [C]
Tc20=50; % Minimum exit temperature of the hot fluid (charging) [C]
C=STHMAX*1e6/(Tc1-Tc20);% Fluid heat capacity m.Cp for charging fluid [W/K]

xp(1)=( UAint*(90-x(1))/(1+UAint/(2*STHCHAR/STHMAX*C)) +...
0*STHCHAR*1e6 - STHDISC*1e6 - UAamb *(x(1)-Tamb))/(M*Cp);
heatloss=UAamb *(x(1)-Tamb)/1e6;
```

## *Lingo optimization subroutine (schedule optimizer for rolling horizon)*

```
! Last Update 21 Jan 2016;
! Author: Alberto Romero;
! Title: Operation optimization algorithm for a mine energy system;
! Features;;
!   - Hybrid wind-diesel power plant;
!   - Energy storage: gas fuel, heat, electricity;
!   - Demand side management through dewatering system;
!   - Heat storage dynamic model to emulate actual plant;
!   - Wind and temperature forecast (24 hours);

MODEL:
    TITLE Selection of technologies;

DATA:
! Imports from .txt file that are not modified by matlab function;
! A very big number compared to the energy flows of the system;
    BIGR = 2000.;
! Note that we changed this from 200 to 2000 because when using different
    unities, i.e., m3/h, the constraints has to accept it
! A very big number compared to the number of pieces of equipment in the
system;
    BIGN = 2000;    ! Idem
! YVE Sale of electricity allowed (no/yes = 0/1);
    YVE    = @FILE('modelinput.ldt');
! YCE Purchase of electricity allowed (no/yes = 0/1);
    YCE    = @FILE('modelinput.ldt');
! YDQ Waste of heat allowed (no/yes = 0/1);
    YDQ    = @FILE('modelinput.ldt');
! ACEMIN Minimum self-consumption of electricity;
    ACEMIN = @FILE('modelinput.ldt');
! PCG Market price for natural gas ($/MWh);
    PCG    = @FILE('modelinput.ldt');
! PCE Purchase price of electricity($/MWh);
    PCE    = @FILE('modelinput.ldt');
! CECP/CECV On-peak/Off-peak coefficient for purchase of electricity;
    CECP, CECV = @FILE('modelinput.ldt');
! PVE Sale price of self-generated electricity($/MWh);
    PVE    = @FILE('modelinput.ldt');
! CEVP/CEVV On-peak/Off-peak coefficient for sale of electricity;
    CEVP, CEVV = @FILE('modelinput.ldt');
! Factor of indirect inversion costs;
    FCI = @FILE('modelinput.ldt');
! Maintenance and capital recovery factor;
    FAM = @FILE('modelinput.ldt');
! Purchase price of diesel;
    PDI = @FILE('modelinput.ldt');
! Purchase price of biomass;
    PBM = @FILE('modelinput.ldt');
ENDDATA

SETS:
! Utilities (j)      1. CG natural gas;
```

```

!           2. VA high pressure steam;
!           3. WC hot water;
!           4. WR cooling water;
!           5. AA ambient air;
!           6. WF cold water;
!           7. EE electricity;
!           8. DI diesel;
!           9. BM biomass;
!          10. DW dewatering;
!          11. AV acconditioned ventilation;
!          12. Mobile work;
UTIL /CG,VA,WC,WR,AA,WF,EE,DI,BM,DW,AV,MW/: INDPUR, INDDDEM, INDSEL, INDWAS;
ENDSETS

```

```

DATA:
INDPUR,          INDDDEM,          INDSEL,          INDWAS          =          @OLE(
'C:\Users\aromero.CORP\Desktop\PhD\MPC\Lingo\P2H\modelinput.xlsx', 'INDPUR',
'INDDDEM', 'INDSEL', 'INDWAS');
ENDDATA

```

```

SETS:
! Technologies (i) 1. TGVA gas turbine           - cogenerates high
pressure steam;
!                 2. MGWC gas engine           - cogenerates hot water;
!                 3. CGVA steam boiler         - produces high
pressure steam;
!                 4. CGWC gas boiler           - produces hot water;
!                 5. ICVA heat exchanger      - high pressure
steam-->hot water;
!                 6. ICWC heat exchanger      - hot water-->cold
water;
!                 7. FAVA DE absorption chiller - operates on high
pressre steam;
!                 8. FAWC SE absorption chiller - operates on hot
water;
!                 9. FMWR enfriadora mecanica - operates on
electricity;
!                 10. ICWR Cooling tower      - cooling water--
>ambient air;
!                 11. DIWC Diesel engine      - See utility
exchanges below;
!                 12. GFBM Gasifier           - ...;
!                 13. FTDI FT unit;
!                 14. BMWC Biomass boiler;
!                 15. DIBO Diesel boiler;
!                 16. EEWC Hot water electric boiler;
!                 17. TGDI Diesel fuelled gas turbine;
!                 18. BMVA Biomass steam boiler;
!                 19. STVA Steam turbine;
!                 20. PMDW Dewatering pump;
!                 21. FNAV Fan acconditioned ventilation;
!                 22. DIMW Diesel fuelled vehicle;
!                 23. EEMW Electric fuelled vehicle;
!                 24. STVA Natural gas fuelled vehicle;
!                 25. EENG Power to gas technology;

```

```

TECN /TGVA, MGWC,CGVA, CGWC,ICVA, ICWC,FAVA, FAWC, FMWR,

```

```

ICWR, DIWC, GFBM, FTDI, BMWC, DIBO, EEWC, TGDI, BMVA,
STVA, PMDW, FNAV, DIMW, EMMW, NGMW, EENG/: YPT, NET,
PET, PIN, CBM, FOV, CIN, PRA;

! YPT Presence of equipment          ( no/yes = 0/1 );
! NET Number of pieces of equipment  ( 0, 1, .... );
! PET Nominal power of equipment      (MW);
! PIN Installed power                 (MW);
! CBM Cost of installed equipment     ($);
! FOV Variable maintenance and operation costs ($/MWh);
! CIN Investment                      ($);
! PRA Annual production               (MWh/year);
ENDSETS

SETS:
! Days (kd)          1. January          ;
  DAYS/ JANUARY
    /: NDA, IDT_INV,
      DVAD, DWCD, DWFD, DEED, DDID,
      CCGD, CEED, VEED, CDID, CBMD,
      CTECGD, CTECED, INGVED, CTEOMD, CVARID, CTEDID, CTEBMD,
      GA, GAO, LD, DDWD ,VDWD, CAVD, DAVD, DMWD, DWIND, DWINDWASTE;

! NDA      Number of days per year (days/year);
! IDT_INV Indicates that the day corresponds to winter electric invoicing (
no/yes = 0/1 );
! DVAD     Steam demand                (MWh/day);
! DWCD     How water demand             (MWh/day);
! DWFD     Cold water demand           (MWh/day);
! DEED     Electricity demand          (MWh/day);
! DDID     Diesel demand;
! CCGD     Purchase of natural gas     (MWh/day);
! CEED     Purchase of electricity     (MWh/day);
! VEED     Sale of electricity         (MWh/day);
! CDID     Purchase of diesel          (MWh/day);
! CBMD     Purchase of biomass         (MWh/day);
! CTECGD   Natural gas cost            ($/day);
! CTECED   Electricity cost            ($/day);
! INGVED   Profit with sale of electricity ($/day);
! CTEOMD   Variable Operation and maintenance cost ($/day);
! CVARID   Total variable cost        ($/day);
! CTEDID   Diesel cost                 ($/day);
! CTEBMD   Biomass cost                ($/day);

! Hours (kh)  1.      1AM 00.00 -> 00.59;
!
!              ...
!              12. 12PM 23.00 -> 23.59;
HOURS /1AM 2AM 3AM 4AM 5AM 6AM 7AM 8AM 9AM 10AM 11AM 12AM
      1PM 2PM 3PM 4PM 5PM 6PM 7PM 8PM 9PM 10PM 11PM 12PM
      /: NHD;
ENDSETS

DATA:
NHD = @OLE (
'C:\Users\aromero.CORP\Desktop\PhD\MPC\Lingo\P2H\modelinput.xlsx', 'NHD');
NDA = @OLE (
'C:\Users\aromero.CORP\Desktop\PhD\MPC\Lingo\P2H\modelinput.xlsx', 'NDA');

```

```

PET,          CBM,          FOV          =          @OLE (
'C:\Users\aromero.CORP\Desktop\PhD\MPC\Lingo\P2H\modelinput.xlsx', 'PET',
'CBM', 'FOV');
NET          =          @OLE (
'C:\Users\aromero.CORP\Desktop\PhD\MPC\Lingo\P2H\modelinput.xlsx', 'NET');
ENDDATA

```

SETS:

```
! TecnUtil (i,j);
```

```

TEUT      (TECN,UTIL)/          TGVA,CG          TGVA,VA          TGVA,WC
TGVA,EE
MGWC,EE          MGWC,CG          MGWC,VA          MGWC,WC          MGWC,WR
CGVA,CG  CGVA,VA
CGWC,CG          CGWC,WC
ICVA,VA  ICVA,WC
ICWC,WC  ICWC,WR
FAVA,VA          FAVA,WR          FAVA,WF
FAVA,EE          FAWC,WC  FAWC,WR          FAWC,WF
FAWC,EE          FMWR,WR          FMWR,WF
FMWR,EE          ICWR,WR          ICWR,AA
ICWR,EE          DIWC,WC          DIWC,WR
DIWC,EE  DIWC,DI          GFBM,CG          GFBM,VA
GFBM,BM          FTDI,CG          FTDI,VA
FTDI,DI          BMWC,WC
BMWC,BM          DIBO,WC
DIBO,DI          EEWC,WC
EEWC,EE          TGDI,VA          TGDI,WC
TGDI,EE  TGDI,DI          BMVA,VA
BMVA,BM          STVA,VA          STVA,WR
STVA,EE          PMDW ,EE          PMDW
,DW          FNAV ,WR          FNAV ,WF          FNAV ,EE
FNAV ,AV          DIMW,WC
DIMW,DI          DIMW, AV          DIMW,MW
EMMW, AV          EMMW,MW          EMMW,WC          EMMW,EE
NGMW,CG          NGMW,WC
NGMW,AV  NGMW,MW          EENG,CG  EENG,WC  EENG,EE
/: INDC, INDP, RIJV,INDC1, INDP1, RIJV1;

```

```
! INDC Fuel indicator;
```

```

! INDP Product indicator;
! RIJV Flow/Production;

! Cogeneration fuel;
FCIJ (TECN,UTIL)/TGVA,CG
      MGWC,CG
      DIWC,DI  TGDI,DI
      STVA,VA/;

! Cogenerated work;
WCIJ (TECN,UTIL)/TGVA,EE
      MGWC,EE
      DIWC,EE  TGDI,EE
      STVA,EE/;

! Cogenerated heat;
QCIJ (TECN,UTIL)/TGVA,VA  TGVA,WC
      MGWC,VA  MGWC,WC
                        DIWC,WC
                        TGDI,WC  TGDI,VA/;

! Waste heat;
QDIJ (TECN,UTIL)/ICWC,WR/;

! Production of heat by steam boiler;
VABO (TECN,UTIL)/CGVA,VA/;

! Consumption of gas by VA boiler;
VAFF (TECN,UTIL)/CGVA,CG/;

! Production of heat by FTDI;
VATT (TECN,UTIL)/FTDI,VA/;

! Production of heat by HW boiler;
HWBO (TECN,UTIL)/CGWC,WC/;

! Production of heat by BM boiler;
BOBM (TECN,UTIL)/BMWC,WC/;

! Biomass input to boiler;
BMBB (TECN,UTIL)/BMWC,BM/;

! Production of heat by EE boiler;
BOEE (TECN,UTIL)/EEWC,WC/;

! Electricity to boiler;
EEBB (TECN,UTIL)/EEWC,EE/;

! Production of heat by DI boiler;
BODI (TECN,UTIL)/DIBO,WC/;

      DIII (TECN,UTIL)/DIBO,DI/;

! Consumption of heat by gasifier;
GAHE (TECN,UTIL)/GFBM,VA/;

! Production of syndiesel;
PRDI (TECN,UTIL)/FTDI,DI/;

! Production of syngas;

```

```

PRSY (TECN,UTIL)/GFBM,CG/;

! WR of engine;
WRMO (TECN,UTIL)/MGWC,WR
      DIWC,WR/;

! Boiler fuel;
COCA (TECN,UTIL)/CGWC,CG/;

! WC of hot water heat exchanger;
WCII (TECN,UTIL)/ICWC,WC/;

! EE of absorption chiller;
EEAB (TECN,UTIL)/FAWC,EE/;

! WC of absorption chiller;
WCAB (TECN,UTIL)/FAWC,WC/;

! WR of absorption chiller;
WRAB (TECN,UTIL)/FAWC,WR/;

! WF of absorption chiller;
WFAB (TECN,UTIL)/FAWC,WF/;

! EE of mechanical chiller;
EEFM (TECN,UTIL)/FMWR,EE/;

! WR of mechanical chiller;
WRFM (TECN,UTIL)/FMWR,WR/;

! WF of mechanical chiller;
WFFM (TECN,UTIL)/FMWR,WF/;

! WR of the cooling tower;
WRTO (TECN,UTIL)/ICWR,WR/;

! EE of the cooling tower;
EETO (TECN,UTIL)/ICWR,EE/;

! AA of the cooling tower;
AATO (TECN,UTIL)/ICWR,AA/;

! Gas production of gasifier;
GASS (TECN,UTIL)/GFBM,CG/;

! Biomass input to gasifier;
GABM (TECN,UTIL)/GFBM,BM/;

! FT syngas input;
FTGA (TECN,UTIL)/FTDI,CG/;

! Electricity produced by TGVA;
TGEE (TECN,UTIL)/TGVA,EE/;

! Syngas input to TGVA;
TGGA (TECN,UTIL)/TGVA,CG/;

```

```

! Steam by turbine;
  TGSS (TECN,UTIL)/TGVA,VA/;

! Hot Water by turbine;
  TGHW (TECN,UTIL)/TGVA,WC/;

! Electricity by DITG;
  TDEE (TECN,UTIL)/TGDI,EE/;

! Diesel input to DITG;
  TDFU (TECN,UTIL)/TGDI,DI/;

! Steam by DI turbine;
  TDSS (TECN,UTIL)/TGDI,VA/;

! Hot Water by DI turbine;
  TDHH (TECN,UTIL)/TGDI,WC/;

! Electricity by gas engine;
  MGEE (TECN,UTIL)/MGWC,EE/;

! Gas input to gas engine;
  MGGG (TECN,UTIL)/MGWC,CG/;

! WR by gas engine;
  MGRR (TECN,UTIL)/MGWC,WR/;

! Hot Water by gas engine;
  MGHH (TECN,UTIL)/MGWC,WC/;

! Steam by gas engine;
  MGSS (TECN,UTIL)/MGWC,VA/;

! Electricity by DI engine;
  DIEE (TECN,UTIL)/DIWC,EE/;

! DI input to DI engine;
  DIGG (TECN,UTIL)/DIWC,DI/;

! WR by DI engine;
  DIRR (TECN,UTIL)/DIWC,WR/;

! Hot Water by DI engine;
  DIHH (TECN,UTIL)/DIWC,WC/;

! Steam into ICVA;
  AAAA (TECN,UTIL)/ICVA,VA/;

! Hot water into ICWC;
  BBBB (TECN,UTIL)/ICWC,WC/;

! Biomass by biomass boiler VA;
  DDDD (TECN,UTIL)/BMVA,BM/;

! Steam production by biomass boiler VA;
  EEEE (TECN,UTIL)/BMVA,VA/;

```

```

! Steam consumption by STVA;
FFFF (TECN,UTIL)/STVA,VA/;

! WR production by STVA;
GGGG (TECN,UTIL)/STVA,WR/;

! Electricity production by STVA;
HHHH (TECN,UTIL)/STVA,EE/;

! Electricity consumed by pump;
PMEE (TECN,UTIL)/PMDW,EE/;
ENDSETS

DATA:
INDC, INDP , RIJV = @OLE(
'C:\Users\aromero.CORP\Desktop\PhD\MPC\Lingo\P2H\modelinput.xlsx', 'INDC', 'IND
P' , 'RIJV ');
STEO, STH0, STW0, STG0 , STEE, STH, STW,STG, NWT,penalty , heatloss= @OLE(
'C:\Users\aromero.CORP\Desktop\PhD\MPC\Lingo\P2H\modelinput.xlsx', 'STE', 'STH'
, 'STW', 'STG', 'STEMAX', 'STHMAX',
'STWMAX', 'STGMAX', 'NWT', 'penalty', 'heatloss');
ENDDATA

SETS:
! DaysHours (kd, kh);
DIHO(DAYS,HOURS): DVAH, DWCH,DWCH2, DWFH, DEEH,DEEH2, DDIH,DDIH2,
PCEDH, PVEDH, CCGH, CEEH, VEEH, CDIH, CBMH,
YCEH, YVEH, NTS, NMS, NMDS,
CTECGH, CTECEH, INGVEH, CTEOMH, CVARIH, CTEDIH, CTEBMH,
SEE, SEF,SHE, SHF, SGE, SWE, SWF, IEC, SEC, SED,
DDWH, PDWH, VDWH ,PMEEH, DAVH, CAVH,PAVH, DMWH, CEEMH,
NPS, PPV, FNWR, FNWF,TURB ,TBEEH , DIEEH, DIMWH, EMMWH, DIMWS, EMMWS,
DIBOH,NWTS,PWIND,EWIND,EDGEN,PWINDLOW,NMDSR,PURDIHSR,EENGH,DIWCWASTE;

! DVAH Steam demand (MWh/h);
! DWCH Hot water demand (MWh/h);
! DWFH Cold water demand (MWh/h);
! DEEH Electricity demand (MWh/h);
! DDIH Diesel demand (MWh/h);
! PCEDH Purchase price electricity ($/MWh);
! PVEDH Sale price electricity ($/MWh);
! CCGH Purchase natural gas (MWh/h);
! CEEH Purchase electricity (MWh/h);
! VEEH Sale electricity (MWh/h);
! CDIH Purchase of diesel (MWh/h);
! CBMH Purchase of biomass (MWh/h);
! YCEH Indicator of electricity purchase (0/1);
! YVEH Indicator of electricity sale (0/1);
! NTS Number of turbines in service (0, 1, ...);
! NMS Number of engines in service (0, 1, ...);
! NMDS Number of diesel engines in service (0, 1, ...);
! CTECGH Natural gas cost ($/h);
! CTECEH Electricity cost ($/h);
! INGVEH Profit with sale of electricity ($/h);
! CTEOMH Variable Operation and maintenance cost ($/h);
! CVARIH Total variable cost ($/h);
! CTEDIH Diesel cost ($/h);

```

```

! CTEBMH Biomass cost ($/h);
! SEF Stored Electricity Flow positive or negative energy flow in each
hour (MWh);
! SEE Stored Electricity Energy total energy stored in each hour (MWh);
ENDSETS

```

```
SETS:
```

```

! DaysHoursUtility (kd,kh,j);
DHU(DAYS,HOURS,UTIL): DEMDHU, PURDHU, CONDHU, PRODHU, SELDHU, WASDHU;
! DEMDHU Demand (MWh/h);
! PURDHU Purchase (MWh/h);
! CONDHU Consumption (MWh/h);
! PRODHU Production (MWh/h);
! SELDHU Sale (MWh/h);
! WASDHU Waste (MWh/h);
! DaysHoursTechnologies (kd,kh,i);
DHT(DAYS,HOURS,TECN): PRODHT;
! PRODHT Production (MWh/h);
! DaysHoursTechnologiesUtilities (kd,kh,i,j);
DHTU(DAYS,HOURS,TECN,UTIL): FDHTU;
! FDHTU Production (MWh/h);
ENDSETS

```

```
CALC:
```

```

! Various inputs;
GAO,OPMAX = @OLE('C:\Users\aromero.CORP\Desktop\PhD\MPC\Lingo\P2H\HOEP.xlsx','GAO','OPMAX');
PCEDH = @OLE('C:\Users\aromero.CORP\Desktop\PhD\MPC\Lingo\P2H\HOEP.xlsx','PCEDH');
PVEDH = @OLE('C:\Users\aromero.CORP\Desktop\PhD\MPC\Lingo\P2H\HOEP.xlsx','PCEDH');
DEEH,DWCH,DDIH,PDWH,DAVH,DMWH,DWFH = @OLE('C:\Users\aromero.CORP\Desktop\PhD\MPC\Lingo\P2H\UD.xlsx','DEEH','DWCH','DDIH','PDWH','DAVH','DMWH','DWFH');
FNWR,FNWF = @OLE('C:\Users\aromero.CORP\Desktop\PhD\MPC\Lingo\P2H\UD.xlsx','FNWR','FNWF');
!Electrical power from each PV installed;
PPV,CPV,AP,effPV = @OLE('C:\Users\aromero.CORP\Desktop\PhD\MPC\Lingo\P2H\PV.xlsx','PPV','CPV','AP','effPV');
!Wind power available per wind turbine;
CWT,PWIND,PWINDLOW = @OLE('C:\Users\aromero.CORP\Desktop\PhD\MPC\Lingo\P2H\WIND.xlsx','CWT','PWIND','PWINDLOW');

```

```
! Calculating the daily and annual demands;
```

```

@FOR (DAYS(kd):
    DVAD(kd) = @SUM(HOURS(kh): NHD(kh) * DVAH(kd,kh));
    DWCD(kd) = @SUM(HOURS(kh): NHD(kh) * DWCH(kd,kh));
    DWFD(kd) = @SUM(HOURS(kh): NHD(kh) * DWFH(kd,kh));
    DEED(kd) = @SUM(HOURS(kh): NHD(kh) * DEEH(kd,kh));
    DDID(kd) = @SUM(HOURS(kh): NHD(kh) * DDIH(kd,kh));
    DAVD(kd) = @SUM(HOURS(kh): NHD(kh) * DAVH(kd,kh));
);
DVAA = @SUM(DAYS(kd): NDA(kd) * DVAD(kd));

```

```

DWCA = @SUM(DAYS(kd): NDA(kd) * DWCD(kd));
DWFA = @SUM(DAYS(kd): NDA(kd) * DWFD(kd));
DEEA = @SUM(DAYS(kd): NDA(kd) * DEED(kd));
DDIA = @SUM(DAYS(kd): NDA(kd) * DDID(kd));
DAVA = @SUM(DAYS(kd): NDA(kd) * DAVD(kd));
ENDCALC

! Our Objective -> Minimize annual cost ($/year);
MIN = ANNUAL_COST;

! Economic balance;
@FREE ( ANNUAL_COST );
! Penalty costs optional;
ANNUAL_COST = FMWREXTRA*CBM(@INDEX(FMWR)) + ICWREXTRA*CBM(@INDEX(ICWR)) +
0*AFIXC + AVARC + 0.0*(SGE(1,24)-penalty)^2 + 0*QCD + 10*DWINDWASTE(1);
! Annual investment cost ($/year);
INVESTMENT = FCI * (@SUM (TECN(i): CIN(i)) + CPV * NPV + EESTORAGE +
SYSTORAGE +PMSTORAGE);
EESTORAGE = (BSTEE * 0.4* 1e6*0 + 0.1900 * STEE * 1e6);
HESTORAGE = 10^3 * (37*STH*0.5 );
SYSTORAGE = 0.25 * 1e6 * BSTG + 0.00682 * STG * 1e6 ;
PMSTORAGE = 100 * STW;

DTRANS = 100; !km;
EECONX = 3*(PCONXMAX * 1e6 + DTRANS * PCONXMAX * 10e3);
DEEMAX=@MAX(DIHO:DEEH);

PCONXMAX <= YCE*BIGR*INDPUR(@INDEX(EE));
!PCONXMAX = 16;

AFIXC = FAM * (INVESTMENT + 1.02 * EECONX);
! Annual operation cost ($/year);
! CTECGA;
CTECGA = @SUM(DAYS(kd): NDA(kd) * CTECGD(kd));
! CTECEA;
CTECEA = @SUM(DAYS(kd): NDA(kd) * CTECED(kd));
! INGVEA;
INGVEA = @SUM(DAYS(kd): NDA(kd) * INGVED(kd));
! CTEOMA;
CTEOMA = @SUM(DAYS(kd): NDA(kd) * CTEOMD(kd));
! CTEDIA;
CTEDIA = @SUM(DAYS(kd): NDA(kd) * CTEDID(kd));
! CTEBMA;
CTEBMA = @SUM(DAYS(kd): NDA(kd) * CTEBMD(kd));
! CVARIA;
@FREE (AVARC);
AVARC = CTECGA + CTECEA - INGVEA + CTEOMA + CTEDIA + CTEBMA;

! Daily operation cost ($/day);
@FOR (DAYS(kd):
! CTECGD;
CTECGD(kd) = @SUM(HOURS(kh): NHD(kh) * CTECGH(kd, kh)) ;
! CTECED;
CTECED(kd) = @SUM(HOURS(kh): NHD(kh) * CTECEH(kd, kh)) +
0*GA(kd)/NDA(kd);
! INGVED;

```

```

INGVED(kd) = @SUM(HOURS(kh): NHD(kh) * INGVEH(kd, kh));
! CTEOMD;
CTEOMD(kd) = @SUM(HOURS(kh): NHD(kh) * CTEOMH(kd, kh));
! CTEDID;
CTEDID(kd) = @SUM(HOURS(kh): NHD(kh) * CTEDIH(kd, kh));
! CTEBMD;
CTEBMD(kd) = @SUM(HOURS(kh): NHD(kh) * CTEBMH(kd, kh));
! CVARID;
@FREE (CVARID(kd));
CVARID(kd) = CTECGD(kd) + CTECED(kd) - INGVED(kd) + CTEOMD(kd) +
CTEDID(kd) + CTEBMD(kd);
);
! Hourly operation cost ($/hour);
@FOR (DIHO(kd, kh):
! CTECGH;
CTECGH(kd, kh) = PCG * CCGH(kd, kh); ! + 0*SGE(kd, kh)*1 ;
! CTECEH;
CTECEH(kd, kh) = (PCEDH(kd, kh) + 40) * (CEEH(kd, kh) +
CEEH(kd, kh)*3e6/(115e3)^2*0.5*DTRANS);
! INGVEH;
INGVEH(kd, kh) = (PVEDH(kd, kh) + 40) * VEEH(kd, kh);
! CTEOMH;
CTEOMH(kd, kh) = @SUM(TECN(i): FOV(i) * PRODHT(kd, kh, i));
! CTEDIH;
CTEDIH(kd, kh) = PDI * (CDIH(kd, kh) +
0*NMDSR(kd, kh)*PET(@INDEX(DIWC))/0.40048*0.1 );
PURDIHSR(kd, kh) = (CDIH(kd, kh) +
NMDSR(kd, kh)*PET(@INDEX(DIWC))/0.40048*0.1 );
! CTEBMH;
CTEBMH(kd, kh) = PBM * CBMH(kd, kh);
! CVARIH;
@FREE (CVARIH(kd, kh));
CVARIH(kd, kh) = CTECGH(kd, kh) + CTECEH(kd, kh) - INGVEH(kd, kh) +
CTEOMH(kd, kh) + CTEDIH(kd, kh) + CTEBMH(kd, kh);
);
@BIN (YCE); ! In case is not a decision variable;
!Technologies;
@FOR (TECN(i):
@BIN (YPT(i)); @GIN (NET(i));
NET(i) <= YPT(i) * BIGN;
CIN(i) = NET(i) * CBM(i);
PRA(i) = @SUM (DHT(kd, kh, i): NDA(kd)*NHD(kh)*PRODHT(kd, kh, i));
);
! Fixed design constrained technologies;
@FOR (TECN(i)|(i#LE#8)#OR#(i#GE#11):
PIN(i) = NET(i) * PET(i);
);
! Dynamic design;
!FMWREXTRA=0; ! If the mechanical chillers cannot change;
!ICWREXTRA=0; ! If the cooling towers cannot change;
! If the cooling towers AND mechanical chillers can change;
@GIN (FMWREXTRA);@GIN (ICWREXTRA);
@FOR (TECN(i)|(i#EQ#9):
PIN(i) = (NET(i) + FMWREXTRA ) * PET(i);

```

```

);
@FOR (TECN(i) | (i#EQ#10):
    PIN(i) = (NET(i) + ICWREXTRA ) * PET(i);
);

! Do not sell electricity if there is no cogeneration;
YVE <= YPT(@INDEX(TGVA)) + YPT(@INDEX(MGWC)) ;

! Production limits;
@FOR(DAYS(kd):
    @FOR(HOURS(kh):
        @GIN(NTS(kd, kh));          NTS(kd, kh)          <=          NET(@INDEX(TGVA));
PRODHT(kd, kh, @INDEX(TGVA)) <= NTS(kd, kh)          * PET(@INDEX(TGVA));
        @GIN(NMS(kd, kh));          NMS(kd, kh)          <=          NET(@INDEX(MGWC));
PRODHT(kd, kh, @INDEX(MGWC)) <= NMS(kd, kh)          * PET(@INDEX(MGWC));
        @GIN(NMDS(kd, kh));         NMDS(kd, kh)         <=          NET(@INDEX(DIWC));
PRODHT(kd, kh, @INDEX(DIWC)) <= NMDS(kd, kh) * PET(@INDEX(DIWC));

PRODHT(kd, kh, @INDEX(DIWC)) >= (NMDS(kd, kh) - 1) * PET(@INDEX(DIWC));
        @GIN(DIMWS(kd, kh));         DIMWS(kd, kh)         <=          NET(@INDEX(DIMW));
PRODHT(kd, kh, @INDEX(DIMW)) <= DIMWS(kd, kh) * PET(@INDEX(DIMW));
        @GIN(EMMWS(kd, kh));         EMMWS(kd, kh)         <=          NET(@INDEX(EMMW));
PRODHT(kd, kh, @INDEX(EMMW)) <= EMMWS(kd, kh) * PET(@INDEX(EMMW));
        @FOR (TECN(i):
            PRODHT(kd, kh, i) <= PIN(i);
        );
    );
);

!PV panels installed and simltaneous;
NPV=0;
@GIN(NPV);
NPV <= 1500;
@FOR(DAYS(kd):
    @FOR(HOURS(kh):
        !@GIN(NPS(kd, kh));
        NPS(kd, kh) <= NPV;
    );
);

! Wind turbines installed and operating simultaneously;
!NWT=4;
@GIN(NWT);
NWT <= 200;      ! Wind turbines limitation! *****;
@FOR(DAYS(kd):
    @FOR(HOURS(kh):
        !@GIN(NWTS(kd, kh));
        @GIN(NMDSR(kd, kh));
        NWTS(kd, kh) <= NWT;
        EWIND(kd, kh)=NWTS(kd, kh) * PWIND(kd, kh);
        !Spinning reserve equations;
        ! (NMDS(kd, kh) * PET(@INDEX(DIWC)) - EDGEN(kd, kh) + SEE(kd, kh)) +
        NMDSR(kd, kh) * PET(@INDEX(DIWC))
        >= NWTS(kd, kh) * (PWIND(kd, kh) - PWINDLOW(kd, kh));
        !NMDS(kd, kh) + NMDSR(kd, kh) <= NET(@INDEX(DIWC));
        !EWIND(kd, kh) <= 0.5 * (CONDHU(kd, kh, @INDEX(EE)) +
        DEMDHU(kd, kh, @INDEX(EE)));
    );
);

```

```

        EDGEN(kd, kh) = PRODHU(kd, kh, @INDEX(EE));
        EENGH(kd, kh) = PRODHU(kd, kh, @INDEX(CG));
    );
    DWIND(kd) = @SUM(HOURS(kh) : NWTs(kd, kh) * PWIND(kd, kh));
    DWINDWASTE(kd) = @SUM(HOURS(kh) : (NWT - NWTs(kd, kh)) * PWIND(kd, kh));
);

! Additional constraints in equipment installed;
!NET(@INDEX(FAVA))=0;
!NET(@INDEX(FAWC))=0;
!NET(@INDEX(TGVA))=0;
!NET(@INDEX(MGWC))=0;
!NET(@INDEX(DIWC))=0;
!NET(@INDEX(STVA))=0;
!NET(@INDEX(TGDI))=0;
!NET(@INDEX(PMDW))=0;
!NET(@INDEX(EMMW))=0;
!NET(@INDEX(DIMW))=0;
!NET(@INDEX(GFBM))=0;
!NET(@INDEX(FTDI))=0;
!NET(@INDEX(EMMW))+NET(@INDEX(DIMW))=30;

POTMOT = PIN(@INDEX(TGVA)) + PIN(@INDEX(MGWC)) + PIN(@INDEX(DIWC)) ;

!Waste heat for hot gases of the diesel generator;
@FOR(DAYS(kd) :
    @FOR(HOURS(kh) :
        @FOR(TEUT(i, j) | (i#LE#10) :
            FDHTU(kd, kh, i, j) = PRODHT(kd, kh, i) * RIJV(i, j);
        );););
@FOR(DAYS(kd) :
    @FOR(HOURS(kh) :
        @FOR(TEUT(i, j) | (i#EQ#11)#AND#(j#EQ#3) :
            FDHTU(kd, kh, i, j) = PRODHT(kd, kh, i) * RIJV(i, j) - 0*DIWCWASTE(kd, kh);
        );
        @FOR(TEUT(i, j) | (i#EQ#11)#AND#(j#LT#3#OR#j#GT#3) :
            FDHTU(kd, kh, i, j) = PRODHT(kd, kh, i) * RIJV(i, j);
        );););
@FOR(DAYS(kd) :
    @FOR(HOURS(kh) :
        @FOR(TEUT(i, j) | (i#GT#11)#AND#i#LE#20)#OR#(i#GE#22) :
            FDHTU(kd, kh, i, j) = PRODHT(kd, kh, i) * RIJV(i, j);
        );););

!Temperature coefficients;
@FOR(DAYS(kd) :
    @FOR(HOURS(kh) :
        @FOR(TEUT(i, j) | (i#EQ#21)#AND#(j#EQ#7#OR#j#EQ#11) :
            FDHTU(kd, kh, i, j) = PRODHT(kd, kh, i) * RIJV(i, j);
        );
        @FOR(TEUT(i, j) | (i#EQ#21)#AND#(j#EQ#4) :
            FDHTU(kd, kh, i, j) = PRODHT(kd, kh, i) * FNWR(kd, kh);
        );
        @FOR(TEUT(i, j) | (i#EQ#21)#AND#(j#EQ#6) :
            FDHTU(kd, kh, i, j) = PRODHT(kd, kh, i) * FNWF(kd, kh);
        );););

```

```

! Utility balances;
@FOR(DAYS(kd) :
  @FOR(HOURS(kh) :
    @FOR(UTIL(j) :
      !@FREE(FDHTU(kd,kh,20,10));
      !@FREE(CONDHU(kd,kh,10));
      CONDHU(kd,kh,j) = @SUM(TEUT(i,j) : INDC(i,j)*FDHTU(kd,kh,i,j));
      PRODHU(kd,kh,j) = @SUM(TEUT(i,j) : INDP(i,j)*FDHTU(kd,kh,i,j));
      PURDHU(kd,kh,j) <= INDPUR(j) * BIGR;
      DEMDHU(kd,kh,j) <= INDDEM(j) * BIGR;
      SELDHU(kd,kh,j) <= INDSEL(j) * BIGR;
      WASDHU(kd,kh,j) <= INDWAS(j) * BIGR;
    );
  );
);

@FOR(DAYS(kd) :
  @FOR(HOURS(kh) :
    @FOR(UTIL(j) | (j#EQ#7) :
      PREEH(kd,kh) = @SUM(PMEE(i,j) : INDC(i,j)*FDHTU(kd,kh,i,j));
    );
    DIEEH(kd,kh) = PRODHT(kd,kh,@INDEX(DIWC) );
    DIMWH(kd,kh) = PRODHT(kd,kh,@INDEX(DIMW) );
    EMMWH(kd,kh) = PRODHT(kd,kh,@INDEX(EMMW) );
    DIBOH(kd,kh) = PRODHT(kd,kh,@INDEX(DIBO) );
  ););

!=====;
! Balance for utilities without storage;
@FOR(DAYS(kd) :
  @FOR(HOURS(kh) :

@FOR(UTIL(j) | (j#EQ#8)#OR#(j#EQ#2)#OR#(j#EQ#4)#OR#(j#EQ#5)#OR#(j#EQ#6)#OR#(j#EQ#9)#OR#(j#EQ#11)#OR#(j#EQ#12) :
  PURDHU(kd,kh,j) + PRODHU(kd,kh,j) = CONDHU(kd,kh,j) + DEMDHU(kd,kh,j)
  + SELDHU(kd,kh,j) + WASDHU(kd,kh,j);!BALANCE OF PRODUCTION,SALE,... FOR
EACH UTILTY EXCEPT ELECTRICITY (j=7) ;
);
);
);

!=====;
! Balance for utilites with storage;
! Storage intital conditions;
SEE(1,1)=STE0;
SHE(1,1)=STH0;
SWE(1,1)=STW0;
SGE(1,1)=STG0;

!Electricity storage definitions;
@FOR(DAYS(kd) :
  @FOR(HOURS(kh) :
    @FOR(UTIL(j) | (j#EQ#7) :
      PURDHU(kd,kh,j) + PRODHU(kd,kh,j) = CONDHU(kd,kh,j) +
      DEMDHU(kd,kh,j)

```

```

+ SELDHU(kd, kh, j) + WASDHU(kd, kh, j) + SEF(kd, kh) - NPS(kd, kh) * AP
* PPV(kd, kh) * effPV/1000 - 0.8*NWTS(kd, kh) * PWIND(kd, kh) ; !BALANCE OF
PRODUCTION, SALE, ... FOR ELECTRICITY (j=7) ;
!SEC for EV battery when present;
);
);
);
@FOR(DAYS(kd) :
@FOR(HOURS(kh) :
@FREE(SEF(kd, kh));
@BIN(BSTEE);
@GIN(IEC(kd, kh));
!BSTEE=0;
!STEE = 0;
SEF(kd, kh) <= IEC(kd, kh)*1e4;
SEF(kd, kh) >= -(1-IEC(kd, kh))*1e4;
SEF(kd, kh) = SEC(kd, kh) - SED(kd, kh);
SEC(kd, kh) <= IEC(kd, kh)*1e4;
SED(kd, kh) <= (1-IEC(kd, kh))*1e4;
SEF(kd, kh) >=-0.25*STEE ;
SEF(kd, kh) <=0.51*STEE ;
STEE <= BSTEE*1e4;
SEE(kd, kh) <= STEE;
SEE(kd, kh) >= 0.1*STEE;
);
);
@FOR(DAYS(kd) :
@FOR(HOURS(kh) | (kh#GE#2) #AND# (kh#LE#6) :
SEE(kd, kh)=SEE(kd, kh-1)*0.999 - SED(kd, kh-1)*1 + SEC(kd, kh-1)*0.9;
);
);
! Constraints for charge and discharge with electric vehicles;
!@FOR(DAYS(kd) :
@FOR(HOURS(kh) | (kh#LE#5) #OR# (kh#GE#21) :
SEC(kd, kh)=0;
!);
!);
!@FOR(DAYS(kd) :
@FOR(HOURS(kh) | (kh#GE#9) #AND# (kh#LE#17) :
SEC(kd, kh)=0;
!);
!);
!@FOR(DAYS(kd) :
@FOR(HOURS(kh) :
CEEMH=FDHTU(kd, kh, @INDEX(EMMW), @INDEX(ee));
!CEEMH(kd, kh)=SED(kd, kh);
!);
!);
! Terminal constraint;
!@FOR(DAYS(kd) :
@FOR(HOURS(kh) | (kh#EQ#1) :
SEE(kd, kh)=SEE(kd, 24)*0.999 - SED(kd, 24)*1 + SEC(kd, 24)*0.9;

```

```

!);
!);

!SYNGAS storage definitions;
@FOR(DAYS(kd):
  @FOR(HOURS(kh):
    @FOR(UTIL(j) | (j#EQ#1):
      PURDHU(kd, kh, j) + PRODHU(kd, kh, j) = CONDHU(kd, kh, j) + DEMDHU(kd, kh, j)
      + SELDHU(kd, kh, j) + WASDHU(kd, kh, j) +
SGF(kd, kh); !BALANCE OF PRODUCTION, SALE, ... FOR SYNGAS (j=1) ;
      !PRODHU(kd, kh, j) = CONDHU(kd, kh, j) + SGF(kd, kh); !BALANCE OF
PRODUCTION, SALE, ... FOR SYNGAS (j=1) ;
    );
  );
);
@FOR(DAYS(kd):
  @FOR(HOURS(kh):
    @FREE(SGF(kd, kh));
    @BIN(BSTG);
    !BSTG=0;
    !STG =12.8;
    STG <= BSTG*10000;
    SGE(kd, kh) <= STG;
    !SGF(kd, kh) > = -0.995*STG;
    !SGF(kd, kh) < = 0.995*STG;
    !SGE(kd, kh) <= LD(kd)*1000;
  );
);
@FOR(DAYS(kd):
  @FOR(HOURS(kh) | (kh#GE#2)#AND#(kh#LE#24):
    SGE(kd, kh)=SGE(kd, kh-1) + SGF(kd, kh-1);
  );
);
! Terminal constraint;
!@FOR(DAYS(kd):
  @FOR(HOURS(kh) | (kh#EQ#1):
    SGE(kd, kh)=SGE(kd, 24) + SGF(kd, 24);
  !);
!);

! Heat storage;
@FOR(DAYS(kd):
  @FOR(HOURS(kh):
    @FOR(UTIL(j) | (j#EQ#3):
      PURDHU(kd, kh, j) + PRODHU(kd, kh, j) = CONDHU(kd, kh, j) + DEMDHU(kd, kh, j)
      + SELDHU(kd, kh, j) + WASDHU(kd, kh, j) +
SHF(kd, kh); !BALANCE OF PRODUCTION, SALE, ... FOR SYNGAS (j=1) ;
    );
  );
);
@FOR(DAYS(kd):
  @FOR(HOURS(kh):
    @FREE(SHF(kd, kh));
    @BIN(BSTH);

```

```

        !BSTH=0;
        !STH =12.8;
        STH <= BSTH*10000;
        SHE(kd,kh) <= STH;
        SHF(kd,kh) >= -0.995*STH;
        !SHF(kd,kh) <= 0.995*STH;
        !SHE(kd,kh) <= LD(kd)*1000;
    );
);

!@FOR (DAYS(kd):
    LD(kd) =@SUM(HOURS(kh): @ABS(SHF(kd,kh)));
    !);
!LL= @SUM(DAYS(kd): LD(kd) );
@FOR(DAYS(kd):
    @FOR (HOURS(kh) | (kh#GE#2)#AND#(kh#LE#24):
        SHE(kd,kh)=SHE(kd,kh-1)*0.99 + SHF(kd,kh-1) - heatloss;
    );
);
!@FOR(DAYS(kd):
    @FOR (HOURS(kh) | (kh#EQ#1):
        SHE(kd,kh)=SHE(kd,24) + SHF(kd,24);
    !);
!);

! Water storage definitions;

@FOR(DAYS(kd):
    @FOR(HOURS(kh):
        @FOR(UTIL(j) | (j#EQ#10):
            PURDHU(kd,kh,j) + PDWH(kd,kh) - PRODHU(kd,kh,j) = +
SWF(kd,kh) ; !BALANCE OF PRODUCTION, SALE, ... FOR WATER (j=10) ;
            PURDHU(kd,kh,j)=CONDHU(kd,kh,j);
        );
        !@FREE(PRODHU(kd,kh,10));
    );
);

!@FOR(DAYS(kd):
    @SUM(HOURS(kh): PRODHU(kd,kh,@INDEX(DW)))=90*24;
!);

BSTW=1;
@FOR(DAYS(kd):
    @FOR(HOURS(kh):
        @FREE(SWF(kd,kh));
        @BIN(BSTW);
        BSTW=1;
        !STW = 2;
        !STW = 0*0.984*5 * 4 * 50 * BSTW;
        SWE(kd,kh) <= 0.99*STW;
        SWE(kd,kh) >= 0.05*STW;
        !SWF(kd,kh) >= -0.995*STW;
        !SWF(kd,kh) <= 0.995*STW;
        !SWE(kd,kh) <= LD(kd)*1000;
    );
);

```

```

);
@FOR (DAYS (kd) :
    @FOR (HOURS (kh) | (kh#GE#2) #AND# (kh#LE#24) :
        SWE (kd, kh) = SWE (kd, kh-1) + SWF (kd, kh-1);
    );
);

! Terminal constraint;
!@FOR (DAYS (kd) :
    @FOR (HOURS (kh) | (kh#EQ#1) :
        SWE (kd, kh) = SWE (kd, 24) + SWF (kd, 24);
    !);
!);

!End of storage equations;
!=====;

@FOR (DAYS (kd) :
    @FOR (HOURS (kh) :
        DEMDHU (kd, kh, @INDEX (va)) = DVAH (kd, kh);
        DEMDHU (kd, kh, @INDEX (wc)) = DWCH (kd, kh);
        DEMDHU (kd, kh, @INDEX (wf)) = DWFH (kd, kh);
        DEMDHU (kd, kh, @INDEX (ee)) = DEEH (kd, kh);
        DEMDHU (kd, kh, @INDEX (di)) = DDIH (kd, kh);
        DEMDHU (kd, kh, @INDEX (AV)) = DAVH (kd, kh);
        DEMDHU (kd, kh, @INDEX (MW)) = DMWH (kd, kh);

        CCGH (kd, kh) = PURDHU (kd, kh, @INDEX (cg));
        CEEH (kd, kh) = PURDHU (kd, kh, @INDEX (ee));
        YCE*PCONXMAX ; !CEEH (kd, kh) <= YCE*BIGR; ! CEEH (kd, kh) = 0;
        VEEH (kd, kh) = SELDHU (kd, kh, @INDEX (ee));
        YVE*PCONXMAX ; !VEEH (kd, kh) <= YVE*BIGR;
        CDIH (kd, kh) = PURDHU (kd, kh, @INDEX (di)); !CDIH (kd, kh) <= 8;
        CBMH (kd, kh) = PURDHU (kd, kh, @INDEX (bm));
        VDWH (kd, kh) = SELDHU (kd, kh, @INDEX (DW));
    );
);
! Daily and yearly results;
@FOR (DAYS (kd) :
! CCGD;
    CCGD (kd) = @SUM (HOURS (kh) : NHD (kh) * CCGH (kd, kh));
! CEED;
    CEED (kd) = @SUM (HOURS (kh) : NHD (kh) * CEEH (kd, kh));
! VEED;
    VEED (kd) = @SUM (HOURS (kh) : NHD (kh) * VEEH (kd, kh));
! CDID;
    CDID (kd) = @SUM (HOURS (kh) : NHD (kh) * CDIH (kd, kh));
! CBMD;
    CBMD (kd) = @SUM (HOURS (kh) : NHD (kh) * CBMH (kd, kh));
! ASDF;
    VDWD (kd) = @SUM (HOURS (kh) : NHD (kh) * VDWH (kd, kh));

);
CCGA = @SUM (DAYS (kd) : NDA (kd) * CCGD (kd));
CEEA = @SUM (DAYS (kd) : NDA (kd) * CEED (kd));
VEEA = @SUM (DAYS (kd) : NDA (kd) * VEED (kd));
CDIA = @SUM (DAYS (kd) : NDA (kd) * CDID (kd)); !CDIA <= 100000;

```

```

CBMA = @SUM(DAYS(kd): NDA(kd) * CBMD(kd));
VDWA = @SUM(DAYS(kd): NDA(kd) * VDWD(kd));

! Global adjustment equations;

!CONMAX = (0.027*PURDHU(7,9,@INDEX(ee))+0.045*PURDHU(7,10,@INDEX(ee))+
0.079*PURDHU(7,11,@INDEX(ee))+0.101*PURDHU(7,12,@INDEX(ee))+
0.118*PURDHU(7,13,@INDEX(ee))+0.121*PURDHU(7,14,@INDEX(ee))+
0.163*PURDHU(7,15,@INDEX(ee))+0.157*PURDHU(7,16,@INDEX(ee))+
0.108*PURDHU(7,17,@INDEX(ee))+0.081*PURDHU(7,18,@INDEX(ee))+
0*PURDHU(7,13,@INDEX(ee)));
CONMAX = 0;
!CONMAX = PURDHU(7,16,@INDEX(ee));

@FOR (DAYS(kd):
GA(kd) = GAO(kd)*(CONMAX/OPMAX)*1e6;
);
!Limit storage for diesel;

!@FOR(DAYS(kd)|kd#GE#3:
@SUM(DAYS(kd): NDA(kd) * CDID(kd)) <= 80000;
! CACA = @SUM(DAYS(kd): NDA(kd) * CDID(kd));
! );
!@FOR(DAYS(kd)|kd#EQ#1#OR#kd#GE#3:
@SUM(DAYS(kd): NDA(kd) * CDID(kd)) <=30000 ;
! );
!@FOR(DAYS(kd)|kd#EQ#1:
LIMIT2 = @SUM(DAYS(kd): NDA(kd) * CDID(kd)) ;
! );

WASTE=PRA(@INDEX(ICWR));

!Limit storage for biomass;
! CBMA <=400000;

! More results;
! Annual fuel consumed by cogeneration equipment;
!FCO = @SUM(FCIJ(i,j): PRA(i)* RIJV(i,j) );
! Annual cogenerated work;
!WCO = @SUM(WCIJ(i,j): PRA(i)* RIJV(i,j) );
! Annual cogenerated heat;
!QCO = @SUM(QCIJ(i,j): PRA(i)* RIJV(i,j) );
! Annual waste heat;
QCD = @SUM(QDIJ(i,j): PRA(i)* RIJV(i,j) );
! 3. DO NOT waste thermal energy;
!QCD <= YDQ*BIGR*8760;
! Consumed cogenerated heat;
!QCC = QCO - QCD;
! Fuel attributable to cogenerated work;
!FWC = FCO - QCC/0.9;
! Minimum Equivalent Electrical Efficiency;
! WCO >= FWC*RTOMIN;
!Total consumption of electricity;
!CONT = WCO - VEEA;
! Self-consumption of electricity (must be at least...);

```

!CONT>=WCO\*ACEMIN;

!\*\*\*\*\*;

BOB = @SUM(BOBM(i,j) : PRA(i)\*RIJV(i,j) );  
BOE = @SUM(BOEE(i,j) : PRA(i)\*RIJV(i,j) );  
EEB = @SUM(EEBB(i,j) : PRA(i)\*RIJV(i,j) );  
BOD = @SUM(BODI(i,j) : PRA(i)\*RIJV(i,j) );  
HWB = @SUM(HWBO(i,j) : PRA(i)\*RIJV(i,j) );  
VAT = @SUM(VATT(i,j) : PRA(i)\*RIJV(i,j) );  
VAF = @SUM(VAFF(i,j) : PRA(i)\*RIJV(i,j) );  
VAB = @SUM(VABO(i,j) : PRA(i)\*RIJV(i,j) );  
PRD = @SUM(PRDI(i,j) : PRA(i)\*RIJV(i,j) );  
PRS = @SUM(PRSY(i,j) : PRA(i)\*RIJV(i,j) );  
WRM = @SUM(WRMO(i,j) : PRA(i)\*RIJV(i,j) );  
COC = @SUM(COCA(i,j) : PRA(i)\*RIJV(i,j) );  
WCI = @SUM(WCII(i,j) : PRA(i)\*RIJV(i,j) );  
EEA = @SUM(EEAB(i,j) : PRA(i)\*RIJV(i,j) );  
WCA = @SUM(WCAB(i,j) : PRA(i)\*RIJV(i,j) );  
WRA = @SUM(WRAB(i,j) : PRA(i)\*RIJV(i,j) );  
WFA = @SUM(WFAB(i,j) : PRA(i)\*RIJV(i,j) );  
EEF = @SUM(EEFM(i,j) : PRA(i)\*RIJV(i,j) );  
WRF = @SUM(WRFM(i,j) : PRA(i)\*RIJV(i,j) );  
WFF = @SUM(WFFM(i,j) : PRA(i)\*RIJV(i,j) );  
WRT = @SUM(WRTO(i,j) : PRA(i)\*RIJV(i,j) );  
EET = @SUM(EETO(i,j) : PRA(i)\*RIJV(i,j) );  
AAT = @SUM(AATO(i,j) : PRA(i)\*RIJV(i,j) );  
GAH = @SUM(GAHE(i,j) : PRA(i)\*RIJV(i,j) );  
GAS = @SUM(GASS(i,j) : PRA(i)\*RIJV(i,j) );  
GAB = @SUM(GABM(i,j) : PRA(i)\*RIJV(i,j) );  
FTG = @SUM(FTGA(i,j) : PRA(i)\*RIJV(i,j) );  
TGE = @SUM(TGEE(i,j) : PRA(i)\*RIJV(i,j) );  
TGG = @SUM(TGGA(i,j) : PRA(i)\*RIJV(i,j) );  
TGS = @SUM(TGSS(i,j) : PRA(i)\*RIJV(i,j) );  
TGH = @SUM(TGHW(i,j) : PRA(i)\*RIJV(i,j) );  
TDE = @SUM(TDEE(i,j) : PRA(i)\*RIJV(i,j) );  
TDF = @SUM(TDFU(i,j) : PRA(i)\*RIJV(i,j) );  
TDS = @SUM(TDSS(i,j) : PRA(i)\*RIJV(i,j) );  
TDH = @SUM(TDHH(i,j) : PRA(i)\*RIJV(i,j) );  
MGE = @SUM(MGEE(i,j) : PRA(i)\*RIJV(i,j) );  
MGG = @SUM(MGGG(i,j) : PRA(i)\*RIJV(i,j) );  
MGR = @SUM(MGRR(i,j) : PRA(i)\*RIJV(i,j) );  
MGS = @SUM(MGSS(i,j) : PRA(i)\*RIJV(i,j) );  
MGH = @SUM(MGHH(i,j) : PRA(i)\*RIJV(i,j) );  
DIR = @SUM(DIRR(i,j) : PRA(i)\*RIJV(i,j) );  
DIE = @SUM(DIEE(i,j) : PRA(i)\*RIJV(i,j) );  
DIG = @SUM(DIGG(i,j) : PRA(i)\*RIJV(i,j) );  
DIH = @SUM(DIHH(i,j) : PRA(i)\*RIJV(i,j) );  
DII = @SUM(DIII(i,j) : PRA(i)\*RIJV(i,j) );  
AAA = @SUM(AAAA(i,j) : PRA(i)\*RIJV(i,j) );  
BBB = @SUM(BBBB(i,j) : PRA(i)\*RIJV(i,j) );  
DDD = @SUM(DDDD(i,j) : PRA(i)\*RIJV(i,j) );  
EEE = @SUM(EEEE(i,j) : PRA(i)\*RIJV(i,j) );  
FFF = @SUM(FFFF(i,j) : PRA(i)\*RIJV(i,j) );  
GGG = @SUM(GGGG(i,j) : PRA(i)\*RIJV(i,j) );  
HHH = @SUM(HHHH(i,j) : PRA(i)\*RIJV(i,j) );

```

NETTGVA=NET (@INDEX (TGVA) );
NETMGWC=NET (@INDEX (MGWC) );
NETCGVA=NET (@INDEX (CGVA) );
NETCGWC=NET (@INDEX (CGWC) );
NETICVA=NET (@INDEX (ICVA) );
NETICWC=NET (@INDEX (ICWC) );
NETFAVA=NET (@INDEX (FAVA) );
NETFAWC=NET (@INDEX (FAWC) );
NETFMWR=NET (@INDEX (FMWR) );
NETICWR=NET (@INDEX (ICWR) );
NETDIWC=NET (@INDEX (DIWC) );
NETGFBM=NET (@INDEX (GFBM) );
NETFTDI=NET (@INDEX (FTDI) );
NETBMWC=NET (@INDEX (BMWC) );
NETDIBO=NET (@INDEX (DIBO) );
NETEEWC=NET (@INDEX (EEWC) );
NETTGDI=NET (@INDEX (TGDI) );
NETBMVA=NET (@INDEX (BMVA) );
NETSTVA=NET (@INDEX (STVA) );
NETPMDW=NET (@INDEX (PMDW) );
NETFNAV=NET (@INDEX (FNAV) );
NETDIMW=NET (@INDEX (DIMW) );
NETEMMW=NET (@INDEX (EMMW) );
NETNGMW=NET (@INDEX (NGMW) );
NETEENG=NET (@INDEX (EENG) );

```

CALC:

```

! @SET( 'TERSEO', 1);
! @SET( 'LINLEN', 120);
!Solving the model;
! @SOLVE( );
!Print results in file;
  @DIVERT( 'montreal_SY.txt', 'A' );

```

ENDCALC

!;

SETS:

```

PINTT(DAYS,HOURS): DVAH_p, DWCH_p, DWFH_p, DEEH_p, CCGH_p, CEEH_p, VEEH_p,
CDIH_p, CBMH_p;

```

ENDSETS

CALC:

```

@FOR (DAYS (kd) :

```

```

  @FOR (HOURS (kh) :

```

```

    DVAH_p(kd, kh) = @FLOOR( DVAH(kd, kh) );
```

```

    DWCH_p(kd, kh) = @FLOOR( DWCH(kd, kh) );
```

```

    DWFH_p(kd, kh) = @FLOOR( DWFH(kd, kh) );
```

```

    DEEH_p(kd, kh) = @FLOOR( DEEH(kd, kh) );
```

```

    CCGH_p(kd, kh) = @FLOOR( CCGH(kd, kh) );
```

```

    CEEH_p(kd, kh) = @FLOOR( CEEH(kd, kh) );
```

```

    VEEH_p(kd, kh) = @FLOOR( VEEH(kd, kh) );
```

```

    CDIH_p(kd, kh) = @FLOOR( CDIH(kd, kh) );
```

```

    CBMH_p(kd, kh) = @FLOOR( CBMH(kd, kh) );

```

```
);  
);
```

ENDCALC

DATA:

```
@OLE('C:\Users\aromero.CORP\Desktop\PhD\MPC\Lingo\P2H\Results.xlsx','TGVA','M  
GWC','CGVA','CGWC','ICVA','ICWC','FAVA','FAWC','FMWR','ICWR','DIWC','GFBM','F  
TDI') =  
NETTGVA,NETMGWC,NETCGVA,NETCGWC,NETICVA,NETICWC,NETFAVA,NETFAWC,NETFMWR,NETIC  
WR,NETDIWC,NETGFBM,NETFTDI;
```

```
@OLE('C:\Users\aromero.CORP\Desktop\PhD\MPC\Lingo\P2H\Results.xlsx','BMWC','D  
IBO','EEWC','TGDI','BMVA','STVA','PMDW','FNAV','DIMW','EMMW','NGMW','EENG') =  
NETBMWC,NETDIBO,NETEEWC,NETTGDI,NETBMVA,NETSTVA,NETPMDW,NETFNAV,NETDIMW,NETEM  
MW,NETNGMW,NETEENG;
```

```
@OLE('C:\Users\aromero.CORP\Desktop\PhD\MPC\Lingo\P2H\Results.xlsx','  
INVESTMENT','ANNUAL_COST','AFIXC','AVARC','CTEOMA') = INVESTMENT,  
ANNUAL_COST,AFIXC,AVARC,CTEOMA;
```

```
@OLE('C:\Users\aromero.CORP\Desktop\PhD\MPC\Lingo\P2H\Results.xlsx','  
PCONXMAX','DEEMAX') = PCONXMAX,DEEMAX;
```

```
@OLE('C:\Users\aromero.CORP\Desktop\PhD\MPC\Lingo\P2H\Results.xlsx','  
DWCA','DWFA','DEEA','DDIA','CCGA','CEEA','CDIA','CBMA','GAS','PRD','VEEA')  
= DWCA,DWFA,DEEA,DDIA,CCGA,CEEA,CDIA,CBMA,GAS,PRD,VEEA;
```

```
@OLE('C:\Users\aromero.CORP\Desktop\PhD\MPC\Lingo\P2H\Results.xlsx','STEE  
,','STH','STW','STG','VDWA') = STEE,STH,STW,STG,VDWA;
```

```
@OLE('C:\Users\aromero.CORP\Desktop\PhD\MPC\Lingo\P2H\Results.xlsx','CEEH')  
= CEEH;
```

```
@OLE('C:\Users\aromero.CORP\Desktop\PhD\MPC\Lingo\P2H\Results.xlsx','EECONX  
) = EECONX;
```

```
@OLE('C:\Users\aromero.CORP\Desktop\PhD\MPC\Lingo\P2H\Results.xlsx','SEE')  
= SEE;
```

```
@OLE('C:\Users\aromero.CORP\Desktop\PhD\MPC\Lingo\P2H\Results.xlsx','SGE')  
= SGE;
```

```
@OLE('C:\Users\aromero.CORP\Desktop\PhD\MPC\Lingo\P2H\Results.xlsx','SHE')  
= SHE;
```

```
@OLE('C:\Users\aromero.CORP\Desktop\PhD\MPC\Lingo\P2H\Results.xlsx','SWE') =  
SWE;
```

```
@OLE('C:\Users\aromero.CORP\Desktop\PhD\MPC\Lingo\P2H\Results.xlsx','SWF') =  
SWF;
```

```
@OLE('C:\Users\aromero.CORP\Desktop\PhD\MPC\Lingo\P2H\Results.xlsx','PMEEH')  
= PMEEH;
```

```
!@OLE('C:\Users\aromero.CORP\Desktop\PhD\MPC\Lingo\P2H\Results.xlsx','TBEEH')  
) = TBEEH;
```

```
@OLE('C:\Users\aromero.CORP\Desktop\PhD\MPC\Lingo\P2H\Results.xlsx','DIEEH','  
NMDS','DIMWH','DIMWS','EMMWH','EMMWS','DIBOH','CDIH') = DIEEH,NMDS,DIMWH,  
DIMWS,EMMWH,EMMWS,DIBOH,CDIH;
```

```
@OLE('C:\Users\aromero.CORP\Desktop\PhD\MPC\Lingo\P2H\Results.xlsx','  
CTECEA','CTEDIA','CTEBMA','WASTE') = CTECEA,CTEDIA,CTEBMA,WASTE;
```

```

@OLE('C:\Users\aromero.CORP\Desktop\PhD\MPC\Lingo\P2H\Results.xlsx',
'NPV','NWT','EWIND','NWTs','EENGH') = NPV,NWT,EWIND,NWTs,EENGH;

@OLE('C:\Users\aromero.CORP\Desktop\PhD\MPC\Lingo\P2H\Results.xlsx',      'NPS',
'effPV','AP') = NPS , effPV, AP;

@OLE('C:\Users\aromero.CORP\Desktop\PhD\MPC\Lingo\P2H\Results.xlsx',
'NMDSR','QCD') = NMDSR,QCD;
@OLE('C:\Users\aromero.CORP\Desktop\PhD\MPC\Lingo\P2H\Results.xlsx',      'SHF')
= SHF;

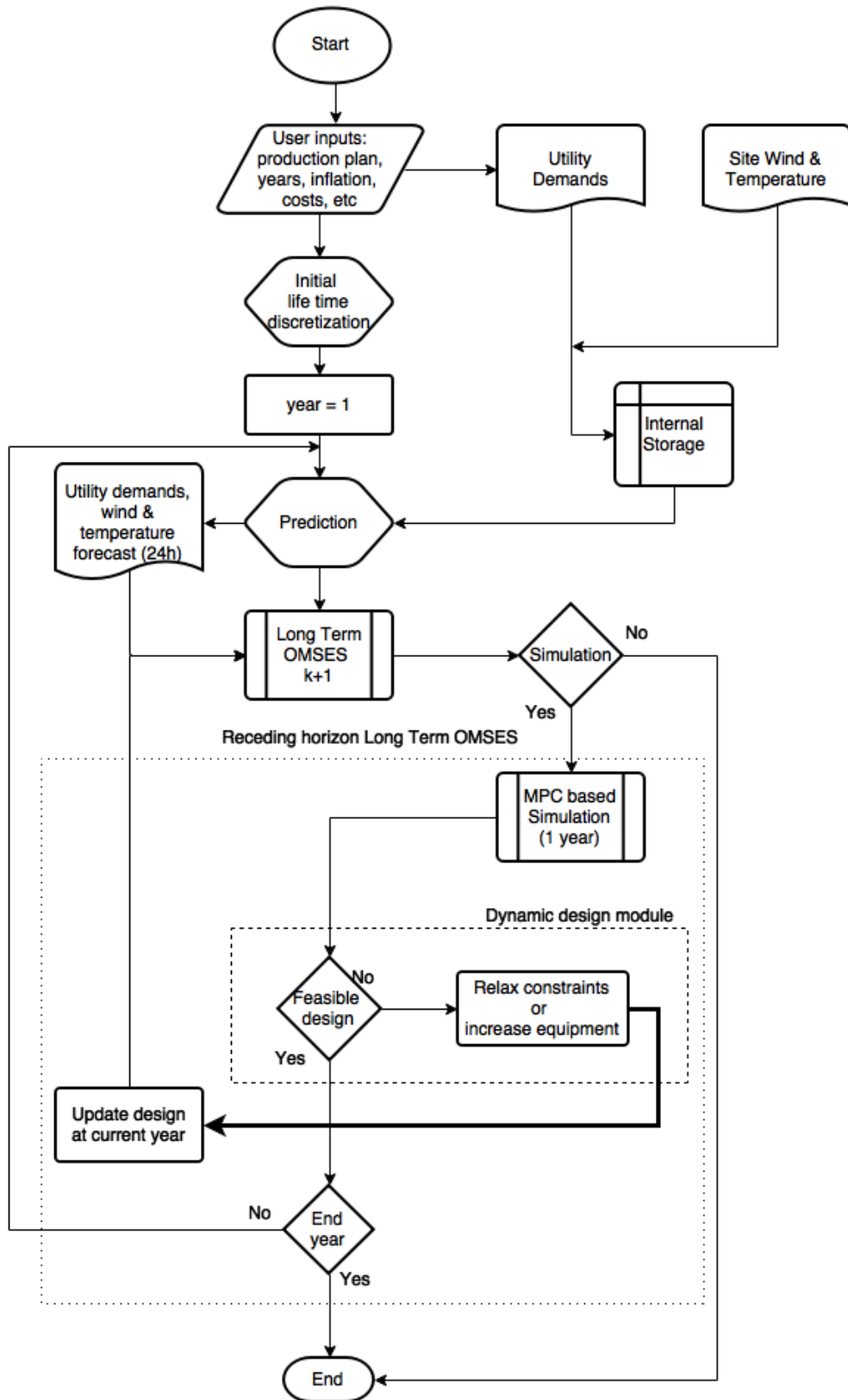
@OLE('C:\Users\aromero.CORP\Desktop\PhD\MPC\Lingo\P2H\Results.xlsx',
'FMWREXTRA','ICWREXTRA') = FMWREXTRA,ICWREXTRA;

ENDDATA
END

```

## **A8.2. Long Term OMSES with simulation algorithm**

Flowchart



## *MATLAB (code for long term OMSES without MPC, i.e., no simulation)*

```
function matlinLTOMSES
clc
clear all

%% Excel connections
% Create object.
ExcelApp = actxserver('Excel.Application');
% Show window (optional).
ExcelApp.Visible = 0;
% Open file connection
file = ExcelApp.Workbooks.Open(fullfile(pwd, 'data2.xlsm'));
file2 = ExcelApp.Workbooks.Open(fullfile(pwd, 'demandsMMC.xls'));
file3 = ExcelApp.Workbooks.Open(fullfile(pwd, 'results.xlsx'));

%% Mine community consolidation
Nco=0; % Number of communities
Nsc=0; % services demand multiplier
Nop=1; % open pit mines multiplier
Nug=0; % underground mines multiplier
file2.Activate
eActivsheetRange = ExcelApp.Activesheet.get('Range', 'F1:F4');
eActivsheetRange.Value = [Nco Nsc Nop Nug]';

%% Energy prices
PDI=130; % Diesel [CAD/MWh]
PBM=50; % Biomass [CAD/MWh]
PPR=80; % Propane [CAD/MWh]
PCG=15; % Natural gas [CAD/MWh]
file.Activate
eActivsheetRange = ExcelApp.Activesheet.get('Range', 'A1:A4');
eActivsheetRange.Value = [PDI PBM PPR PCG]';

%% Demand multipliers
DM1Y=1; % First annual series compared to full demand [-]
DM2Y=1; % Second annual series compared to full demand [-]
DM3Y=1; % Third annual series compared to full demand [-]
file2.Activate
% First year series
eActivsheetRange = ExcelApp.Activesheet.get('Range', 'AG1');
eActivsheetRange.Value = DM1Y;
% Second year series
eActivsheetRange = ExcelApp.Activesheet.get('Range', 'AN1');
eActivsheetRange.Value = DM2Y;
% Third year is always 1 (excel does not need to be updated)

%% Annual intervals
AI1Y=5; % First annual series [year]
AI2Y=5; % Second annual series [year]
AI3Y=10; % Third annual series [year]
AI=[AI1Y AI2Y AI3Y];
```

```

%% Economic data
id=0.1;      % Discount rate [-]
jr=.05;     % General inflation [-]
je=.08;     % Fuel inflation [-]
idp=(id-jr)/(1+jr);
idpp=(id-je)/(1+je);

pwfe=zeros(1,sum(AI));
for i=1:sum(AI)
    pwfe(1,i)=1/(1+idpp)^(i-1);
end

EIR=zeros(1,3);
empieza=[1 AI(1)+1 AI(1)+AI(2)+1];
life=[sum(AI(1:3)) sum(AI(2:3)) AI(3)];
for i=1:3
    FAY(1,i)=1/(1+idp)^(empieza(i)-1)*1;
    for j=1:AI(i)
        EIR(1,i)=EIR(1,i)+pwfe(1,empieza(i)+j-1);
    end
end

file.Activate
eActivsheetRange = ExcelApp.Activesheet.get('Range', 'F2:F4');
eActivsheetRange.Value = FAY';
eActivsheetRange = ExcelApp.Activesheet.get('Range', 'G2:G4');
eActivsheetRange.Value = EIR';

%% Degradation factor
DF=[1 2 3]; % Dimensionless
file.Activate
eActivsheetRange = ExcelApp.Activesheet.get('Range', 'K2:M2');
eActivsheetRange.Value = DF;

%% Matlab to Excel.
NET=zeros(19,1);
scenarios=1;
ANNUAL_COST=zeros(scenarios,1);

tic
for i=1:scenarios
    i;
    PDI=PDI;
    PPR=PPR;
    PCG=PCG;
    Caux(i)=PCG;
    file.Activate
    eActivsheetRange = ExcelApp.Activesheet.get('Range', 'A1');
    eActivsheetRange.Value = PDI;
    eActivsheetRange = ExcelApp.Activesheet.get('Range', 'A2');
    eActivsheetRange.Value = PBM;
    eActivsheetRange = ExcelApp.Activesheet.get('Range', 'A3');
    eActivsheetRange.Value = PPR;
    eActivsheetRange = ExcelApp.Activesheet.get('Range', 'A4');
    eActivsheetRange.Value = PCG;
    %% Execute Lingo %%%%%%%%%%%%%%

```

```

system('C:\LINGO11\RunLingo
C:\Users\aromero.CORP\Documents\Demands_Calculation\LINGO_MODELS\LTOMSES\ltom
ses.ltf')
%%%%%%%%%%%%%%%%%%%%%%%%%%%%%%%%%%%%%%%%%%%%%%%%%%%%%%%%%%%%%%%%%%%%%%%%
file3.Activate
eSheets = ExcelApp.ActiveWorkbook.Sheets;
eSheet1 = eSheets.get('Item', 1);
eSheet1.Activate;
Activesheet = ExcelApp.Activesheet.get('Range', 'B3:D21');
NET(:,i:i+3-1) = round(cell2mat(Activesheet.value));
Activesheet = ExcelApp.Activesheet.get('Range', 'B22');
ANNUAL_COST(i) = (Activesheet.value);
end
toc

%% Close excel files
file.Save;
file.Close;
file2.Save;
file2.Close;
file3.Save;
file3.Close;
ExcelApp.Quit;
ExcelApp.release;

%% Results output
TECH=zeros(19,1);
TECH=['TGVA '
'MGWC '
'CGVA '
'CGWC '
'ICVA '
'ICWC '
'FAVA '
'FAWC '
'FMWR '
'ICWR '
'DIWC '
'GFBM '
'FTDI '
'BMVA '
'DIBO '
'EEWC '
'STVA '
'MPWC '
'CPWC '];
S1 = horzcat( TECH,num2str(NET))
ANNUAL_COST
plot(Caux,ANNUAL_COST,'-or')
hold on

[NET(:,1,:)
NET(:,2,:)
NET(:,3,:)
ANNUAL_COST
AI1Y
AI2Y

```

AI3Y  
DM1Y  
DM2Y  
DM3Y  
DF(1)  
DF(2)  
DF(3)  
id  
jr  
jel

*Lingo optimization subroutine (investment plan optimizer)*

MODEL:

MIN = ANNUAL\_COST;

SETS:

UTIL /CG,VA,WC,WR,AA,WF,EE,DI,BM,PR/: INDCOM, INDDDEM, INDVEN, INDDDES;

DAYS/ JANUARY, FEBRUARY, MARCH, APRIL, MAY, JUNE!, JULY, AUGUST, SEPTEMBER,  
OCTOBER, NOVEMBER, DECEMBER;

/: NDA;

HOURS /1AM 2AM 3AM 4AM 5AM 6AM 7AM 8AM 9AM 10AM 11AM 12AM 1PM 2PM 3PM 4PM 5PM  
6PM 7PM 8PM 9PM 10PM 11PM 12PM /: NHD ;

YEAR /YEAR1, YEAR2, YEAR3/:NAY, FAY, AFIXC, AVARC,  
DVAA, DWCA, DWFA, DEEA, DDIA,  
INVESTMENT,  
CTECGA, CTEPRA, CTECEA, INGVEA, CTEOMA, CTEDIA, CTEBMA,  
CCGA, CPRA, CEEA, VEEA, CDIA, CBMA, EIR, PWF;

TEUT (TECN,UTIL)/TGVA,CG	TGVA,VA	TGVA,WC		TGVA,EE
	MGWC,CG	MGWC,VA	MGWC,WC	MGWC,WR
MGWC,EE				
	CGVA,CG	CGVA,VA		
	CGWC,CG		CGWC,WC	
		ICVA,VA	ICVA,WC	
			ICWC,WC	
		FAVA,VA		ICWC,WR
FAVA,EE			FAVA,WR	FAVA,WF
		FAWC,WC	FAWC,WR	FAWC,WF
FAWC,EE				
			FMWR,WR	FMWR,WF
FMWR,EE				
			ICWR,WR	ICWR,AA
ICWR,EE				
		DIWC,WC		DIWC,WR
DIWC,EE	DIWC,DI			
	GFBM,CG			GFBM,VA
GFBM,BM				
	FTDI,CG			FTDI,VA
FTDI,DI				
		BMWC,VA		
BMWC,BM				
		DIBO,WC		
DIBO,DI				
		EEWC,WC		
EEWC,EE				
			STVA,VA	STVA,WR
STVA,EE				
	MPWC,VA	MPWC,WC	MPWC,WR	MPWC,EE
MPWC,PR				

CPWC,WC

CPWC,PR

/: INDC, INDP, RIJV;

DHU(YEAR,DAYS,HOURS,UTIL): DEMDHU, COMDHU, CONDHU, PRODHU, VENDHU, DESDHU;

DHT(YEAR,DAYS,HOURS,TECN): PRODHT, alpha, betha, PRODHT1,PRODHT2,PRODHT3;

DHTU(YEAR,DAYS,HOURS,TECN,UTIL): FDHTU;

DIHO(DAYS,HOURS): DVAH, DWCH, DWFH, DEEH, DDIH,  
DVAH1Y, DWCH1Y, DWFH1Y, DEEH1Y, DDIH1Y,  
DVAH2Y, DWCH2Y, DWFH2Y, DEEH2Y, DDIH2Y,  
PCEDH, PVEDH;

#####  
####;

YETE(YEAR,TECN): CIN, PRA, NET2Y, PIN, FOV2Y;

YEDI(YEAR,DAYS):

DVAD,DWCD,DWFD,DEED,DDID,  
CCGD,CPRD,CEED,VEED,CDID,CBMD,  
CTECED,INGVED,CTECGD,CTEPRD,CTEDID,CTEBMD,CTEOMD,CVARID;

YEDIHO(YEAR,DAYS,HOURS): CCGH,CPRH,CEEH,VEEH,CDIH,CBMH,  
NTS,NMS,NMDS,NMPS,  
CTECEH,INGVEH,CTECGH,CTEPRH,CTEDIH,CTEBMH,CTEOMH,CVARIH;

#####  
####;

ENDSETS

DATA:

BIGR = 500; BIGN = 500;

YVE,YCE,YDQ,ACEMIN,PCG2,PPR2,PCE,CECP,CECV,PVE,CEVP,CEVV,FCI,FAM =  
@FILE('ltomses.ldt');

INDCOM,INDDEM,INDVEN,INDDES = @FILE('ltomses.ldt');

YPT,NET,PET,CBM,FOV = @FILE('ltomses.ldt');

NDA = @FILE('ltomses.ldt');

NHD = @FILE('ltomses.ldt');

INDC = @FILE('ltomses.ldt');

INDP = @FILE('ltomses.ldt');

RIJV = @FILE('ltomses.ldt');

DVAH, DWCH, DWFH, DEEH, DDIH =  
@OLE('C:\Users\aromero.CORP\Documents\Demands\_Calculation\LINGO\_MODELS\LTOMSE  
S\demandsMMC.xls','DVAH','DWCH','DWFH','DEEH','DDIH');

PDI, PBM, PPR, PCG=  
@OLE('C:\Users\aromero.CORP\Documents\Demands\_Calculation\LINGO\_MODELS\LTOMSE  
S\data2.xlsm','PDI','PBM','PPR','PCG');

DVAH1Y, DWCH1Y, DWFH1Y, DEEH1Y, DDIH1Y =  
@OLE('C:\Users\aromero.CORP\Documents\Demands\_Calculation\LINGO\_MODELS\LTOMSE  
S\demandsMMC.xls','DVAH1y','DWCH1y','DWFH1y','DEEH1y','DDIH1y');

DVAH2Y, DWCH2Y, DWFH2Y, DEEH2Y, DDIH2Y =  
@OLE('C:\Users\aromero.CORP\Documents\Demands\_Calculation\LINGO\_MODELS\LTOMSE  
S\demandsMMC.xls','DVAH2y','DWCH2y','DWFH2y','DEEH2y','DDIH2y');

```
NAY, FAY, FOV2Y, EIR, PWF=
@OLE('C:\Users\aromero.CORP\Documents\Demands_Calculation\LINGO_MODELS\LTOMSE
S\data2.xlsm', 'NAY', 'FAY', 'FOV2Y', 'EIR', 'PWF');
```

```
ENDDATA
```

```
@FOR (DAYS(kd) :
```

```
@FOR (HOURS(kh) :
```

```
PCEDH(kd, kh) = PCE ;
```

```
PVEDH(kd, kh) = PVE ;
```

```
););
```

```
@FOR (YEDI(ky, kd) | ky#EQ#3 :
```

```
DVAD(ky, kd) = @SUM(HOURS(kh) : NHD(kh) * DVAH(kd, kh));
```

```
DWCD(ky, kd) = @SUM(HOURS(kh) : NHD(kh) * DWCH(kd, kh));
```

```
DWFD(ky, kd) = @SUM(HOURS(kh) : NHD(kh) * DWFH(kd, kh));
```

```
DEED(ky, kd) = @SUM(HOURS(kh) : NHD(kh) * DEEH(kd, kh));
```

```
DDID(ky, kd) = @SUM(HOURS(kh) : NHD(kh) * DDIH(kd, kh));
```

```
);
```

```
@FOR (YEDI(ky, kd) | ky#EQ#2 :
```

```
DVAD(ky, kd) = @SUM(HOURS(kh) : NHD(kh) * DVAH2Y(kd, kh));
```

```
DWCD(ky, kd) = @SUM(HOURS(kh) : NHD(kh) * DWCH2Y(kd, kh));
```

```
DWFD(ky, kd) = @SUM(HOURS(kh) : NHD(kh) * DWFH2Y(kd, kh));
```

```
DEED(ky, kd) = @SUM(HOURS(kh) : NHD(kh) * DEEH2Y(kd, kh));
```

```
DDID(ky, kd) = @SUM(HOURS(kh) : NHD(kh) * DDIH2Y(kd, kh));
```

```
);
```

```
@FOR (YEDI(ky, kd) | ky#EQ#1 :
```

```
DVAD(ky, kd) = @SUM(HOURS(kh) : NHD(kh) * DVAH1Y(kd, kh));
```

```
DWCD(ky, kd) = @SUM(HOURS(kh) : NHD(kh) * DWCH1Y(kd, kh));
```

```
DWFD(ky, kd) = @SUM(HOURS(kh) : NHD(kh) * DWFH1Y(kd, kh));
```

```
DEED(ky, kd) = @SUM(HOURS(kh) : NHD(kh) * DEEH1Y(kd, kh));
```

```
DDID(ky, kd) = @SUM(HOURS(kh) : NHD(kh) * DDIH1Y(kd, kh));
```

```
);
```

```
@FOR (YEAR(ky) :
```

```
DVAA(ky) = @SUM(DAYS(kd) : NDA(kd) * DVAD(ky, kd));
```

```
DWCA(ky) = @SUM(DAYS(kd) : NDA(kd) * DWCD(ky, kd));
```

```
DWFA(ky) = @SUM(DAYS(kd) : NDA(kd) * DWFD(ky, kd));
```

```
DEEA(ky) = @SUM(DAYS(kd) : NDA(kd) * DEED(ky, kd));
```

```
DDIA(ky) = @SUM(DAYS(kd) : NDA(kd) * DDID(ky, kd));
```

```
);
```

```
! Our Objective -> Minimize annual cost (euros/year);
```

```
@FREE ( ANNUAL_COST );
```

```
ANNUAL_COST = @SUM(YEAR(ky) : AFIXC(ky)) + @SUM(YEAR(ky) : EIR(ky)
*AVARC(ky));
```

```
@FOR (YEAR(ky) :
```

```
INVESTMENT(ky) = FCI * @SUM (TECN(i) : CIN(ky, i));
```

```
AFIXC(ky) = FAY(ky) * INVESTMENT(ky);
```

```
CTECGA(ky) = @SUM(DAYS(kd) : NDA(kd) * CTECGD(ky, kd));
```

```

CTEPRA (ky) = @SUM(DAYS (kd) : NDA (kd) * CTEPRD (ky, kd) );
CTECEA (ky) = @SUM(DAYS (kd) : NDA (kd) * CTECED (ky, kd) );
INGVEA (ky) = @SUM(DAYS (kd) : NDA (kd) * INGVED (ky, kd) );
CTEOMA (ky) = @SUM(DAYS (kd) : NDA (kd) * CTEOMD (ky, kd) );
CTEDIA (ky) = @SUM(DAYS (kd) : NDA (kd) * CTEDID (ky, kd) );
CTEBMA (ky) = @SUM(DAYS (kd) : NDA (kd) * CTEBMD (ky, kd) );

);

@FOR (YEAR (ky) :

@FREE (AVARC (ky) );
AVARC (ky) = CTECGA (ky) + CTEPRA (ky) + CTECEA (ky) - INGVEA (ky) +
CTEOMA (ky) + CTEDIA (ky) + CTEBMA (ky) ;
);

@FOR (YEDI (ky, kd) :
CTECGD (ky, kd) = @SUM(HOURS (kh) : NHD (kh) * CTECGH (ky, kd, kh) );
CTEPRD (ky, kd) = @SUM(HOURS (kh) : NHD (kh) * CTEPRH (ky, kd, kh) );
CTECED (ky, kd) = @SUM(HOURS (kh) : NHD (kh) * CTECEH (ky, kd, kh) );
INGVED (ky, kd) = @SUM(HOURS (kh) : NHD (kh) * INGVEH (ky, kd, kh) );
CTEOMD (ky, kd) = @SUM(HOURS (kh) : NHD (kh) * CTEOMH (ky, kd, kh) );
CTEDID (ky, kd) = @SUM(HOURS (kh) : NHD (kh) * CTEDIH (ky, kd, kh) );
CTEBMD (ky, kd) = @SUM(HOURS (kh) : NHD (kh) * CTEBMH (ky, kd, kh) );

@FREE (CVARID (ky, kd) );
CVARID (ky, kd) = CTECGD (ky, kd) + CTEPRD (ky, kd) + CTECED (ky, kd) -
INGVED (ky, kd) + CTEOMD (ky, kd) + CTEDID (ky, kd) + CTEBMD (ky, kd) ;
);

@FOR (YEDIHO (ky, kd, kh) :
CTECGH (ky, kd, kh) = PCG * CCGH (ky, kd, kh) ;
CTEPRH (ky, kd, kh) = PPR * CPRH (ky, kd, kh) ;
CTECEH (ky, kd, kh) = PCEDH (kd, kh) * CEEH (ky, kd, kh) ;
INGVEH (ky, kd, kh) = PVEDH (kd, kh) * VEEH (ky, kd, kh) ;
CTEDIH (ky, kd, kh) = PDI * CDIH (ky, kd, kh) ;
CTEBMH (ky, kd, kh) = PBM * CBMH (ky, kd, kh) ;
@FREE (CVARIH (ky, kd, kh) );
CVARIH (ky, kd, kh) = CTECGH (ky, kd, kh) + CTEPRH (ky, kd, kh) + CTECEH (ky, kd, kh) -
INGVEH (ky, kd, kh) + CTEOMH (ky, kd, kh) + CTEDIH (ky, kd, kh) + CTEBMH (ky, kd, kh) ;
);

@FOR (DIHO (kd, kh) :
CTEOMH (@INDEX (YEAR1) , kd, kh) = @SUM (TECN (i) :
FOV (i) * FOV2Y (@INDEX (YEAR1) , i) * PRODHT1 (@INDEX (YEAR1) , kd, kh, i) );
);

@FOR (DIHO (kd, kh) :
CTEOMH (@INDEX (YEAR2) , kd, kh) = @SUM (TECN (i) :
FOV (i) * (
FOV2Y (@INDEX (YEAR2) , i) * PRODHT1 (@INDEX (YEAR2) , kd, kh, i) +
FOV2Y (@INDEX (YEAR1) , i) * PRODHT2 (@INDEX (YEAR2) , kd, kh, i) ) ;
);

@FOR (DIHO (kd, kh) :
CTEOMH (@INDEX (YEAR3) , kd, kh) = @SUM (TECN (i) :

```

```

FOV(i)*(
FOV2Y(@INDEX(YEAR3),i)*PRODHT1(@INDEX(YEAR3),kd,kh,i) +
FOV2Y(@INDEX(YEAR2),i)*PRODHT2(@INDEX(YEAR3),kd,kh,i)+
FOV2Y(@INDEX(YEAR1),i)*PRODHT3(@INDEX(YEAR3),kd,kh,i));
);

@BIN (YCE);
! Tecnologias;
@FOR (TECN(i):
    @BIN (YPT(i));
);

@FOR (YEAR(ky):
@FOR (TECN(i):
    @GIN (NET2Y(ky,i));
    NET2Y(ky,i) <= YPT(i) * BIGN;
    !PRA(ky,i) <= YPT(i) * BIGN * 24 * 12 *10;
    PIN(ky,i) = NET2Y(ky,i) * PET(i);
    CIN(ky,i) = NET2Y(ky,i) * CBM(i) ;
    PRA(ky,i) = @SUM (DHT(ky,kd,kh,i) : NDA(kd)*NHD(kh)*PRODHT(ky,kd,kh,i));
););

!=====;

@FOR (YEAR(ky) :
NET2Y(ky,@INDEX(TGVA )) =0;
!NET2Y(ky,@INDEX(MGWC )) =0;
NET2Y(ky,@INDEX(MPWC )) =0;
!NET2Y(ky,@INDEX(DIWC )) = 0;
!NET2Y(ky,@INDEX(CPWC )) =0;
!NET2Y(ky,@INDEX(CGWC )) =3;

!NET2Y(ky,@INDEX(ICVA )) =0;
!NET2Y(ky,@INDEX(ICWC )) =0;
NET2Y(ky,@INDEX(FAVA )) =0;
!NET2Y(ky,@INDEX(FAWC )) =0;
!NET2Y(ky,@INDEX(FMWR)) =4;

!NET2Y(ky,@INDEX(EEWC )) =0;
!NET2Y(ky,@INDEX(STVA )) =0;
!NET2Y(ky,@INDEX(DIBO )) =0;

!NET2Y(ky,@INDEX(GFBM )) =0;
!NET2Y(ky,@INDEX(FTDI )) =0;
);
!=====;

! Production limits;
@FOR (YEAR(ky) :
    @FOR (DAYS(kd) :
        @FOR (HOURS(kh) :
            @GIN (NTS(ky,kd,kh)); NTS(ky,kd,kh) <= NET2Y(ky,@INDEX(TGVA));
! PRODHT(kd,kh,@INDEX(TGVA)) = NTS(kd,kh) * PET(@INDEX(TGVA));
            @GIN (NMS(ky,kd,kh)); NMS(ky,kd,kh) <= NET2Y(ky,@INDEX(MGWC));
! PRODHT(kd,kh,@INDEX(MGWC)) = NMS(kd,kh) * PET(@INDEX(MGWC));

```

```

                @GIN (NMDS (ky, kd, kh) ) ;                NMDS (ky, kd, kh)                <=
NET2Y (ky, @INDEX (DIWC) ) ;                ! PRODHT (kd, kh, @INDEX (DIWC) )                =                NMDS (kd, kh)                *
PET (@INDEX (DIWC) ) ;
                @GIN (NMPS (ky, kd, kh) ) ;                NMPS (ky, kd, kh)                <=
NET2Y (ky, @INDEX (MPWC) ) ;
) ; ) ; ) ;

@FOR (YEAR (ky) | ky#EQ#1 :
    @FOR (DAYS (kd) :
        @FOR (HOURS (kh) :
            @FOR (TECN (i) :
                ! PRODHT (ky, kd, kh, i) <= PIN (ky, i) ;

                PRODHT (ky, kd, kh, i)                =
PRODHT1 (ky, kd, kh, i) + PRODHT2 (ky, kd, kh, i) + PRODHT3 (ky, kd, kh, i) ;
                PRODHT1 (ky, kd, kh, i) <= PIN (ky, i) ;
                PRODHT2 (ky, kd, kh, i) = 0 ;
                PRODHT3 (ky, kd, kh, i) = 0 ;
            ) ; ) ; ) ; ) ;

@FOR (YEAR (ky) | ky#EQ#2 :
    @FOR (DAYS (kd) :
        @FOR (HOURS (kh) :
            @FOR (TECN (i) :
                PRODHT (ky, kd, kh, i)                =
PRODHT1 (ky, kd, kh, i) + PRODHT2 (ky, kd, kh, i) + PRODHT3 (ky, kd, kh, i) ;
                PRODHT1 (ky, kd, kh, i) <= PIN (@INDEX (YEAR1) , i) ;
                PRODHT2 (ky, kd, kh, i) <= PIN (ky, i) ;
                PRODHT3 (ky, kd, kh, i) = 0 ;
            ) ; ) ; ) ; ) ;

@FOR (YEAR (ky) | ky#EQ#3 :
    @FOR (DAYS (kd) :
        @FOR (HOURS (kh) :
            @FOR (TECN (i) :
                PRODHT (ky, kd, kh, i)                =
PRODHT1 (ky, kd, kh, i) + PRODHT2 (ky, kd, kh, i) + PRODHT3 (ky, kd, kh, i) ;
                PRODHT1 (ky, kd, kh, i) <= PIN (@INDEX (YEAR1) , i) ;
                PRODHT2 (ky, kd, kh, i) <= PIN (@INDEX (YEAR2) , i) ;
                PRODHT3 (ky, kd, kh, i) <= PIN (ky, i) ;
            ) ; ) ; ) ; ) ;

@FOR (YEAR (ky) :
    @FOR (DAYS (kd) :
        @FOR (HOURS (kh) :
            @FOR (TECN (i) :
                @GIN (alpha (ky, kd, kh, i) ) ;    @GIN (betha (ky, kd, kh, i) ) ;
            ) ; ) ; ) ; ) ;

! Flows;
@FOR (YEAR (ky) :
    @FOR (DAYS (kd) :
        @FOR (HOURS (kh) :
            @FOR (TEUT (i, j) :

```

```

                FDHTU(ky, kd, kh, i, j) = PRODHT(ky, kd, kh, i) * RIJV(i, j);
););););

! Utility balances;
@FOR(YEAR(ky) :
    @FOR(DAYS(kd) :
        @FOR(HOURS(kh) :
            @FOR(UTIL(j) :
                CONDHU(ky, kd, kh, j) = @SUM(TEUT(i, j) :
INDC(i, j) * FDHTU(ky, kd, kh, i, j));
                PRODHU(ky, kd, kh, j) = @SUM(TEUT(i, j) :
INDP(i, j) * FDHTU(ky, kd, kh, i, j));
                COMDHU(ky, kd, kh, j) <= INDCOM(j) * BIGR;
                DEMDHU(ky, kd, kh, j) <= INDDEM(j) * BIGR;
                VENDHU(ky, kd, kh, j) <= INDVEN(j) * BIGR;
                DESDHU(ky, kd, kh, j) <= INDDDES(j) * BIGR;
                COMDHU(ky, kd, kh, j) + PRODHU(ky, kd, kh, j) = CONDHU(ky, kd, kh, j)
+ DEMDHU(ky, kd, kh, j) + VENDHU(ky, kd, kh, j) + DESDHU(ky, kd, kh, j);
);););););

@FOR(DAYS(kd) :
    @FOR(HOURS(kh) :
        DEMDHU(@INDEX(YEAR1), kd, kh, @INDEX(va)) = DVAH1Y(kd, kh);
        DEMDHU(@INDEX(YEAR1), kd, kh, @INDEX(wc)) = DWCH1Y(kd, kh);
        DEMDHU(@INDEX(YEAR1), kd, kh, @INDEX(wf)) = DWFH1Y(kd, kh);
        DEMDHU(@INDEX(YEAR1), kd, kh, @INDEX(ee)) = DEEH1Y(kd, kh);
        DEMDHU(@INDEX(YEAR1), kd, kh, @INDEX(di)) = DDIH1Y(kd, kh);

        DEMDHU(@INDEX(YEAR2), kd, kh, @INDEX(va)) = DVAH2Y(kd, kh);
        DEMDHU(@INDEX(YEAR2), kd, kh, @INDEX(wc)) = DWCH2Y(kd, kh);
        DEMDHU(@INDEX(YEAR2), kd, kh, @INDEX(wf)) = DWFH2Y(kd, kh);
        DEMDHU(@INDEX(YEAR2), kd, kh, @INDEX(ee)) = DEEH2Y(kd, kh);
        DEMDHU(@INDEX(YEAR2), kd, kh, @INDEX(di)) = DDIH2Y(kd, kh);

        DEMDHU(@INDEX(YEAR3), kd, kh, @INDEX(va)) = DVAH(kd, kh);
        DEMDHU(@INDEX(YEAR3), kd, kh, @INDEX(wc)) = DWCH(kd, kh);
        DEMDHU(@INDEX(YEAR3), kd, kh, @INDEX(wf)) = DWFH(kd, kh);
        DEMDHU(@INDEX(YEAR3), kd, kh, @INDEX(ee)) = DEEH(kd, kh);
        DEMDHU(@INDEX(YEAR3), kd, kh, @INDEX(di)) = DDIH(kd, kh);
);););

@FOR(YEAR(ky) :
@FOR(DAYS(kd) :
    @FOR(HOURS(kh) :
        CCGH(ky, kd, kh) = COMDHU(ky, kd, kh, @INDEX(cg));
        CPRH(ky, kd, kh) = COMDHU(ky, kd, kh, @INDEX(PR));
        CEEH(ky, kd, kh) = COMDHU(ky, kd, kh, @INDEX(ee)); CEEH(ky, kd, kh) <=
YCE*BIGR; !CEEH(kd, kh) = 0;
        VEEH(ky, kd, kh) = VENDHU(ky, kd, kh, @INDEX(ee)); VEEH(ky, kd, kh) <=
YVE*BIGR;
        CDIH(ky, kd, kh) = COMDHU(ky, kd, kh, @INDEX(di)); !CDIH(kd, kh) <= 8;
        CBMH(ky, kd, kh) = COMDHU(ky, kd, kh, @INDEX(bm));
););););

!standing#####;

```

```

! Daily and yearly results;
@FOR (YEAR (ky) :
@FOR (DAYS (kd) :
  CCGD (ky, kd) = @SUM (HOURS (kh) : NHD (kh) * CCGH (ky, kd, kh) );
  CPRD (ky, kd) = @SUM (HOURS (kh) : NHD (kh) * CPRH (ky, kd, kh) );
  CEED (ky, kd) = @SUM (HOURS (kh) : NHD (kh) * CEEH (ky, kd, kh) );
  VEED (ky, kd) = @SUM (HOURS (kh) : NHD (kh) * VEEH (ky, kd, kh) );
  CDID (ky, kd) = @SUM (HOURS (kh) : NHD (kh) * CDIH (ky, kd, kh) );
  CBMD (ky, kd) = @SUM (HOURS (kh) : NHD (kh) * CBMH (ky, kd, kh) );
);

CCGA (ky) = @SUM (DAYS (kd) : NDA (kd) * CCGD (ky, kd) );
CPRA (ky) = @SUM (DAYS (kd) : NDA (kd) * CPRD (ky, kd) );
CEEA (ky) = @SUM (DAYS (kd) : NDA (kd) * CEED (ky, kd) );
VEEA (ky) = @SUM (DAYS (kd) : NDA (kd) * VEED (ky, kd) );
CDIA (ky) = @SUM (DAYS (kd) : NDA (kd) * CDID (ky, kd) ); !CDIA <=100000;
CBMA (ky) = @SUM (DAYS (kd) : NDA (kd) * CBMD (ky, kd) );
);

!@SUM (YEAR (ky) : CDIA (ky) * NAY (ky) ) <= 70000 * @SUM (YEAR (ky) : NAY (ky) );
!@SUM (YEAR (ky) : CBMA (ky) * NAY (ky) ) <= 400000 * @SUM (YEAR (ky) : NAY (ky) );

@FOR (YEAR (ky) :
@FOR (DAYS (kd) | kd#GE#1 :
  @SUM (DAYS (kd) : NDA (kd) * CDID (ky, kd) ) <= 30000;
););

@FOR (YEAR (ky) :
@FOR (DAYS (kd) | kd#GE#1 :
  @SUM (DAYS (kd) : NDA (kd) * CBMD (ky, kd) ) <= 450000;
););

! Annual fuel consumed by cogeneration equipment;

!@FOR (YEAR (ky) :
FCO = @SUM (FCIJ (i, j) : PRA (ky, i) * RIJV (i, j) );
! Annual cogenerated work;
!WCO = @SUM (WCIJ (i, j) : PRA (ky, i) * RIJV (i, j) );
! Annual cogenerated heat;
!QCO = @SUM (QCIJ (i, j) : PRA (ky, i) * RIJV (i, j) );
! Annual waste heat;
!QCD = @SUM (QDIJ (i, j) : PRA (ky, i) * RIJV (i, j) );
! 3. DO NOT waste thermal energy;
!QCD <= YDQ*100*8760;
!QHO = @SUM (QHIJ (i, j) : PRA (ky, i) * RIJV (i, j) );
!);

!@FOR (YEAR (ky) :
@FOR (TEUT (i, j) :
  TOTO2 (ky, i, j) = PRA (ky, i) * RIJV (i, j) ;
!);!);

NETTGVA =NET2Y (@INDEX (YEAR1 ), @INDEX (TGVA ) );
NETMGWC=NET2Y (@INDEX (YEAR1 ), @INDEX (MGWC) );
NETCGVA =NET2Y (@INDEX (YEAR1 ), @INDEX (CGVA ) );

```

NETCGWC=NET2Y (@INDEX (YEAR1 ) , @INDEX (CGWC ) );  
 NETICVA =NET2Y (@INDEX (YEAR1 ) , @INDEX (ICVA ) );  
 NETICWC=NET2Y (@INDEX (YEAR1 ) , @INDEX (ICWC ) );  
 NETFAVA =NET2Y (@INDEX (YEAR1 ) , @INDEX (FAVA ) );  
 NETFAWC =NET2Y (@INDEX (YEAR1 ) , @INDEX (FAWC ) );  
 NETFMWR =NET2Y (@INDEX (YEAR1 ) , @INDEX (FMWR ) );  
 NETICWR =NET2Y (@INDEX (YEAR1 ) , @INDEX (ICWR ) );  
 NETDIWC =NET2Y (@INDEX (YEAR1 ) , @INDEX (DIWC ) );  
 NETGFBM =NET2Y (@INDEX (YEAR1 ) , @INDEX (GFBM ) );  
 NETFTDI =NET2Y (@INDEX (YEAR1 ) , @INDEX (FTDI ) );  
 NETBMWC =NET2Y (@INDEX (YEAR1 ) , @INDEX (BMWC ) );  
 NETDIBO =NET2Y (@INDEX (YEAR1 ) , @INDEX (DIBO ) );  
 NETEEWC =NET2Y (@INDEX (YEAR1 ) , @INDEX (EEWC ) );  
 NETSTVA=NET2Y (@INDEX (YEAR1 ) , @INDEX (STVA ) );  
 NETMPWC=NET2Y (@INDEX (YEAR1 ) , @INDEX (MPWC ) );  
 NETCPWC=NET2Y (@INDEX (YEAR1 ) , @INDEX (CPWC ) );

NETTGVA2 =NET2Y (@INDEX (YEAR2 ) , @INDEX (TGVA ) );  
 NETMGWC2 =NET2Y (@INDEX (YEAR2 ) , @INDEX (MGWC ) );  
 NETCGVA2 =NET2Y (@INDEX (YEAR2 ) , @INDEX (CGVA ) );  
 NETCGWC2 =NET2Y (@INDEX (YEAR2 ) , @INDEX (CGWC ) );  
 NETICVA2 =NET2Y (@INDEX (YEAR2 ) , @INDEX (ICVA ) );  
 NETICWC2 =NET2Y (@INDEX (YEAR2 ) , @INDEX (ICWC ) );  
 NETFAVA2 =NET2Y (@INDEX (YEAR2 ) , @INDEX (FAVA ) );  
 NETFAWC2 =NET2Y (@INDEX (YEAR2 ) , @INDEX (FAWC ) );  
 NETFMWR2 =NET2Y (@INDEX (YEAR2 ) , @INDEX (FMWR ) );  
 NETICWR2 =NET2Y (@INDEX (YEAR2 ) , @INDEX (ICWR ) );  
 NETDIWC2 =NET2Y (@INDEX (YEAR2 ) , @INDEX (DIWC ) );  
 NETGFBM2 =NET2Y (@INDEX (YEAR2 ) , @INDEX (GFBM ) );  
 NETFTDI2 =NET2Y (@INDEX (YEAR2 ) , @INDEX (FTDI ) );  
 NETBMWC2 =NET2Y (@INDEX (YEAR2 ) , @INDEX (BMWC ) );  
 NETDIBO2 =NET2Y (@INDEX (YEAR2 ) , @INDEX (DIBO ) );  
 NETEEWC2 =NET2Y (@INDEX (YEAR2 ) , @INDEX (EEWC ) );  
 NETSTVA2 =NET2Y (@INDEX (YEAR2 ) , @INDEX (STVA ) );  
 NETMPWC2 =NET2Y (@INDEX (YEAR2 ) , @INDEX (MPWC ) );  
 NETCPWC2 =NET2Y (@INDEX (YEAR2 ) , @INDEX (CPWC ) );

NETTGVA3 =NET2Y (@INDEX (YEAR3 ) , @INDEX (TGVA ) );  
 NETMGWC3 =NET2Y (@INDEX (YEAR3 ) , @INDEX (MGWC ) );  
 NETCGVA3 =NET2Y (@INDEX (YEAR3 ) , @INDEX (CGVA ) );  
 NETCGWC3 =NET2Y (@INDEX (YEAR3 ) , @INDEX (CGWC ) );  
 NETICVA3 =NET2Y (@INDEX (YEAR3 ) , @INDEX (ICVA ) );  
 NETICWC3 =NET2Y (@INDEX (YEAR3 ) , @INDEX (ICWC ) );  
 NETFAVA3 =NET2Y (@INDEX (YEAR3 ) , @INDEX (FAVA ) );  
 NETFAWC3 =NET2Y (@INDEX (YEAR3 ) , @INDEX (FAWC ) );  
 NETFMWR3 =NET2Y (@INDEX (YEAR3 ) , @INDEX (FMWR ) );  
 NETICWR3 =NET2Y (@INDEX (YEAR3 ) , @INDEX (ICWR ) );  
 NETDIWC3 =NET2Y (@INDEX (YEAR3 ) , @INDEX (DIWC ) );  
 NETGFBM3 =NET2Y (@INDEX (YEAR3 ) , @INDEX (GFBM ) );  
 NETFTDI3 =NET2Y (@INDEX (YEAR3 ) , @INDEX (FTDI ) );  
 NETBMWC3 =NET2Y (@INDEX (YEAR3 ) , @INDEX (BMWC ) );  
 NETDIBO3 =NET2Y (@INDEX (YEAR3 ) , @INDEX (DIBO ) );  
 NETEEWC3 =NET2Y (@INDEX (YEAR3 ) , @INDEX (EEWC ) );  
 NETSTVA3 =NET2Y (@INDEX (YEAR3 ) , @INDEX (STVA ) );  
 NETMPWC3 =NET2Y (@INDEX (YEAR3 ) , @INDEX (MPWC ) );  
 NETCPWC3 =NET2Y (@INDEX (YEAR3 ) , @INDEX (CPWC ) );

DATA:

@TEXT

('C:\Users\aromero.CORP\Documents\Demands\_Calculation\LINGO\_MODELS\LTOMSES\results.txt') = @TABLE( alpha );

@OLE('C:\Users\aromero.CORP\Documents\Demands\_Calculation\LINGO\_MODELS\LTOMSES\results.xlsx', ' NETTGVA ', 'NETMGWC','NETCGVA','NETCGWC')= NETTGVA, NETMGWC,NETCGVA,NETCGWC ;

@OLE('C:\Users\aromero.CORP\Documents\Demands\_Calculation\LINGO\_MODELS\LTOMSES\results.xlsx', 'NETICVA', 'NETICWC','NETFAVA',' NETFAWC', 'NETFMWR', 'NETICWR', 'NETDIWC' )= NETICVA, NETICWC,NETFAVA, NETFAWC, NETFMWR, NETICWR, NETDIWC;

@OLE('C:\Users\aromero.CORP\Documents\Demands\_Calculation\LINGO\_MODELS\LTOMSES\results.xlsx', 'NETGFBM', 'NETFTDI', 'NETBMWC', 'NETDIBO', 'NETEEWC', 'NETTGDI','NETMPWC','NETCPWC')= NETGFBM, NETFTDI, NETBMWC, NETDIBO, NETEEWC, NETSTVA,NETMPWC,NETCPWC ;

@OLE('C:\Users\aromero.CORP\Documents\Demands\_Calculation\LINGO\_MODELS\LTOMSES\results.xlsx', ' NETTGVA2 ', 'NETMGWC2','NETCGVA2','NETCGWC2')= NETTGVA2, NETMGWC2,NETCGVA2,NETCGWC2 ;

@OLE('C:\Users\aromero.CORP\Documents\Demands\_Calculation\LINGO\_MODELS\LTOMSES\results.xlsx', 'NETICVA2', 'NETICWC2','NETFAVA2',' NETFAWC2', 'NETFMWR2', 'NETICWR2', 'NETDIWC2' )= NETICVA2, NETICWC2,NETFAVA2, NETFAWC2, NETFMWR2, NETICWR2, NETDIWC2;

@OLE('C:\Users\aromero.CORP\Documents\Demands\_Calculation\LINGO\_MODELS\LTOMSES\results.xlsx', 'NETGFBM2', 'NETFTDI2', 'NETBMWC2', 'NETDIBO2', 'NETEEWC2', 'NETTGDI2','NETMPWC2','NETCPWC2')= NETGFBM2, NETFTDI2, NETBMWC2, NETDIBO2, NETEEWC2, NETSTVA2,NETMPWC2,NETCPWC2 ;

@OLE('C:\Users\aromero.CORP\Documents\Demands\_Calculation\LINGO\_MODELS\LTOMSES\results.xlsx', ' NETTGVA3 ', 'NETMGWC3','NETCGVA3','NETCGWC3')= NETTGVA3, NETMGWC3,NETCGVA3,NETCGWC3 ;

@OLE('C:\Users\aromero.CORP\Documents\Demands\_Calculation\LINGO\_MODELS\LTOMSES\results.xlsx', 'NETICVA3', 'NETICWC3','NETFAVA3',' NETFAWC3', 'NETFMWR3', 'NETICWR3', 'NETDIWC3' )= NETICVA3, NETICWC3,NETFAVA3, NETFAWC3, NETFMWR3, NETICWR3, NETDIWC3;

@OLE('C:\Users\aromero.CORP\Documents\Demands\_Calculation\LINGO\_MODELS\LTOMSES\results.xlsx', 'NETGFBM3', 'NETFTDI3', 'NETBMWC3', 'NETDIBO3', 'NETEEWC3', 'NETTGDI3','NETMPWC3','NETCPWC3')= NETGFBM3, NETFTDI3, NETBMWC3, NETDIBO3, NETEEWC3, NETSTVA3,NETMPWC3,NETCPWC3 ;

@OLE('C:\Users\aromero.CORP\Documents\Demands\_Calculation\LINGO\_MODELS\LTOMSES\results.xlsx','PDI', 'PBM', 'PCG', 'PPR' )= PDI, PBM, PCG, PPR ;

@OLE('C:\Users\aromero.CORP\Documents\Demands\_Calculation\LINGO\_MODELS\LTOMSES\results.xlsx','AFIXC','AVARC','ANNUAL\_COST')= AFIXC,AVARC,ANNUAL\_COST;

ENDDATA

END







